Remote sensing the distribution and spatiotemporal changes of major lichen communities in the Central Namib Desert

Vom Fachbereich Biologie der Universität Kaiserslautern zur Verleihung des akademischen Grades "Doktor der Naturwissenschaften" genehmigte Dissertation.

vorgelegt von
Christoph Schultz

Kaiserslautern, 2006.
(D 386)

Tag der wissenschaftlichen Aussprache
8. Februar, 2006.

Prüfungskommission:

1. Gutachter: Prof. Dr. Burkhard Büdel

2. Gutachter: Dr. Bianca Hörsch

Vorsitzender: Prof. Dr. Matthias Hahn

I, Christoph Schultz, do hereby declare that this submission is my own work and that, to the best of my knowledge and belief, it contains no material previously published by another person nor material which to a substantial extent has been accepted for the award of any other degree or diploma of a university or other institute of higher learning.

Hiermit erkläre ich, Christoph Schultz, dass ich diese Dissertation selbständig verfasst habe und dass ich keine anderen Quellen und Hilfsmittel als die angegebenen benutzt und die Stellen der Arbeit, die anderen Werken dem Wortlaut oder dem Sinn nach entnommen sind, in jedem Fall als Entlehnung kenntlich gemacht habe. Das gleiche gilt auch für beigegebene Zeichnungen, Karten, Skizzen und Abbildungen.

Kaiserslautern, im Dezember 2005.

Acknowledgements

There are many persons I owe to thank for their support and encouragement during my PhD thesis. This was a long and difficult period, which I might not have managed without them.

Firstly, I would like to thank Prof. Dr. Burkhard Büdel for accepting me as a PhD student and for supporting me along the way that led to my PhD work. Secondly, I am highly indebted to Dr. Bianca Hörsch for her continued support, valuable guidance.

I also thank Dr. Michael Schmidt, Dr. Gerald Braun and Prof. Dr. Stefan Dech for the possibility to work in the Biota project which has been a great experience about real life science.

In particular, I thank Dr. Jo Henschel, Dr. Kurt Loris and Prof. Dr. Dirk Wessels for their expertise and cheerful contribution to my work, as well as Elke Erb, Roger Braby and Ben Strohbach for providing me with expert knowledge on their country's ecology.

This list would not be complete without mentioning my present and former colleagues of the German Remote Sensing Data Center and the Unit of Remote Sensing, University of Würzburg: Among others Thilo Wehrmann, Rene Colditz, Martin Bachmann, Michael Bock, Michael Wissen, Godela Roßner, Ralf Hanatschek and Robert Backhaus for prolific discussions and scientific support.

Last but not least I want to thank my family. First of all I thank my wife Margret Schultz for she knows how difficult it is having a husband writing a PhD thesis. She always gave me strength and encouragement as well as practical advises and was always there for me. I also feel a deep sense of gratitude for my parents. The happy memory of my mother still provides a persistent inspiration for my journey in this life.

Thank you all.

Abstract

Biological Soil Crusts (BSCs), composed of lichens, mosses, green algae, microfungi and cyanobacteria are an ecological important part of the perennial landcover of many arid and semiarid regions (Belnap et al. 2001a), (Büdel 2002). In many arid and hyperarid areas BSCs form the only perennial "vegetation cover" largely due to their extensive resistance to drought (Lange et al. 1975).

For the Central Namib Desert (Namibia), BSCs consisting of extraordinary vast lichen communities were recently mapped and classified into six morphological classes for a coastal area of 350 km x 60 km. Embedded into the project "BIOTA" (www.biota-africa.org) financed by the German Federal Ministry of Education and Research the study was undertaken in the framework of the PhD thesis by Christoph Schultz.
Some of these lichen communities grouped together in so called "lichen fields" have already been studied concerning their ecology and diversity in the past (Lange et al. 1994), (Loris & Schieferstein 1992), (Loris et al. 2004), (Ullmann & Büdel 2001a), (Wessels 1989).

Multispectral LANDSAT 7 ETM+ and LANDSAT 5 TM satellite imagery was utilized for an unitemporal supervised classification as well as for the establishment of a monitoring based on a combined retrospective supervised classification and change detection approach (Bock 2003), (Weiers et al. 2003). Results comprise the analysis of the mapped distribution of lichen communities for the Central Namib Desert as of 2003 as well as reconstructed distributions for the years 2000, 1999, 1992 and 1991 derived from retrospective supervised classification.

This allows a first monitoring of the disturbance, destruction and recovery of the lichen communities in these arid environments including the analysis of the major abiotic processes involved. Further analysis of these abiotic processes is key for understanding the influence of Namib lichen communities on overall aeolian and water induced erosion rates, nutrient cycles, water balance and pedogenic processes (Belnap & Gillette 1998), (Belnap et al. 2001b), (Belnap 2001c), (Evans & Lange 2001), (McKenna Neumann & Maxwell 1999).
In order to aid the understanding of these processes SRTM digital elevation model data as well as climate data sets were used as reference. Good correlation between geomorphological form elements as well as hydrological drainage system and the disturbance patterns derived from individual post classification change comparisons between the timeframes could be observed. Conjoined with the climate data sets sporadic foehn-like windstorms as well as extraordinary precipitation events were identified to largely affect the distribution patterns of lichen communities.

Therefore the analysis and monitoring of the diversity, distribution and spatiotemporal change of Central Namib BSCs with the means of Remote Sensing and GIS applications proof to be important tools to create further understanding of desertification and degradation processes in these arid regions.

"Warum interessierren Sie sich eigentlich so sehr für diese Geschichte, Mr. Bulero? Haben Sie eine, äh, besondere Vorliebe für Flechten?"
"Nein, Mister Hepburn-Gilbert, ich bin nur ein um das Gemeinwohl besorgter Bürger des Sol-Systems. Und ich verlange, daß Sie etwas unternehmen."

Philip K. Dick, Die drei Stigmata des Palmer Eldritch.

CURRICULUM VITAE

Personal Information

CHRISTOPH SCHULTZ
Theodor-Litt-Str. 9
53121 Bonn
E-Mail: christoph@familie-schultz.de
born in Bergisch Gladbach, Germany (Jan. 6, 1974)
married

Education

since 06/2001	Research Assistent at the German Aerospace Center (DLR), German Remote Sensing Data Center (DFD), Department of Environment and Geoinformation, Cologne / Munich, Germany.
04/1994 - 04/2001	Studies at the Department of Geography, University of Bonn, Germany (Specialization in Ecology and Environmental Sciences). Final Degree: Diplom Geographer. Thesis: "Fernerkundungs- und GIS-gestützte Untersuchung der Zusammenhänge zwischen Phytodiversität und Geofaktoren Afrikas".
10/1993 - 03/1994	Studies at the Department of Geography University of Cologne, Germany.
1984 - 06/1993	Dietrich-Bonhöffer-Gymnasium, Bergisch Gladbach, Germany.
08/1990 - 12/1990	Coronado High School, Colorado Springs, Colorado, United States of America
1980 - 1984	Primary School: Gemeinschafts-Grundschule Hand-Paffrath, Bergisch Gladbach, Germany.

Employment

01/1996 - 03/1999	Student Assistent at the Department of Geography, Prof. Winiger, University of Bonn, Germany.
09/1999 - 08/2000	Student Assistent at the Institute for the Study of Labor (IZA) Bonn, Germany.
since 06/2001	Research Assistent at the German Aerospace Center (DLR), German Remote Sensing Data Center (DFD), Department of Environment and Geoinformation, Cologne / Munich, Germany. Focus: BIOTA Southern-Africa Project, funded by the German Ministry of Research and Education.
since 2002	Ph.D. studies at the Department of General Botany, Technical University of Kaiserslautern, Germany.

International Experience

02/1999 - 03/1999	DFG-Research-Project in the Kalahari Desert, South Africa.
03/2002 - 04/2002	Field work for the Biota-Southern-Africa Project within the Central Namib Desert, Namibia.
04/2003 - 05/2003	Field work for the Biota-Southern-Africa Project within the Central Namib Desert, Namibia.
02/2005 - 04/2005	Field work for the Biota-Southern-Africa Project within Central- and Northern Namibia as well as the Central Namib Desert, Namibia.
09/2005 - 10/2005	Field work for the Biota-Southern-Africa Project within the Namaqualand, South Africa, Central Namibia and the Central Namib Desert, Namibia.

Publications

Schultz, C. (2001): Fernerkundungs- und GIS-gestützte Untersuchung der Zusammenhänge zwischen Phytodiversität und Geofaktoren Afrikas. Diplomarbeit, Bonn.

Mutke, J., Kier, G., Braun, G., Schultz, C. & Barthlott, W. (2001): Patterns of African vascular plant diversity - a GIS based analysis. In: Systematics and Geography of Plants. Bd. 71, 1125-1136.

Hörsch, B., Schultz, C., Hanatschek, R. & Vogel, M. (2002): Remote Sensing and GIS based Survey of Spatial and Temoporal Biodiversity Dynamics in Southern and West Africa. Proceedings of the Second Workshop of the EARSeL Special Interest Group on Remote Sensing for Developing Countries, Bonn.

Hörsch, B., Schultz, C., Hanatschek, R. & Vogel, M. (2003): The Potential of Remote Sensing and GIS for Biodiversity Monitoring in Southern Africa. GTÖ 2003 - 16. Jahrestagung, Rostock.

Büdel, B., Deutschewitz, K., Dojani, S. Hörsch, B., Loris, K., Rambold, G., Reisser, W., Salisch, M., Schultz, C., Weber, B., Wirth, V. & Zedda, L. 2004. Biodiversity and ecology of biological soil crusts (BSCs): from the micro-scale to the ecosystem scale. In Beck, E., Berendsohn, W.G., Boutros, M., Denich, M., Henle, K., Jürgens, N., Kirk, M. & Wolters, V. (eds.), Sustainable use and conservation of biological diversity - a challenge for society. - 142-144. Bonn.

Becker, T., Schultz, C., Vogel, M., Hörsch, B., Strohbach, M. & Hanatschek, R. (2005): Zum Stand der Vegetationskartierung im Rahmen des BIOTA Southern Africa-Projektes. Basic and Applied Dryland Research I - Beiträge des Arbeitskreises Wüstenökologie. M. Veste, Akhtar-Schuster, M., Wissel, C. Leipzig, UFZ.

Weber, B., Deutschewitz, K., Schultz, C., Dojani, S. & Büdel, B. (2005): Development and Implementation of Remote Sensing Techniques for Long-Term Monitoring of Biological Soil Crusts (BSCs) - Utilization of CHRIS-Proba Data for Upscaling and Classification. In: B. Hörsch: 3rd CHRIS-Proba Workshop, ESRIN, Frascati, Italy, ESA. pp 6.

Schultz, C. & B. Weber (2005): Multi-scale remote sensing techniques for long-term monitoring of Biological Soil Crusts (BSCs). In: BMBF: Biodiversity and Global Change - Statusreport 2005, Wuerzburg, PT-DLR Environmental Research and Technology. pp 141.

Schultz, C. (2006): Remote sensing of the distribution and spatiotemporal changes of major lichen communities in the Central Namib Desert. PhD Thesis, Kaiserslautern.

List of Abbreviations

AODA	Attitude and Orbit Determination Avionics
ASI	Agenzia Speziale Italiana
ASD	Analytical Spectral Devices field spectrometer
	FR Full Range
ATCOR	Atmospheric Correction Algorithm
AVHRR	Advanced Very High Resolution Radiometer
AVIRIS	Airborne Visible and Infra-Red Imaging Spectrometer
BIOTA	Biodiversity Monitoring Transekt Analysis in Africa
BMBF	German Federal Ministry of Education and Research
BSC	Biological Soil Crusts
BSCI	Biological Soil Crust Index (spectral)
CASI	Compact Airborne Spectrographic imager
CCA	Canonical Correspondence Analysis
CHRIS-Proba	Compact High Resolution Imaging Spectrometer - Project for On-Board Autonomy
CI	Crust Index
CIR	Colour Infra Red
DAIS	Digital Airborne Imaging Spectrometer
DEM	Digital Elevation Model
DIVERSITAS	International Biodiversity Taskforce of the UN
DLR	German Aerospace Center
DFD	German Remote Sensing Data Center
DN	Digital Numbers
DRFN	Desert Research Foundation Namibia
DSU	Derivative Spectral Unmixing Mode
EONN	Environmentala Obervatories Network of Namibia
ETM+	Enhanced thematic mapper
F-Distribution	Fisher-Distribution
FOV	Field of View
GCP	Ground Control Points
GFZ	Germany's National Research Centre for Geoscience
GPS	Global Positioning System
HPLC	High Pressure Liquid Chromatography
JM	Jeffries-Matusita (divergence measure)
JPL	Jet Propulsion Laboratory
LF	Lichen Field
MMS	Monolithic Miniature Spectrometer
MSS	Multispectral Scanner
MODIS	Moderate Resolution Imaging Spectrometer
MSAVI	Modified Soil-Adjusted Vegetation Index
MVC	Maximum Value Compositing

NDVI	Normalized Difference Vegetation Index
NOAA	National Oceanic and Atmospheric Administration
NPP	Net Primary Production
NWCTRA	National West Coast Tourist Recreation Area
ODT	Ocean Data Takes
PADR	Position and Attitude Data Record
PAM	Pulse-Amplitude-Modulation
PCA	Principal Component Analysis
	sPCA selective PCA
PIF	Pseudo-Invariant Features
R-NIR	Red Near infra red
SAR	Synthetic Aperture Radar
SASI	Shortwave Infrared Spectrographic Imager
SAVI	Soil-Adjusted Vegetation Index
SCL	Scan Line Corrector
SMA	Spectral Mixture Analysis
TFV	Treshold Friction Velocities
TM	Thematic mapper
TOA	Top of Atmosphere
UNCBD	International Convention on Biodiversity
ULX, ULY	upper left X-coodinate, upper left Y-coordinate
UTM	Universal Transverse Mercator (projection)
USGS	US Geological Survey
WGS 84	World Geodetic System 1984 (projection)
WRS	World Reference System (projection)
X-SAR/SRTM	X-Band Synthetic Aperture Radar / Shuttle Radar Topography Mission

Contents

Figures

Formulas

Maps

Photos

Tables

1 Introduction

Biological soil crusts, composed of lichens, mosses, green algae, microfungi and cyanobacteria are an important ecological part of the perennial land cover in many arid regions of the world (BELNAP ET AL. 2001A, BÜDEL 2002).

They are defined as follows: "Biological soil crusts result from an intimate association between soil particles and cyanobacteria, algae, microfungi, lichens, and bryophytes which live within, or immediately on top of, the uppermost millimetres of soil. Soil particles are aggregated through the presence and activity of these biota, and the resultant living crust covers the surface of the ground as a coherent layer" (BELNAP ET AL. 2001A).

Biological soil crusts are often referred to as cryptogamic, cryptobiotic, microbiotic, microfloral, microphytic or organogenic soil crusts as well. In contrast to these terms "biological soil crusts" is the broadest term which clearly states that these crusts are dependent on the activity of living organisms, in contrast to physical or chemical crusts. It includes no taxonomic implications and is applicable to soil crusts regardless of their species composition. Moreover this term may also be used to address communities, closely related to biological soil crusts, but excluded by a strict interpretation of the definition. This includes communities unassociated to soil particles, growing on top of organic material, or where the majority of biomass is located above the soil surface (BELNAP ET AL. 2001A).

In many desert biomes biological soil crusts form the only perennial "vegetation cover" largely due to their extensive resistance to drought (LANGE ET AL. 1975). Therefore biological soil crusts also have a strong influence on desert ecosystems regarding their soil stability, build up, fertility and water regime. In addition species forming soil crusts are often the only organisms capable of nitrate-fixation while at the same time providing significant carbon input into ecosystems (EVANS & LANGE 2001A, WARREN 2001B, BELNAP ET AL. 2001B).

In-situ measurements of maximal daily carbon gains of three crustose Namib Desert lichen species by LANGE ET AL. (1994) amounted in 158 to 290 mg C m^{-2} day^{-1}, while maximal chlorophyll contents ranged from 236 to 508 mg m^{-2}. Considering that average chlorophyll contents of semi-arid and arid regions range from 100 to 1500 mg m^{-2}, biological soil crusts contribute significantly to the biomass of these biomes (BÜDEL 2002). In addition, observed maximal daily carbon gains are remarkable given the hostility of the Namib environment (LANGE ET AL. 1990).

However, most ecosystem balances do not account for biological soil crust at the level of CO_2 sinks. Therefore it is extremely interesting to learn more about the role of biological soil crusts towards their possible role as part of global carbon cycles (BÜDEL 2002). Yet, the knowledge of the distribution of biological soil crusts, their ecological function, as well as information on their role in ecosystems is still limited and often reflects the geographic preference of researchers (ULLMANN & BÜDEL 2001A, BÜDEL 2001B).

On a regional scale biological soil crusts occur in many different biomes worldwide (BÜDEL 2001B). In particular, the highly diverse biological soil crust communities of the Namib Desert can be considered unique on a global scale (WALTER 1985, ULLMANN & BÜDEL 2001A, SEELY 2004[3]). Dominated by phycol-

ichens and differing in composition and structure they also form numerous large lichen fields within the fog zone of the Central Namib Desert due to almost ideal environmental conditions (WESSELS & VAN VUUREN 1986, ULLMANN & BÜDEL 2001A, LORIS ET AL. 2004, WALTER & BRECKLE 1999?).

Although widespread, these biological soil crusts are extremely vulnerable to disturbance or destruction. As they protect the upper soil surface, small anthropogenic and natural disturbances often lead to a severe increase of soil erosion rates following corrasion and deflation by windstorms as well as water runoff (BELNAP & GILLETTE 1998, BELNAP & ELDRIDGE 2001). Due to slow recovery rates, reduction of carbon and nitrate influx into corresponding ecosystems will also reduce their fertility which is undoubtedly one of the most definitive and serious aspects of desertification (EVANS ET AL. 2001, BELNAP 2001).

Over the past years several efforts have been made to emphasize the need for the conservation of these unique lichen fields (GIESS 1989). Following a scientific symposium held at Swakopmund in 1987, efforts to educate and inform the general public about the fragility of the Namib ecosystem and need for its conservation were initiated (HEINRICH 1986). Consequently site-specific ecological studies included the description of new lichen species, and the structure, composition, biomass and distribution of lichen communities in the Central Namib Desert (BÜDEL & WESSELS 1986, WESSELS & VAN VUUREN 1986,KÄRNEFELT 1988, SCHIEFERSTEIN 1989, WESSELS 1989, LANGE ET AL. 1990, LORIS & SCHIEFERSTEIN 1992, LANGE ET AL. 1994, LALLEY & VILES 2005).
Regard being had to their nature, biological soil crusts have been considered an important management issue, in particular with the gradually increasing anthropogenic land-use of arid and semi-arid territories forming a great potential thread (ULLMANN & BÜDEL 2001A, BELNAP & ELDRIDGE 2001). As a consequence spatial patterns of soil crusts can also be employed to indicate changes in the utilization and function of landscapes. Furthermore, a much better understanding of the large-scale distribution patterns is crucial for desertification and climate change studies as well as conservation measures (BÜDEL 2001B).
Therefore it is essential to identify the occurrence and distribution of biological soil crusts and monitor their spatiotemporal changes on a regional scale complementary to site-specific ecological studies (KARNIELI ET AL. 2001B, BELNAP ET AL. 2001A, ULLMANN & BÜDEL 2001B, BELNAP 2002, CHEN ET AL. 2005). However all of these objectives are difficult to accomplish, in particular regarding the spatial extend, the repeat frequency and the need to access remote and difficult terrain (WYATT 2000).

In compliance with these requirements remote sensing data and classification techniques have become an indispensable tool for any spatially extensive survey of vegetation or land cover on many scales (JENSEN 2000). Supplementary multi-date satellite imagery has also successfully been used to determine spatial patterns of land cover changes in the past (PILON ET AL. 1988, MUCHONEY & HAACK 1994, JENSEN ET AL. 1995, COPPIN & BAUER 1996, LEVIEN ET AL. 1998, EKLUND ET AL. 2000).

However, despite these benefits there have been relatively few studies published on the use of remote sensing to detect and to map the distribution and spatiotemporal changes

of biological soil crusts (KARNIELI ET AL. 2001B).
WESSELS & VAN VUUREN (1986) were the first to use multispectral LANDSAT data for the assessment of the biological soil crust communities dominated by phycolichens. Solely based on visual analysis, this study emphasized the possible use of satellite imagery to map the distribution of Namib Desert lichen community coverage. Furthermore they suggested that extensive ground reference data must be available for an accurate differentiation of lichen communities.

Subsequently various types of remotely sensed data have been used for the assessment of biological soil crusts. Airborne orthoimages and hyperspectral, and spaceborne multispectral remote sensing datasets have been employed to map their distribution patterns at various scales. Applied methods and techniques included regression analysis (WASER ET AL. 2003), spectral indexing (KARNIELI 1997, CHEN ET AL. 2005), and spectral feature analysis based on spectroscopic measurements (KOKALY ET AL. 1994, KARNIELI ET AL. 2001B).

Other studies including the spectral analysis of laboratory or in-situ reflectance measurements of biological soil crusts were presented by AGER & MILTON (1987), KARNIELI & TSOAR (1995), KARNIELI ET AL. (1996), KARNIELI (1997), KARNIELI ET AL. (1999), SCHMIDT & KARNIELI (2000), GARTY ET AL. (2001), OKIN ET AL. (2001), BECHTEL ET AL. (2002), KARNIELI ET AL. (2002), and REES ET AL. (2004).
However, neither laboratory or in-situ reflectance measurements, nor results of local regression analysis and site-specific spectral indices allow biological soil crusts to be mapped and detected on a regional scale regardless of location. On the contrary, only airborne hyperspectral remote sensing datasets offer the ability to precisely resolve and identify surface materials based on spectral absorption and reflectance features. Although superior to both airborne orthoimages and spaceborne multispectral datasets, it does not share all of the benefits for mapping and monitoring large areas. Due to its airborne character acquisition is costly and spatial coverage is usually limited to a small strip. In addition repeated acquisition usually requires a large budget.

On the contrary multispectral remote sensing provides consistent, high resolution and reproducible information combined with high repeat frequencies needed to detect, map and monitor biological soil crusts on a regional scale. However, despite these considerable advantages preceding studies have focussed on the visual, site-specific and monotemporal analysis of these datasets. They did not include the utilization of contiguous multispectral datasets to detect and map the spatial distribution of biological soil crusts on a regional scale, while at the same time analyse their spatiotemporal changes based on multiple acquisition dates.

Based on the presented objectives this thesis will focus on the remotely sensed detection and mapping of the distribution of the lichen dominated biological soil crust communities of the Central Namib Desert, Namibia, using multispectral LANDSAT 7 ETM+ data. Furthermore spatiotemporal changes of the distribution patterns of lichen communities are analysed using multi-date LANDSAT 5 TM and LANDSAT 7 ETM+ data.

1.1 Objectives and innovations of this thesis

The objectives and innovations of this thesis are as follows:

- **Detecting and mapping the spatial distribution of major lichen communities in the Central Namib Desert**

Subsequent to preliminary studies of the past and supplemental to site-specific ecological studies the first objective of this thesis will focus on the analysis of the current spatial distribution of the lichen communities in the Central Namib Desert based on multispectral LANDSAT 7 ETM+ satellite imagery. Utilizing fuzzy enhanced supervised classification techniques in conjunction with a hierarchical classification scheme, derived from the concept of morphological groups, determination among differing lichen communities is accomplished.

Eliminating the need for complex, often confusing changes in nomenclature the concept of morphological groups also allows the transfer of the applied methodology to different regions and continents (e.g. Atacama, Chile). Based on this conceptual framework and extensive ground reference a hierarchical classification scheme is derived, enabling the classification of Central Namib Desert lichen communities. Supplementary mean spectral reflectance curves obtained from in-situ spectroradiometer measurements of selected lichen communities are analysed to support the findings. In order to overcome the various uncertainties still present in satellite derived land cover classifications, probabilities of class memberships will be used to gather additional information on overall classification stability, reliability and class separability. Thus fuzzy classification techniques will be used in addition to conventional maximum-likelihood methodology for improved results and accuracy assessment.

Based on this approach a first map describing the distribution of major lichen communities of the Central Namib Desert is presented for the year 2003. Furthermore areal statistics will be discussed. The presented distribution map of 2003 also intends to assist future conservation measures as coherent and unaltered existence of most lichen communities is increasingly endangered by anthropogenic utilization and recreational activities.

- **Identifying spatiotemporal changes in the distribution of major lichen communities in the Central Namib Desert**

Almost no ecosystem is at equilibrium but fluctuates in response to various forms of disturbance. Frequent intense disturbances may permanently alter lichen distribution patterns due to slow recovery rates, while others may only cause fluctuations.

Therefore a first approach to identify spatiotemporal changes in the distribution of major lichen communities in the Central Namib Desert is presented. Based on post classification change detection, multi-date LANDSAT 7 ETM+ and LANDSAT 5 TM satellite imagery will be used to determine these variations. The identification of spatiotemporal changes in the distribution of lichen communities is also supported by the weakly developed climatic seasonality of the coastal regions of the Central Namib Desert. In order to accomplish multitemporal classification, ground reference information acquired during field campaigns is analysed using selective PCA (sPCA) change detection techniques. Thus sPCA based information of changes between corresponding image pairs, is calculated on all training samples already

utilized for the unitemporal classification. Based on the individual yet consecutive comparison of mean changes, invariant training samples are identified. Following this procedure, a validated set of reference information is derived, allowing the supervised classification of multitemporal satellite imagery. Subsequently individual classification stability, reliability, class separability and accuracy are assessed in correspondence to the unitemporal classification approach. Thus requirements for a post-classification comparison are met. Therefore spatiotemporal changes in the distribution of lichen communities will be presented for the study area using change matrix computations of corresponding multitemporal classification results. Supplementary areal statistics are calculated and discussed.

- **Analysing disturbance patterns of major lichen communities in the Central Namib Desert**

As a result of the change matrix computations of the multitemporal classification, disturbance patterns are outlined. However, their origins are unclear as no long-term studies on the spatiotemporal changes of lichen distributions in the Central Namib Desert exist. However, the impact of a given disturbance always depends on the biotic and abiotic characteristics of the site and the severity, frequency, and type of the disturbance. Therefore disturbance patterns of major lichen communities in the Central Namib Desert are analysed using auxiliary spatiotemporal information on biotic, abiotic, and site-specific aspects of the study area.

Hence climate data obtained from automatic weather stations, orographic data derived from a digital elevation model (DEM), and field observations are utilized. In addition information available from previous studies addressing the structure, composition and distribution of lichen communities is incorporated. Moreover studies featuring vegetation dynamics and climate of the Central Namib Desert in general are also included to support the findings.

As a whole, this analysis will focus on the identification of spatiotemporal coherences between observed disturbance patterns and auxiliary reference information obtained for the study area. Thereby different natural and anthropogenic forms of disturbances affecting the distribution of lichen communities of the Central Namib Desert are identified. As some of the observed disturbance patterns have evolved in the absence of human impacts, analysis will also contribute to the identification of ecological factors controlling lichen distribution patterns based on remotely sensed data. A schematic overview of this thesis is also depicted in figure1.

1.2 Programmatic framework of this thesis

This thesis is embedded into the "BIOTA Southern Africa" project (Biodiversity Monitoring Transect Analysis in Africa), which is part of the BIOLOG program framework funded by the German Federal Ministry of Education and Research (BMBF).

As a whole, BIOTA-Africa aims to create a significant contribution to the International Convention on Biodiversity (UNCBD) and follows the guidelines of the international biodiversity task force of the United Nations (UN), called DIVERSITAS.

"There is an increasing awareness that biodiversity is intimately interconnected with long-term health and vigour of the biosphere, as an indicator of the global environment but

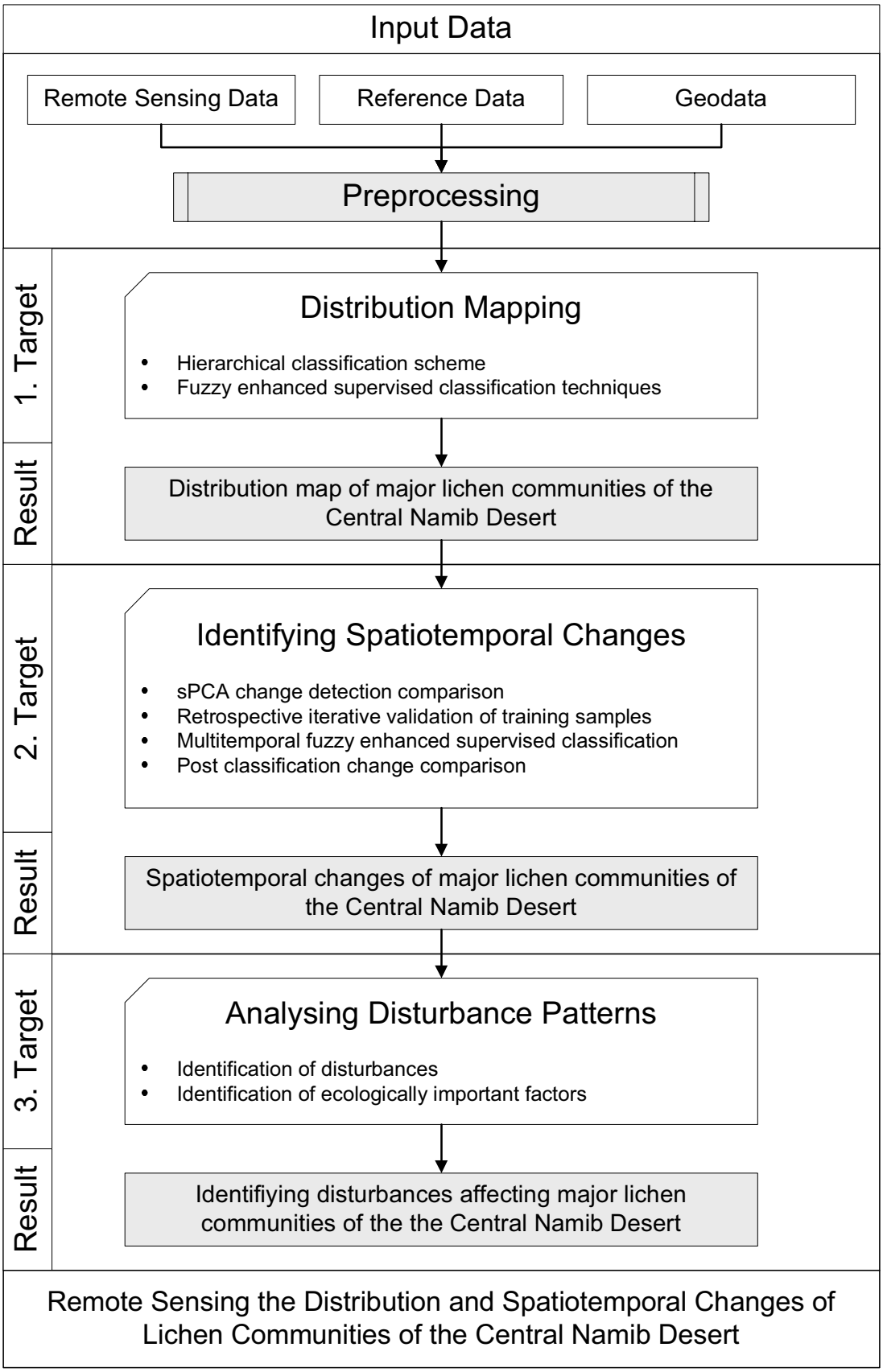

Figure 1: Workscheme of this thesis.

also as a regulator of ecosystem functioning" (SOLBRIG 1991 in STOMS & ESTES 1993).

Therefore the BIOTA Southern Africa project aims to analyse the changes of biodiversity in the most important biomes by means of an interdisciplinary and integrative approach including numerous African as well as German research institutions and universities. The overall goal of the project is the achievement of knowledge for decision-makers for a practical, efficient and sustainable management of the different aspects of biodiversity, taking into account the functioning of ecosystems as well as the socio-economic framework. Feasible socio-economic land use practises will be analysed in combination with scientifically based conservation concepts in order to preserve the resource biodiversity.
Along the most important climatic gradient, following the rainfall gradient from the dry forests to arid savannah and further to the winter rainfall zones in southern Africa (Namibia and South Africa), transect study areas were created (compare figure 2). This also includes the observatory site of Wlotzkasbaken situated within the study area addressed in this thesis.

This study ties in with three subprojects of Biota-Africa addressing remote sensing (S01 and W01) as well as biological soil crusts (S05). It is based on a cooperation between German Remote Sensing Data Centre (DFD), institute of German Aerospace Centre (DLR) and the Plant Ecology and Systematics research group of Prof. Dr. Burkhard Büdel located at the Technical University of Kaiserslautern.

Subprojects S01 and W01 create the basis for a system in which both, remote sensing and GIS applications form an analysis and monitoring system for the assessment of human

Figure 2: Schematic overview of the "BIOTA Southern Africa" research transects and study areas.

impacts on biological diversity. In addition subproject S05 addresses the biodiversity, functional diversity, their environmental determinants and ecosystematic role of biological soil crusts.
Multi-scale remote sensing as well as GIS datasets are utilized to allow the analysis of spatial patterns of biodiversity, its temporal changes and the mutual dependency of geodiversity and biological diversity. Thus development and implantation of remote sensing techniques for long-term monitoring of biological soil crusts is conducted.

Socio-economic activity has led to various degradation levels of natural ecosystems. In addition human impact also affects the

dynamics and diversity of biological soil crusts. Therefore comparative studies of natural and degraded ecosystems in regards of the functional ecology of biological soil crust and their influence on nutrient cycling are accomplished.

Thus the detection and indications of spatial patterns and diversity changes of biological soil crusts, using remote sensing techniques, will contribute to future monitoring and conservation concepts.

2 Current state of research

This chapter focuses on presenting the current knowledge published by numerous researchers on and being relevant for this thesis. Specific aspects such as the description of new lichen species, and the structure, composition, biomass, distribution, remote sensing and possible monitoring of lichen communities for the study area of the Central Namib Desert are presented, in relation to the objectives, inventions and general contributions to the research topic of this thesis.

2.1 Relation of the Namib Desert lichen flora with other fog desert lichen communities

Reviewed by ROGERS (1977), RUNDEL (1978) and BÜDEL (2001a) comprehensive information on lichens in the coastal fog deserts of the world is available to date. However, little is known about the distribution, vegetation patterns and morphological as well as ecophysiological adaptations of lichen communities of the Namib Desert (ULLMANN & BÜDEL 2001A). To date LANGE ET AL. (1990), LANGE ET AL. (1991) and LANGE ET AL. (1994) were the only ones to report on water relations, CO_2 exchange, and assimilation rates of selected Namib Desert lichen species. On the contrary many studies have addressed the fog deserts of the New World. REDON & LANGE (1983), for example, described habitat conditions and distribution patterns of epiphytic lichens in a Chilean fog oasis and the CO_2 exchange and water relations of typical fog lichens in this area. Whereas NASH ET AL. (1979) reported on the fruticose lichens of the coastal region of Baja California and MATTHES-SEARS ET AL. (1986) described water relations and primary production of *Ramalina menziesii* which grows along the western coast of the United States. Furthermore FOLLMANN (1966) and FOLLMANN & REDON (1972) presented information on the species composition of lichen communities of the fog zone of the Atacama Desert.

Based on studies reported on in DOIDGE (1950), ROGERS (1977) proposed that the Namib lichen flora is related to the lichen flora of drier areas of Australia. These findings have also been verified by BÜDEL (2001B). According to BÜDEL (2001B) African lichen genera show large floristic similarities to asian and middle-eastern populations (60 – 90 %), but no conclusions are drawn on the phytogeographic relationships of southern African lichens in particular, on the basis of present knowledge.

Nonetheless has the significance of the vast lichen communities of the fog zone of the Central Namib Desert been recognised by botanists like WESSELS & VAN VUUREN (1986), GIESS (1989), SCHIEFERSTEIN (1989), LORIS & SCHIEFERSTEIN (1992), LORIS ET AL. (2004), and LALLEY & VILES (2005) as well as geographers like WALTER (1976), WALTER (1985), AND WALTER & BRECKLE (1999[7]) for several decades.

2.2 Uniqueness of the Namib Desert lichen flora and endemism

Due to their age and the effects of plate tectonics, lichen genera and families have wide distribution ranges. In general distribution patterns follow major climatic and vegetation zones (BÜDEL 2001B). Nevertheless differentiation has been observed for geographically or ecologically isolated populations.

Confirmed by many authors, the lichen flora of the Namib Desert can also be characterized by its endemism. WESSELS & VAN VUUREN (1986) also pointed out that speciation and specialization can be considered well advanced. Endemic genera include *Coronoplectrum* and *Santessonia*, as well as a variety of

species. Regarding the genus of *Santessonia* two out of three species are known to occur exclusively in the Namibian Desert, whereas the third species, *S. hereroensis*, occurs in both the Namibian and Angolan parts of the Namib Desert. On the contrary *Pertusaria salax* is endemic to the Diamond area located in vicinity of Oranjemund in the southern parts of the Namib Desert. Other lichen species endemic to the Namib Desert include *Coronoplectrum namibicum*, *Caloplaca elegantissima* (Nyl.) Zahlbr., *Caloplaca eudoxa* (Müll. Arg.) Zahlbr., *Caloplaca namibensis* Kärnefelt, *Caloplaca volkii* Wirth & Vezda, *Lecidella crystallina* Wirth & Vezda, *Xanthoparmelia luderitziana* Hale, *Xanthoparmelia serusiauxii* Hale, *Xanthoparmelia walteri* Knox and *Xanthomaculina convoluta* (Wessels 1989). In addition, continued identification of new lichen species help to increase the knowledge Namib lichen flora, while at the same time emphasizing its uniqueness.

In total about 100 lichen species are known to exist in the Namib Desert with many of them endemic and the actual total number assumed to be much higher (Henschel 2003). As members of the lichen association at least 26 algae genera are described.

Ninety lichen species have been reported for the Sperrgebiet (Loris et al. 2004). However, due to the inaccessibility and as a consequence of continued surveys of many areas in the Namib, it is expected that these numbers will increase. On the contrary some of the known lichen species are already considered endangered by the Swedish Species Information Center. In the "Preliminary Global Red List of Lichens" *Santessonia lagunebergii* and *Santessonia namibiensis* Hale & Vobis are already listed (Swedish Species Information Center 2003). Therefore a rapid assessment of lichen distribution on a regional scale will be needed to identify distribution hotspots and assist future conservation measurements to preserve the uniqueness of the Namib Desert lichen flora.

2.3 Subject specific studies on Namib Desert lichen species

2.3.1 Taxonomy of Namib Desert lichens

The lichen flora of the Namib has firstly been described by Leonard Schultze (1907) (in Schieferstein 1989). In his article "Aus Namaland und Kalahari" he describes the lichen fields between Swakopmund and Cape Cross. Subsequently, limited species lists have been published by Zahlbrucker (1926) (in Schieferstein 1989), Doidge (1950) and Mattick (1970). New species of the fog zone of the Namib Desert were described by Wirth & Vézda (1975), Hale & Vobis (1978), Knox & Brusse (1983), Serusiaux & Wessels (1984) (all in Loris & Schieferstein 1992), Kärnefelt (1988), Hale (1990) (in Zedda & Rambold 2004), and Lalley & Viles (2005) amongst others. Feurerer (2005) also provides an online checklist of lichens and lichenicolous fungi of Namibia at the University of Hamburg, Germany.

Although the majority of species have been collected and described from the Central Namib Desert (Ullmann & Büdel 2001a), this might not be due to extraordinary species richness, but merely reflect the increased accessibility of this part of the Namib Desert. However, despite these publications, present day knowledge of the taxonomy of Namibia's lichen flora (coastal as well as inland) is still incomplete. Nevertheless, one can be certain that new species will inevitably be found in the Skeleton Coast National Park and lichen islands in the sand desert, as recent studies of Lalley & Viles (2005) have shown. In addition to these sites a number of interesting type

localities also occur in the Central Namib Desert. However, it obliges Namibian conservation authorities to preserve these sites in their original conditions.

2.3.2 Anatomical studies of Namib Desert lichens

Distinctive specializations of endemic lichen species have been reported by BÜDEL & WESSELS (1986) for the thalli of *Xanthomaculina convoluta* (as *Parmelia hueana Gyeln.*) common to the vagrant habitat. Specializations include modifications of the upper cortex, algal layer and medulla. Supplementary they also discussed the way in which the thallus unrolls during wet periods and reproduce through phyllidia. Furthermore, the unhindered movement of thalli during windy days was stressed out, as these conditions seem to favour the distribution and reproduction of the species.
The habitat and morphological features of a chasmoendolithic *Lecidea* species inhabiting cracks in quartz was discussed by WESSELS (1989). In addition to these studies he also described how this lichen weathers quartz by mechanical and chemical actions and discussed the possible advantages of its habitat.
In correspondence to KÄRNEFELT (1988), many species have various anatomical adaptations which aid in the reduction of light intensity and evaporation.
His studies also showed that *Teloschistes capensis* (L.f.) Müll. Arg. populations in the Namib have a deeper pigmentation and a denser tomentum than those in South Africa. Such a dense tomentum presumably favours the absorption of water derived from fog (KÄRNEFELT 1988). General adaptive phenomena such as thallus form and colour, thickness of the cortex and other adaptations of desert lichens have been also been discussed by LANGE ET AL. (1975).

2.3.3 Ecophysiological studies of Namib Desert lichens

Lichens apparently have no special mechanisms for the uptake or conservation of water but their thallus. It enables them to extract water from the air with almost their entire surface (WALTER & BRECKLE 1999[7]). Available water is absorbed very rapidly and lost again. They outlast drought in a dry latent state without loosing their viability. Yet extended drought can be destructive on them as field experiments have shown (LANGE ET AL. 1975).
LANGE ET AL. (1990), LANGE ET AL. (1991), and LANGE ET AL. (1994) reported on the microclimatic conditions, water content and CO_2 exchange of several lichen species, characteristic to the Central Namib Desert. They postulated fog being the most important source of water for Namib lichens. In addition, dew condensation is second most important, as it also resulted in high degrees of hydration. Thus, water contents of more than 100 % of thallus dry weight were recorded. Although initially influenced by the increase in photosynthetically active radiation, hydrated thalli showed a strong increase in net photosynthesis subsequent to sunrise. Two to four hours after sunrise, when thallus water contents decreased to less than 10 %, photosynthetic activity also ceased due to the dehydration of the lichen thallus.
Even though CO_2 uptake is limited to these periods, water vapour uptake by lichen thalli is also induced by increased air humidity during the late afternoon. According to the studies cited above, such diurnal patterns of photosynthetic activity are nonetheless influenced by the prevailing weather. However photosynthesis rates showed similar values in both autumn and spring. Hence photosynthetic production can considered independent of season (LANGE ET AL. 1994).

Results of LANGE ET AL. (1991) also showed that morphological characteristics may be influencing the maximal rate of photosynthesis and the ability of the lichens to gain from available moisture. Higher rates of photosynthesis were recorded for multi branched thalli of *Teloschistes capensis* (L.f.) Müll. Arg., *Alectoria* sp., and *Ramalina lacera* compared to the more compact foliose lichens *Xanthomaculina convoluta*, *Xanthomaculina hottentotta,* and *Xanthoparmelia walteri* Knox. Therefore microclimate, water relations, and photosynthesis of ten characteristic lichen species of the Namib Desert were observed. Light saturation of thalli under natural conditions varied between 583 (*Xanthomaculina hottentotta*) and 1856 µE m^{-2} s^{-1} (*Ramalina lacera*), whereas light compensation point of these species varied between 16.3 (*Caloplaca elegantissima* (Nyl.) Zahlbr. (Nyl.) Zahlbr.) and 31.5 µE m^{-2} s^{-1} (*Xanthomaculina hottentotta*). They also showed that moisture compensation point of the species varied between 15.0 (*Santessonia hereroensis*) and 25.6 % (*Ramalina lacera*) water content relative to dry mass of thalli.

Supplementary to these findings, (Lange et al. 1991) observed assimilation rates of 44 to 240 mg CO_2 m^{-2} h^{-1} within the *Teloschistes capensis* (L.f.) Müll. Arg. fields. Although such rates are only attained for a short period of time during the morning, following the formation of fog and dew during the night, they are similar to those of a closed layer of *Fagus sylvatica* (beech) leaves in a forest in Germany. Thus, they found *Teloschistes capensis* (L.f.) Müll. Arg. to be the most productive of the species they investigated, with a maximal daily carbon gain of about 0.25 % of thallus carbon content.

In addition soil crust lichens cover large areas of the Central Namib Desert and show chlorophyll contents and photosynthetic rates (under optimal conditions and based on an area basis) nearly equal to that of typical higher plants (LANGE ET AL. 1994). The relatively high light compensation point of these species (28-43 µmol m^{-2} s^{-1} photon flux density) they ascribed to light interception by non-photosynthetic pigments in the cortices of the lichen species.

Maximal daily carbon gains amounted in 158 to 290 mg C m^{-2} day^{-1}, while maximal chlorophyll contents ranged from 236 to 508 mg m^{-2} Considering that average chlorophyll content of semi-arid and arid regions ranges from 100 to 1500 mg m^{-2}, biological soil crusts contribute significantly to the biomass of these biomes (BÜDEL 2002). According to them a rough first estimate of the annual carbon balance of the soil crust lichens, *Acarospora schleicheri* (Ach.) A. Massal., *Caloplaca volkii* Wirth & Vezda, and *Lecidella crystallina* Wirth & Vezda is 16 g C m^{-2} yr^{-1}. Considering the hostility of the Namib environment including the near absence of precipitation this carbon balance is remarkable (LANGE ET AL. 1990). The importance of lichens in the ecology of the Namib is further discussed in LORIS & SCHIEFERSTEIN (1992), WALTER & BRECKLE (1999[7]) and LORIS ET AL. (2004).

2.4 Ecological studies of Namib Desert lichens

2.4.1 Lichen-Animal Interactions

As a form of pioneering vegetation, lichens reduce deflation, enrich the soil with nitrates, and serve as food and habitat to insects (HENSCHEL 2003).

Some lichen species of the Namib Desert have been analysed by JOUBERT ET AL. (1982) regarding their chemical composition. Thereby highest protein contents were observed for *Xanthomaculina hottentotta* (as *Parmelia hottentotta*) thalli (16.24 %), followed by *Xanthomaculi-*

na convoluta (as *Omphalodium convolutum*) comprising 14.42 % and *Teloschistes capensis* (L.f.) Müll. Arg. including 13.45 %. In addition thalli contained fructose, galactose, glucose, and a number of amino acids.

According to their findings, multibranched fruticose thalli of *Teloschistes capensis* (L.f.) Müll. Arg. serve as a supplementary food source to Springbok (*Antidorcas marsupialis*) during years of drought in the interior of the country.

Previous studies by WESSELS ET AL. (1979) had also discussed a lichen-animal interaction including *Teloschistes capensis* (L.f.) Müll. Arg.. They showed that two lichen-feeding arthropod Coleoptera species (*Calosis amabilis* Deyrolle and *Stenocara eburnea* Pascoe) were closely associated to *Teloschistes capensis* (L.f.) Müll. Arg.. According to them these insects might play an important part in the lichen's dispersal.

MITCHEL (1984) (in SCHIEFERSTEIN 1989) also considered several mite species to be associated with the coastal lichen fields. Nonetheless mites also form an important source of food for birds which are commonly observed in the coastal lichen communities. Lichen-bird associations were studied by FROST & SHAUGNESSY (1976) and CLINNING (1978). They concluded that lichen fields along Namibia's coast provide windbreaks, camouflage and shade for the nests of *Sterna balaenarum,* a rare migrant sea-bird.

Due to the above findings lichen-animal interactions indirectly emphasize the ecological significance of lichen communities in the otherwise mostly barren landscape of the Central Namib Desert. Furthermore these associations also reveal the possible utilization of lichen distribution patterns to indicate patterns of overall biodiversity.

2.4.2 Disturbance and recovery

Disturbance can severely affect the cover, species composition, and the physiological functioning of a biological soil crust, while the impact of a given disturbance depends on the soil, plant and climate characteristics of the site and the severity, frequency, and type of the disturbance (BELNAP & ELDRIDGE 2001; BELNAP ET AL. 2001C).

GARCIA-PICHEL & BELNAP (1996) showed that in typical biological soil crust more than 75 % of the photosynthetic biomass, and almost all photosynthetic productivity, is located within organisms in the top 3 mm of the soil, making it very vulnerable to mechanical disturbance. Although differing from conventional biological in species composition and structure, lichen communities of the Central Namib Desert also suffer from mechanical disturbance. Prevailing anthropogenic disturbances include mechanical disturbances created by off-road driving, mining, and hiking. Major natural disturbance can result from precipitation and subsequent water run-off, deflation, and corrasion by windstorms.

Although assessing disturbance and recovery of biological soil crust can visually be accomplished for moss and lichen cover, differentiation between crustal components is still important, as alteration of species composition can heavily influence ecological functioning of the crust (BELNAP ET AL. 2001C). However, knowledge on the disturbance and recovery of biological soil crusts has been mostly limited to site-specific studies. These studies addressed the impacts of various potential disturbances both natural and anthropogenic in differing biomes worldwide. Due to the differences in species composition, abiotic characteristics, and land-use practices, various disturbances were analysed. For example, SCUTURI ET AL. (2004) analysed

the potential of lichen groups and species for the assessment of rangeland disturbances in north-eastern Patagonia. They observed sites of three different grazing levels grouped into non-grazed, regularly grazed and heavily grazed sites. Results of correlations between the grazing intensity and lichen species denoted two crustose lichen groups being most sensitive to grazing disturbance, while groups of terricolous lichen species with dark foliose thalli and lichens growing on siliceous gravel were indicated most resistant. Therefore the lichen groups being most sensitive to grazing disturbances are proposed as bioindicators for continued overgrazing (SCUTURI ET AL. 2004).

On the contrary ORLOVSKY ET AL. (2004) suggested that the effects of an increase of biological crust on the structure and biomass of vegetation communities, in areas commonly affected by grazing, could as well be negative. Based on 40 years of field observation in the Karrakyl area of the Karakorum Desert, Turkmenistan, they conclude that a protective regime causes a wide-spreading of biological soil crusts. Though the initial rehabilitation of biological soil crusts can have positive effects at first, it will negatively affect the development and productivity of valuable higher plants, being palatable forage to livestock. According to these findings under-, as well as over-grazing, can be considered a degradation factor within that area.

Although the effects of anthropogenically induced grazing and associated trampling are of no great relevance for the current study addressing the hyper-arid coastal vicinity of the Central Namib Desert, differences in the above findings are. It becomes apparent that the categorization of disturbances does all too often include human perception due to land-use practices. As one may think of the biological soil crust being a disturbance itself, others may be dependent on their existence.

Supplementary to testing the effects of mechanical disturbance on species composition and structure of biological soil crusts, BELNAP & GILLETTE (1998) utilized a portable wind tunnel to obtain threshold friction velocities (TFV) of undisturbed as well as disturbed crust communities. TFVs of undisturbed crusts were well above natural wind forces, whereas the stability threshold of recently disturbed sites or soils with less developed crusts was frequently exceeded by these wind speeds. Applied disturbances by foot or vehicle-tracks were found to decrease threshold friction velocity by up to 93 % within the first year, and 31 – 82 % in the second year, relative to wind speeds commonly occurring in the investigation sites (BELNAP & GILLETTE 1998). Another study comparing the strength, stability and resistance to abrasion of monospecific sand crusts formed by three species of free-living fungi species was performed by MCKENNA NEUMANN & MAXWELL (1999). It showed that two of three fungal crusts were stable at wind-velocities of up to 10 m s^{-1} which compared to the threshold friction velocities obtained by BELNAP & GILLETTE (1998) for such soil crust types.

In respect to the studies of BELNAP & GILLETTE (1998) addressing the relationship of "recreational" anthropogenic disturbances and wind speed, ELDRIDGE (1998) focussed on the correlation of "economic" anthropogenic disturbances and erosion rates. Therefore effects of trampling by livestock were observed by using an artificial sheep-hoof, for the winter-rainfall dominated areas of eastern Australia where soil crusts are dominated by lichens and bryophytes. Observed erosion rates for rain-impacted water-flow showed high correlation to "trampling" rates, however well-developed crust showed an increased resistance to this

mechanical disturbance (ELDRIDGE 1998). Micromorphological investigations revealed that, especially trampling followed by rainfall events resulted in considerable surface sealing and sorting of sediments, loss of fine material and deposition of coarse material in micro-depressions (ELDRIDGE 1998).
As a consequence of these studies it becomes obvious that anthropogenic disturbances, whether economic or recreational, are likely to increase the effects of natural disturbances resulting from windstorm or heavy precipitation events.
In particular the studies of BELNAP & GILLETTE (1998), regarding TFVs of are important to understand the severity of deflation and abrasion by windstorm events frequently occurring in the Central Namib Desert. In addition to these disturbances aeolian deposits are also known to fully destroy lichen dominated soil crusts of the Namib. Buried by e.g. sands photosynthetic activity is permanently prohibited (compare photo 1).

Already causing severe damage among soil crust communities and phanerogamic vegetation, effects of these disturbances will most likely aggravate as anthropogenic disturbances increase.

As small-scale land-use practices are mostly limited to the linear oasis of ephemeral riverbeds, studies addressing anthropogenic disturbances were mostly limited to the effects of off-road driving. Foremost caused by recreational activities, off-road driving is also a problematic aspect of legal, and illegal mining activities, and maintenance of power- as well as water-lines dissecting lichen covered areas. Site-specific effects of off-road driving on crust communities of the Namib were performed by SEELY & HAMILTON (1978), DANEEL (1992), and JARROLD (2001).

For the dune/interdune system of the southern Central Namib Desert SEELY & HAMILTON (1978) analyzed the durability of vehicle tracks on three substrates. Vehicles were repeatedly driven over sand dunes, gravel-covered sand and calcrete rubble. While all signs of tracks had disappeared on the dune sands after one week, tracks dissecting the gravel-covered sands and the calcrete rubble were still visible after three months.
In 1992 DANEEL (1992) repeated this experiment on the gravel-plains between Khan and Kuiseb River for a time-span of two years. Her results also showed that impact was worst on unstabilized gravel-covered sands. Lichen communities, dominated by crustose species, occurring on the slightly undulating coarse gravel plains of the central Namib, were observed to be severely vulnerable to the damaging effects of off road vehicles travelling through them. Although some terri-

Photo 1: Costal lichen community covered by aeolian sand deposits in the vicinity of Cape Cross, Central Namib Desert, Namibia.

colous crustose species were found to be increasing along the cutlines of vehicle tracks, overall lichen community showed no sign of recovery during the two year period (compare photo 2). These findings were also confirmed by the studies of JARROLD (2001).

Supplemental to the mechanical disturbance by off-road vehicles described by Seely & HAMILTON (1978), DANEEL (1992), and JARROLD (2001), studies of BELNAP & GILLETTE (1998) also analysed the effects on the nitrogen cycle of various regional soil crusts of the western United States of America. Their results depicted reduced nitrogen fixation rates on all disturbed sites. However, statistically significant results were only obtained for 12 of the 26 sites observed, with cool deserts showing greater decline than hot deserts (BELNAP 2002). Therefore strong implications for ecosystems depending on soil crusts for nitrogen input are considered inevitable.
In general, noticeable recovery has only been described for semi-arid environments of Turkmenistan and Patagonia (e.g. ORLOVSKY ET AL. 2004), SCUTURI ET AL. 2004). On the contrary no noticeable recovery could be recorded by for test-sites located within the southern part study area (e.g. DANEEL 1992, JARROLD 2001).
Hence it is important to identify the effects of disturbance both natural and anthropogenic disturbances beyond site-specific studies. Though minor disturbances can not be detected using remotely sensed data on a regional scale, many natural disturbances vastly affecting the distribution of Namib Desert lichen communities can, including floods and storm damages. Furthermore the results of these studies also emphasize the need to limit anthropogenic utilization of those parts of the study area densely covered by lichen communities.
Therefore the identification of distribution patterns of lichen communities is essential. In addition specifying ecological factors controlling their distribution patterns will contribute to the current state of knowledge. Thus current and future conservation measurements on a regional scale are assisted.

For northern area the Tourism Officer of the Municipality of Henties Bay recently laid out a marked path through the area and published several brochures describing it with included turnoff GPS-coordinates to prevent off-road enthusiasts from driving off-track (TOURISM

Photo 2: Exemplary photo of vehicle tracks created from illegal off-road driving dissecting and destroying lichen communities in vicinity of Jakkalsputz.

Officer of Municipality of Henties Bay 2003a, Tourism Officer of Municipality of Henties Bay 2003b). This method of semi-controlled access might be one way to preserve the unique lichen fields until further conservation measures are implemented.

Contrasting to most of the study area, conservation already exists in the southern part of the study area. Within the Namib Naukluft Park area off-road driving is strictly prohibited and access is only granted on a daily basis. However, public through roads exist. Based on the close proximity to the touristic centre of Swakopmund as well as the natural scenic landscapes of the Swakop Canyon and the heavily frequented Welwitschia drive much disturbance arises from vehicle traffic in the southern part of the study area. Dust plumes caused by high-speed traffic obviously degrade the lichen communities alongside the roads with the repeated dust cover, thus obscuring their photosynthetic systems and causing inevitable die back (compare photo 3).
However, these minor disturbances caused by regular tourist traffic seem inevitable as the tourism industries can be considered an important economical factor. On the contrary sustainable tourism may also create awareness and generate revenues for environmental conservation within the framework of sustainable use (Barnard 1998). Nevertheless it must be kept in mind that Namibia strongly relies on its natural landscape and biota as a tourism draw-card (Barnard & Shikongo 2000).

2.5 Geographical distribution of Namib Desert lichen communities

The Namib coastal zone's impressive lichen fields are often mentioned in the literature (Mattick 1970, Wessels & van Vuuren 1986, Giess 1989, Schieferstein 1989, Wessels 1989, Loris & Schieferstein 1992, Jürgens & Niebel-Lohmann 1995, Loris et al. 2004).
Although the exact definition of biological soil crust does not include the rich stands of foliose and fruticose lichens found in the area as no "soil" particles are aggregated by these organisms, the boundaries between these communities and biological soil crusts are fluent.
This is also expressed by the multiple names by which biological soil crusts have been syn-

Photo 3: Dust plumes created by high speed traffic, covering the lichen fields of the Namib Naukluft Park area along the roadside.

onymously referred to in the past: cryptogamic, cryptobiotic, microbiotic, microfloral, microphytic or organogenic soil crusts. Today the term biological soil crust is used as it lacks taxonomic implications, is broadly applicable to all soil crusts and implicates that these crust are dependent on living organisms (BELNAP ET AL. 2001a).

Lichen community encrustations cover nearly the whole area of the central Namib Desert but are concentrated to numerous larger lichen fields in a globally unique way (WESSELS & VAN VUUREN 1986, ULLMANN & BÜDEL 2001A). For example, the *Teloschistes capensis* (L.f.) Müll. Arg. lichen community north-east of Wlotzkasbaken, covers an area of approximately 200 km². Also noteworthy, are the lichen community east of Cape Cross which covers an area of more than 400 km² and the soil crust lichen community east of Swakopmund covering an even greater area.
Following the definition by SCHIEFERSTEIN (1989) and LORIS & SCHIEFERSTEIN (1992) a lichen field is an extended plain area comprising a minimum area of 4 km² which is densely covered by lichens excluding small occurrences such as rocky slopes of favourable exposition. This definition was substantiated by JÜRGENS & NIEBEL-LOHMANN (1995) to the following that lichen fields are "plant formations of considerable surface area, in which epilithic (saxicolous) to episammic (terricolous) lichens play the dominant role with respect to structure, cover and biomass, if compared with ferns and seed plants". The distribution of large lichen fields is known to date to be limited to the central Namib Desert in between Kuiseb and Huab River (SCHIEFERSTEIN 1989). MEYER (1910) (in LORIS & SCHIEFERSTEIN 1992) was the first to describe the extent of the lichen covered areas of the Namib. This was followed by MATTICK (1970), who described the floristics of a few lichen communities in the Central Namib Desert.
South of this area only some lichen fields, however considerably smaller in size, are known for the Lüderitz peninsula, the coastal Sperrgebiet-Area between Chamais and Elizabeth Bay, and for Alexanderbay with the latter being the only reviewed one (LORIS & SCHIEFERSTEIN 1992, JÜRGENS & NIEBEL-LOHMANN 1995, LORIS ET AL. 2004).

The first analysis of the distribution of lichen communities was presented by WESSELS & VAN VUUREN (1986) who were as well the first to use satellite imagery. Based on a visual approach, an estimation of the distribution of lichen communities for the Central Namib Desert was discussed. Two prominent lichen communities within the spatial extend of the satellite image were described with the first stretching along the Khomas Hochland road east of Swakopmund and the road leading to Goanikontes. The second community mentioned by WESSELS & VAN VUUREN (1986) stretches in the hinterland northeast of Cape Cross in a slightly undulating terrain dissected by washes. In contrast to the first lichen community which is dominated by crustose species, it is dominated by shrub-like fruticose and foliose species.
However, despite the use of satellite imagery no map depicting the extent and distribution of lichen communities was presented.
Therefore SCHIEFERSTEIN (1989) and LORIS & SCHIEFERSTEIN (1992) mapped the extent and distribution of some lichen communities in the Central Namib Desert, based on field visits and long distance transects located along the coast between the Namib Naukluft Park area in the vicinity of the Swakop River and the Huabmond. They recorded number, geographic location, characteristics and estimated the extent of eight (SCHIEFERSTEIN 1989), and six (LORIS & SCHIEFERSTEIN 1992) major

lichen fields in the Central Namib Desert by the means of field surveys. In addition they also reported on site-specific aspects of the ground coverage, species composition and distribution as well as biomass rates for the lichen field of Wlotzkasbaken. As a result four zones, each characterized by either dominance of a growth form, a growth type or a lichen species, were outlined for the coastal vicinity of the lichen field of Wlotzkasbaken. Preceding the analogue mapping of SCHIEFERSTEIN (1989) and LORIS & SCHIEFERSTEIN (1992), SEELY (2004[3]) also reported on considerable lichen cover for some coastal areas near the Huabmond in the first edition of her book in 1987.

For the northern Namib Desert LALLEY & VILES (2005) recently presented a survey of the terricolous lichens of the northern Namib Desert between the Hoarusib and the Munutum River. This first known survey of the northern Namib Desert delineated seven soil crust habitat types comprising a total of twenty-eight soil crust lichen species many of the of them presumably unique to this area. In addition lichen distribution patterns were analysed with the means of Canonical Correspondence Analysis (CCA) and Spearman's Rank Correlation. While the environmental variable of soil crust thickness showed highest correlations, CCA also revealed gravel clast size as an important determinant followed by slope and soil crust thickness. Based on the inter-regional differences of geomorphology, fog deposition and lichen community development between the northern, central and southern Namib, LALLEY & VILES (2005) also proposed the separate consideration of the three biomes, as far as ecological studies are concerned.

ZEDDA & RAMBOLD (2004) discussed site-specific changes in diversity of soil-growing lichens along a climate gradient in Southern Africa. Based on the observations from 22 selected observatories, effects of the different summer- / winter-rain regimes, fog frequency, soil properties and man-made disturbance was examined for 59 terricolous lichen species. Observed diversity was generally higher along the coast resulting from increased fog frequency and air-humidity. Unfortunately neither LALLEY & VILES (2005) nor ZEDDA & RAMBOLD (2004) presented distribution maps delineating lichen species or lichen community distribution based on their field-work regardless of scale.

In a nutshell only SCHIEFERSTEIN (1989) and LORIS & SCHIEFERSTEIN (1992) presented valuable information on the distribution patterns of Namib lichen communities. Although solely based on field observations and aggravated as GPS-navigation was still inexistent, their results provide a good survey of lichen covered territories alongside their research transect in the Central Namib Desert. However, despite a small-scale mapping approach for the costal vicinity of Wlotzkasbaken no differentiation of lichen community coverage was presented. Moreover, not all lichen fields previously mentioned in the literature were taken into account, considering the preliminary results of WESSELS & VAN VUUREN (1986).Yet their work is highly relevant to this thesis as it represents the only comprehensive mapping approach of lichen distribution patterns within the Central Namib Desert to date.

2.6 Detection and monitoring of Biological Soil Crusts including lichens

Despite the well recognized ecological importance of biological soil crusts, relatively few studies have been published on the use of remote sensing systems to detect and map their distributions. Following the study of WESSELS & VAN VUUREN (1986) who used LANDSAT MSS, acquired 1981, and visual

analysis to receive an estimation of the distribution of lichen communities for the Central Namib Desert, a relatively small number of publications have presented the spectral properties of BSCs or applied remote sensing techniques to map them (KARNIELI ET AL. 2001).
The objective of the following paragraphs is to present an overview of studies dedicated to the remote sensing of BSCs with relevance for this thesis.

2.6.1 Monitoring of Biological Soil Crusts including lichens

The only long-term survey on the temporal dynamics and productivity of biological soil crusts was performed by ORLOVSKY ET AL. (2004) for the central Karakum desert of Turkmenistan. Based on field samplings collected within the time-span of 1960 to 2000 and aerial photography's for the years of 1964, 1977 and 1999 the effect of biological soil crusts (BSC) on the vegetation communities was studied within a fenced off area. Results showed that BSCs were significantly influencing plant communities as positive effects of the BSCs changed to negative effects on the structure and biomass of higher vegetation after some 15 years. Thus undergrazing as well as overgrazing was considered to be a desertification facto for these areas (ORLOVSKY ET AL. 2004). However most of the findings were based on the field samples while aerial photographs were only analysed visually to illustrate the results.

Supplementary short-term studies addressing the monitoring of biological soil crust communities have been focussing for example on Australia and North America, no comparable studies exist for Southern Africa (ZEDDA & RAMBOLD 2004).

With few exceptions such as the study presented by (ORLOVSKY ET AL. 2004), most of these studies based on the biological collection and analysis of repeated observations to assess changes over time, precluding the use of remote sensing (ROSENTRETER ET AL. 2001).
However land-cover classifications derived from spacecraft or airborne datasets rely in many ways on extensive ground reference data which can be extraordinary difficult to obtain for biological soil crusts, particularly for broad-scale monitoring programs. Biological field research on crusts has been facing the same problems with the in situ identification of species for a long time. As identification is problematic, monitoring can be a daunting task to all but the most experienced (ELDRIDGE & ROSENTRETER 1999).
Strong relationships exist between the form (morphology) of crust organisms and their ecological function in relation to erosion and water retention, as well as their tolerance to and recover from physical disturbance (ROGERS 1977). Morphological groups have thus been proposed for the assessment and monitoring of biological soil crusts in arid areas (ELDRIDGE & ROSENTRETER 1999).
Morphological groups are biologically and ecologically efficient and convey a better image of the organismal form and its potential impact to non-specialists. True, in different regions and continents these relationships eliminate the need for complex, often confusing changes in nomenclature (ROSENTRETER ET AL. 2001). Despite the ease of identification, which is independent of sexual reproductive structures, the concept of morphological groups enables less specialized staff to monitor sites more quickly, record cover and abundance measures more rapidly, allowing the assessment of more sites per time unit (ELDRIDGE & ROSENTRETER 1999). Though appropriate for broad-scale studies and

regional monitoring, specific goals of individual studies might however find this concept too coarsely meshed as it ignores the detection of individual species, particularly rare or uncommon taxa (BELNAP ET AL. 2001A).
In terms of remote sensing, the adaptation of this framework for monitoring microphytic crusts in arid lands could not only be the key to a rapid and comprehensive regional collection of ground reference data, but also prepare the ground for the establishment of monitoring approaches based on remotely sensed data.

2.6.2 Remote Sensing of Biological Soil Crusts including lichens

In the past differing approaches have been used regarding the remote sensing of biological soil crust including lichens.
AGER & MILTON (1987) were the first to use laboratory reflectance measures of collected lichen species from the Extremadura region of Spain to report on their characteristic spectral absorption features. Three broad absorption features at 1730, 2100 and 2300 nm wavelength were found to represent the presence of cellulose. Based on the analysis of modelled laboratory lichen spectra and from a geological point of view they suggested the use of LANDSAT 5 TM band ratios of 3 : 4 and 5 : 2 to minimize lichen effects in TM image analysis.

In addition, earlier works by WESSELS & VAN VUUREN (1986) used spaceborne multispectral LANDSAT MSS (WRS-1: 193-75 & 192-76) data from 1981 for visual analysis to receive an estimation of the distribution of lichen communities for the southern part of the Central Namib Desert. Although this proved to WESSELS & VAN VUUREN (1986) the possible use of satellite imagery as an additional mapping aid for the Namib Desert lichen vegetation they also suggested that extensive ground reference data must be available for a true differentiation of lichen communities.

In contrast to all other studies presented, WASER ET AL. (2003) build multiple linear regression models containing ecological meaningful variables extracted from colour infra-red (CIR) orthoimages in conjunction with lichen expert knowledge and stepwise variable selection to predict lichen species richness represented by lichen relevés for six test sites in the Swiss Pre-Alps. Observed correlations for the potential absence or presence ranged from r = 0.79 for lichens on trees to 0.48 for lichens on the ground, while these measures were then utilized to calculate potential lichen species richness.
However transferability of all derived models is limited to neighbouring regions with similar landscape structures. In fact it might probably be the only study known to assess lichen distribution patterns by remote sensing and multiple regression techniques.

On the contrary the approach presented by AGER & MILTON (1987) more or less reflects the different aspects, subsequently utilized by many authors for the analysis of biological soil crusts using remote sensing techniques and remotely sensed data, in part or as a whole. At the foremost site-specific spectral absorption features would be obtained from either laboratory or in-situ spectrometer measurements. In the following, distinctive absorption features of individual species or communities were correlated to characteristic chemical substances or physiological parameters. Based on these results existing spectral indices were tested or new site-specific ones developed.
However, only a few studies, addressing the remote sensing of biological soil crusts, have

considered mapping their spatial distribution on a regional scale, following the proposal of WESSELS & VAN VUUREN (1986).

Therefore still little is known about the relationship between the spectral reflectance of biological soil crusts and the potential of mapping them with the medium spectral and spatial resolution of multispectral LANDSAT MSS, TM and ETM+ sensors. Although the potential of discriminating different biological soil crust cover utilizing LANDSAT data have been tested by AGER & MILTON (1987), KARNIELI & TSOAR (1995), KARNIELI (1997), REES ET AL. (2004), and CHEN ET AL. (2005) most of the studies were either based upon visual interpretation and or regression models when it came to classification and mapping of biological soil crusts (e.g. WESSELS & VAN VUUREN 1986, WASER ET AL. 2003), or reported on the spectral absorption features derived from laboratory or in-situ spectroradiometer measurements with few utilizing hyperspectral remote sensing systems in addition (e.g. AGER & MILTON 1987, KOKALY ET AL. 1994, KARNIELI & TSOAR 1995, KARNIELI ET AL. 1996, KARNIELI 1997, KARNIELI ET AL. 1999, SCHMIDT & KARNIELI 2000, GARTY ET AL. 2001, KARNIELI ET AL. 2001, OKIN ET AL. 2001, BECHTEL ET AL. 2002, KARNIELI ET AL. 2002, REES ET AL. 2004, CHEN ET AL. 2005).
Among all the authors who have contributed to the remote sensing of biological soil crust, Arnon Karnieli's work must be emphasized. Since the study of KARNIELI & TSOAR (1995), his work has continuously addressed the remote sensing of biological soil crusts. Head of the remote sensing laboratory of the Jacob Blaustein Institutes for Desert Research at the Ben-Gurion University of the Negev, many of his studies were focussed on the soil crusts of the Negev/Sinai region located between Israel and Egypt. Along with studies in other regions of world, he has without a doubt published or co-authored most of the literature available on the topic. Therefore much of the review on the state of research on the remote sensing of biological soil crusts will refer to his studies.

KARNIELI & TSOAR (1995) tested the effect of biogenic crusts on imagery acquired by spaceborne sensors with the means of field-spectrometer measurements for the Negev/Sinai region of Israel and Egypt. A Li-Cor LI-1800 portable spectrometer was first used to identify areas of bare dune sand, cyanobacteria crust and higher vegetation in order to explain large differences in reflectance at the Sinai/Negev boundary first observed for a LANDSAT MSS scene acquired 1972. His results showed that the regional differences in reflectance which had been described in existing literature as being caused by the severe anthropogenic impact on the higher vegetation by the Sinai Bedouin, were in fact caused by almost complete cover of biogenic crust on the Israelian side resulting in a lower overall spectral reflectance. This phenomenon has also been reported on for the Namib Desert by WESSELS & VAN VUUREN (1986), who visually delineated lichen distribution patterns, based on the strong natural brightness differences in relation to the surrounding quartz covered gravel plains. However, the higher spectral reflectance on the Egyptian side is caused by continuous anthropogenic activities, preventing the establishment of the biogenic crust and thus rejecting the prevailing theory of any type of overgrazing mechanism.

Subsequently, the importance of an extended study of the distribution patterns of biological soil crusts was emphasized by a study performed by KARNIELI ET AL. (1996) devoted to discrepancies of Normalized Difference Veg-

etation Index (NDVI) values derived from spaceborne satellite data and the phenomenon of desert artefacts described in semi-arid and arid regions. This phenomenon describes the observation of surprisingly high NDVI values in areas where little, if any photosynthetic activity of higher plants exist. Therefore spectral characteristics of several crust types were studied in the field and laboratory using a field-portable spectroradiometer. Findings included the description of spectral reflectance curves of soil crusts, almost resembling those of phanerogamic vegetation. Therefore it was considered that NDVI values may lead to a misinterpretation of the vegetation dynamics and false estimation of ecosystem productivity in desert environments. Due to the quick response of biological soil crusts subsequent to the availability of water, the effects on the remote sensing of the vegetation are even more severe when Maximum Value Compositing (MVC) techniques are used to obtain cloud-free NDVI values.

Due to these findings SCHMIDT & KARNIELI (2000) utilized field spectrometer measurements and monthly NDVI MVC-composites derived from the Advanced Very High Resolution Radiometer (AVHRR) data of the National Oceanic and Atmospheric Administration (NOAA). This data was used to observe the temporal response of different ground cover components to rainfall events at two different study sites in the Sinai region. The field observations showed that all cover components observed – annuals, biogenic crust, perennials – respond differently.
Biological soil crusts and lichens were observed to have a characteristic fast and short response in terms of weighted NDVI peaks, while annuals gave significant response for only a few weeks after the beginning of the rainy season and perennials slightly increasing their overall high spectral response towards the end of the rainy season. In order to correlate both satellite derived NDVI and the NDVI based on spectral ground measurements, the spectral responses of the field measurements were weighted according to the fractional cover of each vegetation component by applying a Linear Mixture Model. Although both sites showed high correlations of up to 0.84 r^2, combined biogenic crust/lichen cover showed only little correlation with high standard errors, which is surprising as fractional cover of microphytes ranged from 45 to 60 % for both study sites. However, one explanation could be the observed fast and short response of this component which might not be reflected by the NDVI composites already observed by KARNIELI ET AL. (1996).

In addition to studies regarding the effects of biological soil crusts on NDVI values, analysis of the relationship between NDVI and ecophysiological parameters of biological soil crusts was conducted. KARNIELI ET AL. (1999) collected five crust communities for laboratory experiments from the Negev Desert, Israel. Analysis of crust communities showed that chlorophyll content of wetted crusts was much higher after 7 days of incubation. Laboratory spectroscopic analysis of spectral features of cyanobacteria soil crusts relative to bare sands and under different moisture conditions revealed that wetted biogenic soil crusts can reach NDVI values of up to 0.3 due to their photosynthetic activity while a shift in position of the infliction point of the observed red edge towards the longer wavelength indicates higher relative abundance and distribution of the microphytic community (KARNIELI ET AL. 1999).
Results also included a high correlation of NDVI values, obtained from continuous laboratory spectral measurements, and chloro-

phyll contents. In addition direct relationships could also be observed between NDVI values and organic matter, polysaccharides content, protein content, and crust thickness (KARNIELI ET AL. 1999).

Upon these findings GARTY ET AL. (2001) focussed on the possible use of NDVI to detect pollutant-induced stress in lichens. They utilized Li-Cor LI-1800 portable spectrometer measurements to obtain the spectral characteristics of lichen samples of the unpolluted Haifa Bay and Mount Carmel region in order to investigate the effect of anthropogenic activity on air quality. Through displacement of some of the lichen samples to a national park area as well as an industrial region for eight month they tried to identify the relationship of physiological parameters of the photosynthetic system with the elemental content of the lichen thalli for the possible establishment of a bio-monitoring network. Their results showed that the photosynthetic rate and chlorophyll K content correlated with the obtained NDVI values but correlated inversely with amounts of heavy metals found in lichens transplanted to the industrial area. This demonstrated the possibility to use NDVI as a non-destructive method to detect pollutant-induced stress in lichens by heavy metals and other substances under laboratory conditions.

Hence, both KARNIELI ET AL. (1999) and GARTY ET AL. (2001) proposed the usage of NDVI as an indicator for many physiological and ecological parameters concerning biological soil crusts.

In order to analyse the relationship between NDVI values and amount of cover components of distinct biological soil crust, studies of BORK ET AL., reported on by KARNIELI ET AL. (2001), were based on the monthly repetitive spectral measurements of ten plots selected to represent the most abundant cover categories of vascular plant and litter thereof, moss, lichen and exposed bedrock. For a location in southern Idaho, United States of America, An ASD Personal Spectrometer (400 – 960 nm) was used to collect all spectra during June, July and August 1995 in the midday of cloud free days. Mean spectral response curves of microphytes, which resembled a complex mixture of mosses, lichens, algae and cyanobacteria of many different species remained spectrally distinct, leading to the conclusion that multiple narrow bands could possibly be used to distinguish them from other cover components.
Based on these observations calibrated predictive relationships between simulated broad-band as well as narrow-band reflectance values and the quantitative amount of cover components were calculated. Their results showed that simple broad-band reflectances were often better predictors than narrow-band data used in companion studies. This is explained by the authors as quantitative changes in soil-based components being more likely to change the overall spectral response curves in magnitude rather than in shape. Lichen dominated microphytic cover which was particularly characterized by broad-band deviations in the R-NIR region around 730 nm. Biological soil crusts in general could be discriminated by four narrow-bands of the blue-green and green regions and only one from the longer wavelength. However no exact wavelength readings of these characteristics are indicated by the authors.

At the same time, distinct yet site-specific spectral reflectance features of biological soil crust were tested, in order to allow the deduction of information regarding their absence, existence and spatial distribution. However

these approaches can be subdivided into studies incorporating either hyperspectral datasets including spectral feature analysis, or the derivation of spectral indices for usage with multispectral remote sensing data.

Surveys by KOKALY ET AL. (1994), which have also been published in KARNIELI ET AL. (2001), included the use of airborne hyperspectral remote sensing data. The study aimed at the identification and mapping using a spectral feature analysis of collected Airborne Visible and Infra-Red Imaging Spectrometer (AVIRIS) data obtained for Arches National Park, Utah, United States of America. In addition to the Tetracoder algorithm a spectral library comprising crust, blackbrush, dune sand and their linear combinations was compiled for spectral feature analysis, resulting in the generation of a map of soil-crust cover. Although light crusts showed great spectral resemblance to bare soil/sand thus being the most difficult to identify and spectral characteristics of rock covering lichens and crusts were very similar, most of the encrusted areas identified could be confirmed by field studies.

ZHANG ET AL. (2004) presented a derivative spectral unmixing model (DSU) as an extension to spectral mixture analysis (SMA) and derivative analysis for the use with hyperspectral remote sensing data. Utilizing the DSU approach it is possible to estimate the fraction of a spectral endmember characterized by certain diagnostic absorption features in contrast to having only a general knowledge of the spectral shapes of the remaining endmembers, sufficient signal to noise ratio and non-conflicting absorption features of the unknown permitting. In their first approach the application of the algorithm presented was limited to laboratory data of green lichen and rock, but showed good correlation between actual abundance obtained from the analysis of a high resolution digital photograph and the predicted endmember abundance. Still experiments with air- and spaceborne hyperspectral imagery will show its true value for quantitative analysis studies.

Unlike the spectral mixture analysis presented by KARNIELI ET AL. (2001) and ZHANG ET AL. (2004), findings of BECHTEL ET AL. (2002) proposed the utilization of hyperspectral remote sensing data to discriminate rock exposures from varying lichen abundances by the simple means of infrared ratios. In the high latitude and subarctic environments of Alberta, Canada, BECHTEL ET AL. (2002) acquired reflectance spectra of rock encrusting crustose and foliose lichens to determine their influence on the reflectance properties of rock exposures. Since overall lichen transmittance was estimated to be less than 3 % through the 350-2500 nm spectral region, they suggest that lichen cover prevents the transmission of light to the underlying rock substrate and thus effectively mask the mineral substrate. In addition to AGER & MILTON (1987) who identified three broad absorption features near 1730, 2100 and 2300 nm, which describe the presence of cellulose in lichen, BECHTEL ET AL. (2002) found more subtle features at 1445 nm and 1860 nm which can be uniquely associated with the lichen species described in their study. While the absorption features around 1730 nm, 2100 nm and 2300 nm report on the presence of cellulose varying in depth for different species, the minimum around 1445 nm is attributed to absorption by the hydroxyl (-OH) group.

BECHTEL ET AL. (2002) further used a plot of the ratio of reflectance at 400/685 nm against 773/685 nm to isolate the spectral characteristics of different colours, types and species of lichen. While the 400 nm was utilized

because all lichens examined in their study showed low reflectance values of < 7 %, the value of 685 nm was used as a general indicator for chlorophyll. 773 nm however served as a numerator as all lichens characteristically show high reflectance at this wavelength with low variation among species.
To discriminate lichen from quartzite rock however an index created from the band ratios 2132/2198 nm and 2232/2198 nm was found to outline the similarity of lichen spectra in the infrared as well as the differences to the spectral features of their quartzite substrate.
Although it is still unclear how many of the hundreds of lichens species known to date can be spectrally identified using the approach published by BECHTEL ET AL. (2002) the proposed infrared ratios can however serve well for the analysis of hyperspectral remote sensing data.
Airborne hyperspectral remote sensing systems, like the Advanced Visible/ Infra-Red Imaging Spectrometer (AVIRIS) utilized by KARNIELI ET AL. (2001), are becoming increasingly available for the mapping of different land-cover units through end-member and spectral analysis. Supported by ground reference data obtained from field spectroradiometer measurements, systems like AVIRIS, Shortwave Infrared Spectrographic Imager (SASI) and Compact Airborne Spectrographic imager (CASI), Digital Airborne Imaging Spectrometer (DAIS) or HyMap hyperspectral scanner provide a greater likelihood of finding an optimal choice of wavebands for discriminating between different land-cover types and relating the various optical properties to the physiology of biological soil crust including lichen's (REES ET AL. 2004). Although superior to both airborne orthoimages and spaceborne multispectral datasets, acquisition of airborne hyperspectral datasets is still very expensive and thus overall spatiotemporal coverage of these datasets remains very limited. Therefore monitoring applications based on these datasets are limited as well. Although providing enhanced spatial coverage and increased repeat frequencies, spaceborne hyperspectral remote sensing systems are still few. Practical limits of hyperspectral remote sensing in arid and semi-arid environments are discussed by OKIN ET AL. (2001).
On the contrary KARNIELI (1997) utilized the unique spectral absorption features of biogenic crust containing cyanobacteria published in KARNIELI & TSOAR (1995), for the development and implementation of a broad-band spectral crust index over dune sands. Based on the fact that the special phycobilin pigment in cyanobacteria contributes to a relatively higher reflectance in the blue spectral region than the same type of substrate without the biogenic crust, his special crust index (CI) focuses on the normalized difference between the RED and the BLUE spectral values. An additional case study on LANDSAT 5 TM imagery proved the applicability of the postulated index to gain information about the absence, existence and spatial distribution of biogenic crusts containing cyanobacteria. However no map was presented.

Based upon the concept by KARNIELI (1997) to use a site-specific spectral broad-band band-ratio, representing the contrasting spectral features of cyanobacteria-dominated soil crust in the Negev Desert Israel, CHEN ET AL. (2005) recently presented a new spectral index (BSCI) for the discrimination of lichen-dominated biological soil crusts from land surfaces consisting of bare sand, dry plant material and higher vegetation.

Based on the spectral reflectance features observed with an MMS-1 field spectrometer in the 400 to 1100 nm range of lichen-domi-

nated soil crust in the Gurbantonggut Desert located in the Xinjiang Uygur Autonomous Region of China the newly developed index basically sets the difference of the broad-band, multispectral red and green bands (LANDSAT bands 3 and 2) in relation to the mean broad-band reflectance at visible- and near-infrared bands (LANDSAT bands 2, 3 and 4). According to the authors this contributes to the in general "flatter" slope between green and red bands and the overall lower reflectance at visible and near-infrared bands than those of bare sand, dry plant material and present higher vegetation.

These assumptions do however rely on a lichen-dominated biological soil crust to alter its background by increased absorption which might for example not be the case for some areas of the Central Namib Desert, where vast lichen cover is situated on flat dark gravel fields. On these territories lichen coverage causes a general increase in reflectance, including a steeper "slope" (compare chapter 5.2.2).

To test the index for sensitivity, they obtained upper and lower detection thresholds, where soil-crust cover is either 100 % or indistinguishable from the background. In addition they used for LANDSAT 7 ETM+ data being atmospherically corrected to surface reflectance and ETM+ data only corrected to Top-of-Atmosphere (TOA) reflectance data, due to a lack of atmospheric optical properties at the time of image acquisition, to test these thresholds.

Results show a steady increase in BSCI values with increasing biological soil crust coverage under all atmospheric conditions. However with increasing simulated aerosol depth the dynamic range indicating solely biological soil crusts is narrowed noticeably. This causes the maximum BSCI threshold value, describing 90 % coverage of biological soil crust, to drop from 6.23 to 5.69, and the minimum to rise from 4.13 to 4.58, which corresponds to a shift in lowest coverage possibly detected from 37 % to 52 %. Therefore CHEN ET AL. (2005) recommended calculating BSCI and determining the lower and upper threshold using surface reflectance after atmospheric correction.

Applied to a LANDSAT-7 ETM+ scene acquired in October 2002 corrected in the above manner the BSCI presented, showed accurate results in the range of 3.69 to 6.59 with an overall accuracy derived from 76 reference points of 94.74 %.

Complementing the possible use of LANDSAT 7 ETM+ data Rees et al. (2004) also discussed the potential discrimination between fruticose and crustose lichens based on these datasets. REES ET AL. (2004) followed the approach of Bechtel et al. 2002) in using a spectroradiometer under laboratory conditions to obtain reflectance spectra of different arctic and sub-arctic Swedish lichen species. As BECHTEL ET AL. (2002) only reported on the spectral reflectance of rock encrusting lichens, REES ET AL. (2004) examined the spectral features of a number of fruticose lichens as well. In comparing the spectral features of fruticose and crustose lichen samples they tried to identify more common features than BECHTEL ET AL. (2002), allowing a more detailed spectral discrimination of different lichen species. However, due to mixing of laboratory spectra obtained for the fruticose lichens and in situ measured spectra for the crustose species results must be judged with caution.

Based on the observed absorption features REES ET AL. (2004) investigated the extent to which spectral discrimination between lichens could be optimally based on a reduced spectral data set with the means of principal component analysis (PCA). In order to practicably calculate the variance-covariance matrix and

eigenvectors they reduced the lichen spectra to 16 "interesting wavelengths" identified in the preceding chapter (400, 470, 520, 570, 680, 800, 1080, 1120, 1200, 1300, 1470, 1670, 1750, 2132, 2198, 2232 nm).

The results of this first analysis show that most of the variation between the spectra can be found in a broad range from about 800 to 1300 nm, while the second principal component is located in a broad band from 1470 to 2232 nm, and the third most variation is reported for the visual range excluding the extreme blue end at 400 nm which is significantly represented only in the fourth principal component. Altogether these first four components represent 98.9 % of the total variance.

In a second approach, PCA was applied on the spectral bands of the LANDSAT 7 ETM+ sensor with all spectral lichen samples being averaged over the six reflective bandpasses 1-5 and 7. The results only broadly resemble that of the first PCA with the major contribution to the first component by LANDSAT-band 4 (760-900 nm) while the second component is predominately located at band 5 (1550-1750 nm). The third principal component however differs as it is represented merely by the difference between band 4 and the average over the visible bands.

As the first two principal components allowed them to differentiate between fruticose and crustose lichen samples despite the limited spectral resolution of the ETM+ bands REES ET AL. (2004) suggested that, although a higher spectral resolution in the range from 900 – 1300 nm would be desirable, limited discrimination utilizing LANDSAT-7 ETM+ data could as well be possible, at least provided that the lichen patches are large enough to be resolved spatially.

Grouping of lichen reflectance spectra into a few "generic lichen spectra", the results obtained by REES ET AL. (2004) allowed the separation of one or two "brown-black" spectra, similar to soil, a well-populated class of "typical light-coloured lichens" and a class of unusually high reflectance lichens.

Although they described this approach somewhat arbitrary, the results showed marked similarities to the average spectra of lichen samples collected by AGER & MILTON (1987) in the Extremadura region of Spain. Since AGER & MILTON (1987) collected their lichen samples in a semi-arid environment contrasting the subarctic Swedish study site, REES ET AL. (2004) also investigated the effect of drying on lichen reflectance spectra. However, their results contradict some previous work to some extent as they found no proof of an increased reflectance at all wavelengths for "dried out" lichen samples which has been reported by AGER & MILTON (1987), KARNIELI ET AL. (1999), and KARNIELI ET AL. (2001). Instead only water absorption features at 1450 and 1900 nm increased.

In general earth-bound spectroscopic, airborne hyperspectral and spaceborne multispectral image analysis show different approaches to differentiate biological soil crusts from other ground components. However, lichen spectra collected from many different locations worldwide were found to have similar absorption features. Still in addition to the studies presented further investigations need to be conducted, to develop site-invariant mapping methods in contrast to site-specific techniques.

This might as well be possible, considering the approaches presented by WESSELS & VAN VUUREN (1986), KARNIELI (1997), REES ET AL. (2004), and CHEN ET AL. (2005). All of these studies proposed the use of multispectral remote sensing data to detect the absence, existence and spatial distribution of biological soil crusts. In addition REES ET AL. (2004) also suggested that discrimination between fruti-

cose and crustose lichen samples would be possible despite the limited spectral resolution of the ETM+ bands. These multispectral remote sensing datasets provide consistent, high resolution and reproducible information combined with high repeat frequencies needed to detect, map and monitor biological soil crusts on a regional scale.

Although requiring the lichen patches to be large enough to be resolved spatially (REES ET AL. 2004), these prerequisites are met by the vast lichen fields of the Central Namib Desert (WESSELS & VAN VUUREN 1986). Permitting that extensive ground reference data would be available, this approach would also be supported by the nearly absence of rain of this hyper-arid region and the very weak seasonality which has been subject to many studies as well (AGER & MILTON 1987, KARNIELI ET AL. 1999, KARNIELI ET AL. 2001, SCHMIDT & KARNIELI 2002, REES ET AL. 2004).

Therefore the quantitative mapping of the spatial distribution of the lichen communities of Central Namib Desert, based on spectral properties, could also significantly contribute to ecological studies and disturbance / response models to support desertification / rehabilitation and climate change studies.

3 Study Area

Existing literature on the study area has been largely focussed on the phanerogamic perennial and ephemeral vegetation occurring scattered throughout the Central Namib Desert.

Special aspects of phanerogamic vegetation were addressed by MOISEL (1971), WALTER (1976), VOGEL & SEELY (1977), SEELY (1978), SOUTHGATE ET AL. (1996), LE HOUERU (1998), HACHFELD (2000), HACHFELD & JÜRGENS (2000), and VON WILLERT ET AL. (1983) for example. Important regional studies on vegetation of ephemeral rivers were published by COWLISHAW & DAVIES (1997) and THERON ET AL. (1980), while WILLIAMSON (1997) addresses the Sperrgebiet.

These studies on the vegetation have been complemented by studies investigating the extraordinary stable yet complicated climatic patterns of the Central Namib Desert. Early climatological studies of the Namib are known from GÜLLAND (1907), KAISERLICHE BERGBEHÖRDE (1912), and BOSS (1941). In recent times the climate of the Namib has been discussed by BESLER (1972), SCHULZE (1976), SEELY & STUART (1976), LANCASTER ET AL. (1984), LINDESAY & TYSON (1990), and LENGOASA ET AL. (1993). Special aspects of the climate were studied by GRAY (1980), ECKARDT & SCHEMENAUER (1998A), ECKARDT & SCHEMENAUER (1998B), and MTULENI ET AL. (1998). However most of these studies were based on temporally and spatially restricted datasets of five to ten years (compare Schulze 1976, SEELY & STUART 1976, NIEMAN ET AL. 1978, LANCASTER ET AL. 1984). Therefore these studies often provided only a preliminary and fragmentary description of the climate of the Central Namib Desert.

As a consequence climatic studies have more frequently been incorporated into studies focused on the geological/geomorphological (e.g. GOUDIE 1972, SELBY 1976, PICKFORD & SENUT 1999) or ecological aspects of the area (e.g. LORIS & SCHIEFERSTEIN 1992, LANGE ET AL. 1994, SEELY ET AL. 1998, HACHFELD 2000, HACHFELD & JÜRGENS 2000).
Nevertheless little information on the soils of the Central Namib Desert exists with only those in the vicinity of Gobabeb described in detail by SCHOLZ (1972). Consecutive the soils within the study area remain largely unclassified.

In concordance to the studies on soils, only a limited number of mostly site specific ecological, ecophysiological and taxonomic studies on the lichen flora of the Namib Desert have been published by MATTICK (1970), JOUBERT ET AL. (1982), BÜDEL & WESSELS (1986), KÄRNEFELT (1988), SCHIEFERSTEIN (1989), WESSELS (1989), LORIS & SCHIEFERSTEIN (1992), JÜRGENS & NIEBEL-LOHMANN (1995), and LALLEY & VILES (2005). Some of the studies also incorporating studies of climatic parameters known to affect lichen community distribution.

Moreover only three of these ecological studies also included first mapping approaches roughly estimating the individual and overall distribution of lichen communities in the Central Namib Desert (compare SCHIEFERSTEIN 1989, LORIS & SCHIEFERSTEIN 1992) while WESSELS & VAN VUUREN (1986) were the first to use visual interpretation of LANDSAT derived images.

3.1 General geographic facts on the study area

The Namib Desert, in width limited to just a narrow strip of 80 – 150 kilometers in width, extends for over 2000 kilometers along the south-west coast of southern Africa. It is bordered by the Olifants River in the north-western part of South Africa (32oS) and the Angolan St. Nicolas-River (14o20's) in the north. The eastern border is formed by the orographic boundary of the Great Escarpment rising to an average of 1200 meters above sea level (LORIS ET AL. 2004).

Various reviews addressing the geography as well as the ecology of the Namib have been published, including the most recent by SEELY ET AL. (1998), LORIS ET AL. (2004), WALTER & BRECKLE (1999[7]), and JÜRGENS ET AL. (1997).

The Namib Desert differs from other deserts because of its estimated age of 25 - 80 Mio years. The present hyper-arid phase has been lasting some 5 Mio years and subsequently it sports a high ecological and biological diversity with a high number of endemic species as well as a great number of organisms extraordinarily well adapted to the arid environment, which is significantly altered by the climatic influence of the Atlantic Ocean (SHACKLEY 1985, LORIS & SCHIEFERSTEIN 1992).

The Namib Desert can roughly be subdivided from south to north into two major parts influenced by summer or winter rainfalls although regional subdivisions exist (compare figure 3). In addition LALLEY & VILES (2005) proposed the separate consideration of northern, central and southern Namib based on inter-regional differences observed during field studies.

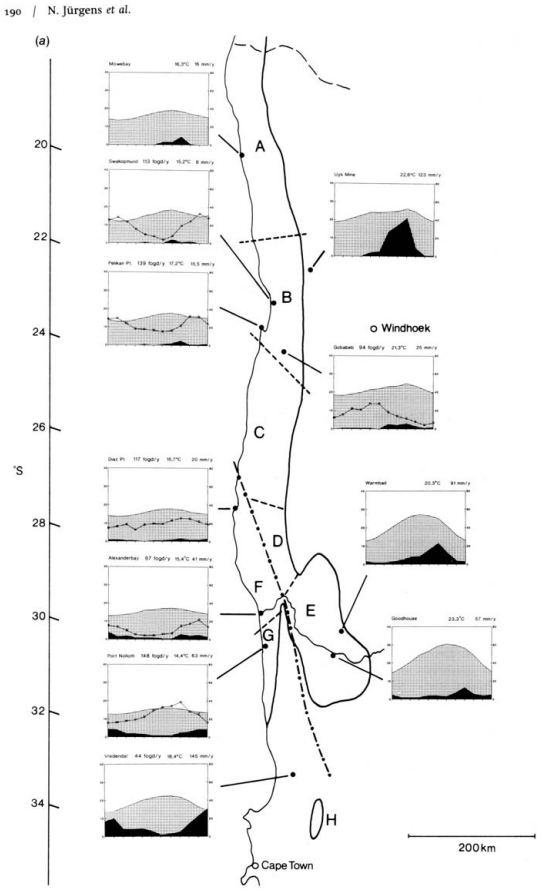

Figure 3: Subdivision of the Namib Desert and corresponding typical climatic diagrams. Source: LORIS ET AL. 2004, PAGE 445.

The summer rainfall is located in the north between the area between St. Nicolas- and Huab-River characterized by coastal dune fields and inland plains covered by rock debris and gravel. South-westerly winds prevail over north-easterly winds in this region (compare areas A, B, C, D, E, figure 3). It is followed by the winter rainfall areas (compare areas F, G, H, figure 3).
The Northern Namib (A) stretches from the Huab- to the Uniab-River in northern directions. Apart from coastal dune-fields large areas are covered by gravel and rock debris. Also noteworthy are south-westerly directed winds prevailing over the north-eastern type.
The Central Namib (B), situated between

Huab- and Kuiseb-River, enfolding the study area of this thesis. It consists primarily of vast almost horizontal gravel plains, only modified by sandy washes, dry river beds (also known as "Riviere") and sporadic inselbergs as well as small rocky ridges extending in a south-west/north-east direction up to 40 kilometers inland (WALTER 1985, LORIS ET AL. 2004). Apart from the extensive lichen cover the plains are almost barren (WESSELS & VAN VUUREN 1986). Therefore vascular plant cover is extremely sparse in areas where most of the lichen dominated biological soil crust cover is situated (ULLMANN & BÜDEL 2001A, WALTER & BRECKLE 1999?). Coherent patches of phanerogamic vegetation are mostly limited to a narrow coastal dune strip and ephemeral river beds (WALTER 1985). As a whole these preconditions favour the use remote sensing techniques for the assessment of lichen distribution patterns.

Directly bordering the southern banks of the Kuiseb-River, the Great Namib dune field (C) extends to the south almost to the town of Luederitz.

South of the erg extends another region influenced by summer rainfall, with plains highly diversified by inselbergs (D). This region ranges from west of Luederitz inland in a slight south-easterly direction and narrows towards its southern border at the base of the escarpment.

In parallel the Sperrgebiet-Namib (F) runs from Luederitz along the coast to Alexanderbay. Yet in a strip of 40 kilometers the Sperrgebiet is characterized by winter rainfalls.

Adjacent the West-Gariep-Namib (G) stretches along the northern and southern parts of the Oranje-River-Valley. As a climatic transition zone it is characterized by a large number of endemic species.

The southernmost part of the Namib Desert is called Namaqualand-Namib (H). It comprises the coastal plains of the northern Namaqualand up to the 100-mm-isohyet. Based on its high vegetation cover this area is often referred to as Succulent-Karoo.

Extending from the Fish-River in the North alongside the mountainous canyon areas of the Oranje-River up towards the region of Warmbad the East-Gariep-Namib (E) is located. This extension is induced by the subtropical high-pressure-belt's convexity between summer and winter rainfall areas (LORIS ET AL. 2004).

3.2 Climate

The climate of the Namib has been of much interest ever since humans first came across it (BESLER 1972). As consequence numerous studies have been published during the past century following its exploration, exploitation and colonisation (PICKFORD & SENUT 1999). However, despite these studies on winter-/summer rainfall regime (e.g. GÜLLAND 1907, NIEMAN ET AL. 1978, SOUTHGATE ET AL. 1996), radiation (e.g. NOTT & SAVAGE 1985), Benguela-Namib interactions (e.g. SHANNON ET AL. 1986), wind-systems (e.g. LINDESAY & TYSON 1990, LENGOASA ET AL. 1993), fog (e.g. BOSS 1941, GRAY 1980, MTULENI ET AL. 1998, SEELY & HENSCHEL 1998, ECKARDT & SCHEMENAUER 1998A, ECKARDT & SCHEMENAUER 1998B) only a few were dedicated to the climate of the Namib as a whole (e.g. BESLER 1972, LANCASTER ET AL. 1984).

Although these studies have made extensive use of the climatological data available, nearly all of them were based upon a series of meteorological stations operated by the Desert Research Foundation Namibia (DRFN) since the establishment of the Gobabeb Research Station in 1962 (compare BESLER 1972, SCHULZE 1976, SEELY & STUART 1976, LANCASTER ET AL. 1984, HENSCHEL 2003). Located in the southern part of the

study area (compare chapter 4.3.5) these studies provide only a preliminary and fragmentary climatic description of the Central Namib Desert.
In order to overcome these shortages climatic studies have also been incorporated into studies addressing ecological aspects of the area (e.g. SCHIEFERSTEIN 1989, LORIS & SCHIEFERSTEIN 1992, LANGE ET AL. 1994, HACHFELD 2000, HACHFELD & JÜRGENS 2000). Although these studies include temporally and spatially restricted information on the climate as well, they have nevertheless helped to understand the occurrence of climatic patterns within the study area.

The Namib Desert, part of the subtropical desert belt, shows only low, erratic and patchy precipitation. In general, total yearly amount of precipitation is comparable to other deserts (SCHIEFERSTEIN 1989).
For the central Namib Desert in particular, annual precipitation is dominated by the summer rainfall climate, but can be influenced by the winter rainfall regime as well. Thus precipitation along the coast can occur yearround, with a maximum of 72% of annual precipitation observed for the period from January to April and a minimum occurring September to December. Rainfall and convective showers are always very variable and highly localized (LANCASTER ET AL. 1984).

Four climatic factors prevail in the central Namib Desert. The high pressure cell of the southern Atlantic Ocean is responsible for the westerly winds blocking humid inland air masses from reaching the Namib Desert. The cold Benguela current running north along the west coast of southern Africa is characterized by the continuous up-welling of cold sea water cooling air masses and thus creating a stable inversion layer at an approximate altitude of 600 meters. Prohibiting the ascent of humid air masses this inversion layer is also directly responsible for the limited formation of clouds. In winter when the high pressure cell weakens warm air masses tend to flow into the Namib Desert from the Great Escarpment resulting in major foehn-/bergwinds (SEELY & HENSCHEL 1998).
The lack of larger topographical barriers within the Namib Plains between the coast and the Great Escarpment also inhibits this macroclimatic situation from being disturbed (LORIS ET AL. 2004). Thus, the overall climatic situation of the central Namib Desert is extraordinary stable, making it unique among the world's greater deserts (LANCASTER ET AL. 1984).

Henschel classifies four main climatic zones following a west-east gradient within the central Namib Desert starting with the Coastal Foggy Zone in the west. This zone reaches as far as 20 kilometers inlands beginning directly at the shore, usually showing cool and moist climatic conditions with a regular occurrence of fog from south-westerly directions in the late afternoon, at night and in the early morning hours. The yearly mean temperature of this zone is about 16°C, while a slight gradient can be acknowledged from the coast to the eastern inland border. An inversion of the above gradient can be observed for the mean yearly humidity of 87%. Mean yearly precipitation is about 15 mm, while fog precipitation can be up to 200% higher and the potential evaporation exceeds rainfalls by 87 times and fog precipitation by 39 times.
Adjacent to the Coastal Foggy Zone lies the Interior Foggy Zone reaching up to 60 kilometers inland. It comprises high daily ranges in temperature and humidity and regular heavy nightly fog precipitation from northerly directions. Potential evaporation exceeds rainfall over 100-fold but fog only 10-fold.
The following Middle Zone covering an area

between 40 and 90 kilometers inland, overlapping with the Interior Foggy Zone, shows almost complimentary climatic parameters, but differs in precipitation and evaporation, making it the driest zone of the Namib. Clouds occur only rarely and average annual precipitation is about 27 mm, with the average annual fog precipitation being of a similar magnitude. Although no strong seasonality in temperature can be observed, averaging around 21°C, mean diurnal temperature amplitude is 17 degrees with a maximum of 26°C. Humidity is significantly lower compared to the Coastal Zone, especially in winter times when cool and moist westerly winds alternate strongly due to the occurrence of dry and warm easterly foehn-/bergwinds. The potential evaporation exceeds rainfall 128-fold and fog 113-fold.
The last region of this zonal classification is the Eastern Zone starting a distance of 70 to 90 kilometers from the coast extending to 120 kilometers, right to the start of the Pro-Namib region. Mean annual precipitation is 87 mm with a very low mean humidity of 36%. Potential evapotranspiration exceeds rainfall 42 times and the mean annual temperature is 22°C. Fog occurs only rarely (HENSCHEL 2003).

Starting with the Pro-Namib LORIS ET AL. (2004) also suggest a climatic classification of the Namib into three zones. The Pro-Namib is followed by the inner Namib reaching up to 50 kilometers towards the coast, where the outer Namib is situated. The outer Namib can be divided into a coastal and an inland section separated by a transition zone at about 30 km coastal distance.
Mean annual rainfalls and temperatures within these zones can be compared to those mentioned by HENSCHEL (2003).

Undisputed by all authors the regular occurrence of fog precipitation in the Namib Desert is considered an ecological key factor (HACHFELD & JÜRGENS 2000, HENSCHEL 2003, WALTER 1976, LANCASTER ET AL. 1984, LANGE ET AL. 1990, LORIS & SCHIEFERSTEIN 1992, JÜRGENS & NIEBEL-LOHMANN 1995, MTULENI ET AL. 1998, SEELY & HENSCHEL 1998, LORIS ET AL. 2004).
As it can influence climatic conditions as far as 100 km inland from the coast it is the most characteristic climatic feature of the central Namib Desert with a multitude of adaptations found in both fauna and flora (LANCASTER ET AL. 1984).
During the night fog banks forming over the cold Benguela current are transported inland by westerly winds usually rising in late afternoon. Insolation usually dissolves the fog in the course of the day. Fog frequency varies spatially within the Namib. The area showing the highest fog frequency of 120 days per year is located between Cape Cross and Conception Bay, while fog frequency declines towards the north and south. Seasonality can be observed for the maximum fog precipitation, shifting from the coast further inland throughout the year (LORIS ET AL. 2004).
Additionally a general coast-inland gradient of fog frequency can be observed. For the central Namib Desert fog frequency at the coast shows a mean of 120 days per year, whereas 40 kilometers inland only 40 days per year can be counted. At 100 kilometers beyond the coastline fog frequency is limited to five days per year. However the overall gradient of the amount of fog water shows a different distribution. LORIS ET AL. (2004) note an increase in fog precipitation along the coast-inland gradient followed by a decrease to further inland areas. This is congruent to observations made by BESLER in 1972 (BESLER 1992).
Measurements within the Topnaar Community resulted in a mean fog precipitation greater

than 1mm/m²/day as far as 50 kilometers inland. A maximum 7mm/m²/day was recorded for fog-precipitation while overall yearly mean values ranged between 40 to 50 mm.
In addition overall spatiotemporal stability of regular fog events, with no major fluctuations is recorded for a period of 10 years, as mentioned by (LORIS ET AL. 2004).
However MTULENI ET AL. (1998) observed yearly variations in fog precipitation evidently following a cyclical 9 year pattern.
Research on the fog water chemistry found the fog itself to be almost sterile (ECKARDT & SCHEMENAUER 1998B). Fog as a source of water can thus be suitable to complement drinking water for animals as well as man (MTULENI ET AL. 1998).
Although precipitation through rain is still the primary water source for the Namib, fog tends to be the more reliable source. Therefore food instead of water can be regarded as the limiting factor in this ecosystem (SEELY ET AL. 1998).
Fog is differentiated by LORIS as a result of its occurrence within the outer Namib climatic zone.

Accordingly to the zonal climatic classification proposed by LORIS ET AL. (2004) the outer Namib can be divided into a coastal and a inland section separated by a transition zone at about 30 km coastal distance. Both sections show different types of fog with varying impacts.
Due to the higher ground- and air-temperatures of the landmass the cloud layer maintains a constant altitude during daytime effectively prohibiting precipitation (SEELY & HENSCHEL 1998; LORIS ET AL. 2004).
After sunset the fog sinks and floats as ground fog as long as westerly winds prevail. With no foehn winds rising this type of fog can cover the whole fog-zone (LORIS ET AL. 2004).
High fog is described by SEELY & HENSCHEL (1998) as a special form of advective fog. Starting from a stratus – and stratocumulus cloud layer over the Atlantic Ocean rising to an altitude of 600m during the day it is detained by a stable atmospheric inversion. Transported up to 60 km inland by strong onshore north-westerly winds it sinks to the ground. This type of fog is of greatest importance to the inner Namib zone (SEELY & HENSCHEL 1998).
The frontal fog, originating from the eastern inland section, evolves from laminar cold air runoff along the Riviere towards the coast. It occasionally is capable of becoming a lively north- north-easterly wind. Frontal fog is not limited to the ground but can also develop into an ample fog-bank if high fog will be present over the landmass in the first place. According to SEELY & HENSCHEL (1998) it forms the most important source of water for the inner Namib zone.
Emerging year-round, this type of fog follows the flow of air masses towards of the coast weakening in the process. During winter it only develops if no foehn winds are blowing. Preceding foehn events thick and extremely wet frontal fog develops usually reaching the coast (LORIS ET AL. 2004).
Drizzle, also developing along with frontal fog, arises from low lying layer clouds. It has a strong influence on both sections of the outer Namib. Especially contributing to the summer-maximum of fog-precipitation for the inland zone, it emerges as well as frontal fog in the early morning hours involving heavy precipitation humidifying all surfaces. Combined with frontal fog events, drizzle plays a prominent role for the lichen vegetation within the coastal section of the outer Namib as it represents a source of water during early morning hours when lighting condi-

tions allow photosynthesis (LORIS ET AL. 2004).
Altogether, advective fog supplies 53 % of the total fog events, followed by 31 % of frontal fog and drizzle contributing 16 % (LORIS ET AL. 2004). Yet measurements of fog precipitation indicated that although advective fog occurs more frequently, the overall amount of precipitated water showed to be higher with high fog events (SEELY & HENSCHEL 1998).

The wind system of the central Namib Desert is characterized by four different types showing diurnal as well as seasonal patterns. All through the year and especially in March and September the south-western onshore sea breeze occurs featuring wind-speeds of 5 – 10 $m*s^{-1}$. At the coast it rises late in the morning and calms at sunset. It is superimposed by north-westerly onshore winds attaining maximum wind-speeds of 10 - 15 $m*s^{-1}$. They are caused by the temperature gradient between the cool outer Namib and the hot inner Namib.
During the night, when the north-westerly winds weaken, moderate south-easterly katabatic winds (bergwinds) start reaching maximum wind-speeds of 5 – 10 $m*s^{-1}$ and climaxing around sunrise. Caused by the inversion of the thermal gradient it is stronger during winter (SEELY & HENSCHEL 1998).
Occasionally and mostly during winter strong dry east-winds (foehn-winds) interrupt the diurnal wind-pattern described above. At an average of eight times a year mostly between May and August these foehn-like bergwinds occur, often becoming severe windstorms. With temperatures of up to 40 °C and gust of winds reaching over 30 $m*s^{-1}$ they severely damage the vegetation by dehydration and aeolian corrasion (LORIS ET AL. 2004). This aeolian corrosion is even strong enough to have erosive impact on exposed rock formations (Photo 4) throughout the central Namib Desert (PICKFORD & SENUT 1999).
The stable atmospheric inversion layer, caused by the cold Benguela current frequently prevents these winds from reaching the coast. At a distance of about 30 – 40 km inlands the windstorm is deflected upwards by the inversion layer thus limiting its severe effects to the inner Namib zone. Hence the Namib is often referred to as Foehn-Desert (LORIS ET AL. 2004).

Photo 4: Image pair showing the aeolian corrosion on exposed rock formations limited to the north-eastern exposition present throughout the study area.

3.3 Geology

Geological development of the study area has been multi-facetted (PICKFORD & SENUT 1999). Various studies have constructed and revised partial geological histories, or published reconstructions of the history of the Namib placing of events of landform history in an order of succession (e.g. MARTIN 1965, OLLIER 1977, HAACK & MARTIN 1983, SCHREIBER 1996, PICKFORD & SENUT 1999). Some aspects of the geology were also addressed by geomorphological and pedological studies (e.g. MARTIN 1963, SCHOLZ 1972, SELBY 1976, SEELY & HAMILTON 1978, DANEEL 1992). Regarding the geologic layout of the study area, mica schists of the Khomas Series of the Precambrian Damara System underlie most of the central Namib Desert (SCHOLZ 1972, PICKFORD & SENUT 1999). It was formed by high temperature – low pressure metamorphism, numerous granite intrusives and intense deformation forming (SCHREIBER 1996).

Within the southern part of the Central (Swakop) Zone the Abbabis Metamorphic Complex form the oldest stratigraphic unit as it outcrops in domes and anticlines. Recognizing distinct stratigraphic units in these rocks is difficult as a result of the high degree of deformation and metamorphism (SCHREIBER 1996).

Eratically the Damara Sequence is overlain by the Abbabis Metamorphic Complex consisting to the most of metasedimentary rocks locally reaching a total thickness of 14 km. The upper portion of the sequence belongs to the Swakop-Group and comprises alternating marble, calc-silicate rock and schists and its basal part belonging to the Nosib Group and dominated by meta-arkoses and calc-silicate rock. Its rocks are found in the cores of antiforms or domes (SCHREIBER 1996).

Photo 5: Dolerite ridges in the hinterland of Wlotzkasbaken, north-east of Swakopmund.

Photo 6: Airborne photography showing dolerite ridges clustered in the hinterland north-east of Swakopmund. Source: SCHIEFERSTEIN 1989

Photo 7: Felsite dyke in the hinterland of Mile 8, north-east of Swakopmund.

A number of granites have intruded into the crystalline basement complex (SCHOLZ 1972). They range in age from late Namibian to Cambrian and Ordovician and are dominated by granites with intrusions of granodiorite, quartz diorite, syenite and gabbro occurring locally (PICKFORD & SENUT 1999). The reddish to light brown, medium-grained and often gneissiv or migamtic granites are often found alongside with the pinkish to grey Salem being the most prevalent one within the study area (SCHREIBER 1996).
Basaltic lavas, being poured onto the surface during upper Triassic and lower Jurassic period, are mainly eroded from the central Namib Desert with only the feeder dykes preserved today (SCHOLZ 1972).
They include abundant dolerite and minor felsite dykes (Photo 5 and Photo 7) for which the dolerite ridges (Photo 5) occur frequently in south-west - north-east directed dyke swarms in the hinterland north-east of Swakopmund (Photo 6) and again inland from Mile 108 and the Brandberg vicinity (PICKFORD & SENUT 1999). However they tend to be less frequent in other regions of the study area.
Cutting through all older metasedimentary and older intrusive units individual dykes are between ten centimetres and several tens of meters wide, often extending for many kilometers (SCHREIBER 1996). Due to their resistance to weathering the larger dolerite dykes tend to form prominent dark ridges of 20 – 40 m in height and extensive scree aprons (PICKFORD & SENUT 1999).

One of the larger dolerite dykes extending for several hundred meters in width is located on the coast at Wlotzkasbaken. In contrast to the dark-brown to black dolerite ridges, the less common felsite ridges are of dark-reddish colour and are only encountered locally (SCHREIBER 1996).

Ecologically all ridges feature an important habitat for higher plants as they not only shield them against devastating windstorms but also act as water reservoirs. Yet in between larger dyke swarms, windstorms can sometimes become even more severe as the air stream gets confined in between the ridges (SCHIEFERSTEIN 1989).
The probably late Cretaceous Henties Bay Alkaline Complex, situated 10 km inland from the coastal town of Henties Bay shows only poor exposures of its light-red to greenish-grey rock due to the extensive sand cover in this part of the central Namib Desert plain. Additionally quaternity deposits of the central Namib Desert plains cover extensive areas along the coast and south of the Swakop River (SCHREIBER 1996).

3.4 Soils

In arid environments soils are typically insufficiently developed showing almost none to little profile while chemical weathering is usually decreased in favour of physical weathering due to lack of water. Therefore raw mineral soils are common within the study area (SCHOLZ 1972).
LORIS & SCHIEFERSTEIN (1992) classically subdivide the Namib Desert into areas of loose sands (erg), gravel-plains (serir) and debris and block covered plains (hamada). Since this classification allows only limited characterisation of the predominant soil-types within the Namib Desert, an updated descriptive classification based on the variation of parent rock and soil substrate is presented by LORIS ET AL. (2004).
These syrosem soils show different phases of weathering of parent rock material especially in the eastern parts where inselbergs are prevalent geomorphological feature (SCHIEFERSTEIN 1989, BESLER 1992).

However based on the large lithological variety of the central Namib Desert soils consist of divers substrates with granite, basalt, sandstone, quartzite, limestone and different conglomerates thus affecting the composition of vegetation (LORIS ET AL. 2004).

Soils based on the weathering of granites are widespread from the Namaqualand to the central Namib Desert and often feature clay subsoil substrates accompanied by a gravel topsoil layer with Aloe dichotoma and Enneapogon scaber forming characteristic elements of their vegetation (LORIS ET AL. 2004).
Basalt weathering proceeds only slowly in an arid environment often forming linear and localized deposits leading to alluvial or aeolian substrates. Ecologically the persistence of basalt is of great importance to the vegetation as it maintains stable habitats protected from windstorms and corrasion. They are mostly restricted to the central Namib.
Weathering of sandstones is found within the East-Gariep-Namib area and the great Namib-Erg. Vegetation cover on these substrates is influenced by an increase in precipitation often causing a rapid increase in soil acidity as well as the accumulation of dune sands.
Comparable to the weathering of basalts, the weathering of quartz proceeds slowly with a reduced formation of substrates in its surrounding. The influence of quartz on the vegetation is thus limited to localized reefs and fragments of gravel and rocks covering vast areas. Nevertheless vegetation on these reefs and plains is highly specialized mainly due to its persistence.

Weathering products of limestone and dolomite can indirectly provide substrates for lime and gypsum crusts (SCHOLZ 1972). Limestone and dolomite themselves, show only sparse specialized vegetation cover whereas many species have adapted to lime and gypsum crusts.
Argillaceous schist and mica are capable of forming favourable substrates, but its vulnerability to weathering on slopes does make colonization by vegetation difficult (LORIS ET AL. 2004).

Figure 4: Hydrogen sulphide eruption along the Central Namib Desert coast observed by MODIS satellite on 16th of October 2003.

In addition to those substrates evolving indirectly from weathering of parent rock, abiotic soil crusts caused by the increase in evaporation over precipitation in arid environments are widespread and often protect the surface against erosive forces. As the actuating water evaporates solid remains of solution and

transportation processes accumulate as a crusted horizon within the affected soil especially at the bottom of slopes and valleys with limestone, gypsum, silicates and NaCl being the major crust forming elements (GOUDIE 1972).

Limestone crusts, also widespread in the Namib Desert, show varying thickness of up to 50 m depending on their age. Since the momentary hyper-arid climatic conditions of the Namib Desert do not allow their formation they date back to when climatic conditions were much more humid. In general limestone crusts are unfavourable to vegetation but large parts of the Namib vegetation, for example Poaceae or Zygophyllaceae, are well adapted (LORIS ET AL. 2004).
Within the central Namib areas covered with limestone crusts are mainly restricted to the inner Namib (BESLER 1992).

The formation of gypsum crusts is caused by biogenic sulphur compounds provided by hydrogen sulphide eruptions from the Benguela sediments along the coast of the Atlantic Ocean (MARTIN 1963) (compare figure 4).

In contrast to previous theses, frequent fog events do not contribute to the build up of gypsum crusts as precipitated water is almost sterile (ECKARDT & SCHEMENAUER 1998a).
Gypsum crust can be located up to a coastal distance of 60 – 70 km which is about complementary to the distribution of the Succulent-Karoo region of the Namib Desert. Many taxa of the inner Namib, like Stipagrostis sibacaulis, have become specialized to gypsum-soils indicating a high age of gypsum soils. The surface of these soils is covered by a layer of fine gravel material amounting to several centimetres with the exception of ephemeral river beds. The gravel material is often embedded into sand by several millimetres and conjoined by salt thus stabilizing the surface against erosive forces. Gypsum soils also tend to produce polygonal soil patterns as well as vesicular top layers (Schaumböden). Compared to other desert areas the distribution of salt crusts is only scarce within the Namib Desert. They are mostly limited to local spring horizons, rivers or other ephemeral waters. However saline soils occur frequently along the central Namib Desert coast.
Silicate crusts are typically found conjoined to sands or silt within the subsoil especially obstructing vegetation after the topsoil has been eroded (LORIS ET AL. 2004).

3.5 Geomorphology

The coastal plains of the central Namib Desert steadily rise by 1 – 2 % in an easterly direction. They are framed by the Atlantic Ocean in the west and the Great Escapement in the east. The Great Escarpment evolved from processes lifting and backwearing the inland. Yet indications of vertical backwasting, having great influence on the development of the coastal plains, were found too. Originally the coastal plain was formed by water as marine sediments indicate, followed by wind becoming the dominant factor as aridity increased during the middle miocene.
Many ephemeral and perennial rivers cut through the Central Namib Desert. While only the larger rivers run off into the Atlantic Ocean, nearly all rivers are south-west – north-east directed complementary to the dolerite ridges (SCHIEFERSTEIN 1989). Therefore general differentiation of rivers is based either on their ability to reach the ocean and those seeping away into inland basins (e.g. Sossus-Vlei) (WALTER & BRECKLE 1999[7]).
However even smaller rivers were observed to even cut through the coastal dune fields of

the Skeleton-Coast park and dewater into the ocean following the extraordinary rainfall events in the year 2000 [BRABY, R., pers. comm.].

Sands are shifted by fluvial forces, as runoff from often heavy but rare local rainfall events causes the larger rivers to flow. Washes cutting through the Namib plains show only local fluvial erosion of their alluvial deposits restricted to heavy rainfall events as well.

Although these traces of fluvial erosion are to be found anywhere, aeolian processes prevail. On the Central Namib Desert plains, topsoil sands are deflated causing gravel to remain on the surface covering vast areas. Ephemeral river beds, dry pans and small channels running in south-west – north-east direction sometimes even intensify deflation processes as the air stream gets confined within their network (BESLER 1992).
Material carried along by surface winds leads to excessive corrasion among bedrock and vegetation as well as anthropogenic matters especially close to the ground where wind driven sands gain maximum momentum (SCHIEFERSTEIN 1989).
On different scales all deflated material becomes deposited again. Sand deposits by the Atlantic Ocean, originally dislocated from the African backcountry by perennial rivers, are usually shifted inlands by the prevailing south-westerly winds (PICKFORD & SENUT 1999).
Thus valley systems and other ancient geomorphologic landforms are covered or persistently altered by those sands. Sand dunes themselves are the only known larger geomorphologic feature created solely by wind-driven sands (saltation) (compare photo 8). On a smaller scale sands are often deposited on the leeward side of perennial vegetation

Photo 8: Coastal sand dunes between Walvisbay and Swakopmund.

Photo 9: Aeolian sand deposits on the leeward site of an Arthraerua leubnitziae accumulated to ripples.

(Nebkha) or found accumulated to ripples (compare photo 9).

Exposed rock is generally weathered by insolation with desquamation and exfoliation having major impact though moisturisation is still an influencing factor as well.
Disintegration and breaking of rock are not solely based on weathering through insolation erosion as they are mainly depending on fissures within the rock which can also evolve as pressure is released from the rock during exhumation processes.
Decompositioned blocks are hollowed by shadow weathering in likely conjunction with fog precipitation as this phenomenon decreases towards inland areas.
Minor cavernous weathering described as tafoni are created when water dries and its minerals form crystals that force small particles to flake off the rock. For the Namib Desert salt weathering induced tafoni are most common along the coast, where seawater and spray brings salt to rock surfaces. However huge abri with cave-like passages are of a different origin. They are produced by prolonged pauses during exhumation in conjunction with subcutaneous weathering within humid soils.
Inselbergs are a characteristic geomorphologic feature of arid environments also found in the Namib as well. Most of them feature exhumated granite intrusions typically forming domes and thus creating surface runoffs in the event of rainfalls and forming natural cisterns leading to extrazonal vegetation within their vicinity (Besler 1992, Loris et al. 2004).
In the Namib Desert endolithic lichen and cyanobacteria colonizing the interior of porous rocks and cracks also cause mechanical and chemical weathering (compare photo 10). For example does the chasmoendolithic Lecidea species contribute to the weathering process of quartz during colonization of this favourable microhabitat (Wessels 1989).

Photo 10: Endolithic crust colonizing crevices and fissures of a quartz rock.

In addition desert varnish is a thin coating of manganese, iron and clays occurring on physically stable rock surfaces that are no longer subject to frequent precipitation, fracturing or sandblasting. Typically found in cold deserts they are formed by colonies of microscopic bacteria living on the rock surface. The bacteria absorb trace amounts of manganese and iron from the atmosphere and precipitate it as a black layer of manganese oxide or reddish iron oxide on the rock surfaces. This thin layer also includes cemented clay particles which help to shield the bacteria against desiccation, extreme heat and intense solar radiation (Krumbein & Jens 1981, Dorn & M. 1982).

3.6 Vegetation

3.6.1 Geographical distribution

In conjunction with the Karoo, the Namib Desert is a paleotropical desert. Consequently its vegetation consists mainly of paleotropic floristic elements. Interspersed floristic elements of the highly divers Capensis floristic realm can be observed congruently to the distribution of winter rainfalls (LORIS ET AL. 2004).

The subordinate floristic regions of the Nama-Karoo and the Succulent-Karoo feature a mostly congruent distribution to the prevailing climatic zones. Nevertheless divergences between climatic and vegetation zones can be observed for the fog-zone of the central Namib Desert as well as for the Richtersveld/Sperrgebiet area. In the first area fog seems to compensate the missing winter rainfalls as floristic elements of the southerly succulent Karoo can also be observed (e.g. *Zygophyllum clavatum, Drosanthemum paxianum, Brownanthus kuntzei*). For the latter area the delineation of vegetation zone is also independent from summer or winter rainfalls. Instead it is primarily triggered by air temperature followed by air humidity. Within the two floristic regions, regional arid centres of endemism are also present, with some of them partly connected (LORIS ET AL. 2004). Accordingly to MAGGS ET AL. (1998) cited by LORIS ET AL. (2004) 275 species are known to be endemic to the Namib Desert.

Despite the obvious aridity of the Namib surprisingly little C4-plants are known to occur whereas many C3-plants are endemic. Even if C4 carbon fixation might be a superior adaptation to arid climates it might not be an imperative (VOGEL & SEELY 1977).

3.6.2 Vegetation of the Namib

Following the classification of LORIS ET AL. (2004) the Namib can roughly be subdivided into five differing habitats.

- **The vegetation of the vast nearly flat plains**

This subsection spreads across both inner and outer Namib region. As stated before, these vast plains are mostly covered by gravel remaining on the surface after topsoil sands have been deflated. With sizes varying between 5 – 20 mm the fine gravel comprises different rock types but is dominated by quartz. Beneath this top layer fine material often conjoined to crusts is deposited (LORIS ET AL. 2004).

In the outer Namib Desert perennial phanerogamic vegetation is extremely sparse and can only be found where stored water from past rainfalls is available within a depth of less than one metre (ULLMANN & BÜDEL 2001A, WALTER & BRECKLE 1999[7]). Upon these gravel plains and in between the ephemeral washes, lichen communities are the prominent vegetation cover often grouped to large lichen fields being rich in species as well as biomass. Lichen are poikilohydric organisms which are able to extract water from fog, dew and high humidity for photosynthetic processes making them independent from precipitation (WALTER & BRECKLE 1999[7]).

Climatic conditions, with the fog in particular not only favour the distribution of lichens but that of green algae and hypolithic cyanobacterial crusts growing on the underside of translucent quartz pebbles (Ullmann & Büdel 2001a). However, special fog plants comparable to the Peruvian Tillandsien are inexistent (LANGE ET AL. 1990).

Subsequent to precipitation species of *Mesenibryantheruni cryptanthum* along with short-lived grasses of the genus *Stipagrostis* are typically found in the central Namib Desert. In the southern Namib species of *Mesenibryantheruni hypertrophicum, M. pellitum* and *M. barklyi* replace the species found in the central part.
Along the coast where temporary flooding and spray increases saline concentrations of the soils, a halophilious Succulent-Karoo plant community including cushions of *Drosanthemum luederitzii, Psilocaulon salicornioides* and *Zygophyllum clavatum* can be located. Moreover these plants are capable to accumulate sands.
Arthraerua leubnitziae, Zygophyllum stapfii, Tetragonia reduplicate and *Salsola tuberculata* dominate the area east of the costal zone with *Arthraerua leubnitziae* becoming less important towards the inner Namib.
For the easterly inner Namib widespread grassland is known to occur subsequently to sparse summer rainfalls, which is dominated by species of the genus *Stipagrostis* (*S. obtusa, S. ciliata*). Occurrence of *Stipagrostis hochstetteriana* and *Stipagrostis uniplumis* is recorded for the Pro-Namib region. Limited to wider washes of the transition zone in between outer and inner-Namib individual plants of *Welwitschia mirabilis* can be located (compare photo 11).

Endemic to the Namib for an area of about 100 km in width and of 1200 km in length this plant consists of a large taproot, a short woody trunk or crown (caudex) protruding above the ground and two livelong growing leaves dying back beyond 2,5 m in length. With their base at the meristematic region the two leaves are split and frayed by wind into bizarre formations allowing them to be interpreted for a multitude. Thickness of leaves ranges from 1 – 2 mm reaching a maximum of 4,2 mm in vicinity of the Brandberg. Welwitschia plants are dioecious, with pollen-bearing and seed-bearing cones (strobili) produced on separate male and female plants. C^{14} analysis revealed larger plants to be older than 2000 years.
Inclined slopes of the East-Gariep-Namib show frequent sheet flooding succeeding rainfall events. Stabilized substrates are covered by a plant association determined by *Calicorema capitata* whereas besieged substrates are colonized by plant communities comparable to ephemeral rivers (*Sisysndite sparteum* or *Prenia tetragonal*) (LORIS ET AL. 2004).

Photo 11: Image pair of a male *Welwitschia mirabilis* situated on the banks of a minor wash in the vicinity of the Messum Crater.

- **Vegetation of the inselbergs**

As Inselbergs tend to accumulate precipitation, ephemeral waters accompanied by extrazonal vegetation subsequently evolve if natural basins are found in their surrounding.
Furthermore rocky ridges function as preferred habitats to succulents with a large variety of species disregarding the size of the formation. Especially the poikilohydric *Chamaegigas intrepidus* shows an extraordinary adaptation to this habitat. For some plants inselbergs also function as retreats with many of them being floristic relicts separated from their original habitats due to climatic changes. East of the arid areas of the outer and inner Namib where ephemeral grasslands prevail and the surface is covered by gravel and debris an area with large *Euphorbia damarana* of up to three metres in height exists (LORIS ET AL. 2004).

- **Vegetation of the ephemeral washes**

The plains of the central Namib Desert are corrugated by smaller runnels also described as washes or wadis. They either dewater into the larger perennial rivers or peter out into wide and shallow pans (LORIS ET AL. 2004).
The runnels themselves are desalted but the pans where water seeps away show a higher saline concentration. Both different habitats evolving also show different plant communities.
The halophobic habitat is commonly colonized by a floristic community comprising Citrullus, Commiphora and Adenolobus supplemented by *Euclea, Parkinsonia Africana* and *Acacia reficiens* shrubs where ground water supply is increased.
On the contrary a halophilic community dominated by *Arthraerua leubnitziae, Zygophyllum stapfii* and *Salsola tuberculata* prevails in the wide and shallow pans. Showing excellent adaptions to this environment the community occurs from the Kuiseb up to south-west Angola. Sands deposited on the leeward side of the perennial vegetation form a typical nebkha-like landscape (LORIS ET AL. 2004).
All these communities are dependent on occasional rainfalls but it is assumed that *Arthraerua* can also assimilate fog (WALTER & BRECKLE 1999?). With the highly specialized phreatophytic *Welwitschia mirabilis,* whose roots are in contact with the water table, being the only exception for the halophobic habitat in the transition zone of outer and inner Namib.

- **Vegetation of the ephemeral / perennial rivers**

For the central Namib Desert this community is generally limited to the linear ephemeral oasis formed by the larger ephemeral riverbeds of the Kuiseb, Swakop, Omaruru, Ugab and Huab (compare photo 12). These

Photo 12: Photo of the linear oasis of the Kuiseb riverbed taken at the desert research station of Gobabeb operated by the Desert Research Foundation of Namibia (DRFN).

rivers are fed by highland summer rainfalls with some carving themselves deeply into the desert surface.

The riverbeds are filled with sands through which flood waters usually seep away quickly. While ephemeral rivers generally flow less in their lower reaches only larger floods actually dewater into the see. But although surface runoff does only occur infrequently subsurface alluvial aquifers are present at most times. And even with water from alluvial aquifers disappearing during severe drought, local fountains are still fed by ground water reservoir. These water resources supplemented by favourable microclimatic conditions allow the occurrence of 14 plant communities comprising 40 variations known to date only in the lower Kuiseb River Valley (THERON ET AL. 1980).

Even with occasional large floods causing the riverbed to be cleared, gallery forest consisting of *Acacia albida, Acacia erioloba, Euclea pseudebenus, Salvadora persica* and various *Tamarix* and *Lycium* species can reach great age in the outward areas of the riverbed (WALTER & BRECKLE 1999[7]).

Within the riverbed itself no perennial vegetation can withstand the erratic floods. Shifting sands show species of *Ricinus communis, Nicotiana glauca, Argemone, Datura* and others while smaller sand dunes are vegetated by the thorny, leafless and endemic *Acanthosicyos horrida* (!Nara) in association with *Eragrostis spinosa* and *Stipagrostis namaquensis* among many other widespread grasses (WALTER & BRECKLE 1999[7]). For several hundred years *Acanthosicyos horrida* has been an important foodsource as it has always been to the wildlife (HENSCHEL 2003). !Nara-Plants tend to accumulate sand, thus leading to dune formation processes at small scales. Since fully grown plants have high water demands their occurrence is always bound to ground water resources (LORIS ET AL. 2004).

Pools and puddles fed by ground comprise species of *Phragmites, Diplachne, Sporobolus* and *Juncellus* (WALTER & BRECKLE 1999[7]).

- **Vegetation of the dune systems**

Vegetation of the large dune formation within the Namib Desert is extremely sparse and concentrates on the fog-zone of the outer Namib along with the easterly Pro-Namib region. Generally an increase in species diversity in conjunction with biomass can be observed. Typical vegetation comprises grasses of *Stipagrostis sabulicola, Stipagrostis seelyae* and *Eragrostis spinosa* diversified by *Kohautia ramosisissima* and *Monsonia ignorata* toward the inland areas and *Trianthema hereroensis* to the seaward limits. They can reach noteworthy coverage after rainfall events.

Dune plant communities being able to fixate the dune system occur as species diversity starts to increase south of Lüderitz mainly caused by rising air humidity and air temperature becoming more moderate. Due to these changes the dune community in this area is largely characterized by the Asteraceae *Othonna cylindrica* and *Othonna sedifolia* accompanied by the Aizoaceae *Stoeberia heetzii* and *Stoeberia*

Photo 13: Photo of Goanikontes oasis situated in the Swakop riverbed, showing small-scale farming by herdsmen.

utilius as well as grasses of *Stipagrostis ciliata* and *Eragrostis spinosa.*
The dune systems of the East-Gariep-Namib clearly show floristic features of the Kalahari dune systems as *Stipagrostis amabilis* grasses in conjunction with shrubs and trees of *Acacia erioloba* and *Acacia haematoxylon* occur (LORIS ET AL. 2004).

3.7 Anthropogenic utilization

Limited utilization by the indigenous hunter and gatherers was prominent to the Namib by the end of the nineteenth century. Today based on its hyper-arid climatic conditions the outer and inner Namib shows only limited potential for agricultural utilization. Only the linear ephemeral oasis of the riverbeds allow small-scale-farming by herdsmen (HENSCHEL 2003) (compare photo 13).

Areas of the Pro-Namib with an emphasis on the riverbeds are only utilized by farmers during periods of extreme drought when pasture is drastically decreased. And though more and more traditionally farmed areas are converted by the owners to serve for tourist needs, overgrazing is still problematic as many farmers do not adjust stocking rates to natural periodicity of rainfall.
For the Central Namib Desert and the area that it is discussed within this study most of the area is situated within the National West Coast Tourist Recreation Area (NWCTRA), with the exception of the Namib-Naukluft Park Area in the south and the Skeleton-Coast Park in the north. Within the NWCTRA tourist interests prevail, as for example the towns of Swakopmund and Hentiesbay almost fully rely on the tourist industry today. Tourist activities include fishing, off-road driving with cross-bikes, quad-bikes and four by four vehicles.
Thus access to the vast plains of the Central Namib is not restricted, except for a few designated areas like the lichen field of Wlotzkasbaken which was at least fenced out from the coastal road (C35), following a symposium held at Swakopmund in 1987 addressing the problem of conservation.
This symposium also compiled a conservation masterplan containing inputs from various stakeholders. In part this has resulted in efforts to educate and inform the general public about the fragility of the Namib ecosystem and need for its conservation. This included various publications (CRAVEN & MARAIS 1986, HEINRICH 1986, WESSELS & VAN VUUREN 1986, GIESS 1989, SCHIEFERSTEIN 1989, WESSELS 1989), as well as the description of marked paths through sensitive areas published by the Tourism Officer of the Municipality of Henties Bay (TOURISM OFFICER OF MUNICIPALITY OF HENTIES BAY 2003A, TOURISM OFFICER OF MUNICIPALITY OF HENTIES BAY 2003B).
However the tourist industry only supplemented former intensive mining in the whole area. While a few mines are still operated today (e.g. Rössing – Uranium, Panther Beacon Salt Works – north of Swakopmund, Walvis Bay Salt Works) many of them have been shut down (Goantagab, Cape Cross Salt Works, Strathford Mine – Tin+Tungsten, Brandberg West – Tin+Tungsten, Uis - Tin+Niobium+Tantalite, Namib Lead Mine, Khan Mine, Huab- and Ida Mine) (MENDELSOHN ET AL. 2002). Due to these widely spread mines an informal road network, consisting of primary and secondary dirt-roads exist. Though this "road-network" often grants the scientist a fairly easy access to remote areas, the disturbances that these roads have created will persist for a long time.

As a third source of disturbance to the Namib ecosystems, constant maintenance of

roads and general construction work within the vicinity of towns can be depicted. While road maintenance is undoubtedly necessary, widely spread acquisition of sand and gravel material should however be avoided, as often untouched areas are disturbed. This disturbance pattern can also be observed in the vicinity of towns with mostly housing construction being responsible for an uncontrolled spatial acquisition of sand and gravel as low-cost building materials.

In general with the increasing off-road traffic and general usage of the NWCTRA for recreation purposes only conservation measures enforced by access restrictions will limit destruction, especially of the lichen communities, by humans.

4. Materials

The structure of the remotely sensed and in situ data conjoined with a detailed description of the preprocessing performed on the data is explained in this chapter. Additionally reference data used for geometric correction of the satellite images are described.
At last the methodology and techniques used for the collection and recording of in situ data is presented. In situ data included the collection of training sites following the concept of morphological groups, sampling of lichen community biomass as well the collection of spectral reflectances for the latter with the means of field spectroradiometer.

4.1 LANDSAT data

LANDSAT data are key or characterizing, quantifying, and mapping the long-term changes that are occurring across the Earth's land surface (VOGELMANN 2003).
The major update to the LANDSAT sensor series including enhancements in geometrical, optical as well as radiometrical resolution was introduced in 1982 with the launch of LANDSAT 4 carrying the first „Thematic Mapper" (TM) in addition to the MSS sensor. The LANDSAT series continued in 1985 with LANDSAT 5 which is still operational today. Unfortunately LANDSAT 6 carrying the first "Enhanced Thematic Mapper" (ETM) was lost on launch in 1993. It was supposed to enhance the TM sensor by adding a 15 x 15 m ground resolution panchromatic band as well as improving the geometrical resolution of the thermal infrared from 120 m to 60 m with both bands being intrinsically registered with the other multispectral bands. Consequently LANDSAT 7 was launched in 1999 with its ETM+ sensor.

However on May 31, 2003, LANDSAT 7 experienced a Scan Line Corrector (SLC) failure during imaging. The SLC is an electromechanical device that compensates the forward motion of the satellite aligning scan lines to minimize overlap and gaps (U.S. GEOLOGICAL SURVEY 2003) (See figure 5 for details).

The report concludes the now inherent artefacts of overlap and underlap caused by the anomaly are likely to have a negative impact on the overall usability of the data.
In addition, the degree to which the scientific usage of this data is sustained is highly dependant on the geometrical position and size of the study area and the scientific application (U.S. GEOLOGICAL SURVEY 2003). Consequently future usage of the LANDSAT

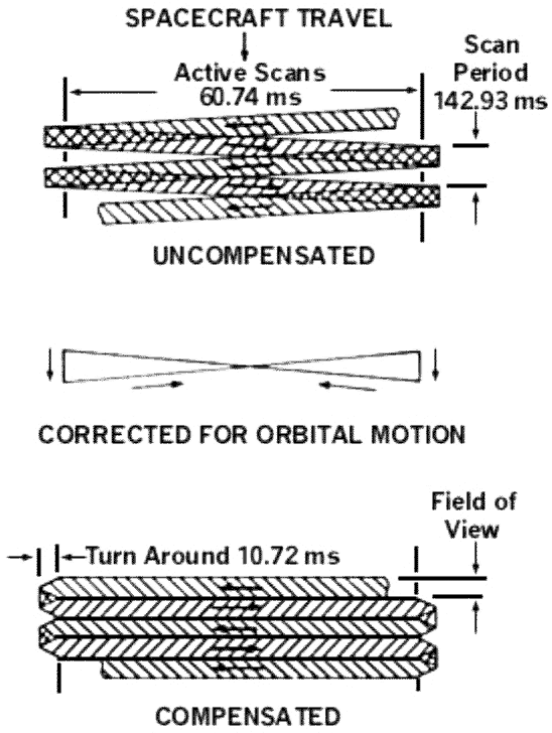

Figure 5: Schematic illustration of SLC functionality. Source: U.S. GEOLOGICAL SURVEY (2003), FIGURE A, PAGE 5.

7 ETM+ SLC-OFF Data starting May 31, 2003, is highly questionable.
For this study LANDSAT 5 Thematic Mapper (TM) and Enhanced Thematic Mapper (ETM) data prior to SLC-Failure was used to calculate both unitemporal and multitemporal classification approaches. In the following both sensors shall thus be described in detail. As the ETM sensor evolved from the TM sensor series, both have a lot more features in common compared to the rather minimal MSS sensor. Both share the same 8 bit quantisation level, 16 days repeat cycle, 705 km of altitude, inclination angle of 98.2°, swath width of 183 km and an equatorial crossing time of 10:00 a.m. +/- 15 min. In addition, they nearly share the same radiometrical and geometrical resolution for the bands 1-5 and 7, facilitating the underlying studies (compare table 1). Though they still differ in geometrical resolution of their thermal infrared band 6, the non-existent panchromatic band for the TM and the enhanced absolute sensor calibration (<10 % on TM and <5 % on ETM+), their almost complementary design makes them ideal for timeseries analysis and change detection studies.

	TM	ETM+
Sensor Parameters		
Technology	Scanning Mirror Spectrometer	
Quantisation Level	8 bit	
Data Rate	85 Mb/s	150 Mb/s
Absolute Calibration	< 10 %	< 5 %
Spectral Resolution		
Band 1 (blue)	0.450 - 0.520 µm	0.450 - 0.515 µm
Band 2 (green)	0.520 - 0.600 µm	0.525 - 0.605 µm
Band 3 (red)	0.630 - 0.690 µm	
Band 4 (NIR)	0.760 - 0.900 µm	0.750 - 0.900 µm
Band 5 (MIR)	1.550 - 1.750 µm	
Band 6 (TIR)	10.42 - 12.50 µm	10.40 - 12.50 µm
Band 7 (MIR)	2.080 - 2.350 µm	
Band 8 (PAN)	-	0.520 - 0.900 µm
Spatial Resolution		
Band 1 (blue)	30 x 30 m^2	30 x 30 m^2
Band 2 (green)	30 x 30 m^2	30 x 30 m^2
Band 3 (red)	30 x 30 m^2	30 x 30 m^2
Band 4 (NIR)	30 x 30 m^2	30 x 30 m^2
Band 5 (MIR)	30 x 30 m^2	30 x 30 m^2
Band 6 (TIR)	120 x 120 m^2	60 x 60 m^2
Band 7 (MIR)	30 x 30 m^2	30 x 30 m^2
Band 8 (PAN)	-	15 x 15 m^2
Orbit Parameters		
Repeat Cycle	16 days / 233 Orbits	
Altitude	705 km ± 5 km	
Period	98.9 min.	
Inclination	98.2 ° ± 0.15 °	
Launch Date	01.04.1985	15.04.1999
Scene Coverage	170 x 183 km	
Swath Width	183 km	
Equat. Cross Time	10:00 a.m. ± 15 min.	
Reference System	WRS-2	

Table 1: Specifications of the Thematic Mapper system.

4.1.1 Acquisition dates, overall environmental conditions and general coverage

Following the WRS-2 geographic reference system, which has catalogued the world's landmass into 57.784 scenes, for LANDSAT 5 TM and LANDSAT 7 ETM+ data, two scenes, had to be used to cover the study area (NASA 1999). For the northern part scenes located on path 180 and row 75 were used, while for the southern part scenes from path 179 and row 76 were acquired (compare figure 6).

Due to the frequent fog events along the coast the number of "cloud-free" scenes was limited noticeably. For example, no satisfactory and coinciding ETM+ scene could be

Sensor	Acquisition Data	Path / Row
TM	15.05.1991	180 / 075
TM	26.05.1992	179 / 076
ETM+	18.09.1999	180 / 075
ETM+	06.04.2000	179 / 076
ETM+	02.07.2000	180 / 075
ETM+	22.04.2003	180 / 075
ETM+	01.05.2003	179 / 076

Table 2: Listing of LANDSAT satellite data acquired for this thesis.

retrieved for the 2002 field-campaign whereas it was possible to acquire two matching scenes for the period of the 2003 field campaign. In order to establish a timeseries for the multitemporal classification approach, which will be discussed later on, additional TM scenes for the years 1991 and 1992 and auxiliary ETM+ scenes for the years 1999 and 2000 were acquired (compare table 2).

4.1.2 Level of processing

The United States Geological Survey (USGS) is currently operating the LANDSAT program. The organisation offers LANDSAT data in three formats hierarchically describing the amount of preprocessing: starting with "level-0" data containing both radiometrical and geometrical uncorrected raw data, followed by the radiometrical but not geometrical corrected "level-1R" data and completed by the fully radiometrical and geometrical corrected "level-1G" datasets (JENSEN 2000). In terms of processing level all LANDSAT data used for this study was acquired as Level 1G Data Product from the USGS, resampled to the user-specified map projection "Universal Transverse Mercator" (UTM) involving WGS 84 (World Geodetic System 1984) for spheroid and projection date. The WGS 84 spheroid uses an equatorial radius (semi-major axis) of 6,378,137.0 m and a polar radius (semi-minor axis) of 6,356,752.31424517929 m. Supplementary UTM-Zone "33-South" was used for all LANDSAT data (ERDAS 2001[5]).

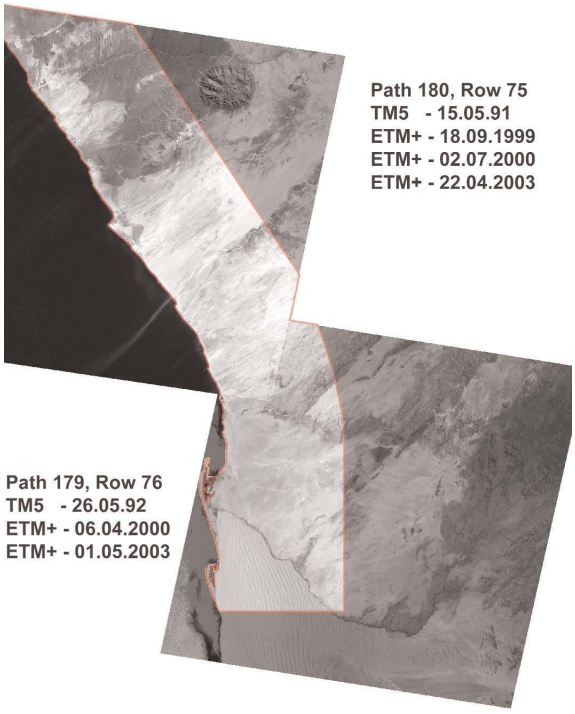

Figure 6: Location and extent of the study area in regards to the spatial coverage of LANDSAT 5 TM and LANDSAT 7 ETM+ data.

Further utilization of these datasets for land cover classification and change detection is however strongly dependant on the extent of the methods and techniques used for preprocessing of these datasets. In regards to preprocessing geometric correction, multitemporal image registration, and radiometric calibration can be considered the most important (COPPIN & BAUER 1996, DU ET AL. 2002).

4.1.3 Geometric correction

As remotely sensed data are generally distorted by the earth curvature, relief displacement and the acquisition geometry of the satellites, it must be the intent of geometric correction to compensate for the distortions introduced by these factors to achieve a geometric integrity equal to that of a map (LILLESAND & KIEFER 2000[5]). Since all LANDSAT data is acquired as being geometrically corrected its accuracy however is insufficient for the underlying studies. The geometric correction

of the raw "level-10" LANDSAT product is obtained without ground control points solely depending on the satellites` orbital parameters. Thus a geodetic error of 250m minimum for flat terrain at sea level can be assigned to the "level-1G" data product (U.S. GEOLOGICAL SURVEY 2004).

As a more accurate geodetic registration is required for the forthcoming classification and change detection studies, "level-1G" datasets have to be manually rerectified using ground-control-points obtained from Namibian topographical maps – scale 1 : 50.000 – and GPS measurements obtained during field campaigns (see also chapter 4.4). This technique is also described as absolute registration and uses polynomial transformations to correct systematic and non-systematic distortions. It was applied to both year 2000 ETM+ scenes of 180/075 and 179/076 creating two master images for relative registration. Relative registration methodology overlays images of the same area which have been acquired at different times or from different satellites registering all other images to the geometry of the one image declared as master (BÄHR & VÖGTLE 1991, HÄBERÄCKER 1994). Because of its higher spatial resolution the panchromatic ETM+ were always used for absolute registration beforehand, thus obtaining a geometric model later applied to all other multispectral bands, except for both TM-scenes missing the panchromatic channel. Nevertheless geometric error was always kept at subpixel niveau for ETM+ as well as TM datasets using second polynomial transformations limiting unnecessary distortions. Nearest-Neighbour-Interpolation was used for resampling in all instances. At last all geometrically corrected data was visually checked for apparent distortions against the reference used for absolute registration and the master images used for relative registration in the first place. An overview of the applied geometric correction techniques as well as error rates is presented in table 3. For more information on interpolation techniques see (ERDAS 2001[5]).

After the successful geometric correction it was also necessary, because of slight geometric errors resulting from the polynomial transformations, to partly shift upper left X (ULX) and upper left Y-coordinates (ULY) of the multispectral datasets to fully match the master images.

However the topographical maps and GPS-Data used for absolute registration always imply horizontal errors themselves which may lead to misclassification at a later stage because of nonthematic errors due to the misregistration between the image classification ground data (FOODY 2002). Thus coregistration of GPS-Data and topographical maps was checked to avoid divergence between training samples recorded by hand-

Dataset	Path / Row	Acqu. Date	Reference	No. of GCP´s	Spatial Resolution	Geodetic Error ±	Polynomial Order
ETM+ pan	179 / 076	06.04.2000	GPS & Topo. Road Map	67	15m	6,4539 m	2
ETM+ mspec.	179 / 076	06.04.2000	GPS & Topo. Road Map	67	30m	6,4539 m	2
ETM+ pan	179 / 076	01.05.2003	ETM+ pan 06.04.2000	87	15m	5,11615 m	2
ETM+ mspec.	179 / 076	01.05.2003	ETM+ pan 06.04.2000	87	30m	5,11615 m	2
TM mspec.	179 / 076	26.05.1992	ETM+ pan 06.04.2000	127	30m	5,75143 m	2
ETM+ pan	180 / 075	02.07.2000	GPS & Topo. Road Map	123	15m	6,45545 m	2
ETM+ mspec.	180 / 075	02.07.2000	GPS & Topo. Road Map	123	30m	6,45545 m	2
ETM+ pan	180 / 075	22.04.2003	ETM+ pan 02.07.2000	153	15m	4,40015 m	2
ETM+ mspec.	180 / 075	22.04.2003	ETM+ pan 02.07.2000	153	30m	4,40015 m	2
ETM+ pan	180 / 075	18.09.1999	ETM+ pan 02.07.2000	152	15m	3,96285 m	2
ETM+ mspec.	180 / 075	18.09.1999	ETM+ pan 02.07.2000	152	30m	3,96285 m	2
TM mspec.	180 / 075	15.05.1991	ETM+ pan 02.07.2000	117	30m	5,80195 m	2

Table 3: Overview of the applied geometric correction and error rates.

held GPS and multitemporal satellite data being registered to the reference of GPS-Data and Namibian topographical maps.

4.1.4 Radiometric correction - ATCOR

For applications where a common radiometric scale is assumed among the multitemporal images, atmospheric correction should generally be taken into consideration in preprocessing (HALL ET AL. 1991). For monitoring applications as the one underlying this thesis where supervised classifiers as well as change detection methods are trained for unitemporal and applied to multitemporal satellite imagery, a full elimination of atmospheric influences is required (SONG ET AL. 2001).
The objective of the so called atmospheric correction is to convert the grey level information (digital numbers or DN) into physical quantities, e.g. surface reflectance and temperature.
With the retrieval of surface reflectances, it is possible to correctly characterize surface properties from remotely sensed imagery since atmospheric effects have been eliminated or at least reduced (CHAVEZ 1989, CHAVEZ 1996). Thus it greatly improves the comparison of multitemporal scenes recorded under different atmospheric conditions as changes observed will be due to changes on the earth's surface and not due to different atmospheric conditions (WOODCOCK ET AL. 2001).

In general atmospheric correction factoring out physical modelling depends on a variety of subsidiary processes. These processes can divided into two main processing steps, which separate atmospheric scattering in constant and varying phenomena.

Effects of the Rayleigh scattering that occur on the optical pathway are therefore regarded as constant. They are quantified based on the height of the atmosphere and the depending atmospheric pressure for a remotely sensed area (JENSEN 2000).
For the ATCOR algorithm these effects are corrected by the use of standard-atmospheres stored in lookup tables previously calculated with MODTRAN-4 and SENSAT-5 radiative transfer codes (RICHTER 1999). In order to allow the algorithm to adapt to the Rayleigh scattering contained within the satellite imagery utilized within this thesis all data was corrected using the preset of "Dry Desert" atmosphere.

Opposed the relatively constant effects of Rayleigh scattering the varying impacts of Mie scattering can not be corrected using atmospheric databases. The Mie theory is a mathematical physical theory of the scattering of electromagnetic radiation by spherical particles, embracing all possible ratios of diameter to wavelength (JENSEN 2000).
Therefore the ATCOR algorithm uses an extended and modified correction algorithm, which focuses on the artificial increase in radiance for known low reflecting surfaces caused by aerosols. Based on theses inflated radiances an aerosol-model can be derived thus, accounting for the correction factor deduced for the Rayleigh scattering, allowing for a recalculation of existing image values (RICHTER 1999).

As this methodology does not allow for the calculation of the actual optical path, additional parameters like sensor-offset and sensor-gain as well as sensor-IFOV (degree), solar-azimuth (degree) and solar-zenith (degree) are considered by the model.
Based upon the modular configuration of the ATCOR program two differing methodologies can be applied for the correction of the imagery. Firstly optical density values of the

image can be entered directly, if they are available from secondary sources. Secondly these values can be derived manually or automatically from the data followed by the recalculation of existing image values. However detailed examination of the obtained correction factors using the "Spectra-Module" is recommended.
With the "Spectra-Module" one can simulate the reflectance of single pixels or areas using different atmospheric conditions. If reference areas of an image are known (e.g. green vegetation, bodies of water or bare ground) one can compare the modelled reflectance values to reference data from spectral libraries or literature thus allowing for the appropriate identification of both atmospheric- and optical density (RICHTER 1999).

In this thesis the "Spectra-Module" was additionally used to compare spectral signatures obtained from the reference imagery of 2003 for unchanged areas with those obtained from the backdated images as the comparison of these elements also known as pseudo-invariant features (PIF) allows for a more precise adjustment if necessary (DU ET AL. 2002). Reference areas comprised gallery forest alongside the ephemeral rivers, areas of bare ground covered by strong reflecting quartz

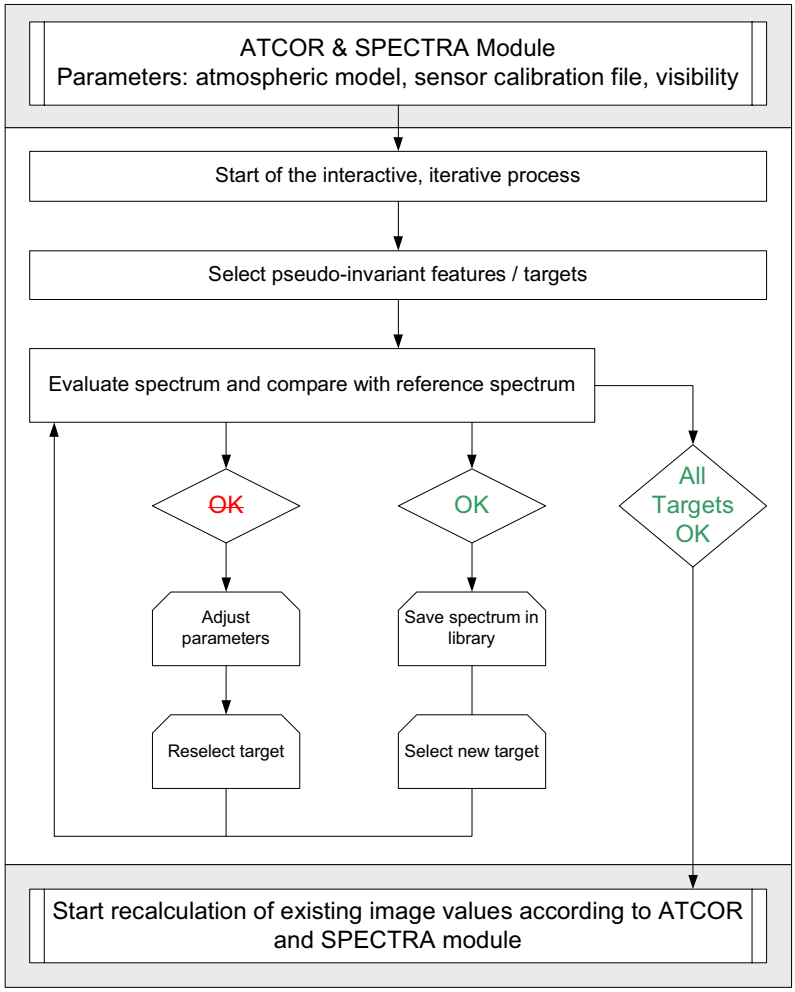

Figure 7: Schematic overview of the atmospheric correction conducted by ATCOR.

gravel plains as well as deep water areas of reservoirs located on the edge of the escarpment.

In combination with the selected standard atmosphere five types of prevailing aerosols can be chosen. This information does not depict the concentration, but describes an approximation of the mixture of aerosols prevailing in regionally different atmospheres, e.g. dust and grime in urban areas and saline crystal in proximity to an ocean. For all scenes the predefined aerosol-type describing "maritime desert" was applied conjoined by a visibility of 100 kilometers and information on acquisition data, solar-azimuth, solar-zenith and mean height above sea level. Automatic retrieval of optical density, additional low-pass-filtering was not utilized. Haze removal and cloud correction were also not applied because of clear sky conditions noted for all satellite scenes. A schematic overview of the atmospheric correction conducted by ATCOR is presented in figure 7.

4.1.5 Calculation of Artificial Channels – NDVI and MSAVI

One of the most frequently used applications of satellite data is the discrimination of vegetation features from soil features using spectral indices. Following the assumption that reflectance patterns of soil and vegetation are unique selected spectral indices are sensitive to reflectance differences (TODD ET AL. 1998).
Spectral indices featuring vegetation and combining two or more spectral bands can generally be subdivided into two categories: slope-based and distance-based vegetation indices (HUETE 1988).
The Normalized Difference Vegetation Index (NDVI) was introduced by ROUSE ET AL. (1973) and ROUSE ET AL. (1974), although the concept of a normalized difference index was first presented by KRIEGLER ET AL. (1969). Today it is one of the most commonly used vegetation indices of this category. However, none of these indices accounts for soil background variations (QI ET AL. 1994).
Based on multispectral satellite imagery, the NDVI has been used for vegetation mapping purposes by many studies on varying scales (JENSEN 2000). Some studies also analysed the NDVI regarding vegetation / rainfall response patterns while others focussed on the variations of phenology in timeseries datasets (NICHOLSON ET AL. 1990, DAVENPORT & NICHOLSON 1993, ROBERTS ET AL. 1994, DALL'OLMO & KARNIELI 2002).
To overcome the problems introduced by the NDVI HUETE (1988) proposed a soil-adjustment factor accounting for first order soil

$$NDVI = \frac{L_{NIR} - L_{RED}}{L_{NIR} + L_{RED}}$$

Formula 1: Normalized Difference Vegetation Index. Source: LILLESAND & KIEFER (2000[5])

background variation. However this Soil-Adjusted Vegetation Index (SAVI) requires prior knowledge about vegetation densities to obtain an optimal constant soil adjustment factor. While a large adjustment-factor would best describe soil-vegetation interactions at low cover values, a dense vegetation cover is best described using a small adjustment factor.
To avoid this and to decrease sensitivity to soil noise as well as minimizing the effect of soil brightness observed for the NDVI, QI ET AL. (1994) introduced a self-adjustable soil line to the SAVI (SCHMIDT & KARNIELI 2001). By increasing the vegetation signal and simul-

taneously lowering soil-induced variations the modified soil-adjusted vegetation index (MSAVI) is recognized as a more sensitive indicator of vegetation than SAVI or NDVI (QI ET AL. 1994).
Based on these findings the MSAVI as proposed by (QI ET AL. 1994) is calculated for all LANDSAT images used within this thesis.

$$MSAVI = \frac{2 * L_{NIR} + 1 - \sqrt{(2 * L_{NIR} + 1)^2 - 8 * (L_{NIR} - L_{RED})}}{2}$$

Formula 2: Modified Soil-Adjusted Vegetation Index. Source: QI ET AL. (1994)

However since the broad usage and acceptance of the standard NDVI it shall also be derived from satellite data as it may provide useful information by comparing its response to the results obtained.

NDVI and MSAVI values theoretically range from -1 to 1. In general all values above zero can be said to determine soil surfaces covered by vegetation whereas all values equal or below zero depict more or less bare ground. To reduce memory usage due to the floating point data obtained for NDVI and MSAVI all datasets were resampled to 8-bit integer values ranging from 0 to 255. However standard maximum-minimum-stretching of the data as implemented in many geoinformation systems is thought to be critical for the analysis and comparison of timeseries. Therefore both NDVI and MSAVI have not been resampled relatively but absolutely, by assigning the floating point value of -1 to the 8-bit value of 0 and 1 to 255 respectively using the following formula:

$$NDVI = \frac{NDVI - (-1)}{(1 - (-1))} * 255$$

Formula 3: 8-bit conversion of NDVI values

4.1.6 Image Stacks

Many authors have shown (compare chapter 2.6.2), that the spectral characteristics allowing for the detection and discrimination of biological soil crusts are widespread in the spectral range between 400 to 2500 nm, also mapped by the LANDSAT sensor. These features might as well be used for the derivation of site-specific crust indices, only depending on defined spectral information (KARNIELI 1997, CHEN ET AL. 2005). Although, delineation of biological soil crust communities towards surrounding areas of bare soils and sands is permitted, spectral discrimination between different crust communities is not incorporated by these approaches based on multispectral LANDSAT datasets. Studies of BORK ET AL., reported on by KARNIELI ET AL. (2001), showed that overall broad-band reflectances were often better predictors of microphytic cover, as quantitative changes in soil-based components are more likely to affect the magnitude of the spectral response rather than its shape. In addition Lichen coverage was particularly delineated from soils due to a deviation in the R to NIR region.
These findings as well as variations in the R to NIR region could also be observed for the mean spectral reflectance curves of different Central Namib Desert lichen communities obtained from broad-band LANDSAT imagery.
Therefore it was decided to allow all six LANDSAT channels of the visible, near-infrared and mid-infrared region to con-

tribute to the spectral supervised classification. Thermal-infrared channels were not taken into account. Instead both NDVI and MSAVI were appended to the final layer stack in order to enhance the detection of the variations in the R-NIR region. Thus the final image stack committed to the classification process comprises eight layers in total. An overview of the entire processing performed on the LANDSAT data is given in figure 8.

4.2 Shuttle Radar Topographic Mission (SRTM) data

The aim of the X-Band Synthetic Aperture Radar / Shuttle Radar Topography Mission (X-SAR/SRTM) was the survey of the 80 % of the land masses between 60° north and 58° south in order to generate a comprehensive and continuous terrain model derived from the recorded topographic data and radar images (PÁC ET AL. 1999).

With the use of the Synthetic Aperture Radar (SAR) instrument, which images the Earth's surface using microwave, the high resolution mapping of land masses is independent of the sun's position, weather and surface contrast. The measurement of actual terrain height and the following derivation of the surface topography was accomplished with a single-pass interferometric measurement setup for two independent sensors.

To obtain the stereo imagery necessary for the derivation of a digital terrain model, both independent sensors were split into a set of two, with one located in the bay of the Space Shuttle and the other on the cap of a 60 m aerial mast. Due to this setup all relevant data

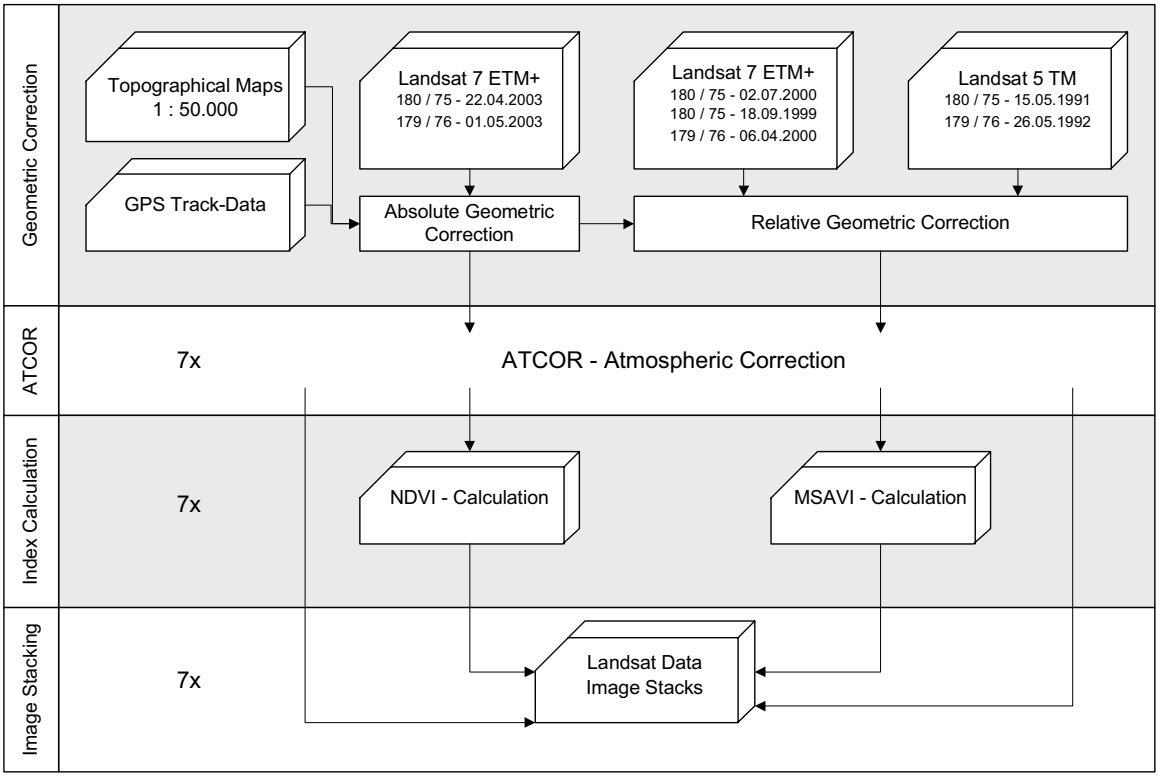

Figure 8: Preprocessing of multispectral LANDSAT datasets.

could be recorded in single-pass mode (MOLL 2003).
Both independent sensor sets recorded independent terrain data as well, resulting in two different digital elevation models. Firstly the C-Band interferometer which has been developed by the Jet Propulsion Laboratory (JPL) was used to scan the Earth's surface at 5.3 GHz for a 255 km wide swath. Secondly the X-Band (X-SAR) flight instrument developed by the German Aerospace Center (DLR) and Agenzia Speziale Italiana (ASI) scanned at 9.6 GHz for a path only 50 km in width but at almost two times the vertical precision of the C-Band (PÁC ET AL. 1999).
Due to this variation on swath width the C-Band data comprises a complete coverage of the surveyed surface area. On the contrary X-Band data was obtained for the complete coverage as well but limited to stripes defined by the swath width. Therefore the overall coverage of the X-Band data is about 50 % of the total area investigated.
With X-Band data available for the study area investigated by this thesis it was preferred to C-Band data because of the advanced spatial resolution and precision.
As all radar data recorded comprised georeferencing information, the position of the Space Shuttle and its sensors in relation to the Earth's surface was determined using Attitude and Orbit Determination Avionics (AODA). Using a GPS-sensor onboard the Shuttle in conjunction with several ground receivers, the Shuttle position could be determined with an accuracy of one meter. The relative position of the sensor sets is then obtained by the determination of the position of the mast cap for an accuracy of five millimetres (PÁC ET AL. 1999).

4.2.1 Mission problems

The terrain model derived from the SRTM X-Band data was analysed by the DLR with the means of Ocean Data Takes (ODT). ODT includes accurate knowledge of the sea-surface based on a geoid elevation model compiled by Germany's National Research Centre for Geoscience (GFZ). Observed deviations between this reference and the newly compiled terrain model must therefore be treated as errors. While absolute accuracy of ± 16 m for more than 90 % of the data was met, relative accuracy of ± 6 m was not achieved for the postulated 90 % (PÁC ET AL. 1999).

This lack of accuracy resulted from a constant rolling motion of the mast and its outer sensor with an amplitude of 4 cm, caused by constant flight path corrections of the Shuttle due to the loss of one of the Shuttle's steering jets. In conjunction with the limited accuracy of the mast cap of 0.5 mm measured by the AODA, errors of ± 2,5 m for the terrain model were observed (PÁC ET AL. 1999).
For Africa and Europe this error was lowered in March 2002 to ± 1.5 m using a new Position and Attitude Data Record (PADR 600) (PÁC ET AL. 1999). These reduced error rates are also included in the data utilized for this thesis.

4.2.2 Validation

SRTM digital elevation data represents the currently best available terrain model for the study area of this thesis regardless of all sources of error discussed in the previous chapter.
Due to the non-existence of absolute geodetic reference data and only scattered GPS-

handheld und barometric measurements of the elevation during the field campaigns as well as only limited information provided by the analogue topographic map sources, accurate validation of the digital terrain model can not be conducted for the study area covering a coastline of almost 300 km.
However due to the almost ideal mean elevation of the study area close to sea level and the limited relief features a horizontal and vertical above average was presumed. This assumption has therefore been exemplarily tested for the geometric location and vertical specification of distinct relief features. All of these control samples showed a good correlation between the terrain model and the investigated features. Nevertheless no absolute measurements will be utilized.

4.2.3 Processing of the digital elevation model data

By visualising the surface of the modelled terrain data, a high frequency error pattern was identified causing model uncertainties for many areas. Due to this high frequency error pattern observed for the original dataset it was decided to try to improve the overall quality using spatially adaptive image filtering techniques.
Standard low-pass filtering offers only limited control on the level of detail that is smoothed out with the broadening of scale arising from the window size used. Moreover many parameters derived from the DEM might inevitably vary with the broadening scale.
To analyse these spatial and scale based variations various low-pass filtered images obtained by varying window sizes would have to be compared concerning their effect on different topographic parameters and to identify the optimal window size.
To avoid such extensive calculations, analysis and filtering of terrain data was realized using a spatially adaptive multi-scale approach offered by the LandSerf application framework version 1.8.0 (Wood 2005).
Basis for most of the analytical functions in LandSerf is the process of quadratic approximation. This is realized using a local moving window of a given size for the DEM cells and fitting the most appropriate continuous quadratic expression through them. This quadratic function is then used to calculate parameters such as aspect, slope and curvature.
In order to gain information on the optimal window size for reducing the high frequency error pattern, while at the same time leaving as much of the original landscape features unchanged, the calculation of "multi-scale parameter variation" is performed on the data followed by a "multi-scale query" (Wood 1996).
The "multi-scale query" allows the graphical analysis of the scale dependency of different topographic parameters for a user defined range of window sizes for an arbitrary point or area. If for example the aspect remains in a relatively constant direction for the range of window sizes at a defined location, aspect is assumed to be scale invariant. If however the aspect tends to vary, the slope must be dependent on the scale at which it is measured (Wood 1996).
Thus critical scales and therefore critical window sizes where parameters do not solely vary over space can be identified.
As a result of the analysis of the scale dependency of the aspect a window size of thirteen was chosen in conjunction with a distance decay component of zero which induces an equal weighting of all values obtained by the kernel window. Following the filter operation on the digital elevation model, it once more exemplarily tested for the geometric location and vertical specification

using distinct relief features (compare chapter 4.2.2).

4.2.4 Topographic parameters

For the further analysis of coherences between the relief and variations on lichen distribution within the study area a set of topographic parameters has been calculated following the extensive approaches on relief classification and parameterization presented by DALY (1984), BROWN (1994), MEIJERINK ET AL. (1994), WOOD (1996), HÖRSCH (2001), MENGELKAMP ET AL. (2003), and WOOD (2005).

4.2.4.1 Landform classification – geomorphological form elements

Since SCHIEFERSTEIN (1989) and LORIS & SCHIEFERSTEIN (1992) also reported on the variations in lichen distribution concerning differences in local and landscape topography a classification of landforms was calculated based on the approach by DIKAU (1988) also conducted by HÖRSCH (2001).
According to DIKAU (1988) form elements can be defined as "relief units with uniform vertical and horizontal curvature-type and feature". Following the framework of classifying morphometric parametrisation provided by EVANS (1980), initial calculations of plan curvature ("aspect change / plan convexity") and profile curvature ("gradient change / profile convexity") were calculated using LandSerf software (WOOD 2005).
Threshold values of curvature-type and feature defined by BRÄNDLI (1997 in HÖRSCH 2001) depict nine different types of geomorphological objects for the study area (compare figure 9).

4.2.4.2 Snow-potential-index

Although initially developed to estimate the potential snow accumulation in an alpine environment based on main-wind-direction, exposition, curvature and height, it might also depict potential areas where accumulation or abrasion during windstorm events occurs. Therefore it was calculated for the study area utilizing the approach presented in BROWN (1994). Further information regarding the snow potential index (SPI) can also be found in BROWN (1994).
Following various observations during field campaigns concerning deflation and corrasion processes affecting lichen distribution patterns in the study area and the synoptic

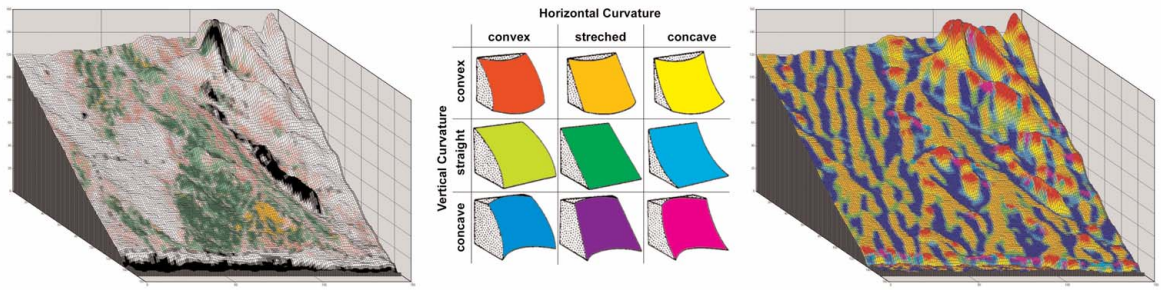

Figure 9: Deduction of 9 geomorphological form elements and their correspondence to terrain and lichen distribution patterns.

analysis of the relief form elements the snow potential index by DALY (1984) was calculated for the study area.
HÖRSCH (2001) found this index to be on one side extremely biased by the main wind direction while it was also totally neglecting the influence of solar radiation and local wind systems on the other side.
While the influences of solar radiation can surely be neglected for this thesis, the shortcomings concerning the consideration of only one prevailing wind direction were corrected by calculating SPI for 12 major winddirections. The derived information was then conjoined according to the weighted occurrence of windstorm-events for the various expositions, derived from climatic datasets for the years 2001 to 2003.
While for some areas synoptic analysis of the obtained SPI-values showed good correspondence to the lichen distribution patterns obtained by the supervised classification approach, it showed extremely unrealistic results for others. This might be due to the fact, that climatic datasets representing windstorm occurrence and direction were only available for distinct areas within the study site, thus neglecting local differences within the wind system. Moreover the spatial resolution of the digital elevation model derived from SRTM x-band data might also not fully depict relevant features of curvature and exposition.
Therefore the SPI was not used for any further analysis within this thesis.

4.2.4.3 Hydrological and fluvial features

The extraction of hydrological and fluvial features from surface models and digital elevation data is probably one of the most widely examined ZEVENBERGEN & THORNE (1987), MOORE ET AL. (1991), JENSEN (1992), and MEIJERINK ET AL. (1994). Since the routing of waters over the surface area, resulting from rainstorm events represents a fundamental geomorphological and ecological process that is presumably tied to lichen distribution and disturbance patterns as well, information about the drainage-network shall be derived from the calculation of flow-direction and flow-accumulation.
Typical problems are artificial depressions, caused by the grid spacing of the digital elevation model (DEM) and errors in the DEM resulting from low precision in flat areas. To overcome these problems filtering of the DEM data can be an option as well as the searching for flow directions across small depressions.
In the following two software-tools developed by the German Aerospace Center (DLR), German Remote Sensing Data Center (DFD) within the ODRAFLOOD-project framework shall be utilized for the compilation of the above parameters (MENGELKAMP ET AL. 2003).
Firstly the flow-direction matrix, depicting water flow direction for each pixel based on the slope of the neighbouring pixels, is calculated to enhance the drainage system precision for the vast undulating plains of the Central Namib Desert.
In case two neighbouring pixel show the same values, the slope of their neighbouring values is decisive whereas null-values depict no discharge at all.
Secondly the flow accumulation matrix is calculated based on a simulation of the "water flow" for each pixel with the means of the previously calculated flow direction matrix and DEM-values assorted by height. Therefore an accumulation map is created with the number of upstream raster elements draining through their neighbouring raster elements. Thus the structure of the drainage network as

well as its hierarchy based on potential "run-off" is clearly demarcated (MENGELKAMP ET AL. 2003).
Although the derived drainage network is still highly correlated to the quality of the DEM s synoptic comparison of the obtained drainage network with topographic map information showed good correspondence.

4.3 Reference data

Most studies using remote sensing are accomplished using some source of reference data, which involves collecting measurements or observations about objects and areas that are being remotely sensed (JENSEN 2000).

4.3.1 Training sites

The approach considered the most accurate for the compilation of a classification and its accuracy assessment is field visit of selected test areas of which the accurate geometric location and its characteristic is known and therefore the classifier can be trained on LILLESAND & KIEFER (2000[5]). This acquisition of knowledge about a study area from field work, also known as ground truthing should be collected at the same time as the remotely sensed data, to ensure good correspondence.
Therefore all lichen community training sites also known as training fields, with its most abundant species shown in annex b, were collected in the Central Namib Desert during the field campaigns of 25.03. – 07.04. 2002 and 01.05. – 25.05. 2003. Each sample was chosen for „vegetational" homogeneity and size.
While for the 2002 field campaign no corresponding LANDSAT image could be acquired two images could be successfully retrieved for the ground truthing obtained in 2003 (see also table XXX, chapter 4.1.1).
The names of the species shown in annex b were verified by two independent experts - Dr. Luciana Zedda and Dr. Kurt Loris. In-situ photos of sampling sites were complemented with laboratory macro photography of lichen samples from the collection of the Museum Botanicum Berolinense, University of Bayreuth and from (ZEDDA & RAMBOLD 2000-2005).
In total 874 training fields and corresponding 900 photos were collected and listed into a database.

4.3.2 ASD-Measurements

The in-situ measurements were taken using a FieldSpec FR spetroradiometer, which operates in the 350-2500nm spectral range and is characterized by a spectal resolution of 1 nm throughout its entire range (ANALYTICAL SPECTRAL DEVICES 2005). Measurements were recorded in reflectance mode as an average of thirty scans in order to minimize instrument noise while each measurement was repeated at least five times and referenced to a white Spectralon reference panel (99 % reflectance) beforehand. For the detailed measurements of all lichens, plants and rocks the field of view (FOV) of the spectroradiometer must be sufficiently small to ensure only a single object is being measured at a given time while for the acquisition of the mixed spectral properties of an entire lichen community the FOV must be large enough to obtain all features present. Therefore all detailed measurements were recorded by bringing the bare fiber optic (FOV 25°) into a position of 1 cm of the object sampled which ensured as well the absence of shadow in the FOV resulting form the tip of the fibre optic. Moreover all objects were sampled using various orientations of the instrument relative to the target to limit differences in illumination.

In opposition the measurement of the lichen communities was accomplished from a distance of 1m perpendicular to the surface using again the bare fiber optic with its FOV of 25°. Additionally measurements of all targets were taken within minutes of the Spectralon reference panel measurement and between 10:00 and 14:00 h local time to minimize the effect of instrument drift.
Since all of the data was measured in situ, the calculated spectra showed strong interferences by atmospheric water in the vicinity of 1400 and 1900 nm while all measurements at wavelength greater > 2400 nm had a low signal-to-noise ratio (S/N). Therefore reflectance bands between 1339 – 1449 nm, 1789 – 1989 nm and beyond 2399 nm were eliminated from the valid band list to avoid errors resulting from possible filtering or interpolation. Mean reflectance for each sample was then calculated as the average of all valid replicates for each sample including up to 240 measurements.
At this point it must also be mentioned that these in-situ measurements were carried out in the course of the Biota-S01 field campaign of March 2005 as a spin-off. Originally addressed to the estimation of biomass along the Biota-South transect including spectroradiometer measurements, four days of this campaign were spend in Central Namib Desert as weather permitted the use of the spectroradiometer in the central parts of the country. If the spectroradiometer could have been utilized for this study from the beginning, analysis and results would have certainly been more extensive.

4.3.3. Biomass data

Destructive biomass samplings of the most prevailing lichen communities were obtained by Dr. Dirk Wessels, S.A., and Dr. Kurt Loris and kindly made available to this thesis. While all plots surveyed by Wessels included coherent standard areas of 1 m 2, Loris sampled the biomass of a distinct lichen community using four independent plots each 0.25 m2 in size (Compare photo 14). Consecutively all destructed plots shall serve for observations of recovery rates among the differing lichen communities in the future.

However Loris and Wessels also used different procedures to obtain the lichen biomass values. While Wessels measured biomass as

Photo 14: Left: Looking North-East – Foliose-crustose lichen community of the Northern Naukluft Plateau previous to sampling in 2003.Right: Looking South-West - Four biomass sampling plots of the foliose-crustose lichen community of the Northern Namib Naukluft Plateau shown to the left. Each plot 0.25 m^2 in size as obtained by Dr. Kurt Loris in 2004.

Oven Dry Weight (OWD) after lichen material was parted from abiotic contents included in the samples, dry oxidation was utilized by Loris in addition. Thereby the Oven Dry Weight (ODW) is known as the weight of biomass mathematically corrected for the amount of moisture present in the sample at the time of weighing whereas dry oxidation at 600 °C can be performed subsequently to derive the inorganic residue left in samples (SLUITER ET AL. 2004). With the means of a Bunsen burner all samples are ashed at 600 °C for four hours. The ash content is a measure of the mineral content and other inorganic matter in biomass samples to determine the total composition of biomass samples and its net weight. Thus measured differences between dry weight and carbon remains were recorded as net biomass per square meter. An overview of the biomass measures obtained by both authors is presented in table 4.

Based on theses differences all samples obtained by Loris and Wessels were used separately for the derivation of biomass estimates with one approximation based on dry weight and the other based on net biomass per square meter.
In order to adjust for slight divergences between samples from Wessels featuring the same lichen community class the arithmetic mean was calculated from the biomass measures for the calculation of the overall biomass of the study area. However for the calculation of the individual biomass contained in distinct areas classified as lichen fields, arithmetic mean values were only used for those communities not specifically sampled for the designated lichen field to adjust for regional disparities. Observed mean divergence between dry weight and net biomass was about 51 %. As only fruticose, fruticose-foliose and foliose-crustose communities were sampled by Loris, measures of missing communities were estimated based on this relationship. Due to these shortcomings all of these measures can only be considered a first rough estimate and shall therefore only be used for discussion.

4.3.4 Geometric reference data

For the geometric correction of the satellite imagery (chapter 4.1.3), 35 analogue topographic maps of Namibia, in a scale of 1 : 25000 were digitized. In addition to the digitized road-network GPS track and point data, which were broadly collected during the field campaigns with eTrex-Summit and Vista handheld receivers, were used to compile an absolute reference layer.
Supplementary to this GIS-layer differing layers comprising dry-pans, river-courses, urban areas, coastline and distinctive rock-forma-

Lichen Community	Mean Dry Weight g/sqm	Mean Net Biomass g/sqm
Fruticose	359,72	192,18
Fruticose / Foliose	188,53	64,90
Foliose	142,62	72,55
Foliose / Crustose	304,22	197,00
Crustose	273,83	139,30
Crustose Sparse	54,77	27,86

Table 4: Mean dry weight and net biomass measures of lichen communities based on the sampling performed by Dr. Dirk Wessels and Dr. Kurt Loris.

tions, were also digitized from the topographic map source of Namibia.

4.3.5 Climatic data

Climatic datasets were kindly made available by various institutions and processed to aid the identification and analysis of the spatiotemporal changes caused by differing natural and anthropogenic disturbances. Sources however differed widely regarding their spatial and temporal coverage and the data sampled making it sometimes difficult to extract valid information in relation to the study area.
Data derived from automatic weather stations were only available from three rather unevenly spread locations within the study area. A list of all climatic data sets and operating institutions is presented in table 5.
While processed climatic data recorded by automatic weather station for the "Wlotzkasbaken" observatory site was kindly made available by the BIOTA Southern Africa Head Office, the Desert Research Foundation Namibia (DRFN) contributed data sets recorded at "Kleinberg" and "Double Three". Both stations are part of the Environmental Observatories Network of Namibia (EONN) program of the DRFN at the Environmental Observatory of Gobabeb. EONN is also a central component of the environmental training program at Gobabeb.
Supplementary personal recordings of the rainy season of 1999/2000 and data published in (HACHFELD 2000) were also kindly made available by the author Dr. Berit Hachfeld from the Biocentre Klein Flottbek & Botanical Garden, Hamburg, Germany.
While all automatic weather stations encountered more or less prolonged malfunctions at differing times, a detailed list of the actually recorded periods is given in annex a figure A1 and A2.
In general it can be stated that although coherent data sets of the DRFN-EONN program are available for the southernmost part of the study area, the overall spatial and temporal coverage remains poor. With the exception of the Wlotzkasbaken lichen field where an automatic weather station was recently installed by the BIOTA Southern Africa Project continuous climatic information was unavailable to this thesis for the rest of the study area.

Name	Lichen Field	Type	Nominal Range	Recording	Operator
Kleinberg	No. 1	Autom. Station	1994 - 2002	Hourly Mean	Desert Research Foundation Namibia (DRFN), Namibia
Double Three	No. 1	Autom. Station	1999 - 2002	Hourly Mean	Desert Research Foundation Namibia (DRFN), Namibia
Transect 1 - 30 km	No. 1	Rain Gauge	1999 - 2000	Single Values	Biocentre Klein Flottbek & Botanical Garden, Hamburg, Germany
Transect 1 - 40 km	No. 1	Rain Gauge	1999 - 2000	Single Values	Biocentre Klein Flottbek & Botanical Garden, Hamburg, Germany
Transect 1 - 50 km	No. 1	Rain Gauge	1999 - 2000	Single Values	Biocentre Klein Flottbek & Botanical Garden, Hamburg, Germany
Transect 1 - 60 km	No. 1	Rain Gauge	1999 - 2000	Single Values	Biocentre Klein Flottbek & Botanical Garden, Hamburg, Germany
Transect 2 - 10 km	No. 2 / No. 3	Rain Gauge	1999 - 2000	Single Values	Biocentre Klein Flottbek & Botanical Garden, Hamburg, Germany
Transect 2 - 20 km	No. 2 / No. 3	Rain Gauge	1999 - 2000	Single Values	Biocentre Klein Flottbek & Botanical Garden, Hamburg, Germany
Transect 2 - 30 km	No. 2 / No. 3	Rain Gauge	1999 - 2000	Single Values	Biocentre Klein Flottbek & Botanical Garden, Hamburg, Germany
Transect 2 - 40 km	No. 2 / No. 3	Rain Gauge	1999 - 2000	Single Values	Biocentre Klein Flottbek & Botanical Garden, Hamburg, Germany
Transect 2 - 50 km	No. 2 / No. 3	Rain Gauge	1999 - 2000	Single Values	Biocentre Klein Flottbek & Botanical Garden, Hamburg, Germany
Swakopmund	No. 3	Rain Gauge	1999 - 2000	Single Values	Biocentre Klein Flottbek & Botanical Garden, Hamburg, Germany
Wlotzkasbaken	No. 5	Autom. Station	2001 - 2003	Hourly Mean	BIOTA Southern Africa Head Office, Hamburg, Germany
Transect 3 - 10 km	No. 6	Rain Gauge	1999 - 2000	Single Values	Biocentre Klein Flottbek & Botanical Garden, Hamburg, Germany
Transect 3 - 20 km	No. 6	Rain Gauge	1999 - 2000	Single Values	Biocentre Klein Flottbek & Botanical Garden, Hamburg, Germany
Transect 3 - 30 km	No. 6	Rain Gauge	1999 - 2000	Single Values	Biocentre Klein Flottbek & Botanical Garden, Hamburg, Germany
Transect 3 - 40 km	No. 7	Rain Gauge	1999 - 2000	Single Values	Biocentre Klein Flottbek & Botanical Garden, Hamburg, Germany
Transect 3 - 50 km	No. 7	Rain Gauge	1999 - 2000	Single Values	Biocentre Klein Flottbek & Botanical Garden, Hamburg, Germany
Transect 3 - 60 km	No. 7	Rain Gauge	1999 - 2000	Single Values	Biocentre Klein Flottbek & Botanical Garden, Hamburg, Germany

Table 5: List of climatic data sets contributing to this thesis.

5 Methods

In the following image processing and statistical methods, applied and developed for assessing the distribution of lichen communities in the Central Namib Desert and their spatiotemporal changes, are explained. At first the applied hierarchical classification scheme is explained as well as the fuzzy enhanced supervised classification approach for the year 2003. Secondly, the newly developed combined retrospective supervised classification and change detection approach, utilizing selective PCA (sPCA) information obtained for training-sites in conjunction with fuzzy enhanced supervised classification techniques is presented. Lastly results comprising the actual distribution of lichen communities for the year 2003 as well as the reconstructed distributions of lichen communities for the years 2000, 1999, 1992 and 1991 are tested for their accuracy.

The derivation of thematic maps from satellite imagery has always been the main objective of studies focussing on the analysis of spatiotemporal changes of the environment. The process of grouping the contents of an image into classes depicting the same characteristics, for example landcover, is known as classification. The automatic classification of satellite imagery in general is based on the hypothesis that objects of the same class show similar spectral reflectance's (JENSEN 2000; LILLESAND & KIEFER 20005).
The information which can be obtained from such a classification product is directly associated with the research objective. The objective depicts the thematic focus of the classification product. In addition the classification is also dependent on the technical prerequisites defined by the sensor system. Conjoined both of these influencing factors set the accuracy of the thematic information depicted by the classification product. Thus, no classification product can be more accurate than the thematic information addressed by the objective and the technical potentials of the sensor system.
Therefore a classification scheme is primarily developed to allow the controlled extraction of thematic information from the satellite imagery based on the objectives of this thesis. Secondly a classification technique is chosen accordingly to obtain the best accuracy and differentiation for the thematic information addressed.
As this methodology focuses on the derivation of distinct thematic information for a single unitemporal state it must be altered if temporal changes of this distinct aspect want to be observed. Along with the thematic and geometric accuracy, the consistency of the utilized classification techniques is of major importance as it allows comparability of the obtained results.
For the detection of quantitative changes of the environment various techniques can be applied including unsupervised cluster-analysis (COHEN ET AL. 1998) and selective principal component analysis (sPCA) (WEIERS ET AL. 2003).
Although these techniques are useful for change detection in general, the artificial classes depicted by these techniques include no information of the underlying thematic changes. As a result in contrast to the real changes in land-cover only the changes detected for these artificial structures would be analysed. Thus all satellite images of a given time-series have to be classified individually to allow for the comparability of the derived thematic maps.

For many areas worldwide where thematic maps for various aspects of land-cover have been continuously updated for many decades

training of these individual classifiers is easily accomplished. For remote areas as the Central Namib Desert, featured in this thesis, this information is basically non-existent, especially concerning the distribution of lichen communities. Therefore a technique allowing the validation of existing thematic reference information for the individual classification of a given time-series has to be developed. With thematic reference data being stored as training-sites the spatiotemporal changes of the spectral properties of these sites need to be analysed to assess their validity.

5.1 Hierarchic classification scheme

Most classifications are performed with a set of target classes in mind. Thus for the derivation of thematic maps from satellite imagery a coherent framework is given by a classification scheme. With the means of the classification scheme, thematic classes are defined and observed by a research objective in a coherent spatiotemporal and thematic way, while also providing a consistent structure (PERDIGAO & ANNONI 1997).

Thus for the study presented a hierarchical classification system was applied. On one hand this was necessary to provide a coarse level classification (hierarchy level 1) which allowed the application to the whole study area of the Central Namib Desert, thus also allowing regional comparison of lichen distribution patterns. On the other hand, the hierarchical classification also potentially allows the assessment on more detailed levels (hierarchy level 2) in order to adjust classification to local conditions.

Moreover the hierarchical system provides an optimal basis for subsequent studies by dividing already existing classes on further hierarchies into even more detailed ones, which can for example be accomplished by expert knowledge.

Although the abilities of discriminating different biological soil crust cover utilizing LANDSAT data have been tested by AGER & MILTON (1987), KARNIELI & TSOAR (1995), KARNIELI (1997), REES ET AL. (2004), and CHEN ET AL. (2005) no classification scheme was given by the authors.

However, land-cover classifications derived from remotely sensed datasets rely on such classification systems, particularly for broad-scale monitoring programs where transferability is an issue.

Therefore this thesis uses a hierarchical classification scheme based on the conceptual framework of morphological groups suggested by ELDRIDGE & ROSENTRETER (1999). Morphological groups are biologically and ecologically efficient and convey a better image of the organismal form and its potential impact to non-specialists. True, in different regions and continents these relationships eliminate the need for complex, often confusing changes in nomenclature (ROSENTRETER ET AL. 2001). Examples of other hierarchical classification systems discriminating landcover classes can also be found within the publications of PERDIGAO & ANNONI (1997) and EUNIS (2005).

On the first hierarchical level seven classes were identified following the framework of morphological groups. On the second level, these seven classes were subclassified into seventeen more detailed classes, which were child classes of the classes above containing semantic descriptions allowing adjustment to local conditions. Both the first and the second hierarchical classes could also be observed in the reference data collected during field works (compare table 6)

Level 1	Level 2
Fruticose Lichen Zone	The Coastal Teloschistes capensis community of the fine quartz gravel plains
	The Inland Teloschistes capensis community of the undulating course quartz gravel plains
Fruticose / Foliose Lichen Zone	The Coastal Teloschistes capensis, Xanthoparmelia walteri community of the fine quartz gravel plains
	The Inland Teloschistes capensis, Xanthoparmelia walteri community of the undulating coarse quartz gravel plains
	The mountainous Xanthomaculina hottentotta community
Foliose Lichen Zone	The Xanthoparmelia walteri community of the fine quartz gravel plains
	The mountainous Saxicolous Xanthoparmelia walteri Lichen community
Foliose / Crustose Lichen Zone	The Xanthoparmelia walteri, Caloplaca, Neofuscelia, Lecidella community of the fine quartz gravel plains
	The mountainous Saxicolous Xanthoparmelia walteri, Caloplca elegantissima Lichen community
	The Xanthoparmelia walteri, Xanthomaculina convoluta, Lecidella crystallina community of the coarse gravel hummocks of the gypsum plains
Crustose Lichen Zone	The Caloplaca, Neosfuscelia, Lecidella community of the fine quartz gravel plains
	Lecidella crystallina, Caloplaca volkii, Xanthomaculina convoluta, community of the gypsum plains
Crustose Sparse Lichen Zone	The sparse Caloplaca, Neosfuscelia, Lecidella community of the fine quartz gravel plains
	The sparse Lecidella crystallina, Caloplaca volkii, Calplaca elegantissima community of the gypsum plains
No Lichen	Non Lichen covered areas of the fine quartz gravel / gypsum plains
	Non Lichen covered areas of the rocky ridges / debris and coarse gravel plains
	Non Lichen covered areas of the rocky and mountainous areas

Table 6: First and second level of the hierarchical classification scheme based on the concept of morphological groups.

However all supervised classifications presented within this thesis shall be restricted to the first hierarchical classification level. This is appropriate to meet on one hand the technical limitations implied by the spectral as well as optical resolutions of the LANDSAT satellite series which is opposed to the increased spatial resolution required for the precise delineation of subclasses. On the other hand, confining the classification to a limited number of sturdy classes enhances its stability to potential sensor noise included in the satellite imagery. At last the reduced class set also supports the aim of this thesis to analyse the spatiotemporal changes of the distribution of lichen fields while at the same time reducing the quantity of reference data collected for supervised classification and the appropriate accuracy assessment.
As future studies will surely include advanced optical satellite sensors as well as an increased database of reference data compiled from the data collected during future field campaigns both classes of the first and the second hierarchy level shall be described in the following.

5.1.1 Fruticose Lichen Zone

5.1.1.1 The Coastal Teloschistes capensis (L.f.) Müll. Arg. community of the fine quartz gravel plains

High cover values of *Teloschistes capensis* (L.f.) Müll. Arg. are a distinct feature of this community. Although cover values decline towards the coast and interior, cover values exceeding 70 % have been recorded in this community. Forming large tufts, cushions, and mats, multibranched fruticose lichen species may reach heights of more than 100 mm (SCHIEFERSTEIN 1989; LORIS & SCHIEFERSTEIN 1992).
Limited to distinct areas along the coast, and varying in size, well developed examples occur in the lichen fields number four, five, six and ten which will be thoroughly discussed in the next chapter.

In particular, the coastal *Teloschistes capensis* (L.f.) Müll. Arg. community north-east of Wlotzkasbaken and located in lichen field number five, has been extensively examined by SCHIEFERSTEIN (1989) and LORIS & SCHIEFERSTEIN (1992). They described different growth forms of *Teloschistes capensis* (L.f.) Müll. Arg. and measured species diversity in the community to be predictable with an average of 12 species per square meter.

In general, this community can mostly be found on fine coastal gravel flats comprising stabilized soils. In softer as well as more unstable patches sand may be found interspersed, where *Teloschistes capensis* (L.f.) Müll. Arg. occurs grouped to large mats. Although these patches show low lichen cover, quartz pebbles are colonized by saxicolous lichen species.

5.1.1.2 The Inland *Teloschistes capensis* (L.f.) Müll. Arg. community of the undulating coarse quartz gravel plains

This extremely species rich lichen community is restricted to the undulating coarse quartz gravel plains in the hinterland of the northern region of the study area. The community is particularly well developed in the area of lichen field number nine. Due to high amounts of fog precipitation, this community represents a mixed terricolous/saxicolous lichen community in which fruticose species occur abundantly.

Fruticose species such as *Teloschistes capensis* (L.f.) Müll. Arg., and unknown species belonging to the genera *Alectoria, Ramalina*

and *Santessonia* are characteristic for this lichen community.

Additionally foliose *Xanthoparmelia walteri* Knox occurs frequently alongside scattered thalli of *Xanthomaculina convoluta* and *Xanthomaculina hottentotta* as well as abundant genera of *Caloplaca, Lecidella, Buellia, Acarospora, Neofuscelia* and *Lecidea.*

5.1.2 Fruticose / Foliose Lichen Zone

5.1.2.1 The Coastal *Teloschistes capensis* (L.f.) Müll. Arg., *Xanthoparmelia walteri* Knox community of the fine quartz gravel plains

The *Teloschistes capensis* (L.f.) Müll. Arg., *Xanthoparmelia walteri* Knox, *Neofuscelia namaensis* (J. Steiner & Zahlbr.) Essl., quartz desert community can be located on bright quartz gravel plains. These territories are dissected by numerous sandy washes and therefore more undulating than the gravel plains on which the previous community occurs.

The presence of thalli of *Teloschistes capensis* (L.f.) Müll. Arg. and *Neofuscelia namaensis* (J. Steiner & Zahlbr.) Essl. distinguishes this community from other lichen communities in the Central Namib Desert. Under dry conditions, the presence of large numbers of *Xanthoparmelia walteri* Knox and *Neofuscelia namaensis* (J. Steiner & Zahlbr.) Essl. results in a black colour clearly distinguishable from the bright quartz gravel plains. Nevertheless fruticose and foliose lichen species dominate in this community. Supplementary, a variety of saxicolous species can also be found on quartz pebbles. Thalli of terricolous *Caloplaca volkii* Wirth & Vezda and *Lecidella crystallina* Wirth & Vezda also occur scattered in the community, but dominate the crustose share on gypsum rich soils.

5.1.2.2 The Inland Teloschistes capensis (L.f.) Müll. Arg., Xanthoparmelia walteri Knox community of the undulating coarse quartz gravel plains

The composition of this community resembles that of the inland *Teloschistes capensis* (L.f.) Müll. Arg. community of the undulating coarse quartz gravel plains described in chapter 5.1.1.2, but differs regarding the decreased abundance of the fruticose *Teloschistes capensis* (L.f.) Müll. Arg. species in favour of foliose species such as *Xanthoparmelia walteri* Knox and *Xanthomaculina hottentotta.*

5.1.2.3 The mountainous *Xanthomaculina hottentotta* community

Examples of this mountainous community occur on elevated yet well eroded outcrops or dolerite ridges of the Namib. Despite the occurrence of accompanying fruticose species *Teloschistes capensis* (L.f.) Müll. Arg., *Ramalina sp.*, and *Santessonia sp.* this mountainous community is distinguished by large quantities of individuals of the foliose lichen *Xanthomaculina hottentotta* (WESSELS 1989).

In some localities, this species forms almost pure stands, whereas most examples of this community occur on rocky ridges and mountains conjoined with *Xanthoparmelia walteri* Knox and *Neofuscelia namaensis* (J. Steiner & Zahlbr.) Essl..

During "dry" state, when lobes of *Xanthomaculina hottentotta* are curled inwards, thus exposing their black underside, the community also takes on a black colour (compare chapter 5.1.2.1). Several crustose lichen species may also occur in variations of this community, depending on the community.

5.1.3 Foliose Lichen Zone

5.1.3.1 The *Xanthoparmelia walteri* Knox community of the fine quartz gravel plains

Ample examples of this lichen community occur east of Hentiesbay in the lichen field of Jakkalsputz (No. 6) on the vast quartz gravel plains of the Omaruru. This type of lichen community is characterised by almost pure stands of the foliose lichen *Xanthoparmelia walteri* Knox combined with terricolous species *Caloplaca volkii* Wirth & Vezda and *Lecidella crystallina* Wirth & Vezda. As these sand binding species are also responsible for the stabilization of the quartz pebble surface layer their abundance triggers the saxicolous growth of *Xanthoparmelia walteri* Knox as well. Where course gravel occurs interspersed scattered species of *Caloplaca namibensis* Kärnefelt, *C. elegantissima* (Nyl.) Zahlbr. and *Neofuscelia sp.* can also be found.

5.1.3.2 The mountainous saxicolous *Xanthoparmelia walteri* Knox lichen community

Dominated by the foliose species of *Xanthoparmelia walteri* and accompanied by scattered *Xanthomaculina hottentotta,* as well as *Neofuscelia, Buellia,* and *Paraparmelia* species this community is most often found on the almost 100 % closed layer of fine to medium dark gravel material covering the substrates in the northern part of the study area (lichen field No. 11). This surface cover of dark gravel material contrasts with the otherwise quartz gravel covered plains or gypsum substrates known for the Central Namib Desert. As the dark gravel material is only loosely embedded into an otherwise sandy substrate the saxicolous growth form prevails in this community. Sand-binding species of *Caloplaca volkii* Wirth & Vezda and *Lecidella crystallina* Wirth & Vezda occur only interspersed where gravel cover is disrupted.

5.1.4 Foliose / Crustose Lichen Zone

5.1.4.1 The *Xanthoparmelia walteri* Knox, *Caloplaca, Neofuscelia, Lecidella* community of the fine quartz gravel plains

Almost resembling the species composition of the *Xanthoparmelia walteri* Knox community of the fine quartz gravel plains this community can be regarded as a transition class between communities either dominated by foliose or crustose species. Due to the decreased abundance of the sand binding terricolous species *Caloplaca volkii* Wirth & Vezda and *Lecidella crystallina* Wirth & Vezda, occurrence of *Xanthoparmelia walteri* Knox also decreases. In contrast saxicolous growth of *Caloplaca namibensis* Kärnefelt, *C. elegantissima* (Nyl.) Zahlbr. and *Neofuscelia sp.* increases as theses species show better adaptation to the increased corrasion in these localities.

5.1.4.2 The mountainous saxicolous *Xanthoparmelia walteri* Knox, *Caloplaca elegantissima* (Nyl.) Zahlbr. Lichen community

This community is characterized by an abundant saxicolous growth of foliose *Xanthoparmelia walteri* Knox and crustose *Caloplaca elegantissima* (Nyl.) Zahlbr. species almost fully overgrowing large dark rock debris. Its distribution within the study area is mainly limited to the well eroded outcrops or dolerite ridges of the Namib. In addition it also covers large areas of the coastal rock debris areas near the Huabmond. Less abundant crustose species occurring within this community are *Caloplaca namibensis* Kärnefelt, *Neofuscelia sp., Buellia sp.* and *Paraparmelia.*

5.1.4.3 The *Xanthoparmelia walteri* Knox, *Xanthomaculina convoluta, Lecidella crystallina* Wirth & Vezda community of the coarse gravel hummocks of the gypsum plains

Terricolous species of *Caloplaca volkii* Wirth & Vezda, *Lecidella crystallina* Wirth & Vezda and foliose *Xanthomaculina convoluta* covering nearly 100 % of the soil surface are the foundation of this community which surpasses the crustose community of the gypsum plains by its abundant growth of *Xanthoparmelia walteri* Knox and scattered *Teloschistes capensis* (L.f.) Müll. Arg. tufts conjoined by *Ramalina sp*. Its distribution is mainly limited to the coarse gravel hummocks of the southern parts of the study area where it represents the most diverse lichen community. Several other crustose species of *Arcarospora*, *Buellia*, *Caloplaca*, *Diplochistes*, and *Lecidea* also occur subordinately.

5.1.5 Crustose Lichen Zone

5.1.5.1 The *Caloplaca, Neofuscelia, Lecidella* community of the fine quartz gravel plains

Predominantly crustose lichen species are present in this community. Various *Caloplaca*, *Lecidella*, *Buellia*, *Neofuscelia*, *Lecidea*, and *Paraparmelia* species are found in this community growing saxicolous on fine quartz gravel. Interspersed coarse quartz gravel is often covered by scattered *Xanthoparmelia walteri* Knox species.
At locations where the gypsum substrate is not covered by a closed quartz gravel layer *Lecidella crystallina* Wirth & Vezda and *Acarospora* species also become abundant.

5.1.5.2 *Lecidella crystallina* Wirth & Vezda, *Caloplaca volkii* Wirth & Vezda, *Xanthomaculina convoluta* community of the gypsum plains

Abundant cover of individuals of *Caloplaca volkii* Wirth & Vezda, *Lecidella crystallina* Wirth & Vezda (both terricolous species), and *Xanthomaculina convoluta* (vagrant) is characteristic for this community. With lichen thalli covering nearly 100 % of the soil surface in some localities, these terricolous species clearly dominate this community. Based on the sand-binding abilities of these soil crust lichen species, they largely contribute to the stabilization of the otherwise only semi-stabilized soil surface
Thalli of foliose and fruticose species such as *Xanthoparmelia walteri* Knox and *Teloschistes capensis* (L.f.) Müll. Arg. occur scattered amongst the crustose species. The sand binding species *Acarospora schleicheri* (Ach.) A. Massal., *Caloplaca volkii* Wirth & Vezda, and *Lecidella crystallina* Wirth & Vezda grow abundantly, thus covering large quantities of the soil surface. Several species of *Arcarospora*, *Buellia*, *Caloplaca*, *Diplochistes*, and *Lecidea* also occur subordinately.

5.1.6 Sparse Crustose Lichen Zone

5.1.6.1 The sparse *Caloplaca, Neofuscelia, Lecidella* community of the fine quartz gravel plains

No fruticose and foliose species are found in this crustose community characterized by the saxicolous growth of *Caloplaca*, *Lecidella*, *Buellia*, and *Neofuscelia* species. In contrast to the comparable crustose community the sparse crustose community shows much lower species abundance, making spectral detection often difficult. Nevertheless it shall be described and included in the classification as

it often forms an important transition zone on the edge of major lichen covered areas reducing deflation and corrasion.

5.1.6.2 The sparse *Lecidella crystallina* Wirth & Vezda, *Caloplaca volkii* Wirth & Vezda, *Xanthomaculina convoluta* community of the gypsum plains

This community is characterized by a definite decrease in the abundance of individuals of the terricolous species *Caloplaca volkii* Wirth & Vezda, *Lecidella crystallina* Wirth & Vezda, and loosely interspersed *Acarospora schleicheri* (Ach.) A. Massal. compared to the *Lecidella crystallina* Wirth & Vezda, *Caloplaca volkii* Wirth & Vezda, *Xanthomaculina convoluta* community of the gypsum plains. Decrease can presumably be attributed to an increased disturbance reflected by observed wind-induced patterns shown in annex a as well as run-off cutlines created by ephemeral water courses at these locations.
Although ground coverage is often below 20 %, thus aggravating the spectral delineation of this class, the ecological importance of this class is characterized by its sand-binding capabilities of otherwise easily deflated surfaces.

5.2 Multilevel supervised classification approach

The process of supervised classification of satellite imagery is generally assigned to a more or less standardized sequence of individual procedures as far as literature on digital image analysis and remote sensing is concerned (BÄHR & VÖGTLE 1991, HÄBERÄCKER 1994, JENSEN 2000, LILLESAND & KIEFER 2000[5]). This sequence is always based on the spectral assignment of image pixels to classes defined by thematic reference data following a confined statistical algorithm in contrast to unsupervised classification approaches (cluster analysis) where no thematic reference information is needed and the assignment of classes is realized post processing.

If this concept of the spectral assignment of image pixels to classes is applied to the electromagnetic radiation being recorded for individual pixels and mapped onto multiple channels within the satellite imagery, every pixel can be devoted to a position in the multidimensional so called image- or feature space and assigned to a certain thematic class. Pixels belonging to similar classes of landscape objects will cluster in this feature space according to the distance measure used.
By calculating the distance of one pixel to a cluster, the pixel can be assigned to the nearest cluster. When the pixel does not belong to any cluster it remains unclassified.

The trained categorization of thematic classes according to feature space is confined by differing parametric rules depending on the underlying classification algorithm. In common Minimum-Distance- and Maximum-Likelihood-Classifiers are used. These classifiers mainly vary in the way that image-elements are assigned to classes in terms of geometric measures or probabilities derived from a statistical distribution function (JENSEN 2000). For remote sensing applications the Maximum-Likelihood-Classifier, usually showing best results, is the most common used algorithm although requiring complex calculations (EHLERS 2002).

In contrast to the Minimum-Distance-Algorithm mentioned above, the Maximum-Likelihood-Classifier assigns each pixel to the class with highest likelihood based on mean vectors and covariance matrices of the classes. Pixels comprising likelihoods below a thresh-

old can also be assigned to a reject class while images of the spatial distribution of these likelihoods can be used to identify areas not described properly by training areas (LILLESAND & KIEFER 2000[5]).

In order to achieve a better approximation of the unimodal and normal distributed classes required for the Maximum-Likelihood-Algorithm spectral subclasses must be identified, which are used in the supervised classification. Spectral subclasses are usually caused by differences in soil type and soil moisture while in an agricultural environment crop development and agricultural practise can also be influencing.

In addition to algorithms operating in a feature space different methods have been proposed. These techniques include Spectral Mixture Analysis (SMA), Binary Encoding Classification and Artificial Neural Networks Classification. As these methods are thoroughly described by for example (ZHANG ET AL. 2004, LILLESAND & KIEFER 2000[5]) and (JENSEN 2000) they shall not be further elaborated at this point. However, one technique which includes fuzzy set theory is discussed in the chapter 5.2.3 as this methodology is partly utilized for the study presented.

Summing up the role of the analysis algorithm is to partition the N-dimensional feature provided by the multispectral, multilayer satellite imagery into M mutually exclusive subregions with each one being a class of surface cover of interest to the study presented. Optimal location of the boundaries of these subregions of interest involves bringing together any reference data and the conditions under which they were collected with an a priori knowledge delineating that information. But rather than achieving this using fully automated analysis methodology, it might still be superior to combine human interaction with the quantitative strengths of machine methods.

5.2.1 Image stratification

Conjoined interpretation of satellite images and ancillary reference data can greatly aid the extraction and evaluation of information. In addition to providing meaningful context for interpretation and analysis, ancillary data can also significantly reduce the physical workload associated with the classification of satellite images (HÄBERÄCKER 1994).

This is accomplished by pre-processing image stratification defined as a procedure by which a region is delineated into sub-area or strata with the objective of grouping homogenous areas regarding one or more specific variables. Benefits from this processing step consist in an overall reduction of image variance as non-substantial image information is assigned to classes obtained from thematic reference data regardless of its radiometric properties. Disadvantages of image stratification based on spectral properties mainly focus on the extensive extraction of auxiliary signatures and the assumption that all stratified features are more or less time-invariant, showing no class-independent changes. The latter is also important for ancillary data as for example urban areas beyond the mapped state are potentially excluded from the strata. Thus topicality of the reference data is crucial (BÄHR & VÖGTLE 1991, HÄBERÄCKER 1994).

For this thesis thematic reference data, obtained from the ancillary topographical maps presented in chapter 4.3.4, was utilized for the extraction and masking of road-networks, urban areas, river courses / gallery forests, dune areas, coastal salt pans and a

general land-sea-mask. The spatial extend of these features was validated and revised, based on an independent signature extraction and supervised classification for the reference LANDSAT images acquired for the year of 2003.

The masking of all strata was accomplished by an overall consolidation of the various sources and a binary recoding. For this reason strata obtained from vector sources had to be converted to raster data beforehand.
This procedure developed a binary raster mask accounting for most of the invariant and variant image objects with no relevance for the study presented. In conjunction with the general confinement of the study area to a maximum coastal distance of about 60 km (compare figure 6 chapter 4.1.1) both overall image variance as well as physical classification workload could be significantly decreased for all satellite images included in this study.

5.2.2 Extraction and analysis of spectral signatures

Supervised classification processes demand for user defined sampling areas, also known as prototype or training set areas, to be collected for each feature type or ground cover of interest to be mapped. The collection of these training set areas is generally accomplished by ground visitations, detailed interpretation of aerial photography or other personal experience.
This acquisition of knowledge about a study area from field work, also known as ground truthing, should coincide with that of the remotely sensed data, to ensure good correspondence.

If training set areas are included in the classification process certain restrictions apply to their utilization for the extraction of spectral signatures from the images to be classified and for the evaluation of the achieved accuracy of the classification. Distinct sites used for the training of a Maximum-Likelihood-Classifier should therefore not only enclose a homogenous area of sufficient spatial extend, but also represent the unique spectral properties of the target class. Statistically the Maximum-Likelihood-Classifier also requires the histogram of such training set areas to show an equal distribution.

For the Central Namib Desert the fulfilment of these aforementioned requirements can be quite difficult during field work. Changes between different lichen communities as well as transition zones and overall patchiness, enforced by water courses and corrasion areas, of areas firstly recognized as homogenous can hardly be overlooked.
In addition differences in class distribution observed during field work may be represented by similar spectral features in the satellite image caused by a significant timely shift between acquisition dates. Moreover differences between observed properties and spectral representation may also be due to geometric shifts between reference and image data.

While thorough geometric correction applied to the LANDSAT imagery tried to limit the effect of geometric divergences (see chapter 4.1.3), irregularities caused by variances in acquisition dates could only be limited for ground truthing obtained during the field campaign of May 2003, where satellite imagery could be acquired within a corresponding timeframe of four weeks (see chapter 4.1.1). In total 874 training areas were collected during both field campaigns.

In order to further minimize the potential deficiencies caused by an over- or underestimation of class variance for the solely user-defined training samples based on field surveys, all training samples were verified and revised in reference to the LANDSAT scenes acquired for the year of 2003.
While preliminary verification merely focussed on the size and spectral homogeneity of the sites, an additional revision was performed by the iterative identification of contiguous pixels with similar spectral characteristics using the Region Grow Algorithm of the Erdas Imagine software suite. For this procedure each previously defined training area served for the collection of seed pixels against which the contiguous pixels are compared up to maximum spectral euclidean distance specified by the user.
As more contiguous pixels are accepted, the mean of the sample is calculated from the pixels and those pixels contiguous to the sample are compared in the same way. Iteratively this process is performed until no pixels that are contiguous to the sample meet the user defined spectral parameters (ERDAS 2001[5]).
If spectral distance, defined as the distance in spectral space computed as euclidean distance in n-dimensions, where n is the number of bands, is iteratively adjusted, the sample grows outward with each repetition thus delineating a polygon of homogenous pixels within or beyond the original training sample.
On the one hand revised training samples mostly decreased regarding their spatial extend but on the other hand showed an equal distribution when tested within the training set editor thus accomplishing the precondition for the Maximum-Likelihood-Classifier.

This combined approach for training sample identification lead to the result that although user control is highest for the initially user-defined samples, potential class variance within these samples could be successfully reduced in combination with the aforementioned auto-assisted approach.

As a result of the accurate verification and revision of the collected training samples numerous were rejected based on the aforementioned requirements. Due to the constrictions of field surveys only 206 of the initially collected 874 samples could be regarded suitable for further use within the classification process (compare chapter 4.3.1).
In order to enhance the extraction of spectral signatures from the multitemporal LANDSAT imagery all training samples firstly stored in vector data format were transformed into thematic raster data. This procedure allows for the creation of spectral signatures based on the thematic raster data values within the training set editor. The result of integrating the training samples into the training set editor is a set of parametric signatures with each signature corresponding to a class of the first hierarchical level of the classification scheme.

In the following all derived signatures were further tested with some of them being aggregated within the training set editor while others were left for assessing the accuracy of the resulting classification.

For many classes defined by the classification scheme spectral subclasses could be observed although signatures were mostly aggregated from various training samples being evenly spread throughout the image, thus allowing for a good representation of the variance within the target class. For these thematically homogeneous but spectrally heterogeneous classes, subclasses had to be included into the classification process.

The identification of these spectral subclasses as well as further testing of the thematic affiliation of the training samples was accomplished by testing the signature separability by comparing the covariance matrixes and the mean vectors of a pair of signatures, based on the assumption that if separability of two samples is not significant they might not be distinct enough to produce successful classification (ERDAS 2001[5]).
Distinct separability of signatures affiliated to the same thematic class may on one hand identify spectral subclasses but on the other hand also detect invalid samples. For this thesis Jeffries-Matusita measures (JM) were used as a distance measure to predict the results of the Maximum-Likelihood classification.
The Jeffries-Matusita (JM) distance comprises an upper (1414) and a lower (0) bound indicating the separability of the signatures. Signatures are entitled to be fully separable if the calculated divergence equals the appropriate upper bound up to a lower limit of 1350 (95 %), whereas signatures characterized by JM-values in between 1350 and 1200 (~85 %) are referred to as fairly separable. As a consequence all signature class-pairs below the threshold of 1200 can comprise delicate separabilities, becoming inseparable the closer the value is located to the lower bound (0) of the JM-distance (LILLESAND & KIEFER 2000[5]). These measures of the computed divergences for every class pair are listed in terms of either best average or best minimum divergence. A full list of all spectral subclasses corresponding to classes of the hierarchical classification scheme is given in figure A3 in annex a.

In order to improve classification results, class separabilities were optimized wherever possible with various means. Firstly new sets of subclasses comprising higher separabilities were created including the substitution of the reference sites utilized to increase separability. Secondly pairs of classes whose separabilities were still too low after complete reassignment were merged using the signature editor. Modification of multispectral band combination was abolished as various reduced band combinations only invoked overall decreased separabilities.

Due to the testing of the signature separability of all training samples a total of 44 spectral signatures were aggregated into 23 signatures describing 6 different types of lichen distribution defined by the classification scheme and 7 signatures describing the surrounding bare soil or rock types for the LANDSAT image of 180 / 75 / 2003, while for the scene of 179 / 76 / 2003, 33 spectral signatures were aggregated into 19 spectral classes describing 3 different types of lichen distribution and 12 signatures of bare soil or rock.
For accuracy assessment 86 training samples were excluded from the classification of 180 / 75 / 2003 while 32 were preserved for the 179 / 76 / 2003 scene amounting for about 57 % in total (118 of 206).

For the spectral separability of all final signatures derived for the supervised classification, best overall separability was observed with all image-stack layers being included in the evaluation. It is assumed that this might be due to the spectrally widespread absorption features of lichen dominated biological soil crusts (compare chapter 3.1.7.1) upon which spectral identification might also depend upon.
Although many signatures showed excellent separability, some Jeffries-Matusita (JM) measured distances were found to be slightly decreased. Therefore all separability measures showing values below a threshold of 1350, delineating the 95 % interval, shall be discussed. Thereby similarities between thematically distinct shall be entitled inter-class rela-

tionships, whereas similarities upon spectral subclasses shall be referred to as intra-class relationships. A full listing of all JM separability measures is given in figure A4 and figure A5 in annex a.

Starting with the separability measures obtained for signatures of the LANDSAT scene 180 / 75 / 2003 only 10 out of 870 possible class-pair combinations could be observed to be below the initially set threshold of 1350 and 2 of them comprising JM-values slightly below the threshold of 1200. Fruticose class 1.1 showed a separability of 1299 compared to the fruticose-foliose class of 1.3. Both the fruticose and the fruticose-foliose class describe coastal communities of the fine quartz gravel plains but differing regarding the community type which is either dominated by the abundance of *Teloschistes capensis* (L.f.) Müll. Arg. or conjoined by *Xanthoparmelia walteri* Knox. Still not regarded crucial, the slightly lowered separability between these thematically distinct classes is likely being caused by its spatial proximity. For all other fruticose classes full separability was reported making it the lichen class best recognized.

Fruticose-foliose classes showed a total of three interclass relationships where spectral separability was decreased. In addition to the decreased separability already discussed above, one class-pair within the fruticose-foliose class, signature 1.2 of the coastal quartz gravel plains and signature 3.1 of the mountainous regions, showed a spectral separability of 1184. As the class type 1.2 is solely observed in the coastal northern areas where gravel plains are often interspersed with dark rock debris, similarities to the rocky mountainous community may be reflected in the separability measure. Another reduction of separability could be observed between the class-pair of fruticose-foliose class 1.1 and foliose class of 1.1. Both found on the costal quartz gravel plains, the similarities expressed by a JM separability measure of about 1319 might be due to the inner class variance typically encountered within both communities, as for example some areas within the fruticose-foliose community may also comprise pure stands of the foliose coastal *Xanthoparmelia walteri* Knox community.

Overall separability of the foliose community classes also shows high values, with the exception of foliose subtype 1.1 and 1.2 showing similarities to the foliose-crustose subtype 1.1 and the non-lichen covered spectral subclass of 1.3 respectively. Both of these slight relationships with JM values of 1194 and 1326 can also be related to a class variance still inherent in these classes.

The same can be observed for the three interclass relationships of the foliose-crustose community diagnosed below the JM threshold of 1350. Already described relationships to spectral foliose subtypes are supplemented by slight correlations of the crustose subclass 1.1 and the none-lichen-covered subtype 2.1 ranging between JM values of 1194 and 1325. For the signatures delineating crustose and crustose sparse lichen distribution, observed relationships comprised a total of four slight similarities identified by the JM algorithm. While three of these slight similarities occurred between crustose and crustose-sparse subclasses of the same ground cover type, only one similarity was encountered for a foliose-crustose subclass described above. Observed slight interclass relationships between crustose and crustose-sparse ranging from 1302 and 1324 reflect the slight difficulties of the classifier to differentiate between the two classes and their inherent transition zones.

Regarding the LANDSAT scene of 179 / 76 / 2003 most of the spectral similari-

ties detected by the JM algorithm focus on the delineation of the foliose-crustose subclasses and the reduced separability between two of the none-lichen-covered classes.
Both foliose-crustose spectral subclasses show slight intra-class similarities reflected by a JM value of 1195. Although slightly below the critical threshold of 1200, test classifications using both signatures showed better results than a single signature created by merging of the two classes. As the first foliose-crustose signature also shows slight correlation (1301) to the crustose subclass 2.1 these two classes were test classified as well with good results regarding their delineation. Comparable to the reasons for the slight similarities between neighbouring classes described for the LANDSAT scene of 180 / 75 / 2003 natural variation inherent in the spectral signature may be the cause of these none-crucial fluctuations.
Regarding the reduced intra-class separability encountered between the two subclasses describing firstly none lichen-covered areas of the fine quartz gravel and gypsum plains and secondly a none lichen-covered area of the rocky and mountainous region, tentative reassignment to differing reference areas, as well as merging did not improve test classifications performed for these two classes. Therefore the similarities of the two signatures were accepted and both subclasses were included in the classification process.

Also noteworthy is the fact that all signatures describing none-lichen-covered areas can be well separated by the classifier from those signatures describing lichen distribution patterns.
This alone can be depicted as a quality measure for the training samples and the derived signatures as lichen distribution itself is likely to be well classified. In total only slightest insecurities for those classes potentially describing transition zones could be observed.

Separability of lichen covered areas from neighbouring sites only comprising bare soils and the correlation of in-situ measurements to LANDSAT derived training samples was also tested using an ASD FieldSpec FR spectroradiometer for in situ measurements obtained on the occasion of the Biota-S01 field campaign of March 2005.

For three selected lichen communities the mean spectral properties of training samples derived from previous reference data were compared to overall mean spectral reflectance of three lichen communities obtained from field spectrometer measurements (compare chapter 4.3.2). To allow for the comparison between the spectral properties of the broad-band LANDSAT 7 ETM+ sensor and those of the high resolution spectrometer data, spectrometer measurements were conducted between 10:00 and 14:00 h local time. In addition all spectroradiometer measurements were also resampled to ETM+ broad-band resolution using the spectral response function for each band integrated into the ENVI program suite.
In addition to the remotely sensed data obtained for the lichen-covered areas, neighbouring none-lichen-covered areas in the vicinity of the reference sites were also sampled during field work to investigate their separability.
Although detailed measurements of the spectral reflectance of various objects were also carried out, only those measurements obtained from a distance of 1 m perpendicular to the surface comprising the lichen community were used for the presented analysis (compare chapter 4.3.2).
Sampled lichen-communities comprised the "fruticose dominated coastal *Teloschistes capen-*

sis (L.f.) Müll. Arg. community of the fine quartz gravel plains" northeast of Cape Cross, the "fruticose-foliose dominated mountainous *Xanthomaculina hottentotta* community" and the "crustose dominated *Lecidella crystallina* Wirth & Vezda, *Caloplaca volkii* Wirth & Vezda, *Xanthomaculina convoluta* community of the gypsum plains".
An overview of the differing mean spectral response curves of the lichen communities as well as their neighbouring none-lichen-covered areas are presented in figure 10 through figure 12.

Concerning all mean reflectance spectra obtained, the offset between corresponding lichen- and none-lichen-covered sites attracts attention. While the fruticose and the foliose community show an increased reflectance for none lichen-covered sites compared to lichen overgrown areas, this relationship is reversed for the fruticose-foliose mountainous community. These differences regarding the modification of ground reflectance by the differing lichen communities are based on the fact that the mountainous fruticose-foliose community featured in this analysis is located on a dark gravel and bedrock cover, whereas the two other communities grow on a bright quartz gravel overlay or gypsum deposits. Therefore the mountainous fruticose-foliose lichen community alters the spectral properties of the underlying ground by increasing the reflectance while at the same time modifying the spectrum with distinct absorption features discussed later.
Through this specific conduct the applicability of the recently proposed spectral index for discriminating lichen-dominated biological soil crusts by CHEN ET AL. (2005), which is based on the assumption that lichen-cover alters its background by increased absorption is regarded at least problematic (compare chapter 3.1.7.1).

Distinct absorption features associated with lichens can be observed in the mean spectral response curves recorded by the spectroradiometer. Firstly the chlorophyll absorption feature is present in the vicinity of 670 nm followed by an increased reflectance in the adjacent near infra-red range. Secondly the three broad absorption features around 1730, 2100 and 2300 nm postulated by AGER & MILTON (1987) and depicting the presence of cellulose can also be recognized. The more subtle features described by laboratory experiments of BECHTEL ET AL. (2002) for the vicinities of 1445 and 1860 nm could not be detected due to interferences of atmospheric water (see chapter 4.3.2). In contrast the low reflectance (< 7 %) described by BECHTEL ET AL. (2002) for the 400 nm region could be clearly depicted, although many of the none-lichen-covered areas also represented this "distinct feature". However the findings of BECHTEL ET AL. (2002) were not only based on laboratory experiments but also featured the spectral reflectance curves of rock encrusting species limiting the comparability to the in-situ community measurements obtained for this study.
In general the detailed description of the spectral response curves of different lichen species as published by REES ET AL. (2004) can not be realized within this study but should be targeted by further studies.

The depiction of the aforementioned distinct features discussed for the spectroradiometer plots can however not be described after resampling to broad-band LANDSAT channels has been performed on the spectra.
The former distinct characteristics inherent in the spectroradiometer plots have merely been degraded to differing levels of reflectance with distinctive variations of slope for different spectral regions which have also been described and utilized by CHEN ET AL. (2005).

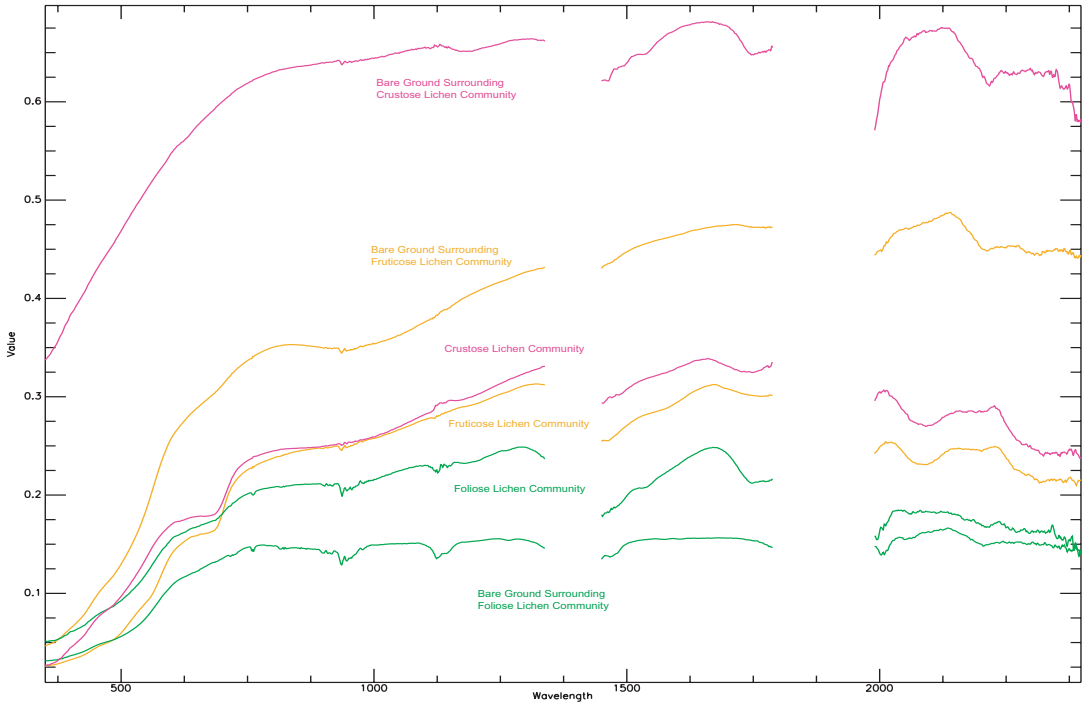

Figure 10: Mean spectral response curves of different lichen communities and their neighbouring none-lichen-covered areas obtained from 785 in-situ spectroradiometer samples. Spectral reflectance is plotted versus spectral range from 350 to 2399 nm with 1 nm resolution.

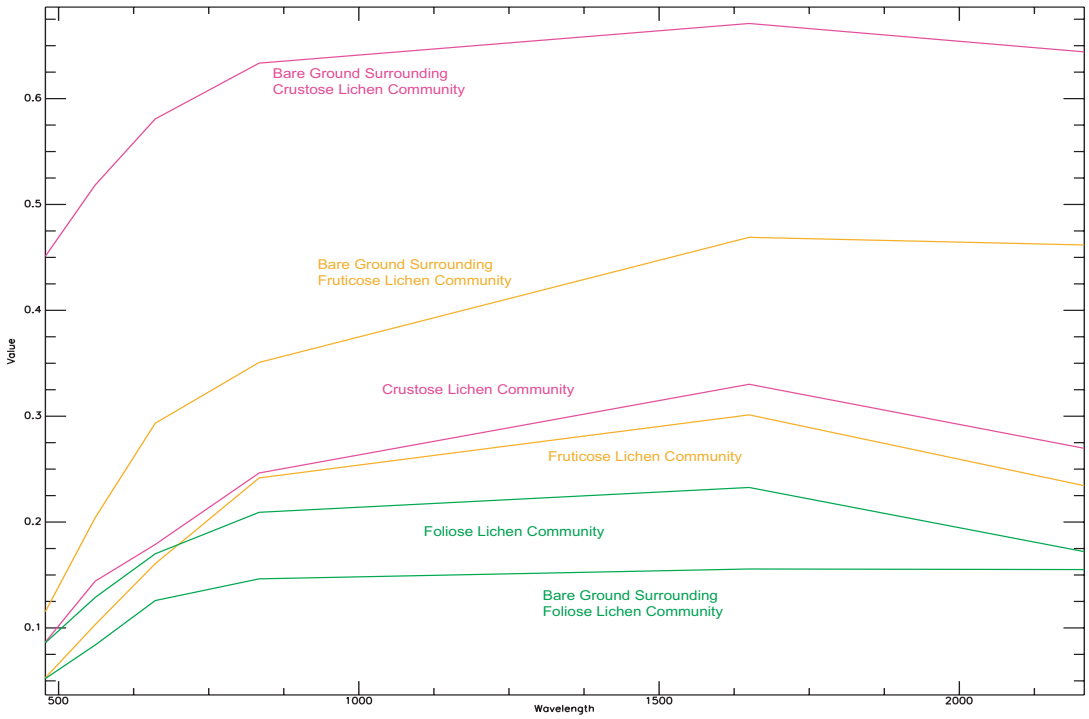

Figure 11: Mean spectral response curves of different lichen communities and their neighbouring none-lichen-covered areas obtained from 785 in-situ spectroradiometer samples resampled to LANDSAT 7 ETM+ broad-band resolution. Spectral reflectance is plotted versus spectral range from 350 to 2399 nm for the LANDSAT 7 ETM+ bands 1-5 and 7.

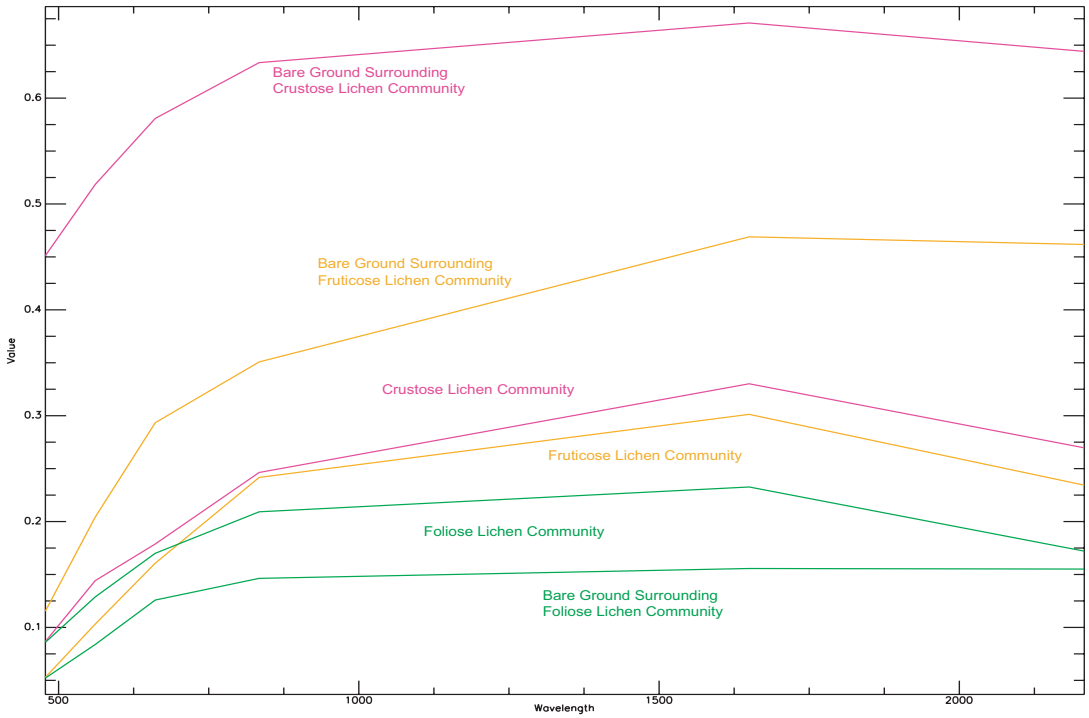

Figure 12: Mean spectral response curves of different lichen communities and their neighbouring none-lichen-covered areas collected from training samples and derived from LANDSAT 7 ETM+ of 2003. Spectral reflectance is plotted versus spectral range from 478.7 to 2208 nm for the LANDSAT 7 ETM+ bands 1-5 and 7.

But although differing in the amount of recorded spectral reflectance, overall reflectance characteristics resemble the mean reflectance spectra collected from training samples and derived from LANDSAT 7 ETM+ of 2003 (compare figure 13 through figure 18).

Therefore an analysis of the correlation between the resampled mean spectroradiometer plots and the mean spectral reflectance curves of the training samples derived from 2003 LANDSAT 7 ETM+ imagery was performed for the first five channels of the LANDSAT sensor. This limitation was chosen because of the increased signal to noise ratio of the spectroradiometer for the spectral vicinity of 2208 nm describing the centre of the seventh LANDSAT channel. The results were scatter plotted and are shown in figure 19 through figure 24.

Although offset, the correlation of the mean spectral reflectance curves showed high values ranging from 0.9841 to 0.9965 r^2 for lichen-covered- and 0.966 to 0.9981 r^2 for the none-lichen-covered areas for a confidence and prediction interval of 95 %. The standard deviation which is indicated in the figures as well, was observed lowest for the coastal fruticose community and neighbouring bare ground.

Based on these findings for the different exemplary lichen communities widely spread over the study area, it can be stated that not only general spectral distinction of lichen-communities from bare soil is feasible but also spectral discrimination between differing communities can be achieved by using LANDSAT imagery conjoined with a supervised classification approach.

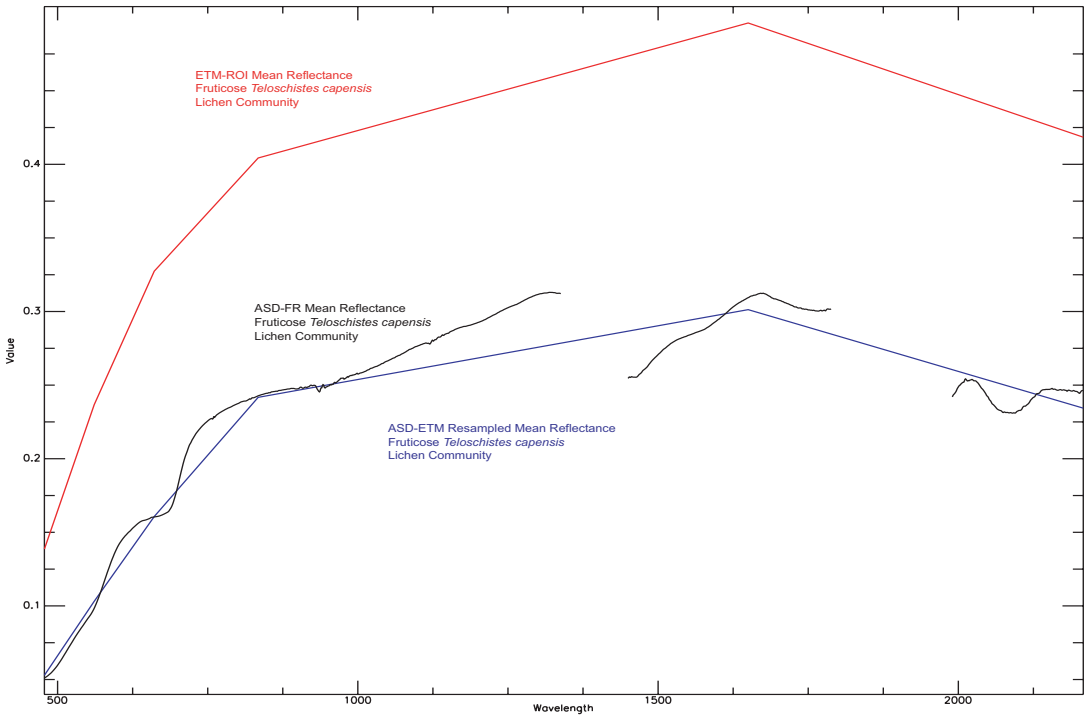

Figure 13: Fruticose lichen community. Comparison of the mean spectral reflectance curves of the spectroradiometer, resampled spectroradiometer and LANDSAT training sample for the spectral range of 478.7 to 2208 nm.

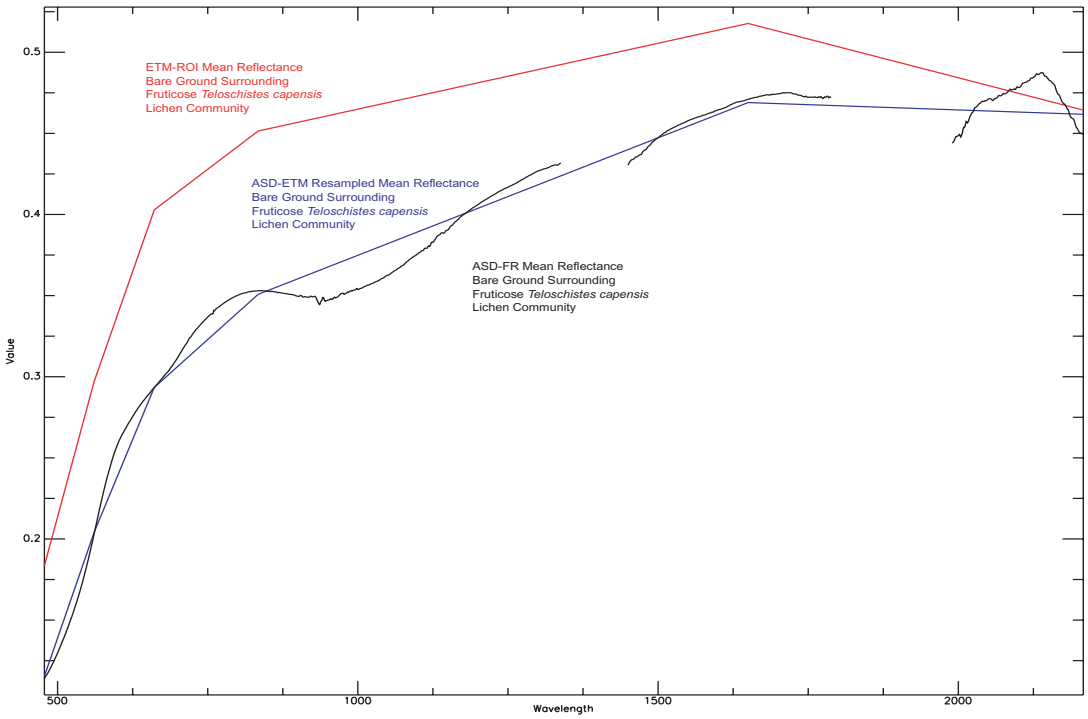

Figure 14: Neighbouring bare ground of fruticose lichen community. Comparison of the mean spectral reflectance curves of the spectroradiometer, resampled spectroradiometer and LANDSAT training sample for the spectral range of 478.7 to 2208 nm.

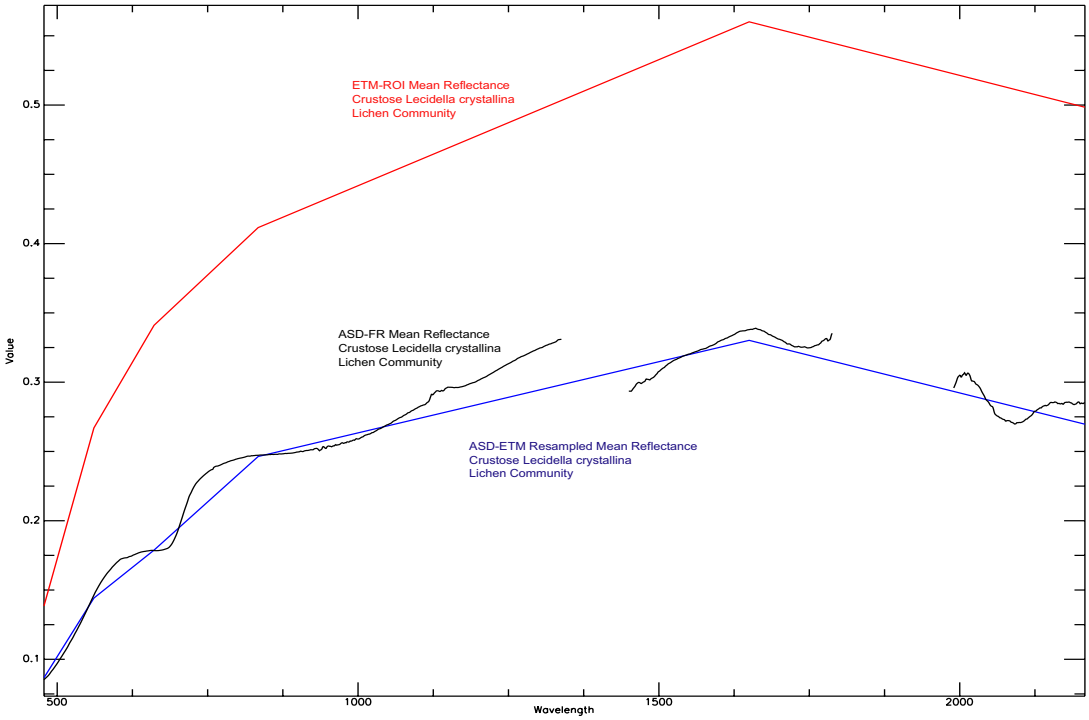

Figure 15: Crustose lichen community. Comparison of the mean spectral reflectance curves of the spectroradiometer, resampled spectroradiometer and LANDSAT training sample for the spectral range of 478.7 to 2208 nm.

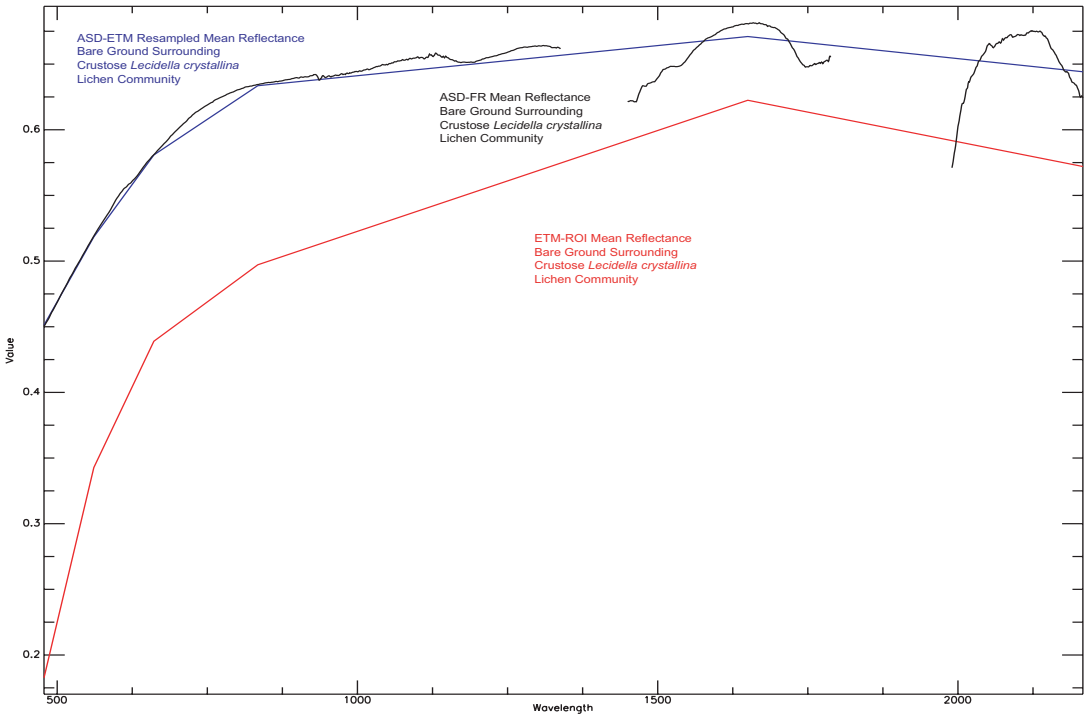

Figure 16: Neighbouring bare ground of crustose lichen community. Comparison of the mean spectral reflectance curves of the spectroradiometer, resampled spectroradiometer and LANDSAT training sample for the spectral range of 478.7 to 2208 nm.

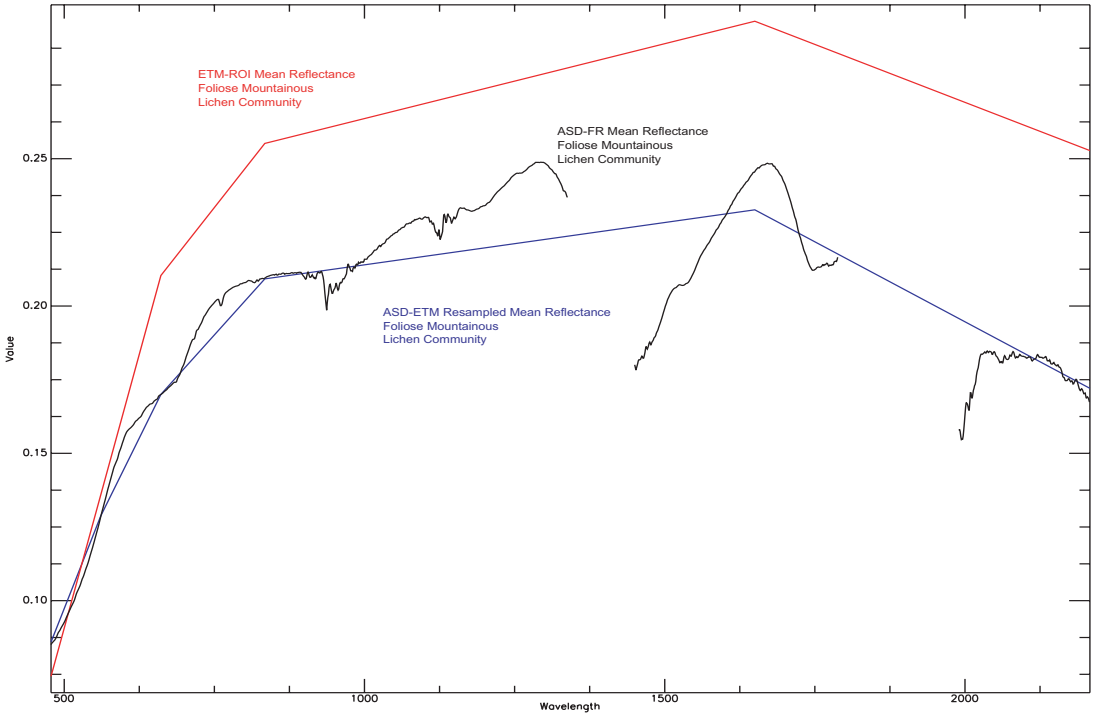

Figure 17: Fruticose-foliose lichen community. Comparison of the mean spectral reflectance curves of the spectroradiometer, resampled spectroradiometer and LANDSAT training sample for the spectral range of 478.7 to 2208 nm.

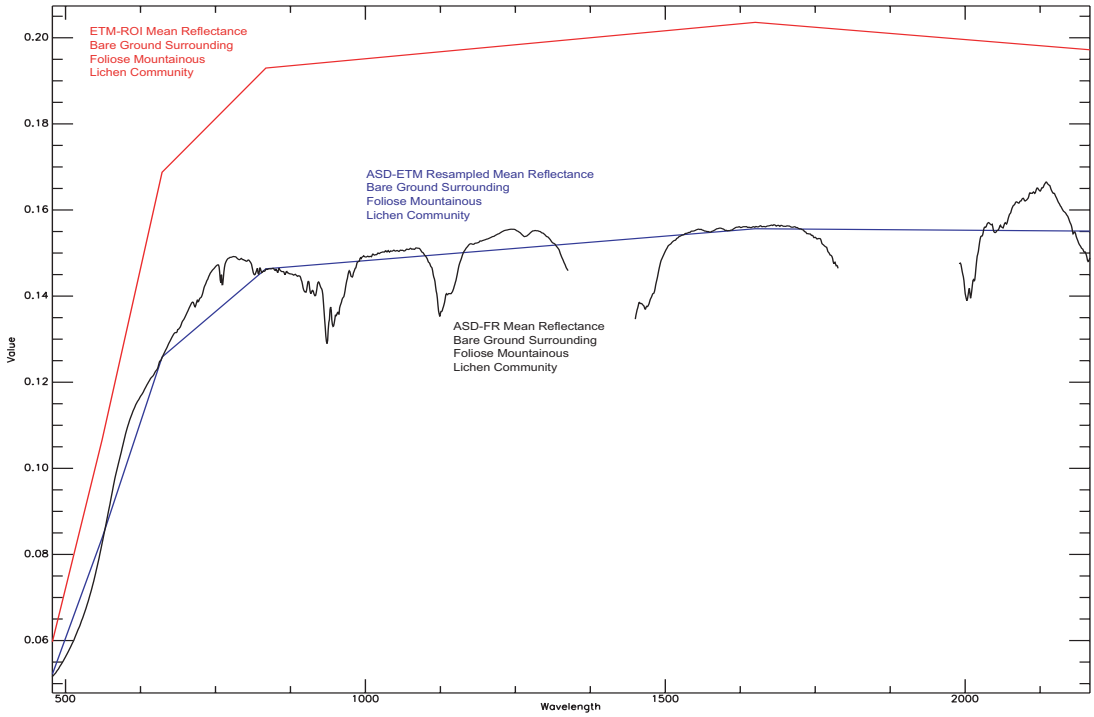

Figure 18: Neighbouring bare ground of fruticose-foliose lichen community. Comparison of the mean spectral reflectance curves of the spectroradiometer, resampled spectroradiometer and LANDSAT training sample for the spectral range of 478.7 to 2208 nm.

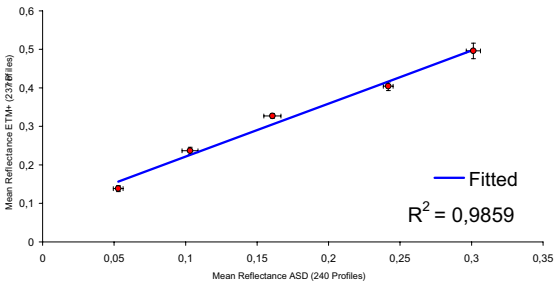

Figure 19: Correlation between LANDSAT 7 ETM+ broadband-channels 1 - 5 and resampled mean spectroradiometer reflectance of the fruticose lichen community.

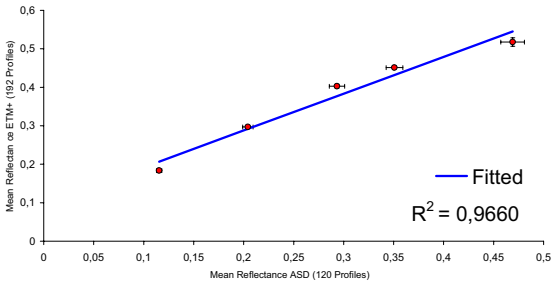

Figure 20: Correlation between LANDSAT 7 ETM+ broadband-channels 1 - 5 and resampled mean spectroradiometer reflectance of the bare ground surrounding the fruticose lichen community.

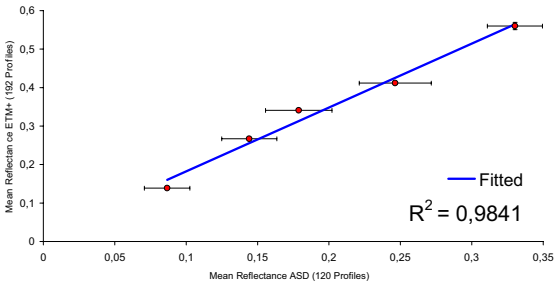

Figure 21: Correlation between LANDSAT 7 ETM+ broadband-channels 1 - 5 and resampled mean spectroradiometer reflectance of the crustose lichen community.

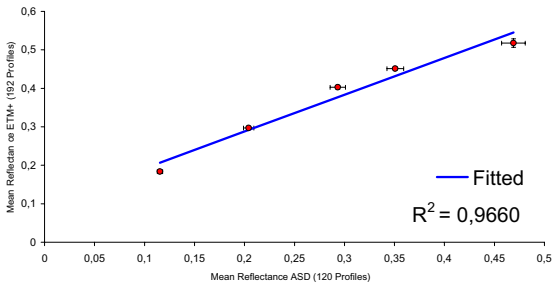

Figure 22: Correlation between LANDSAT 7 ETM+ broadband-channels 1 - 5 and resampled mean spectroradiometer reflectance of the bare ground surrounding the crustose lichen community.

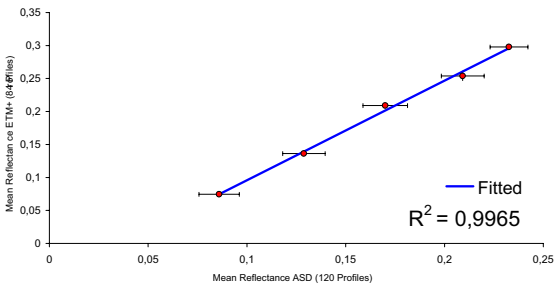

Figure 23: Correlation between LANDSAT 7 ETM+ broadband-channels 1 - 5 and resampled mean spectroradiometer reflectance of the mountainous fruticose-foliose lichen community.

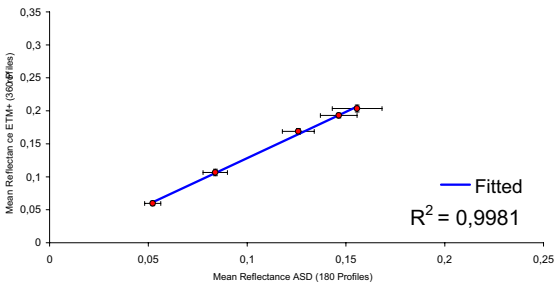

Figure 24: Correlation between LANDSAT 7 ETM+ broadband-channels 1 - 5 and resampled mean spectroradiometer reflectance of the bare ground surrounding the mountainous fruticose-foliose lichen community.

5.2.3 Statistical fuzzy likelihood classification approach

Since remotely sensed images often confront the user with various uncertainties arising from for example local atmospheric disturbances, errors for the sensor calibration, problems of class assignment caused by natural transition zones, mixed-pixel-problems due to limitations in spatial resolution as well as selective spectral acquisition and inner class variability, accounting for these uncertainties is proposed by various authors (TIZHOOSH 1998).
In the conventional maximum-likelihood per-pixel algorithm, the class to which the pixel is assigned is that of the highest probability. However probabilities of class membership, on which the assignment is based, are usually disregarded. Therefore no information on the probabilities is available after the classification and consequently no information whether a strong or weak membership exists (ABKAR ET AL. 2000).

Fuzzy classification therefore applies a fuzzy logic concept, introduced by Lotfi Zadeh in the 1960's, to overcome the above described problems of hard classification algorithms where a given pixel might have partial membership to more than one class or category (LILLESAND & KIEFER 2000[5]). The fuzzy logic concept being a superset of Boolean logic allows the survey of partial truth values between "completely true" and "completely false" (BUCKLEY & ESLAMI 2002).
While traditional classification techniques utilizing "hard classifiers" assign each pixel to only one class, with fuzzy classification techniques, often referred to as "soft classifiers", only a membership grade is assigned to the classified pixel (ZHANG & KIRBY 1999). Thus a fuzzy partitioning includes a large amount of quantitative information where a traditional crisp classifier only provides qualitative information (MATSAKIS ET AL. 2000).
Within a fuzzy classification a pixel can as well belong to one category with 75 % membership and to another class with 25 % membership, where hard classifiers would only report on the class with the highest membership. Supplementary information obtained for the pixel-memberships can also be used to gather information on overall classification stability, reliability and class separability (FOODY 1999).
Following this transition from the "hard" classification system to the "soft" classification system, also known as fuzzification, and the analysis of the degrees of membership, defuzzification is used to translate the fuzzy membership values back into hard values in order to visualize the classification results. Therefore the maximum fuzzy class-membership is assigned to a pixel as the class value to be presented (EKLUND ET AL. 2000).

For the integration of fuzzy theory into the multi-level pixel-based classification approach presented within this thesis the fuzzy convolution classification features by the Erdas Imagine software suite were depicted.
However the fuzzy convolution classification offered by Erdas Imagine can not be regarded as a real fuzzy classification technique on strict terms. The assignment of pixels to classes is described by the Mahalanobis-distances in fuzzy way, as no I/O information is given, but information describing a "more or less" membership. Still these class-membership probabilities of pixels are only obtained for adjacent classes while no fuzzy information is given on the memberships of all pixels to all classes.
Rule-based defuzzification based on the membership-values is thus limited to "convolution filtering" where kernel size and weight-

ed distance to its central pixel can be adjusted. As a result no new fuzzy-class-membership-information is obtained permitting the use of defuzzification techniques proposed in literature. Instead the fuzzy membership values are translated back into "hard" unambiguous class values accompanied by image filtering.
Therefore the "fuzzy convolution classification" offered by Erdas Imagine does not represent an own classification strategy, but can only be referred to as special post-processing technique taking fuzzy concepts into account.

5.2.4 Unitemporal fuzzy enhanced classification

The program suite of Erdas Imagine offers the fuzzy convolution classification for enhancing pixel-based classifications by obtaining information on both the most likely pixel to class assignment as well as the corresponding Mahalanobis-distances.

Starting with the transition from the hard system to the soft system also known as fuzzification, a layer-stack is generated which hierarchically depicts the best class value assigned to a pixel according to a user-defined number of best classes. In accordance Mahalanobis-distances depicting the class-membership in terms of fuzzy logic are also calculated for every pixel of each of the hierarchically ordered best class assignments.
Therefore, the number of best classes directly defines the number of class-memberships obtained for each pixel. Thus the number of best classes also defines the number of layers needed to store the information of all class-assignments and corresponding Mahalanobis-distances. For this analysis the six best classes were calculated for each pixel.

While pixel to class assignments are stored as a thematic layer-stack, Mahalanobis distances representing probabilities are stored in a layer-stack of 32-bit offset continuous raster layers in which each data file value represents the result of the spectral distance equation.
Pixels containing higher distance file values h are spectrally farther from the signature means for the classes to which they were assigned whereas pixels comprising low values are spectrally nearer. Therefore higher distances represent potentially misclassified pixels while low distances are likely to be classified correctly with the lowest distances usually assigned to the training samples themselves. The histogram of these distance file values resembles that of a none-symmetrical chi-square distribution opposed to a normal distribution with its symmetrical bell curve (ERDAS 2001[5]).

Thus the analysis of the relationship of the probabilities is proposed preceding further processing of the imagery in order to find out whether the allocation of the differing classes can be regarded equiprobable or if the assignment of all classes other than the first can be regarded insecure. Therefore all computed Mahalanobis distances h for the first to sixth best class are utilized according to FRANZEN ET AL. (1998).

However direct comparison of the probabilities is difficult. FRANZEN ET AL. (1998) therefore propose the use of the chi-square distribution of the Mahalanobis-distance of a pixel to obtain its actual probability of class-membership. In addition the class-memberships to be included in the classification can be selected using this approach.
As the relationship of two chi-square distributions can be regarded F-(Fisher) distributed a threshold value extracted from a F-distribution table can be used to measure the degree

by which the two chi-square distributions differ significantly for a given statistical significance. The degrees of freedom are defined by the number of bands of the data used. Since all image-stacks used within this study comprise eight layers, the threshold value extracted from the F-distribution table is 3.44 for a statistical significance of 95 % (SCHÖNWIESE 1985).

Hence the hierarchically ordered chi-square distributions of the second to sixth best class to pixel assignments are compared to the distribution of the class assignment of the first, using the F-test approach to analyse their similarities.
As a result 82 % of the class assignments of the second order, 49 % of the third order, 24 % of the fourth order, 8 % of the fifth order and only 2 % of the sixth order did not differ from the first class assignment with the highest probability for LANDSAT scene of 180/75 from 22nd of April of 2003.
For the LANDSAT scene of 179/76 from the 1st of May of 2003, 87 % of the class assignments of the second order, 65 % of the third order, 41 % of the fourth order, 19 % of the fifth order and only 5 % of the sixth order did not differ from the first class assignment with the highest probability (compare table 7).

These results reflect the overall stability of the class-assignments as probabilities by which classes other than that of the first probability are allocated steadily decrease. Moreover it also depicts the class-memberships to be included in the classification as the compliance of class-assignments rapidly decreases for the fourth, fifth and sixth probability. Even though the third probability shows a large degree of equiprobable allocation for both scenes it is excluded from further processing as tests revealed an increasing confusion between the classes of foliose-crustose, crustose and crustose-sparse. Therefore only the first two probabilities shall be included into the fuzzy likelihood classification.

Following the preceding analysis, the Mahalanobis-distances as well as the proposed class to pixel assignments of the two best classes per pixel, defuzzification is performed using fuzzy convolution filtering.
While defuzzification in general describes the translation of the fuzzy membership values back into hard values in order to visualize the classification results, convolution filtering alone is defined as "mathematically determining the data value for a new cell in an $n * m$ neighbourhood of cells" (MICROIMAGES' SCIENTIFIC WRITERS 2003).
The qualities of the aforementioned approaches are combined in the fuzzy convolution utility which allows the three dimensional application of a moving window convolution filtering, with the defined size of

	Distance 1-2	Distance 1-3	Distance 1-4	Distance 1-5	Distance 1-6
180 / 75 / 2003	82%	49%	24%	8%	2%
179 / 76 / 2003	87%	65%	41%	19%	5%

Table 7: Analysis of the similarities of the chi-square distributions of the second to sixth best class to pixel assignments compared to the distribution of the class assignment of the first order using an F-test approach and a statistical significance of 95 %.

n * *n* * *m* Pixel and *m* defining the number of bands, on a fuzzy classification with multiple output class assignments. It utilizes the multilayer classification and distance file to create a new single class output file by calculating a total weighted inverse distance for all the classes within a moving window of 3 * 3 pixels. As a result it assigns the class with the largest total inverse distance summed over the entire set of fuzzy classification layers to the centre pixel.
As a consequence pixels with small distance values remain unchanged whereas pixels with higher distance may be changed to a neighbouring class value if there are a sufficient number of adjacent pixels with class values and small corresponding distance values (ERDAS 2001[5]).
Therefore this special post-processing technique creates a context-based classification that effectively reduces classification noise by taking fuzzy concepts into account. In order to create a coherent mapping product of the study area both unitemporal classifications were assembled into a mosaic using an overlay function for the overlapping peripheral areas post-processing. Therefore individual as well as conjoined accuracy assessment of the classification results is discussed subsequently and analysed in chapter 6.
After all both fuzzy enhanced classification as well as post-processing techniques lead to an improved result of the unitemporal supervised classification and present the first distribution map of the lichen communities of the Central Namib Desert for the year of 2003 (compare chapter 6.4).

5.2.5 The retrospective classification strategy

Although the approaches presented for the accomplishment of the unitemporal supervised classification can as well be utilized for the multitemporal retrospective classification, methodological differences apply.

In general multitemporal classification has often been utilized to accurately classify land-cover strongly affected by seasonality. For example, field samplings of biomass, in-situ spectral reflectance measurements of vegetation types, or other reference information can be used for the assessment of the phenological state represented of each individual time-series images. Based on this knowledge and on the summary of the individual information extracted from the remotely sensed images an accurate vegetation classification is obtained.
Contrasting with many ecosystems, only a very weak seasonality can be observed for the Central Namib Desert (WALTER & BRECKLE 1999[7]). In addition studies of LANGE ET AL. (1991) and LANGE ET AL. (1994) showed that photosynthesis and water relations of lichen communities are virtually not affected by these minor climatic fluctuations. Thereby alterations of lichen communities can be mostly ascribed to slow natural growth rates as well as event driven natural and anthropogenic disturbances.

However, in contrast to most multitemporal classifications focussing on land cover variations and changes, no spatially referenced thematic information describing some previous state is available for the Central Namib Desert (compare MUCHONEY & HAACK 1994, JENSEN ET AL. 1995, COPPIN & BAUER 1996, LEVIEN ET AL. 1998, WEIERS ET AL. 2003).
Thus information describing the lichen community distribution as obtained from the field-campaigns and transferred into training samples depicts the only source of reference for this study. However recently derived spectral signatures or training samples, acquired

for a specific image or timeframe potentially deviate from the information inherent in previous satellite imagery, thus rendering them useless for retrospective supervised classification (REES & WILLIAMS 1997). Still some of these recently collected training areas might have been unaffected for a longer period, foregoing its collection event. Thus rendering them useful for retrospective supervised classification as their reference information might also be valid for previously recorded imagery. Based on these assumptions methodologies allowing for the assessment and identification of changed and unchanged reference information need to be applied and developed.

Change detection algorithms which can be utilized for the analysis and the quantification of the spectral changes in respect to multitemporal imagery are decidedly the best. However, utilized algorithms will have to allow the verification of reference samples to support retrospective supervised classification. Therefore the selected approach will have to incorporate sensitivity to gradual changes, minimize the loss of information, and allow the identification of gradual changes.

Selective Principal Component Analysis (sPCA) can both reduce the dimensionality of a dataset while at the same time minimize the loss of information naturally associated with standard PCA analysis or univariate image differencing (compare SINGH 1989). Due to selective analysis of all input bands, and the model-specific options introduced by WEIERS ET AL. (2003), assessment of the extent and intensity of gradual changes is accomplished. Thus change intensity can serve as an indicator for updating and monitoring priority. On the contrary no information about the direction or nature of the detected change is provided.

Instead Post Classification Comparison also known as Post Classification Change Differencing based on multitemporal supervised classifications is utilized. The advantage of this change detection methodology is the production of change maps comprising a complete matrix of changes based on the classification results. Subsequently discussed in detail, intensity as well as direction of changes will be identified based on the combined approach.

Reviews and surveys of available change detection techniques for the assessment of land-cover variations were also presented by SINGH (1989), FUNG (1990), BEEBER (2000), WOODCOCK ET AL. (2001), CIVCO ET AL. (2002), and ROGAN ET AL. (2002).

5.2.5.1 Selective Principal Component Analysis

The main purpose of the multivariate Principal Component Analysis (PCA) is to condense the information contained in a large number of original variables into a smaller set of variables with a minimum loss of information. In regards of satellite image processing, PCA is used to reduce the correlation between bands of data and enhance features that are unique to each band. Characteristically information common to all input bands is mapped to the first principal component while subsequent principal components comprise progressively less of the total scene variance. If the PCA is applied to multitemporal datasets, defined as satellite images depicting the same area at different times, the first principal component will contain all information that has not changed between the two dates, while the second principal component will contain all the information that has been changed with the areas of

greatest change found in the tails of the image histogram (SINGH 1989).

As problems include the loss of information that is mapped to a component not being used in the analysis and the concurrent difficulties of clearly delineating corresponding change classes, CHAVEZ & MACKINNON (1994) postulated the use of sPCA to overcome these problems.

Based on the objective that it might be far more interesting to the user to obtain the information that is unique to each spectral band as compared to information that is common to all the bands of a given multispectral dataset, sPCA is used to map the spectral contrast between different spectral bands (CHAVEZ & KWARTENG 1989). As the contrast is mostly limited to the second principal component also containing information of inherent changes, a band-wise extraction of this information is accomplished. Moreover every selectively obtained second principle component derived from the comparison of multitemporal and multispectral satellite images approximately represents the spectral differences of two identical bands acquired at different times (CHAVEZ & KWARTENG 1989).

Based on these findings WEIERS ET AL. (2003) developed a pixel oriented change detection approach within the Mobio Project (Monitoring in Biotopes) for the change analysis of timely differing satellite image pairs of a common area using sPCA and fuzzy membership transformation. Comprising change information as well as noise, they utilize the second principle component (compare SINGH 1989, CHAVEZ & MACKINNON 1994). However the Gaussian distribution of the second principal component creates a threshold problem as the change information is found in the tails of the histogram and the noise around the peak of the unimodal distribution. With no precise decision rule possible WEIERS ET AL. (2003) propose the use of a fuzzy transformation where the histogram values of each individual second principle component layer are transformed into fuzzy membership values by a transfer function. A value of one, representing completely changed pixels, is assigned to the tails of the histogram and a value of zero,

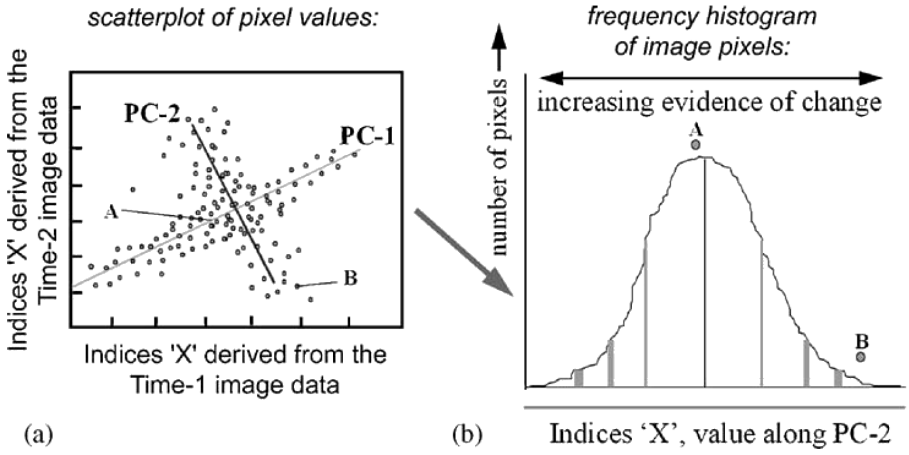

Figure 25: The diagram illustrates the effect of principal component transformation. On image (a) alongside the axis of the first principal component (PC-1) all information common to both images is gathered. The length of the axis indicates the relative amount of total variance explained by it. The shorter axis of the second principle component (PC-2) defines a mixture of change and noise information. The histogram on image (b) illustrates an increasing evidence of change from the peak (maximum of noise) to the tails of the histogram. Source: WEIERS ET AL. (2003), FIG.4, PP. 15.

corresponding with pixels fully unchanged, is allocated to the peak of the distribution (compare figure 25).
At last all transformed index layers are aggregated using an 'OR' condition, e.g. averaging, thus creating an index-layer comprising a normative value describing change intensities ranging from zero to one for the analysed image pair (WEIERS ET AL. 2003).

To utilize this change detection methodology for the assessment of the suitability of reference samples collected for the timeframe of 2003 some preconditions have to be fulfilled. Since image pairs are compared band-wise, the radiometric as well as spatial resolution of the sensor of the underlying multispectral satellite imagery must be identical (compare chapter 4.1). Further all images need to be geometrically and atmospherically corrected to allow observed changes to be due to changes on the earth's surface (compare chapter 4.1.3 and 4.1.4).

With all these prerequisities fulfilled two differing approaches can be chosen for the evaluation of the reference data regarding its suitability for retrospective supervised classification.
Firstly it is possible to analyse the inherent changes in between two image-pairs for their full spatial extend. Therefore a master-scene for which the recently derived training-samples were obtained is classified according to that reference data and its classification scheme.
With the means of the sPCA change detection approach presented by WEIERS ET AL. (2003) the spectral differences between that master-scene and a back-dated image are computed and stored in the above described normative measure. This measure then depicts all areas which have been spectrally altered to a greater or lesser degree between the master and its back-dated counterpart. If inverted this product also depicts those areas where corresponding to their spectral response no changes have occurred.
If these spectrally constant areas are intersected with the supervised classification of the master-scene new training-samples can be derived for the back-dated scene based on the assumption that the underlying surface has remained spectrally and thus thematically unchanged.
However assets and drawbacks arise from this procedure. One disadvantage results from the fact that the full images are compared regarding their spectral differences. As the minimum and the maximum of the index developed by WEIERS ET AL. (2003) emerges from the minimum and maximum spectral difference between the two images, slight changes between the two timeframes might be suppressed by the dynamic of strongly altered areas. Thus slight changes occurring within a lichen community training sample might not be detected due to its limited dynamic range. In addition all uncertainties of the supervised classification of the master-scene will be included in the process as its thematic information serves as a reference.
Opposed to these disadvantages the simple derivation of numerous large training sites can be regarded as an asset.

To overcome the problems of the first approach a second methodology based on the above findings was considered. For the target specific identification of spectral modifications caused by the differing acquisition dates of the satellite imagery all time-series images were firstly masked according to the final set of training samples stored in the aforementioned thematic raster layer. Due to this confinement only the spectral changes of objects, featured within this study, are compared. Thus the sensitivity of the change index

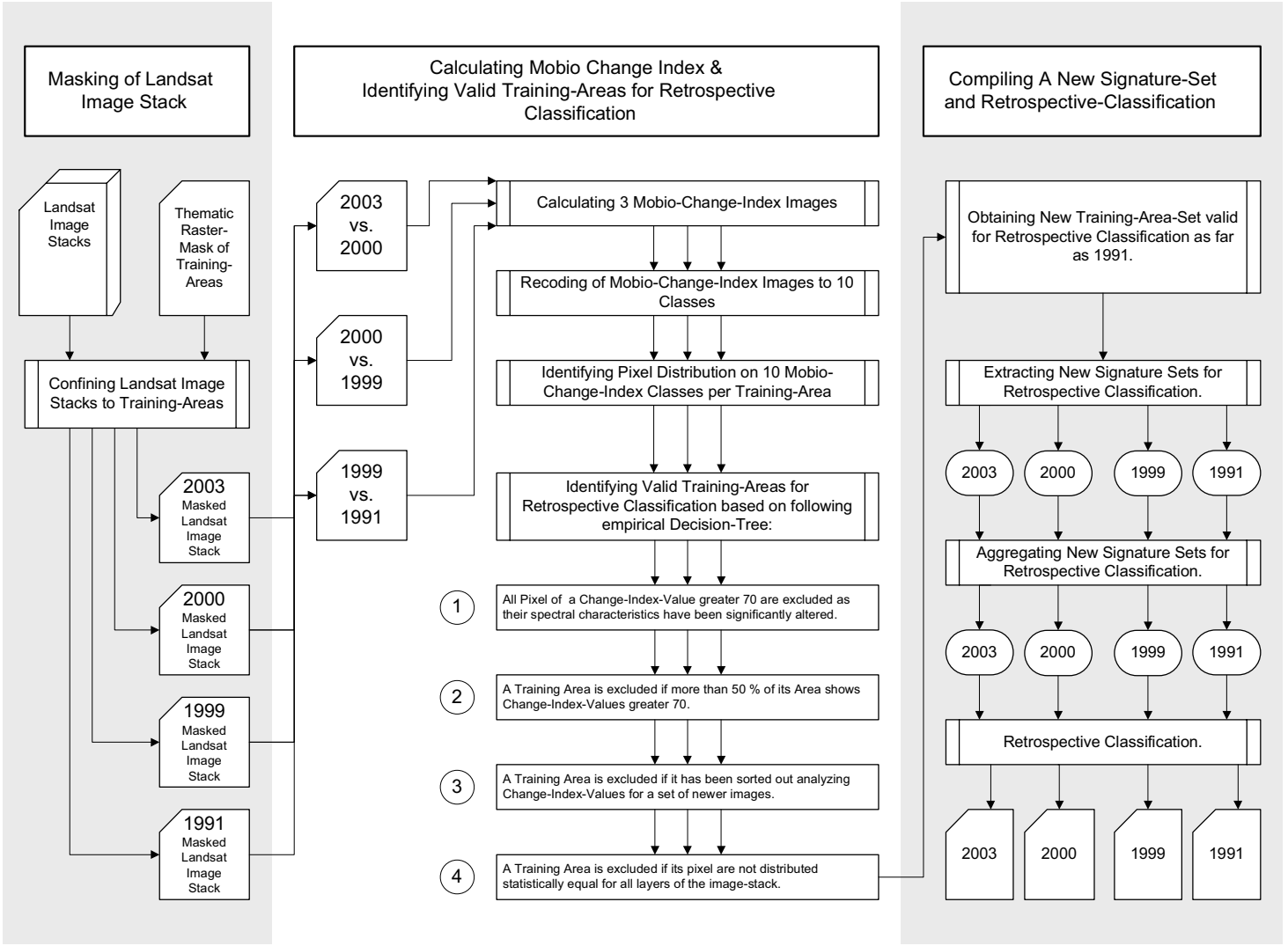

Figure 26: Flow-chart displaying the retrospective classification strategy..

developed by WEIERS ET AL. (2003) is not only strongly increased but also "thematically calibrated".
Areas unchanged were identified by progressively running backward change detection, utilizing the algorithm proposed by WEIERS ET AL. (2003).
The same sets of training sites, obtained for the unitemporal classifications in chapter 5.2.2, therefore form the basis for all back-dated images included in this study, with the exception of those samples and pixels showing high change values within the repeated analysis.

If this approach is iteratively applied to the multitemporal imagery obtained for the study area the number of approved reference samples showing no change in spectral response will certainly decrease the greater the acquisition of the reference and its back-dated counterpart differ in time.
In addition many samples might comprise spectrally constant as well as variable areas due to the fact that the computation of the change detection indices is performed on a pixel basis. Moreover the computed index, ranging from fully constant (0) to fully changed (1), requires a threshold to be set to discriminate between true change information and noise.
Both of these observed problems can however only be solved conjointly. As much of the true changes depicted by the change detection index are located within the outer areas of the training samples they are likely to be caused by uncertainties of the geometric correction if images are compared pixel-wise. However the change index values inherent in these "coronal-like" error-areas also help to depict an adapted threshold value for which the spectral information of the compared pixels can be regarded as significantly altered.
It could be observed that for those training samples where change index values were found to have a heterogeneous distribution, values were generally above 0.7 for the outer areas while core areas comprised values well below that threshold level. On the other hand training samples comprising a nearly homogeneous distribution of high change values also showed values comparable to the outer areas. Training samples comprising a homogenous distribution of low change index values could only be observed for training samples thematically assigned to objects considered invariant.

Based on these findings the evaluation and confinement of each training sample on a per pixel basis is proposed. According to the empirically obtained threshold value discriminating between true change and noise for the computed change index, the in- or exclusion of each specific pixel is decided. As this first pixel based decision rule does not consider the overall distribution of change values within a reference sample, a second criteria accounting for the abundance of changed pixels in relation to the size of the reference sample is established. To enhance the analysis of the change detection values derived from the comparison of the timeframes all normative change index values were recoded into ten classes ranging from 0 to 100 % likelihood of change.
With the change value depicting a normative likelihood for which a pixel has changed its spectral properties, this value was set to likelihood greater than 70 % empirically based on the above findings and testing of various threshold values. This conservatively set threshold value for the pixel based change detection is accompanied by the decision rule where a complete training sample is excluded from the classification if more than 50 % of its total area comprises pixel values succeed-

ing the previously set change index value of 70 %.
Moreover training samples are also subsequently excluded from the classification process if additional restrictions resulting from the selected supervised classification algorithm apply.

On one hand this conjoined iterative identification of both pixel-based and sample-based changes does not only decrease the amount of training samples but also, due to the distinct exclosure of modified pixels, the total amount of available reference area (compare chapter 5.2.6).
On the other hand a validated and adapted set of training samples is acquired which serves all time-series images of the study area and successfully accounts for both spectral and geometric error rates. In addition future information on reference areas can be evaluated for their suitability, thereby constantly increasing the reference information available for all time-series images. Thus the only disadvantage of this technique where a potentially decreased number of training samples might restrict the supervised classification of some far back-dated imagery might as well be overcome in the future by a steadily increasing amount of available reference information.

With the validated set of training samples and the resulting independent supervised classification of all images included in this study, requirements for a post-classification comparison are met. The advantage of this most obvious change detection methodology is the production of change maps comprising a complete matrix of changes based on the classification results. Moreover selective grouping of classification results allows the analyst to observe any subset of changes which may be of interest (SINGH 1989). An overview of the full methodological approach is presented in figure 26.

In addition to the accuracy assessment of the classified results with the means of independent reference data, change detection indices obtained from the aforementioned first sPCA approach can as well be utilized. Patterns identified from the spectral change detection comparison of the full image pairs can serve for the verification of the spatial differences of the differing classification results.
In conjunction with the fuzzy enhanced supervised classification approach described for the unitemporal classification, the application of the retrospective multitemporal classification strategy and its effects are presented and discussed in the following chapter.

5.2.6 Extraction and analysis of retrospective signature sets

As shown above the derivation and analysis of change intensity information can serve as an indicator whether existing or newly obtained training samples can in theory be utilized for the retrospective classification of back-dated imagery. This chapter comprises the implementation of the retrospective classification strategy discussed in chapter 5.2.5.1 with regard to the multitemporal LANDSAT 5 TM and LANDSAT 7 ETM+ dataset presented in chapter 4.1. One advantage arising from the utilization of the LANDSAT 5 TM and LANDSAT 7 ETM+ sensor is based on their virtually identical geometrical, optical, as well as radiometrical resolution allowing for full comparability of their information products (compare chapter 4.1).

The application of the methodology discussed before can generally be assigned to a sequence of three individual procedures as

shown above in figure 26. Firstly all obtained satellite images are stratified to the area of the reference set of training samples compiled for the unitemporal classification of the year 2003. Secondly pixel-based computation and analysis of the Mobio change detection index is performed according to the decision rules established in the previous chapter. Thirdly the newly computed reference set of training samples, consistent for all back-dated images, is utilized for a fuzzy enhanced classification approach.

After all spectral information inherent in the time-series images of the study area is spatially confined to the area of the training samples which have previously been transformed into thematic raster data (compare chapter 5.2.2) thus allowing for the comparative computation and analysis of the Mobio change detection index for all time-series images. In contrast to the LANDSAT scene covering the WRS-2 tile of 180/75 where four time-series images for the years of 1991, 1999, 2000 and 2003 only three – 1992, 2000 and 2003 could be obtained for the scene of 176 / 79.

The information on changes, inherent in the training samples still remains comparable although an additional validation layer exists for the northern half of the study area. The missing 179/76 scene of 1999 only inhibits a coherent mapping of this state as no supervised classification product can be derived for the southern part of the study area.

For the previously defined threshold value of 70 %, training samples positively evaluated by the change index values of the compared time-series images decreased from the original number of 138 for the unitemporal classification to 108 valid samples for the year 2000, 93 for the 1999 and 80 for the time-series image of 1991 for the study area covered by the WRS-2 scene of 180/75.
From the 68 reference samples originally derived for the coverage of the satellite scenes of 179/76, 56 could be considered suitable for the timeframe of 2000 while 52 were positively evaluated for the year of 1992. Therefore the final set of valid training-areas obtained for the timeframe of 1991 and 1992 respectively forms the basis for all time-series imagery.
Both reference scenes of the year 2003 are also classified using this reduced training set to allow for comparison with the unitemporal classification utilizing the full reference set. Thereby emerging classifications shall in the following be referred to as retrospective or multitemporal classification in contrast to the unitemporal classification performed beforehand.

Although all time-series images are classified using the same set of 80 (180/75) and 52 (179/76) training-samples identified by the iterative procedure, the progressive decrease of reference area, due to the pixel-based change detection approach also becomes apparent (compare figure A6, annex a).

Despite those reference samples describing non-lichen covered areas all other samples associated with classes of the first hierarchical classification level show a total decline of more than 50 % of their initial coverage for the time-span from 2003 to 91/92. As the virtual invariance of the none-lichen covered areas is not astonishing, strongest variations of the lichen-covered areas can be regionally observed for the southern part of the study-area with a mean decrease of about 76 % of the total reference area in contrast to the northern part where mean decrease is about 62 %. Conjoined the overall decrease of reference area inherent in the training samples is about 64 %. Strongest class based reduction

could be observed for the fruticose-crustose lichen zone for the northern part of the study area (74 %) and the crustose lichen zone of the southern part (84 %) (compare figure A6, annex a).
Although this pixel-based spectral variability is quite noteworthy, a total of 36 % of the recently obtained reference information on lichen-covered areas was considered to be spectrally and thus thematically stable across all four different satellite images and a time period of twelve years.

In the following all signatures derived from the valid set of 132 training samples were further tested for all time-series images with some of them being aggregated within the training set editor while others were left for assessing the accuracy of the resulting classifications.
Due to the prerequisitions of the selected supervised Maximum-Likelihood classification algorithm another 22 training samples had to be subsequently excluded from the classification process. Thereby the total number of reference samples was reduced to 110, with 70 samples assigned to the spatial extend of the scene of 180/75 and 40 assigned to the coverage of the scene of 179/76.

As previously described for the unitemporal supervised classification spectral subclasses could be observed for many classes defined by the classification scheme although signatures were mostly aggregated from various training samples being evenly spread throughout the image thus allowing for a good representation of the variance within the target class. For these thematically homogeneous but spectrally heterogeneous classes, subclasses had to be included into the classification process.
Identification of spectral subclasses as well as further testing of the thematic affiliation of the training samples was accomplished analogue to the methodology described in chapter 5.2.2 by testing the signature separability based on the comparison of the covariance matrixes and the mean vectors for a pair of signatures. Again Jeffries-Matusita measures (JM) were used as a distance measure to predict the results of the Maximum-Likelihood classification (compare chapter 5.2.2).
In order to improve classification results, class separabilities were optimized wherever possible with various means. Firstly new sets of subclasses comprising higher separabilities were created including the substitution of the reference sites utilized to increase separability. Secondly pairs of classes whose separabilities were still too low after complete reassignment were merged using the signature editor. All of these measures were identically applied to all retrospective signature sets in order to allow best comparison of the classification results. This postulated comparability of the miscellaneous retrospective signature sets additionally required the consensus on some compromises regarding the aggregation and reassignment of reference samples.
Due to the testing of the signature separability of all training samples, signatures were aggregated into 19 signatures describing 6 different types of lichen community distribution defined by the classification scheme and 5 signatures describing the surrounding bare soil or rock types for all LANDSAT time-series images covering the WRS-2 scene of 180/75, while for all scenes of 179/76, spectral signatures were aggregated into 5 spectral classes describing 3 different types of lichen community distribution and 10 signatures of bare soil or rock. For accuracy assessment purposes 65 % of the training samples were excluded from the multitemporal classification process (71 of 110).
Alike the unitemporal signature set, many signatures of the retrospective set showed good

separability, but the number of class-pairs for which Jeffries-Matusita (JM) measured distances were slightly lowered, progressively increased for the retrospective signature sets. Therefore distinct separability measures showing values below the threshold of 1200 from which on separability decays, shall be discussed in the following. A full listing of the separability measures is shown in figure A7 through figure A13 in annex a.

Regarding the separability of the retrospective signature sets computed for the classification of the WRS-2 scene of 180/75 and its time-series images of 1991, 1999, 2000 and 2003 some congruencies and discrepancies as well as tendencies can be observed.
Compared to the unitemporal signature set which comprised a total of 30 spectral subclasses for the discrimination of 7 topclasses, only the number of distinguishable subclasses was reduced to 24 spectral signatures for all retrospective signature sets.
While all spectral subclasses of the foliose topclass as well as the crustose and crustose sparse topclass could still be discriminated by the reduced set, only two instead of four subclasses were determined for the foliose-crustose topclass. For the topclasses describing the fruticose and fruticose-foliose lichen the number of recognized subclasses was lessened by one.
Still the evaluation of the separability measures must be realized individually for each timeframe and topclass.
For the fruticose subclasses describing the coastal communities of the fine quartz gravel plain and the inland community of the undulating course gravel flats both dominated by the abundance of *Teloschistes capensis* (L.f.) Müll. Arg. excellent intra-class separability was realized throughout all retrospective signature sets. Slightly lowered inter-class separability can only be observed for the fruticose-foliose subclasses. As the coastal subclass 1.1 was well separable from all classes throughout the entire set, the inland subclass 2.1 shows fluctuating but slightly decreased values for the fruticose-foliose subclasses. This inter-class relationship shows lowest separability for the retrospective signature set of the year 2000 where one class-pair comprises a JM-value below the threshold of 1200. This contrasts with signature sets of the years 2003, 1999 and 1991 where no more than one class-pair of lowered separability can be observed.
This observation may be explained by the strong temporary modifications of the Central Namib Desert caused by substantial and extraordinary precipitation events preceding the satellite image of the year 2000 and the fact that with the exception of a few, all classes suffer from reduced inter-class separability within this timeframe. Also compare HACHFELD (2000).
The intra-class separability of the fruticose-foliose topclass was well accomplished for all retrospective signature sets, except 2000, where in accordance to its unitemporal counterpart slight deviations from the maximum separability can be observed.
For the retrospective set of 2000 three class-pairs of the fruticose-foliose topclass comprise JM-values slightly below the threshold of 1200. In contrast to the mountainous fruticose-foliose subclass 3.1 showing full separability for all timeframes, an overall reduced separability can be observed between the coastal and the inland subclasses.
Although some of these intra-class separability measures for the year 2000 are below the threshold of 1200 (85 %) of the maximum JM separability measure where separability becomes limited, all signatures were utilized for the classification process as test classifications showed insufficient results after affected signatures were either merged or excluded.
After all only intra-class separability was

affected while at the same time inter-class separability showed good results, although a lowered separability between the fruticose-foliose and foliose subclasses were observed for the retrospective signature set of 1991.
In total overall inter-class separability of the fruticose-foliose topclass was lowest for the timeframe of 1991 where 4 % of all inter-class relationships showed values below the threshold of 1200 and highest for the retrospective signature set of the timeframe of 2003 where no inter-class relationships below the threshold of 1200 could be observed. Excellent separability measures for classes describing none lichen-covered areas were accomplished for all timeframes.
For the foliose topclass intra-class separability was best for the retrospective signature sets of 2003 and 1991. The intra-class separability was lowest for the timeframes of 1999 and 2000 although still well above the threshold of 1200. In fact no JM-values below the 1200 threshold could be observed for the intra-class separability at all.
Inter-class separability of the foliose topclass steadily decreased from excellent for the timeframe of 2003 to a maximum of 3 class-pair values below the threshold of 1200 for the timeframe of 1991. These lowered measures emerge from the class-pairs with fruticose-foliose subclasses and were already discussed above. Another lowered separability measure was only encountered between the foliose-crustose subclass 1.3 describing the *Xanthoparmelia walteri* Knox, *Caloplaca, Neofuscelia, Lecidella* community of the fine quartz gravel plains and the foliose subclass 1.3 located on the same substrate but dominated by *Xanthoparmelia walteri* Knox. The lowered JM-value of 1184 for the class-pair was solely observed for the timeframe of 2000 and might as well also be caused by the already discussed strong temporary disturbances indicated in the image.
Inter-class separability of the foliose-crustose topclass can be considered very good throughout the signature sets with the slight exception of the timeframe of 2000. Supplementary to the already lowered separability determined for one of the foliose subclasses mentioned before and an observed separability measure slightly lowered for one of the crustose subclasses, the only landmark case of reduced separability between any class describing lichen-covered areas and those describing none-lichen covered areas can be observed. For the class-pair of the foliose-crustose subclass 2.1 describing the mountainous saxicolous *Xanthoparmelia walteri* Knox, *Caloplaca elegantissima* (Nyl.) Zahlbr. community and the none-lichen covered areas of the rocky ridges, rock debris and coarse gravel plains a separability of 1159 was observed. This is astonishing as all other separabilities of this class-pair are found ranging between 1374 and the full separability of 1414.
It is difficult to speculate what may have altered the reflectance for the particular timeframe of 2000 in such a way that distance measures between some signatures were reduced slightly below the threshold value of 1200 as reassignment of differing reference sites to these particular class-pairs also showed no positive effect on the JM-value. However test classification showed good delineation of the affected classes. Therefore it was decided to agree on a compromise and retain the class-pairs as changes to the retrospective signature set of the 2000 timeframe would have also affected all other signature sets and moreover involved the exclusion of an elementary subclass of the foliose-crustose community.

The intra-class separability of the crustose topclass was considered excellent throughout the entire retrospective signature set. Inter-

class separability comprises JM-values mostly above all thresholds with the exception of the slight positive relationship with one of the neighbouring foliose-crustose subclasses already mentioned above.
For the crustose sparse topclass intra-class separability can also be regarded excellent for all retrospective signature sets. In addition inter-class relationships also comprised good to excellent separability measures throughout the signature sets for all three subclasses identified. Good intra- as well as inter-class separability measures observed for the crustose-sparse topclass also applied to the five subclasses identified for the none-lichen covered areas, with the exception of one foliose-crustose subclass comprising only a fairly good distance value for the timeframe of the year 2000.

As far as the LANDSAT scene of 179 / 76 / 2003 was concerned most of the spectral similarities detected by the JM algorithm within the retrospective signature sets focussed on the delineation of the foliose-crustose subclasses and the reduced separability between two of the none-lichen-covered classes which were previously under discussion for the unitemporal classification.
Best overall separability was observed for the retrospective signature set assigned to the timeframe of 2003. In accordance to its unitemporal counterpart only two subclasses of the none lichen-covered topclass showed distinct similarities. Expressed by reduced JM-values these similarities were also observed within the retrospective signature sets of the year 2000 and 1992.
In addition the slight intra-class similarities of the foliose-crustose as well as their positive inter-class relationship with the crustose subclass 2.1 which were both previously discussed for the unitemporal classification for the year of 2003 were also observed. Both inter- and intra-class values of these relationships show their lowest JM separability measures for the timeframe of 2000 followed by 1992 and 2003. Alike the unitemporal signature set neither tentative reassignment to differing reference areas did improve the separability, nor did the merging of subclasses enhance the classification results compared to test classification performed with the full signature set. All signatures were therefore included in the classification.
Supplementary all signatures describing none-lichen-covered areas were well separated by the classifier form those signatures describing lichen distribution patterns.
Again this can be depicted as a quality measure for the training samples and the derived signature sets as lichen distribution itself is likely to be well classified with only slight insecurities for those classes potentially describing transition zones.

Recapitulating the similarity of both unitemporal and multitemporal signature sets for the year 2003 the observed congruencies and discrepancies expressed by the JM-values were not astonishing as most of the reference samples identified for use with the retrospective classification included full reference samples successfully utilized for the unitemporal classification beforehand. The retrospective signature set for the year 2000 performed surprisingly low in terms of intra- and inter-class separability measures especially if compared to the further back-dated sets for the years 1999, 1992 and 1991. Although in some cases class separability comprised lowered JM-distance measures, all test classifications utilizing the Maximum-Likelihood algorithm showed good delineation of all classes of the first hierarchical level of the classification scheme. The same overall picture emerged for the signature sets derived for the timeframes of 1999, 1992 and 1991. Although overall class

separability was superior for the timeframe of 1999 neither the signature set of 1992 nor 1991 showed delicate performance during test classifications. After all the delineation of all signatures describing none-lichen-covered areas form those signatures describing lichen distribution patterns was accomplished by all retrospective signature sets. Therefore the evaluation of the derived JM-distance values predicted a fairly good performance of the aspired Maximum-Likelihood algorithm, despite the reduced number of reference samples for the retrospective signature sets.

5.2.7 Multitemporal fuzzy enhanced classification

In the following the validated retrospective training sets were utilized for the independent supervised classifications of all time-series images included in this study. In compliance with the unitemporal approach, the supervised fuzzy convolution classification post processing technique, offered by the Erdas Imagine program suite, was used to obtain information on most likely pixel to class assignment as well as the corresponding Mahalanobis-distances. Additionally this information obtained for the pixel-memberships was used to gather information on overall classification stability according to FOODY (1999) (compare chapters 5.2.3 and 5.2.4).
Therefore the fuzzification of class membership and the analysis of the degree of membership using Mahalanobis-distances were performed on all time-series images.
As class-memberships in terms of Mahalanobis-distances as well as the best class values assigned to a pixel were derived for the user-defined order of six best classes and thereafter hierarchically stored within a layer-stack, the actual probability of class-memberships was again analysed utilizing the relationships of chi-square distributions of the Mahalanobis-distances proposed by FRANZEN ET AL. (1998).
Thus the hierarchically ordered chi-square distributions of the second to sixth best class to pixel assignments were compared to the distribution of the class assignment of the first order using the F-test approach to analyse their similarities (compare table 8).

With the exception of both LANDSAT scenes for the year 2003, whose compliances mostly resembled those of the unitemporal analysis (compare table 7 chapter 5.2.4.), all

180 / 75	Distance 1-2	Distance 1-3	Distance 1-4	Distance 1-5	Distance 1-6
2003 TS	81%	56%	30%	11%	3%
2000 TS	90%	72%	48%	21%	6%
1999 TS	83%	62%	37%	13%	4%
1991 TS	92%	75%	47%	21%	7%
179 / 76					
2003 TS	81%	60%	38%	18%	3%
2000 TS	91%	82%	59%	34%	15%
1992 TS	91%	81%	66%	42%	20%

Table 8: Analysis of the similarities of the chi-square distributions of the second to sixth best class to pixel assignments compared to the distribution of the class assignment of the first order using an F-test approach for a statistical confidence of 95 %.

other time-series imagery showed strong compliances of the third and fourth probability in regards of the first. Testing revealed strong influence of the third probability layer on the classification results as confusion in overall class allocation was strongly increased following its exclusion. Thus its utilization for all time-series images is proposed. Contrasting the fourth probability layer mostly introduced the same confusion of the foliose-crustose, crustose and crustose-sparse classes which had already been observed for the unitemporal fuzzy enhanced classification. It was therefore excluded. Thus the first three probability layers were utilized whereas for the time-series imagery of 2003 only the first two probability layers were included into the fuzzy likelihood classification.

Based on these results defuzzification of the fuzzy membership values back into hard values was performed in order to visualize the classification results. Hence the fuzzy convolution utility of the Erdas GIS suite which allowed the application of a moving window convolution filtering on a fuzzy classification with multiple output class assignments was utilized for computing a single class output file for each of the time-series images on the basis of the multilayer classification and distance file (ERDAS 2001[5]) (compare chapter 5.2.4).

With the creation of individual supervised classifications for all time-series images, the requirements for a Post Classification Change Differencing are met, whose greatest advantage is the production of change maps comprising a complete matrix of changes based on the classification results (SINGH 1989).
For the creation of retrospective distribution maps fully covering the study area the coherently mapped timeframes of 2003, 2000 and 1991/1992 were assembled into mosaics using an overlay function for the overlapping peripheral areas post-processing (compare chapter 6.5). Thus individual as well as conjoined accuracy assessment of the classification products is discussed subsequently. A result of this evaluation as well as analysis of the observed change patterns of the multitemporal classification is presented in chapter 6.
Finally the retrospective classification strategy as well as post-processing techniques lead to good results of the multitemporal classification products and present a first estimate of the temporal alterations of the distribution of the lichen communities of the Central Namib Desert for the time-span of 1991 to 2003.

5.2.8 Accuracy Assessment

The accuracy of remotely sensed data and all thematic products derived from it is critical to any successful mapping project. As the user of land-cover maps depends on the knowledge of how accurate the product is in order to use the inherent information efficiently, accuracy assessment is an important tool (TATEM ET AL. 2005). With various methodologies of accuracy assessment available some of them are generally accepted for remote sensing studies and can thus be regarded as standard approaches. Extensive information on assessing the accuracy of thematic maps derived from remotely sensed data is presented by CONGALTON (1991), JANSSEN & VAN DER WEL (1994), STEHMAN (1997), STEHMAN & CZAPLEWSKI (1998), and FOODY (2002).

While the non-thematic accuracy by which processing of the remotely sensed data was carried out has already been discussed in chapter 4.1 including its special influence (e.g. geocoding) on the multitemporal classification (chapter 5.2.5.1), the accuracy by which

the classification has transformed spectral pixel values into nominal classes has not been determined yet. This thematic accuracy reports on the correspondence between the class labels assigned to a pixel by the classification algorithm and the true class verified by reference data. Reference data either derived from the collection of ground truth data, auxiliary thematic maps or aerial photographs can therefore be regarded as a prerequisites for estimating the thematic accuracy (STEHMAN & CZAPLEWSKI 1998, POWELL ET AL. 2004).

If reference data were collected from ground truth within a study the common utilization for training of the classification as well as testing the accuracy of its results is realized by portioning the data in a training and test set prior to classification (compare chapter 5.2.2 and 5.2.6). Thus in-sample accuracy resulting from only testing the classification with the training set is avoided by using an independent reference set providing out-sample accuracy for testing of the overall classification precision (FOODY 2002). The necessary independent reference information, utilized within this study, was conjointly obtained labelled and statistically tested in the same manner as those reference sites included into the classification process during field visits (compare chapter 5.2.2).

In addition to theses prerequisites regarding general classification accuracy, certain particularities of the multitemporal need to be discussed. Although the same independent reference set is provided for the calculation of the contingency matrix, size of individual samples may vary due to the retrospective evaluation process applied to both training and reference samples (compare chapter 5.2.5).

On one hand this methodology allows for comparison of both retrospective classification and accuracy assessment result. On the other hand the average loss of 60 % of the original multitemporal valid reference samples due to the retrospective evaluation inevitably entails a limited credibility of the accuracy parameters derived. However, the number of reference samples and therefore the credibility of the accuracy parameters will increase as future field studies will produce additional reference samples also accomplishing the retrospective evaluation (compare chapter 5.2.5).

Supplementary to the provision of basic accuracy assessment components information on issues such as sampling design used for the acquisition of the reference set, the confidence in the ground data labels and their lineage might be helpful as it allows the evaluation of the procedures used (FOODY 2002). The polygonal sampling units of homogenous spectral information, forming the fundamental unit on which the accuracy assessment is based, are directly associated with the mapped land-cover features. Errors resulting from the in situ misclassification of reference data can be regarded low since all, truly subjective, in situ collection of reference areas were solely carried out by the author, thus increasing the confidence of the class labelling in the reference data. In addition all reference samples used for the accuracy assessment of the multitemporal classification were iteratively tested and spatially modified conjointly with the extraction of the retrospective signature sets described in chapter 5.2.6. The disadvantages of polygonal sampling units being solely associated with a particular map, are therefore avoided as only spatially adapted and thematically unaltered sampling units are utilized for validation purposes. Caused by the limited amount of reference samplings all accuracy measures were solely derived for the seven classes of the first hierarchical level of the classification scheme.

The sampling design however could not be based on random sampling for the accuracy assessment of the thematic maps as the very large study area in combination with the physically restricted access to many sites of the study area and the timely restrictions of field campaigns rendered such sampling design impracticable. Instead it is proposed to balance statistical requirements with practicalities in a way that practical issues shall not reduce the credibility of the accuracy statement derived (STEHMAN & CZAPLEWSKI 1998).

As neither a thematic reference map nor any other source of reference depicting past or present land- and lichen-cover was available to this study, the sampling design was accomplished by a non-probability sampling based on reference samples practically collected during field work preceding the classification process. Although it is virtually impossible to approve with confidence that these purposefully collected reference samples have the same attributes as the entire region, field visit of selected test areas of which the accurate geometric location is known, still forms one of the best approaches for assessing the accuracy of a classification (JANSSEN & VAN DER WEL 1994, STEHMAN & CZAPLEWSKI 1998, FOODY 2002, TATEM ET AL. 2005).

For subsequent studies and field campaigns it is nevertheless intended to utilize stratified probability sampling based on maps of accessibility zones, as this will diminish the pragmatic problems of inaccessibility while at the same time providing random probability sampling design (STEHMAN & CZAPLEWSKI 1998).

Based on these remarks on the sampling design a pixel based testing of the accuracy of the produced classifications is performed. This is realized with the cross tabulation of a unitemporal as well as multitemporal set of independent reference image pixels and the results of both unitemporal and multitemporal automatic classifications. As a consequence an extreme misclassification would inevitably result in a misallocation of the majority of reference pixels and thereby entail low accuracies.

This cross tabulation also known as contingency matrix, confusion matrix or error matrix is a table of numbers set out in rows and columns, which represent the number of reference units assigned to a particular class relative to the class verified by the ground truth. This matrix provides a basic description of the classification accuracy in different ways while at the same time allowing comparison of accuracies (FOODY 2002).

Firstly the overall accuracy describes the agreement of the correctly classified objects to the total number of the points of reference. It is calculated by dividing the sum of correctly classified samples, indicated by the major diagonal of the matrix, by the total number of samples taken. The obtained overall classification accuracy is a measure of the classification as a whole not indicating the distribution of accuracy across individual classes. Therefore further measures need to be calculated.

Secondly the probability by which an object of the reference data will be correctly classified is indicated by the producer's accuracy. It is calculated by the division of the correctly classified objects of a class by the total number of reference samples for that particular class (column total).

Thirdly the probability that a sample of the classified image actually represents the class indicated by the reference data is known as user's accuracy. In other words the user's accuracy gives information about the reliability of the classified maps and shows if an object was assigned according to the class reality. It is calculated by the division of the correctly classified objects by the number of

all classified objects of that class (row total) (CONGALTON 1991, JANSSEN & VAN DER WEL 1994, STEHMAN 1997, STEHMAN & CZAPLEWSKI 1998, FOODY 2002).

Directly related to class specific accuracy based on both user's and producer's accuracy the simple measures of error of omission and commission can also be derived. While error of commission in percent is the difference between 100 and the user's accuracy, the error of omission is obtained from the difference between 100 and the producer's accuracy (JANSSEN & VAN DER WEL 1994). However these two simple measures shall not be utilized in the following.

Instead an additional measure for the overall thematic accuracy shall be calculated. The Kappa coefficient of agreement utilizes all elements of the contingency matrix in contrast to the overall accuracy described above. Forming a measure of the difference between the actual agreement between the reference data and an automated classifier as well as the chance agreement between the reference data and a random classifier it is computed as presented in formula 4 (LILLESAND & KIEFER 2000[5]).

$$\kappa = \frac{N\sum_{i=1}^{r} \chi_{ii} - \sum_{i=1}^{r} (\chi_{i+} \cdot \chi_{+i})}{N^2 - \sum_{i=1}^{r} (\chi_{i+} \cdot \chi_{+i})}$$

Formula 4: Calculation of the Kappa coefficient of agreement Source: LILLESAND & KIEFER (2000[5]), P. 574.

r = number of rows in the confusion matrix

X_{ii} = total number of observations in row i and column I (on the major diagonal)

X_{i+} = total observations in row i (shown as marginal total to right of the matrix)

X_{+i} = total observations in column i (shown as marginal total at bottom of the matrix)

N = total number of observations included in matrix

5.2.9 Assessing classification accuracy using class-membership probabilities

Although the accuracy assessment of both unitemporal and multitemporal classifications with the means of confusion matrices and derived accuracy parameters as well as metrics provides good insight into the overall prosperity of the classifications and its thematic classes, only a site specific assessment of the correspondence between the image classification and ground truth is obtained (FOODY 2002). Therefore, spatial distribution of error is not analysed by these quantitative measures. For the supplemental determination of the spatial distribution of error the establishment of a regional accuracy assessment, on the account of the spatial extend of the twelve major lichen field units identified within this thesis, is proposed (compare chapter 6.1). Due to the lack of unequally distributed area-wide reference data the use of stratified error matrices can be regarded unsuitable. However lichen field specific classification accuracy can partly be derived from the analysis of the probabilities contained in the Mahalanobis-distances computed for each of the fuzzy enhanced classifications (compare chapters 5.2.4 and 5.2.7).

Firstly used to assess information on strong or weak memberships between pixels and their assigned classes exist by analysing the probability of allocation, the given information shall in the following be utilized in a lichen field specific framework. By depicting whether all pixels grouped into a specific lichen field show strong or weak member-

ships to their designated classes in terms of their probability, an accuracy accounting for the spatial distribution of error for all classifications is presented and analysed. These observed regional disparities are of special importance to the multitemporal classifications produced as inevitable regional uncertainties within the classification are directly incorporated into the monitoring of changes. With the analysis of the similarities of the chi-square distributed Mahalanobis distances on a per lichen field basis it is tested whether the allocation of the differing classes can be regarded equiprobable or if the assignment of all other classes other than the first can be regarded insecure. Therefore all computed Mahalanobis distances h for the first to sixth best class are utilized according to FRANZEN ET AL. (1998).

Thereby sturdy high equiprobability values encountered for layers (classes) otherwise given a low overall probability, in comparison to the most probable layer (class), depict an insecure class assignment. Whereas head on low or rapidly decreasing equiprobability values predict good and stable class-assignments and classification results. The results of this approach are presented in chapter 6 (results).

6 Results

This chapter presents the results of both unitemporal and multitemporal classification approaches. Based on the methodology presented in the previous chapters 5.2.8 and 5.2.9, the accuracy of the classification results shall be analysed firstly. In addition to accuracy parameters and metrics derived from confusion matrices, the results of a regional accuracy assessment accounting for the spatial distribution of error shall be discussed.
For the unitemporal classification a first map depicting the distribution of lichen communities in the Central Namib Desert is presented while at the same time twelve coherent lichen field were found to exist in the study area using the underlying approach. They shall be presented and discussed subsequently. For the multitemporal classification approach maps depicting the results a change matrix computation of the image pairs 2003 – 2000 and 2000 – 1991/92 are presented for the study area. To reduce the overall workload the lichen field of Wlotzkasbaken will serve as an example for the detailed and extended analysis of the spatiotemporal changes caused by differing natural and anthropogenic disturbances involving digital elevation model (DEM) derived data as well as climate data, and field observations. Comprehensive descriptive statistics of complete and lichen field specific distribution patterns are presented in annex c, d, and e.
Mapping of the results was accomplished with the Erdas program suite. The six lichen communities which had previously been identified on the basis of morphological groups are described by differing colours as well listed in the legend included with every map. The none lichen covered areas were blinded out and their coverage was filled with grey-scale information derived from the panchromatic channels of the appropriate LANDSAT timeframes. Conjoined with the overlay of major and minor roads and the labelling of important landmarks map orientation is strongly enhanced. The Atlantic Ocean bordering the study area to the west was masked as well to limit printing expenses.

6.1 Analysing accuracy parameters of the unitemporal classification

The analysis of the accuracy of the unitemporal classification presented in chapter 5.2.4 focuses on the accuracy parameters discussed in chapter 5.2.8. These accuracy measures present differing estimates of misclassifications inherent in both LANDSAT scenes classified. Although their accuracy is discussed separately an area-wide accuracy covering the whole study area is also presented.
For the extraction of the contingency matrix a thematic data layer containing independent reference samples previously excluded from the supervised classification was used for accuracy assessment. User's and producer's accuracy as well as the Kappa coefficient were derived using spreadsheet calculations. Starting with the analysis of the unitemporal classification accuracy measured for the LANDSAT scene of the WRS-2 position 180 / 75 acquired 22nd of April of 2003 its contingency matrix is presented in table 9.

The overall accuracy encountered for this classification was 87 % rounded off. This overall accuracy exceeds the commonly recommended target accuracy of 85 % proposed by FOODY (2002). Accuracy measures of the overall producer's accuracy ranged from 37 % to 100 % while overall user's accuracy varied between 59 % and 99 %.
The variation observed for the probability by which an object of the reference data was

correctly classified, also known as producer's accuracy, can mainly be ascribed to the fourth class indicating the foliose-crustose lichen zone. With all other classes showing values ranging from 70 % to 100 %, the producer's accuracy of the foliose-crustose lichen zone measures only 37 %. This is being caused by an obvious confusion of the foliose-crustose lichen zone with the neighbouring classes of the foliose- and the crustose lichen-zone who account for more than 40 % of the foliose-crustose reference samples. In addition 15 % of the reference pixels were ascribed to the class 7 depicting no lichen cover.
While the producer's accuracy of this class is truly disappointing, it might as well be explained by the composition of the reference samples themselves. As the foliose-crustose lichen zone is considered a transition zone within the classification scheme of lichen distribution its in-situ delineation can be quite difficult, as previously discussed in chapter 5.2.2. Although the classification process solely involved those samples comprising the most homogenous and genuine characterization of each class, reference samples of this difficult class might not. This assumption is also supported by the very good user's accuracy of 78 % of this class demarcating the probability that a sample of the classified image actually represents the class indicated by the reference data.
The same relationship between producer's and user's accuracy can also be observed for the crustose-sparse lichen zone (class 6) whose adjacency and often smooth transition to bare or gravel-covered top-soils is expressed in the differing class-specific accuracy measures.

Information about the reliability by which the classified thematic maps and its inherent classes reflect the reality indicated by the reference samples is expressed by the user's accuracy. Although lowest for the foliose-lichen zone (class 3) with 59 % all other classes depicting lichen community distribution patterns showed values ranging from 78 % to 99 % with best accuracies observed for the fruticose lichen zone and the none lichen-covered areas.

These promising results are also reflected by the Kappa coefficient measuring the difference between the actual agreement between the reference data and an automated classifier as well as the chance agreement between the reference data and a random classifier according to LILLESAND & KIEFER (2000[5]).

	Class 1	Class 2	Class 3	Class 4	Class 5	Class 6	Class 7	Sum	Users
Class 1	3287	28	0	0	0	0	0	3315	99%
Class 2	278	2773	283	93	28	0	0	3455	80%
Class 3	22	458	1191	259	85	0	10	2025	59%
Class 4	0	28	31	552	72	0	26	709	78%
Class 5	1	35	42	368	1716	18	0	2180	79%
Class 6	0	0	1	6	138	898	18	1061	85%
Class 7	28	165	119	234	53	370	12065	13034	93%
Sum	3616	3487	1667	1512	2092	1286	12119	25779	Matrix Sum
Producers	91%	80%	71%	37%	82%	70%	100%		22482
			Overall-Classification-Accuracy			87%			
			Overall-Kappa-Statistics			0,82000196			

Table 9: Contingency matrix of the unitemporal supervised classification of LANDSAT scene of the WRS-2 position 180 / 75 acquired 22nd of April of 2003.

According to ORTIZ ET AL. (1997) who proposed a benchmark system for the evaluation of thematic classifications based on the Kappa coefficient, values ranging from 0.60 to 0.80 surely characterize a very good classification. With the discussed classification comprising a Kappa coefficient of 0.82 it even exceeds the interval of very good classifications delineated by this metric. Therefore the Kappa coefficient proposes that the discussed classification is by 82 % better than a random classifier applied to the same original data set.

Overall accuracy of the unitemporal classification of lichen communities based on the LANDSAT scene of WRS-2 position 179/76 acquired 1st of May of 2003 is specified by 87 %, conterminous to the classification of its neighbouring counterpart. It is presented in table 10.

Calculation of class specific producer's and user's accuracy was limited to classes four to seven as the classes indicating fruticose-, fruticose-foliose and foliose lichen communities could not be observed for the area covered. In contrast to the somewhat low producer's accuracy encountered for the foliose-crustose class within the northern part of the study area, this class was very well characterized by the reference data for the southern part of the study area. In addition user's accuracy for this class featured a rounded 100 %. This is explained by the contrasting occurrence of the foliose-crustose class within the southern part of the study area. Differing from the often patchy distribution of this class found on the fine quartz gravel plains and course rock debris areas in the northern part of the study area, its distribution pattern on the gravel hummocks and gypsum plains of the southern part is mainly homogenous, thus enhancing delineation and classification of this particular lichen community.
On the other hand both user's as well as producer's accuracy of the crustose-sparse lichen community were largely decreased to values of 48 % and 43 % respectively, due to environmental characteristics of the southern part of the study area. Here the natural patchiness and the adjacency and often smooth transition to barren gypsum soils (class 7) are not only expressed by the producer's accuracy values but also by the user's accuracy with 52 % of the classified objects belonging to the seventh class. Therefore the mapped distribution of this class must be critically questioned for all areas south of the Swakop River.

	Class 1	Class 2	Class 3	Class 4	Class 5	Class 6	Class 7	Sum	Users
Class 1	0	0	0	0	0	0	0	0	0
Class 2	0	0	0	0	0	0	0	0	0
Class 3	0	0	0	0	0	0	0	0	0
Class 4	0	0	0	687	1	0	0	688	100%
Class 5	0	0	0	161	566	36	0	763	74%
Class 6	0	0	0	0	0	113	121	234	48%
Class 7	0	0	0	11	19	111	1809	1950	93%
Sum	0	0	0	859	586	260	1930	3635	Matrix Sum
Producers	0	0	0	80%	97%	43%	94%		3175

Overall-Classification-Accuracy	87%
Overall-Kappa-Statistics	0,79976709

Table 10: Contingency matrix of the unitemporal supervised classification of LANDSAT scene of the WRS-2 position 179/76 acquired 1st of May of 2003.

Nevertheless the Kappa coefficient of a rounded 0.80 indicated the observed classification is 80 % better than one resulting from chance.

For the area-wide accuracy assessment and the combination of both independent classifications discussed above, the following picture emerges (compare table 11):

The overall accuracy of the classes of the first hierarchical level of the classification scheme measured 87 % for the combined accuracy assessment of southern and the northern part of the study areas. However, it must be kept in mind, that combined accuracy assessment of the individual classifications can also affect accuracy measures due to regional disparities. Best classification results according to user's accuracy are obtained for the fruticose lichen zone (99 %), and the none lichen-covered (93 %) zone, followed by the crustose-foliose lichen zone (89 %), and the foliose-lichen zone (80 %). These good results are as well reflected in the combined Kappa coefficient of 0.82 by which the presented distribution map of the lichen communities of the Central Namib Desert for the year of 2003 is better than one resulting from chance.

6.2 Analysing accuracy parameters of the multitemporal classification

In the following the accuracy of the seven retrospective classifications performed in chapter 5.2.7 is analysed. For the WRS-2 scene of 180/75 four time-series classifications for the years of 2003, 2000, 1999 and 1991 are analysed conjointly with the southern scene of 179/76 classified for the timeframes of 2003, 2000 and 1992. Thus a combined accuracy assessment addressing the whole study area could only be carried out for the conjointly classified timeframes of 2003, 2000, and 1991/1992.
The combined overall accuracy for the multitemporal classification varied between 79 % and 86 %. While area-wide overall accuracy for the timeframes of 2003 and 2000 was above the threshold value of 85 % proposed by FOODY (2002), it was below that value for the timeframe of 91/92 (compare figure A14, A15, and A16, annex a)

Supplementary the Kappa coefficient confirmed these findings, reporting a rounded 0.79 for the combined multitemporal classification of 2003, 0.80 for the year of 2000 and 0.72 for the timeframe of 91/92. Despite all

	Class 1	Class 2	Class 3	Class 4	Class 5	Class 6	Class 7	Sum	Users
Class 1	3287	28	0	0	0	0	0	3315	99%
Class 2	278	2773	283	93	28	0	0	3455	80%
Class 3	22	458	1191	259	85	0	10	2025	59%
Class 4	0	28	31	1239	73	0	26	1397	89%
Class 5	1	35	42	529	2282	54	0	2943	78%
Class 6	0	0	1	6	138	1011	139	1295	78%
Class 7	28	165	119	245	72	481	13874	14984	93%
Sum	3616	3487	1667	2371	2678	1546	14049	29414	Matrix Sum
Producers	91%	80%	71%	52%	85%	65%	99%		25657

Overall-Classification-Accuracy	87%
Overall-Kappa-Statistics	0,82003858

Table 11: Contingency matrix of the combined unitemporal supervised classifications for the year of 2003.

three values of the Kappa coefficient describing a very good to excellent result according to ORTIZ ET AL. (1997) and overall accuracy either above or only slightly below the proposed accuracy measures by FOODY (2002), class-specific as well as individual accuracy comprised mixed results.

Starting with the producer's accuracy of the combined multitemporal classifications the reference samples of the foliose-crustose lichen zone (class 4) comprised insufficient accuracies for all timeframes progressively decreasing form 18 % to 17 % to 8 % for the timeframe of 91/92. This is also reflected by the producer's accuracies obtained for that class from individual testing of the seven multitemporal classifications (compare figure A14 through figure A23 in annex a).

Similarly the producer's accuracy for these classifications decreased for the foliose-crustose lichen zone in a progressive downward manner from a maximum of 20 % to a minimum of 8 %. In addition user's accuracy for this class comprised somewhat higher but still disappointing values ranging from 47 % down to 23 % for the combined and 44 % down to 19 % for the individual contingency matrices. Despite this decrease of accuracy matching the time gradient, overall accuracy measures of the foliose-crustose lichen class were slightly raised though still inadequate for the northern part of the study area.
The same could be observed for the user's accuracy of the sparse crustose lichen zone (class 6). The class specific error rates of the sparse crustose lichen zone for the area-wide user's accuracy values ranged from 39 % down to only 29 %. Lowest values could however be encountered for the individual accuracy assessments of the multitemporal classification results. With user's accuracy measures reaching down to a mere 6% of accuracy in the southern part of the study area and reference objects mainly being allocated to neighbouring classes the sparse crustose lichen zone proved to be the most difficult to classify.
For the timeframes of 1999 and 1991 and solely limited to the northern part of the study area a low user's and producer's accuracy of the crustose lichen zone (class 5) could also be observed. Conjoined with the high user's accuracy of 72 % for that class obtained for the southern part of the study area and the timeframe of 1992 the combined user's accuracy for the timeframe of 91/92 was measured to be only 38 % area-wide.
Weakest individual multitemporal classification according to class-specific parameters was achieved for the timeframe of 1999, while lowest reliability according to overall classification measures and Kappa coefficient was obtained for the timeframe of 1991 with both timeframes covering the northern part of the study area. In contrast the best time-series classification, utilizing the reduced training, was also obtained for the northern part but for the timeframe of 2003 according to all accuracy measures.

Classes best classified according to accuracy measures obtained for the southern part of the study area (WRS-2 scene of 179 / 76) comprised the crustose lichen zone (class 5) with an average 67 % and the none-lichen covered areas (class 7) averaging at 98 %. For the northern part and the scene of 180 / 75 the classes considered best classified by the obtained measures included the fruticose lichen zone (class 1) averaging at 99 % user's accuracy, the fruticose-foliose lichen zone (class 2) averaging at 72 % and again the none-lichen covered areas averaging at a rounded 87 % accuracy.
Therefore it can be stated that land-cover changes derived for the crustose-foliose and

sparse crustose lichen communities and in part the foliose lichen community must be regarded insufficiently characterized according to user's and producer's accuracy. On the contrary promising insights into land-cover changes of lichen communities can be derived for the fruticose-, the fruticose-foliose- and the crustose lichen community according to these measures. In addition changes regarding the expansion and formation of none lichen-covered areas can also be precisely mapped using this retrospective classification approach, although a large number of erroneous change indications can be produced since an error on either date can give a false indication of change (SINGH 1989).

6.3 Analysing classification accuracy using class-membership probabilities

Compared to the area-wide analysis of class assignment probabilities already accomplished for unitemporal and multitemporal classifications where overall stability of class assignments was reflected, the lichen field specific probability measures show mixed results (compare figure A24, annex a).

Very little differences regarding the stability of lichen field specific class-assignments can be observed between the unitemporal and multitemporal of the timeframe of 2003. With the exception of the third lichen field all lichen field areas depict rapidly decreasing equiprobability values for classes given a low probability of assignment. Thereby a good overall class-assignment can be stated for the unitemporal und multitemporal classifications of the timeframe of 2003.
The slightly raised equiprobabilities observed for the third lichen field are mainly based upon its unfortunate position on the respective edges of the bordering LANDSAT scenes utilized for this thesis and can also be observed for all subsequent timeframes of the multitemporal classification.
Although being of different origin, raised equiprobabilities of classes otherwise given low probabilities of assignment can also be observed for the southernmost lichen fields one and two. The lichen field of the southern Naukluft Plateau (No. 1) depicted a compliance of 90 % of chi-square distribution between the first and the third probability and a compliance of 74 % between the first and the fourth for the timeframe of 1992. This could also be observed for the lichen field of the northern Naukluft Plateau (No. 2) where a compliances value of 91 % and 76 % are reported between the same probability layers for the same timeframe. This is as well supported by the previously obtained accuracy measures for the area-wide classification product where confusion between classes depicting lichen distribution resulted in low user accuracies and best separability measures depicting slight inter-class similarities beforehand to classification (compare chapter 5.2.6). Still all problems focused on the differentiation of lichen distribution patterns whereas differentiation of lichen distribution and none-lichen covered areas was accomplished at all times.
For the lichen field of Mile 8/Mile 12 (No. 4) located in the northern part of the study area rapidly decreasing measures of equiprobability were obtained for all timeframes although a constant gradient of weakened class-memberships towards anterior classification could be observed. Even better equiprobability measures also following the backward gradient could be observed for the adjacent lichen fields of Wlotzkasbaken (No. 5), Jakkalsputz (No. 6), the Omaruru gravel plain (No. 7) and Mile 72 (No. 8). Excellent relationship of

probability measures could be obtained for the area of the Cape Cross lichen field (No. 10).
Probably due to the multitude of spectral characteristics, the highly diverse lichen field of the Messum Crater / Orawab (No. 9) comprised high equiprobability values of the third and fourth probability for the multitemporal classifications of 2000 and 1991. Many of the insecurities reflected by high probabilities of class-memberships might be based on the foliose- and foliose-crustose lichen zone abundantly covering the outer reaches of this lichen field also providing low class-specific accuracy measures for the timeframes under discussion.
In regards of the lichen fields of the Brandberg-West-Road (No. 11) and the northernmost lichen-field of the Huabmond (No. 12) mixed results were obtained for the approach presented. Strong inter-annual variations of the probability of class-membership potentially reflect strong fluctuations of classification accuracy. In combination with the lowered accuracies obtained for the foliose- and foliose-crustose lichen zone prevailing in theses lichen field the results obtained from a change detection based on post-processing classification comparison should be evaluated with care.

In contrast to these obvious findings, where the combination of the differing accuracy measures resulted in a clear proposal, ambiguous coherences could also be observed. An example for the ambiguity of the differing accuracy measures can be found in the time-series classifications of 1999 and 1991 of the WRS-2 scene of 180/75.
In the same way as the "standard" accuracy assessment performed in the previous chapter indicated the time-series classification of 1999 to be problematic regarding its user's and producer's accuracy, the analysis of class-membership probabilities depicted good to very good class-assignments for this timeframe. Class-specific accuracy measures derived for the time-series classification of 1991 nearly were as problematic but additionally included lower overall accuracy measures. Contrasting to the good class-membership values derived for the timeframe 1999, class-assignment for this timeframe was significantly weaker except for lichen field number eleven. Whether the observed discrepancies can be assigned to the differing scale inherent in both approaches with most of classification uncertainties located outside the delineated lichen fields can only be assumed.
However the very fact that these lichen fields show very high equiprobabilities for classes given a low overall probability at these particular timeframes does not render the obtained classifications useless but reflects a potential uncertainty which might or not might not have been previously observed for the contingency matrix derived accuracy parameters. In addition the differing number of classes of the first hierarchical classification level as well as spectral subclasses inherent in the differing lichen fields might also affect the spatially confined probabilities of class-memberships.

Recapitulatory it can therefore be stated that the spatially adaptive analysis of potential classification error with the means of class-membership probabilities gives good insight into the regional disparities regarding the accuracy of the produced thematic classifications. In combination with accuracy measures obtained from individual or combined contingency matrices a good evaluation of the classifications can be accomplished.
In addition to the good reproduction of natural lichen distribution patterns accomplished by the unitemporal classification, the multitemporal classification products also reflect the high potential of the presented retrospec-

tive classification strategy towards a highly detailed future semi-automatic monitoring.

6.4 Unitemporal classification

In the following chapter results of the unitemporal supervised classification of lichen distribution of the Central Namib Desert are discussed in detail. Therefore a first map depicting the assessed lichen distribution patterns is presented for the study area of the Central Namib Desert. This map is enclosed to this thesis and serves as the basis of all subsequent discussions.
To aid the statistical analysis of the study area the result of the full regional classification extending from Gobabeb (south) to Huabmond (north) was subdivided into twelve major coherent lichen field units. In total the delineated lichen fields in the year 2003 consisted of a lichen coverage of 1825 km². The remaining area outside of these coherent lichen fields also covering an impressive 875 km² shall not be discussed in the following because of its incoherent spatial patterns mostly dominated by crustose lichen communities.
Maps describing the spatial extend of the dissected lichen field units, statistically and thematically referred to as 'lichen fields', can be found in figure A25, annex a.
Areal statistics addressing these coherent lichen field are presented in annex c.
In addition densely overgrown inselberg structures are not discussed in the following as these orographic habitats are not defined as lichen fields, although species richness often exceeds that of the 'flat' terrains covered by lichens (MATTICK 1970). Good examples of these inselberg structures comprise the Lagunenberg near Cape Cross, various mountain ranges surrounding Messum Crater in the northern part as well as large dolerite ridges, felsite dykes and the area of the Swakop and Kuiseb Canyon in the southern part of the study area.
Similarities observed for all lichen fields include main species composition and zonation, whereas strong distinctions were found in the spatial extend, distance to coast and top soil cover.

6.4.1 Lichen field of the Southern Naukluft Plateau (No. 1)

Extending alongside the dirt road C14, southeast of Walvis Bay, in northerly and southerly direction a coherently lichen covered area of about 231 square kilometers (23091 hectares) is located. Neither SCHIEFERSTEIN (1989), LORIS & SCHIEFERSTEIN (1992), nor WESSELS & VAN VUUREN (1986) reported on this lichen field south of the Tumas Rivier (compare map 1).
Crustose lichens constitute the overall dominant growth form (covering about 221 km²) interspersed with a mixture of foliose and crustose lichens (covering about 10 km²).

The areas covered by the crustose lichen zone (130 km²) are characterised by the terricolous species of *Caloplaca volkii* Wirth & Vezda, *Lecidella crystallina* Wirth & Vezda, and the sand-binding species *Acarospora schleicheri* (Ach.) A. Massal. dominating with nearly 100 % cover firmly attached to fine quartz gravel and encrusted sandy gypsum substrate.

The sparse crustose lichen zone comprising about the same species composition as the crustose lichen zone, however covering only about 20 % of the ground, is found on non-stabilized sandy gypsum substrates (91 km²). Where *Lecidella crystallina* Wirth & Vezda and *Caloplaca volkii* Wirth & Vezda are prevailing lichen cover can show strong wind induced

'wave patterns' (compare figure B35 and B36, annex b).

The areas where the foliose-crustose lichen community is abundant are mostly found about 20 km inland of Walvis Bay in the northern part of the lichen field limited to gypsum and mica rich coarse gravel hummocks. In addition to the species found in the crustose lichen community *Xanthoparmelia walteri* Knox and *Xanthomaculina convoluta* together with scattered *Teloschistes capensis* (L.f.) Müll. Arg. and *Ramalina* sp. occur.

Phanerogames are scare and scattered in this lichen field. Individuals of *Zygophyllum stapfii* and *Arthraerua leubnitziae* are the only shrubby inhabitants, mainly confined to sandy washes. Although located within the Namib Naukluft Park power lines and several untarred primary and secondary roads dissect the lichen field. Due to the close proximity of Walvis Bay and Walvis Bay International Airport there is heavy traffic encountered through this lichen field. This increases as well the frequency of vehicles leaving the roads, criss-crossing through the desert, destroying the lichen communities. This is exceptionally pronounced in the southern part of the lichen field, where a lot of 4 X 4 tourist vehicles cross the sensitive area towards the Kuiseb River Canyon.

6.4.2 Lichen field of the Northern Naukluft Plateau (No. 2)

Described as the southernmost lichen field of the Central Namib Desert by SCHIEFERSTEIN (1989), LORIS & SCHIEFERSTEIN (1992) and

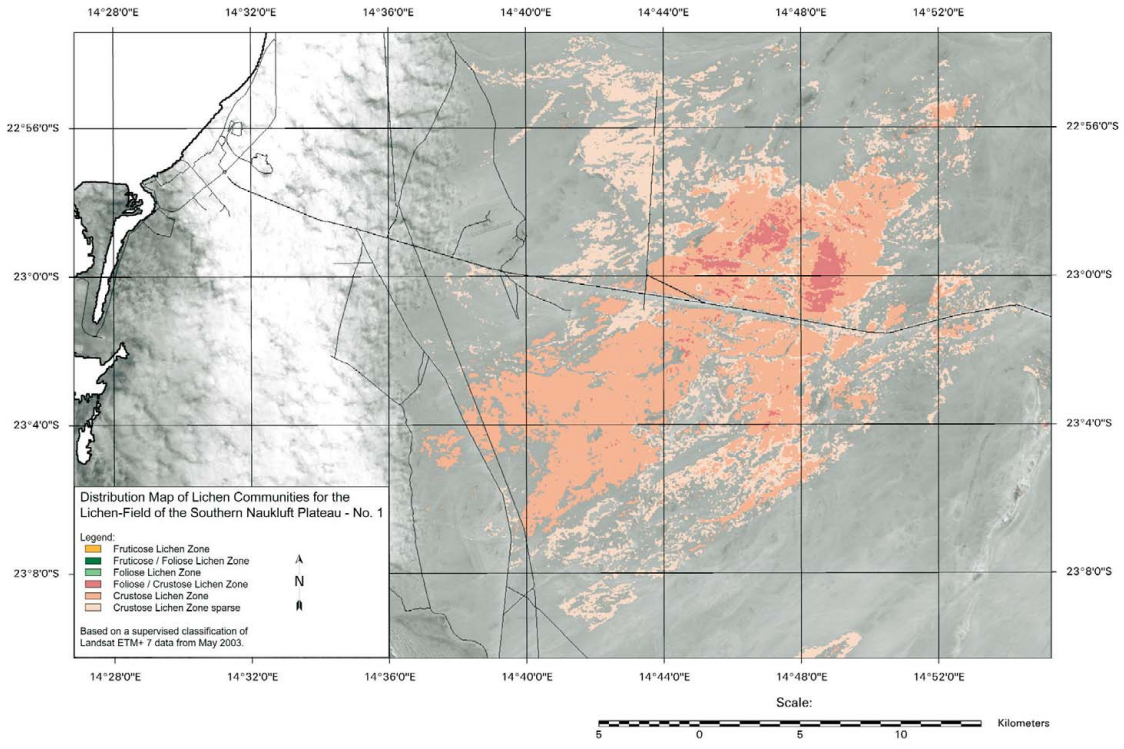

Map 1: Lichen field of the Southern Naukluft Plateau (No. 1), Central Namib Desert, Namibia.

WESSELS & VAN VUUREN (1986) the second lichen field of the northern Naukluft Plateau is bordered by the Swakop Canyon in the north and the Tumas Rivier in the south, a coastal dune belt in the west and by the limited outreach of the coastal fog zone to the east (about 30 km inland). It is dissected by the Khomas Hochland (compare map 2)

Congruently to the lichen field no 1 crustose lichens constitute the overall dominant growth form (covering about 255 km^2), interspersed with a mixture of foliose and crustose lichens (covering about 16 km^2).

The crustose lichen community resembles the species composition of lichen field no. 1 with abundant cover of *Lecidella crystallina* Wirth & Vezda and *Caloplaca volkii* Wirth & Vezda of the terricolous sand-binding species on the slightly undulating gypsum and mica rich plains. Found within sandy washes the anatomically interesting vagrant lichen species *Xanthomaculina convoluta* is well represented in this community. *X. convoluta* has become well adapted to this environment with individuals blown by wind (GIESS 1989). Unknown species of *Arcarospora, Buellia, Caloplaca, Diplochistes,* and *Lecidea* also occur subordinately.

The sparse crustose lichen community is mostly found on the outskirts of the crustose lichen zone, where abundance and ground cover decrease due to disturbances by washes and strong winds (SCHIEFERSTEIN 1989).

Throughout this lichen field with a slight accumulation within the area fenced by the Goanikontes and C28 road abundant patches of the foliose-crustose lichen community can be observed, limited to the gypsum and mica rich coarse gravel hummocks.

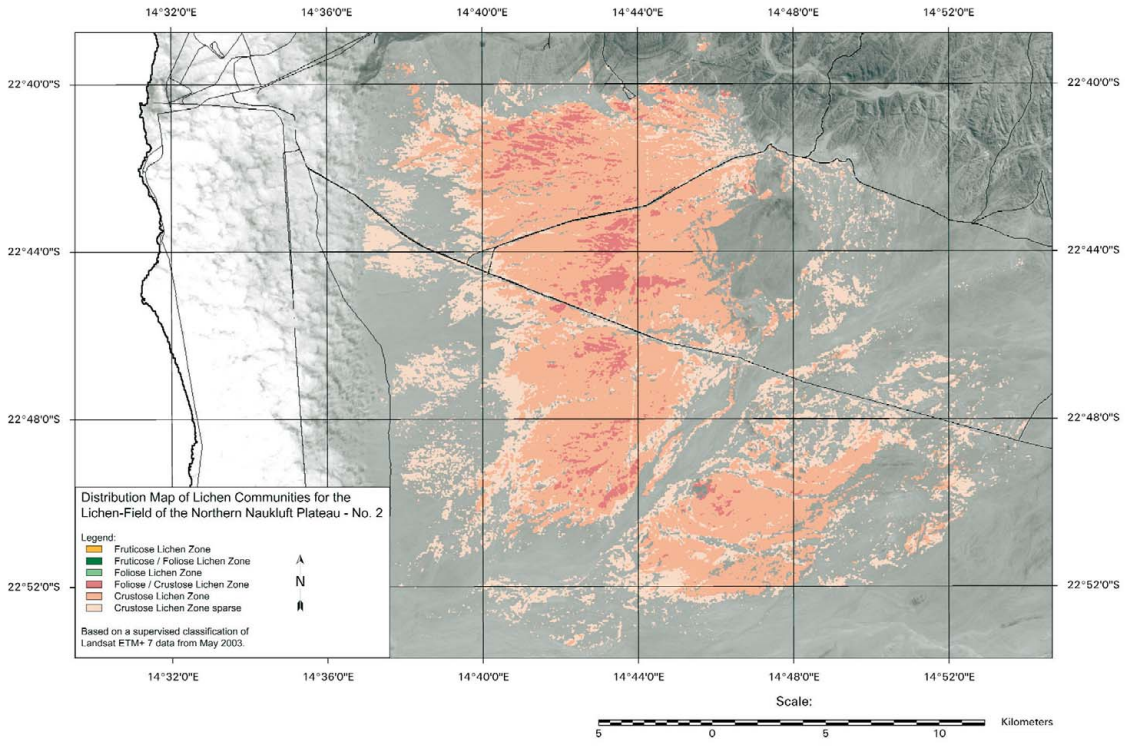

Map 2: Lichen field of the Northern Naukluft Plateau (No. 2), Central Namib Desert, Namibia.

Scattered within this community *Teloschistes capensis* (L.f.) Müll. Arg. and *Ramalina sp.* can be found from up a coastal distance between 15 and 20 km. The almost total absence of these fruticose species with the exception for south-westerly facing slopes on a local scale strongly reflects the heavy easterly winds frequently occurring within this area. Whereas *Xanthoparmelia walteri* Knox is obviously less affected by this disturbance, taking its abundance within this lichen zone as an indicator.
As in the first lichen field the phanerogame vegetation can be observed in sandy washes.
Based on the close proximity to the touristic centre of Swakopmund as well as the natural scenic landscapes of the Swakop Canyon and the heavily frequented Welwitschia drive much disturbance arises from vehicle traffic. Although off-road driving is strictly prohibited within the Namib Naukluft Park area dust plumes caused by high-speed traffic obviously degrade the lichen communities alongsides the roads. Obscuring their photosynthetic systems with the repeated dust cover lichen communities are condemned to die back.

6.4.3 Lichen field of Nonidas (No. 3)

Although partly covered by fog clouds in the unitemporal supervised classification of 2003 the mappable north-eastern part of the lichen field of Nonidas is discussed here. Located north of the tar road B2 (Swakopmund - Okahandja) and dissected by the railroad most of the lichen distribution covering 26 km² in total is limited to a range of outcrops (compare map 3).
Dominated by crustose communities as well sparse crustose communities nearly equal the

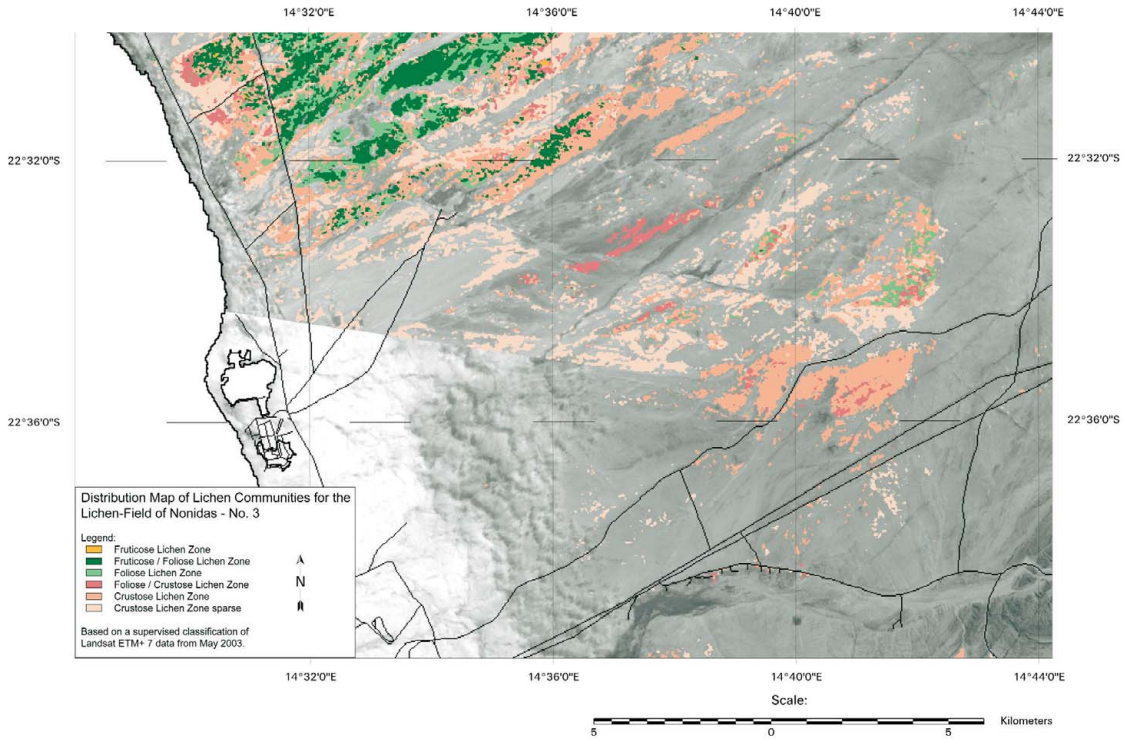

Map 3: The Nonidas lichen field (No. 3), Central Namib Desert, Namibia. Partly covered by fog clouds.

distribution of the crustose lichen zone, reflecting the overall patchy distribution pattern, which can be as well observed in the rather low extent of the foliose-crustose lichen zone (2 km²). However patches of the lichen community dominated by foliose species of *Xanthoparmelia sp.* can be observed on rocky outcrops in contrast to the larger southern lichen fields where this community is absent. Their existence indicates a possible transition zone between the crustose dominated southern lichen fields of the Namib Naukluft Park and the adjacent northern lichen fields dominated by fruticose and foliose communities.

With the crustose communities merely reflecting the species composition of lichen field no 1 and 2, fine quartz gravel increases its fraction of total ground cover. Thus saxicolous crustose species like *Caloplaca namibensis* Kärnefelt and *Caloplaca elegantissima* (Nyl.) Zahlbr., as well as *Neofuscelia sp.* show increased occurrence. Therefore observed changes in community patterns within the area of third lichen field may also reflect an overall change of substrate.

Anthropogenic disturbance can be regarded as a very strong impact factor. Bordered to the west by town of Swakopmund and its airport, this proximity not only increases off-road driving within the area, but littering as well. Littering has also become a severe problem for phanerogame vegetation since the usual prevailing south-westerly winds distribute non-decomposing plastic litter in an inland direction from the communal dump site.

In addition the B2 tar road forming the southern border allows easy access to the whole area for cross and quad bikes which is not at all restricted since the area lies within the National West Coast Tourist Recreation Area (NWCTRA).

6.4.4 Lichen field of Mile 8/Mile 12 (No. 4)

Lichen field no. 4 is bordered by the coastal road C34 to the north-east between Mile 8 and Mile 12. These measurements show the northerly distance from Swakopmund and are present alongside the whole northern coast, giving orientation to fishermen. SCHIEFERSTEIN (1989) referred to this lichen field as 'lichen field No. 2 and 3', but it was combined by LORIS & SCHIEFERSTEIN (1992), now referred to as lichen field No. 2.

Extending over gypsum encrusted quartz gravel planes and dissected in many ways by washes and riviers as well as some dolerite ridges and felsite dykes in south-west - north-east direction, the lichen field shows abundant occurrence of foliose and fruticose lichen communities for the first time. Its south-west - north-east extension from up the coast is about 15 km, while the extension from south to north amounts to about ten km (compare map 4).

The foliose lichen community is characterised by almost pure stands of foliose lichen *Xanthoparmelia walteri* Knox (14 km²), however accompanied by the terricolous *Caloplaca volkii* Wirth & Vezda, *C. elegantissima* (Nyl.) Zahlbr., *C. namibiensis* Kärnefelt, *Neofuscelia sp.* and *Lecidella crystallina* Wirth & Vezda. Throughout the study area this lichen community occurs on alluvial plains and areas with semi-stabilized to stabilized sands, primarily paved with fine quartz gravel varying between 2 to 20 mm in diameter. In some areas more than 90 % of the soil service may be paved.

Towards the higher, more stabilized reaches of the terrain this community is socialised with abundant small lichen tufts of *Teloschistes capensis* (L.f.) Müll. Arg., therefore referred to as fruticose-foliose lichen zone (19 km²).

Within this community pure stands of fruticose *Teloschistes capensis* (L.f.) Müll. Arg. forming large cushions and mats are scarcely found (0.37 km²). Outer boundaries of these fruticose/foliose patches show a hierarchical and spatial sequence of foliose/crustose, crustose and sparse crustose lichen communities, which is mostly based on the increased disturbance of washes and riviers. In total 14 km² are covered by foliose/crustose communities, while 54 km² are covered by crustose and 63 km² are covered by sparse crustose communities.

In contrast to the lichen fields discussed above fine non-encrusted/unstabilized quartz gravel where saxicolous lichen species adhere to abundantly covers the ground. Many of these quartz pebbles are completely overgrown by thalli of *Caloplaca elegantissima* (Nyl.) Zahlbr. and *C. namibiensis* Kärnefelt. This interesting phenomenon results from the periodic rolling-over of such pebbles by strong easterly berg winds. The substrate underneath the quartz pebbles ranges from unstabilized sands to stabilized sandy gypsum. State of stabilisation in top-soils generally reflects lichen community cover as well since increasing abundance of lichens reinforces soil stabilisation processes and vice versa.

Anthropogenic impact within the lichen field comes from a power line as well as a pipeline dissecting the lichen field in north-south direction. Additionally within the coastal parts vehicle tracks destroying the lichens from tourists and local fishermen can be observed.

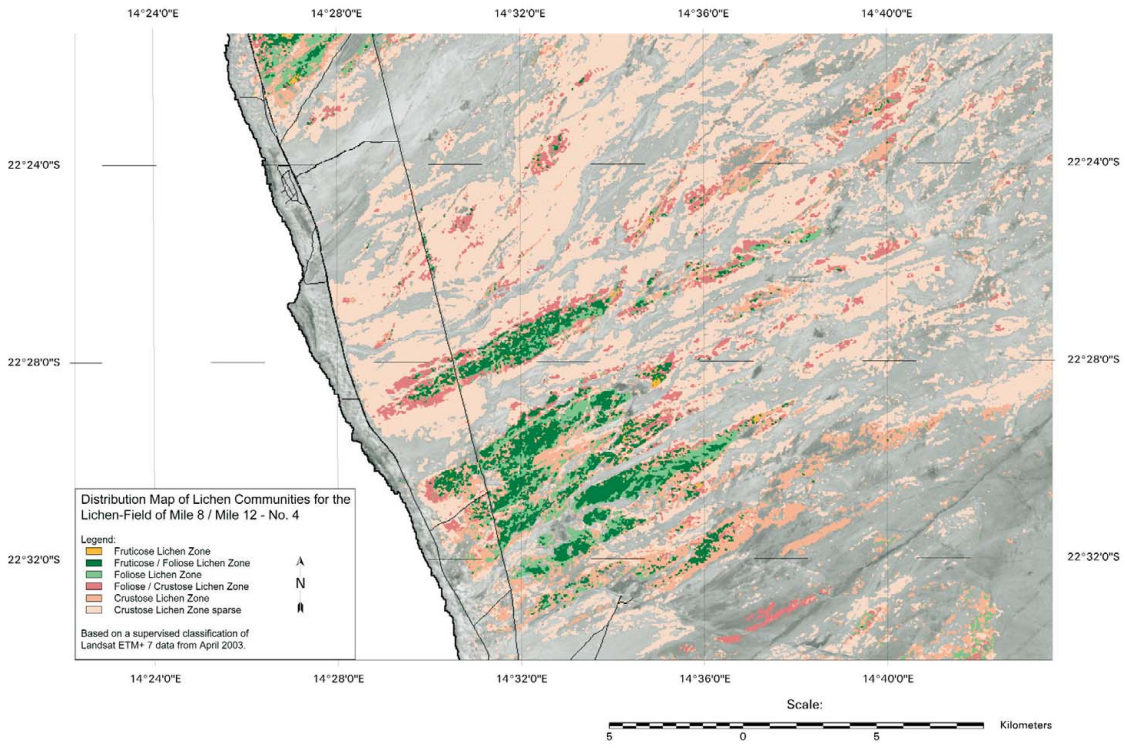

Map 4: Lichen field of Mile 8 / Mile 12 (No. 4), Central Namib Desert, Namibia.

6.4.5 Lichen field of Wlotzkasbaken (No. 5)

Three kilometers north of the Wlotzkasbaken village or 37 km from Swakopmund the lichen field of Wlotzkasbaken extends for about 30 km in north-easterly direction from the coast comprising lichen covered areas of 185 km² in total. Referred to as lichen field No. 3 by LORIS & SCHIEFERSTEIN (1992) and No. 4 by SCHIEFERSTEIN (1989) it is bordered by flat coastal dunes with shrub vegetation to the west while distribution ends in a riverbed system to the north and east. The eastern extension is however not as clearly marked as reported by SCHIEFERSTEIN (1989) but is loosely connected to an adjacent system of scattered dolerite ridges. To the south a three to ten centimetre thick layer of sand, presumably deposited by seasonal east winds, prohibits further lichen distribution (compare map 5).

Throughout this lichen field all lichen communities derived from the concept of morphological groups are well represented. In fact, the Wlotzkasbaken lichen field is one of the few to show vast coverage of the coastal *Teloschistes capensis* (L.f.) Müll. Arg. dominated community classified as fruticose lichen zone. In the outer areas of the lichen field and on the banks of riviers and washes the crustose lichen community prevails (107 km²). It shows the same Caloplaca/Neofuscelia/Lecidella community of the fine quartz gravel plains encountered and described for lichen field No. 3, which decreases in coverage as natural disturbance increases. In these areas the crustose lichen community is predominated by the sparse crustose lichen community (57 km²).

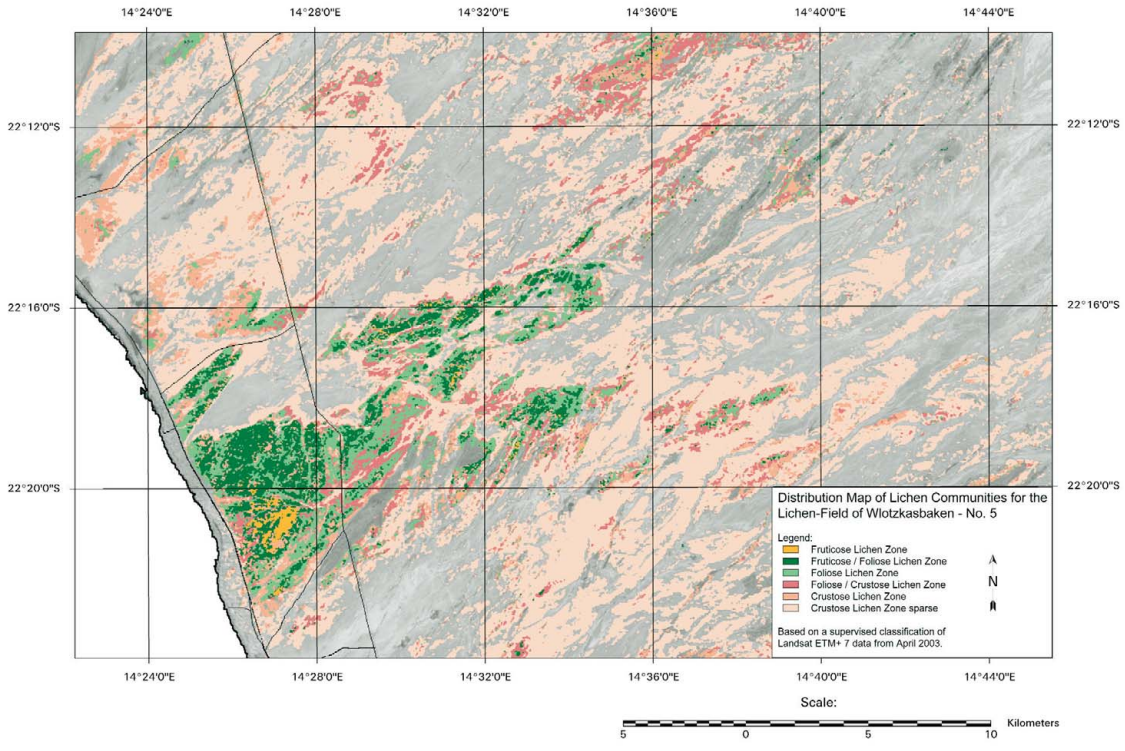

Map 5: Lichen field of Wlotzkasbaken (No. 5), Central Namib Desert, Namibia.

On stabilized sandy substrates covered by fine quartz gravel the prevailing species in the crustose lichen zone are complemented by foliose species of *Xanthoparmelia*. This foliose-crustose lichen community covers 18 km² in total. However in the north-eastern area where dolerite ridges as well as rock debris dominate the landscape this foliose-crustose lichen community does not only comprise of *Xanthoparmelia walteri* Knox but also of *Xanthomaculina hottentotta* indicating a shift towards the mountainous saxicolous community. Anchored to rocks with the centre of its large thallus this species shows a higher stability against strong sand blowing winds LORIS & SCHIEFERSTEIN (1992). A fully developed mountainous saxicolous community belonging to the topclass of foliose lichen communities can as well be observed in the vicinity of dolerite ridges.

For the more coastal extend of the Wlotzkasbaken lichen field up to 15 km inland the foliose lichen community and the fruticose-foliose lichen community are characterized by the same composition in species and coverage as encountered in lichen field No. 4. The foliose lichen community covers an area of 34 km², whereas the foliose-fruticose lichen community covers 24 km².

The fruticose-foliose community can also be encountered on the same stabilized higher reaches of the terrain, especially in the area located about 10 km inland, which is strongly dissected by small washes and riverbeds.

The fruticose lichen zone community is to a large amount limited in its distribution to a large sink opened to and located near the coast, covering 2 km² in total. With the fruticose lichen *Teloschistes capensis* (L.f.) Müll. Arg. attaining high cover values of more than 70 % in this area, it has been intensively investigated by SCHIEFERSTEIN (1989) and LORIS & SCHIEFERSTEIN (1992). LORIS & SCHIEFERSTEIN (1992) described different growth forms of *T. capensis* (L.f.) Müll. Arg., called 'tufts', 'cushions' and 'mats', varying in size and height. Though mats are only found in this special coastal area large cushions also are found in other spots as well, often grouped together with tufts. Tufts also characterize the fruticose-foliose lichen zone.

The overall structure of the Wlotzkasbaken lichen field observed by supervised classification derived from satellite imagery only loosely resembles the distribution patterns mapped by LORIS & SCHIEFERSTEIN (1992). Though the overall spatial extent of the lichen field initially mapped by SCHIEFERSTEIN (1989) reflects the newly obtained coverage quite well, the inner fragmentation and distribution of lichen communities clearly exceeds the anterior mapping due to overall system advantages.

The unique coastal *Teloschistes capensis* (L.f.) Müll. Arg. dominated fruticose lichen zone with its limited distribution forced local authorities to set up a fence against the coastal salt road C34 to limit the amount of damage already caused by off-road driving. Still, this fence does only protect the lichen field to a certain amount, since access is still granted from the dirt road accompanying the power line and the pipeline dissecting the field at about 5 km coastal distance. Nevertheless vehicle tracks are not as abundant as in other lichen fields, due to the remote position between Swakopmund and Hentiesbay. Therefore further conservation measures should be installed.

6.4.6 Lichen field of Jakkalsputz (No. 6)

Starting at about six kilometers south from Hentiesbay and extending into the north-eastern area of the vast Omaruru gravel plain the lichen field of Jakkalsputz is located. By the main roads C34, C35 and D1918, as well as many first and secondary dirt roads and the Omaruru River bed itself, the lichen field is dissected (compare map 6).

The predominant saxicolous lichen community of the fine quartz gravel plains is not rich in species. This might be due to the fact that unstabilized substrates in many parts may act as a limiting factor and also form the natural borders to all directions except the south, where salt pans and heavily disturbed dolerite ridges occur.

Lichen species such as *Caloplaca namibensis* Kärnefelt, *C. elegantissima* (Nyl.) Zahlbr., *Xanthoparmelia walteri* Knox, *Neofuscelia sp.* dominate this area. This is represented in the distribution of the morphological groups as well, as crustose communities and sparse crustose communities are found on 107 km² and 105 km² respectively. Only at the southernmost extension of the lichen field and in an area located about six kilometers inland of Hentiesbay increased coverage of *X. walteri* Knox and *Teloschistes capensis* (L.f.) Müll. Arg. tufts form small areas of foliose (19 km²) and fruticose-foliose (2.5 km²) lichen communities. These isolated areas are only sparsely surrounded by about 8 km² of foliose-crustose lichen communities.

Phanerogame vegetation of *Arthraerua leubnitziae* and *Zygophyllum stapfii,* as well as *Salsola sp.* bushes can be found on the banks of riviers and washes varying in size.

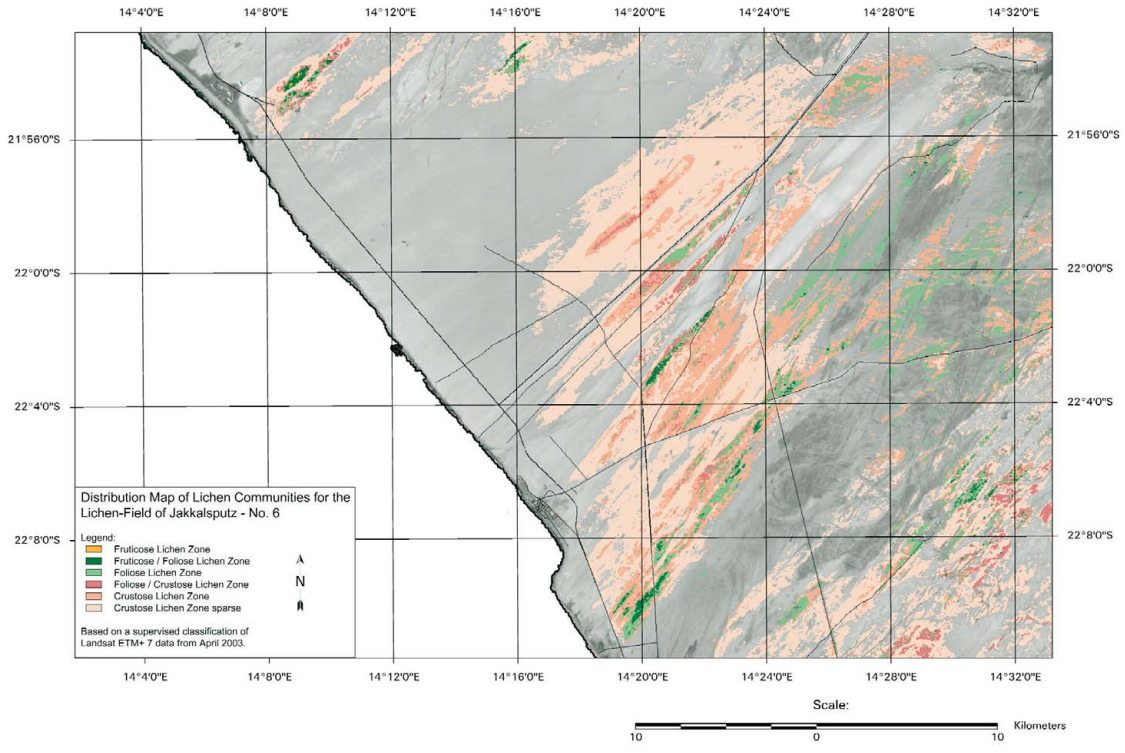

Map 6: Lichen field of Jakkalsputz (No. 6), Central Namib Desert, Namibia.

6.4.7 Lichen field of the Omaruru gravel plain (No. 7)

Located as far as 30 km inland and east of the Omaruru gravel plain upon a large area of small hummocks and dolerite ridges the lichen field No. 7, which has not been described in literature up to date, comprises a total coverage of 261 km² (compare map 7)

It features a compact extension of the fruticose-foliose and the foliose lichen zone upon extensive hummocks, whereas dolerite ridges are thoroughly covered by foliose-crustose (22 km²) and crustose (80 km²) lichen communities, interspersed by large extends of the sparse crustose lichen zone (121km²). Due to the far inland position of the lichen field species composition shows many aspects of a mountainous saxicolous community.

Foliose (28 km²) and fruticose-foliose (10 km²) lichen zones are complemented by abundant *Xanthomaculina hottentotta* and surprisingly abundant coverage of *Lecidella crystallina* Wirth & Vezda accompanied by *Parmelia sp.* and *Buellia sp.*

Human impact in this area is scarcely found as the lichen field is located in a sufficient distance from road C35. The only dissection occurs by a hard to find dirt road leading to the former Strathmore mine located in northern direction towards the Messum Crater region.

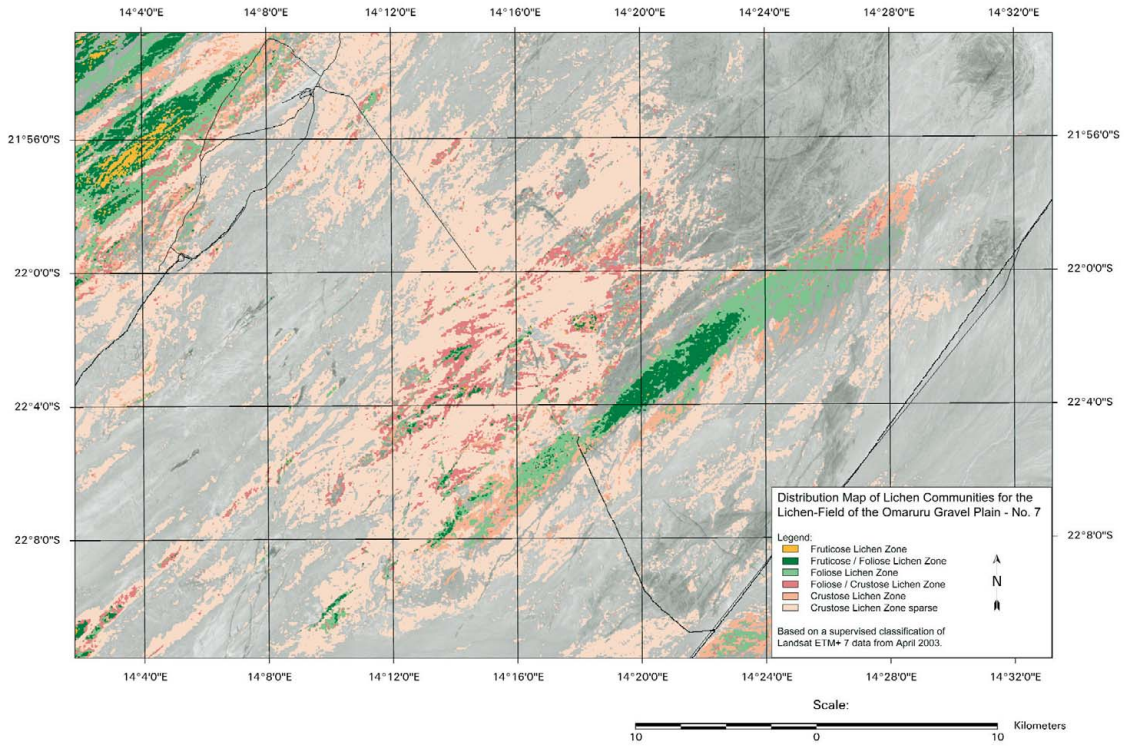

Map 7: Lichen field of the Omaruru Gravel Plain (No. 7), Central Namib Desert, Namibia.

6.4.8 Lichen field of Mile 72 (No. 8)

Lichen field no. 8 is bordered by the coastal road C34 to the north-east at 72 Miles distance from Swakopmund in northerly directions. Encompassing a total spatial lichen coverage of only 12 km², that has also not been noted in literature, it represents the smallest of the lichen fields discussed in this study. Although small in size it still extends for more 8 kilometers inland and shows a maximum width of almost 2 kilometers (compare map 8).

As the outer areas of the lichen field are mainly covered by the crustose lichen community (4 km²) and the sparse crustose lichen community (4 km²) growing on fine quartz gravel, loosely lying on a top soil of semi-stabilized sands on top of gypsum substrate, the inner area is characterized by small but densely lichen covered hummocks. Lower slopes of these hummocks are overgrown by 1.6 km2 of the foliose-crustose lichen community, while the slopes themselves are mainly covered by foliose (0.88 km²) and fruticose-foliose (1 km²) dominated lichen communities, depending on which direction slopes are facing. In small sheltered spots even the fruticose lichen community (0.06 km²) can be found within the lichen field. Species composition resembles that of the other lichen fields accessing the shore in a more or less distinct way.

Signs of anthropogenic impact were not detected within this area during field work, which could be based on the remote position in regards to the touristic attractions of Cape Cross or Hentiesbay. Additionally it can hard-

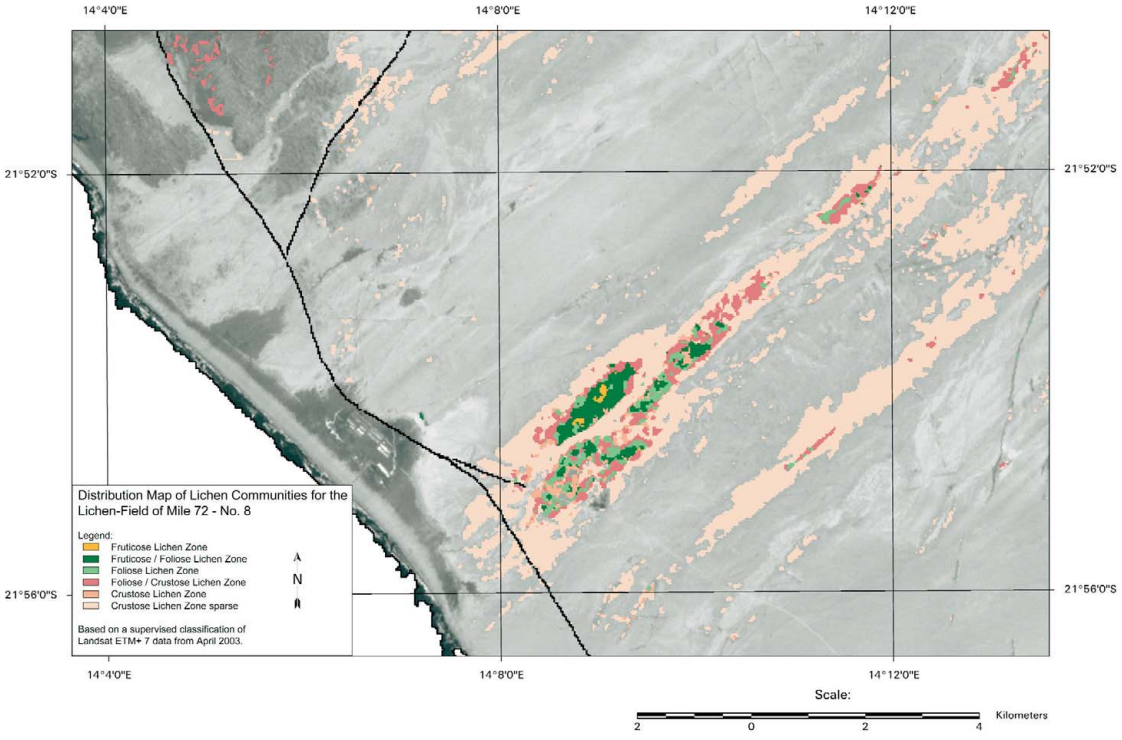

Map 8: Lichen field of Mile 72 (No. 8), Central Namib Desert, Namibia.

ly be encountered from the C35 coastal road, due to the more inland position of the densely lichen covered areas. Salt Work located close by at the shore also did not seem to have had any impact.

6.4.9 Lichen field of the Messum Crater / Orawab (No. 9)

Comprising a total lichen covered area of about 373 km² and extending for more than 25 km in length and about 20 km in width, this lichen field is the largest and by far the most diverse reported on in this study.
It was first mentioned by WESSELS & VAN VUUREN (1986) who synoptically analysed LANDSAT-MSS imagery of this area recorded 1981. They described it as a shrub-lichen dominated community with species such as *Teloschistes capensis* (L.f.) Müll. Arg., *Santessonia sp., Alectoria sp.* and *Ramalina sp.* found to grow abundant in an otherwise barren landscape based on field observations. During their field studies they also accounted dense stands of *Xanthomaculina hottentotta* on rocky outcrops along the northern periphery. Additionally *Xanthoparmelia walteri* Knox occurred frequently in dense patches on the plains alongside scattered thalli of *Xanthomaculina convoluta* as well as genera of *Buellia, Caloplaca* and *Lecidea* (WESSELS & VAN VUUREN 1986).
Dry, mostly shallow watercourses show denser phanerogame population than the surrounding flats consisting of *Arthraerua leubnitziae, Zygophyllum stapfii* and *Welwitschia mirabilis* along the northern boundary (WESSELS & VAN VUUREN 1986) (compare map 9).

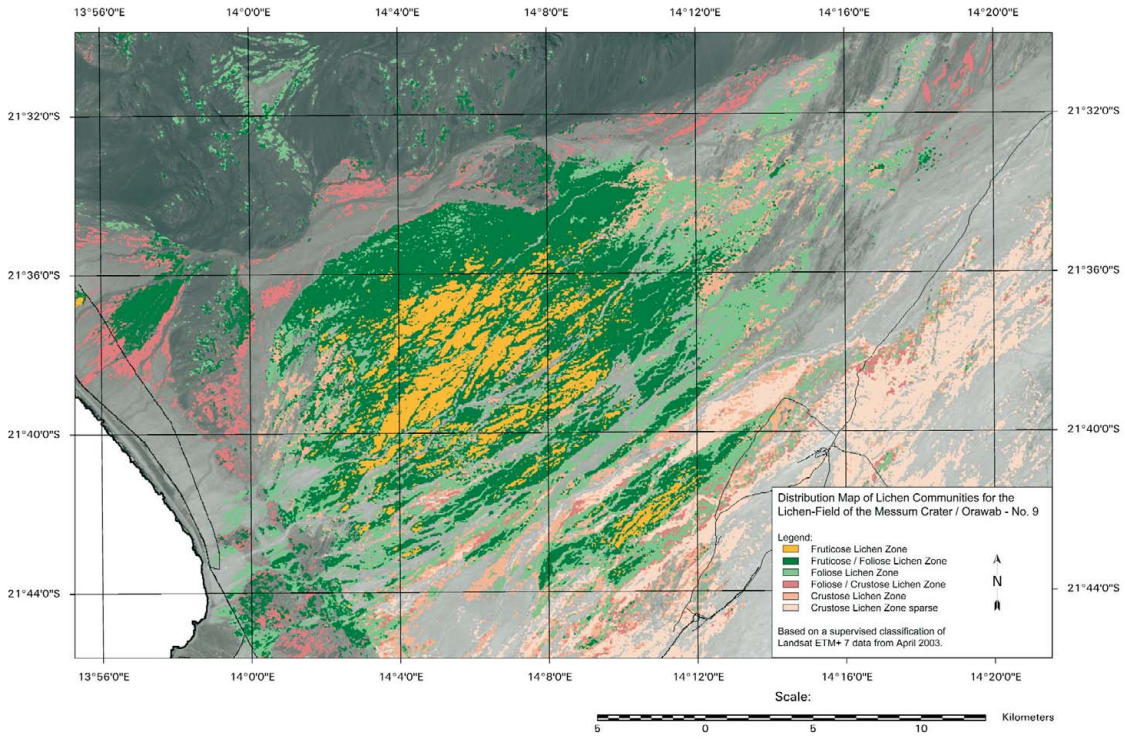

Map 9: Lichen field of the Messum Crater / Orawab (No. 9), Central Namib Desert, Namibia.

Although field work was obviously carried out within the lichen field no information is given on its exact position and extend. To the north the lichen field is bordered by the ephemeral runnings of the Orawab Rivier, while in the easterly direction overall lichen distribution tends to fade away for no orographic reason. It is therefore assumed that the easterly extend of the lichen field is limited by the occurrence or non-occurrence of humidating coastal fog. To the south it borders the vast unstabilized gravel plains of the Omaruru River and almost connecting to the northern extensions of lichen field No. 7. Towards the coast increasing destabilization of soils in conjunction with coastal rocky outcrops and ridges delimits the distribution of lichen communities at five kilometers from the coast.
Towards the Omaruru gravel plain lichen distribution is widely dissected by watercourses and washes forming more or less isolated lichen covered patches extending in south-west - north-east direction. As watercourses narrow towards the northern parts of the lichen field large coherent lichen covered plains can be found.

In accordance to the observations made by WESSELS & VAN VUUREN (1986) the classification depicts large areas dominated by fruticose lichen communities. These are however not comparable to their coastal equivalent regarding prevailing species. In contrast to the coastal fruticose lichen community this inland fruticose community is not only characterized by the large abundance of *Teloschistes capensis* (L.f.) Müll. Arg. tufts, but also comprises large amounts of *Santessonia sp., Ramalina sp.,* and foliose *Xanthomaculina convoluta, Xanthoparmelia sp.,* and *Paraparmelia sp.* growing on top of a well developed crustose layer consisting of various *Caloplaca, Lecidella, Buellia, Arcarospora, Neofuscelia* and *Lecidea* species. This community covers an already impressive 43 km² , whereas the fruticose-foliose lichen community covers an immense 148 km², followed by the foliose lichen community with a coverage of 105 km².

Both latter lichen communities differ from the fruticose lichen community only by an increasing absence of fruticose species in favour of foliose. Towards the rocky outcrops the foliose fraction of these communities tends to shift towards a more abundant distribution of *Xanthomaculina hottentotta.*

Crustose lichen communities forming the bases for all foliose and fruticose growth forms show only limited distribution. Although strong pure crustose stands can be observed alongside shallow watercourses in the densely covered northern area the spatial resolution of the satellite imagery might not be capable of detecting these patterns. Therefore distribution of foliose-crustose (10 km²), crustose (49 km²) and sparse crustose (18 km²) lichen communities is somewhat limited to the western and southern areas where overall lichen distribution is fading or watercourses are widening.

Anthropogenic impact on the area is due to its remote position very limited, and since the closure of the southerly adjacent Strathfore Mine industrial impact no longer exists. Still, the beauty of the area and the nearby Messum Crater attract off-road enthusiasts. To prevent these enthusiasts from driving off-track the Tourism Officer of the Municipality of Henties Bay recently laid out a marked path through the area and published a brochure describing it with included turnoff GPS-coordinates (TOURISM OFFICER OF MUNICIPALITY OF HENTIES BAY 2003B). This method of semi-controlled access might be the best way for the preservation of this unique lichen field as it is still located within the NWCTRA.

6.4.10 Lichen field of Cape Cross (No. 10)

First described by SCHIEFERSTEIN (1989) and LORIS & SCHIEFERSTEIN (1992) as a coherent lichen field starting with its southernmost extension alongside the coastal road (C35) at Mile 88 and reaching up to Horingbay at Mile 97 to the point where the Brandberg-West road forks east in this thesis it became obvious that it actually consist of three spatially dissected lichen fields. The small southernmost extensions described by SCHIEFERSTEIN (1989) are clearly outlined on the total distribution map, as well as the northern part, which shall be described later as lichen field no. 11. Subsequently only the lichen community densely and cuneiformly overgrowing the coastal alluvial fan of a rivier originating in the Messum Crater area, located about 10 km northeast of Cape Cross, is described. The total lichen coverage amounts to 17 km² (compare map 10)

Starting at about 1 to 2 km inland this lichen field is naturally delineated by large amounts of wind-borne unstabilized sands apparently suppressing further colonization by lichens. The north-eastern border results from a small coastal mountain range and the cleared out riverbed narrowed by the hilly landscape in this area.

Due to the unstable alluvial and wind-borne deposits the sparse crustose and crustose lichen communities cannot be observed.
The foliose-crustose and foliose communities, covering about 9 km² and 0.73 km² respectively, therefore form the 'lowest' type

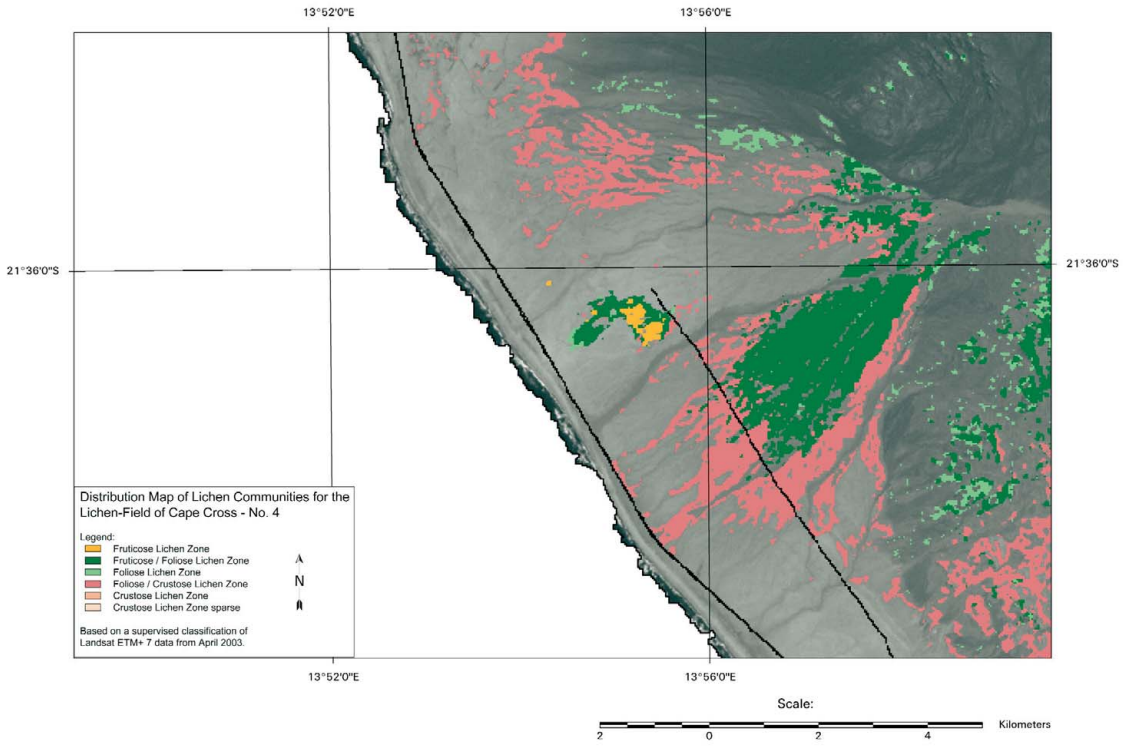

Map 10: Lichen field of Cape Cross (No. 10), Central Namib Desert, Namibia.

of lichen cover mostly prevailing in between small riverbeds and washes. They are either dominated by *Xanthoparmelia walteri* Knox, or consist of a well-developed crustose quartz gravel community with *Caloplaca* species prevailing.
Gypsum soils in these area tend to produce vesicular top layers (Schaumböden) which are stabilized best by coastal fruticose-foliose lichen community (7.4 km_2), dominated by small-growing *Teloschistes capensis* (L.f.) Müll. Arg. tufts and *Xanthoparmelia walteri* Knox.

In a limited area, which is dissected from the main alluvial fan by large washes, pure stands of the coastal fruticose lichen community as described for lichen field no. 5 can be observed on a more sandy substrate. Dominated by *Teloschistes capensis* (L.f.) Müll. Arg., large tufts, cushions and even mats consisting of this species, in conjunction with *Ramalina sp.* and interspersed with *Xanthoparmelia, Caloplaca* and *Buellia* species, are found attached to scattered gravel. Covering about 0.27 km^2, which is 15 % of the extend of the coastal fruticose community found at Wlotzkasbaken, it could be observed during field work that the overall extension of this community must have been a lot larger in former times, as large areas showed dead remains of *Teloschistes*-mats, almost fully covered by sand. Despite the observed natural impacts anthropogenic influence is confined to an old secondary dirt road crossing the lichen field from north to south, parallel to the coastal salt road (C35). Due to its distance from the latter no further disturbances are known to occur.

6.4.11 Lichen field of the Brandberg-West-Road (No. 11)

The lichen field consists of three major parts, for which one is located at about 5 km from the coast at Mile 105 and dissected by the Brandberg-West road (D2303) in north-easterly direction. The second part is located further east behind a small coastal mountain range extending on the stabilized banks in between numerous washes in otherwise almost flat terrain. The third part is confined to the large southerly banks of the Messum Rivier, starting at about 4 km east of the Brandberg-West road in a coastal distance of almost 15 km, only accessible via a small dirt road forming its southern border in conjunction with a small rivier (compare map 11).

The major difference between these and all previously described lichen fields is the dominating coverage of fruticose/foliose mountainous lichen community and the mountainous saxicolous lichen community. This is indicated by the large abundance of the foliose species *Xanthomaculina hottentotta,* and *Xanthoparmelia walteri* Knox as well as an overall extraordinary species richness assumed to be due to the various ecological niches.

Supplementary all three lichen fields differ distinctively from all previous lichen fields regarding the substrate. The sandy gypsum substrate is no longer covered by fine quartz gravel as observed in the southern regions, but is covered by an almost 100 % closed layer of fine to medium dark gravel material amounting several centimetres. The gravel material is only loosely embedded into the sand but acts as a protection to the wind's erosive forces. Being only loosely connected to the ground it is however easily disturbed by off-road driving.

These rocky substrates are therefore the main cause for the widespread distribution of the saxicolous foliose mountain community (25 km²). Additional species observed in this community are *Teloschistes capensis* (L.f.) Müll. Arg., *Santessonia sp., Ramalina sp.* and foliose *Xanthomaculina convoluta, Xanthoparmelia sp.* attached to solitary rocks and *Paraparmelia sp., Caloplaca, Buellia,* and *Neofuscelia* species overgrowing the dark gravel cover.

In sheltered places the abundance of fruticose component of this community increases, hence reflected by 4 km² of fruticose-foliose lichen community occurring scattered throughout the lichen field.

Because of the strong spectral absorption of the dark gravel material foliose-crustose, crustose and sparse crustose communities could not be spectrally separated from the background signal, although encountered during field work. This results in the foliose lichen community depicting the lower limit for the supervised classification of lichen communities in these area.

Only alongside the large riverbanks of the Messum Rivier for example, where the above described top-layer is mostly substituted by large rock debris and gypsum deposits, the lighter color of the background allows the detection of a abundant foliose-crustose lichen community (0.7 km²) with *Arcarospora sp., Lecidella crystallina* Wirth & Vezda complementing the above described crustose layer.

Phanerogamous vegetation is mostly restricted to ephemeral watercourses and washes with an large population of *Welwitschia mirabilis* occurring in the eastern parts of the lichen field.

Anthropogenic impact is mostly refined to

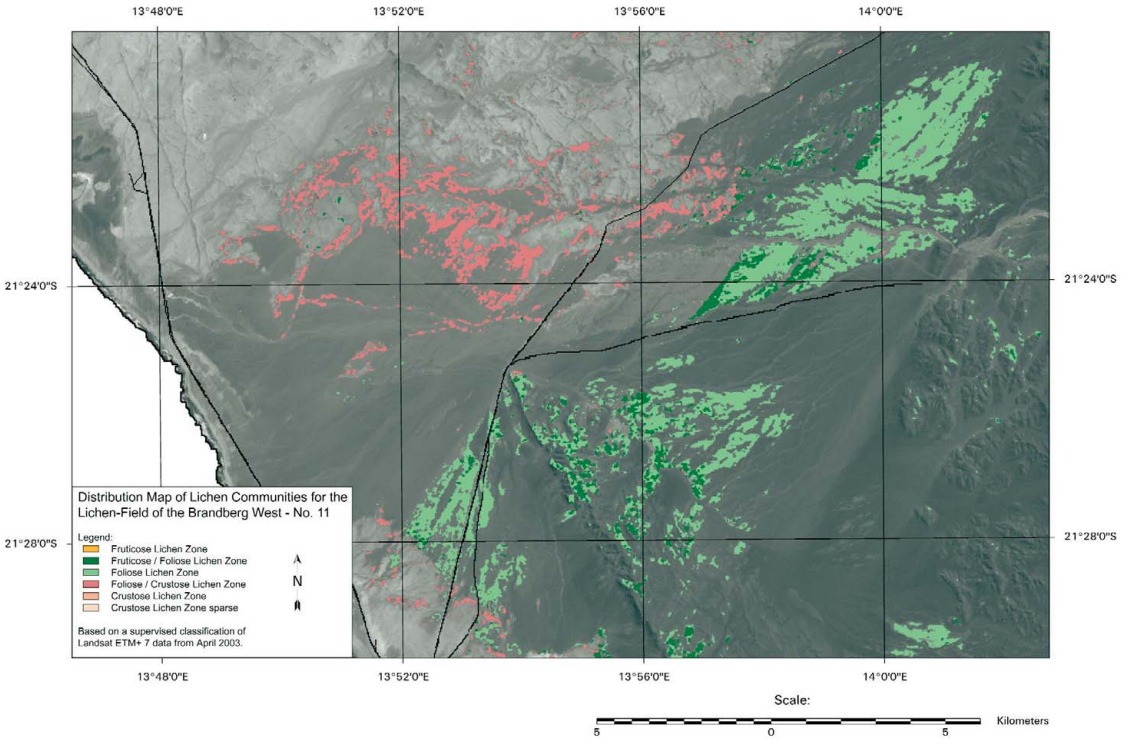

Map 11: Lichen field of Brandberg West Road (No. 11), Central Namib Desert, Namibia.

the newly established Messum Crater 4X4-Trail (Tourism Officer of Municipality of Henties Bay 2003b) running along the southern border of the above described easternmost part of the lichenfield. The Brandberg-West dirt road (D2303) dissects the southernmost part but does not seem to have a major impact on the lichen fields, assumably because of generally low traffic.

6.4.12 Lichen field of Huabmond (No. 12)

The twelfth lichen field is known to SCHIEFERSTEIN (1989) as no. 8 and LORIS & SCHIEFERSTEIN (1992) referred to is as no. 6. It was first mentioned in the 1st edition of SEELY (2004[3]) in the year of 1987 as cited in SCHIEFERSTEIN (1989). It depicts the northernmost lichen field presented in this study and is situated south of the Huab River in the Skeleton Coast Park, its total lichen coverage amounts to about 11 km² (compare map 12). It extends for about 8 km alongside the coastal park road and throughout the hilly coastal areas covered by a gravel layer almost reflecting the composition of lichen field no. 11. It is bordered by coastal dune systems to the west and a widely ramified watercourse system accompanied by salt pans towards all other directions.

The foliose-crustose community (11.5 km²) of this lichen field could be very well delineated due to the lichen communities almost fully overgrowing the dark rock debris contrasting with the lichen field of the Brandberg-West road.

Again foliose (0.02 km²) and fruticose-foliose (0.5 km²) lichen communities occur scattered

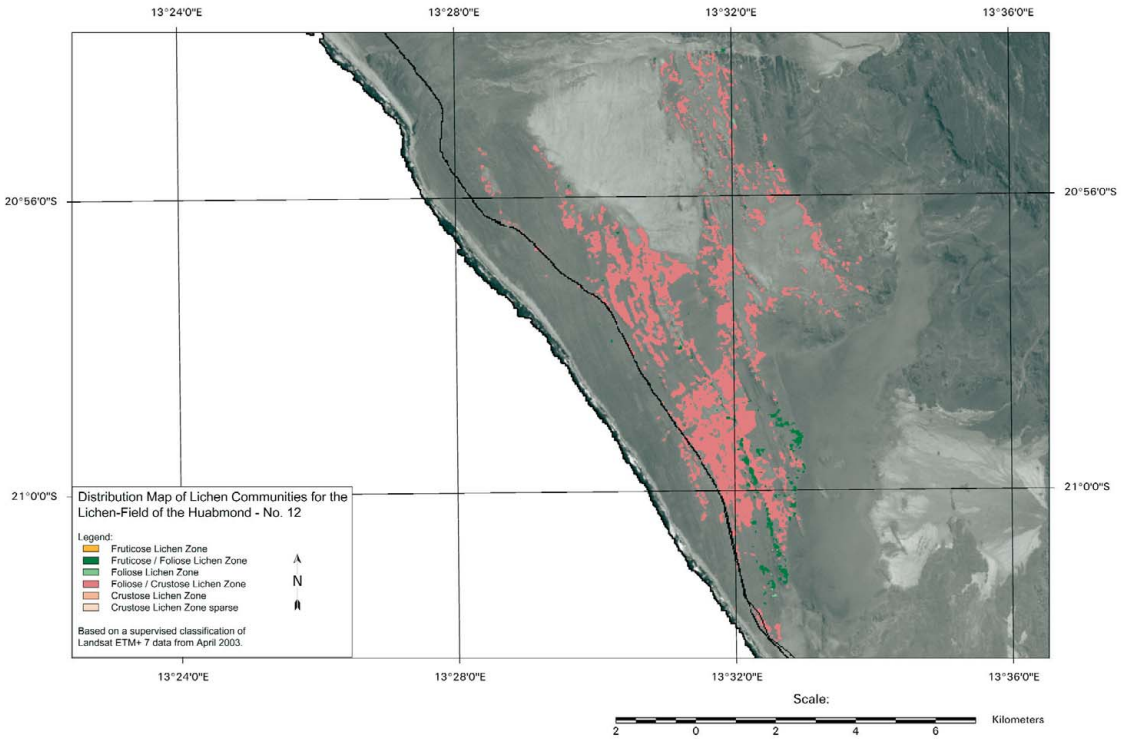

Map 12: Lichen field of Huabmond (No. 12), Central Namib Desert, Namibia.

throughout the area mostly confined to wind-sheltered places. The species composition of the described lichen communities resembles that of lichen field no. 11. Located within the Skeleton Coast National Park anthropogenic impact is restricted by park rules.

6.2 Multitemporal classification

Consecutively the results of the multitemporal supervised classification of the lichen distribution of the Central Namib Desert are discussed in detail. With the means of Post-Classification Change Differencing, areal statistics as well as maps comprising a complete matrix of changes, the classification results of different timeframes are presented and analysed. To aid the analysis of the large study area and to balance workload with practicalities the observed changes are examined and presented at two different mapping scales.

Firstly the coherently mapped timeframes of 2003, 2000 and 1991/92 which were assembled into individual mosaics beforehand are compiled into two maps depicting the observed changes between timeframes for the full study area. Each of these maps graphically depicts the results of the computation of a change matrix of the images pairs 2003 – 2000 and 2000 – 1992/92. Attached to this thesis in DIN-A1 format these maps shall in the following be used for the discussion of detected changes identified on the second mapping scale.

In order to balance the requirements of a detailed discussion of the observed alterations in lichen distribution patterns with practicalities the second mapping scale is confined to the lichen field of Wlotzkasbaken (No. 5). In contrast to the discussion of three to four time-series images for twelve individual lichen fields inescapable encompassing no less than 46 chapters, the lichen field of Wlotzkasbaken shall be used exemplary. For the rest of the lichen fields which will not be individually mapped, descriptive statistics comprising their alterations are presented in annex d and annex e, to allow for comparative discussion. Resembling most of the lichen distribution characteristics also found in the remaining areas identified for the unitemporal classification and due to its vast and divers extent the lichen field of Wlotzkasbaken was selected. Moreover it features the only lichen-field of the Central Namib Desert where major ecological research has been carried out by SCHIEFERSTEIN (1989), LORIS & SCHIEFERSTEIN (1992), as well as LORIS ET AL. (2004) and still progresses due to the observatory site of the Biota Southern-Africa project also including a permanent climate station erected in 2001 (compare ZEDDA & RAMBOLD 2004). Supplementary to his ecological and climatological studies, the work of Dr. Kurt Loris from the German University of Stuttgart-Hohenheim also included a constant photo-documentation of the lichen distribution patterns from fixed view points as well as a recent biomass assessment of selected lichen communities which were kindly provided for this thesis to serve the discussion of remotely sensed areas. Advanced information on the biomass of differing lichen communities was also provided by Dr. Dirk Wessels (University of Limpopo, South Africa), while additional climatic data were kindly made available Dr. Jo Henschel (Desert Research Foundation, Namibia) and Dr. Berit Hachfeld (University of Hamburg, Germany) to serve for discussion of lichen distribution patterns.

Mapping of all multitemporal timeframe is performed in accordance with the unitemporal classification. However maps comprising additional information based on the compu-

tation of change matrices comprise extended information. Supplementary to the already established legend colours, degraded, recovered and destructed territories are presented.
Degradation is defined as a negative alteration of the previous lichen coverage towards a sparse crustose community while recovery describes the alteration of lichen coverage towards a fruticose community. This approach is necessary due to a deficit of subcategories describing natural and abiotic alterations of the main classes for the study area as well as an overall lack of knowledge on the succession of Central Namib Desert lichen communities.
As a consequence the post classification change detection comparison of the differing timeframes is only able to address patterns of degradation and recovery based on the existing classes of the classification system which is likely to result in a retrospective misclassification of an existing area although an alteration of that area was detected correctly.

In order to reduce these shortcomings of the post classification change detection approach and to allow for the examination of change patterns solely based on the comparison of spectral information provided by the time-series images area-wide maps of changes based on sPCA change comparison analysis (compare chapter 5) are presented to replenish the detailed discussion of changes for the lichen field of Wlotzkasbaken (No. 5).
Supplementary to the description of alterations of the distribution of lichen communities, the "destructed lichen area" identified by the post classification change comparison

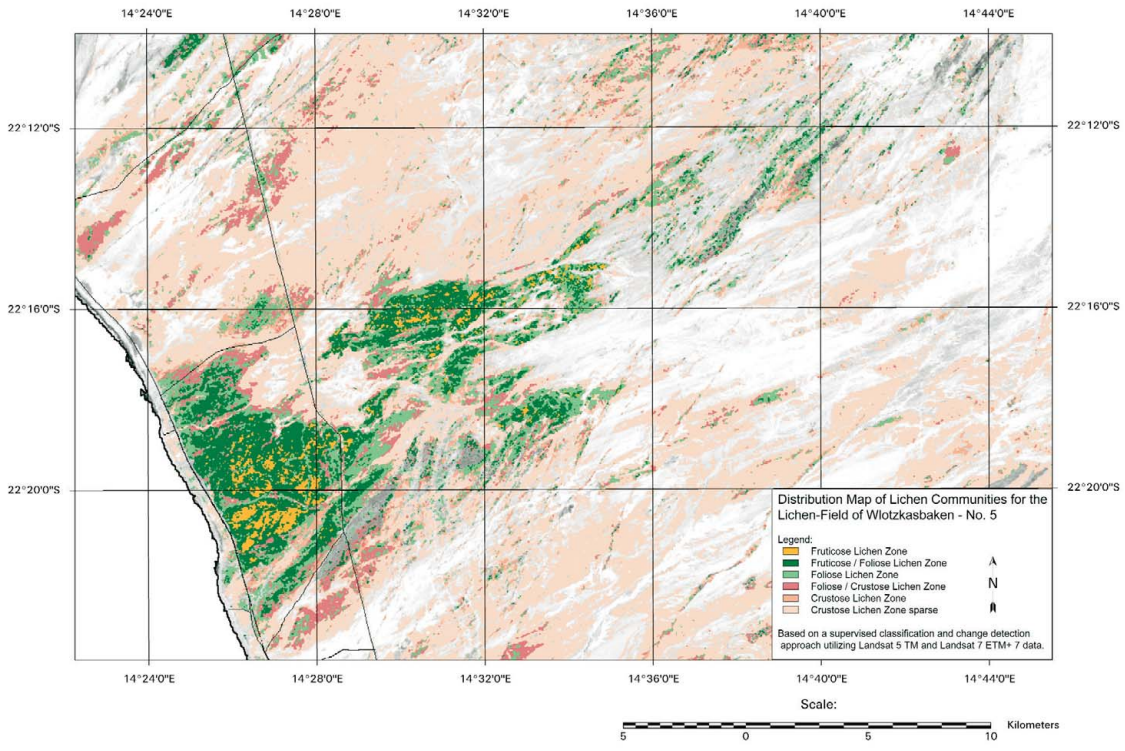

Map 13: Map depicting the distribution patterns of the lichen communities of the lichen field of Wlotzkasbaken (No. 5) for the timeframe of 1991 based on a retrospective classification approach.

depicts all none lichen-covered areas formerly covered by lichens according to the classification, with none lichen covered areas known as areas where no spectral separability from bare ground is given by the satellite data. Due to bare ground being defined by the detection limit, insecurities may arise if lichen community coverage is temporally decreased or if coverage is low in general. As the sparse crustose lichen community generally comprises low lichen coverage and decreased measures of separability all alterations between that class and none-lichen covered areas were excluded from mapping in order to retain a precise delineation of significant changes and their patterns. Nevertheless the obtained measures are fully listed in the statistics located in annex d and e.

6.5.1 Post classification change differencing between 1991 and 1999

For the detailed study of variations in the distribution of lichen communities of the lichen field of Wlotzkasbaken (No. 5) two maps displaying the results of the retrospective classification approach are provided for either timeframe (compare map 13 and map 14).

Variations in the distribution of lichen communities for the lichen field of Wlotzkasbaken (No.5) observed for the post classification change comparison of the retrospective classification results of 1991 and 1999 include a large variety of differing patterns. If retrospective classifications are spatially compared using the computation of a matrix image the

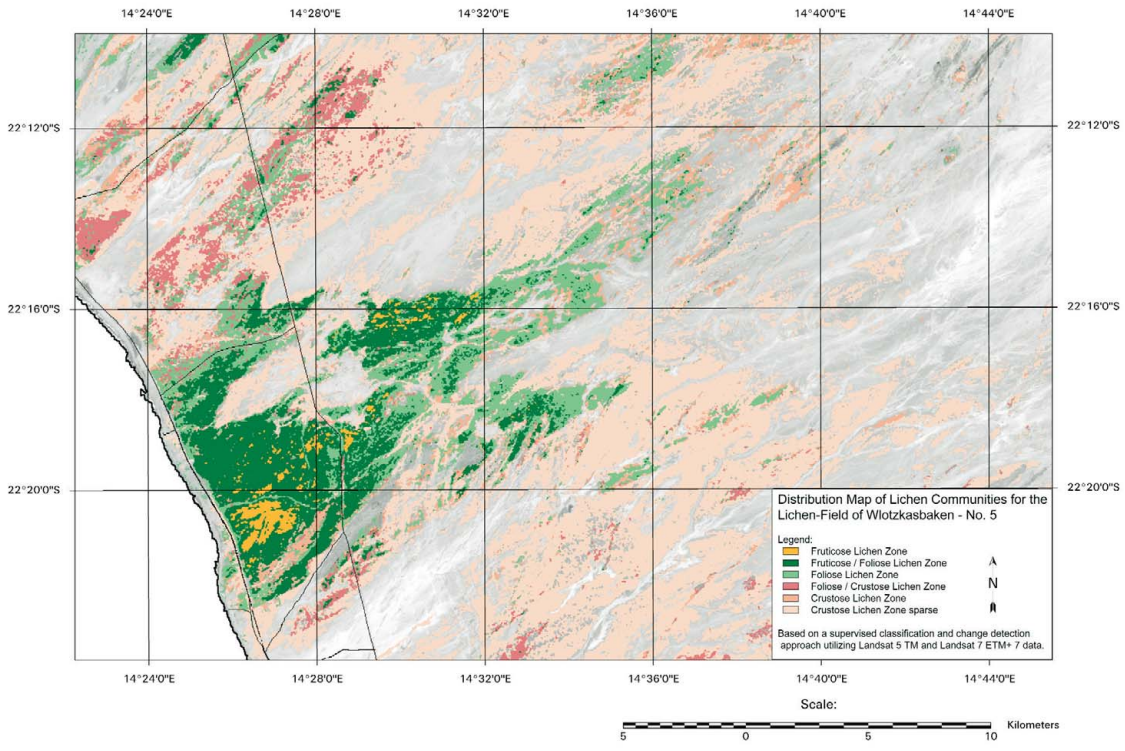

Map 14: Map depicting the distribution patterns of the lichen communities of the lichen field of Wlotzkasbaken (No. 5) for the timeframe of 1999 based on a retrospective classification approach.

result can be used to depict degraded, recovered and destructed territories based on lichen distribution patterns. The result of this computation is presented in map 15.

At first sight those areas where lichen communities have been eliminated on the northern (alongside 22.16°S and 22.18°S) and southern rims (14.28E & 22.22°S) of the lichen field as well as in the vicinity of the dolerite dykes at about 20 km coastal distance (14.36°E-14.40°E and 22.12°S-22.16°S), all indicated by red colour, catch the viewers eye.

Despite these widespread and plane patterns of destruction, small patches of degraded areas are mostly confined to the area located at a coastal distance of 10 km. They are located in an area where numerous washes of all sizes tend to dissect the lichen distribution patterns (14.32°E and 22.16°S).

On the contrary a widespread "recovery" or "upgrade" is visible for the "northernmost branch" of the lichen field (14.24°E-14.28°E and 22.16°S) as well as for the inner parts and certain area of the north-eastern outreach. In fact the comparison of the two timeframes reflects the largest amount of coherent upgrade patterns of any of the change differencing images obtained for the lichen field of Wlotzkasbaken.

In order to confirm the change patterns depicted by the comparison of the two retrospective classifications they shall also be compared to those change patterns based solely on spectral differences obtained from the

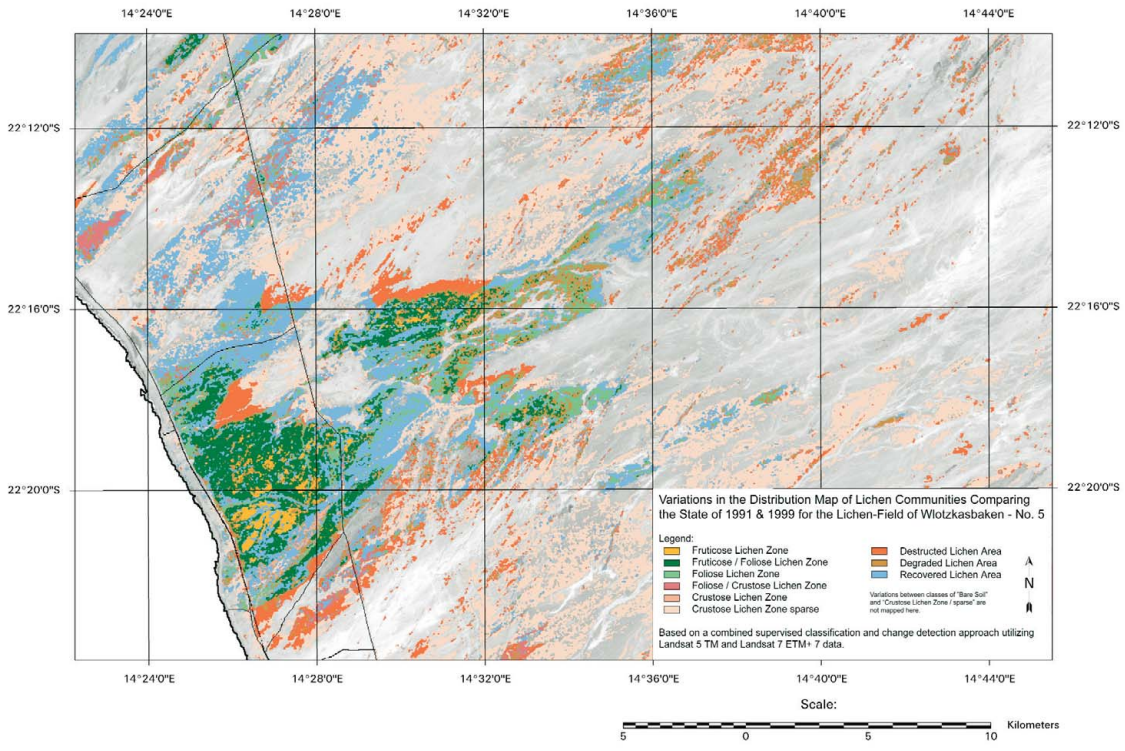

Map 15: Detailed map showing the variations in the distribution of lichen communities for the lichen field of Wlotzkasbaken based on the matrix of post classification change comparison of the timeframes of 1991 and 1999.

sPCA change detection approach previously presented in chapter 5.2.3.1. Although a different, spatially confined approach was used for the extraction of retrospective signature sets later on, subsets of the area-wide sPCA approach form a good source of validation. In compliance with the retrospective classification strategy a threshold of 70 was set to discriminate change information and noise. The map is presented in map 16.

In correspondence with the variations of lichen distribution patterns encountered by the classification, map 16 also delineates those areas where changes were most severe. Especially for the northern and southern rim and those patches at about 10 km coastal distance where fruticose-foliose and foliose communities were degraded and destroyed, a strong agreement of patterns can be observed. The strong patterns occurring in the eastern areas between 14.36°E-14.40°E and 22.16°S-20.20°S could also be observed by the classification as changes affecting the relationship between the crustose-sparse community and none lichen-covered areas. However as stated in the introduction to this chapter, all alterations between the sparse crustose community and none lichen-covered class were excluded from mapping to retain a precise delineation of significant changes and their patterns.

In addition to the usage of maps for the localization of change patterns, areal statistics were calculated to gain further information on interclass variations. During the long period from 1991 to 1999, 8046 ha (42 %) of the

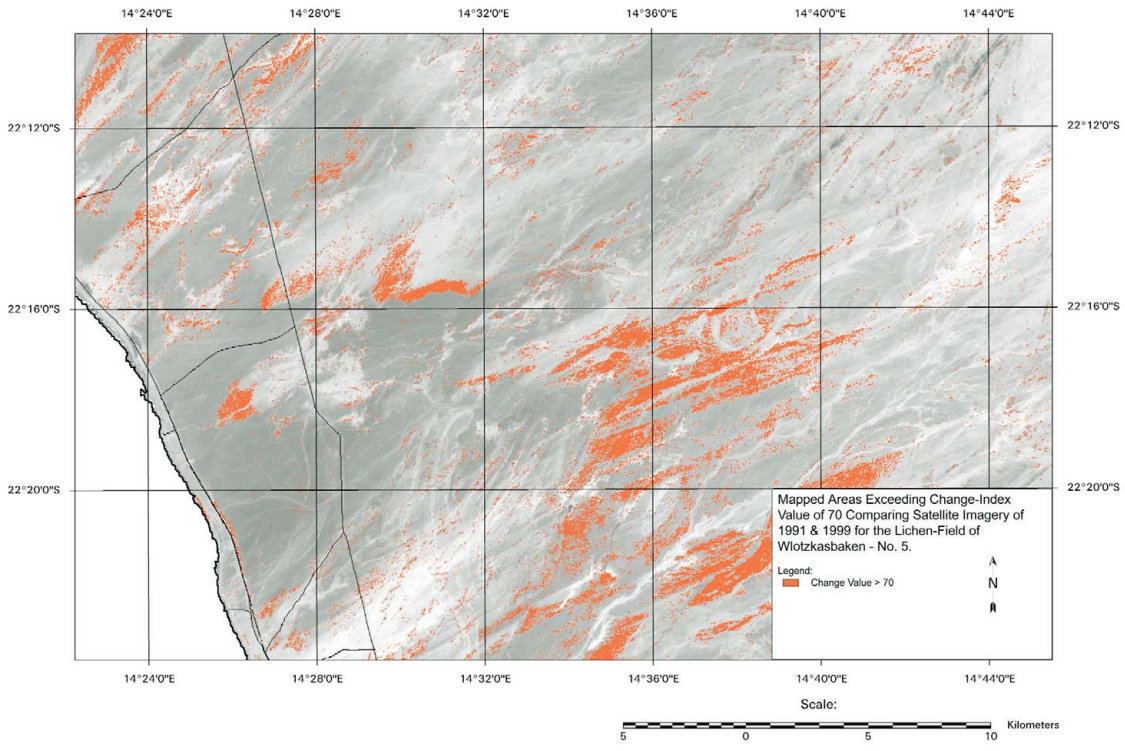

Map 16: Detailed map of the lichen field of Wlotzkasbaken (No. 5) depicting areas exceeding a change-index value of 70 comparing the timeframes of 1991 and 1999 based on the approach of WEIERS ET AL. (2003).

lichen coverage and 14913 ha (50 %) of the total lichen field area registered in 1999 remained identical to that of 1991. 3944 ha of lichen communities were lost while at the same time 2433 ha of lichen coverage arose on formerly none lichen-covered areas (compare figure E18, annex e). Within this second measure the combined sudden increase of fruticose-foliose and foliose communities of altogether 250 ha draws ones attention. This enforced shifting of classes towards the fruticose-foliose and foliose classes can also be identified for the crustose-sparse community (1103 ha), the crustose (392 ha) and the foliose-crustose community (914 ha). At the same time the *Teloschistes capensis* (L.f.) Müll. Arg. dominated fruticose communities were degraded by 53 % (compare figure E18, annex e) again in favour of the fruticose-foliose and foliose communities (306 ha).
On a broader scale these intra-class variability also leads to an overall increase of the fruticose-foliose and foliose communities by 690 ha and 473 ha respectively (compare figure D21of annex d).

Based on these descriptive statistics a dislocation of fruticose as well as foliose lichen thalli material is considered to have formed the widespread changes in lichen distribution observed for the lichen field of Wlotzkasbaken for the time-span between 1991 and 1999. Considering the spatial information provided by the map depicting the post classification change comparison of the direction by which dislocation of lichen material was accomplished from a north-easterly towards a south-westerly direction. As this direction

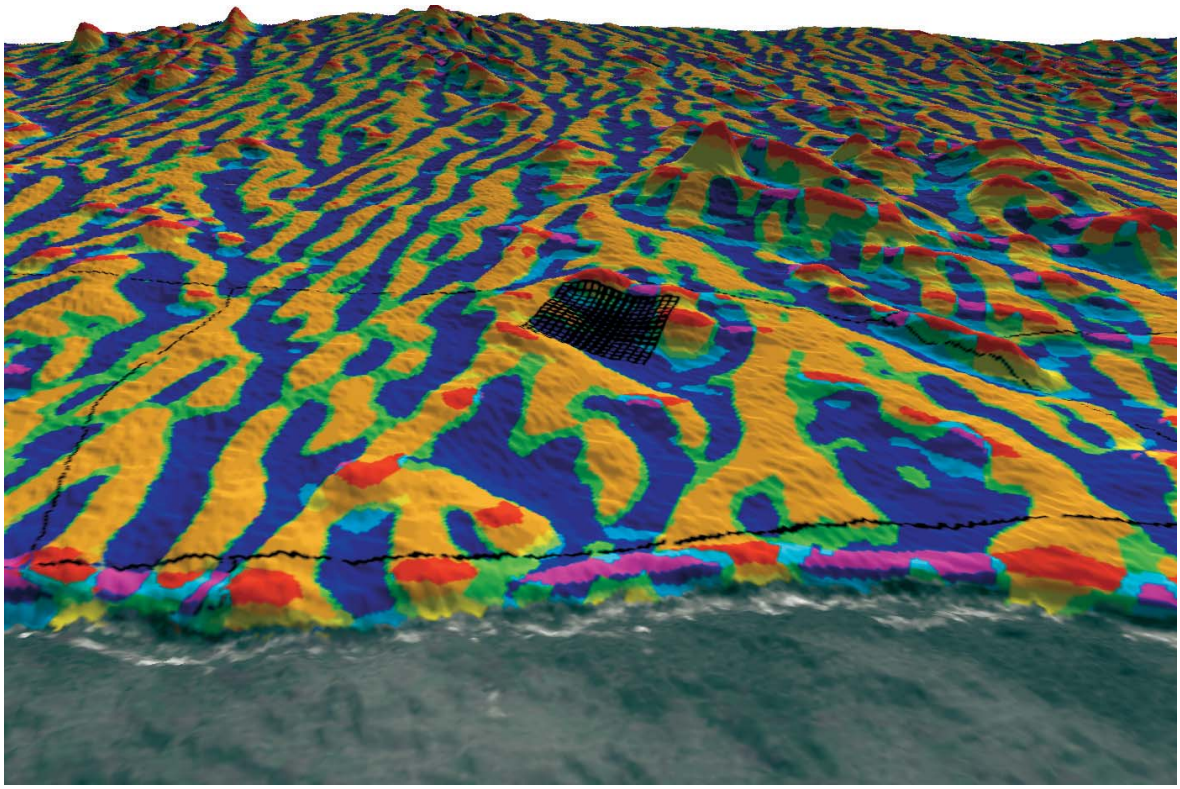

Figure 27: Image drape rendering of the computed geomorphological form elements and the SRTM digital elevation model for the vicinity of the lichen field of Wlotzkasbaken (No. 5) also showing the BIOTA Southern-Africa observatory site.

mostly resembles the rise of terrain of the Central Namib Desert plains towards north-easterly directions and therefore also forms the main direction of run-offs created from rare precipitation events, it most of all constitutes the cardinal heading of episodic foehn-like bergwinds, frequently becoming severe windstorm events during winter (LORIS ET AL. 2004). The aeolian corrosion of the winds reaching over 30 m*s^{-1} can severely damage higher vegetation and is often strong enough to have erosive impact on exposed rock formations (PICKFORD & SENUT 1999). Contrasting to the higher vegetation studies by MCKENNA NEUMANN & MAXWELL (1999) showed that two out of three monospecific sand crusts were stable at wind velocities of up to 10 m*s-1 only which also compared to the threshold friction velocities obtained by BELNAP & GILLETTE 1998). This underlines the potential effects of the frequent windstorm events observed for the lichen communities of the Central Namib Desert in general and the Wlotzkasbaken lichen field in particular (also compare figure 40, chapter 6.5.3).

As fluvial destruction by widened or newly created washes dissecting the lichen field would have formed more linear destructive patterns, the fact that all major change patterns depicted by either map 15 or 16 are merely widespread and plane leads to the conclusion that these patterns were most likely caused by aeolian deflation and accumulation processes.
This is also supported by the surveys performed by SCHIEFERSTEIN (1989), LORIS & SCHIEFERSTEIN (1992) and LORIS ET AL.

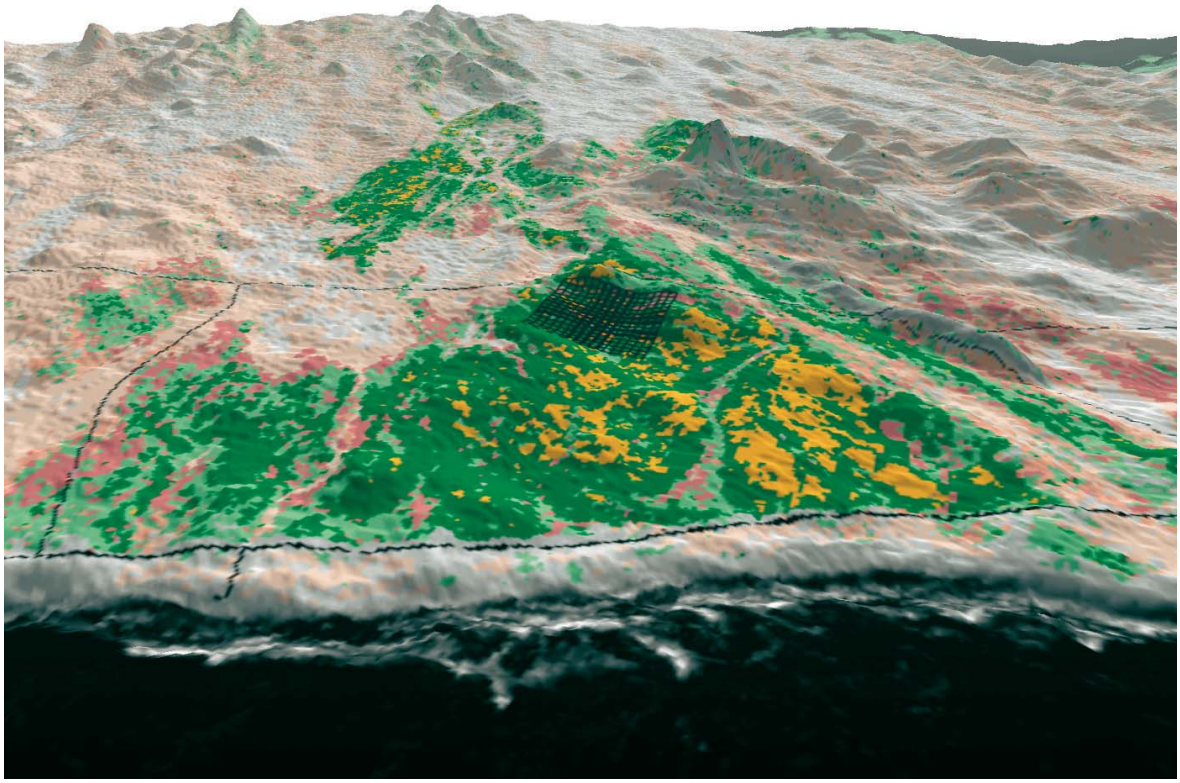

Figure 28: Image drape rendering of the multitemporal classification of 1991 and the SRTM digital elevation model for the vicinity of the lichen field of Wlotzkasbaken (No. 5) also showing the BIOTA Southern-Africa observatory site.

(2004) who considered the southern border of the Wlotzkasbaken lichen field being defined by windstorm abrasion and sand accumulation, which is also reflected by the destructive patterns outlined by the results of this thesis.

The effects of deflation and accumulation of windstorms on the distribution of lichen thalli was studied by SCHIEFERSTEIN (1989) and LORIS ET AL. (2004) with the means of various small nets which were closely attached to the ground and spread throughout the coastal areas of the lichen field of Wlotzkasbaken in 1987 and 1990. Results of SCHIEFERSTEIN (1989) showed that dislocation of lichen material by north-easterly foehn-winds greatly outperformed that of the steady south-easterly winds blowing onshore, with a maximum of 13.6 gm of lichen material intercepted by one net on a single windstorm occasion. LORIS ET AL. (2004) also presented additional evidence that large amounts of lichen fragments disassociated by windstorms are sometimes even removed to the Atlantic Ocean. By extrapolation of material intercepted on the shoreline of Wlotzkasbaken Loris estimated the total loss of lichen material to be around 4 tons for the year of 1990. Although no information regarding the species composition intercepted by the nets is given, its main portion can be considered fruticose and foliose species due to their reduced wind resistance. However many deflated thalli segments are able to resettle after dislocation as repeated observations on permanent sites have shown (LORIS ET AL. 2004).

Therefore it seems likely that the wind-induced dislocation of fruticose and foliose

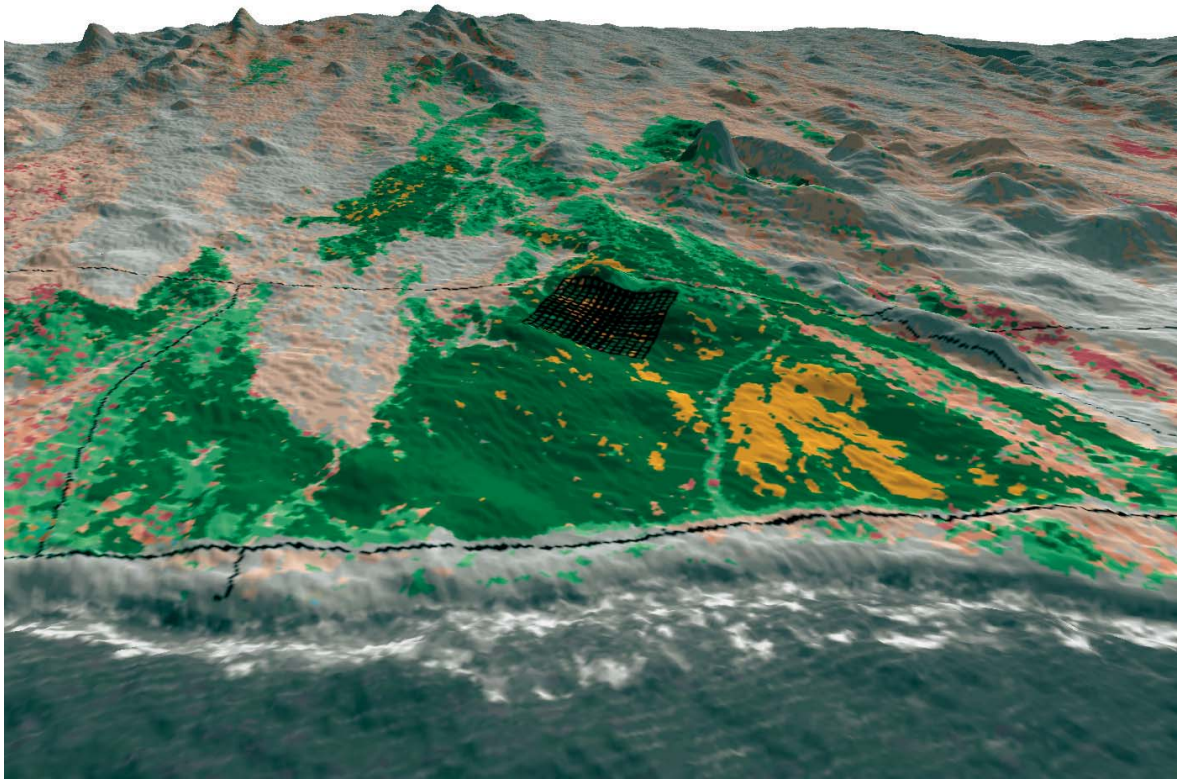

Figure 29: Image drape rendering of the multitemporal classification of 1999 and the SRTM digital elevation model for the vicinity of the lichen field of Wlotzkasbaken (No. 5) also showing the BIOTA Southern-Africa observatory site.

lichen thalli lead to an increase of the fruticose-foliose and foliose lichen communities while at the same time fruticose and foliose-crustose lichen communities coverage decreased (compare figure D21 of annex d).
Thereby fruticose and foliose lichen material was accumulated along the coast due to the north-easterly direction of foehn-storm events although some areas were also strongly affected by wind abrasion in this area (compare 14.26°E and 22.18°S).
On the contrary many of the fruticose-foliose and foliose-crustose communities of the hinterland (14.34°E, 22.16°S and 14.38°E, 22.14°S) were degraded to either foliose or crustose lichen communities due to deflation processes and according to the retrospective classification.

As the deflation and accumulation of lichen material induced by windstorm events can thus be considered a major ecological factor influencing lichen distribution patterns the identification of potential areas prone to deflation of accumulation seems desirable.
Therefore the relationship between the major changes in the distributions of lichen communities and geomorphological form elements was analysed. Although some obvious relationships could be examined no overall correlation was found to exist. Nevertheless an image drape of the distribution of geomorphological form elements and the SRTM digital elevation model is presented for the vicinity of the Wlotzkasbaken lichen field in figure 27 for discussion. To further aid the visual interpretation of the distribution patterns of the form elements obtained from the

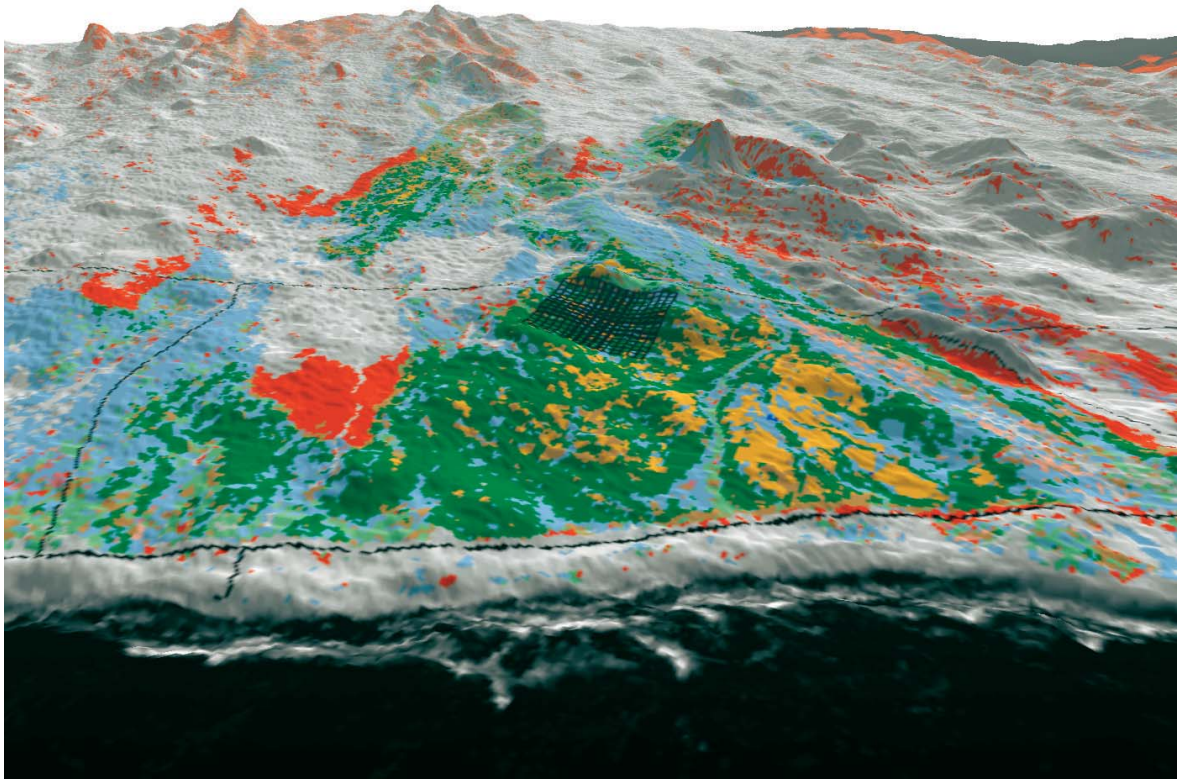

Figure 30: Image drape rendering of the variations in the distribution of lichen communities based on the matrix of post classification change comparison of the timeframes of 1991 and 1999 and the SRTM digital elevation model for the vicinity of the lichen field of Wlotzkasbaken (No. 5) also showing the BIOTA Southern-Africa observatory site.

landform classification and to allow for comparison with subsequent timeframes, drape images were also created for the multitemporal classification results of the years 1991 and 1999 as well as the matrix image obtained from the post classification change comparison for the vicinity of the Wlotzkasbaken lichen field (compare figure 28, 29, and 30).

In addition to the thematic information provided by the various classification results, the drape images also depict an exaggerated approximation of the terrain obtained from the SRTM digital elevation model from an elevated viewpoint looking inland, with the shoreline in the foreground. The images are dissected left to right by the coastal road in the foreground and the road following the powerline in the background as well as smaller dirt roads on either side of the main lichen field running in north-easterly - south-westerly directions. Supplementary the BIOTA Southern-Africa site covering exactly 1 km² is plotted for orientation and scale.

As geomorphological form elements such as ditches and moulds are indicated by blue and magenta colours while ridges and peaks are outlined by yellow, orange and read colours, green colour highlights merely flat terrain. Compared to the drape images obtained for the multitemporal classifications of 1991 and 1999 an obvious relationship between the major fruticose lichen community dominated by *Teloschistes capensis* (L.f.) Müll. Arg. and a long stretched concave mould can be observed (compare figure 27 and figure 29). This mould is encircled by a long-stretched ridge indicated by orange colour except for its seaside.
However the coastal fruticose communities are not evenly spread throughout the mould but are slightly off centred towards the south-western (SW) facing slopes of the north-north-easterly (NNE) ridges encircling them (compare figure 29). This largely coincides with the observations made by SCHIEFERSTEIN (1989) and LORIS & SCHIEFERSTEIN (1992) who firstly described the dominance of fruticose and foliose lichens on SW-exposed, ocean-facing habitats.
In addition LORIS ET AL. (2004) also noted that the aeolian accumulation of lichen material was strongest in between the coastal distance of 0.5 and 1.5 km which also corresponds to the various ocean-facing moulds identified within the area.
Supplementary these habitats are more or less sheltered from north-easterly winds by a range of higher ridges and peaks extending from the vicinity of the BIOTA observatory site towards the coast. Therefore this harboured area extending towards northern (N) and north-easterly (NE) directions in regards of the unique accumulation of the coastal fruticose community also appends to the prominent coastal part of the lichen field of Wlotzkasbaken roughly located between 14.26°E-14.28°E and 22.18°S-22.22°S.

The same interaction of terrain and lichen distribution patterns can also be observed for a small area located north of the observatory site at 14.30°E-22.18°S and to a lesser degree for the lichen patches located alongside the latitude of 22.18°S at a coastal distance of 10 to 15 km.
In these eastern parts of the lichen field natural barriers are less distinct leading to an increase of potential abrasion by sand-transporting east winds which is also reflected by the destructed areas clearly visible in the image drape of the matrix of the two timeframes (compare figure 30). Supplementary it is also increased due to its adjacency to vast areas dissected by washes and covered by unstabilized topsoil layers of quartz gravel and sands located in NNE directions.

Hot and sand-transporting easterly foehn-storms are also responsible for the formation of the southern border of the lichen field of Wlotzkasbaken. With the large dolerite ridge located south-east of the main lichen field area and its adjacent formations clearly outlined by the terrain classification, gaps in these formations are known to channel the windstorms, thereby creating strong gusts and detaching lichens from their anchoring points or covering them with sand (LORIS & SCHIEFERSTEIN 1992). In addition this area is also disturbed by large ephemeral river beds comprising unstabilized vesicular top layers (Schaumböden).

Regarding the terrain structure presented by the geomorphological classification presented in figure 27, all of the above features are clearly outlined. The large ephemeral river bed, also functioning as a wind channel creating the southern border of the lichen field, is located south of the ridge encircling the coastal *Teloschistes capensis* community and stretching further inland alongside the northern face of the dolerite ridge. Indicated by a long stretch of blue colour it is almost continuously depicted (compare figure 27). To the south mostly fruticose and foliose lichen communities are located alongside the face of the dolerite ridge and a gentle bulge in terrain indicated by orange colour before lichen cover is completely averted on an adjacent windswept gravel plain. In these areas steady south-westerly inshore winds can also cause inland accumulations of seaside sands sometimes covering lichen communities as well.

These disturbances caused by the south-westerly winds can also be observed within the Cape Cross lichen field (No. 10). The map of the study area attached to this thesis shows the variations of lichen community distribution patterns and depicts the destruction of vast areas within the 10th lichen field between the years of 1991 and 1999. Based on field observations performed in the years 2002 and 2003 these areas were found to have been fully covered by sands from a south-westerly direction during that period (compare overview image in photo 15).

Underneath the sand cover all lichen communities die back eventually and regeneration is aggravated due to the unstabilized material (compare detailed image in photo 15).

Abrasion and deflation patterns of lichen communities similar to those observed for

Photo 15: Overview and detailed picture of the coastal fruticose community of the lichen field of Cape Cross (No. 10) being covered by sands. Deposition of sands indicates a south-westerly wind direction.

the lichen field of Wlotzkasbaken can also be found in the north-eastern areas of the lichen field of the Omaruru Gravel Plain (No. 7) and the outer areas of the divisions of the lichen field of Mile 8 / Mile 12 (No. 4) (compare map attached to this thesis). Although mixed with the fluvial features of the year 2000 in the map, the plane and widespread abrasion patterns can clearly be observed within the 4th lichen field.
Contrasting with the 4th, the 7th lichen field is located as far as 30 km inland on hummocks which are only prone to fluvial erosion alongside their edges (compare photo 16).

Photo 16: Photo taken in May 2003 showing a couple of hummocks on the south-eastern border of the lichen field of the Omaruru Gravel Plain (No. 7).

Therefore the vast degradation pattern created in the centre of the lichen field is most likely based on abrasion and deflation caused by windstorm events during the period of 1991 through 1999. Unfortunately no climatic data of the study area was available to validate these findings except for the recordings of the Kleinberg (1994 – 2002) and the Double Three (1999 – 2002) weather stations operated by the Desert Research Foundation of Namibia (DRFN) located in the southernmost part of the study area (compare figure A1 and A2, annex a). However the loggings can not be utilized for the discussion of changes observed within the rest of the study area covering almost 300 km of coastline as climatic conditions differ widely throughout the study area.
As an example the direction of windstorms exceeding mean hourly wind velocities of 10 $m*s^{-1}$ at the Kleinberg and Double Three station are compared to those of Wlotzkasbaken on a long-term basis (compare figure 39, chapter 6.5.3).
While the main north-eastern direction of windstorm is complemented by a strong northern component (21 %) for Wlotzkasbaken, Kleinberg station includes large fraction of windstorms coming from south-westerly (9 %) and eastern (8 %) directions although the north-eastern direction of windstorms is still prominent at this station (compare figure 31).
However a fully different picture emerges at the Double Three station which more or less resembles the position of the Wlotzkasbaken station in terms of coastal distance (compare figure 32). For this station the north-eastern wind direction becomes sub-dominant (17 %) in favour of south-western windstorms dominating by 68 %. This is also confirmed by the findings of SEELY & STUART (1976), LINDESAY & TYSON (1990), SEELY & HENSCHEL (1998), and HENSCHEL (2003).

Still it is difficult to speculate about the factors causing changes in the early years of the period between 1991/92 and 2000 as only fragmentary information on climate and ecology has been recorded or published in literature. Moreover due to these differences and the limited spatial and temporal coverage of climate stations for the study area no detailed assertion of the observed variations of the distribution of lichen communities can be realized. Instead the analysis is limited to the interpretation of observed patterns according to the findings of localized studies mainly describing the area of the lichen field of

Wlotzkasbaken (No. 5) (compare (SCHIEFERSTEIN 1989, LORIS & SCHIEFERSTEIN 1992, LORIS ET AL. 2004).

Recapitulating it can be stated that although some large lichen territories alongside the windswept northern and southern borders of the Wlotzkasbaken lichen field were destroyed between the years of 1991 and 1999 the inner structure of the lichen field shielded by geomorphological formations remained mostly intact. At the same time large amounts of lichen fragments were presumably disassociated by windstorms resulting in an increase of lichen territories alongside the coast and distinct areas in the hinterland.
Regarding the remaining study area similar patterns could also be observed within the lichen fields of Mile 8 / Mile 12, the Omaruru Gravel Plain and Cape Cross (No. 4, 7 and 10) for the northern study area. Because of a missing satellite scene of the timeframe of 1999 for the southern part of the study area (WRS-2 179/76) no correlating spatial patterns could be derived for the lichen fields of the Northern- and Southern Naukluft Plateau (No. 1 and 2). Therefore discussion will be limited to the comparison of the multitemporal classifications of 1992 and 2000 which is performed in the following chapter.

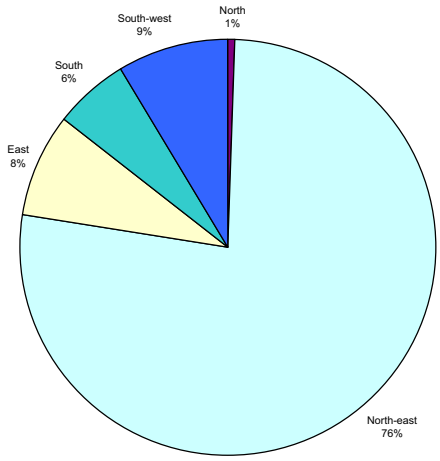

Figure 31: Proportionate occurrence of wind-directions for mean hourly wind-velocities greater 10 m/s, between 01.07.1994 and 31.12.2002 at the Kleinberg automatic weather station within the lichen field of the Southern Namib-Naukluft Plateau (No. 1).

6.5.2 Post classification change differencing between 1999 and 2000

In addition to the previously presented retrospective classifications of the timeframes of 1991 and 1999, a detailed map displaying the distribution of lichen communities of the Wlotzkasbaken lichen field (No. 5) is also provided for the timeframe of the year 2000 (compare map 17).

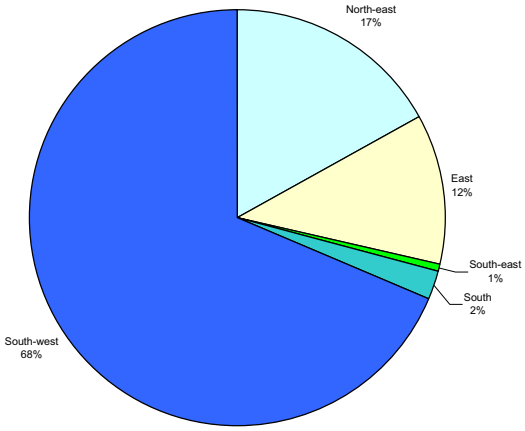

Figure 32: Proportionate occurrence of wind-directions for mean hourly wind-velocities greater 10 m/s, between 03.02.1999 and 13.11.2002 at the Double Three automatic weather station on the western edge of the lichen field of the Southern Namib-Naukluft Plateau (No. 1).

Compared to the variations observed between the timeframes of 1991 and 1999, dissimilar alterations can be depicted between the subsequent image-pair of 1999 and 2000. The results of the computation of a change matrix between the two image pairs are presented in map 18. This matrix image allows for the identification and spatial registration of degraded, destructed and recovered territories based on the lichen distribution patterns obtained from the two classification results.

In contrast to the merely widespread, plane and divers patterns discussed the period of 1991-1999 which were most likely caused by aeolian deflation and accumulation processes, linear features of degradation and destruction are prominent in the image of the post classification comparison of the timeframes of 1999 and 2000. Well developed examples of these patterns can be observed in the hinterland of the lichen field (14.28°E-14.32°E and 22.16°S; 14.36°E and 22.14°S) as well as within the coastal vicinity of its "northernmost" branch" (14.24°E-14.28°E and 22.16°S-22.18°S). Although coherent in shape linearity prevails within the structure of these patterns.

Although subordinate to the previously discussed features, patterns indicating upgraded/recovered territories can also be observed within the gravel plains in the northern area of the lichen field (14.26°E-14.30°E and 22.12°S-22.16°S) and the south-eastern area partly obstructed by dolerite ridges (14.28°E-14.32°E and 22.18°S-22.22°S).

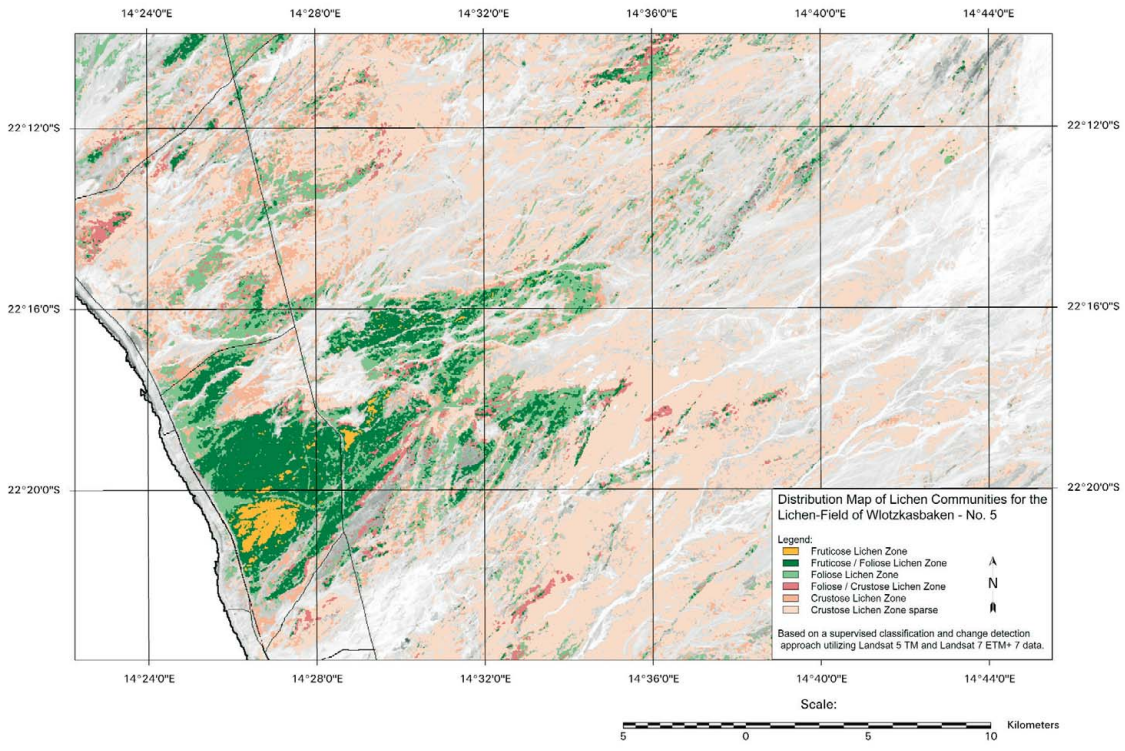

Map 17: Map depicting the distribution patterns of the lichen communities of the lichen field of Wlotzkasbaken (No. 5) for the timeframe of 2000 based on a retrospective classification approach.

These differences are also reflected by the image obtained from the area-wide sPCA approach (compare map 19), discriminating spectral changes from noise for the threshold of 70 in compliance with the retrospective classification strategy (compare chapter 5.2.5.1, figure 26).

Agreement between the map product of the matrix image and the change-index image can be considered strong as the change-index image furthermore emphasizes the dominance of linear features already observed for the matrix image. Especially for the coastal area of 14.26°E and 22.18°S as well as for the region 14.30°E and 22.18°S at about 10 km coastal distance where fruticose-foliose and foliose communities were dissected a strong agreement of destructive change-patterns can be observed. In addition prominent destructive features in the hinterland areas between 14.32°E-14.36°E and 22.12°S-22.16°S as well as 14.36°E-14.44°E and 22.14°S-22.20°S could be observed to reflect changes between the crustose-sparse lichen community and non lichen-covered areas although alterations between these classes were excluded from mapping to underline outstanding changes. Moreover it becomes obvious that almost all of the linear change patterns seem to correspond to washes and river beds clearly outlined by the underlying panchromatic information provided by the LANDSAT 7 ETM+ imagery of the year 2000. Secondary upgrade/recovery patterns were also clearly depicted by the change-index image although patterns were not quite as coherent as obtained from the matrix image of the two classifications (compare 14.28°E-14.32°E and

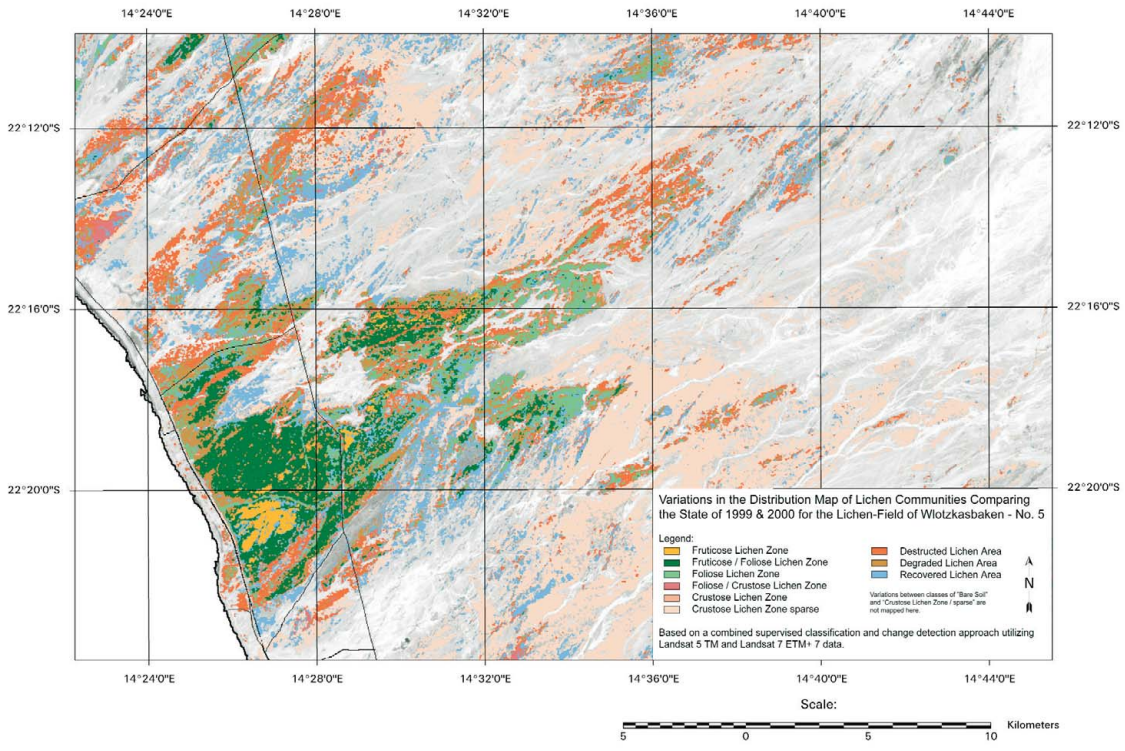

Map 18: Detailed map showing the variations in the distribution of lichen communities for the lichen field of Wlotzkasbaken based on the matrix of post classification change comparison of the timeframes of 1999 and 2000.

22.18°S-22.22°S; 14.26°E-14.30°E and 22.12°S-22.16°S).

As before areal statistics were calculated and analysed to obtain information regarding interclass variations thus complementing localization of change patterns realized with the mapping of the differing classification results. Within the one year period between 1999 and 2000, 8379 ha (46 %) of the lichen coverage and 16733 ha (56 %) of the total lichen field area appointed in 2000 was considered identical to that of 1999. A total of 4294 ha of lichen community coverage was destructed whereas 3488 ha of lichen coverage evolved on formerly none lichen-covered areas resulting in a total loss of 806 ha (compare figure E15, annex e).

However, the increase of lichen community coverage is mostly due to the strong increase of the sparse crustose lichen community (2525 ha, 72 %) which also accounts for most of the lost lichen coverage (2435 ha, 57 %) as well. Due to the high variability of the sparse crustose community an adjusted measure excluding the alterations of this class is proposed. With 1859 ha of lichen cover lost by all other classes and only 963 ha gained by those classes a total of 896 ha of lichen cover is lost within the first five classes in between the years of 1999 and 2000. Compared to the eight year period of 1991 to 1999 where this adjusted measure would have depicted a loss of lichen of 780 ha among the first five classes, a reduction of 896 ha within only one year is impressive.

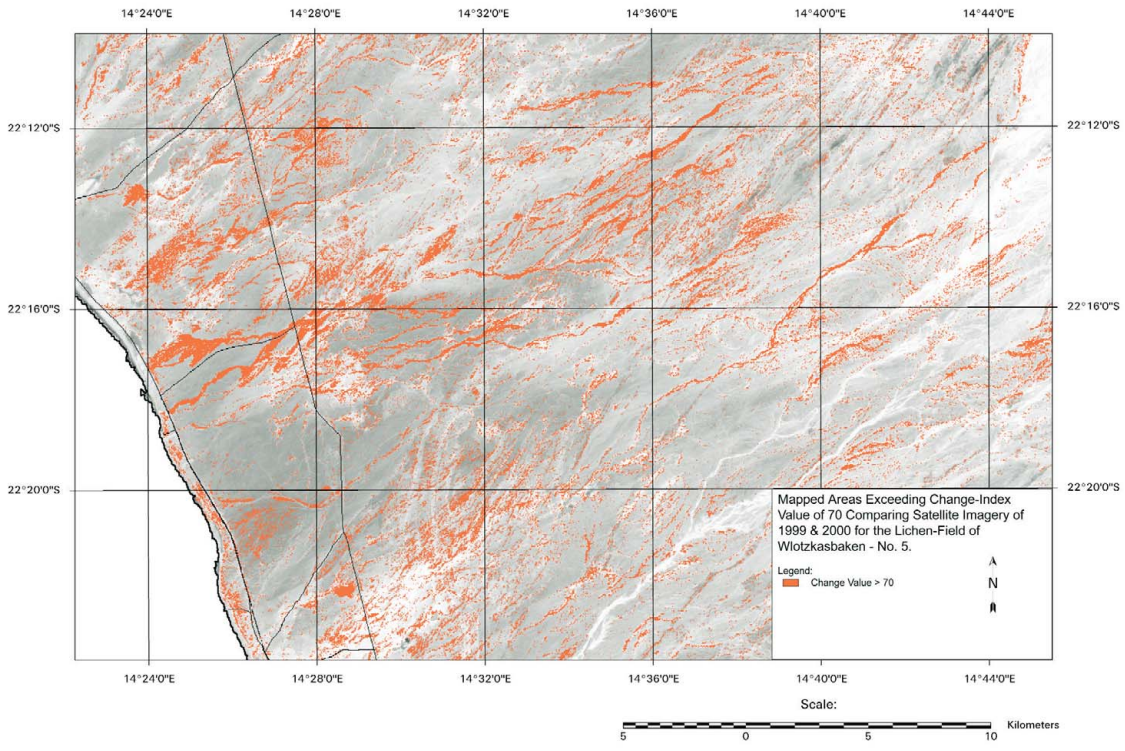

Map 19: Detailed map of the lichen field of Wlotzkasbaken (No. 5) depicting areas exceeding a change-index value of 70 comparing the timeframes of 1999 and 2000 based on the approach of WEIERS ET AL. (2003).

Unlike the preceding eight year period where a sudden increase of fruticose-foliose, foliose communities against a decrease of mostly foliose-crustose communities was predominant the opposite can be observed for the one year period currently under discussion. Both fruticose-foliose and foliose communities are decreased by 619 ha and 401 ha respectively whereas foliose-crustose and crustose community coverage increased by 362 ha and 138 ha (compare figure D13, annex d). However this increase encountered for the "crustose" communities is partly based on degradation of the foliose communities and a sudden upgrade of sparse crustose communities and none lichen-covered areas (compare figure E15, annex e).

Based on these measures and the prominent change patterns encountered by both matrix- and change-index imagery depicting widespread linear features, only unusual run-offs arising from rare precipitation events can be considered as an explanation. Extending in a mostly north-easterly, south-westerly direction and following the general gradient of slope towards the coast some larger washes can be observed to dewater into the Atlantic Ocean while some seem to seep away into inland basins (compare map 18)
Dissecting inner as well as outer lichen field territories washes show fluvial erosion alongside their banks (compare photo 17).
In addition the upswelling of smaller washes produces aggravated degradation and destruction among adjacent lichen communities where no disturbance could be observed for the multitemporal classifications preceding the state of the year 2000 (compare map 18
Furthermore the rainpulse could have also triggered the germination of phanerogamous species which might as well be the reason for the existence of upgrade / recovery patterns among inland basins and dolerite ridges of

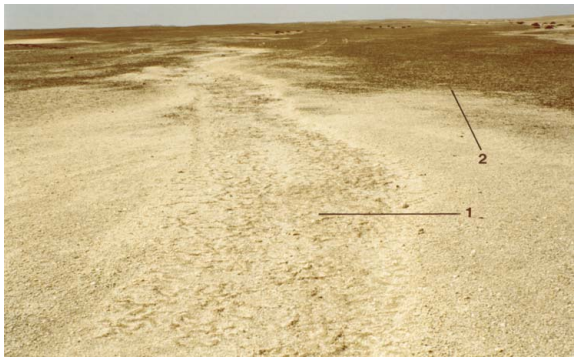

Photo 17: Detailed photo of a small wash dissecting the lichen field of Wlotzkasbaken (No. 5), indicating the wash itself (1) and the lichen cover (2). The banks located in between the two are also disturbed as the fluctuating lichen coverage shows.
Source: SCHIEFERSTEIN (1987).

the lichen field of Wlotzkasbaken due to the increased water supply.

In fact the rainy season of 1999/2000 showed a couple of very rare rain pulse events which were responsible for one of the most exceptional rainfalls events over the Central Namib Desert. After repeated smaller precipitation events recorded for November and December of 1999 (1 – 5 mm) and February of 2000 (1 – 2 mm), a total of 98 mm was recorded by automatic weather station at Swakopmund for the 24th and 25th of March (HACHFELD & JÜRGENS 2000).

Following these rainfall events the routing of waters through all differing kinds of washes and rivers with many of them dewatering into the Atlantic Ocean could be observed (compare photo 18).

Some of the smaller rivers of the Skeleton-Coast Park were also observed cutting through the coastal dune fields during that period [BRABY, R., pers. comm.].
Supplementary to precipitation (HACHFELD 2000) also measured the rainpulse triggered germination of several species along three

coast to inland transects using a nested plot design with four different plot sizes ranging from 1 to 1000 m². Her results showed that cover of ephemeral plant species was almost doubled in favourable areas compared to 1999 while at the same time none-favoured areas showed virtually no increase in ephemeral plant cover.

As the multitemporal classification result for the timeframe of 2000 is based on LANDSAT 7 ETM+ scenes acquired 6th of April (180/75) and 2nd of July (179/76) the effects of ephemeral vegetation cover due to the extraordinary rainfall events are most likely also included in the remotely sensed data.

The routing and accumulation of waters over the surface area subsequent to rainstorm events can be regarded as a fundamental ecological process directly influencing lichen distribution. Therefore additional information on the hydrological and fluvial features shall in the following be utilized for the analysis of the observed disturbance patterns.

Photo 18: Airborne photo of the numerous washes and water channel dissecting the lichen field of Wlotzkasbaken (No. 5).
Source: SCHIEFERSTEIN (1987).

In the following, the relationship between the observed disturbance patterns and the hydrological drainage network derived from flow-direction and flow-accumulation data obtained from the SRTM digital elevation model is analysed. map 20 comprises an overlay of the computed drainage system and the matrix image of the multitemporal classifications of 1999 and 2000.

As the area enclosed by the lichen field of Wlotzkasbaken (No. 5) is located within the northern half of the study area the timeframe of 1999 is available in addition to the area-wide timeframes of 91/92 and 2000. Therefore the utilization of the post classification change comparison of the timeframes 1999 and 2000 is employed as this time-span is likely to include nothing but runoff disturbance patterns.
Unfortunately and probably due to limitations regarding the spatial resolution of the supervised classification and the DEM, no significant statistical correlation between the hydrological drainage network and the disturbance patterns obtained from the post classification change comparison could be observed. Nonetheless a visual analysis is performed for the lichen field of Wlotzkasbaken (No. 5).

Visual correlation between the disturbance patterns and the potential drainage network are evident as nearly all of the water channels coincide with the disturbance patterns obtained from the matrix image (compare map 19). Especially in the “northern” coastal

area of 14.26°E and 22.18°S as well as in the "southern" border around 14.26°E and 22.22°S of the lichen field of Wlotzkasbaken where ephemeral water channels have cut through mostly fruticose-foliose and foliose lichen communities a good level of agreement can be depicted. In addition, degradation patterns along the coastal road (C34) can be associated with the potential run-off arising from the water channels. Nevertheless correlation of destructive patterns also exist for the region 14.30°E and 22.16°S-22.18°S at about 10 km coastal distance where similar communities were dissected by run-off.

In addition the aggregation of drainage lines in the hinterland areas between 14.32°E-14.36°E and 22.12°S-22.16°S as well as 14.36°E-14.44°E and 22.14°S-22.20°S could be observed to reflect changes between the crustose-sparse lichen community and non lichen-covered areas. Nevertheless alterations between these classes were excluded from mapping to underline outstanding changes. Still these destructive patterns are clearly outlined by the change-index image (compare map 19).

Obviously affected by the run-off processes, these areas can also be depicted by comparing image drape renderings of the drainage system, the multitemporal classification result of the year 2000 as well as its matrix image computed from the classification of 1999 and 2000 (compare figure 33, 34 and 35)

Supplementary to the thematic information presented by the different two-dimensional maps, three-dimensional drape images give a

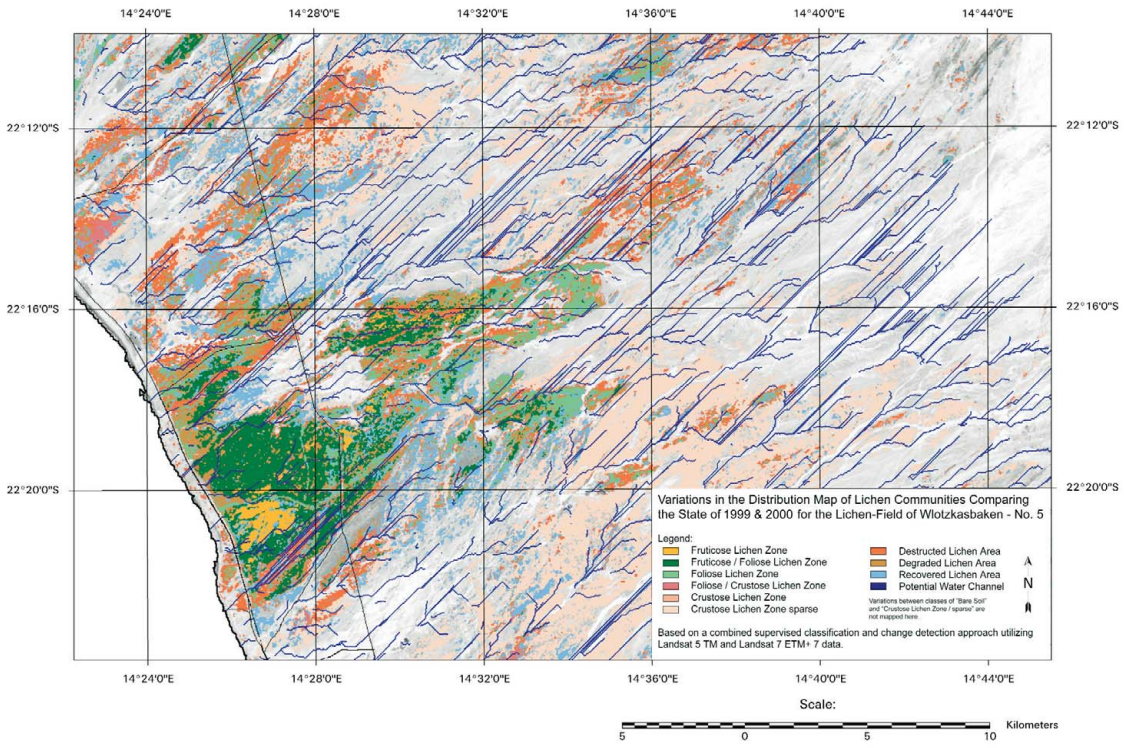

Map 20: Detailed map showing the variations in the distribution of lichen communities for the lichen field of Wlotzkasbaken based on the matrix of post classification change comparison of the timeframes of 1999 and 2000 in conjunction with the potential drainage network derived from SRTM digital elevation model data.

much more vivid impression of the landscape features and relationships.
Within the rendering depicting the flow-accumulation features (figure 33) differing amounts of potentially routed run-off waters are also assigned different shades of blue colour with light colours depicting low quantities and dark ones representing high quantities.

As a side effect, the algorithm utilized for the derivation of the drainage network also tends to accumulate drainage features on flat terrain as no distinct flow-direction is given for the simulation of "water flow" for each pixel. Thereby flat areas with little run-off but increased infiltration rates are indirectly identified. Supplementary these areas are also characterized by widely spread but reduced water quantities as indicated by the light blue colours (figure 33). Conjoined with areas of no apparent drainage in regards of the derived network (compare 14.28°E-14.32°E and 22.18°S-22.22°S, map 20) these areas of high water supply are favourable for ephemeral plant species to occur thus leading to misclassification (also compare 14.26°E-14.30°E and 22.12°S-22.16°S as well as drape image renderings).

These misclassifications also occur scattered among the main agglomeration of the coastal *Teloschistes capensis* (L.f.) Müll. Arg. as some fruticose-foliose areas were upgraded to become part of the *Teloschistes* community (compare map 35). As ephemeral plant species are known to have been present among the community as their remains were still traceable among the lichen communities

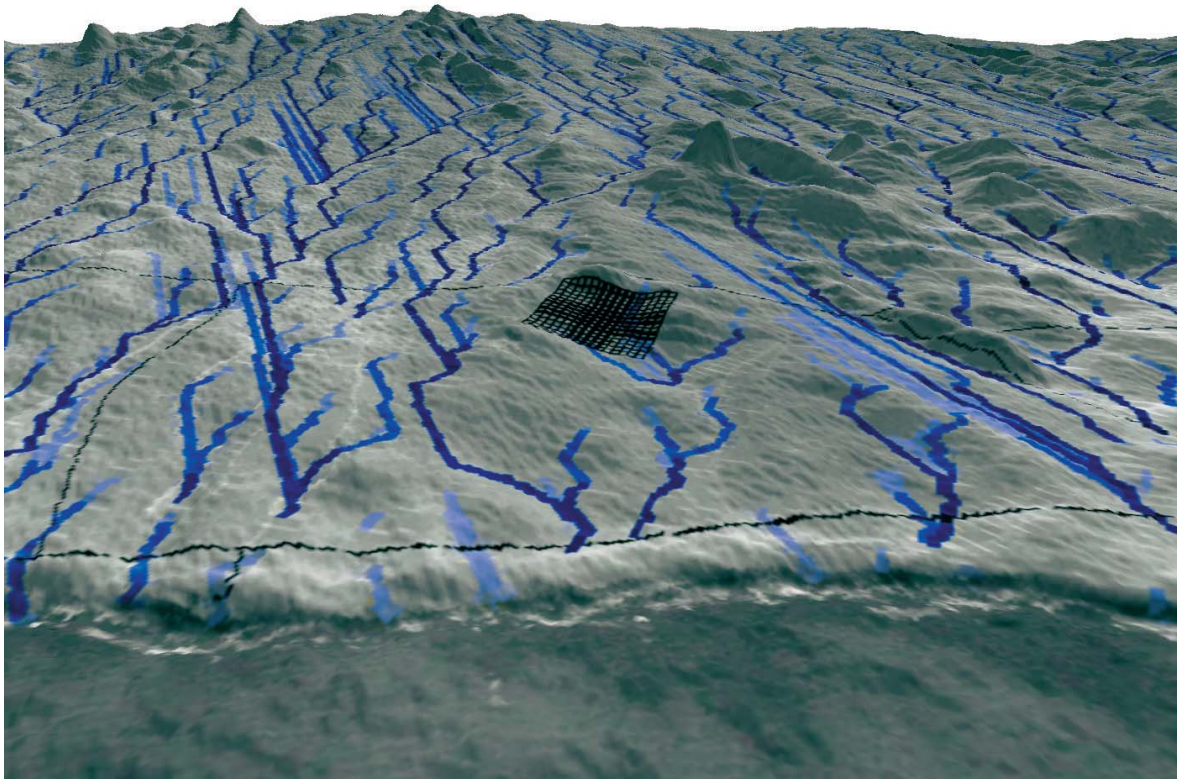

Figure 33: Image drape rendering of the computed potential drainage network and the SRTM digital elevation model for the vicinity of the lichen field of Wlotzkasbaken (No. 5) also showing the BIOTA Southern-Africa observatory site.

during the field campaign of 2002 the concave mould identified earlier presumably collected water as well. However no degradation patterns based on run-off events could be examined in this area.
A similar increase in ephemeral vegetation cover resulting in misclassification can also be observed for the lichen field of Jakkalsputz (No. 6) (compare map attached to this thesis). According to the northernmost transect of HACHFELD (2000) running alongside C35 dirt-road from Hentiesbay to Usakos and dissecting the lichen field of Jakkalsputz (No. 6), rainfall amounted in an average of about 40 mm for the two westernmost zones closest to the coast. Although the relationship between species richness and rainfall events was low, the total cover of ephemeral species was more than twice as high in 2000 compared to 1999, amounting in a maximum of 5.3 %. The remains of this extraordinary increase in ephemeral vegetation could still be observed in May of 2003 (compare photo 19).

On the contrary results of HACHFELD (2000) differed for the Namib-Naukluft Park transect running alongside C14 dirt road and dissecting the lichen field no.1.
In both lichen- (20-30 km coastal distance) and minimum zone (40-50 km coastal distance) delineated by HACHFELD (2000), which correspond to the outer and inner Namib defined by LORIS ET AL. (2004), ephemeral species response did not correlate with rainfall amount. Compared to the measured rainfall amount of 15 mm for the year 1999 neither ephemeral species richness nor cover rates were significantly increased although

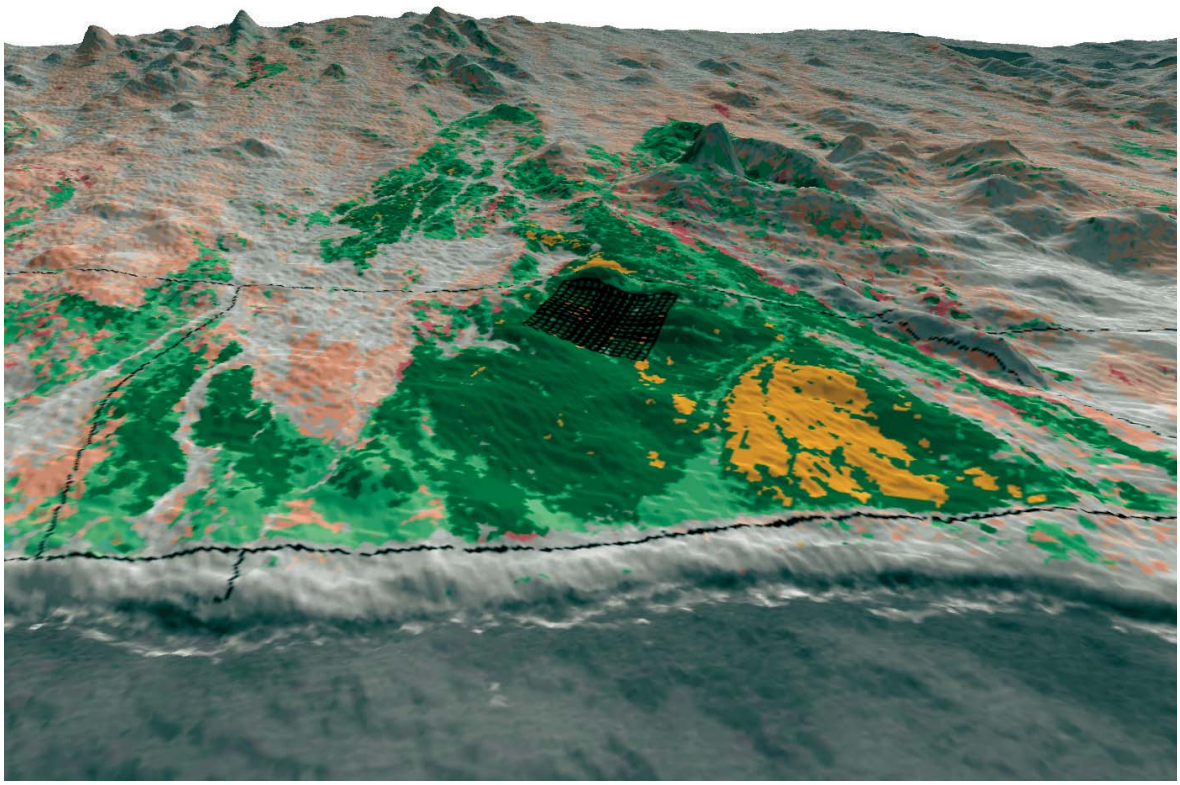

Figure 34: Image drape rendering of the multitemporal classification of 2000 and the SRTM digital elevation model for the vicinity of the lichen field of Wlotzkasbaken (No. 5) also showing the BIOTA Southern-Africa observatory site.

precipitation in March 2000 amounted in 70 - 80 mm for that area which was also confirmed by the Kleinberg weather station. Maximum cover of ephemeral species for the two westernmost zones was measured at a maximum of only 1.6 % in 2000.

This is also reflected by the post classification change comparison of the timeframes of 1992 and 2000 attached to this thesis, also covering the lichen field of the Southern Naukluft Plateau (No. 1). With slight upgrade patterns only found alongside the north-eastern rim of the lichen field none of them could be directly related to the rainfall events during field observations. In addition most of them were stable for the consecutive timeframe of 2003 showing no degradation patterns typical for ephemeral vegetation.

Therefore it can be stated the results on the increase of ephemeral vegetation published by HACHFELD (2000) show good correspondence to the results of the matrix of the post classification change comparison where overmodulation of the classification could be observed for the vicinity of the lichen field of Jakkalsputz (No. 6) and the northern parts of lichen field of Wlotzkasbaken (No. 5) whereas no oversteering could be observed for the lichen fields of the Southern Naukluft Plateau (No. 1) due to an increase of ephemeral vegetation cover among lichen communities.

Although an areal overmodulation of the classification due to extraordinary rainfall events and subsequent increase of ephemeral vegetation was only clearly observed for the

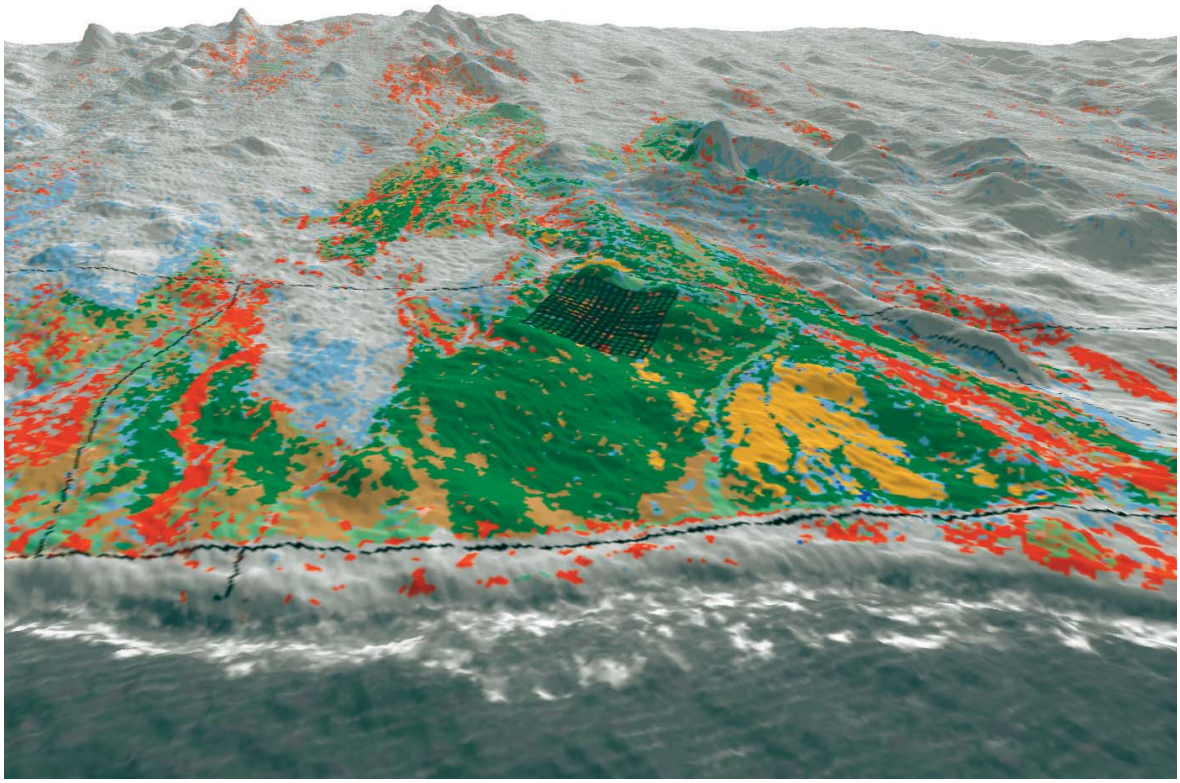

Figure 35: Image drape rendering of the variations in the distribution of lichen communities based on the matrix of post classification change comparison of the timeframes of 1999 and 2000 and the SRTM digital elevation model for the vicinity of the lichen field of Wlotzkasbaken (No. 5) also showing the BIOTA Southern-Africa observatory site.

lichen field of Jakkalsputz (No. 6) and some outer areas of the lichen field of Wlotzkasbaken (No. 5) additional disturbance patterns resulting from the routing of water of these precipitation events can be observed throughout the study area.

These disturbance patterns show no areal shape but form linear features of destructed lichen area which can be best observed within the lichen field of the Northern-Namib-Naukluft Plateau (No. 2) where larger and smaller washes, presumably broadened by the increased runoff, have clearly destructed crustose lichen communities located on its waterssides (compare map attached to this thesis). Opposed to these findings no such patterns could be observed for the neighbouring and southernmost lichen field of the Southern Naukluft Plateau (No. 1).

Within the northern part of the study area the large lichen field of the Messum Crater / Orawab (No. 9) stretching on vast undulating gravel plains widely dissected by watercourses and washes forming more or less isolated lichen covered patches extending in south-west - north-east direction also depicts disturbance patterns from precipitation runoff (compare map attached to this thesis).
On a smaller scale these effects can also be observed for the lichen fields of Mile 8 / Mile 12 (No. 4) where shallow as well as larger washes have clearly cut through the foliose and foliose-fruticose lichen communities (compare map attached to this thesis).

Summarizing the above findings it can be stated that although extraordinary precipitation paired with intense run-offs the inner structure of the Wlotzkasbaken lichen field (No. 5) remained mostly intact although some areas where ephemeral rivers dewatered into the Atlantic Ocean forming small river mouth

Photo 19: Detailed photo taken in May of 2003 showing the remains of ephemeral vegetation resulting from the extraordinary precipitation events of the rainy season 1999/2000.

areas where lichen communities were degraded or destroyed. Meanwhile large lichen territories were washed away by ephemeral rivers of differing sizes dissecting the coherent lichen areas due to extraordinary precipitation events. Lichen communities affected by the run-offs were identified alongside the northern and southern borders of the Wlotzkasbaken lichen field where large ephemeral river structures are predominant as well as in the hinterland where numerous smaller washes prevail.

These disturbance patterns could also be observed for many areas of the study area outside the vicinity of Wlotzkasbaken. While an increase in ephemeral vegetation was clearly observed within the Jakkalsputz lichen field (No. 5), elongated run-off patterns were most prominent for the lichen fields of the Northern Naukluft Plateau (No. 2), the Messum Crater / Orawab (No. 9) and the lichen fields of Mile 8 / Mile 12 (No. 4). All of these findings were also verified by climatic data obtained from HACHFELD (2000), the Desert Research Foundation of Namibia (DRFN) as well as drainage data derived from SRTM digital elevation data.

6.5.3 Post classification change differencing between 2000 and 2003

As the multitemporal classification of the timeframe of 2003 shall in the following serve as reference for the discussion of change patterns arising from the post classification change comparison, this short digression on the analysis of the differences between the uni- and multitemporal classification is intended to outline its potentials and limitations in regards of the unitemporal classification.

In contrast to the retrospective classification of the timeframes of 1991, 1999 and 2000 a unitemporal as well as multitemporal classification of the timeframe of 2003 depending on the utilized signature set is available for the computation of a change differencing. Although representing the same timeframe and only differing slightly in terms of accuracy both classifications serve individual purposes.

While the unitemporal classification represents the best possible result regarding individual class and overall regional accuracy, the multitemporal classification provides slightly lowered accuracy but also time-series comparability based on its reference set only comprising invariant samples. If the unitemporal classification is assumed to comprise the best possible classification result and is therefore referred to as reference, over- and underestimations can be observed for the multitemporal classification, which help putting the

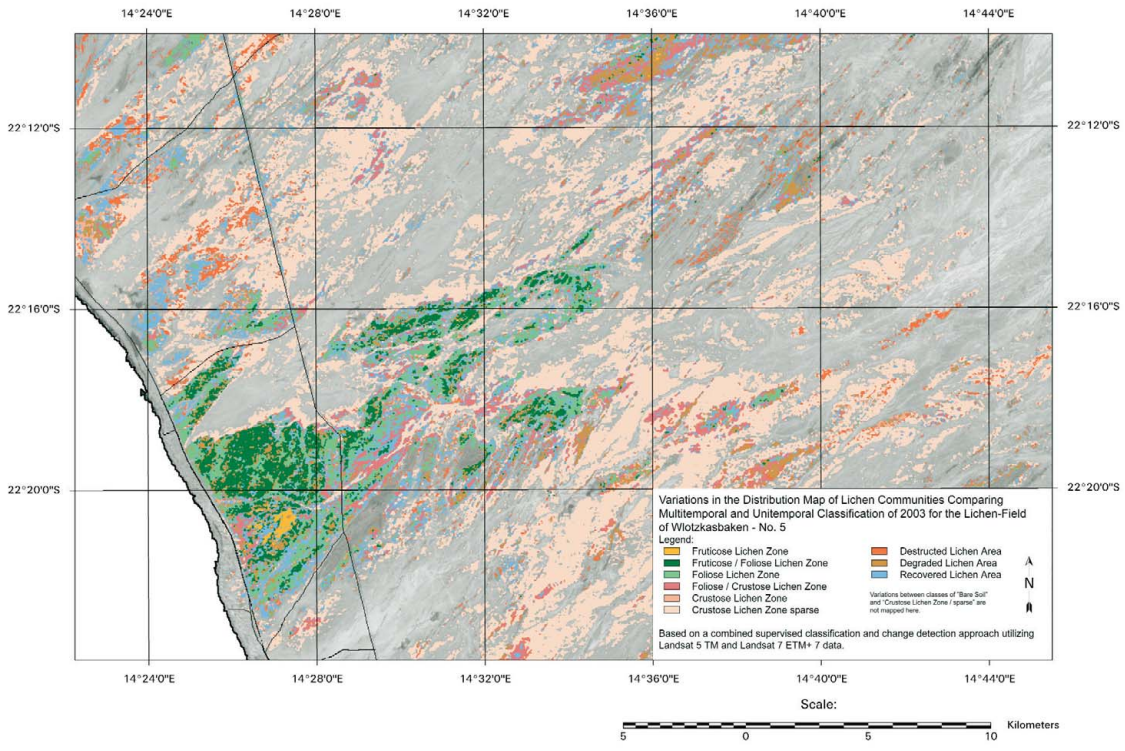

Map 21: Detailed map showing the variations in the distribution of lichen communities for the lichen field of Wlotzkasbaken based on the matrix of post classification change comparison of the multitemporal and unitemporal classification of 2003.

results of the limited retrospective reference set in perspective.

In annex d, figure D4 the total lichen covered areas of the two classification results are compared on a per lichen field basis. It can be observed that the majority of lichen fields are slightly underestimated by the multitemporal classification regarding its total lichen coverage. In total the multitemporal classification comprises about 25778 ha (14.1 %) less lichen cover within the delineated lichen fields in relation to the unitemporal classification which encloses a total of 182457 ha of lichen cover within the confined lichen fields.

If these overall underestimations of the multitemporal classification are split up into individual classes on a per lichen field basis, as shown in figure D5 of annex d, the observed decrease can obviously be averted to an underestimation of the crustose and crustose-sparse lichen communities in favour of neighbouring classes. Both lichen fields of the Naukluft Plateau (No. 1 & No. 2) show the strongest decrease (15610 ha) of crustose classes being allocated to none lichen-covered areas. For the rest of the lichen fields, misallocation is mostly limited to classes neighbouring none lichen-covered areas with the lichen field of the Messum Crater / Orawab (No. 9) showing a significant increase of the foliose community. At the same time the foliose dominated lichen field of the Brandberg West (No. 11) shows a reduction of foliose communities for none-lichen covered territories (compare figure C1, annex c and figure D3, annex d).

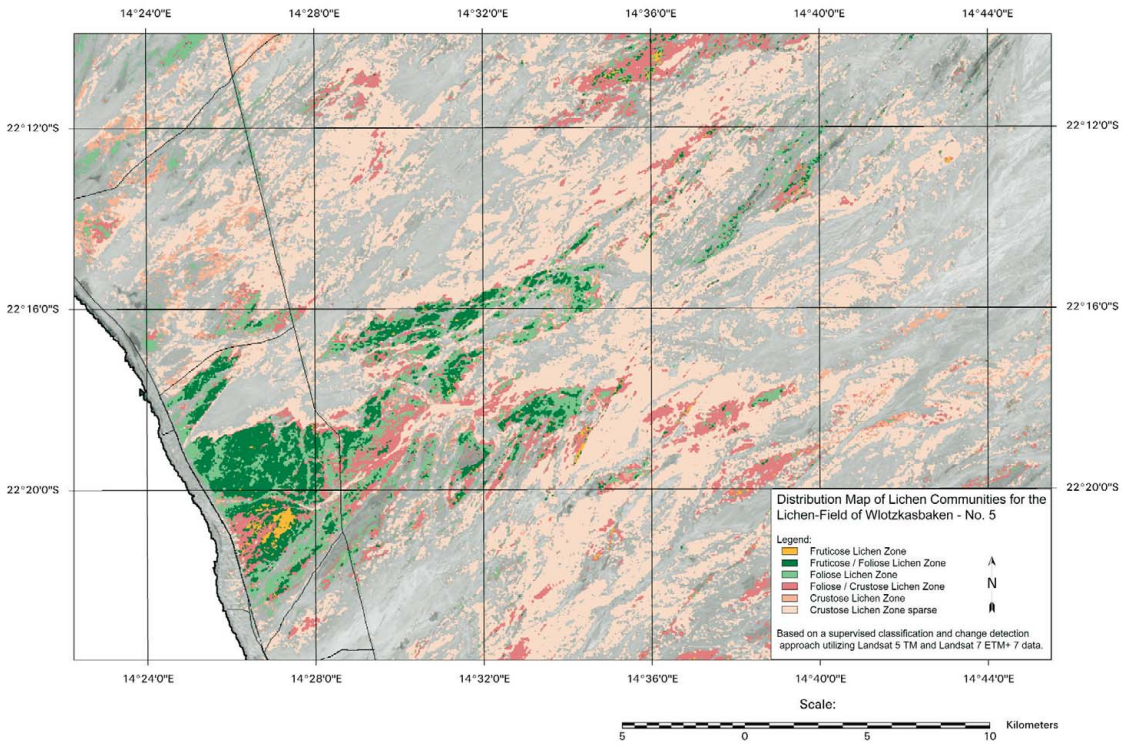

Map 22: Map depicting the distribution patterns of the lichen communities of the lichen field of Wlotzkasbaken (No. 5) for the timeframe of 2003 based on a retrospective classification approach.

What is interlinking these differences is the fact that all underestimated classes are more or less directly bordering none lichen-covered areas if observation is focussed on the particular lichen fields (compare individual lichen field maps of chapter 6.1). This is also shown in map 21, where a detailed post classification change differencing map of the two classifications is exemplary given for the lichen field of Wlotzkasbaken (No. 5).

Therefore it is assumed that the identification of lichen covered areas located in transition zones adjacent to none lichen-covered territory is aggravated and decreased due to the reduced reference set. This however denotes that transition zones of lichen fields are likely to enclose an additional lichen cover of about 265 km² represented by the unitemporal classification. Nevertheless central areas of lichen distributions are clearly outlined and show mostly identical distribution patterns.

Recapitulating it can be stated that if transition zones of lichen covered areas adjacent to none lichen-covered territories are underestimated by the multitemporal classification, degradation patterns will also include these shortcomings. Therefore disturbance patterns arising from post classification change comparison of the multitemporal classification of 2003 will presumably differ by some degree for these territories as if compared to the unitemporal classification result.
Although a map of the lichen field of Wlotzkasbaken (No. 5) has already been presented on the basis of the unitemporal classification in chapter 6.4.5 an additional map displaying the results of the multitemporal classification is presented in map 22. In the following this map will be utilized for the detailed discussion of the variations of lichen distribution patterns between the timeframe of 2000 and 2003.

Based on a post classification change comparison strong spatial variations regarding the distribution of lichen communities between the timeframes of 2000 and 2003 can be observed. In contrast to the periods discussed beforehand, extensive and plane patterns of destruction as well as linear disturbance patterns can be identified. Supplementary these patterns are no longer confined to the windswept borders of the lichen field but affect the inner structure of the lichen field as well. (compare map 23).

In particular the widespread destructive patterns alongside the northern rim of the lichen field (14.26E-14.28E and 22.18°S; 14.28E-14.32E and 22.16°S) are quite noteworthy as coherent patterns of almost the same shape could also be observed in this area for the period between 1991 and 1999 (compare chapter 6.5.1).
In the hinterland of the lichen field at a coastal distance of 10 km which had been widely dissected by washes during the extraordinary precipitation events of the year 2000 additional degradation patterns can also be observed (compare 14.28°E-14.32°E and 22.17°S). Existing water channels seemed to have been widened once more allowing the progression of degradation and destruction among adjacent lichen communities already described beforehand. However all of these patterns seem secondary compared to the extensive degradation found in the inner structure of the lichen field also affecting the agglomeration of the coastal *Teloschistes capensis* (L.f.) Müll. Arg. community (compare 14.26°E-14.39°E and 22.18°S-22.20°S). Although smaller degraded patches have previously

been observed in this vicinity, effects of deflation, abrasion or fluvial erosion have only occurred scattered in this area so far.

Some plane areas of upgrade/recovery also occur subordinate in the hinterland (compare 14.34°E-14.40°E and 22.10°S-22.26°S; 14.34°E-14.44°E and 22.18°S-22.22°S) and alongside the southern rim of the lichen field in the vicinity of the coast (14.26°E and 22.22°S). These patterns are also supported by the area-wide change-index image obtained from the sPCA approach presented in chapter 5.2.3.1 (compare map 24).
With the exception of the subordinate upgrade/recovery, a high correspondence between the change-index image and the matrix image of the classification results can be observed for areas where severe changes of lichen distribution patterns were detected by the post classification change comparison. With all spatial information of potential changes combined within the change-index image and indicated by red colour the extent by which the structure of the Wlotzkasbaken lichen field was affected is accentuated.

During the three year period between 2000 and 2003 only 7177 ha (40 %) of the lichen coverage and 14660 ha (49 %) of the total lichen field area detected for year of 2003 remained unaltered compared to that of 2000 as the analysis of areal statistics shows. In total 4284 ha of lichen communities were lost while at the same time 4445 ha of lichen coverage arose on for-

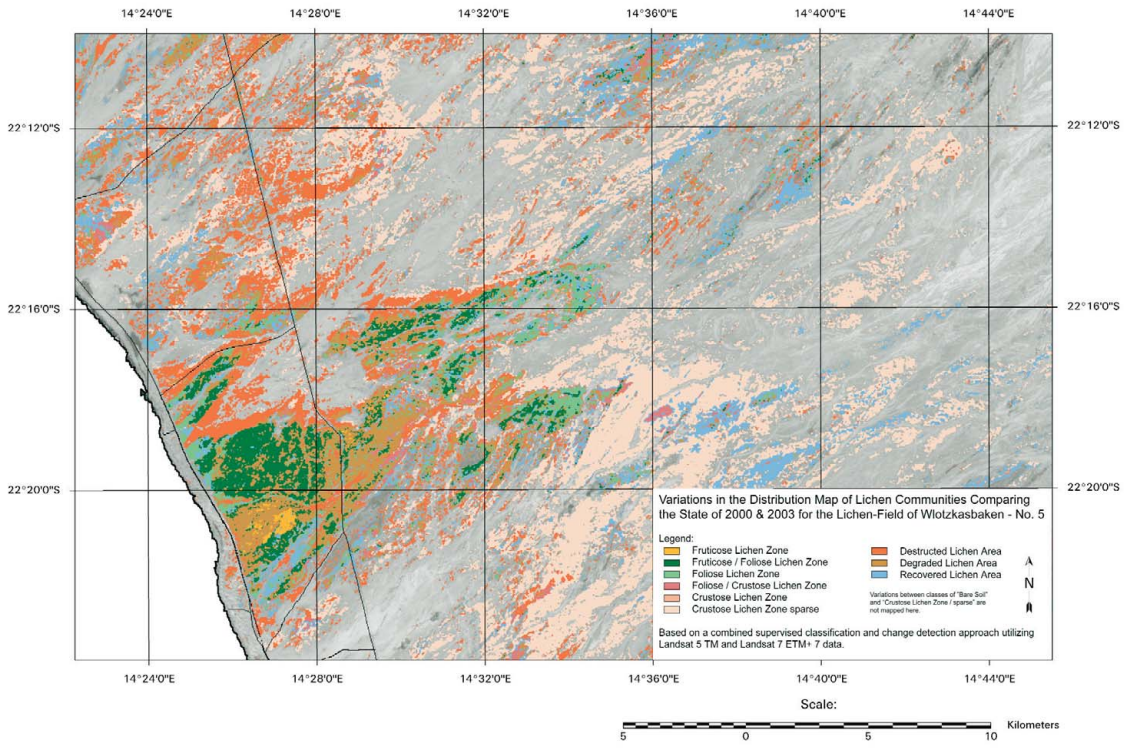

Map 23: Detailed map showing the variations in the distribution of lichen communities for the lichen field of Wlotzkasbaken based on the matrix of post classification change comparison of the timeframes of 2000 and 2003.

merly none lichen-covered areas (compare figure E14, annex e).

However as stated before, this increase of lichen community coverage which would result in a gross gain of 161 ha of lichen coverage is once again due to the strong increase of the highly variable sparse crustose lichen community (3540 ha, 80 %). This community also accounts for most of the lost lichen coverage (2392 ha, 56 %) as well. If this class is excluded from the computation of profits and losses the adjusted loss of lichen communities amounts in 1892 ha, whereas the gain of lichen communities is reduced to 905 ha resulting in a total loss of 987 ha of lichen coverage among the first five classes within a three year period. Compared to the time periods analysed previously where loss of lichen cover amounted in 780 ha (1991-1999) and 896 ha (1999-2000) respectively for the lichen field of Wlotzkasbaken (No. 5) the loss of 987 ha of lichen coverage outnumbers these measures by 27 % and 10 % (compare figure E14, annex e).

In almost the same manner as observed for the one year period between 1999 and 2000 fruticose-foliose and foliose communities were largely decreased. However the observed reduction amounting in a loss of 1443 ha of fruticose-foliose and 1086 ha of foliose lichen communities was more than doubled for the most recent period. In addition the contrasting increase of the foliose-crustose communities can clearly be attributed to areas formerly covered by

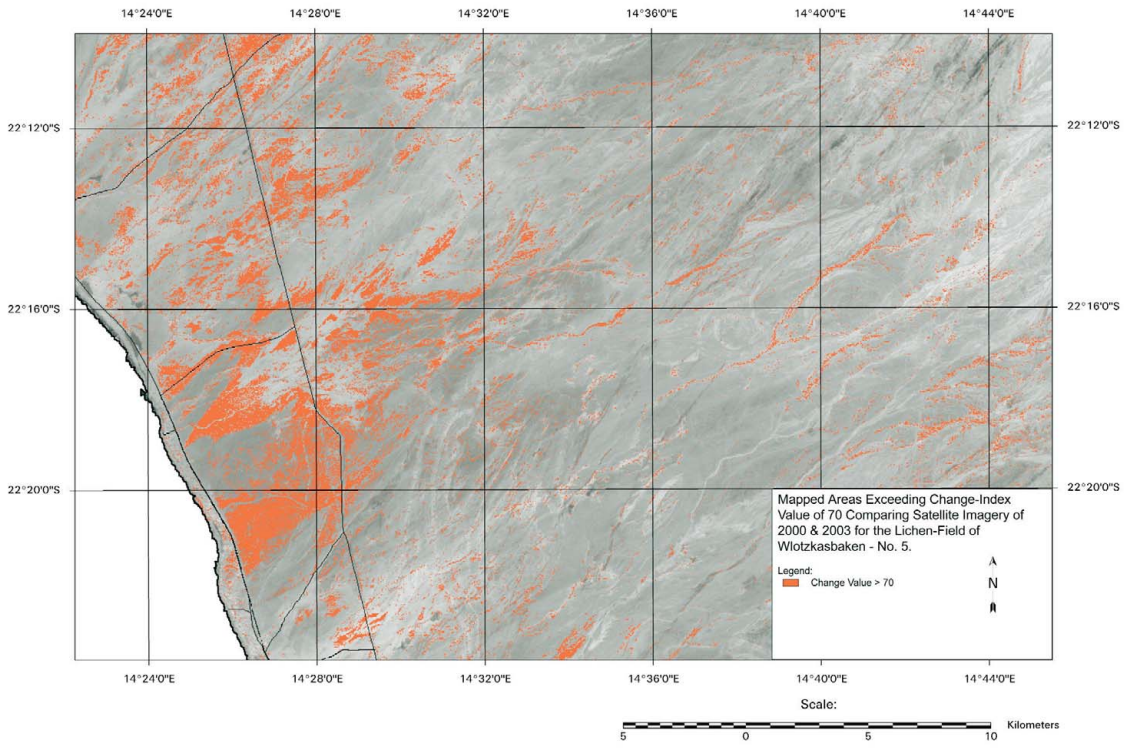

Map 24: Detailed map of the lichen field of Wlotzkasbaken (No. 5) depicting areas exceeding a change-index value of 70 comparing the timeframes of 2000 and 2003 based on the approach of WEIERS ET AL. (2003).

fruticose-foliose and foliose lichen communities (compare map 23).
Moreover fruticose lichen community coverage was reduced to 142 ha, resulting in a loss of 68 % of the coverage observed for the timeframe of 2000 (450 ha) and a reduction to 29 % of the coverage obtained for the timeframe of 1999 (491 ha) and 20 % of the initial coverage obtained for the timeframe of 1991 (701 ha).
Based on the close connection between the descriptive measures previously presented for the period of 1991 to 1999 and the ones currently under discussion as well as due to the widespread and plane disturbance patterns encountered by both matrix- (map 23) and change-index imagery (map 24) it is concluded that these patterns were most likely caused by severe aeolian deflation and abrasion processes. Still the vigorousness by which deflation occurred during the period of 2000 to 2003 must have exceeded that of previous events by multiple times.
This theory is as well supported by the three-dimensional drape image created for the matrix image as well as the result of the multitemporal classification of 2003 (compare figure 36 and figure 37).
Upon examination of the disturbance patterns in relationship to the terrain structure it becomes obvious that most significant disturbance patterns indicated by red colour, are with only few exceptions located on the north-north-west (NNW) facing slopes of minor and major ridges. (compare figure 27 and figure 37).

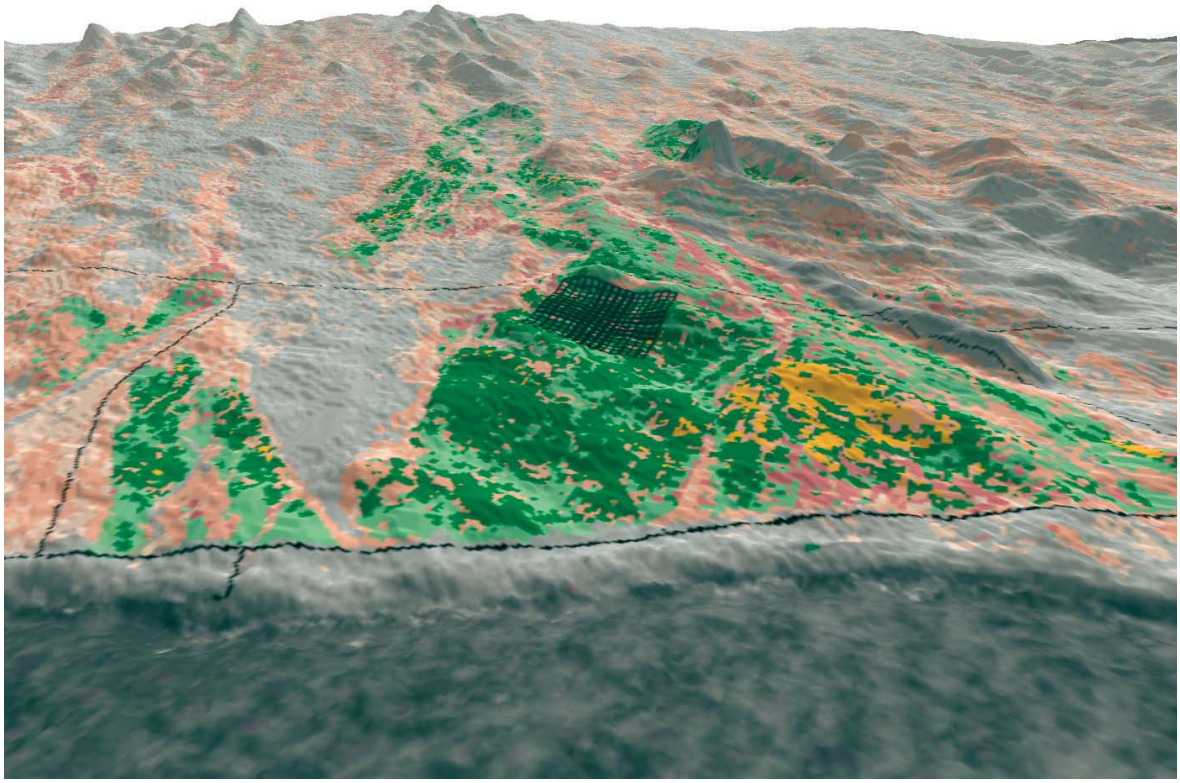

Figure 36: Image drape of the unitemporal classification of 2003 and the SRTM digital elevation model for the vicinity of the lichen field of Wlotzkasbaken (No. 5) also showing the BIOTA Southern-Africa observatory site.

In particular this relationship is visible in the widely dissected lichen covered area in the hinterland at about 10 km coastal distance as well as for the northern border of the lichen field and the agglomerated fruticose community adjacent to the costal road.

For the hinterland area (compare 14.28°E-14.32°E and 22.17°S) previously described disturbance patterns can be largely assigned to the NNW-facing banks of ephemeral rivers and washes which dissected the lichen communities as a result of the precipitation events of the year 2000. As many of these washed out areas are vulnerable to the deflation caused by windstorms due to its missing stabilization by lichen communities of differing types, deflated material carried along by surface winds leads to excessive corrasion among the adjacent lichen communities still remaining.

BESLER (1992) also noted that ephemeral river beds, dry pans and small channels can sometimes even intensify deflation processes as the air stream gets confined within their network. In addition increased corrasion can also arise from extensive areas comprising large amounts of unstabilized materials and bordering lichen community coverage as the amount of wind driven sands and gravel material as well as its momentum is largely increased.

Regarding the terrain associated rendering of the matrix image this effect can be well observed for the vicinity of the northern border of the lichen field where most likely corrasion of materials collected from

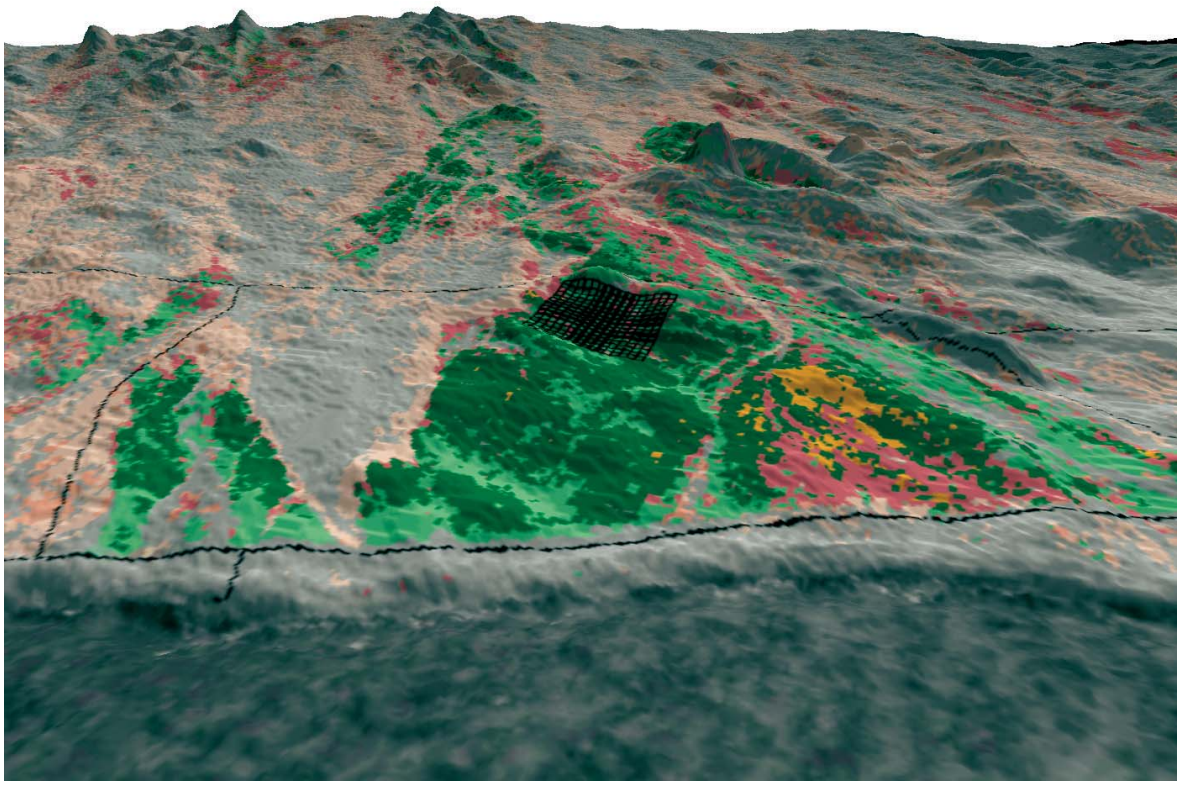

Figure 37: Image drape of the multitemporal classification of 2003 and the SRTM digital elevation model for the vicinity of the lichen field of Wlotzkasbaken (No. 5) also showing the BIOTA Southern-Africa observatory site.

adjacent plains destroyed the lichen coverage forming a large triangular pattern (compare figure 38).

But although many of the observed destruction patterns seem to largely correlate with wind induced abrasion processes no apparent explanation is given for the extensive degradation of the inner lichen field structure including the agglomerated fruticose community adjacent to the coastal road. Irrespective of the detailed changes observed for the lichen field of Wlotzkasbaken by the multitemporal classification of 1991, 1999 and 2000 the inner structure remained almost unaltered up to the most recent timeframe acquired on April 22nd 2003.

In contrast to the limited information available for the detailed discussion of the preceding timeframes of 1991, 1999 and 2000 large amounts of reference information were collected during the field campaign of 2003 only shortly after the acquisition date of the satellite image. In addition most of the reference data could also be compared to samples obtained during the preceding field campaign of 2002 as well as reference information obtained by SCHIEFERSTEIN (1989) and LORIS & SCHIEFERSTEIN (1992) during a 1987 field-study for the vicinity of the Wlotzkasbaken lichen field (No. 5). Thereby photographic documentation of lichen distribution patterns of the Wlotzkasbaken lichen field dating back to the year of 1987 was kindly made available to this thesis by Dr. Kurt Loris. Consistently collected local climatic data from the recently installed automatic

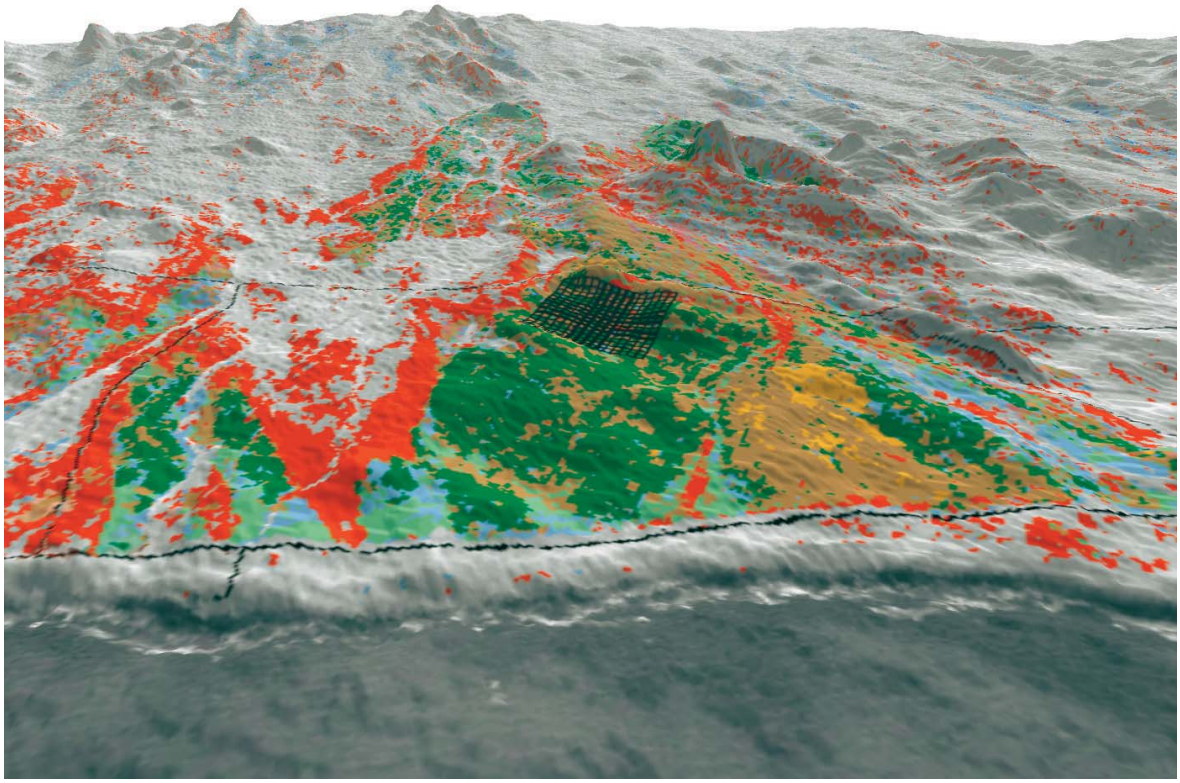

Figure 38: Image drape of the variations in the distribution of lichen communities based on the matrix of post classification change comparison of the timeframes of 2000 and 2003 and the SRTM digital elevation model for the vicinity of the lichen field of Wlotzkasbaken (No. 5) also showing the BIOTA Southern-Africa observatory site.

weather station located in the centre of the BIOTA Southern-Africa observatory site of the Wlotzkasbaken lichen field was also available for the first time. They were provided by the Biocentre Klein Flottbek & Botanical Garden, Hamburg, Germany.
If storm events with wind velocities exceeding hourly mean values of 10 m*s^{-1} recorded by this climate station are mapped into a graph together with mean wind-direction and precipitation values interesting patterns can be observed (compare figure 39).

The threshold value of 10 m*s^{-1} was chosen according to the studies of (Belnap & Gillette 1998) and (McKenna Neumann & Maxwell 1999) who found this value to be critical to most biological soil crusts during wind-channel testing even though hourly mean values of wind velocities exclude gusts which might eventually be much stronger.
Although storm events with very high mean hourly wind-speeds were recorded at the weather station for the period of July through August of 2001 and 2002 prior to that of 16.-17.04.2003 none of them coincided with a rainfall event. With a mean air-temperature value 32.1 °C and prominent north-easterly wind-directions all events prior to the extraordinary storm event of April of 2003 were more or less expressions of the foehn-like bergwinds occurring regularly during the winter. In difference the 2003 storm event included a mean air-temperature value of 22.7 °C, 8.4 mm of rainfall and wind-direction varying

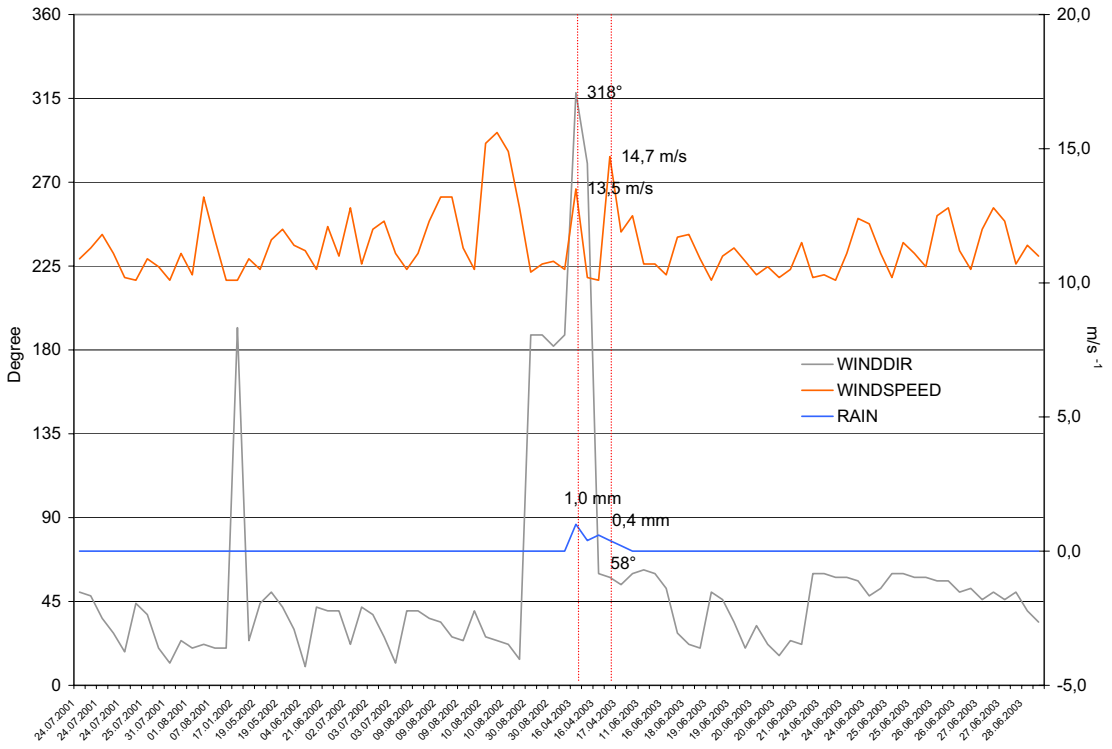

Figure 39: Mean wind-directions and precipitation values for mean hourly wind-velocities greater 10 m*s, between 07.07.2001 and 29.06.2003 at the Biota Southern-Africa observatory site within the Wlotzkasbaken lichen field (No. 5).

between north-westerly and north-easterly directions. Thereby the north-westerly direction of the windstorm is one most uncommon to the area of Wlotzkasbaken as analysis shows (compare figure 40). In fact this wind-direction was only recorded once within a two year period whereas north (21 %) and north-easterly (71 %) prevailed.

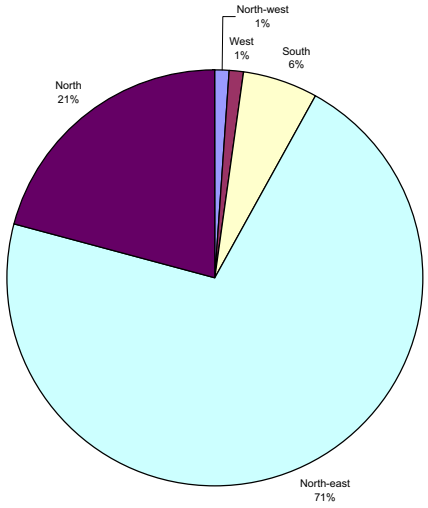

Figure 40: Proportionate occurrence of wind-directions for mean hourly wind-velocities greater 10 m*s^{-1}, between 07.07.2001 and 29.06.2003 at the Biota Southern-Africa observatory site within the Wlotzkasbaken lichen field (No. 5).

Conjoined with the occurrence of rainfall a scenario arises where a storm front must have moved towards the coast coming from the sea in the evening hours of the 16th of April, 2003 resulting in different wind-direction and rainfall during its passage. This is also affirmed by coincidental photos taken by Melanie Vogel from the BIOTA S01 project during that evening (compare photo 20 and photo 21).
In the first picture (photo 20), which is taken from a crest of the costal dune strip in northern direction towards Swakopmund the storm front with its low rain clouds can be clearly outlined moving towards the coast. Most unusual low hanging clouds as well as the formation of rainfall is visible in the second picture (photo 21) which was taken later that evening from the sandy gypsum plains east of the coastal dune strip in western direction towards the vicinity of Swakopmund. This picture also shows that the wind storm was gaining strength towards the evening hours of the 16th of April.
This is also reflected in the climate data recorded by the automatic weather station located within the coastal area of the Wlotzkasbaken lichen field (No. 5). After an unusual hot day with maximum air-temperature of 36.9 °C with hardly any wind from varying directions, wind-speed suddenly rose from 5.1 m*s^{-1} to 13.5 m*s^{-1} for the hourly mean between 18.00 and 19.00 hours and wind-direction changed from south, south-westerly directions to north-westerly directions all of a sudden conjoined with the 1st mm of rainfall. In the following hours between 19.00 and 21.00, wind speed decreased from 10.2 to 5.1 m*s^{-1} while at the same time a total of 6.2 mm of rainfall was recorded by the automatic rain gauge. Wind-direction also changed back towards south, south-westerly directions (196 °).
In concordance with the observation of thunder of lightning during the evening and the early hours of the night (pers. comm. E. Erb and M. Vogel) the thunderstorm must have obviously climaxed between 18.00 and 21.00 hours.
Then wind-direction changed again between 22.00 hours and 3.00 hours of the 17th of April by more than 220 ° towards north-easterly directions (58 °) while wind speed rose to an impressive hourly mean of

14.7 $m*s^{-1}$ between 23.00 and 0.00 hours of the 16th of April. In addition it was still accompanied by slight rainfall totalling in 1.2 mm.
But although the wind storm changed towards the typical north-eastern direction it may not be regarded as such as no foehn-like increase of air-temperature could be observed. Therefore it seems likely that the thunderstorm must have more or less circled over the area thus resulting in strong north-easterly winds as it approached towards the coast from inland territories during the early hours of the 17th of April 2003.
This unique combination of strong winds and rainfall resulting from the thunderstorm caused great damage among lichen communities of the Wlotzkasbaken lichen field (No. 5). As most of the wind resistance of foliose and fruticose lichens in particular is based on the strong and withstanding linkage between the thalli, gravel material and top soil abrasion, deflation by windstorm events is mostly limited to thallus pieces. In addition deflation of thallus pieces may also be a distribution strategy for some species (SCHIEFERSTEIN 1989, LORIS & SCHIEFERSTEIN 1992).

However with the ground softened by the rainfall, as it would never occur during the typical eastern windstorm event, the linking between lichen thalli, gravel material and top soil was strongly weakened. Therefore the windstorm did not only provoke the deflation of thallus pieces but resulted in a widespread "uprootal" of lichen thalli, fully dislocating them from their original territories. Supplementary the most uncommon north-westerly windstorm direction also allowed for the damage of the inner lichen field structure including the agglomerated fruticose community as the "range" of higher ridges and peaks extending alongside the north-eastern coastal border of the lichen field had no protective function (compare figure 27).

This widespread uprootal can also be well observed in images taken after the windstorm event. In addition some of the sites shown in the pictures have also been documented by photographs at differing times preceding the windstorm thus allowing for

Photo 20: Photo taken from a crest of the costal dune strip in northern direction towards Swakopmund. The storm front with its low rain clouds can be clearly outlined in the background moving towards the coast. Source: MELANIE VOGEL (2003).

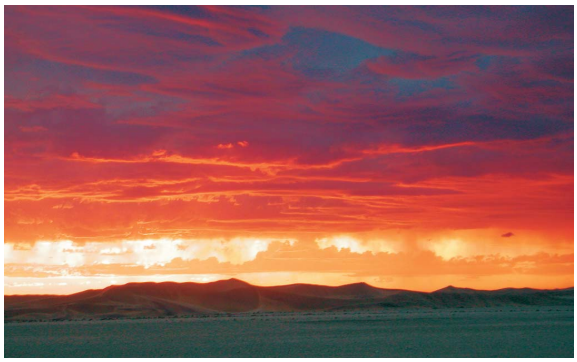

Photo 21: Photo taken from the gypsum plains east of the coastal dune strip in western direction towards the vicinity of Swakopmund showing a massive storm front moving towards the coast with the sun setting behind it. In addition the formation of rainfall is clearly visible. Source: MELANIE VOGEL (2003).

photographic comparison of the differing states.
The first image pair shows a hillock located almost in the centre of the agglomerated coastal fruticose community at the geographic coordinates S 22° 20´ 46.1´´ and E 14° 26´ 20.9´´ (photo 22).

It becomes obvious that the entire fruticose and foliose fraction of the lichen community dominated by the fruticose *Teloschistes capensis* (L.f.) Müll. Arg. was fully dislocated in the period between the two images were taken. An agglomeration of dislocated thalli fragments now forming a large matt of lichen material is also clearly visible on the south-western slope of the hillock.
It is mostly composed of thalli fragments of *Teloschistes capensis* (L.f.) Müll. Arg. as this area is located close to the coast but pieces of *Ramalina sp., Xanthoparmelia walteri* Knox and *Xanthomaculina hottentotta* as well as intact thalli of the vagrant lichen species *Xanthoparmelia convoluta* can also be observed towards the hinterland of the lichen field (compare photo 22 and photo 23).

The second picture also reveals that no interlinking exists between the newly formed lichen mats and the top soil cover as it can be curled up with no force applied. Another image pair depicting the formation of lichen mats induced by the windstorm is presented in photo 24.

While the first picture taken in May of 2000 after the extensive rainfall shows a perfectly healthy fruticose community dominated by tufts of *Teloschistes capensis* (L.f.) Müll. Arg., the second picture shows no such a thing. Again all lichen thalli have been dislocated and it also reveals that precipitation alone does not have much impact on the lichen communities except when it is paired with windstorm.

In concordance with the first image pair presented, patterns formed by lichen fragments run elongated in north-easterly / south-westerly direction, indicating that the abrasion and deflation of the "second"

Photo 22: Image pair documenting the changes observed between September 1987 and August 2003 looking south for the geographic coordinates of S 22° 20´ 46.1´´ and E 14° 26´ 20.9´´ located almost in the centre of the agglomerated coastal fruticose lichen community of the lichen field of Wlotzkasbaken. Source: Dr. Kurt Loris (2003).

north-easterly directed windstorm event must have the degradation also observed by the retrospective classification time-frames under discussion.

Although much of the fruticose lichen biomass of the inner lichen field structure remained in the lichen field after it was dislocated and might as well be able to resettle as stated by LORIS ET AL. (2004), statistics of the retrospective classifications performed for the years of 2000 and 2003 previously revealed a loss of lichen community coverage by 68 %. Due to observations made in the field it can be assumed that this biomass was blown into the sea by the off-shore north-easterly winds. This has also been noted been noted by LORIS ET AL. (2004). The image pair presented in photo 25 shows agglomerations of thalli fragments alongside the shoreline. While the first image shows large amount of mostly *Teloschistes capensis* (L.f.) Müll. Arg. thalli fragments agglomerated in a coastal salt pan, the other image depicts lichen thalli blown up to the coastal dune strip in large amounts.

Supplementary higher vegetation was also affected by the degradation of lichen communities as much of the thalli fragments was accumulated within their branches thus prohibiting photosynthetic activity eventually causing the plant to die. The image pair presented in photo 26 shows a large Arthraerua leubnitziae within the coastal fruticose lichen community of the lichen field of Wlotzkasbaken in September 1987 and after the thunderstorm event in August 2003. While the first image shows the plant in a healthy state surrounded by a widespread cover of fruticose lichen tufts the second image shows the plant being fully covered by dislocated mostly fruticose lichen thalli fragments. In addition it is now

Photo 22: Detailed photo taken May 2003 showing the composition of an agglomeration of thalli fragments dislocated by the windstorm event of 2003 at the “power-line” dissecting the lichen field of Wlotzkasbaken.

Photo 23: Detailed photo taken May 2003 showing a newly formed lichen mat created from dislocated thalli fragments being easily curled up as no interlinking to top soil exists.

Photo 24: Image pair documenting the changes observed between May 2000 and August 2003 looking north-east for the geographic coordinates of S 22° 20´58.6´´ and E 14° 26´10.5´´ located in the agglomerated coastal fruticose lichen community of the lichen field of Wlotzkasbaken. Source: Dr. Kurt Loris (2003).

Photo 25: Image pair of photographs taken in May 2003 depicting agglomerations of thalli fragments along the shoreline and the coastal dune strip.

Photo 26: Image pair documenting the changes observed between September 1987 and August 2003 for the geographic coordinates of S 22° 20´ 40,3´´ and E 14° 26´34,5´´ showing the effects of lichen community degradation on an Arthraerua leubnitziae within the lichen field of Wlotzkasbaken. Source: Dr. Kurt Loris (2003).

mostly surrounded by bare ground except for some scattered lichen coverage.

Considering the above references it can be stated that large amounts of lichen cover were either destroyed or degraded by unusual thunderstorm event comprising rainfall as well as strong north-westerly and north-easterly winds. As the interlinking of top-soil, gravel material and lichen thalli was weakened by a total of 8.4 mm of rainfall, deflation and abrasion of lichen communities by winds comprising hourly mean velocities of up to 14.7 $m*s^{-1}$ was strongly increased. This is also verified by previous observations for the years 1991, 1999 and 2000 where no exclusive rainfall or windstorm event affected the inner structure of the Wlotzkasbaken lichen field. While some of the lichen thalli fragments accumulated into newly formed mats loosely attached the ground or were collected within natural gutters, a large amount of lichen biomass was also blown off-shore as observations following the thunderstorm indicated.

In total fruticose communities were reduced by 68 % while fruticose-foliose communities suffered a loss of 35 %. In combination with the reduction of the foliose communities by 25 % most of the deflated areas were degraded to the foliose-crustose community type which increased by almost 200 % compared to the state of the year 2000.
In comparison to the unitemporal classification of 2003, gains and losses indicated by the multitemporal classification differed between 2 and 13 % for all classes except the foliose-crustose and crustose type. Due to the limitations of the retrospective signature set utilized for the multitemporal classification, the identification of lichen covered areas located in transition zones adjacent to none lichen-covered territory is aggravated resulting in differences of up to 82 % for the two classes compared to the timeframe of 2000. Therefore the unitemporal classification shows much better plausibility for these classes as it reflects the gain of the foliose-crustose class (113 %) due to the degradation of fruticose and foliose classes as well as the stability of the classes dominated by crustose lichens (16 %) due to their increased resistance to abrasion and deflation.

Subsequently to the detailed discussion of the extensive degradation patterns identified by the post classification change comparison of the timeframes of 2000 and 2003 for the lichen field of Wlotzkasbaken (No. 5), change patterns shall also be analysed on the scale of the study area. Therefore discussion shall be based on a map, graphically depicting the results of the computation of a change matrix of the image pairs of 2003 and 2000 in DIN-A1 format attached to this thesis.

In addition to the matrix map of the study area the spatial distribution of changes can also analysed utilizing the information derived from the sPCA computation of the training samples (compare chapter 5.2.6). Bar plots indicating spatial membership in regards of identified lichen fields as well as observed change intensity were created for the comparison of the timeframes of 2003 and 2000 (compare figure 41 and figure 42). Lichen field membership resulted from the delineation of lichen covered areas used for the discussion of the results of the unitemporal classification (compare chapter 6.1).

Both bar plots calculated form the southern (WRS-2 179/76) and the northern (WRS-2 180/75) LANDSAT 7 ETM+ image pairs give a first impression of the rather heterogeneous spatial distribution of changes between the two timeframes. With strong spectral alterations of training samples mostly confined to the area of the lichen fields two to six these results are also reflected by the matrix map of the two time-series classifications.

Starting with the vicinity of the lichen field of Jakkalsputz (No. 6) change intensities indicated by the training samples agree with the widespread patterns of destruction outlined for the hinterland at about 10 km coastal distance by the map of the study area attached to this thesis. However these spectral changes are no result of the degradation of lichen communities but a consequence of the die back of ephemeral vegetation triggered by the extraordinary rainfall events of 2000. These patterns were also discussed for the image-pairs of 1999 and 2000 where in opposition to the degradation patterns and overmodulation of the classification could be observed and related to rainfall events. Although not as widespread in shape these "degradation" patterns due to ephemeral vegetation can also be observed within the lichen fields seven through twelve indicated by the matrix map and reflected by scattered spectral divergence of training samples obtained during the 2003 field campaign. Also noteworthy are the scattered elongated upgrade patterns within the lichen fields

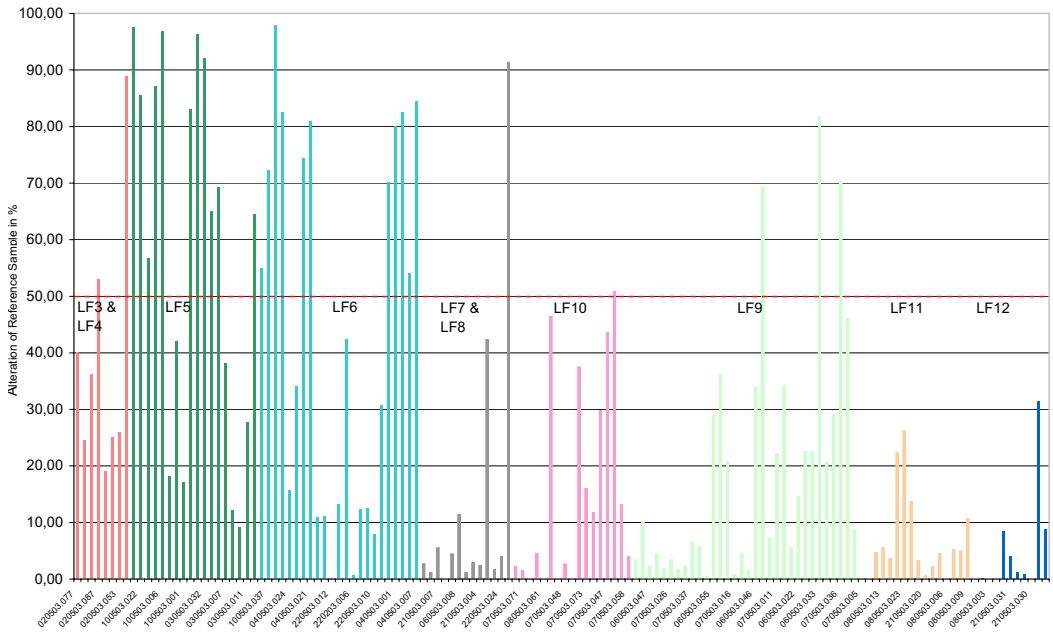

Figure 41: Observed normalized change intensities of reference samples between the timeframes of 2003 and 2000 mapped according to lichen field (LF) membership for the coverage of WRS-2 scene 180 / 75.

nine, ten and eleven where lichen communities seemed to have recovered alongside the washes dissecting them earlier in 2000.

The lichen field of Mile 8 / Mile 12 (No. 4) seems to reflect the changes of lichen distribution patterns which have previously been discussed for the lichen field of Wlotzkasbaken (No. 5). Patterns of degradation and destruction are once again not only confined to the northern rims of the elongated divisions of the lichen field but are also affect the inner structures alongside the coast. Although reference samples show slightly lowered change intensities for this lichen field as they are mostly confined to the inner lichen structures of the hinterland of the lichen field, remains of blown lichen thalli fragments could also be found alongside the coastal-road C34 in May of 2003 two weeks after the passage of the thunderstorm (compare photo 29).

The Nonidas lichen field (No. 3) located east of Swakopmund alongside the tar road B2 could have served as an interlink between the vast gravel covered plains of the northern study area and the undulating gypsum plains of the south. However local cloud cover for the year 2003 did not allow for comparison with the previous timeframe of 2000.

Subsequently change patterns of the lichen field of the Northern Naukluft Plateau (No. 2) are discussed. Although dominated by the by a crustose lichen community consisting of terricolous sand-binding species with largely increased wind resistance compared to the erected thalli of most fruti-

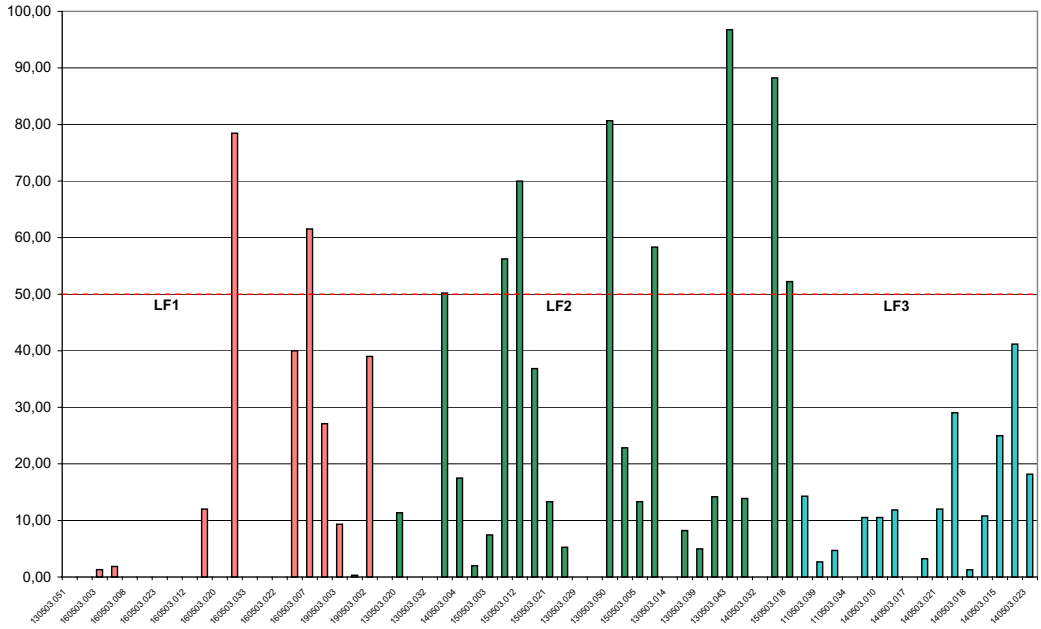

Figure 42: Observed normalized change intensities of reference samples between the timeframes of 2003 and 2000 mapped according to lichen field (LF) membership for the coverage of WRS-2 scene 179 / 76.

cose and foliose species strong degradation patterns are depicted the matrix map alongside its the western border.

The image pair presented in photo 27 depicts such an area where the terricolous crustose community has been fully removed. Only scattered saxicolous species can still occur scattered. In addition extremely wind blown thalli fragments with maximum diameters of 1 cm can also be observed lying loosely on the ground alongside the newly created western border of the lichen field no. 2 (compare photo 28).

Due to a lack of localized climatic data for the area it can only be assumed that the combined effects of rainfall weakening the interlinking between the terricolous lichen cover and subsequent abrasion by windstorm was responsible for the observed degradation patterns in much the same way as previously discussed for the lichen field of Wlotzkasbaken. However all photography's of the thunderstorm presented earlier in photo 20 and photo 21 were taken from this area, thereby indicating that the thunderstorm did most likely affect this

Photo 28: Wave-pattern of extremely wind blown thalli fragments of the terricolous sand-binding crustose community alongside the newly created western border of the lichen field of Northern Naukluft Plateau (No. 2).

Photo 27: Image pair of photographs taken in May 2003 depicting abrasion patterns within the former western parts of the lichen field of the Northern Naukluft Plateau (No. 2) where the terricolous sand-binding crustose community has been fully removed.

area as well. This is also supported by the strong change intensities of the reference samples in this area (compare figure 42).
Contrasting with the degradation patterns encountered on the western border of the lichen field no. 2 recovery patterns alongside larger and smaller washes are also depicted by the matrix image of the two multitemporal classifications of 2003 and 2000 within the inner area of the lichen field. Therefore it seems likely that the lichen coverage alongside the banks of the washes which was previously degraded by the extensive run-offs caused by the extraordinary precipitation of the summer of 1999 / 2000 has started to recover.

Photo 29: Photo taken May 2003 showing an agglomeration of thalli fragments dislocated by the windstorm event of 2003 alongside the coastal-road C34 west of the lichen field of Mile 8 / Mile 12 (No. 4).

Opposed to the climatically induced change patterns observed for the previously discussed lichen fields the southernmost lichen field of the study area (No. 1) comprises some change patterns due to the expansion of a power-line dissecting the lichen field (compare photo 30).
Following the erection of a large construction site office at 22 55 08.31 S and 14 43 33.11 E about 9.6 km north-east of the airport of Walvisbay (turn-off from C14: 23 00 27.55 S and 14 43 03.01 E) and an the obviously increased frequentation of an electric power substation located at 23 02 29.95 S and 14 40 26.21 E lichen communities were obviously degraded alongside the access routes. However considering the size of the lichen field and the actual areas affected the effect seems negligible as long as disturbance remains confined to these routes.

Photo 30: Power-line dissecting the lichen fields of the Naukluft Plateau and destroying the lichen communities along its way due to off-road driving required for service and maintenance.

7 Summary and discussion

This chapter summarizes and highlights the implication of the results presented by this thesis. Potentials and limitations of the presented mapping products are explained, and advantages and disadvantages of the methodology and techniques used for image processing are discussed. In addition major contributions of this thesis are listed.

7.1 Detecting and mapping the spatial distribution of major lichen communities in the Central Namib Desert

Identified earlier, it is essential to map the occurrence and distribution of biological soil crusts on a regional scale. Increased knowledge on the large scale distribution patterns yields better understanding of desertification and climate change processes and may also indicate changes in the utilization and function of landscapes. Therefore the first part of this thesis successfully addressed the mapping and detection of the spatial distribution of major lichen communities in the Central Namib Desert, Namibia.

Perennial vascular cover is extremely sparse in the outer Namib Desert where most of the lichen dominated biological soil crust cover is situated (ULLMANN & BÜDEL 2001A, WALTER & BRECKLE 1999[7]). In addition the Central Namib Desert shows almost horizontal, hummocky gravel plains, dissected by numerous sandy washes and dry river beds, only interrupted by scattered inselbergs and rocky ridges. Combined with the extraordinary vast coverage by lichen dominated biological soil crusts representing up to 100 % of living cover, these preconditions set by the vegetation and geomorphology also favour this study area among others.

With the study area covering a costal strip of more than 21480 km², remotely sensed LANDSAT 7 ETM+ datasets were utilized for the presented approach. Acquired on April 22nd and May 1st of 2003, two scenes referred to as 180/75 and 179/76, based on the WRS-2 reference system, were processed in order to conduct a supervised classification approach. Ground reference information was obtained from two field campaigns in 2002 and 2003, with the latter ones being collected almost simultaneously to the acquisition of the satellite data. Chosen for homogeneity and size during field work, a total of 874 well documented training samples describing lichen communities were collected within the study area. Most abundant species are also described in annex b.

In regard to the digitized Namibian topographical maps – scale 1 : 50.000 – and GPS measurements obtained during field campaigns, pre-processing of the satellite images also involved absolute geometric correction. By means of Ground-Control-Points and polynomial reprojection, the spatial error of the original "level-1G" products obtained from the U.S. Geological Survey was greatly reduced. In addition to the very low "mean square root error" reported by the polynomial function, good spatial alignment towards reference information could also be reported (compare chapter 4.1.3). As a consequence an excellent spatial registration between ground truth data obtained during the field campaigns of 2002 and 2003 and the satellite imagery could be achieved. In order to assume a common radiometric scale among the neighbouring satellite scenes covering the study area, atmospheric correction was applied subsequently using the ATCOR algorithm (compare chapter 4.1.4).

In order to further enhance homogeneity, all training sites were revised using the iterative identification of contiguous pixels with simi-

lar spectral characteristics by means of a Region Grow Algorithm. As a result of this verification process a total of 206 optimized training samples could be identified. The large discrepancy to the original amount of 874 samples can be fully related to the constrictions of field surveys, where true homogeneity of areas intended to consist of several hectares in size is hardly overlooked completely.

Based on the results of the field campaigns and the concept of morphological groups introduced by ELDRIDGE & ROSENTRETER (1999), a hierarchical classification scheme was successfully developed. On a community level, it proved to be an important pre-condition for the coherent assessment of lichen distribution patterns in the study area.

Consisting of a course first level and a detailed second level, this classification scheme allowed for the assessment of the whole study area while at the same time being able to adjust to local conditions.

However, all thematic classification products presented in this thesis, focus on the first level classification hierarchy consisting of a limited number of sturdy classes. Besides the obvious delineation of lichen-covered- and none-lichen-covered areas this level focuses on the identification of three lichen communities either dominated by fruticose, foliose or crustose cover as well as their transition classes fruticose/foliose, foliose/crustose and crustose sparse.

Due to this standardization, regional comparison of lichen distribution patterns is ensured and robustness to potential sensor noise included in the satellite imagery is enhanced. In addition transferability of the classification products was successfully facilitated to allow for the development of a broad-scale monitoring of spatiotemporal changes in the distribution of lichen community patterns.

Spectral discrimination between different lichen communities as well as towards surrounding bare soil and rock cover was verified using spectral separability analysis for all training sites and field spectrometer measurements of selected sites throughout the study area (compare chapter 4.3.2).

Spectral separability analysis focussed on the spectral delineation of classes previously identified by the hierarchical classification scheme. Therefore Jeffries-Matusita (JM) best average values were used as a distance measure to predict the results of the Maximum-Likelihood classification algorithm. This analysis showed best separability measures using an image stack comprising of eight layers derived from the LANDSAT-7 ETM+ datasets (compare chapter 4.1.6). Based on the full spectral information provided by the LANDSAT 7 ETM+ sensor discrimination between all lichen community classes of the hierarchical classification scheme could be realized with only slight inconsistencies among spectral subclasses. Spectral discrimination between lichen-covered- and none-lichen-covered areas was excellent at all times (compare chapter 5.2.2).

However field spectrometer measurements were used to verify the findings of the separability analysis of mean broad-band reflectances. To allow for the comparison between the mean spectral reflectance curves of LANDSAT 7 ETM+ and field spectrometer measurements regarding homogeneous reference areas, mean values of the high resolution spectrometer data were resampled to broad-band resolution using the spectral transfer function for each band. Although reflectances of the two sensors were observed to be offset, results of this analysis showed good correspondence between the space-borne and in-situ reflectance measurements. This is expressed by r^2 values ranging from 0.9841 to 0.9965 for lichen-covered- and 0.966 to 0.9981 r^2 for the none-lichen-

covered areas for a confidence and prediction interval of 95 % (compare chapter 5.2.2).
Confirmed by these results it is stated that not only general spectral discrimination of lichen communities from surrounding bare soil can be achieved using spaceborne broad band LANDSAT 7 ETM+ reflectances but also spectral delineation of differing communities is feasible.
In addition to the Maximum-Likelihood classification approach, fuzzy post-processing techniques were utilized mainly to account for problems of pixel assignments in transitional lichen community classes. Based on the comparison of chi-square distributed Mahalanobis distance measures for the hierarchically ordered six best pixel-to-class-assignments as proposed by FRANZEN ET AL. (1998), overall stability of the class-assignments was reflected. Due to the steady decrease of probabilities, by which classes other than that of the first probability are assigned to each pixel, it also depicted the class-memberships to be included in the defuzzification process (compare chapter 5.2.4). Therefore defuzzification was based upon the Mahalanobis-distances as well as the proposed class to pixel assignments of the two best classes per pixel and performed using fuzzy convolution filtering.
As a result of this multilevel supervised classification approach the first distribution map of major lichen communities in the Central Namib Desert for the year 2003 is presented. In total 12 major coherent lichen fields, comprising a total cover of 1824.6 km², could be identified within the study area extending form the vicinity of Gobabeb up to the Huabmond. Among these lichen fields mapped by classification approach, six have not been at all or only partly been described in literature so far.
The lichen fields of the Southern Naukluft (No. 1), Nonidas (No. 3), Omaruru (No. 7) and Mile 72 (No. 8) have neither been described by SCHIEFERSTEIN (1989) and LORIS & SCHIEFERSTEIN (1992) nor WESSELS (1989) - whereas the lichen fields of the Messum Crater (No. 9) and the Brandberg West (No. 11) have partly been described by SCHIEFERSTEIN (1989) and WESSELS (1989) respectively.
While SCHIEFERSTEIN (1989) underestimated the extend of lichen cover in the hinterland and alongside the Brandberg West road, the lichen field of the Messum Crater (No. 9) was only partly mentioned in the visual analysis of LANDSAT MSS data performed by WESSELS (1989). Located in the hinterland of Cape Cross and covering a total of 373 km², lichen field No. 9 is in fact the largest of the Central Namib Desert followed by the lichen fields No. 2, 7, 6 and 1. A full list of the areal statistics is presented in table 12, whereas a schematic overview of their location is shown in figure 43.
Outside of these coherent lichen fields another 875.5 km² of lichen coverage could be identified, adding up to a rounded total of 2700 km² of lichen coverage found within the study area which is almost equivalent to the extend of the German state of Saarland covering 2569 km² (HARTMANN 1997[3]). However, outside of the lichen fields, areas are mostly dominated by crustose lichen communities whereas most of the foliose and fruticose communities are found within the 68 % of lichen coverage grouped into coherent lichen fields (compare chapter 6.2).
In addition to the coherent lichen fields identified within this thesis, several azonal but extraordinary lichen communities should also be included by conservation measures although accurate identification was problematic by the approach presented. Among them, the Lagunenberg coastal mountain range in the vicinity of Cape Cross, as well as mountainsides along the Brandberg West road and

within the Messum Crater region, comprise outstandingly divers lichen communities. Variations of these community patches have also been observed for the numerous large dolerite ridges and felsite dykes.

Nevertheless, the six lichen communities which had previously been identified on the basis of the hierarchical classification scheme and the spectral separability analysis could be delineated with an overall classification accuracy of 87 % based on independent reference samples excluded form the classification process. Minor insecurities, expressed in differing class-specific producer's and user's accuracy measures, could mostly be related to transitional classes or where separability towards bare soil was limited due to direct adjacency or smooth transition to bare or gravel-covered top-soils.

In total best classification results according to user's accuracy measures could be obtained for the fruticose lichen zone (99 %), and the none-lichen-covered (93 %) zone, followed by the crustose-foliose lichen zone (89 %), and the foliose-lichen zone (80 %). These measures are also reflected in the very good Kappa coefficient of 0.82, stating that the combined classification product is 82 % better than one resulting from chance (compare chapter 6.1).

In addition to these measures reflecting the site-specific assessment of the correspondence between the image classification and ground truth, spatial distribution of error within the lichen fields was analysed using class-membership probabilities.

Based on the analysis of lichen field specific high or low equiprobabilities of class-memberships, otherwise given a low overall probability in comparison to the most probable class-memberships, the spatial distribution of error was assessed (compare chapter 5.2.9 and 6.3). Except for the Nonidas lichen field (No. 3), where slight insecurities were

No.	Name	Coverage
1	Southern Naukluft	230,9 km^2
2	Northern Naukluft	271,9 km^2
3	Nonidas	26,3 km^2
4	Mile 8 / Mile 12	164,0 km^2
5	Wlotzkasbaken	185,2 km^2
6	Jakkalsputz	241,3 km^2
7	Omaruru	261,0 km^2
8	Mile 72	12,0 km^2
9	Messum Crater	372,6 km^2
10	Cape Cross	17,5 km^2
11	Brandberg West	30,4 km^2
12	Huabmond	11,5 km^2
	Subtotal	1824,6 km^2
	Outside	875,5 km^2
	Total	2700,0 km^2

Table 12: List of lichen fields and areal statistics of lichen coverage per lichen field

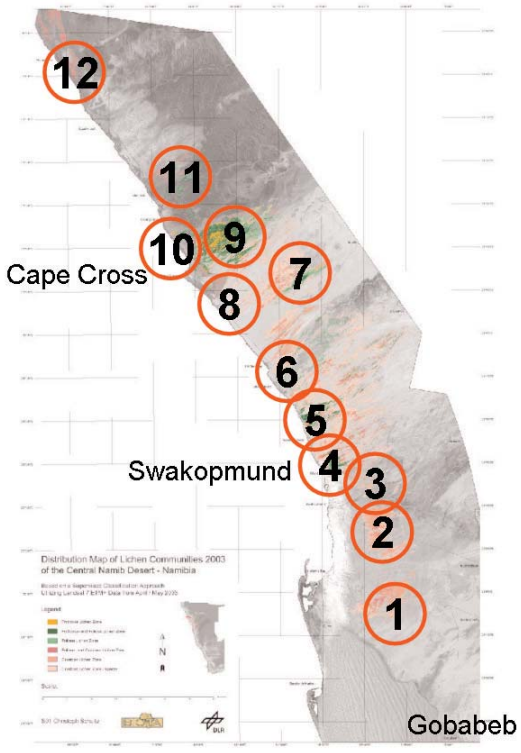

Figure 43: Schematic overview of the location of major coherent lichen fields within the study area.

expressed by a high equiprobability of the third- and fourth-most probable class assignment, good relationships of probabilities could be obtained for all other lichen fields.
Recapitulating, it can therefore be stated that site-specific as well as regional distribution of error inherent in the unitemporal classification product can be considered minor; in particular and in respect of the broad-band satellite sensors and the scale addressed by the supervised classification products.
Compared to previous studies addressing the distribution mapping of biological soil crusts in general and lichen distribution patterns in particular, the utilization of broad-band LANDSAT-7 ETM+ reflectances did not only serve for the detection and mapping of biological soil crusts but also for the discrimination of different communities on a regional scale. Thus a first map depicting the spatial distribution of major lichen communities in the Central Namib Desert could be successfully derived.

7.2 Identifying spatiotemporal changes in the distribution of major lichen communities in the Central Namib Desert

In addition to the unitemporal approach this thesis also focussed on the identification of spatiotemporal changes in the distribution of major lichen communities in the Central Namib Desert. Due to the special ecological and climatic conditions supporting this objective a multitemporal classification approach was aspired for the years of 2000, 1999, 1992 and 1991, utilizing LANDSAT-7 ETM+ and LANDSAT-5 TM data. Due to the virtually identical geometrical, optical, as well as radiometrical resolution of the two sensor products, full comparability of the two sensor products is realized, thus enabling their utilization for time-series analysis (compare chapter 4.1).
Based on individual supervised classifications of the time-series images, Post Classification Comparison is postulated for the identification of mostly event driven change intensities and directions.
However no spatially referenced information describing any past distribution patterns of lichen communities according to the satellite imagery is available for the study area. Therefore a retrospective classification strategy had to be developed allowing for the utilization of reference information acquired during the field campaigns already incorporated into the unitemporal classification approach. Based on this objective, the analysis focussed on the identification of spectrally invariant training areas.
As a prerequisite all multitemporal LANDSAT imagery of the study area was geometrically rectified, relatively in regards to the 2003 master scenes utilized for the unitemporal approach. In addition atmospheric correction using the ATCOR algorithm was applied to the multitemporal imagery, thus ensuring a common radiometric scale among them and towards the master scenes.
In order to account for the spatial extent and intensity of gradual changes within the reference samples and to minimize the loss of information naturally associated with standard PCA analysis or univariate image differencing, a change detection approach based on Selective Principal Component Analysis (sPCA) and fuzzy membership transformation postulated by WEIERS ET AL. (2003) was utilized. Thereby specific analysis of all previously derived training samples allowed for the detection of changes, sensitive to site-specific spectral alterations and spatial misalignment among the satellite imagery. Based on error thresholds obtained from the "coronal-like" error-distributions resulting from spatial mis-

alignment in some cases, adapted threshold values for which the spectral information of the compared pixels of every training sample can be regarded significantly altered could be derived.

However, if iteratively applied to the multi-temporal imagery obtained for the study area the number of approved reference samples showing no change in spectral response will certainly decrease the greater the acquisition of the reference and its back-dated counterpart differ in time. Moreover the derivation and analysis of change intensity information can serve as an indicator whether existing or newly obtained training samples can in theory be utilized for the retrospective classification of back-dated imagery. Thus the amount of available reference information for all time-series images is steadily increased as a result of continued field surveys. As a result a total set of 132 invariant training samples serving for the supervised classification of the time-series images acquired for the study area could be derived. Furthermore this set successfully accounts for both spectral and geometric error rates inherent in all input data.

In the following the extraction of "times-series" signature sets was performed on an individual basis for all timeframes including the timeframe of 2003. Although class separabilities were optimized wherever possible, some inconsistencies could be observed by the analysis of Jeffries-Matusita distance measures as a consequence of the limited number of training samples.

Due to the event driven alterations of the Central Namib Desert Environment these inter-class and intra-class separabilities also varied between the differing timeframes (compare chapter 5.2.6).

As expected, best overall class separability could be obtained for the timeframe of 2003. For the backdated imagery best overall class separability could be obtained for the timeframe of 1999 while the retrospective signature set for the year 2000 performed lowest in terms of intra-class separability measures. The signature set addressing the timeframes of 1992 and 1991 showed lowest separability measures among various top-classes. However, good separability measures between classes describing lichen- and none lichen-covered areas were accomplished for all timeframes. Therefore the evaluation of the derived JM-distance values predicted a fairly good performance of the aspired Maximum-Likelihood algorithm for the timeframes of 1999 and 2000, despite the reduced number of reference samples for the retrospective signature sets. However aspired classifications of the timeframes 1992 and 1991 must be critically evaluated regarding the delineation of the differing lichen communities specified by the hierarchical classification system.

Following the joined aggregation and selection of training samples the validated retrospective training sets were utilized for the independent supervised classifications of all time-series images included in this study. Supervised classification strategy resembled that of the unitemporal approach. Contrasting to the unitemporal classification approach for the year of 2003, the first three probability layers were included into the fuzzy likelihood classification to stabilize class to pixel assignments.

Measures regarding the site specific and regional accuracy of the multi-date classifications were also derived following the methodology presented beforehand. Overall site-specific accuracies varied between 79 % and 86 %, but showed mixed results for the individual classifications. For the northern half of the study area, addressed by the 180/75 WRS-2 scene, site-specific accuracy was best for the timeframe of 2003 (84 %), followed by the timeframe of 2000 (83 %). Contrasting with these very good results the timeframes of

1999 (73 %) and 1991 (67 %) performed well below the threshold value of 85 % proposed by FOODY (2002). However this steady decrease of overall accuracy measures could not be observed for the southern part of the study area (179/76). Accuracy measures for all timeframes only varied between 88 % and 89 %. It is assumed that these high values of site-specific classification accuracy are driven by the lowered variability of lichen communities dominated by crustose species, also averting misclassification.

Results from the varying producer's and user's accuracy measures derived from the contingency matrices showed that the crustose-foliose and sparse crustose lichen communities and in part the foliose lichen community must be regarded insufficiently characterized towards neighbouring classes. On the contrary good to excellent delineation of the fruticose-, the fruticose-foliose-, and the crustose lichen community and none lichen covered areas were obtained according to these measures.

However, several aspects have to be kept in mind when assessing the accuracies of the multitemporal image classifications presented in this work. Due to the reduced number of independent training samples, site-specific error rates only provide limited information on actual accuracies and do not provide information on the spatial distribution of error at all. Therefore the analysis of class-memberships was used in addition to the analysis of class-assignment probabilities in concordance to the unitemporal approach (compare chapter 6.3).

Analysis showed excellent relationship of probability measures for the lichen field of the Cape Cross lichen field (No. 10). Very good results could be achieved for the lichen fields of Wlotzkasbaken (No. 5), Jakkalsputz (No. 6), the Omaruru gravel plain (No. 7) and Mile 72 (No. 8). Good results can be expected for Messum Crater / Orawab (No. 9), whereas average results were obtained for the lichen field of the southern Naukluft Plateau (No. 1) and northern Naukluft Plateau (No. 2). Weakest overall results could be derived for the lichen fields of the Brandberg-West-Road (No. 11) and the northernmost lichen-field of the Huabmond (No. 12).

Surprisingly though, much of the error reported by the contingency matrix for the timeframe of 1991 could not be observed analysing class-memberships probabilities. However, whether much of the previously observed error rates results from uncertainties located outside the delineated lichen fields can only be assumed.

Although some uncertainties can be expected for the timeframes addressing the lichen distribution patterns in the years 1991/92 discrimination among lichen covered and none lichen-covered areas was ensured for all timeframes according to error matrices. Therefore strong "degradation" and "recovery" resulting in an increase or decrease of none lichen-covered areas should be clearly outlined.

7.3 Analysing disturbance patterns of major lichen communities in the Central Namib Desert

Results of the multitemporal classification approach were presented and discussed using maps depicting the results of Post Classification Change Differencing of the image pairs 2003 – 2000 and 2000 – 1991/92 for the complete study area. The greatest advantage of this technique is the production of change maps comprising a complete matrix of changes based on the classification results. Lichen field specific descriptive statistics of the observed spatiotemporal changes in distribution patterns are presented in annex d and e.

In order to reduce the overall workload the lichen field of Wlotzkasbaken will serve as an example for the detailed and extended analysis of the spatiotemporal changes. Therefore secondary reference data involving digital elevation model (DEM) derived data as well as climate data, ecology and field observations were utilized to aid the identification and analysis of natural and anthropogenic disturbances.

Regarding the comparison of the timeframes of 1991 and 1999, fragmentary information on climate and ecology formerly recorded or published in literature did not suffice to fully explain the changes observed throughout the study area. For the lichen field of Wlotzkasbaken (No. 5) it can only be assumed that widespread and plane disturbance patterns alongside the northern and southern rims of the lichen field are related to severe windstorm events noted by LORIS & SCHIEFERSTEIN (1992). Despite these degradation patterns the inner structure of the lichen field remained mostly intact. Analysis of geomorphological form elements, derived from DEM data, showed that this could be most likely due to ridge structures shielding it from the north-north-eastern windstorm events.

Similarities for such an event driven disturbance could also be observed for the lichen fields of Cape Cross (No. 10), the Omaruru Gravel Plain (No. 7), and the outer areas of the divisions of the lichen field of Mile 8 / Mile 12 (No. 4). Because of a missing satellite scene of the timeframe of 1999 for the southern part of the study area (WRS-2 179/76) no correlating spatial patterns could be derived for the lichen fields of the Northern- and Southern Naukluft Plateau (No. 1 and 2).

In contrast to the indistinct identification of change patterns for the timeframes 1991 and 1999, extraordinary precipitation events paired with intense run-offs could be related to the disturbance patterns observed between the timeframes of 1999 and 2000.

These precipitation events verified by climatic data obtained from HACHFELD (2000), the Desert Research Foundation of Namibia (DRFN) as well as drainage data derived from SRTM digital elevation data. In the results, fluvial disturbance by widened or newly created washes, dissecting the lichen field of Wlotzkasbaken (No. 5) could be observed to create linear destructive patterns using the Post Classification Change Detection approach.

Thereby the utilization of area-wide sPCA data was necessary as the comparison of the differing timeframes is only able to address patterns of degradation and recovery based on the existing classes of the classification scheme. Thus classification results are likely to result in a retrospective misclassification in terms of lichen communities of an existing area, although an alteration of that area was detected correctly. As area-wide sPCA products are solely based on the comparison of the spectral information provided by the corresponding timeframes, correspondence of observed patterns successfully served as a source of validation for the observed run-off patterns.

In addition to sPCA data, analysis of the potential drainage network, derived from DEM data, also supported these findings, although no direct correlation could be obtained.

Regarding the overall study area, elongated run-off patterns affecting the distribution of lichen communities could also be observed within the lichen fields of Mile 8 / Mile 12 (No. 4), the Northern-Namib-Naukluft Plateau (No. 2), and the Messum Crater / Orawab (No. 9) (compare chapter 6.5.2).

Supplementary to the destructive force of surface waters, data from HACHFELD (2000)

also served for the identification of rainpulse triggered germination of annuals within the study area causing areal misclassification for the year 2000. Thereby prominent "recovery" patterns among the inner Wlotzkasbaken lichen field (No. 5) and the lichen field of Jakkalsputz (No. 6) could be related to an extraordinary increase in ephemeral vegetation whose remains were also observed during the field campaigns of 2002 and 2003. In accordance to the findings of HACHFELD (2000), no misclassifications could be observed for the lichen fields of the Southern Naukluft Plateau (No. 1).

Based on these findings the routing and accumulation of waters over the surface area subsequent to rainstorm events can be regarded as a fundamental ecological process directly influencing lichen distribution patterns.

Regarding the comparison of the classifications obtained for the timeframes 2000 and 2003, plane and coherent disturbance patterns alongside the northern rim of the lichen field of Wlotzkasbaken (No. 5) were of similar shape as the ones observed for the period 1991 to 1999. However, despite these similarities extensive plane degradation within the inner lichen field area of Wlotzkasbaken could be observed for the first time. This degradation mainly affected the agglomeration of the coastal *Teloschistes capensis* (L.f.) Müll. Arg. community dominating this area.

Analysis of the spatial distribution of spectral changes among reference samples, in respect of the delineated lichen field areas, depicted a rather heterogeneous distribution of change intensities throughout the study area. It could be shown that strong spectral alterations resulting in the disturbance lichen communities were mostly limited to the lichen fields of Wlotzkasbaken (No. 5), Mile 8 / Mile 12 (No. 4), and the Northern Naukluft Plateau (No. 2), which was also reflected by the matrix map of the two time-series classifications – due to local cloud cover in 2003 no coherent information could be retrieved for the Nonidas lichen field (No. 3).

Based on these observations and considering the analysis of climate data it became obvious that large amounts of lichen cover were strongly disturbed by a localized and unusual thunderstorm event on late April 16th to early 17th of 2003. It could be investigated that a total of 8.4 mm of rainfall must have weakened the interlinking of top-soil, gravel material, and lichen thalli, while subsequent north-westerly and north-easterly winds comprising hourly mean velocities of up to 14.7 $m*s^{-1}$ caused extensive deflation and abrasion mostly among fruticose and foliose lichen communities. Analysis of climate data showed that the north-westerly direction of the windstorm is one most uncommon to the area of Wlotzkasbaken. In fact this wind-direction was only recorded once within a two year period whereas north (21 %) and north-easterly (71 %) prevailed.

While some of the lichen thalli fragments accumulated into newly formed mats loosely attached the ground or were collected within natural gutters, a large amount of lichen biomass was also blown off-shore as observations following the thunderstorm indicated.

Contrasting with the limited information available for the detailed discussion of the preceding timeframes of 1991/92, 1999 and 2000, good reference information describing these degradation patterns could be acquired during the 2003 field campaign shortly after the thunderstorm event. This information also served for the comparison with data collected during the 2002 field campaign and reference information obtained by SCHIEFERSTEIN (1989) and LORIS & SCHIEFERSTEIN (1992) during a 1987 field-study for the vicinity of the Wlotzkasbaken lichen field (No. 5). Due to photographic evidence it became obvious that much of the fruticose and

foliose fraction of the lichen community dominated by the fruticose *Teloschistes capensis* (L.f.) Müll. Arg. was fully dislocated during the storm event.
However, much of the fruticose lichen biomass of the inner lichen field structure remained in the lichen field after it was dislocated and might as well be able to resettle as stated by LORIS ET AL. (2004). Nevertheless statistics of the retrospective classifications performed for the years of 2000 and 2003 showed that 68 % of the fruticose lichen community, 35 % of the fruticose-foliose and 25 % of the original foliose coverage of the lichen field of Wlotzkasbaken (No. 5) was affected by the thunderstorm event.
Based on these findings, storm events could also be identified as a fundamental ecological process directly influencing lichen distribution patterns, especially when paired with precipitation.

Altogether scene classification techniques must continue to evolve regarding the improved discrimination of successional stages of lichen communities beyond multispectral image analysis. Therefore continued efforts must include the integration of air- and spaceborne hyperspectral sensor data, allowing for a more detailed delineation of lichen communities in conjunction with field spectrometer measurements and ecological parameters. The utilization of theses techniques will also provide further insight into the relationship between in-situ biomass, productivity, and spectral response. In addition further improvements in multitemporal image classification are still required in order to minimize the ratio between the detection of significant alterations and classification accuracy. Nevertheless the major contributions of this thesis specify as follows.

Major contributions of this thesis:

- Development and implementation of a hierarchical classification scheme allowing for the regional assessment of Central Namib Desert lichen communities.

- Successful utilization of multispectral satellite imagery for the detection, discrimination, and spatial mapping of six lichen dominated biological soil crust communities mostly confined to twelve major lichen fields.

- Development and implementation of a methodology allowing for the extraction of invariant reference information from a multi-date image stack, thus enabling multitemporal image classification.

- Successful utilization of multispectral satellite imagery for the delineation of spatiotemporal changes regarding the distribution of six lichen dominated biological soil crust communities defined by the hierarchical classification scheme.

- Identification of two major ecological factors controlling lichen distribution based on disturbance patterns obtained from the post classification change comparison of multitemporal satellite images and secondary reference information.

8 Conclusion and future prospects

In recent years, many authors have denoted the significance of the existing distribution of the lichen communities to the arid ecosystem of the Central Namib Desert. However, many of them also concluded, that a much better understanding regarding the large-scale distribution patterns beyond site-specific ecological studies would be desirable. Especially when discussing the potentials of conservation measures addressing the unique lichen flora.
Nevertheless the production of land cover and vegetation maps has always been one of the most common uses of remotely sensed data. However, the level of classification precision is directly related to the remote sensing instrument and its spatial and spectral resolution (STOMS & ESTES 1993). Therefore, land cover maps derived from satellite imagery with the means of classification techniques always contain some error due to map generalization and misclassification when spectral classes do not map perfectly into information classes. Yet they represent an important tool supporting the rapid assessment of land cover distribution and variation with spatial precision.

Results presented within this thesis also revealed the great potential of remote sensing in detecting, mapping, and change detection of Central Namib Desert lichen communities. It could be shown that remote sensing represents a time and cost effective tool for assessing lichen distribution patterns while also providing potentials for the development of monitoring applications addressing the their spatiotemporal variations. Based on image classification techniques, a first map delineating several new and known coherent lichen fields could be successfully derived according to a hierarchical classification scheme.

In addition to the stabilization of the soil surface, species forming these biological soil crusts are often the only organisms providing significant carbon input into the ecosystem of the Central Namib Desert. Based on these findings their possible role as part of global carbon cycles has also been of much interest in recent times (BÜDEL 2002). Although measures of biomass and productivity can not be directly assessed by remote sensing, lichen communities mapped within the framework of this thesis could well be related to biomass samplings and productivity coefficients derived from field samples stratified by community.

Based on the biomass samplings conducted by Dr. Dirk Wessels and Dr. Kurt Loris mean dry weight and net biomass measures can be obtained for the lichen communities delineated in the framework of this thesis (compare chapter 4.3.3).
Extrapolated to the spatial extend of lichen coverage identified by the classification approach, gross dry weight of total lichen biomass within the study area would result in a first very rough estimate of 493612 tons, with a rounded 80 % (396508 tons) of that biomass included in the delineated lichen fields (compare figure A26 through A28, annex a). Supplemental a very rough first estimate of net lichen biomass would result in 255731 tons with a comparable rounded 80 % (203442 tons) located within the coherent lichen fields identified within this thesis (compare figure A29 through A31, annex a).
In regards of the total study, this would result in an estimated mean dry weight of lichen biomass of 23 tons * km^{-2}, while mean net lichen biomass would account for about 12 tons * km^{-2}.

In addition to these biomass estimates, LANGE ET AL. (1994) were the first to provide a very rough yet area-related approximation of annual carbon balance for soil-crust lichen amounting in a positive 16 g C * m^{-2} * $year^{-1}$ (photosynthetic gain minus respiratory losses, at 100 % coverage). Based on the assumption of 250 fog days per year and providing an average coverage of 20 % for all lichen covered areas identified within this thesis, the annual carbon gain of lichen communities located within the study area would amount in an estimated 8640 tons * year-1 with about 68 % (5839 tons * $year^{-1}$) confined to the twelve lichen fields (compare figure A32, annex a).
Alternative productivity estimates were also derived from species specific daily carbon gains obtained by LANGE ET AL. (1991). Although far from complete, these values describing 10 lichen species, can be related to species specific cover fractions obtained by Wessels in the course of the biomass sampling of the different lichen communities (compare figure A33 to figure A39 in annex a). Calculated on a community basis using the environmental prerequisites set by LANGE ET AL. (1994) an estimated annual carbon gain of 8120 tons * $year^{-1}$ can be derived. Although based on a species-specific approach the amount resembles the above values by almost 94 %. However, it should be emphasized, that all of theses numbers represent no more than a very rough estimate.

Nevertheless it becomes obvious, that, given the magnitude of their photosynthetic productivity, reduction or loss of these biological soil crusts due to anthropogenic as well as natural disturbances will cause a definite decrease of ecosystem productivity as recovery rates are slow. For example burial of these most dominant primary producers caused by natural or traffic induced aeolian sediments inevitably causes the death of all photosynthetic components. Thereby reducing the fertility of the whole system which is undoubtedly one of the most definitive and problematic aspects of desertification BELNAP (2001). In addition long term changes in cover and species composition in response to increased CO_2 and UV radiation will affect abundance, species composition, and function of biological soil crusts as highly specialized crustal organisms will not likely be replaced by other more resistant species. Thus, impacts evolving from global change processes might as well affect biological soil crusts which in turn will have dire effects on the stability, biodiversity, and biogeochemistry of the ecosystems where they occur (EVANS ET AL. 2001).

However, the nature of impact being investigated will always influence the monitoring methods used for their identification. Future studies focussing on species composition and biomass fluctuations will undoubtedly require spectroscopic analysis and micro plot sampling. On the contrary forceful natural disturbances or other large scale disturbances on biological soil crusts may still be best examined using multispectral remote sensing data, providing consistent, high resolution, and reproducible information combined with high repeat frequencies.
For the Central Namib Desert, ecological drivers including occasional windstorm and precipitation events have been pointed out by several authors conducting ecological studies in this region (SCHIEFERSTEIN 1989, LORIS & SCHIEFERSTEIN 1992). These major drivers could also be successfully identified analysing the disturbance patterns of major lichen communities based on multitemporal image classifications and secondary reference information. However, various limitations apply.
In general, observed spectral changes between satellite images of multiple dates have to be related to changes of lichen com-

munities types and subtypes. However, in the absence of knowledge on successional stages and subtypes, post classification change detection comparison is currently only able to denote patterns of degradation and recovery based on the existing classes of the classification system. Thus further improvements are still required in order to allow for the discrimination of small but statistically significant levels of change and noise introduced by classification errors. Otherwise various uncertainties will continue to plague monitoring activities based on multispectral datasets.

In addition to these limitations, many changes in the structure and function of biological crusts can often not be assessed during field surveys (BELNAP ET AL. 2001C). However, to monitor trends in land-cover distribution patterns with remote sensing instruments exemplary knowledge on the expected magnitude of changes will be needed to evaluate results; provided that changes have been significant enough to be detected by remote sensing sensors (STOMS & ESTES 1993). In this context, remote sensing will never be able to directly monitor species-specific extinctions or changes of biological soil crusts. Instead only changes in land or habitat cover and biophysical factors can be observed over time to infer or predict effects on certain species.
Therefore continued site-specific research and surveys on the lichen communities of the Central Namib Desert is needed to identify habitat preferences and to improve small-scale modelling (e.g. SCHIEFERSTEIN 1989, DANEEL 1992, LORIS & SCHIEFERSTEIN 1992, LANGE ET AL. 1994, JARROLD 2001, LORIS ET AL. 2004, ZEDDA & RAMBOLD 2004, LALLEY & VILES 2005).
Complementing these studies, additional methods should be used to analyse biological responses of soil crust to disturbance or management change. These methods should include the determination of chlorophyll contents using spectroscopic analysis on species and community level or high pressure liquid chromatography (HPLC) as an efficient and reliable measure for monitoring changes in photosynthetic biomass, even when cover is difficult to detect or differentiate during field surveys (BELNAP ET AL. 2001C).

Therefore future ecological and spectroscopic analysis utilizing in-situ spectrometer measurements and hyperspectral remote sensing should be conducted to increase our understanding of the relationship between photosynthetic activity, spectral reflectance properties, carbon fluxes, and biomass measures. Within this research context, it will also be important to identify the effects of disturbances, both natural and anthropogenic, among different scales, although these factors tend to overlap with other dynamic factors. In turn this will allow for the stepwise and scale-based identification of ecological factors controlling lichen distribution patterns, especially as rates of disturbance are known in the absence of human impacts.
Based on these finding, additional studies introducing spaceborne hyperspectral CHRIS-Proba datasets in conjunction with isochronous in-situ spectroscopic and biomass samplings are already initialized. Supplemental chlorophyll contents obtained from Pulse-Amplitude-Modulation (PAM) Fluorometers on the species and community level will be included in an approach focussing on the lichen field of Wlotzkasbaken. Multiplicity of surveys is thought to contribute to an integrated approach, allowing for the combination of site-specific ecological studies and remote sensing surveys. In addition CHRIS-Proba data providing 62 spectral bands (406 – 1003 nm) will also help to refine results based on the multispectral datasets presented within this thesis.

Nevertheless, all of these studies will be conducted within the multidisciplinary research framework of the BIOTA Southern-Africa project. Thus close cooperation with lichenologists and ecologists of the Universities of Limpopo, South Africa (Prof. Dr. Dirk Wessels), Stuttgart-Hohenheim (Dr. Kurt Loris) and Kaiserslautern (Prof. Dr. Burkhard Büdel), Germany, is facilitated.

In the end all of these research initiatives addressing the unique Central Namib Desert lichen communities in the past, present and future have been conducted with the objective of promoting extended conservation measures.

Known to be severely vulnerable to the damaging effects of off road vehicles travelling through them and in regards of their ecological importance, the need for conservation has been repeatedly emphasized by many authors (e.g. MATTICK 1970, SEELY & HAMILTON 1978, HEINRICH 1986, WESSELS & VAN VUUREN 1986, GIESS 1989, SCHIEFERSTEIN 1989, DANEEL 1992, LORIS & SCHIEFERSTEIN 1992, JÜRGENS & NIEBEL-LOHMANN 1995, JÜRGENS ET AL. 1997, JARROLD 2001, LORIS ET AL. 2004, LALLEY & VILES 2005).

Often inseparable, lichen-animal interactions observed by many authors (e.g. FROST & SHAUGNESSY 1976, CLINNING 1978, WESSELS ET AL. 1979, JOUBERT ET AL. 1982) are mainly ascribed to their role as the most dominant primary producers in their hyper-arid environment. Nevertheless some of the known lichen species being endemic to the Namib are already at risk considering the "Preliminary Global Red List of Lichens" (SWEDISH SPECIES INFORMATION CENTER 2003).
However, despite their well discussed ecological importance and uniqueness, one of the many reasons for conserving these communities also lies in the very likely possibility that towns including Swakopmund, Wlotzkasbaken and Hentiesbay will suffer from aggravated dust storms, should further large scale anthropogenic impacts inflict damage upon these communities. Recently addressed by ECKARDT & KURING (2005), these dust storms will be fed by additional sources of dust arising from territories formerly stabilized and fertilized by extensive lichen communities (compare figure 44).

Figure 44: Dust plumes along the Central Namib Desert coast observed by MODIS satellite on 09th of August 2002.

Although natural disturbances can also induce large-scale spatiotemporal changes among lichen communities, only anthro-

pogenic disturbances including mining, road construction and off-road driving are known to reduce the quantity of natural habitats and their structural diversity to a large degree. As a consequence this habitat fragmentation will undoubtedly affect regional distribution patterns as species find it increasingly difficult to recolonize isolated patches.

Albeit pending, a conservation master-plan is still inexistent, even though it has initially been envisaged in the following of a scientific symposium held at Swakopmund in 1987 [LORIS, K., pers. comm.]. The very fact is even more surprising, as Namibia is well known for its well established network of protected areas consisting of many parks including a high species diversity and endemicity (BARNARD 1998). Therefore, additional areas need to be identified allowing for the protection of the unique lichen communities alongside the arid Namibian coastline.

However, the implementation of conservation measures addressing an area the size of the Central Namib Desert and consisting of large touristic and economic value will always include trade-offs. Therefore, priority areas, equivalent to the twelve coherent lichen fields identified by this thesis, need to be identified to support the decision-making-process.
Nevertheless, Namibia's tourism sector relies strongly on the country's biodiversity and scenic beauty. Therefore sustainable tourism attracted to by these conservancies may also create awareness and generate revenues for environmental conservation within the framework of sustainable use (BARNARD 1998).

Literature

Abkar, A. et al. (2000): Liklihood-based image segmentation and classification: a framework for the integration of expert knowledge in image classification procedures. In: International Journal of Applied Earth Observation and Geoinformation 2 (2): pp 104 - 119.

Ager, C. M. & N. M. Milton (1987): Spectral reflectance of lichens and their effects on the reflectance of rock substrates. In: Geophysics 52: pp 898 - 906.

Analytical Spectral Devices (2005): www.asdi.com. Access Day: 14.04.2005.

Bähr, H. P. & T. Vögtle (1991): Digitale Bildverarbeitung: Anwendung in Photogrammetrie, Kartographie und Fernerkundung. Wichmann, Karlsruhe.

Barnard, P. (ed.) (1998): Biological diversity in Namibia: a country study. Windhoek, Namibian National Biodiversity Task Force.

Barnard, P. & S. T. Shikongo (2000): Namibia's National Report - to the Fifth Conference of Parties on implementation of the Convention on Biological Diversity. Nairobi, Kenya, Namibian National Biodiversity Programme, Directorate of Environmental Affairs, Ministry of Environment & Tourism: pp 1 - 22.

Bechtel, R. et al. (2002): Spectral properties of foliose and crustose lichens based on laboratory experiments. In: Remote Sensing of the Environment 82: pp 389 - 396.

Beeber, G. (2000): Change Detection Techniques Using Landsat Data. http://www.ae.utexas.edu/courses/ase389/midterm/gregg/greggmid.html, Access Day: 07.01.2000.

Belnap, J. & D. A. Gillette (1998): Vulnerability of desert biological soil crusts to wind erosion: the influences of crust development, soil texture, and disturbance. In: Jounal of Arid Environments 39: pp 133 - 142.

Belnap, J. (2001): Biological Soil Crusts and Wind Erosion. In: J. Belnap & O. L. Lange (eds): Biological Soil Crusts: Structure, Function, and Management. Ecological Studies 150: pp 339 - 348. Springer-Verlag.

Belnap, J. & D. J. Eldridge (2001): Disturbance and Recovery of Biological Soil Crusts. In: J. Belnap & O. L. Lange (eds): Biological Soil Crusts: Structure, Function, and Management. Ecological Studies 150: pp 363 - 384. Springer-Verlag.

Belnap, J. et al. (2001a): Biological Soil Crusts: Characteristics and Distribution. In: J. Belnap & O. L. Lange (eds): Biological Soil Crusts: Structure, Function, and Management. Ecological Studies 150: pp 3 - 30. Springer-Verlag.

Belnap, J. et al. (2001b): Influence of Biological Soil Crusts on Soil Environments and Vascular Plants. In: J. Belnap & O. L. Lange (eds): Biological Soil Crusts: Structure, Function, and Management. Ecological Studies 150: pp 281 - 302. Springer-Verlag.

Belnap, J. et al. (2001c): Biological Soil Crusts: Ecology and Management. U.S. Department of the Interior, Denver, Colorado.

Belnap, J. (2002): Impacts of off-road vehicles on nitrogen cycles in biological soil crusts: resistance in different U.S. deserts. In: Journal of Arid Environments 52: pp 155 - 165.

Besler, H. (1972): Klimaverhältnisse und klimamorphologische Zonierung der zentralen Namib (Südwestafrika). In: Stuttgarter geographische Studien 83 (1-209): pp.

Besler, H. (1992): Geomorphologie der ariden Gebiete. Erträge der Forschung; Bd. 280, Wissenschaftliche Buchgesellschaft, Darmstadt.

Boss, G. (1941): Niederschlagsmenge und Salzgehalt des Nebelwassers an der Küste Deutsch-Südwestafrikas. In: Bioklimatische Beiblätter (1): pp 1 - 15.

Brown, D. G. (1994): Predicting vegetation types at treeline using topography and biophysical disturbance variables. In: Journal of Vegetaion Science 5: pp 641 - 656.

Buckley, J. J. & E. Eslami (2002): An Introduction to Fuzzy Logic and Fuzzy Sets. Heidelberg / New York.

Büdel, B. & D. C. J. Wessels (1986): Parmelia hueana Gyeln., a vagrant lichen from the Namib Desert, SWA/Namibia. Anatomical and reproductive adaptions. In: Dinteria 18: pp 3 - 15.

Büdel, B. (2001a): Biological Soil Crusts of South America. In: J. Belnap & O. L. Lange (eds): Biological Soil Crusts: Structure, Function, and Management. Ecological Studies 150: pp 51 - 56. Springer-Verlag.

Büdel, B. (2001b): Synopsis: Comparative Biogeography and Ecology of Soil-Crusts Biota. In: J. Belnap & O. L. Lange (eds): Biological Soil Crusts: Structure, Function, and Management. Ecological Studies 150: pp 141 - 154. Springer-Verlag.

Büdel, B. (2002): Diversity and Ecology of Biological Crusts. In: Progress in Botany 63: pp 386 - 404.

Chavez, P. S. (1989): Radiometric Calibration of Landsat Thematic Mapper Multispectral Images. In: Photogrammetric Engineering and Remote Sensing 55 (9): pp 1285 - 1294.

Chavez, P. S. & A. Y. Kwarteng (1989): Extraction Spectral Contrast in Landsat Thematic Mapper Image Data Using Selective Principal Component Analysis. In: Photogrammetric Engineering and Remote Sensing 55 (3): pp 339 - 348.

Chavez, P. S. & D. J. MacKinnon (1994): Automatic Detection of Vegetation Changes in the Southwestern United States Using Remotely Sensed Images. In: Photogrammetric Engineering and Remote Sensing 60 (5): pp 571 - 583.

Chavez, P. S. (1996): Image-Based Atmospheric Corrections - Revisited and Improved. In: Photogrammetric Engineering and Remote Sensing 62 (9): pp 1025 - 1036.

Chen, J. et al. (2005): A new index for mapping lichen-dominated biological soil crusts in desert areas. In: Remote Sensing of the Environment 96: pp 165 - 175.

Civco, D. L. et al. (2002): A comparison of land use and landcover change detection methods. In: ASPRS-ACSM Annual Conference and FIG XXII Congress. pp

Clinning, C. F. (1978): The biology and conservation of the Damara Tern in South West Africa. In: Madoqua 11 (31 - 39): pp.

Cohen, W. B. et al. (1998): An Efficient and Accurate Method for Mapping Forest Clearcuts in the Pacific Northwest Using Landsat Imagery. In: Photogrammetric Engineering and Remote Sensing 64 (4): pp 293 - 300.

Congalton, R. G. (1991): A review of assessing the accuracy of classifications of remotely sensed data. In: Remote Sensing of Environment 37 (1): pp 35-46.

Coppin, P. R. & M. E. Bauer (1996): Digital change detection in forest ecosystems with remote sensing imagery. In: Remote Sensing Reviews 13: pp 207 - 234.

Cowlishaw, G. & J. G. Davies (1997): Flora of the Pro-Namib Desert Swakop River catchment, Namibia: community classification and implications for desert vegetation sampling. In: Journal of Arid Environments 36: pp 271 - 290.

Craven, P. & C. Marais (1986): Namib Flora. Swakopmund to the giant Welwitschia via Goanikontes. Gamsberg Macmillan Publishers, Windhoek.

Dall'Olmo, G. & A. Karnieli (2002): Monitoring phenological cycles of desert ecosystems using NDVI and LST data derived from NOAA-AVHRR imagery. In: International Journal of Remote Sensing 23 (19): pp 4055 - 4071.

Daly, C. (1984): Snow Distribution Patterns in the Alpine Krummholz Zone. In: Progress in Physical Geography 8 (2): pp 157 - 176.

Daneel, J. L. (1992): The Impact of Off-Road Vehicle Traffic on the Gravel Plains of the Central Namib Desert, Namibia. Department of Agronomy. Pietermaritzburg, University of Natal, Namibia: pp 75.

Davenport, M. L. & S. E. Nicholson (1993): On the relation between rainfall and the Normalized Difference Vegetation Index for diverse vegetation types in East Africa. In: International Journal of Remote Sensing 14 (12): pp 2369 - 2389.

Dikau, R. (1988): Entwurf einer geomorphgraphisch-analytischen Systematik von Reliefeinheiten. In: Heidelberger Geographische Bausteine 5: pp 45.

Doidge, E. M. (1950): The South-African fungi and lichens to the end of 1945. In: Bothalia 5: pp 1-1094.

Dorn, R. I. & O. T. M. (1982): Rock Varnish. In: Progress in Physical Geography 6: pp 317-367.

Du, Y. et al. (2002): Radiometric normalization of multitemporal high-resolution satellite images with quality control for land cover change detection. In: Remote Sensing of Environment 82 (1): pp 123-134.

Eckardt, F. D. & N. Kuring (2005): SeaWiFS identifies dust sources in the Namib Desert. In: International Journal of Remote Sensing 26 (19): pp 4159 - 4167.

Eckardt, F. D. & R. Schemenauer (1998a): Fog water chemistry in the Namib Desert, Namibia. In: Atmospheric Environment 32 (14/15): pp 2595 - 2599.

Eckardt, F. D. & R. S. Schemenauer (1998b): The chemistry of Namib Desert fog in comparison with coastal desert fog of Chile and Oman. In: R. Schemenauer & H. Bridgman (eds): International Conference on Fog and Fog Collection: pp 187 - 190.

Ehlers, M. (2002): Fernerkundung für GIS-Anwender - Sensoren und Methoden zwischen Anspruch und Wirklichkeit. In: T. Blaschke (ed): Fernerkundung und GIS. Neue Sensoren - innovative Methoden: pp 10 - 23, Heidelberg.

Eklund, P. et al. (2000): Mining Remote Sensing Image Data: An Integration of Fuzzy Set Theory and Image Understanding Techniques for Environmental Change Detection. In: Proceedings of SPIE 2000: Knowledge and Data Discovery. pp 66 - 67.

Eldridge, D. J. (1998): Trampling of microphytic crusts on calcareous soils, and its impact on erosion under rain-impacted flow. In: Catena 33: pp 221 - 239.

Eldridge, D. J. & R. Rosentreter (1999): Morphological groups: a framework for monitoring microphytic crusts in arid landscapes. In: Jounal of Arid Environments 41: pp 11 - 25.

ERDAS (2001[5]): Erdas Imagine Field Guide. Georgia, USA.

EUNIS (2005): Habitat Classification System. European Environment Agency, European Topic Centre for Nature Protection and Biodiversity. http://eunis.eea.eu.int/habitats.jsp, Access Day: 06.02.

Evans, I. S. (1980): An integrated system of terrain analysis and slope mapping. In: Zeitschrift fur Geomorphologie 36: pp 274 - 295.

Evans, R. D. et al. (2001): Global Change and the Future of Biological Soil Crusts. In: J. Belnap & O. L. Lange (eds): Biological Soil Crusts: Structure, Function, and Management. Ecological Studies 150: pp 417 - 430. Springer-Verlag.

Evans, R. D. & O. L. Lange (2001): Biological Soil Crusts and Ecosystem Nitrogen and Carbon Dynamics. In: J. Belnap & O. L. Lange (eds): Biological Soil Crusts: Structure, Function, and Management. Ecological Studies 150: pp 263 - 280. Springer-Verlag.

Feurerer, T. (2005): Checklists of lichens and lichenicolous fungi. Version 1 October 2005. http://www.checklists.de, Access Day: 21.10.2005

Follmann, G. (1966): Chilenische Wanderflechten. In: Ber. Deut. Bot. Ges. 79: pp 453-462.

Follmann, G. & J. Redon (1972): Erganzungen zur flechtenflora der nordchilenischen nebeloasen fray jorge und talinay. In: Willdenowia 6 (3): pp 431-459.

Foody, G. M. (1999): The continuum of classification fuzziness in thematic mapping. In: Photogrammetric Engineering and Remote Sensing 65 (4): pp 443 - 451.

Foody, G. M. (2002): Status of land cover classification accuracy assessment. In: Remote Sensing of the Environment 80: pp 185 - 201.

Franzen, M. et al. (1998): Ergänzung und Fortführung des Digitalen Landschaftsmodells des BEV mit Fernerkundung. In: Österreichische Zeitschrift für Vermessung und Geoinformation 3: pp 161 - 166.

Frost, P. G. H. & E. Shaugnessy (1976): Breeding adaptations of the Damara Tern Sterna balaenarum. In: Madoqua 9 (33 - 39): pp.

Fung, T. (1990): An Assessment of TM Imagery for Land-Cover Change Detection. In: IEEE Transactions on Geoscience and Remote Sensing 28 (4): pp 681 - 684.

Garcia-Pichel, F. & J. Belnap (1996): Microenvironments and microscale productivity of cyanobacterial desert crusts. In: Journal of Phycology 32: pp 774-782.

Garty, J. et al. (2001): Photosynthesis, Chlorophyll Integrity, and Spectral Reflectance in Lichens Exposed to Air Pollution. In: Journal of Environmental Quality 30: pp 884 - 893.

Giess, W. (1989): Einiges zu unserer Flechtenflora. In: Dinteria 20: pp 30 - 32.

Goudie, A. (1972): Climate, weathering, crust formation, dunes, and fluvial features of the Central Namib Desert, near Gobabeb, South West Africa. In: Madoqua 1: pp 15 - 31.

Gray, V. (1980): Fog Precipitation in the Central Namib Desert: A short-term project. In: Bulletin van die Woestyn Ekologiese Navorsingseenheid (10): pp 6 - 8.

Gülland, A. (1907): Das Klima von Swakopmund. In: Mitteilungen aus den deutschen Schutzgebieten 20 (3): pp 17 - 164.

Haack, U. & H. Martin (1983): Geochronology of the Damara Orogon - a review. In: H. Martin & F. W. Eder (eds): Intracontinental fold belts: pp 839 - 846. Springer-Verlag.

Häberäcker, P. (1994): Digitale Bildverarbeitung: Grundlagen und Anwendungen., München, Wien.

Hachfeld, B. (2000): Rain, fog and species richness in the Central Namib Desert in the exceptional rainy season of 1999/2000. In: Dinteria 26 (11): pp 113 - 146.

Hachfeld, B. & N. Jürgens (2000): Climate patterns and their impact on the vegetation in a fog driven desert: The Central Namib Desert in Namibia. In: Phytocoenologia 30 (3 - 4): pp 567 - 589.

Hall, F. G. et al. (1991): Radiometric Rectification: Toward a Common Radiometric Response Amonge Multidate Multisensor Images. In: Remote Sensing of the Environment 35: pp 11 - 27.

Hartmann, J. (1997[3]): Handbuch der deutschen Bundesländer. Bundeszentrale für Politische Bildung, Bonn.

Heinrich, D. (1986): Flechtenfelder - Stolz SWA/Namibias. Allgemeine Zeitung Namibia: pp 5 - 13.

Henschel, J. R. (2003): The Climate of the Central Namib. In: K. Bender (ed): Coastal profile of the Erongo region. Integrated Coastal Zone Management Programme: pp 214. Erongo Regional Council, Swakopmund, Namibia.

Henschel, J. R. (2003): The Vegetation of the Central Namib including Lichen Fields. In: K. Bender (ed): Coastal profile of the Erongo region. Integrated Coastal Zone Management Programme: pp 214. Erongo Regional Council, Swakopmund, Namibia.

Hörsch, B. (2001): Zusammenhang zwischen Vegetation und Relief in alpinen Einzugsgebieten des Wallis (Schweiz). Ein multiskaliger GIS- und Fernerkundungsansatz. Mathematisch-Naturwissenschaftlichen Fakultät, Universität Bonn: pp 213.

Huete, A. R. (1988): A Soil-Adjusted Vegetation Index (SAVI). In: Remote Sensing of the Environment 25: pp 295 - 309.

Janssen, L. L. F. & J. M. van der Wel (1994): Accuracy Assessment of Satellite Derived Land-Cover Data: A Review. In: Photogrammetric Engineering and Remote Sensing 60 (4): pp 419 - 428.

Jarrold, J. (2001): The Impacts of Off-Road Traffic on the Lichen Fields of the Central Namib Desert. Department of Geography, University of Oxford, UK: pp 124.

Jensen, J. R. (2000): Remote Sensing of the Environment. An Earth Resource Perspective., Prentice Hall, Upper Saddle River, New Jersey.

Jensen, J. R. et al. (1995): Inland Wetland Change Detection in the Everglades Water Conservation Area 2A Using a Time Series of Normalized Remotly Sensed Data. In: Photogrammetric Engineering and Remote Sensing 61 (2): pp 199 - 209.

Jensen, S. K. (1992): Applications of hydrologic information automatically extracted from digital elevation models. In: K. J. Beven & I. D. Moore (eds): Terrain analysis and distributed modelling in hydrology: pp 35 - 48. John Wiley & Sons Ltd., Chichester.

Joubert, J. J. et al. (1982): Chemical composition of some lichen species occurring in the Namib Desert, South West Africa. In: Dinteria 16 (33-42): pp.

Jürgens, N. et al. (1997): Desert. In: R. M. Cowling et al. (eds): Vegetation of Southern Africa: pp 198 - 214. Cambridge University Press.

Jürgens, N. & A. Niebel-Lohmann (1995): Geobotanical Observations on Lichen Fields of the Southern Namib Desert. In: Mitt. Inst. Allg. Bot. Hamburg 25: pp 135 - 156.

Kaiserliche Bergbehörde (1912): Jahresbericht über das meteorologische Beobachtungswesen im südwestafrikanischen Schutzgebiet für die Zeit vom 1. Juli 1910 bis 30. Juni 1911. Mitteilungen aus den deutschen Schutzgebieten. 25: pp 56 - 71.

Kärnefelt, I. (1988): Two closely related species of Caloplaca (Teloschistaceae, Lichens) from the Namib Desert. In: Bothalia 18 (1): pp 51 - 56.

Karnieli, A. & H. Tsoar (1995): Spectral reflectance of biogenic crust developed on desert dune sand along the Israel-Egypt border. In: International Journal of Remote Sensing 16 (2): pp 369 - 374.

Karnieli, A. et al. (1996): The Effect of Microphytes on the Spectral Reflectance of Vegetation in Semiarid Regions. In: Remote Sensing of the Environment 57: pp 88 - 96.

Karnieli, A. (1997): Development and implementation of spectral crust index over dune sands. In: International Journal of Remote Sensing 18 (6): pp 1207 - 1220.

Karnieli, A. et al. (1999): Spectral Characteristics of Cyanobacteria Soil Crust in Semiarid Environments. In: Remote Sensing of the Environment 69: pp 67 - 75.

Karnieli, A. et al. (2001): Remote Sensing of Biological Soil Crusts. In: J. Belnap & O. L. Lange (eds): Biological Soil Crusts: Structure, Function, and Management. Ecological Studies 150: pp 431 - 456. Springer-Verlag.

Karnieli, A. et al. (2002): Temporal dynamics of soil and vegetation spectral responses in a semi-arid environment. In: International Journal of Remote Sensing 23 (19): pp 4073 - 4087.

Kokaly, R. F. et al. (1994): Vegetation and cryptobiotic soils mapping in arid regions. Spectral Analysis Workshop: The Use of Vegetation as an Indicator of Environmental Contamination, Desert Research Institute, Reno, NV. http://speclab.cr.usgs.gov/PAPERS.arches.crypto.94/arches.crypto.dri.html, Access Day: 26.10.2005

Kriegler, F. J. et al. (1969): Preprocessing transformations and their effects on multispectral recognition. In: Proceedings of the Sixth International Symposium on Remote Sensing of Environment, Ann Arbor, MI, University of Michigan. pp 97 - 131.

Krumbein, W. E. & K. Jens (1981): Biogenic rock varnishes of the Negev Desert (Israel), an ecological study of iron and manganese transformation by cyanobacteria and fungi. In: Oecologia 50 (25 - 38): pp.

Lalley, J. S. & H. A. Viles (2005): Terricolous lichens in the northern Namib Desert of Namibia: distribution and community composition. In: The Lichenologist 37 (1): pp 77 - 91.

Lancaster, J. et al. (1984): Climate of the central Namib Desert. In: Madoqua 14 (1): pp 5 - 61.

Lange, O. L. et al. (1991): Mikroklima, Wassergehalt und Photosynthese von Flechten in der küstennahen Nebelzone der Namib-Wüste: Messungen während der herbstlichen Witterungsperiode. In: Flora 185: pp 233 - 266.

Lange, O. L. et al. (1975): Adaptions of desert lichens to drought and extreme temperatures. In: N. F. Hadley, (ed): Environmental Physiology of Dersert Organisms: pp 20 - 37. Dowden, Hutchinson and Ross, Inc., Stroudsburg, Pennsylvania.

Lange, O. L. et al. (1990): Eight days in the life of a desert lichen: water relations and photosynthesis of Telochistes capensis in the coastal fog zone of the Namib Desert. In: Madoqua 17 (1): pp 17 - 30.

Lange, O. L. et al. (1994): Photosynthesis and water relations of lichen soil crusts: field measurements in the coastal fog zone of the Namib Desert. In: Functional Ecology 8: pp 253 - 264.

Le Houeru, H. N. (1998): Fog-dependent vegetation and ecosystems in the dry lands of Africa. In: R. Schemenauer & H. Bridgman (eds): International Conference on Fog and Fog Collection: pp 175 - 178.

Lengoasa, J. R. et al. (1993): The influence of a synoptic-scale disturbance on topographically induced boundary layer circulations over the central Namib Desert. In: Madoqua 18 (2): pp 71 - 78.

Levien, L. M. et al. (1998): Statewide change detection using multitemporal remote sensing data. In: Seventh Forest Service Remote Sensing Applications Conference, Nassau Bay, Texas. pp

Lillesand, T. M. & R. W. Kiefer (2000[5]): Remote Sensing and Image Interpretation., New York.

Lindesay, J. A. & P. D. Tyson (1990): Climate and Near-surface Airflow Over the Central Namib. In: M. K. Seely (ed): Namib ecology: 25 years of Namib research. Transvaal Museum Monograph No. 7: pp 27 - 37. Transvaal Museum, Pretoria.

Loris, K. et al. (2004): Zonobiom III: Die Namib-Wüste im südwestlichen Africa (Namibia, Südafrika, Angola). In: H. Walter & S.-W. Breckle (eds): Ökologie der Erde: pp 441 - 497. Spektrum Akademischer Verlag.

Loris, K. & B. Schieferstein (1992): Ecological investigations on lichen fields of the Central Namib. In: Vegetatio 98: pp 113 - 128.

Martin, H. (1963): A suggested theory for the origin and a brief description of some gypsum deposits of South West Africa. In: The Transactions of the Geological Society of South Africa LXVI: pp 345 - 351.

Martin, H. (1965): The Precambrian geology of South West Africa and Namaqualand. Precambr. Res. Unit., University of Cape Town: pp 159.

Matsakis, P. et al. (2000): Evaluation of fuzzy partitions. In: Remote Sensing of Environment 74: pp 516 - 533.

Matthes-Sears, U. et al. (1986): The ecology of Ramalina menziesii. IV. In situ photosynthetic patterns and water relations of reciprocal transplants between two sites on a coastal-inland gradient. In: Canadian Journal of Botany 64: pp 1183-1187.

Mattick, F. (1970): Flechtenbestände der Nebelwüste und Wanderflechten der Namib. In: Namib und Meer 1: pp 35 - 43.

McKenna Neumann, C. & C. Maxwell (1999): A wind tunnel study of the resilience of three fungal crusts to particle abrasion during aeolian sediment transport. In: Catena 38: pp 151 - 173.

Meijerink, A. M. J. et al. (1994): Introduction to the use of geographic information systems for practical hydrology. ITC Publication Number 23, Enschede.

Mendelsohn, J. et al. (2002): Atlas of Namibia. A Portratit of the Land and its People., David Philip Publishers, Capetown, South Africa.

Mengelkamp, H. T. et al. (2003): Überflutung von Stadtgebieten: ARCHE (DLR). In: GKSS-Forschungszentrum (ed): Simulation von Hochwasser im Einzugsgebiet der Oder mit einem gekoppelten Modellsystem (ODRAFLOOD). Abschlussbericht: pp 76 - 86, Geesthacht.

Microimages' Scientific Writers (2003): Glossary for Geospacial Science. www.microimages.com, Access Day: 15.01.2004.

Moisel, L. (1971): Beobachtungen an einigen Namibpflanzen und ihrer Wasserversorgung. In: Namib und Meer 20: pp 65 - 75.

Moll, A. (2003): Shuttle Radar Topography Mission (SRTM/X-SAR) – ein radarinterferometrisches Höhenmodell und seine Validierung am Beispiel des Bonner Raumes. Geographisches Institut, Universität Bonn: pp 110.

Moore, I. D. et al. (1991): Digital terrain modelling: A review of hydrological, geomorphological and biological applications. In: Hydrological Process 5: pp 3 - 30.

Mtuleni, V. et al. (1998): Evaluation of Fog-Harvesting potential in Namibia. In: R. Schemenauer & H. Bridgman (eds): International Conference on Fog and Fog Collection: pp 179 - 182.

Muchoney, D. M. & B. N. Haack (1994): Change Detection for Monitoring Forest Defoliation. In: Photogrammetric Engineering and Remote Sensing 60 (10): pp 1243 - 1257.

NASA (1999): Landsat 7 Fact Sheet. Release No: 99-34, National Aeronautics and Space Administration, Press Kit.

Nash, I., T.H. et al. (1979): Lichen vegetational gradients in relation to the Pacific coast of Baja California: The maritime influence. In: Madroño 26: pp 149-163.

Nicholson, S. E. et al. (1990): A comparison of the vegeteion response to rainfall in the Sahel and East Africa, using Normalized Difference Vegetation Index fom NOAA AVHRR. In: Climatic Change 17: pp 209 - 241.

Nieman, W. A. et al. (1978): A note on precipitation at Swakopmund. In: Madoqua 11 (1): pp 69 - 73.

Nott, K. & M. Savage (1985): Radiation measurements from the Namib Desert. In: Madoqua 14 (2): pp 165 - 172.

Okin, G. S. et al. (2001): Practical limits on hyperspectral vegetation discrimination in arid and semiarid environments. In: Remote Sensing of the Environment 77: pp 212 - 225.

Ollier, C. D. (1977): Outline geological and geomorphic history of the Central Namib Desert. In: Madoqua 10 (3): pp 207 - 212.

Orlovsky, L. et al. (2004): Temporal dynamics and productivity of biogenic soil crusts in the central Karakum desert, Turkmenistan. In: Jounal of Arid Environments 56: pp 579 - 601.

Ortiz, M. J. et al. (1997): Classification of croplands through integration of remote sensing, GIS, and historical database. In: International Journal of Remote Sensing 8 (1): pp 95 - 105.

Pác, R. et al. (1999): X-SAR/SRTM Shuttle Radar Topography Mission. Mapping the Earth from Space., Deutsches Zentrum für Luft- und Raumfahrt (DLR): pp 24.

Perdigao, V. & A. S. A. I. Annoni, AIS Unit, JRC. (1997): Technical and methodological guide for updating the CORINE landcover database., Space Application Institute, AIS Unit, JRC.

Pickford, M. & B. Senut (1999): Geology and Paleaebiology of the Namib Desert, Southwestern Africa. Memoir 18, Geological Survey of Namibia, Ministry of Mines and Energy.

Pilon, P. G. et al. (1988): An Enhanced Classification Approach to Change Detection in Semi-Arid Environments. In: Photogrammetric Engineering and Remote Sensing 54 (12): pp 1709 - 1716.

Powell, R. L. et al. (2004): Sources of error in accuracy assessment of thematic land-cover maps in the Brazilian Amazon. In: Remote Sensing of Environment 90 (2): pp 221-234.

Qi, J. et al. (1994): A Modified Soil Adjusted Vegetation Index. In: Remote Sensing of the Environment 48: pp 119 - 126.

Redon, J. & O. L. Lange (1983): Epiphytic lichens in the region of a Chilean "Fog Oasis" (Fray Jorge). I. Distributional patterns and habitat conditions. In: Flora 174: pp 213-243.

Rees, W. G. et al. (2004): Reflectance spectra of subarctic lichens between 400 and 2400 nm. In: Remote Sensing of the Environment 90: pp 281 - 292.

Rees, W. G. & M. Williams (1997): Monitoring changes in land cover induced by atmospheric pollution in the Kola Peninsula, Russia, using Landsat-MSS data. In: International Journal of Remote Sensing 18 (8): pp 1703 - 1723.

Richter, R. (1999): Atmospheric correction algorithm for flat terrain: Modell ATCOR2. Wessling, DLR: pp.

Roberts, M. et al. (1994): Component Analysis for Interpretation of Time Series NDVI Imagery. In: ASPRS/ACSM. pp 538 - 550.

Rogan, J. et al. (2002): A comparison of methods for monitoring multitemporal vegetation change using Thematic Mapper imagery. In: Remote Sensing of the Environment 80: pp 143 - 156.

Rogers, R. W. (1977): Lichens of hot arid and semi-arid lands. In: M. R. D. Seaward (ed): Lichen Ecology: pp 211-252. Academic Press, New York.

Rosentreter, R. et al. (2001): Monitoring and Management of Biological Soil Crusts. In: J. Belnap & O. L. Lange (eds): Biological Soil Crusts: Structure, Function, and Management. Ecological Studies 150: pp 457 - 470. Springer-Verlag.

Rouse, J. W. et al. (1974): Monitoring the vernal advancement and retrogradation (green wave effect) of natural vegetation. NASA/GSFC Type III Final Report. Greenbelt, MD.: pp 371.

Rouse, J. W. et al. (1973): Monitoring vegetation systems in the great plains with ERTS. In: Third ERTS Symposium, NASA SP-351. pp 309 - 317.

Rundel, P. W. (1978): Ecological relationships of desert fog zone lichens. In: The Bryologist 81 (2): pp 277-293.

Schieferstein, B. (1989): Ökologische Untersuchungen an den Flechtenfeldern in der Namib-Nebelwüste. Institut für Botanik. Hohenheim, Universität Hohenheim: pp 1 - 171.

Schmidt, H. & A. Karnieli (2000): Remote sensing of seasonal variability of vegetation in a semi-arid environment. In: Journal of Arid Environments 45: pp 43 - 59.

Schmidt, H. & A. Karnieli (2001): Sensitivity of vegetation indices to substrate brightness in hyper-arid environment: the Makhtesh Ramon Crater (Israel) case study. In: International Journal of Remote Sensing 22 (17): pp 3503 - 3520.

Schmidt, H. & A. Karnieli (2002): Analysis of the temporal and spatial vegetation patterns in a semi-arid environment observed by NOAA AVHRR imagery and spectral ground measurements. In: International Journal of Remote Sensing 23 (19): pp 3971 - 3990.

Scholz, H. (1972): The soils of the Central Namib Desert with special consideration of the soils in the vicinity of Gobabeb. In: Madoqua 2 (1): pp 33 - 51.

Schönwiese, C. D. (1985): Praktische Statistik für Meteorologen und Geowissenschaftler. Gebrüder Borntraeger, Berlin, Stuttgart.

Schreiber, U. M. (1996): The geology of the Walvis Bay Area. Explanation of Sheet 2214 (Scale 1: 250 000). Ministry of Mines and Energy / Geological Survey of Namibia.

Schulze, B. R. (1976): The Climate of Gobabeb. In: Scient. Pap. Namib Desert Res. Stn. (38): pp 5 - 11.

Scuturi, N. C. et al. (2004): Soil-associated lichens in rangelands of north-eastern Patagonia. Lichen groups and species with potential as bioindicators of grazing disturbance. In: The Lichenologist 36 (6): pp 405 - 412.

Seely, M. K. (1978): Standing crop as an index of precipitation in the Central Namib grassland. In: Madoqua 11 (1): pp 61 - 68.

Seely, M. K. (2004[3]): The Namib. Natural History of an Ancient Desert. Desert Research Foundation of Namibia, Windhoek.

Seely, M. K. & W. J. Hamilton (1978): Durability of vehicle tracks on three Namib Desert substrates. In: South-African Journal on Wildlife Research 8 (3): pp 107-111.

Seely, M. K. & J. R. Henschel (1998): The climatology of Namib fog. In: R. Schemenauer & H. Bridgman (eds): International Conference on Fog and Fog Collection: pp 353 - 356.

Seely, M. K. et al. (1998): The Ecology of Namib desert dunes. In: R. Schemenauer & H. Bridgman (eds): International Conference on Fog and Fog Collection: pp 183 - 186.

Seely, M. K. & P. Stuart (1976): Namib climate: 2. The climate of Gobabeb, ten-year summary 1962/72. In: Bulletin of the Desert Ecological Research Unit (8): pp 7 - 9.

Selby, M. J. (1976): Some thoughts on the geomorphology of the Central Namib Desert. In: Bulletin of the Desert Ecological Research Unit (8): pp 5 - 6.

Shackley, M. (1985): Palaeolithic achaeology of the Central Namib Desert. A preliminary survey of chronology, typology and site location. Cimbebasia Memoir No. 6, State Museum, Windhoek.

Shannon, L. V. et al. (1986): On the existence of an El Nino-type phenomenon in the Benguela System. In: Journal of Marine Research 44: pp 495 - 520.

Singh, A. (1989): Digital change detection techniques usinge remotely-sensed data. In: International Journal of Remote Sensing 10 (6): pp 989 - 1003.

Sluiter, A. et al. (2004): Determination of ash in biomass. Biomass Analysis Technology Team Laboratory Analytical Procedure, National Bioenergy Center, U S. Department of Energy: pp 6.

Solbrig, O. T. (1991): The origin and function of biodiversity. In: Environment 33: pp 16 - 20 and 34 - 38.

Song, C. et al. (2001): Classification and Change Detection Using Landsat TM Data: When and How to Correct Atmospheric Effects? In: Remote Sensing of the Environment 75: pp 230 - 244.

Southgate, R. I. et al. (1996): Precipitation and biomass changes in the Namib Desert dune ecosystem. In: Journal of Arid Environments 33: pp 267 - 280.

Stehman, S. V. (1997): Selecting and interpreting measures of thematic classification accuracy. In: Remote Sensing of Environment 62 (1): pp 77-89.

Stehman, S. V. & R. L. Czaplewski (1998): Design and Analysis for Thematic Map Accuracy Assessment: Fundamental Principles. In: Remote Sensing of Environment 64 (3): pp 331-344.

Stoms, D. M. & J. E. Estes (1993): A remote sensing research agenda for mapping and monitoring bodiversity. In: International Journal of Remote Sensing 14 (10): pp 1839 - 1860.

Swedish Species Information Center (2003): Preliminary Global Red List of Lichens. http://www.artdata.slu.se/guest/global3.htm, Access Day: 10.09.2003.

Tatem, A. J. et al. (2005): Assessing the accuracy of satellite derived global and national urban maps in Kenya. In: Remote Sensing of Environment 96 (1): pp 87-97.

Theron, G. K. et al. (1980): Vegetation of the lower Kuiseb River. In: Madoqua 11 (4): pp 327 - 345.

Tizhoosh, H. R. (1998): Fuzzy-Bildverarbeitung: Einführung in Theorie und Praxis., Heidelberg.

Todd, S. W. et al. (1998): Biomass estimation on grazed and ungrazed rangelands using spectral indices. In: International Journal of Remote Sensing 19 (3): pp 427 - 438.

Tourism Officer of Municipality of Henties Bay (2003a): Omaruru River 4 X 4 Trail. Municipality Henties Bay, Namibia.

Tourism Officer of Municipality of Henties Bay (2003b): Messum Crater 4 X 4 Trail. Municipality of Henties Bay.

U.S. Geological Survey (2003): Preliminary Assessment of the Value of Landsat 7 ETM+ Data following Scan Line Corrector Malfunction. Sioux Falls, USA.

U.S. Geological Survey (2004): USGS Landsat Project - Landsat 7 Homepage. http://landsat.usgs.gov, Access Day: 07.10.04.

Ullmann, I. & B. Büdel (2001a): Biological Soil Crusts of Africa. In: J. Belnap & O. L. Lange (eds): Biological Soil Crusts: Structure, Function, and Management. Ecological Studies 150: pp 107 - 118. Springer-Verlag.

Ullmann, I. & B. Büdel (2001b): Ecological Derterminants of Species Composition of Biological Soil Crusts on a Landscape Scale. In: J. Belnap & O. L. Lange (eds): Biological Soil Crusts: Structure, Function, and Management. Ecological Studies 150: pp 203 - 216. Springer-Verlag.

Vogel, J. C. & M. K. Seely (1977): Occurrence of C-4 plants in the Central Namib Desert. In: Madoqua 1007 (1): pp 75 - 78.

Vogelmann, J. E. (2003): Reports from the Science Community. In: U. S. G. Survey (ed): Preliminary Assessment of the Value of Landsat 7 ETM+ Data following Scan Line Corrector Malfunction: pp 19 - 53, Sioux Falls, USA.

von Willert, D. J. et al. (1983): CO_2 exchange of CAM exhibiting succulents in the southern Namib desert in relation to microclimate and water stress. In: Photosynthesis Research 42: pp 289 - 298.

Walter, H. (1976): Gibt es in der Namib Nebelpflanzen? In: Namib und Meer 7: pp 5 - 14.

Walter, H. (1985): The Namib Desert. In: M. Evenari et al. (eds): Hot Deserts and Arid Shrublands, B. Ecosystems of the World 12B: pp 245-282. Elsevier, Amsterdam.

Walter, H. & S.-W. Breckle (1999[7]): Vegetation und Klimazonen. UTB, Stuttgart.

Warren, S. D. (2001b): Synopsis: Influence of Biological Soil Crusts on Arid Land Hydrology and Soil Stability. In: J. Belnap & O. L. Lange (eds): Biological Soil Crusts: Structure, Function, and Management. Ecological Studies 150: pp 349 - 362. Springer-Verlag.

Waser, L. et al. (2003): Rapid Assessment of Lichens Diversity - Correlation of Remote Sensing Data with Field Samples. In: E. Feldmeyer-Christe (ed): State of the Art in Vegetation Monitoring Approaches. Abstracts. International Symposium, March 24 - 26 2003., Birmensdorf, Swiss Federal Research Institute WSL. pp 38.

Weiers, S. et al. (2003): Mapping and indicator approaches for the assessment of habitats at different scales using remote sensing and GIS methods. In: Landscape and Urban Planning 1007: pp 1 - 23.

Wessels, D. C. J. (1989): Lichens of the Namib Desert, South West Africa/Namibia. In: Dinteria 20: pp 3 - 22.

Wessels, D. C. J. & D. R. J. van Vuuren (1986): Landsat imagery - its possible use in mapping the distribution of major Lichen Communites in the Namib Desert, South West Africa. In: Madoqua 14 (4): pp 369 - 373.

Wessels, D. C. J. et al. (1979): A preliminary report on lichen feeding coleoptera occurring on Teloschistes capensis Malme in the Namib Desert, South West Africa. In: Bryologist 82 (270-273): pp.

Williamson, G. (1997): Preliminary account of the Floristic Zones of the Sperrgebiet (Protected Diamond Area) in southwest Namibia. In: Dinteria 25: pp 1 - 68.

Wirth, V. & A. Vézda (1975): Drei neue Flechtenarten aus SWA. In: Stuttgarter Beitr. Naturk. Serie A: pp 284.

Wood, J. (1996): The Geomorphological Characterisation of Digital Elevation Models, University of Leicester: pp 185.

Wood, J. (2005): LandSerf. http://www.landserf.org/, Access Day: 17.02.2005.

Woodcock, C. E. et al. (2001): Monitoring large areas for forest change using Landsat: Generalization across space, time and Landsat sensors. In: Remote Sensing of the Environment 78: pp 194 - 203.

Wyatt, B. K. (2000): Vegetation Mapping from Ground, Air and Space - Competitive or Complementary Techniques? In: R. Alexander & A. C. Millington (eds): Vegetation Mapping: From Patch to Planet: pp 3 - 18. John Wiley & Sons Ltd.

Zedda, L. & G. Rambold (2000-2005): BIOTA Southern Africa Subproject S04 - Diversity of Lichens. http://141.84.65.132/UBT-Mycology/Biota/DataFind.cfm, Access Day: 15.01.2005.

Zedda, L. & G. Rambold (2004): Diversity change of soil-growing lichens along a climate gradient in Southern Africa. In: Döbbeler, P. & G. Rambold (eds.): Contributions to Lichenology. Festschrift in Honour of Hannes Hertel. 88: pp 701 - 714.

Zevenbergen, L. W. & C. R. Thorne (1987): Quantitative Analysis of Land Surface Topography. In: Earth Surface Processes and Landforms 12: pp 47 - 56.

Zhang, J. & R. P. Kirby (1999): Alternative Criteria for Defining Fuzzy Boundaries Based on Fuzzy Classification of Aerial Photographs and Satellite Images. In: Photogrammetric Engineering and Remote Sensing 62 (12): pp 1379 - 1387.

Zhang, J. et al. (2004): Derivative Spectral Unmixing of Hyperspectral Data Applied to Mixtures of Lichen and Rock. In: IEEE Transactions on Geoscience and Remote Sensing 42 (9): pp 1934 - 1940.

Kleinberg	30 km E of Walvis Bay	182 m	23°00.996'S; 14°43.435'E
Operator	Desert Research Foundation Namibia (DRFN), Gobabeb, Namibia		
Hourly	AirT, RH, Rain, Wspd, Wdir		
1994	01.07.1994 – 31.12.1994		
1995	01.01.1995 – 31.12.1995		
1996	01.01.1996 – 01.04.1996 12.06.1996 – 30.08.1996 27.09.1996 – 07.12.1996		
1997	18.03.1997 – 09.05.1997 03.09.1997 – 27.09.1997 10.10.1997 31.10.1997		
1998	24.02.1998 – 06.10.1998 03.11.1998 – 31.12.1998		
1999	03.02.1999 – 03.11.1999		
2000	25.01.2000 – 31.12.2000		
2001	01.01.2001 – 31.12.2001		
2002	01.01.2002 – 05.07.2002 02.08.2002 – 12.11.2002 04.12.2002 – 31.12.2002		

Figure A1: Details of Kleinbeg automatic climate station.

Double-Three	10 km E of Walvis Bay	27 m	22°59.655'S; 14°34.121'E
Operator	Desert Research Foundation Namibia (DRFN), Gobabeb, Namibia		
Hourly	AirT, RH, Rain, Wspd, Wdir, Sol.Rad, RokT, Wetness, Fog		
1999	03.02.1999 – 03.11.1999		
2000	25.01.2000 – 31.12.2000		
2001	01.01.2001 – 14.11.2001		
2002	04.02.2002 – 13.11.2002		

Wlotzkasbaken	30 km N of Swakopmund	60 m	22° 19" 09.96 S; 14° 27" 50.31 E
Operator	BIOTA Southern Africa Head Office, Hamburg, Germany		
Hourly	AIRTEMP, SOILTEMP, AIR_RH, SOLARRAD, WINDDIR, WETNESS, WINDSPEED, RAIN		
2001	07.07.2001 – 16.08.2001 03.10.2001 – 31.12.2001		
2002	01.01.2002 – 31.12.2002		
2003	01.01.2003 – 29.06.2003		

Figure A2: Details of Double Three and Wlotzkasbaken automatic climate stations

Level 1	Level 2	Type Classes
Fruticose Lichen Zone	The Coastal *Teloschistes capensis* community of the fine quartz gravel plains	Type 1.1
		Type 1.2
	The Inland *Teloschistes capensis* community of the undulating course quartz gravel plains	Type 2.1
Fruticose / Foliose Lichen Zone	The Coastal *Teloschistes capensis, Xanthoparmelia walteri* community of the fine quartz gravel plains	Type 1.1
		Type 1.2
		Type 1.3
		Type 1.4
	The Inland Teloschistes capensis, Xanthoparmelia walteri community of the undulating coarse quartz gravel plains	Type 2.1
		Type 2.2
	The mountainous Xanthomaculina hottentotta community	Type 3.1
Foliose Lichen Zone	The *Xanthoparmelia walteri* community of the fine quartz gravel plains	Type 1.1
		Type 1.2
		Type 1.3
	The mountainous Saxicolous Xanthoparmelia walteri Lichen community	Type 2.1
Foliose / Crustose Lichen Zone	The *Xanthoparmelia walteri, Caloplaca, Neofuscelia, Lecidella* community of the fine quartz gravel plains	Type 1.1
		Type 1.2
		Type 1.3
	The mountainous Saxicolous Xanthoparmelia walteri, Caloplca elegantissima Lichen community	Type 2.1
	The *Xanthoparmelia walteri, Xanthomaculina convoluta, Lecidella crystallina* community of the coarse gravel hummocks of the gypsum plains	Type 3.1
		Type 3.2
Crustose Lichen Zone	The Caloplaca, Neosfuscelia, Lecidella community of the fine quartz gravel plains	Type 1.1
		Type 1.2
	Lecidella crystallina, Caloplaca volkii, Xanthomaculina convoluta, community of the gypsum plains	Type 2.1
		Type 2.2
		Type 2.3
Crustose Sparse Lichen Zone	The sparse Caloplaca, Neosfuscelia, Lecidella community of the fine quartz gravel plains	Type 1.1
		Type 1.2
		Type 1.3
	The sparse Lecidella crystallina, Caloplaca volkii, Calplaca elegantissima community of the gypsum plains	Type 2.1
		Type 2.2
No Lichen	Non Lichen covered areas of the fine quartz gravel / gypsum plains	Type 1.1
		Type 1.2
		Type 1.3
		Type 1.4
		Type 1.5
		Type 1.6
		Type 1.7
		Type 1.8
		Type 1.9
		Type 1.10
	Non Lichen covered areas of the rocky ridges / debris and coarse gravel plains.	Type 2.1
		Type 2.2
	Non Lichen covered areas of the rocky and mountainous areas.	Type 3.1
		Type 3.2
		Type 3.4
		Type 3.5
		Type 3.6
		Type 3.7
		Type 3.8

Figure A3: Hierarchical Classification Scheme: spectral subclasses according to the first and second level of the hierarchical classification scheme based on the concept of morphological groups.

	1 Foliose Crustose Type 3.1	2 Foliose Crustose Type 3.2	3 Crustose Type 2.1	4 Crustose Type 2.2	5 Crustose Type 2.3	6 Crustose Sparse Type 2.1	7 Crustose Sparse Type 2.2	8 No Lichen Type 1.5	9 No Lichen Type 1.6	10 No Lichen Type 1.7	11 No Lichen Type 1.8	12 No Lichen Type 1.9	13 No Lichen Type 1.10	14 No Lichen Type 1.11	15 No Lichen Type 3.4	16 No Lichen Type 3.5	17 No Lichen Type 3.6	18 No Lichen Type 3.7	19 No Lichen Type 3.8
1 Foliose Crustose Type 3.1	0	1195,01578	1301,39896	1382,47827	1413,84417	1414,21356	1414,21354	1414,21356	1414,21356	1414,21356	1414,21355	1414,21356	1414,21356	1414,21356	1413,80423	1414,21356	1414,21356	1414,1361	1414,21218
2 Foliose Crustose Type 3.2	1195,01578	0	1409,48742	1395,42125	1414,21312	1414,21356	1414,21356	1414,21356	1414,21356	1414,21356	1414,21356	1414,21356	1414,21356	1414,21356	1413,26137	1414,21356	1414,21356	1414,09764	1414,18622
3 Crustose Type 2.1	1301,39896	1409,48742	0	1390,64029	1370,28856	1414,21356	1414,16142	1414,21337	1414,21356	1414,21356	1414,2114	1414,21356	1414,21356	1414,21356	1411,24898	1414,21323	1414,21356	1414,03085	1414,21316
4 Crustose Type 2.2	1382,47827	1395,42125	1390,64029	0	1411,89437	1414,21356	1414,18411	1414,20684	1414,21356	1414,21356	1414,21356	1414,21353	1414,21356	1414,21356	1414,18624	1414,2123	1414,21354	1414,08381	1414,21353
5 Crustose Type 2.3	1413,84417	1414,21312	1370,28856	1411,89437	0	1414,21353	1365,52493	1413,36053	1414,21329	1414,21356	1414,05667	1414,21324	1414,21356	1414,21356	1413,97879	1413,59719	1414,21356	1414,13478	1414,21356
6 Crustose Sparse Type 2.1	1414,21356	1414,21356	1414,21356	1414,21356	1414,21353	0	1413,90188	1403,02081	1396,97902	1368,95815	1414,18752	1414,15704	1414,21356	1414,21356	1414,21356	1376,43054	1411,27382	1414,21215	1414,21356
7 Crustose Sparse Type 2.2	1414,21354	1414,21356	1414,16142	1414,18411	1365,52493	1413,90188	0	1399,10894	1397,31642	1414,21014	1388,3848	1414,21337	1414,21356	1414,21356	1414,20815	1354,662	1414,20045	1414,18524	1414,21356
8 No Lichen Type 1.4	1414,21356	1414,21356	1414,21337	1414,20684	1413,36053	1403,02081	1399,10894	0	1412,74109	1414,20154	1414,21125	1414,18151	1414,21356	1414,21356	1414,21355	896,304172	1408,7667	1414,19727	1414,21356
9 No Lichen Type 1.5	1414,21356	1414,21356	1414,21356	1414,21356	1414,21329	1396,97902	1397,31642	1412,74109	0	1380,14166	1375,50364	1414,21342	1414,21356	1414,21356	1414,21315	1402,25637	1405,0922	1414,17721	1414,21356
10 No Lichen Type 1.6	1414,21356	1414,21356	1414,21356	1414,21356	1414,21356	1368,95815	1414,21014	1414,20154	1380,14166	0	1414,11826	1414,21339	1414,21226	1414,21356	1414,21356	1414,00242	1412,22482	1414,21228	1414,21356
11 No Lichen Type 1.7	1414,21355	1414,21356	1414,2114	1414,21356	1414,05667	1414,18752	1388,3848	1414,21125	1375,50364	1414,11826	0	1414,21356	1414,21356	1414,21356	1414,12835	1413,82618	1414,21348	1414,18666	1414,21356
12 No Lichen Type 1.8	1414,21356	1414,21356	1414,21356	1414,21353	1414,21324	1414,15704	1414,21337	1414,18151	1414,21342	1414,21339	1414,21356	0	1414,21356	1414,21356	1414,21356	1414,17994	1414,21208	1414,21356	1414,21356
13 No Lichen Type 1.9	1414,21356	1414,21356	1414,21356	1414,21356	1414,21356	1414,21356	1414,21356	1414,21356	1414,21356	1414,21226	1414,21356	1414,21356	0	1411,24854	1414,21356	1414,21356	1414,21356	1414,21356	1414,21356
14 No Lichen Type 1.10	1414,21356	1414,21356	1414,21356	1414,21356	1414,21356	1414,21356	1414,21356	1414,21356	1414,21356	1414,21356	1414,21356	1414,21356	1411,24854	0	1414,21356	1414,21356	1414,21356	1414,21356	1414,21356
15 No Lichen Type 3.4	1413,80423	1413,26137	1411,24898	1414,18624	1413,97879	1414,21356	1414,20815	1414,21355	1414,21315	1414,21356	1414,12835	1414,21356	1414,21356	1414,21356	0	1414,21259	1414,21356	1407,95687	1258,3659
16 No Lichen Type 3.5	1414,21356	1414,21356	1414,21323	1414,2123	1413,59719	1376,43054	1354,662	896,304172	1402,25637	1414,00242	1413,82618	1414,17994	1414,21356	1414,21356	1414,21259	0	1407,8269	1414,17046	1414,21356
17 No Lichen Type 3.6	1414,21356	1414,21356	1414,21356	1414,21354	1414,21356	1411,27382	1414,20045	1408,7667	1405,0922	1412,22482	1414,21348	1414,21208	1414,21356	1414,21356	1414,21356	1407,8269	0	1414,19858	1414,21356
18 No Lichen Type 3.7	1414,1361	1414,09764	1414,03085	1414,08381	1414,13478	1414,21215	1414,18524	1414,19727	1414,17721	1414,21228	1414,18666	1414,21356	1414,21356	1414,21356	1407,95687	1414,17046	1414,19858	0	1407,71401
19 No Lichen Type 3.8	1414,21218	1414,18622	1414,21316	1414,21353	1414,21356	1414,21356	1414,21356	1414,21356	1414,21356	1414,21356	1414,21356	1414,21356	1414,21356	1414,21356	1258,3659	1414,21356	1414,21356	1407,71401	0

Figure A4: Full listing of the Jeffries-Matusita (JM) separability measures obtained for the unitemporal classification of WRS-2 scene 179 / 76 for the year of 2003.

	1 Fruticose Type 1.1	2 Fruticose Type 1.2	3 Fruticose Type 2.1	4 Fruticose Foliose Type 1.1	5 Fruticose Foliose Type 1.2	6 Fruticose Foliose Type 1.3	7 Fruticose Foliose Type 1.4	8 Fruticose Foliose Type 2.1	9 Fruticose Foliose Type 2.2	10 Fruticose Foliose Type 3.1	11 Foliose Type 1.1	12 Foliose Type 1.2	13 Foliose Type 1.3	14 Foliose Type 2.1	15 Foliose Crustose Type 1.1	16 Foliose Crustose Type 1.2	17 Foliose Crustose Type 1.3	18 Foliose Crustose Type 2.1	19 Crustose Type 1.1	20 Crustose Type 1.2	21 Crustose Sparse Type 1.1	22 Crustose Sparse Type 1.2	23 Crustose Sparse Type 1.3	24 No Lichen Type 1.1	25 No Lichen Type 1.2	26 No Lichen Type 1.3	27 No Lichen Type 2.1	28 No Lichen Type 2.2	29 No Lichen Type 3.1	30 No Lichen Type 3.2
1 Fruticose Type 1.1	0	1414,21356	1414,21345	1410,46243	1414,21356	1299,45013	1412,72791	1410,78126	1414,21356	1414,21356	1413,99058	1414,21234	1413,60999	1414,21356	1414,21356	1414,21356	1414,21356	1414,21356	1414,21356	1414,21356	1414,21356	1414,21356	1414,21356	1414,21356	1414,21356	1414,21356	1414,21356	1414,21356	1413,99431	1414,21356	1414,21356
2 Fruticose Type 1.2	1414,21356	0	1414,21356	1414,21356	1414,21356	1414,21356	1414,21356	1414,21356	1414,21327	1414,21356	1414,21356	1414,21356	1414,21356	1411,99957	1414,21356	1414,21199	1414,21356	1414,21356	1414,21356	1414,21356	1414,21356	1414,21356	1414,21356	1414,21356	1414,21356	1414,21356	1414,21356	1414,21356	1414,21255	1414,21356	1414,21356
3 Fruticose Type 2.1	1414,21345	1414,21356	0	1414,21356	1414,21356	1411,62972	1411,82396	1412,16535	1402,91002	1414,21356	1414,21356	1414,21356	1414,20364	1413,91155	1414,21356	1414,21356	1414,21356	1414,21356	1414,21356	1414,21356	1414,21356	1414,21356	1414,21356	1414,21356	1414,21356	1414,21356	1414,21356	1414,21356	1414,20309	1414,21356	1414,21356
4 Fruticose Foliose Type 1.1	1410,46243	1414,21356	1414,21356	0	1414,21356	1411,60523	1413,41669	1414,07551	1414,21356	1414,21356	1318,99691	1413,46069	1386,01525	1414,21356	1409,45191	1414,21356	1414,16342	1414,21356	1414,21356	1414,15624	1414,21356	1414,21356	1414,21337	1414,21356	1414,21356	1414,21356	1414,14698	1414,21356	1414,10825	1414,21356	1414,21356
5 Fruticose Foliose Type 1.2	1414,21356	1414,21356	1414,21356	1414,21356	0	1414,21356	1414,21356	1414,21356	1414,21356	1184,34652	1414,21356	1414,21356	1414,21356	1414,21356	1414,21356	1414,21356	1414,21356	1414,21179	1414,21356	1414,21356	1414,21356	1414,21356	1414,21356	1414,21356	1414,21356	1414,21356	1414,21356	1414,21356	1414,21356	1392,18028	1414,21356
6 Fruticose Foliose Type 1.3	1299,45013	1414,21356	1411,62972	1411,60523	1414,21356	0	1361,64768	1383,7408	1414,1521	1414,21356	1414,10175	1414,20288	1408,56821	1414,21353	1414,21319	1414,21356	1414,21356	1414,21356	1414,21356	1414,21356	1414,21356	1414,21356	1414,21356	1414,21356	1414,21356	1414,21356	1414,21356	1414,21356	1413,60882	1414,21356	1414,21356
7 Fruticose Foliose Type 1.4	1412,72791	1414,21356	1411,82396	1413,41669	1414,21356	1361,64768	0	1402,34597	1405,24462	1414,21356	1414,18453	1412,79663	1385,64466	1414,16302	1414,21349	1414,21341	1414,21354	1414,21356	1414,21354	1414,21356	1414,21356	1414,21356	1414,21356	1414,21356	1414,21356	1414,21356	1414,21258	1414,21356	1408,03296	1414,21356	1414,21356
8 Fruticose Foliose Type 2.1	1410,78126	1414,21356	1412,16535	1414,07551	1414,21356	1383,7408	1402,34597	0	1412,5205	1414,21356	1412,83124	1414,21188	1407,9765	1414,2044	1414,21355	1414,21356	1414,21351	1414,21356	1414,21356	1414,21356	1414,21356	1414,21356	1414,21356	1414,21356	1414,21356	1414,21356	1414,21356	1414,21356	1414,15707	1414,21356	1414,21356
9 Fruticose Foliose Type 2.2	1414,21356	1414,21327	1402,91002	1414,21356	1414,21356	1414,1521	1405,24462	1412,5205	0	1414,21356	1414,21356	1414,17351	1414,20118	1398,7634	1414,21356	1414,21355	1414,21356	1414,21356	1414,21356	1414,21356	1414,21356	1414,21356	1414,21356	1414,21356	1414,21356	1414,21356	1414,2135	1414,21356	1413,1555	1414,21356	1414,21356
10 Fruticose Foliose Type 3.1	1414,21356	1414,21356	1414,21356	1414,21356	1184,34652	1414,21356	1414,21356	1414,21356	1414,21356	0	1414,21356	1414,21356	1414,21356	1414,21356	1414,21356	1414,21356	1414,21356	1413,07456	1414,21356	1414,21356	1414,21356	1414,21356	1414,21356	1414,21356	1414,21356	1414,21356	1414,21356	1414,20827	1414,21356	1377,97473	1414,21356
11 Foliose Type 1.1	1413,99058	1414,21356	1414,21356	1318,99691	1414,21356	1414,10175	1414,18453	1412,83124	1414,21356	1414,21356	0	1413,90069	1401,51717	1414,21356	1194,3672	1414,21356	1380,75019	1414,21356	1376,75467	1414,13906	1414,21264	1414,21323	1414,15663	1410,80135	1414,21356	1414,11099	1414,21356	1414,21356
12 Foliose Type 1.2	1414,21234	1414,21356	1414,21356	1413,46069	1414,21356	1414,20288	1412,79663	1414,21188	1414,17351	1414,21356	1413,90069	0	1398,41793	1414,21356	1414,18597	1414,21314	1414,21055	1414,21356	1414,21356	1414,20127	1414,21356	1414,21356	1414,21176	1325,881	1414,21356	1405,15548	1414,21356	1414,21356
13 Foliose Type 1.3	1413,60999	1414,21356	1414,20364	1386,01525	1414,21356	1408,56821	1385,64466	1407,9785	1414,20118	1414,21356	1401,51717	1398,41793	0	1414,21356	1413,47284	1414,21356	1410,95358	1414,21356	1411,04683	1414,21291	1414,21356	1414,21356	1414,21326	1413,35383	1414,21356	1413,5669	1414,21356	1414,21356
14 Foliose Type 2.1	1414,21356	1411,99957	1413,91155	1414,21356	1414,21356	1414,21353	1414,16302	1414,2044	1398,7634	1414,21356	1414,21356	1414,21356	1414,21356	0	1414,21356	1414,20976	1414,21356	1414,21356	1414,21356	1414,21356	1414,21356	1414,21356	1414,21356	1414,21356	1414,21356	1414,21356	1414,21356	1414,07649	1414,21356	1414,21356
15 Foliose Crustose Type 1.1	1414,21356	1414,21356	1414,21356	1409,45191	1414,21356	1414,21319	1414,21349	1414,21355	1414,21356	1414,21356	1194,3672	1414,18597	1413,47284	1414,21356	0	1414,21356	1402,92215	1414,21356	1386,54098	1414,03758	1414,21335	1406,36738	1414,21356	1414,21355	1414,21117	1413,41314	1414,21356	1414,19074	1414,21356	1414,21356
16 Foliose Crustose Type 1.2	1414,21356	1414,21199	1414,21356	1414,21356	1414,21356	1414,21356	1414,21341	1414,21356	1414,21355	1414,21356	1414,21356	1414,21314	1414,21356	1414,20976	1414,21356	0	1414,21356	1414,21356	1414,21356	1414,21356	1414,21356	1414,21356	1414,21356	1414,21356	1414,21356	1414,08641	1414,21356	1324,87171	1414,21356	1414,21356
17 Foliose Crustose Type 1.3	1414,21356	1414,21356	1414,21356	1414,16342	1414,21356	1414,21356	1414,21354	1414,21351	1414,21356	1414,21356	1380,75019	1414,21055	1410,95358	1414,21356	1402,92215	1414,21356	0	1414,21356	1251,8998	1413,27806	1414,21196	1412,72158	1414,21356	1414,21324	1414,21356	1414,21356	1414,21354	1414,21356	1414,21356
18 Foliose Crustose Type 2.1	1414,21356	1414,21356	1414,21356	1414,21356	1414,21179	1414,21356	1414,21356	1414,21356	1414,21356	1413,07456	1414,21356	1414,21356	1414,21356	1414,21356	1414,21356	1414,21356	1414,21356	0	1414,21356	1414,21356	1414,21356	1414,21356	1414,21356	1414,21356	1414,21356	1414,21356	1402,53221	1414,18824	1405,46517	1414,21356
19 Crustose Type 1.1	1414,21356	1414,21356	1414,21356	1414,15624	1414,21356	1414,21356	1414,21354	1414,21356	1414,21356	1414,21356	1376,75467	1414,20127	1411,04683	1414,21356	1386,54098	1414,21356	1251,8998	1414,21356	0	1392,69508	1413,8159	1302,4383	1414,21355	1414,19757	1413,94402	1413,67517	1414,21356	1414,21225	1414,21356	1414,21356
20 Crustose Type 1.2	1414,21356	1414,21356	1414,21356	1414,21356	1414,21356	1414,21356	1414,21356	1414,21356	1414,21356	1414,21356	1414,13906	1414,21356	1414,21291	1414,21356	1414,03758	1414,21356	1413,27806	1414,21356	1392,69508	0	1312,8283	1234,02396	1413,83531	1410,45647	1413,55836	1414,21147	1414,21356	1414,21355	1414,21356	1414,21356
21 Crustose Sparse Type 1.1	1414,21356	1414,21356	1414,21356	1414,21356	1414,21356	1414,21356	1414,21356	1414,21356	1414,21356	1414,21356	1414,21264	1414,21356	1414,21356	1414,21356	1414,21335	1414,21356	1414,21196	1414,21356	1413,8159	1312,8283	0	1412,18269	1410,91381	1402,69175	1367,08598	1414,21321	1414,21356	1414,21356	1414,21356	1414,21356
22 Crustose Sparse Type 1.2	1414,21356	1414,21356	1414,21356	1414,21337	1414,21356	1414,21356	1414,21356	1414,21356	1414,21356	1414,21356	1412,68037	1414,21356	1414,21253	1414,21356	1406,36738	1414,21356	1412,72158	1414,21356	1302,4383	1234,02396	1412,18269	0	1414,21346	1414,14596	1414,18483	1414,15911	1414,21356	1414,21342	1414,21356	1414,21356
23 Crustose Sparse Type 1.3	1414,21356	1414,21356	1414,21356	1414,21356	1414,21356	1414,21356	1414,21356	1414,21356	1414,21356	1414,21356	1414,21356	1414,21356	1414,21356	1414,21356	1414,21356	1414,21356	1414,21356	1414,21356	1414,21355	1413,83531	1410,91381	1414,21346	0	1350,13011	1413,43197	1414,21356	1414,21356	1414,21356	1414,21356	1414,21356
24 No Lichen Type 1.1	1414,21356	1414,21356	1414,21356	1414,21356	1414,21356	1414,21356	1414,21356	1414,21356	1414,21356	1414,21356	1414,21323	1414,21356	1414,21356	1414,21356	1414,21355	1414,21356	1414,21324	1414,21356	1414,19757	1410,45647	1402,69175	1414,14596	1350,13011	0	1413,8732	1414,21355	1414,21356	1414,21356	1414,21356	1414,21356
25 No Lichen Type 1.2	1414,21356	1414,21356	1414,21356	1414,21356	1414,21356	1414,21356	1414,21356	1414,21356	1414,21356	1414,21356	1414,15663	1414,21176	1414,21326	1414,21356	1414,21117	1414,21356	1414,20294	1414,21356	1413,94402	1413,55836	1367,08598	1414,18483	1413,43197	1413,8732	0	1413,98193	1414,21356	1414,2077	1414,21356	1414,21356
26 No Lichen Type 1.3	1414,21356	1414,21356	1414,21356	1414,14698	1414,21356	1414,21356	1414,21258	1414,21356	1414,2135	1414,21356	1410,80135	1325,881	1413,35383	1414,21356	1413,41314	1414,08641	1414,10532	1414,21356	1413,67517	1414,21147	1414,21321	1414,15911	1414,21356	1414,21355	1413,98193	0	1414,21356	1383,31607	1414,21356	1414,21356
27 No Lichen Type 2.1	1414,21356	1414,21356	1414,21356	1414,21356	1414,21356	1414,21356	1414,21356	1414,21356	1414,21356	1414,20827	1414,21356	1414,21356	1414,21356	1414,21356	1414,21356	1414,21356	1414,21356	1402,53221	1414,21356	1414,21356	1414,21356	1414,21356	1414,21356	1414,21356	1414,21356	1414,21356	0	1414,17634	1414,21307	1414,21356
28 No Lichen Type 2.2	1413,99431	1414,21255	1414,20309	1414,10825	1414,21356	1413,60882	1408,03296	1414,15707	1413,1555	1414,21356	1414,11099	1405,15548	1413,5669	1414,07649	1414,19074	1324,87171	1414,21354	1414,18824	1414,21225	1414,21355	1414,21356	1414,21342	1414,21356	1414,21356	1414,2077	1383,31607	1414,17634	0	1414,21354	1414,21356
29 No Lichen Type 3.1	1414,21356	1414,21356	1414,21356	1414,21356	1392,18028	1414,21356	1414,21356	1414,21356	1414,21356	1377,97473	1414,21356	1414,21356	1414,21356	1414,21356	1414,21356	1414,21356	1414,21356	1405,46517	1414,21356	1414,21356	1414,21356	1414,21356	1414,21356	1414,21356	1414,21356	1414,21356	1414,21356	1414,21307	1414,21354	0	1414,21356
30 No Lichen Type 3.2	1414,21356	1414,21356	1414,21356	1414,21356	1414,21356	1414,21356	1414,21356	1414,21356	1414,21356	1414,21356	1414,21356	1414,21356	1414,21356	1414,21356	1414,21356	1414,21356	1414,21356	1414,21356	1414,21356	1414,21356	1414,21356	1414,21356	1414,21356	1414,21356	1414,21356	1414,21356	1414,21356	1414,21356	1414,21356	1414,21356	0

Figure A5: Full listing of the Jeffries-Matusita (JM) separability measures obtained for the unitemporal classification of WRS-2 scene 180 / 75 for the year of 2003.

180 / 75	2003	2003 TS	2000 TS	1999 TS	1991 TS	
Fruticose Lichen Zone	323	298	278	214	204	ha
Fruticose / Foliose Lichen Zone	352	217	196	158	152	ha
Foliose Lichen Zone	111	77	60	42	41	ha
Foliose / Crustose Lichen Zone	136	110	101	83	81	ha
Crustose Lichen Zone	188	188	180	162	114	ha
Crustose Sparse Lichen Zone	116	113	96	67	53	ha
No Lichen	993	621	601	432	242	ha

179 / 76	2003	2003 TS	2000 TS	1999 TS	1992 TS	
Foliose / Crustose Lichen Zone	55	55	44		40	ha
Crustose Lichen Zone	114	53	50		45	ha
Crustose Sparse Lichen Zone	53	26	26		19	ha
No Lichen	563	537	408		336	ha

Unified	2003	2003 TS	2000 TS	1999 TS	91/92 TS	
Fruticose Lichen Zone	323	298	278	214	204	ha
Fruticose / Foliose Lichen Zone	352	217	196	158	152	ha
Foliose Lichen Zone	111	77	60	42	41	ha
Foliose / Crustose Lichen Zone	191	165	145	83	121	ha
Crustose Lichen Zone	302	242	231	162	159	ha
Crustose Sparse Lichen Zone	169	139	122	67	72	ha
No Lichen	1556	1158	1009	432	578	ha
Sum	3005	2296	2041	1156	1328	ha

Figure A6: The decrease of the total as well as class-based reference area for the differing time-series images (TS) of the satellite scenes of 180 / 75 and 179 / 76 in contrast to those available for the unitemporal classification is displayed, based on the training samples evaluated for the timeframes of 1991 and 1992 respectively.

	1 Foliose Crustose Type 3.1	2 Foliose Crustose Type 3.2	3 Crustose Type 2.1	4 Crustose Type 2.2	5 Crustose Sparse Type 2.2	6 No Lichen Type 1.4	7 No Lichen Type 1.5	8 No Lichen Type 1.6	9 No Lichen Type 1.9	10 No Lichen Type 1.10	11 No Lichen Type 3.4	12 No Lichen Type 3.5	13 No Lichen Type 3.6	14 No Lichen Type 3.7	15 No Lichen Type 3.8
1 Foliose Crustose Type 3.1	0	1133,88407	1315,59751	1411,17743	1413,64891	1414,21356	1414,21356	1414,21356	1414,21356	1414,21356	1412,10403	1414,21355	1414,21356	1414,21356	1413,62524
2 Foliose Crustose Type 3.2	1133,88407	0	1216,52476	1374,25328	1395,72783	1414,20339	1414,21356	1414,21356	1414,21356	1414,21356	1411,65037	1414,17464	1414,20856	1414,206	1413,53516
3 Crustose Type 2.1	1315,59751	1216,52476	0	1413,2732	1338,61063	1414,20675	1414,21356	1414,21355	1414,21356	1414,21356	1405,54423	1414,08026	1414,21292	1414,21346	1412,96535
4 Crustose Type 2.2	1411,17743	1374,25328	1413,2732	0	1413,10378	1414,0278	1414,21356	1414,21356	1414,21356	1414,21356	1414,20352	1414,13259	1412,71526	1414,09219	1414,20815
5 Crustose Sparse Type 2.2	1413,64891	1395,72783	1338,61063	1413,10378	0	1413,87092	1414,21356	1414,20878	1414,21356	1414,21356	1413,30724	1410,86531	1414,1746	1414,21337	1414,21225
6 No Lichen Type 1.4	1414,21356	1414,20339	1414,20675	1414,0278	1413,87092	0	1414,18736	1413,83154	1414,18736	1414,21356	1414,21353	854,991019	1272,86853	1414,21356	1414,21356
7 No Lichen Type 1.5	1414,21356	1414,21356	1414,21356	1414,21356	1414,21356	1414,18736	0	1413,296	0	1394,49489	1414,21356	1414,1985	1414,03962	1414,21356	1414,21356
8 No Lichen Type 1.6	1414,21356	1414,21356	1414,21355	1414,21356	1414,20878	1413,83154	1413,296	0	1413,296	1411,27041	1414,21356	1412,86262	1414,0897	1414,21356	1414,21356
9 No Lichen Type 1.9	1414,21356	1414,21356	1414,21356	1414,21356	1414,21356	1414,18736	0	1413,296	0	1394,49489	1414,21356	1414,1985	1414,03962	1414,21356	1414,21356
10 No Lichen Type 1.10	1414,21356	1414,21356	1414,21356	1414,21356	1414,21356	1414,21356	1394,49489	1411,27041	1394,49489	0	1414,21356	1414,21356	1414,21356	1414,21356	1414,21356
11 No Lichen Type 3.4	1412,10403	1411,65037	1405,54423	1414,20352	1413,30724	1414,21353	1414,21356	1414,21356	1414,21356	1414,21356	0	1414,21347	1414,21355	1413,85896	1058,07496
12 No Lichen Type 3.5	1414,21355	1414,17464	1414,08026	1414,13259	1410,86531	854,991019	1414,1985	1412,86262	1414,1985	1414,21356	1414,21347	0	1335,74641	1414,21356	1414,21356
13 No Lichen Type 3.6	1414,21356	1414,20856	1414,21292	1412,71526	1414,1746	1272,86853	1414,03962	1414,0897	1414,03962	1414,21356	1414,21355	1335,74641	0	1414,21331	1414,21356
14 No Lichen Type 3.7	1414,21356	1414,206	1414,21346	1414,09219	1414,21337	1414,21356	1414,21356	1414,21356	1414,21356	1414,21356	1413,85896	1414,21356	1414,21331	0	1413,801
15 No Lichen Type 3.8	1413,62524	1413,53516	1412,96535	1414,20815	1414,21225	1414,21356	1414,21356	1414,21356	1414,21356	1414,21356	1058,07496	1414,21356	1414,21356	1413,801	0

Figure A7: Full listing of the Jeffries-Matusita (JM) separability measures obtained for the multitemporal classification of WRS-2 scene 179 / 76 for the year of 1992.

	1 Foliose Crustose Type 3.1	2 Foliose Crustose Type 3.2	3 Crustose Type 2.1	4 Crustose Type 2.2	5 Crustose Sparse Type 2.2	6 No Lichen Type 1.4	7 No Lichen Type 1.5	8 No Lichen Type 1.6	9 No Lichen Type 1.9	10 No Lichen Type 1.10	11 No Lichen Type 3.4	12 No Lichen Type 3.5	13 No Lichen Type 3.6	14 No Lichen Type 3.7	15 No Lichen Type 3.8
1 Foliose Crustose Type 3.1	0	1047,03914	998,41294	1414,19623	1408,64514	1414,20033	1414,21356	1414,21356	1414,21356	1414,21356	1414,21344	1414,03945	1414,21355	1414,21356	1414,21355
2 Foliose Crustose Type 3.2	1047,03914	0	1044,25975	1413,14381	1411,92869	1414,21105	1414,21356	1414,21356	1414,21356	1414,21356	1414,20047	1414,17369	1414,21356	1414,21332	1414,21278
3 Crustose Type 2.1	998,41294	1044,25975	0	1414,12328	1394,53863	1414,06066	1414,21356	1414,21356	1414,21356	1414,21356	1414,1602	1412,20578	1414,21337	1414,21055	1414,20524
4 Crustose Type 2.2	1414,19623	1413,14381	1414,12328	0	1414,21274	1414,20565	1414,21356	1414,21356	1414,21356	1414,21356	1414,21356	1414,19561	1414,1712	1414,21151	1414,21356
5 Crustose Sparse Type 2.2	1408,64514	1411,92869	1394,53863	1414,21274	0	1411,38827	1414,21349	1414,21327	1414,21349	1414,21356	1414,21356	1383,00228	1414,18506	1414,21356	1414,21356
6 No Lichen Type 1.4	1414,20033	1414,21105	1414,06066	1414,20565	1411,38827	0	1414,21355	1414,21356	1414,21355	1414,21356	1414,21356	1184,15415	1390,73076	1414,21354	1414,21356
7 No Lichen Type 1.5	1414,21356	1414,21356	1414,21356	1414,21356	1414,21349	1414,21355	0	1404,81518	0	1411,43346	1414,21356	1414,20831	1414,16731	1414,21356	1414,21356
8 No Lichen Type 1.6	1414,21356	1414,21356	1414,21356	1414,21356	1414,21327	1414,21356	1404,81518	0	1404,81518	1413,79018	1414,21356	1414,17678	1414,20406	1414,21356	1414,21356
9 No Lichen Type 1.9	1414,21356	1414,21356	1414,21356	1414,21356	1414,21349	1414,21355	0	1404,81518	0	1411,43346	1414,21356	1414,20831	1414,16731	1414,21356	1414,21356
10 No Lichen Type 1.10	1414,21356	1414,21356	1414,21356	1414,21356	1414,21356	1414,21356	1411,43346	1413,79018	1411,43346	0	1414,21356	1414,21356	1414,21356	1414,21356	1414,21356
11 No Lichen Type 3.4	1414,21344	1414,20047	1414,1602	1414,21356	1414,21356	1414,21356	1414,21356	1414,21356	1414,21356	1414,21356	0	1414,21356	1414,21337	1412,85191	1126,49001
12 No Lichen Type 3.5	1414,03945	1414,17369	1412,20578	1414,19561	1383,00228	1184,15415	1414,20831	1414,17678	1414,20831	1414,21356	1414,21356	0	1355,26082	1414,21344	1414,21356
13 No Lichen Type 3.6	1414,21355	1414,21356	1414,21337	1414,1712	1414,18506	1390,73076	1414,16731	1414,20406	1414,16731	1414,21356	1414,21337	1355,26082	0	1414,20335	1414,21356
14 No Lichen Type 3.7	1414,21356	1414,21332	1414,21055	1414,21151	1414,21356	1414,21354	1414,21356	1414,21356	1414,21356	1414,21356	1412,85191	1414,21344	1414,20335	0	1409,68388
15 No Lichen Type 3.8	1414,21355	1414,21278	1414,20524	1414,21356	1414,21356	1414,21356	1414,21356	1414,21356	1414,21356	1414,21356	1126,49001	1414,21356	1414,21356	1409,68388	0

Figure A8: Full listing of the Jeffries-Matusita (JM) separability measures obtained for the multitemporal classification of WRS-2 scene 179 / 76 for the year of 2000

	1 Foliose Crustose Type 3.1	2 Foliose Crustose Type 3.2	3 Crustose Type 2.1	4 Crustose Type 2.2	5 Crustose Sparse Type 2.2	6 No Lichen Type 1.4	7 No Lichen Type 1.5	8 No Lichen Type 1.6	9 No Lichen Type 1.9	10 No Lichen Type 1.10	11 No Lichen Type 3.4	12 No Lichen Type 3.5	13 No Lichen Type 3.6	14 No Lichen Type 3.7	15 No Lichen Type 3.8
1 Foliose Crustose Type 3.1	0	1372,75475	1384,9915	1414,21356	1414,21356	1414,21356	1414,21332	1414,21356	1414,21332	1414,21356	1413,98304	1414,21356	1414,21356	1414,21345	1414,21325
2 Foliose Crustose Type 3.2	1372,75475	0	1410,16472	1414,21332	1414,21356	1414,21356	1414,2132	1414,21356	1414,2132	1414,21356	1413,17906	1414,21356	1414,21356	1414,21293	1414,19636
3 Crustose Type 2.1	1384,9915	1410,16472	0	1414,13702	1412,29454	1414,21332	1414,10324	1414,21356	1414,10324	1414,21356	1413,83716	1414,20905	1414,21356	1414,21355	1414,21341
4 Crustose Type 2.2	1414,21356	1414,21332	1414,13702	0	1414,19551	1414,07155	1414,06428	1414,21356	1414,06428	1414,21356	1414,21348	1414,17935	1414,21114	1414,21064	1414,21356
5 Crustose Sparse Type 2.2	1414,21356	1414,21356	1412,29454	1414,19551	0	1408,94184	1388,29615	1414,20432	1388,29615	1414,21356	1414,21354	1315,28087	1414,20045	1414,21353	1414,21356
6 No Lichen Type 1.4	1414,21356	1414,21356	1414,21332	1414,07155	1408,94184	0	1409,22858	1414,21193	1409,22858	1414,21356	1414,21356	1183,29366	1409,94756	1414,21354	1414,21356
7 No Lichen Type 1.5	1414,21332	1414,2132	1414,10324	1414,06428	1388,29615	1409,22858	0	1375,80596	0	1414,21169	1413,71262	1354,59251	1407,39386	1414,11319	1414,21071
8 No Lichen Type 1.6	1414,21356	1414,21356	1414,21356	1414,21356	1414,20432	1414,21193	1375,80596	0	1375,80596	1414,21356	1414,21356	1414,20703	1413,83832	1414,21356	1414,21356
9 No Lichen Type 1.9	1414,21332	1414,2132	1414,10324	1414,06428	1388,29615	1409,22858	0	1375,80596	0	1414,21169	1413,71262	1354,59251	1407,39386	1414,11319	1414,21071
10 No Lichen Type 1.10	1414,21356	1414,21356	1414,21356	1414,21356	1414,21356	1414,21356	1414,21169	1414,21356	1414,21169	0	1414,21356	1414,21356	1414,21356	1414,21356	1414,21356
11 No Lichen Type 3.4	1413,98304	1413,17906	1413,83716	1414,21348	1414,21354	1414,21356	1413,71262	1414,21356	1413,71262	1414,21356	0	1414,21356	1414,21356	1413,57564	1238,48641
12 No Lichen Type 3.5	1414,21356	1414,21356	1414,20905	1414,17935	1315,28087	1183,29366	1354,59251	1414,20703	1354,59251	1414,21356	1414,21356	0	1412,62597	1414,21339	1414,21356
13 No Lichen Type 3.6	1414,21356	1414,21356	1414,21356	1414,21114	1414,20045	1409,94756	1407,39386	1413,83832	1407,39386	1414,21356	1414,21356	1412,62597	0	1414,21226	1414,21356
14 No Lichen Type 3.7	1414,21345	1414,21293	1414,21355	1414,21064	1414,21353	1414,21354	1414,11319	1414,21356	1414,11319	1414,21356	1413,57564	1414,21339	1414,21226	0	1413,86325
15 No Lichen Type 3.8	1414,21325	1414,19636	1414,21341	1414,21356	1414,21356	1414,21356	1414,21071	1414,21356	1414,21071	1414,21356	1238,48641	1414,21356	1414,21356	1413,86325	0

Figure A9: Full listing of the Jeffries-Matusita (JM) separability measures obtained for the multitemporal classification of WRS-2 scene 179 / 76 for the year of 2003.

	1 Fruticose Type 1.2	2 Fruticose Type 2.1	3 Fruticose Foliose Type 1.1	4 Fruticose Foliose Type 1.2	5 Fruticose Foliose Type 1.3	6 Fruticose Foliose Type 2.1	7 Fruticose Foliose Type 2.2	8 Fruticose Foliose Type 3.1	9 Foliose Type 1.1	10 Foliose Type 1.2	11 Foliose Type 1.3	12 Foliose Type 2.1	13 Foliose Crustose Type 1.1	14 Foliose Crustose Type 2.1	15 Crustose Type 1.1	16 Crustose Type 1.2	17 Crustose Sparse Type 1.1	18 Crustose Sparse Type 1.2	19 Crustose Sparse Type 1.3	20 No Lichen Type 1.1	21 No Lichen Type 1.2	22 No Lichen Type 2.1	23 No Lichen Type 2.2	24 No Lichen Type 3.1
1 Fruticose Type 1.2	0	1414,21356	1414,21356	1414,21356	1414,21356	1414,21356	1414,21356	1412,66282	1414,21356	1414,21356	1414,21356	1414,21356	1414,21356	1414,19981	1414,21356	1414,21356	1414,21356	1414,21356	1414,21356	1414,21356	1414,21356	1414,21356	1414,21287	1414,21356
2 Fruticose Type 2.1	1414,21356	0	1413,09949	1371,80654	1335,23285	1386,41632	1356,28907	1414,21356	1413,56848	1414,20383	1397,0318	1407,38326	1413,03642	1414,21356	1414,21335	1414,20833	1414,21356	1414,2095	1414,21356	1414,21356	1414,21356	1414,21205	1414,21356	1356,28907
3 Fruticose Foliose Type 1.1	1414,21356	1413,09949	0	1414,20315	1374,66488	1319,35289	1406,88889	1414,21356	1147,8711	1412,53851	1300,13097	1414,20159	1386,05334	1414,21356	1390,89589	1373,69215	1413,71049	1322,28569	1414,21356	1414,21356	1414,21356	1414,21356	1414,21356	1406,88889
4 Fruticose Foliose Type 1.2	1414,21356	1371,80654	1414,20315	0	1411,00294	1414,09135	1270,76088	1414,21356	1414,1969	1412,1075	1413,49242	1149,17167	1414,03198	1414,21356	1414,21356	1414,21356	1414,21356	1414,21355	1414,21356	1414,21356	1414,21356	1413,12621	1414,16747	1270,76088
5 Fruticose Foliose Type 1.3	1414,21356	1335,23285	1374,66488	1411,00294	0	1305,97127	1385,81658	1414,21356	1398,06919	1414,20573	1260,76778	1412,4984	1412,55678	1414,21356	1414,20142	1413,1849	1414,21283	1413,81818	1414,21356	1414,21356	1414,21356	1414,21204	1414,21356	1385,81658
6 Fruticose Foliose Type 2.1	1414,21356	1386,41632	1319,35289	1414,09135	1305,97127	0	1266,97405	1414,21356	1332,99053	1402,43207	1050,78202	1413,7105	1345,5051	1414,21356	1397,68254	1409,40934	1413,8004	1408,93504	1414,21356	1414,21356	1414,21352	1414,21352	1414,21356	1266,97405
7 Fruticose Foliose Type 2.2	1414,21356	1356,28907	1406,88889	1270,76088	1385,81658	1266,97405	0	1414,21356	1388,10346	1398,13399	1287,69703	1329,32335	1391,35015	1414,21356	1412,53368	1413,93254	1414,19156	1413,6329	1414,21356	1414,21356	1414,21356	1414,17617	1414,21265	1337,87587
8 Fruticose Foliose Type 3.1	1412,66282	1414,21356	1414,21356	1414,21356	1414,21356	1414,21356	1414,21356	0	1414,21356	1414,21356	1414,21356	1414,21356	1414,21356	1414,21356	1414,21356	1414,21356	1414,21356	1414,21356	1414,21356	1414,21356	1414,21356	1414,21356	1414,21356	1414,21356
9 Foliose Type 1.1	1414,21356	1413,56848	1147,8711	1414,1969	1398,06919	1332,99053	1388,10346	1414,21356	0	1375,86572	1265,07453	1414,12543	1285,02279	1414,21356	1221,42568	1353,03281	1400,72186	1248,72089	1414,21356	1414,21356	1414,18718	1414,21355	1414,21325	1388,10346
10 Foliose Type 1.2	1414,21356	1414,20383	1412,53851	1412,1075	1414,20573	1402,43207	1398,13399	1414,21356	1375,86572	0	1369,416	1394,55847	1403,48424	1414,21356	1352,15112	1408,59845	1410,81079	1406,7124	1414,21345	1414,21356	1414,20811	1414,1973	1413,60453	1398,13399
11 Foliose Type 1.3	1414,21356	1397,0318	1300,13097	1413,49242	1260,76778	1050,78202	1287,69703	1414,21356	1265,07453	1369,416	0	1410,18182	1349,44616	1414,21356	1388,44566	1402,20978	1413,77255	1406,23938	1414,21356	1414,21356	1414,21355	1414,21312	1414,21299	1287,69703
12 Foliose Type 2.1	1414,21356	1407,38326	1414,20159	1149,17167	1412,4984	1413,7105	1329,32335	1414,21356	1414,12543	1394,55847	1410,18182	0	1413,87099	1414,21356	1414,19984	1414,21339	1414,21356	1414,21294	1414,21356	1414,21356	1414,21356	1405,17669	1412,00612	1329,32335
13 Foliose Crustose Type 1.3	1414,21356	1413,03642	1386,05334	1414,03198	1412,55678	1345,5051	1391,35015	1414,21356	1285,02279	1403,48424	1349,44616	1413,87099	0	1414,21356	1322,44192	1392,29638	1408,93862	1365,83479	1414,21356	1414,21356	1414,21356	1414,21352	1414,21336	1391,35015
14 Foliose Crustose Type 2.1	1414,19981	1414,21356	1414,21356	1414,21356	1414,21356	1414,21356	1414,21356	1414,21356	1414,21356	1414,21356	1414,21356	1414,21356	1414,21356	0	1414,21356	1414,21356	1414,21356	1414,21356	1414,21356	1414,21356	1414,21356	1414,15423	1413,54843	1414,21356
15 Crustose Type 1.1	1414,21356	1414,21335	1390,89589	1414,21356	1414,20142	1397,68254	1412,53368	1414,21356	1221,42568	1352,15112	1388,44566	1414,19984	1322,44192	1414,21356	0	1297,90095	1400,52624	1226,27738	1414,21356	1414,21356	1414,21356	1414,21356	1414,21299	1412,53368
16 Crustose Type 1.2	1414,21356	1414,20833	1373,69215	1414,21356	1413,1849	1409,40934	1413,93254	1414,21356	1353,03281	1408,59845	1402,20978	1414,21339	1392,29638	1414,21356	1297,90095	0	1404,69566	1296,78266	1414,21356	1414,21356	1414,21274	1414,21356	1414,21356	1413,93254
17 Crustose Sparse Type 1.1	1414,21356	1414,21356	1413,71049	1414,21356	1414,21283	1413,8004	1414,19156	1414,21356	1400,72186	1410,81079	1413,77255	1414,21356	1408,93862	1414,21356	1400,52624	1404,69566	0	1339,67159	1414,21044	1414,21355	1330,39425	1414,21356	1414,21332	1414,19156
18 Crustose Sparse Type 1.2	1414,21356	1414,2095	1322,28569	1414,21355	1413,81818	1408,93504	1413,6329	1414,21356	1248,72089	1406,7124	1406,23938	1414,21294	1365,83479	1414,21356	1226,27738	1296,78266	1339,67159	0	1414,21356	1414,21356	1414,19678	1414,21356	1414,2135	1413,6329
19 Crustose Sparse Type 1.3	1414,21356	1414,21356	1414,21356	1414,21356	1414,21356	1414,21356	1414,21356	1414,21356	1414,21356	1414,21345	1414,21356	1414,21356	1414,21356	1414,21356	1414,21356	1414,21356	1414,21044	1414,21356	0	1414,21356	1414,15909	1414,21356	1414,21356	1414,21356
20 No Lichen Type 1.1	1414,21356	1414,21356	1414,21356	1414,21356	1414,21356	1414,21356	1414,21356	1414,21356	1414,21356	1414,21356	1414,21356	1414,21356	1414,21356	1414,21356	1414,21356	1414,21356	1414,21356	1414,21355	1414,21356	1414,21356	0	1414,21356	1414,21356	1414,21356
21 No Lichen Type 1.2	1414,21356	1414,21356	1414,21356	1414,21356	1414,21356	1414,21352	1414,21356	1414,21356	1414,18718	1414,20811	1414,21355	1414,21356	1414,21356	1414,21356	1414,21356	1414,21274	1330,39425	1414,19678	1414,15909	1414,21356	0	1414,21356	1414,21356	1414,21356
22 No Lichen Type 2.1	1414,21356	1414,21205	1414,21356	1413,12621	1414,21204	1414,21352	1414,17617	1414,21356	1414,21355	1414,1973	1414,21312	1405,17669	1414,21352	1414,15423	1414,21356	1414,21356	1414,21356	1414,21356	1414,21356	1414,21356	1414,21356	0	1347,77098	1414,17617
23 No Lichen Type 2.2	1414,21287	1414,21356	1414,21356	1414,16747	1414,21356	1414,21356	1414,21265	1414,21356	1414,21325	1413,60453	1414,21299	1412,00612	1414,21336	1413,54843	1414,21299	1414,21356	1414,21332	1414,2135	1414,21356	1414,21356	1414,21356	1347,77098	0	1414,21265
24 No Lichen Type 3.1	1414,21356	1356,28907	1406,88889	1270,76088	1385,81658	1266,97405	1337,87587	1414,21356	1388,10346	1398,13399	1287,69703	1329,32335	1391,35015	1414,21356	1412,53368	1413,93254	1414,19156	1413,6329	1414,21356	1414,21356	1414,21356	1414,17617	1414,21265	0

Figure A10: Full listing of the Jeffries-Matusita (JM) separability measures obtained for the multitemporal classification of WRS-2 scene 180 / 75 for the year of 1991.

	1 Fruticose Type 1.2	2 Fruticose Type 2.1	3 Fruticose Foliose Type 1.1	4 Fruticose Foliose Type 1.2	5 Fruticose Foliose Type 1.3	6 Fruticose Foliose Type 2.1	7 Fruticose Foliose Type 2.2	8 Fruticose Foliose Type 3.1	9 Foliose Type 1.1	10 Foliose Type 1.2	11 Foliose Type 1.3	12 Foliose Type 2.1	13 Foliose Crustose Type 1.1	14 Foliose Crustose Type 2.1	15 Crustose Type 1.1	16 Crustose Type 1.2	17 Crustose Sparse Type 1.1	18 Crustose Sparse Type 1.2	19 Crustose Sparse Type 1.3	20 No Lichen Type 1.1	21 No Lichen Type 1.2	22 No Lichen Type 2.1	23 No Lichen Type 2.2	24 No Lichen Type 3.1
1 Fruticose Type 1.2	0	1414,21356	1414,21356	1414,21356	1414,21356	1414,21356	1414,21356	1406,40972	1414,21356	1414,21356	1414,21356	1414,21356	1414,21356	1414,21326	1414,21356	1414,21356	1414,21356	1414,21356	1414,21356	1414,21356	1414,21356	1414,20776	1414,21356	1414,16718
2 Fruticose Type 2.1	1414,21356	0	1413,59379	1403,27923	1403,42316	1382,35158	1225,53267	1414,21356	1413,01231	1414,20482	1401,66479	1411,17894	1414,21356	1414,21356	1414,21356	1414,21356	1414,21356	1414,21356	1414,21356	1414,21356	1414,21356	1414,21355	1414,21356	1414,21356
3 Fruticose Foliose Type 1.1	1414,21356	1413,59379	0	1413,96157	1231,92911	1300,64041	1401,08918	1414,21356	1188,15259	1406,94877	1361,42023	1413,66404	1368,94014	1414,21356	1413,18339	1412,50419	1414,21299	1403,24888	1414,21356	1414,21356	1414,21356	1414,21354	1414,21356	1414,21356
4 Fruticose Foliose Type 1.2	1414,21356	1403,27923	1413,96157	0	1413,53488	1414,10827	1243,7545	1414,21356	1413,41755	1414,01389	1413,73539	1333,92885	1414,21356	1414,21356	1414,21356	1414,21356	1414,21356	1414,21356	1414,21356	1414,21356	1414,21356	1414,20439	1414,21356	1414,21356
5 Fruticose Foliose Type 1.3	1414,21356	1403,42316	1231,92911	1413,53488	0	1042,34656	1381,11907	1414,21356	1367,37993	1410,5144	1125,17515	1413,46229	1411,65263	1414,21356	1414,2007	1414,18685	1414,21356	1414,01028	1414,21356	1414,21356	1414,21356	1414,21353	1414,21356	1414,21356
6 Fruticose Foliose Type 2.1	1414,21356	1382,35158	1300,64041	1414,10827	1042,34656	0	1327,87259	1414,21356	1314,4262	1408,9509	1209,46856	1413,71187	1413,74253	1414,21356	1414,20641	1414,21283	1414,21356	1414,20735	1414,21356	1414,21356	1414,21356	1414,21356	1414,21356	1414,21356
7 Fruticose Foliose Type 2.2	1414,21356	1225,53267	1401,08918	1243,7545	1381,11907	1327,87259	0	1414,21356	1387,00324	1412,80896	1382,72512	1351,82298	1414,21114	1414,21356	1414,21356	1414,21356	1414,21356	1414,21351	1414,21356	1414,21356	1414,21356	1414,20855	1414,21356	1414,21356
8 Fruticose Foliose Type 3.1	1406,40972	1414,21356	1414,21356	1414,21356	1414,21356	1414,21356	1414,21356	0	1414,21356	1414,21356	1414,21356	1414,21356	1414,21356	1414,21355	1414,21356	1414,21356	1414,21356	1414,21356	1414,21356	1414,21356	1414,21356	1414,21356	1414,21356	1414,21304
9 Foliose Type 1.1	1414,21356	1413,01231	1188,15259	1413,41755	1367,37993	1314,4262	1387,00324	1414,21356	0	1287,4446	1285,8858	1411,84663	1339,87234	1414,21356	1370,76448	1412,62566	1413,09067	1408,22908	1414,21356	1414,21356	1414,21255	1414,21344	1414,21348	1414,21356
10 Foliose Type 1.2	1414,21356	1414,20482	1406,94877	1414,01389	1410,5144	1408,9509	1412,80896	1414,21356	1287,4446	0	1346,72036	1382,22411	1396,96746	1414,21356	1392,79323	1413,8727	1413,97449	1411,47857	1414,21356	1414,21356	1414,21351	1414,211	1414,04126	1414,21356
11 Foliose Type 1.3	1414,21356	1401,66479	1361,42023	1413,73539	1125,17515	1209,46856	1382,72512	1414,21356	1285,8858	1346,72036	0	1412,34402	1407,86893	1414,21356	1410,67672	1414,21183	1414,21315	1414,0193	1414,21356	1414,21356	1414,21356	1414,21356	1414,21356	1414,21356
12 Foliose Type 2.1	1414,21356	1411,17894	1413,66404	1333,92885	1413,46229	1413,71187	1351,82298	1414,21356	1411,84663	1382,22411	1412,34402	0	1414,21355	1414,21356	1414,21351	1414,21356	1414,21356	1414,21356	1414,21356	1414,21356	1414,21356	1410,41072	1414,17758	1414,21356
13 Foliose Crustose Type 1.3	1414,21356	1414,21356	1368,94014	1414,21356	1411,65263	1413,74253	1414,21114	1414,21356	1339,87234	1396,96746	1407,86893	1414,21355	0	1414,21356	1244,50422	1406,41507	1413,71956	1400,26489	1414,21356	1414,21356	1414,21328	1414,21356	1414,21356	1414,21356
14 Foliose Crustose Type 2.1	1414,21326	1414,21356	1414,21356	1414,21356	1414,21356	1414,21356	1414,21356	1414,21355	1414,21356	1414,21356	1414,21356	1414,21356	1414,21356	0	1414,21356	1414,21356	1414,21356	1414,21356	1414,21356	1414,21356	1414,21356	1402,99144	1414,20498	1374,99021
15 Crustose Type 1.1	1414,21356	1414,21356	1413,18339	1414,21356	1414,2007	1414,20641	1414,21356	1414,21356	1370,76448	1392,79323	1410,67672	1414,21351	1244,50422	1414,21356	0	1323,766	1402,76297	1301,50824	1414,21356	1414,21356	1414,21311	1414,21356	1414,21356	1414,21356
16 Crustose Type 1.2	1414,21356	1414,21356	1412,50419	1414,21356	1414,18685	1414,21283	1414,21356	1414,21356	1412,62566	1413,8727	1414,21183	1414,21356	1406,41507	1414,21356	1323,766	0	1378,38446	1232,8084	1414,05412	1414,21356	1406,05813	1414,21356	1414,21356	1414,21356
17 Crustose Sparse Type 1.1	1414,21356	1414,21356	1414,21299	1414,21356	1414,21356	1414,21356	1414,21356	1414,21356	1413,09067	1413,97449	1414,21315	1414,21356	1413,71956	1414,21356	1402,76297	1378,38446	0	1408,63404	1414,12463	1414,21356	1396,78405	1414,21356	1414,21354	1414,21356
18 Crustose Sparse Type 1.2	1414,21356	1414,21356	1403,24888	1414,21356	1414,01028	1414,20735	1414,21351	1414,21356	1408,22908	1411,47857	1414,0193	1414,21356	1400,26489	1414,21356	1301,50824	1232,8084	1408,63404	0	1414,21328	1414,21356	1414,20793	1414,21356	1414,21356	1414,21356
19 Crustose Sparse Type 1.3	1414,21356	1414,21356	1414,21356	1414,21356	1414,21356	1414,21356	1414,21356	1414,21356	1414,21356	1414,21356	1414,21356	1414,21356	1414,21356	1414,21356	1414,21356	1414,05412	1414,12463	1414,21328	0	1414,21356	1414,18654	1414,21356	1414,21356	1414,21356
20 No Lichen Type 1.1	1414,21356	1414,21356	1414,21356	1414,21356	1414,21356	1414,21356	1414,21356	1414,21356	1414,21356	1414,21356	1414,21356	1414,21356	1414,21356	1414,21356	1414,21356	1414,21356	1414,21356	1414,21356	1414,21356	0	1414,21356	1414,21356	1414,21356	1414,21356
21 No Lichen Type 1.2	1414,21356	1414,21356	1414,21356	1414,21356	1414,21356	1414,21356	1414,21356	1414,21356	1414,21255	1414,21351	1414,21356	1414,21356	1414,21328	1414,21356	1414,21311	1406,05813	1396,78405	1414,20793	1414,18654	1414,21356	0	1414,21356	1414,21354	1414,21356
22 No Lichen Type 2.1	1414,20776	1414,21355	1414,21354	1414,20439	1414,21353	1414,21356	1414,20855	1414,21356	1414,21344	1414,211	1414,21356	1410,41072	1414,21356	1402,99144	1414,21356	1414,21356	1414,21356	1414,21356	1414,21356	1414,21356	1414,21356	0	1414,21156	1413,65706
23 No Lichen Type 2.2	1414,21356	1414,21356	1414,21356	1414,21356	1414,21356	1414,21356	1414,21356	1414,21356	1414,21348	1414,04126	1414,21356	1414,17758	1414,21356	1414,20498	1414,21356	1414,21356	1414,21354	1414,21356	1414,21356	1414,21356	1414,21354	1414,21156	0	1414,21337
24 No Lichen Type 3.1	1414,16718	1414,21356	1414,21356	1414,21356	1414,21356	1414,21356	1414,21356	1414,21304	1414,21356	1414,21356	1414,21356	1414,21356	1414,21356	1374,99021	1414,21356	1414,21356	1414,21356	1414,21356	1414,21356	1414,21356	1414,21356	1413,65706	1414,21337	0

Figure A11: Full listing of the Jeffries-Matusita (JM) separability measures obtained for the multitemporal classification of WRS-2 scene 180 / 75 for the year of 1999.

	1 Fruticose Type 1.2	2 Fruticose Type 2.1	3 Fruticose Foliose Type 1.1	4 Fruticose Foliose Type 1.2	5 Fruticose Foliose Type 1.3	6 Fruticose Foliose Type 2.1	7 Fruticose Foliose Type 2.2	8 Fruticose Foliose Type 3.1	9 Foliose Type 1.1	10 Foliose Type 1.2	11 Foliose Type 1.3	12 Foliose Type 2.1	13 Foliose Crustose Type 1.1	14 Foliose Crustose Type 2.1	15 Crustose Type 1.1	16 Crustose Type 1.2	17 Crustose Sparse Type 1.1	18 Crustose Sparse Type 1.2	19 Crustose Sparse Type 1.3	20 No Lichen Type 1.1	21 No Lichen Type 1.2	22 No Lichen Type 2.1	23 No Lichen Type 2.2	24 No Lichen Type 3.1
1 Fruticose Type 1.2	0	1414,21356	1414,21356	1414,21356	1414,21356	1414,21356	1414,21356	1388,14122	1414,21356	1414,21356	1414,21356	1414,21356	1414,21356	1412,98479	1414,21356	1414,21356	1414,21356	1414,21356	1414,21356	1414,21356	1414,21356	1414,21355	1414,21336	1399,01644
2 Fruticose Type 2.1	1414,21356	0	1413,01709	1397,53423	1094,03865	1318,18615	1348,4255	1414,21356	1413,05664	1414,20087	1408,05462	1413,01479	1414,21224	1414,21356	1414,2135	1414,21356	1414,21356	1414,21147	1414,21356	1414,21356	1414,21356	1414,21345	1414,21354	1414,21356
3 Fruticose Foliose Type 1.1	1414,21356	1413,01709	0	1412,55464	1365,5575	1126,6717	1352,42928	1414,21356	1014,65289	1315,94273	1208,51838	1402,79181	1328,01455	1414,21356	1298,75615	1413,66899	1414,18979	1370,63361	1414,21356	1414,21356	1414,21319	1414,20926	1414,18133	1414,21356
4 Fruticose Foliose Type 1.2	1414,21356	1397,53423	1412,55464	0	1369,10952	1404,62772	1285,00158	1414,21356	1414,14717	1413,55986	1411,81479	1346,97044	1414,20693	1414,21356	1414,21173	1414,21356	1414,21356	1414,21123	1414,21356	1414,21356	1414,21356	1414,06245	1414,1769	1414,21356
5 Fruticose Foliose Type 1.3	1414,21356	1094,03865	1365,5575	1369,10952	0	1103,49844	1260,61778	1414,21356	1383,86704	1410,37881	1391,29875	1400,38498	1414,08849	1414,21356	1413,84316	1414,2135	1414,21354	1413,574	1414,21356	1414,21356	1414,21356	1414,18505	1414,19403	1414,21356
6 Fruticose Foliose Type 2.1	1414,21356	1318,18615	1126,6717	1404,62772	1103,49844	0	1105,73364	1414,21356	1256,83349	1389,10698	1236,24004	1400,70113	1391,31281	1414,21356	1384,00997	1414,16736	1414,19815	1407,19175	1414,21356	1414,21356	1414,21316	1414,21349	1414,21187	1414,21356
7 Fruticose Foliose Type 2.2	1414,21356	1348,4255	1352,42928	1285,00158	1260,61778	1105,73364	0	1414,21356	1396,27619	1402,98337	1370,59724	1319,7547	1413,16771	1414,21356	1413,23073	1414,21335	1414,21351	1413,58124	1414,21356	1414,21356	1414,21356	1414,20912	1414,19535	1414,21356
8 Fruticose Foliose Type 3.1	1388,14122	1414,21356	1414,21356	1414,21356	1414,21356	1414,21356	1414,21356	0	1414,21356	1414,21356	1414,21356	1414,21356	1414,21356	1414,10013	1414,21356	1414,21356	1414,21356	1414,21356	1414,21356	1414,21356	1414,21356	1414,21345	1414,2134	1411,92307
9 Foliose Type 1.1	1414,21356	1413,05664	1014,65289	1414,14717	1383,86704	1256,83349	1396,27619	1414,21356	0	1347,35431	1314,59167	1413,8304	1353,71608	1414,21356	1295,14601	1412,88182	1413,38142	1278,8639	1414,21356	1414,21356	1414,20948	1414,21356	1414,21247	1414,21356
10 Foliose Type 1.2	1414,21356	1414,20087	1315,94273	1413,55986	1410,37881	1389,10698	1402,98337	1414,21356	1347,35431	0	1397,96629	1272,78964	1386,78674	1414,21356	1245,89589	1413,4962	1414,05259	1362,34037	1414,21356	1414,21356	1414,19942	1413,76569	1392,53217	1414,21356
11 Foliose Type 1.3	1414,21356	1408,05462	1208,51838	1411,81479	1391,29875	1236,24004	1370,59724	1414,21356	1314,59167	1397,96629	0	1412,72675	1187,66345	1414,21356	1340,30981	1412,24717	1413,53282	1390,77577	1414,21356	1414,21356	1414,20888	1414,21356	1414,21345	1414,21356
12 Foliose Type 2.1	1414,21356	1413,01479	1402,79181	1346,97044	1400,38498	1400,70113	1319,7547	1414,21356	1413,8304	1272,78964	1412,72675	0	1414,11353	1414,21356	1412,8365	1414,21356	1414,21356	1414,11624	1414,21356	1414,21356	1414,21356	1406,9619	1378,77572	1414,21356
13 Foliose Crustose Type 1.3	1414,21356	1414,21224	1328,01455	1414,20693	1414,08849	1391,31281	1413,16771	1414,21356	1353,71608	1386,78674	1187,66345	1414,11353	0	1414,21356	1093,937	1406,92719	1412,91	1332,40069	1414,21356	1414,21356	1414,2118	1414,21356	1414,2135	1414,21356
14 Foliose Crustose Type 2.1	1412,98479	1414,21356	1414,21356	1414,21356	1414,21356	1414,21356	1414,21356	1414,10013	1414,21356	1414,21356	1414,21356	1414,21356	1414,21356	0	1414,21356	1414,21356	1414,21356	1414,21356	1414,21356	1414,21356	1414,21356	1414,08958	1413,77218	1159,63424
15 Crustose Type 1.1	1414,21356	1414,2135	1298,75615	1414,21173	1413,84316	1384,00997	1413,23073	1414,21356	1295,14601	1245,89589	1340,30981	1412,8365	1093,937	1414,21356	0	1408,29818	1412,61203	1293,86968	1414,21356	1414,21356	1414,20911	1414,201	1414,21356	1414,21356
16 Crustose Type 1.2	1414,21356	1414,21356	1413,66899	1414,21356	1414,2135	1414,16736	1414,21335	1414,21356	1412,88182	1413,4962	1412,24717	1414,21356	1406,92719	1414,21356	1408,29818	0	1351,72992	1246,29165	1413,66833	1414,21347	1412,16761	1414,21356	1414,21356	1414,21356
17 Crustose Sparse Type 1.1	1414,21356	1414,21356	1414,18979	1414,21356	1414,21354	1414,19815	1414,21351	1414,21356	1413,38142	1414,05259	1413,53282	1414,21356	1412,91	1414,21356	1412,61203	1351,72992	0	1391,74181	1406,43752	1414,19923	1319,16348	1414,21356	1414,21356	1414,21356
18 Crustose Sparse Type 1.2	1414,21356	1414,21147	1370,63361	1414,21123	1413,574	1407,19175	1413,58124	1414,21356	1278,8639	1362,34037	1390,77577	1414,11624	1332,40069	1414,21356	1293,86968	1246,29165	1391,74181	0	1414,20854	1414,21356	1413,94636	1414,21356	1414,21079	1414,21356
19 Crustose Sparse Type 1.3	1414,21356	1414,21356	1414,21356	1414,21356	1414,21356	1414,21356	1414,21356	1414,21356	1414,21356	1414,21356	1414,21356	1414,21356	1414,21356	1414,21356	1414,21356	1413,66833	1406,43752	1414,20854	0	1413,97619	1340,53759	1414,21356	1414,21356	1414,21356
20 No Lichen Type 1.1	1414,21356	1414,21356	1414,21356	1414,21356	1414,21356	1414,21356	1414,21356	1414,21356	1414,21356	1414,21356	1414,21356	1414,21356	1414,21356	1414,21356	1414,21356	1414,21347	1414,19923	1414,21356	1413,97619	0	1414,20137	1414,21356	1414,21356	1414,21356
21 No Lichen Type 1.2	1414,21356	1414,21356	1414,21319	1414,21356	1414,21356	1414,21356	1414,21316	1414,21356	1414,21356	1414,20948	1414,19942	1414,20888	1414,21356	1414,2118	1414,21356	1414,20911	1412,16761	1319,16348	1413,94636	1340,53759	1414,20137	0	1414,21356	1414,21354	1414,21356
22 No Lichen Type 2.1	1414,21355	1414,21345	1414,20926	1414,06245	1414,18505	1414,21349	1414,20912	1414,21345	1414,21356	1413,76569	1414,21356	1406,9619	1414,21356	1414,08958	1414,21356	1414,21356	1414,21356	1414,21356	1414,21356	1414,21356	1414,21356	0	1250,52536	1414,2135
23 No Lichen Type 2.2	1414,21336	1414,21354	1414,18133	1414,1769	1414,19403	1414,21187	1414,19535	1414,2134	1414,21247	1392,53217	1414,21345	1378,77572	1414,2135	1413,77218	1414,201	1414,21356	1414,21356	1414,21079	1414,21356	1414,21356	1414,21354	1250,52536	0	1414,20125
24 No Lichen Type 3.1	1399,01644	1414,21356	1414,21356	1414,21356	1414,21356	1414,21356	1414,21356	1411,92307	1414,21356	1414,21356	1414,21356	1414,21356	1414,21356	1159,63424	1414,21356	1414,21356	1414,21356	1414,21356	1414,21356	1414,21356	1414,21356	1414,2135	1414,20125	0

Figure A12: Full listing of the Jeffries-Matusita (JM) separability measures obtained for the multitemporal classification of WRS-2 scene 180 / 75 for the year of 2000.

	1 Fruticose Type 1.2	2 Fruticose Type 2.1	3 Fruticose Foliose Type 1.1	4 Fruticose Foliose Type 1.2	5 Fruticose Foliose Type 1.3	6 Fruticose Foliose Type 2.1	7 Fruticose Foliose Type 2.2	8 Fruticose Foliose Type 3.1	9 Foliose Type 1.1	10 Foliose Type 1.2	11 Foliose Type 1.3	12 Foliose Type 2.1	13 Foliose Crustose Type 1.1	14 Foliose Crustose Type 2.1	15 Crustose Type 1.1	16 Crustose Type 1.2	17 Crustose Sparse Type 1.1	18 Crustose Sparse Type 1.2	19 Crustose Sparse Type 1.3	20 No Lichen Type 1.1	21 No Lichen Type 1.2	22 No Lichen Type 2.1	23 No Lichen Type 2.2	24 No Lichen Type 3.1
1 Fruticose Type 1.2	0	1414,21356	1414,21356	1414,21356	1414,21356	1414,21356	1414,21356	1239,58345	1414,21356	1414,21356	1414,21356	1414,21356	1414,21356	1414,21058	1414,21356	1414,21356	1414,21356	1414,21356	1414,21356	1414,21356	1414,21356	1414,21356	1414,21356	1401,04775
2 Fruticose Type 2.1	1414,21356	0	1414,21356	1407,47104	1323,75659	1412,66318	1407,54342	1414,21356	1414,21356	1414,21356	1414,20364	1414,09569	1414,21356	1414,21356	1414,21356	1414,21356	1414,21356	1414,21356	1414,21356	1414,21356	1414,21356	1414,21356	1414,21356	1414,21356
3 Fruticose Foliose Type 1.1	1414,21356	1414,21356	0	1414,21356	1414,21165	1411,93383	1414,19529	1414,21356	1318,99691	1413,46069	1386,01525	1414,21356	1414,16342	1414,21356	1414,15624	1414,21356	1414,21356	1414,21353	1414,21356	1414,21356	1414,21356	1414,21356	1414,21356	1414,21356
4 Fruticose Foliose Type 1.2	1414,21356	1407,47104	1414,21356	0	1413,68949	1413,79261	1340,32593	1414,21356	1414,21356	1414,12877	1414,16139	1340,57858	1414,21356	1414,21356	1414,21356	1414,21356	1414,21356	1414,21356	1414,21356	1414,21356	1414,21356	1414,21356	1414,21356	1414,21356
5 Fruticose Foliose Type 1.3	1414,21356	1323,75659	1414,21165	1413,68949	0	1380,95906	1393,36944	1414,21356	1414,19867	1414,21332	1413,70165	1414,16606	1414,21356	1414,21356	1414,21356	1414,21356	1414,21356	1414,21356	1414,21356	1414,21356	1414,21356	1414,21356	1414,21356	1414,21356
6 Fruticose Foliose Type 2.1	1414,21356	1412,66318	1411,93383	1413,79261	1380,95906	0	1264,24663	1414,21356	1413,17462	1413,79287	1350,98402	1414,16743	1414,21352	1414,21356	1414,21356	1414,21356	1414,21356	1414,21356	1414,21356	1414,21356	1414,21356	1414,21356	1414,21356	1414,21356
7 Fruticose Foliose Type 2.2	1414,21356	1407,54342	1414,19529	1340,32593	1393,36944	1264,24663	0	1414,21356	1414,20245	1413,5554	1406,47376	1404,90533	1414,21356	1414,21356	1414,21356	1414,21356	1414,21356	1414,21356	1414,21356	1414,21356	1414,21356	1414,21356	1414,21356	1414,21356
8 Fruticose Foliose Type 3.1	1239,58345	1414,21356	1414,21356	1414,21356	1414,21356	1414,21356	1414,21356	0	1414,21356	1414,21356	1414,21356	1414,21356	1414,21356	1413,43156	1414,21356	1414,21356	1414,21356	1414,21356	1414,21356	1414,21356	1414,21356	1414,21356	1414,21356	1385,27956
9 Foliose Type 1.1	1414,21356	1414,21356	1318,99691	1414,21356	1414,19867	1413,17462	1414,20245	1414,21356	0	1413,90069	1401,51717	1414,21356	1380,75019	1414,21356	1376,75467	1414,13906	1414,21355	1413,07452	1414,21356	1414,21356	1414,21356	1414,21356	1414,21356	1414,21356
10 Foliose Type 1.2	1414,21356	1414,21356	1413,46069	1414,12877	1414,21332	1413,79287	1413,5554	1414,21356	1413,90069	0	1398,41793	1410,81192	1414,21055	1414,21356	1414,20127	1414,21356	1414,21356	1414,21356	1414,21356	1414,21356	1414,21356	1414,21356	1414,20136	1414,21356
11 Foliose Type 1.3	1414,21356	1414,20364	1386,01525	1414,16139	1413,70165	1350,98402	1406,47376	1414,21356	1401,51717	1398,41793	0	1414,20503	1410,95358	1414,21356	1411,04683	1414,21291	1414,21356	1414,21349	1414,21356	1414,21356	1414,21356	1414,21356	1414,21356	1414,21356
12 Foliose Type 2.1	1414,21356	1414,09569	1414,21356	1340,57858	1414,16606	1414,16743	1404,90533	1414,21356	1414,21356	1410,81192	1414,20503	0	1414,21356	1414,21356	1414,21356	1414,21356	1414,21356	1414,21356	1414,21356	1414,21356	1414,21356	1414,2017	1413,21021	1414,21356
13 Foliose Crustose Type 1.1	1414,21356	1414,21356	1414,16342	1414,21356	1414,21356	1414,21352	1414,21356	1414,21356	1380,75019	1414,21055	1410,95358	1414,21356	0	1414,21356	1251,8998	1413,27806	1414,21355	1413,1237	1414,21356	1414,21356	1414,21356	1414,21356	1414,21356	1414,21356
14 Foliose Crustose Type 2.1	1414,21058	1414,21356	1414,21356	1414,21356	1414,21356	1414,21356	1414,21356	1413,43156	1414,21356	1414,21356	1414,21356	1414,21356	1414,21356	0	1414,21356	1414,21356	1414,21356	1414,21356	1414,21356	1414,21356	1414,21356	1414,21042	1414,21317	1403,98522
15 Crustose Type 1.1	1414,21356	1414,21356	1414,15624	1414,21356	1414,21356	1414,21356	1414,21356	1414,21356	1376,75467	1414,20127	1411,04683	1414,21356	1251,8998	1414,21356	0	1392,69508	1414,20749	1339,57888	1414,21355	1414,21356	1414,21354	1414,21356	1414,21356	1414,21356
16 Crustose Type 1.2	1414,21356	1414,21356	1414,21356	1414,21356	1414,21356	1414,21356	1414,21356	1414,21356	1414,13906	1414,21356	1414,21291	1414,21356	1413,27806	1414,21356	1392,69508	0	1407,11226	1358,0803	1413,83531	1414,21356	1414,14352	1414,21356	1414,21356	1414,21356
17 Crustose Sparse Type 1.1	1414,21356	1414,21356	1414,21356	1414,21356	1414,21356	1414,21356	1414,21356	1414,21356	1414,21355	1414,21356	1414,21356	1414,21356	1414,21355	1414,21356	1414,20749	1407,11226	0	1414,21242	1406,79502	1414,21356	1373,56261	1414,21356	1414,21356	1414,21356
18 Crustose Sparse Type 1.2	1414,21356	1414,21356	1414,21353	1414,21356	1414,21356	1414,21356	1414,21356	1414,21356	1413,07452	1414,21356	1414,21349	1414,21356	1413,1237	1414,21356	1339,57888	1358,0803	1414,21242	0	1414,21356	1414,21356	1414,21356	1414,21356	1414,21356	1414,21356
19 Crustose Sparse Type 1.3	1414,21356	1414,21356	1414,21356	1414,21356	1414,21356	1414,21356	1414,21356	1414,21356	1414,21356	1414,21356	1414,21356	1414,21356	1414,21356	1414,21356	1414,21355	1413,83531	1406,79502	1414,21356	0	1414,21356	1412,16608	1414,21356	1414,21356	1414,21356
20 No Lichen Type 1.1	1414,21356	1414,21356	1414,21356	1414,21356	1414,21356	1414,21356	1414,21356	1414,21356	1414,21356	1414,21356	1414,21356	1414,21356	1414,21356	1414,21356	1414,21356	1414,21356	1414,21356	1414,21356	1414,21356	0	1414,21356	1414,21356	1414,21356	1414,21356
21 No Lichen Type 1.2	1414,21356	1414,21356	1414,21356	1414,21356	1414,21356	1414,21356	1414,21356	1414,21356	1414,21356	1414,21356	1414,21356	1414,21356	1414,21356	1414,21356	1414,21354	1414,14352	1373,56261	1414,21356	1412,16608	1414,21356	0	1414,21356	1414,21356	1414,21356
22 No Lichen Type 2.1	1414,21356	1414,21356	1414,21356	1414,21356	1414,21356	1414,21356	1414,21356	1414,21356	1414,21356	1414,21356	1414,21356	1414,2017	1414,21356	1414,21042	1414,21356	1414,21356	1414,21356	1414,21356	1414,21356	1414,21356	1414,21356	0	1408,75109	1414,21356
23 No Lichen Type 2.2	1414,21356	1414,21356	1414,21356	1414,21356	1414,21356	1414,21356	1414,21356	1414,21356	1414,21356	1414,20136	1414,21356	1413,21021	1414,21356	1414,21317	1414,21356	1414,21356	1414,21356	1414,21356	1414,21356	1414,21356	1414,21356	1408,75109	0	1414,21356
24 No Lichen Type 3.1	1401,04775	1414,21356	1414,21356	1414,21356	1414,21356	1414,21356	1414,21356	1385,27956	1414,21356	1414,21356	1414,21356	1414,21356	1414,21356	1403,98522	1414,21356	1414,21356	1414,21356	1414,21356	1414,21356	1414,21356	1414,21356	1414,21356	1414,21356	0

Figure A13: Full listing of the Jeffries-Matusita (JM) separability measures obtained for the multitemporal classification of WRS-2 scene 180 / 75 for the year of 2003.

	Class 1	Class 2	Class 3	Class 4	Class 5	Class 6	Class 7	Sum	Users
Class 1	3287	28	0	0	0	0	0	3315	99%
Class 2	278	2773	283	10	3	0	0	3347	83%
Class 3	22	458	1191	0	31	0	0	1702	70%
Class 4	0	28	31	270	239	1	2	571	47%
Class 5	1	35	42	968	1996	1	0	3043	66%
Class 6	0	0	1	51	404	253	175	884	29%
Class 7	28	165	119	165	234	226	13771	14708	94%
Sum	3616	3487	1667	1464	2907	481	13948	27570	Matrix Sum
Producers	91%	80%	71%	18%	69%	53%	99%		23541

Overall-Classification-Accuracy	85%
Overall-Kappa-Statistics	0,78570774

Figure A14: Contingency matrix of the combined multitemporal supervised classifications for the year of 2003.

	Class 1	Class 2	Class 3	Class 4	Class 5	Class 6	Class 7	Sum	Users
Class 1	3287	28	0	0	0	0	0	3315	99%
Class 2	278	2773	283	5	3	0	1	3343	83%
Class 3	22	458	1191	3	10	0	0	1684	71%
Class 4	0	28	31	209	239	5	12	524	40%
Class 5	1	35	42	847	1959	0	0	2884	68%
Class 6	0	0	1	68	324	291	70	754	39%
Class 7	28	165	119	123	235	106	12095	12871	94%
Sum	3616	3487	1667	1255	2770	402	12178	25375	Matrix Sum
Producers	91%	80%	71%	17%	71%	72%	99%		21805

Overall-Classification-Accuracy	86%
Overall-Kappa-Statistics	0,79947011

Figure A15: Contingency matrix of the combined multitemporal supervised classifications for the year of 2000.

	Class 1	Class 2	Class 3	Class 4	Class 5	Class 6	Class 7	Sum	Users
Class 1	3287	28	0	0	0	0	0	3315	99%
Class 2	278	2773	283	6	0	0	1	3341	83%
Class 3	22	458	1191	18	21	0	0	1710	70%
Class 4	0	28	31	86	232	0	1	378	23%
Class 5	1	35	42	790	443	0	0	1311	34%
Class 6	0	0	1	55	272	237	58	623	38%
Class 7	28	165	119	62	1023	16	6924	8337	83%
Sum	3616	3487	1667	1017	1991	253	6984	19015	Matrix Sum
Producers	91%	80%	71%	8%	22%	94%	99%		14941

Overall-Classification-Accuracy	79%
Overall-Kappa-Statistics	0,71696828

Figure A16: Contingency matrix of the combined multitemporal supervised classifications for the year of 91/92.

	Class 1	Class 2	Class 3	Class 4	Class 5	Class 6	Class 7	Sum	Users
Class 1	3222	18	0	0	0	0	0	3240	99%
Class 2	81	1486	389	10	3	0	0	1969	75%
Class 3	4	385	755	0	31	0	0	1175	64%
Class 4	0	0	101	219	180	1	2	503	44%
Class 5	0	0	0	678	1568	0	0	2246	70%
Class 6	0	0	0	0	157	229	65	451	51%
Class 7	0	78	147	165	153	157	7695	8395	92%
Sum	3307	1967	1392	1072	2092	387	7762	17979	Matrix Sum
Producers	97%	76%	54%	20%	75%	59%	99%		15174

Overall-Classification-Accuracy	84%
Overall-Kappa-Statistics	0,78671269

Figure A17: Contingency matrix of the multitemporal supervised classification of LANDSAT scene of the WRS-2 position 180 / 75 acquired 22nd of April of 2003.

	Class 1	Class 2	Class 3	Class 4	Class 5	Class 6	Class 7	Sum	Users
Class 1	2875	23	0	0	0	0	0	2898	99%
Class 2	211	1232	341	5	3	0	1	1793	69%
Class 3	2	359	526	3	10	0	0	900	58%
Class 4	0	0	18	171	164	5	12	370	46%
Class 5	0	0	6	675	1572	0	0	2253	70%
Class 6	0	0	0	0	95	203	49	347	59%
Class 7	3	272	199	123	160	102	7371	8230	90%
Sum	3091	1886	1090	977	2004	310	7433	16791	Matrix Sum
Producers	93%	65%	48%	18%	78%	65%	99%		13950

Overall-Classification-Accuracy	83%
Overall-Kappa-Statistics	0,7643816

Figure A18: Contingency matrix of the multitemporal supervised classification of LANDSAT scene of the WRS-2 position 180 / 75 acquired 2nd of July of 2000.

	Class 1	Class 2	Class 3	Class 4	Class 5	Class 6	Class 7	Sum	Users
Class 1	2298	20	1	1	3	0	0	2323	99%
Class 2	61	1168	218	4	1	0	0	1452	80%
Class 3	8	359	300	2	1	0	0	670	45%
Class 4	0	0	27	71	165	37	36	336	21%
Class 5	0	0	23	666	85	0	0	774	11%
Class 6	0	0	0	0	1478	146	16	1640	9%
Class 7	8	51	147	62	62	2	5299	5631	94%
Sum	2375	1598	716	806	1795	185	5351	12826	Matrix Sum
Producers	97%	73%	42%	9%	5%	79%	99%		9367

Overall-Classification-Accuracy	73%
Overall-Kappa-Statistics	0,64248799

Figure A19: Contingency matrix of the multitemporal supervised classification of LANDSAT scene of the WRS-2 position 180 / 75 acquired 18th of September of 1999.

	Class 1	Class 2	Class 3	Class 4	Class 5	Class 6	Class 7	Sum	Users
Class 1	1858	20	0	0	0	0	0	1878	99%
Class 2	403	1031	152	6	0	0	1	1593	65%
Class 3	7	430	328	18	21	0	0	804	41%
Class 4	0	2	13	64	138	0	1	218	29%
Class 5	0	2	28	649	83	0	0	762	11%
Class 6	0	0	0	0	74	170	40	284	60%
Class 7	1	51	187	54	956	14	3053	4316	71%
Sum	2269	1536	708	791	1272	184	3095	9855	Matrix Sum
Producers	82%	67%	46%	8%	7%	92%	99%		6587

Overall-Classification-Accuracy	67%
Overall-Kappa-Statistics	0,57224895

Figure A20: Contingency matrix of the multitemporal supervised classification of LANDSAT scene of the WRS-2 position 180 / 75 acquired 15th of May of 1991.

	Class 1	Class 2	Class 3	Class 4	Class 5	Class 6	Class 7	Sum	Users
Class 1	0	0	0	0	0	0	0	0	0%
Class 2	0	0	0	0	0	0	0	0	0%
Class 3	0	0	0	0	0	0	0	0	0%
Class 4	0	0	0	51	59	0	0	110	46%
Class 5	0	0	0	290	428	1	0	719	60%
Class 6	0	0	0	51	247	24	110	432	6%
Class 7	0	0	0	0	81	69	6076	6226	98%
Sum	0	0	0	392	815	94	6186	7487	Matrix Sum
Producers	0%	0%	0%	13%	53%	26%	98%	0	6579

Overall-Classification-Accuracy	88%
Overall-Kappa-Statistics	0,59705846

Figure A21: Contingency matrix of the multitemporal supervised classification of LANDSAT scene of the WRS-2 position 179 / 76 acquired 1st of May of 2003.

	Class 1	Class 2	Class 3	Class 4	Class 5	Class 6	Class 7	Sum	Users
Class 1	0	0	0	0	0	0	0	0	0%
Class 2	0	0	0	0	0	0	0	0	0%
Class 3	0	0	0	0	0	0	0	0	0%
Class 4	0	0	0	38	75	0	0	113	34%
Class 5	0	0	0	172	387	0	0	559	69%
Class 6	0	0	0	68	229	88	21	406	22%
Class 7	0	0	0	0	75	4	4724	4803	98%
Sum	0	0	0	278	766	92	4745	5881	Matrix Sum
Producers	0%	0%	0%	14%	51%	96%	100%	0	5237

Overall-Classification-Accuracy	89%
Overall-Kappa-Statistics	0,66480437

Figure A22: Contingency matrix of the multitemporal supervised classification of LANDSAT scene of the WRS-2 position 179 / 76 acquired 6th of April of 2000.

	Class 1	Class 2	Class 3	Class 4	Class 5	Class 6	Class 7	Sum	Users
Class 1	0	0	0	0	0	0	0	0	0%
Class 2	0	0	0	0	0	0	0	0	0%
Class 3	0	0	0	0	0	0	0	0	0%
Class 4	0	0	0	22	94	0	0	116	19%
Class 5	0	0	0	141	360	0	0	501	72%
Class 6	0	0	0	55	198	67	18	338	20%
Class 7	0	0	0	8	67	2	3871	3948	98%
Sum	0	0	0	226	719	69	3889	4903	Matrix Sum
Producers	0%	0%	0%	10%	50%	97%	100%	0	4320

Overall-Classification-Accuracy	88%
Overall-Kappa-Statistics	0,65460483

Figure A23: Contingency matrix of the multitemporal supervised classification of LANDSAT scene of the WRS-2 position 179 / 76 acquired 26th of May of 1992.

LF-1	Distance 1-2	Distance 1-3	Distance 1-4
2003	85%	62%	36%
2003 TS	85%	62%	36%
2000 TS	96%	86%	64%
1999 TS	-	-	-
1992 TS	98%	90%	74%

LF-2	Distance 1-2	Distance 1-3	Distance 1-4
2003	85%	61%	34%
2003 TS	84%	59%	33%
2000 TS	97%	88%	64%
1999 TS	-	-	-
1992 TS	98%	91%	76%

LF-3	Distance 1-2	Distance 1-3	Distance 1-4
2003	89%	73%	50%
2003 TS	85%	69%	48%
2000 TS	97%	90%	78%
1999 TS	-	-	-
1992 TS	99%	77%	70%

LF-4	Distance 1-2	Distance 1-3	Distance 1-4
2003	88%	58%	30%
2003 TS	84%	63%	41%
2000 TS	95%	80%	64%
1999 TS	80%	59%	36%
1991 TS	97%	79%	56%

LF-5	Distance 1-2	Distance 1-3	Distance 1-4
2003	87%	58%	29%
2003 TS	87%	60%	32%
2000 TS	94%	78%	55%
1999 TS	86%	62%	34%
1991 TS	96%	86%	61%

LF-6	Distance 1-2	Distance 1-3	Distance 1-4
2003	84%	46%	20%
2003 TS	85%	57%	26%
2000 TS	92%	73%	50%
1999 TS	81%	51%	23%
1991 TS	95%	78%	48%

LF-7	Distance 1-2	Distance 1-3	Distance 1-4
2003	88%	54%	26%
2003 TS	87%	65%	35%
2000 TS	93%	76%	55%
1999 TS	82%	59%	33%
1991 TS	95%	82%	51%

LF 8	Distance 1-2	Distance 1-3	Distance 1-4
2003	86%	48%	21%
2003 TS	75%	52%	32%
2000 TS	87%	68%	47%
1999 TS	70%	39%	17%
1991 TS	93%	78%	48%

LF-9	Distance 1-2	Distance 1-3	Distance 1-4
2003	82%	52%	26%
2003 TS	92%	75%	42%
2000 TS	98%	91%	73%
1999 TS	93%	78%	50%
1991 TS	98%	91%	66%

LF-10	Distance 1-2	Distance 1-3	Distance 1-4
2003	73%	35%	10%
2003 TS	78%	47%	20%
2000 TS	88%	59%	31%
1999 TS	73%	47%	26%
1991 TS	86%	57%	25%

LF-11	Distance 1-2	Distance 1-3	Distance 1-4
2003	62%	28%	9%
2003 TS	76%	38%	10%
2000 TS	96%	78%	47%
1999 TS	94%	83%	63%
1991 TS	92%	72%	39%

LF-12	Distance 1-2	Distance 1-3	Distance 1-4
2003	67%	30%	9%
2003 TS	75%	40%	14%
2000 TS	91%	51%	16%
1999 TS	59%	37%	15%
1991 TS	76%	48%	25%

Figure A24: Analysis of the similarities of the chi-square distributions of the second to sixth best class to pixel assignments compared to the distribution of the class assignment of the first order using an F-test approach for a statistical confidence of 95 % on a per lichen field basis.

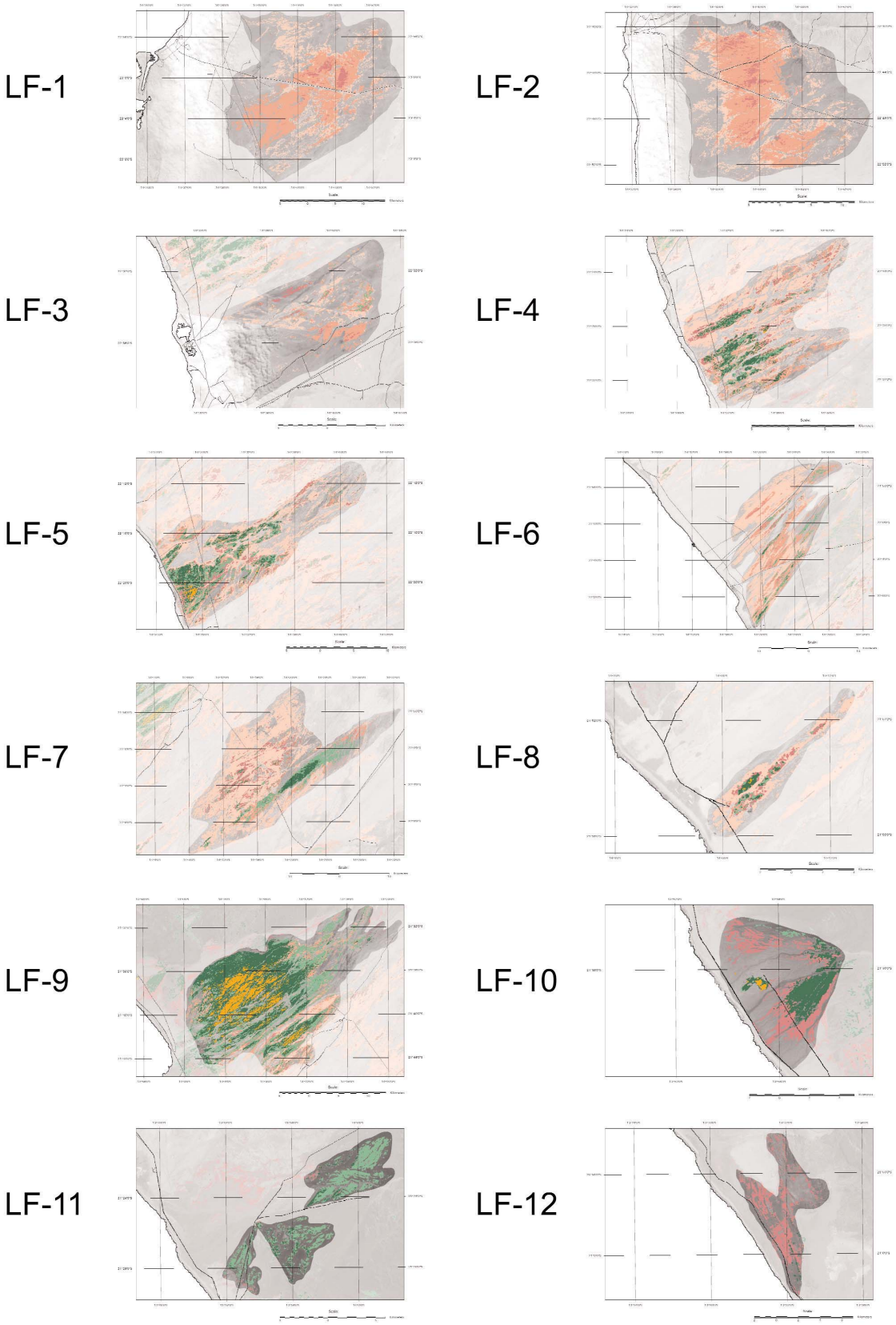

Figure A25: Overview maps depicting the spatial extend of the dissected lichen field units, statistically and thematically referred to as ‘lichen fields’.

Dry weight Biomass acc. to Wessels

Area related Biomass Contributions per Lichen Community (Mean Values)

Class	Lichen Community	Mean Dry Weight g/sqm
Class 1	Fruticose	359,72
Class 2	Fruticose / Foliose	188,53
Class 3	Foliose	142,62
Class 4	Foliose / Crustose	304,22
Class 5	Crustose	273,83
Class 6	Crustose Sparse	54,77

Unitemporal Classification 2003 for all Lichen Fields

Class	Lichen Community	Total Biomass per Lichen Community t	Outside Lichen Fields		
			Area ha	Biomass g/sqm (Mean)	Biomass total t
Class 1	Fruticose	16659,42	20,88	359,72	75,11
Class 2	Fruticose / Foliose	45087,42	2220,93	188,53	4187,12
Class 3	Foliose	42122,73	6714,63	142,62	9576,41
Class 4	Foliose / Crustose	62857,18	8469,54	304,22	25766,03
Class 5	Crustose	156293,98	8717,85	273,83	23872,09
Class 6	Crustose Sparse	73486,85	61402,50	54,766	33627,69
Total		396507,58			97104,45

Figure A26: Estimated total dryweight biomass calculation according to WESSELS.

Dry weight Biomass acc. to Wessels - Unitemporal Classification 2003 for all Lichen Fields (continued)

Class	Lichen Community	Lichen Field 1 - Southern Naukluft Plateau			Lichen Field 2 - Northern Naukluft Plateau		
		Area ha	Biomass g/sqm (Mean)	Total Biomass t	Area ha	Biomass g/sqm (Mean)	Total Biomass t
Class 1	Fruticose	0,00	359,72	0,00	0,00	359,72	0,00
Class 2	Fruticose / Foliose	0,00	188,53	0,00	0,00	188,53	0,00
Class 3	Foliose	0,00	142,62	0,00	0,00	142,62	0,00
Class 4	Foliose / Crustose	970,65	304,22	2952,91	1633,14	304,22	4968,34
Class 5	Crustose	13038,12	273,83	35702,28	15984,72	273,83	43770,96
Class 6	Crustose Sparse	9082,53	54,766	4974,14	9575,01	54,766	5243,85
Total				43629,33			53983,15

Class	Lichen Community	Lichen Field 3 - Nonidas			Lichen Field 4 - Mile 8/Mile 12		
		Area ha	Biomass g/sqm (Mean)	Total Biomass t	Area ha	Biomass g/sqm (Mean)	Total Biomass t
Class 1	Fruticose	0,00	359,72	0,00	37,17	359,72	133,71
Class 2	Fruticose / Foliose	0,99	188,53	1,87	1898,19	188,53	3578,66
Class 3	Foliose	137,25	142,62	195,75	1381,86	142,62	1970,81
Class 4	Foliose / Crustose	215,01	304,22	654,10	1408,95	304,22	4286,31
Class 5	Crustose	1129,41	273,83	3092,66	2981,07	273,83	8163,06
Class 6	Crustose Sparse	1150,56	54,766	630,12	8691,48	54,766	4759,98
Total				4574,49			22892,52

Class	Lichen Community	Lichen Field 5 - Wlotzkasbaken			Lichen Field 6 - Jakkalsputz		
		Area ha	Biomass g/sqm (Mean)	Total Biomass t	Area ha	Biomass g/sqm (Mean)	Total Biomass t
Class 1	Fruticose	201,51	359,72	724,87	2,70	359,72	9,71
Class 2	Fruticose / Foliose	2441,52	188,53	4603,00	248,76	188,53	468,99
Class 3	Foliose	3408,39	142,62	4861,05	1861,56	142,62	2654,96
Class 4	Foliose / Crustose	1796,04	304,22	5463,91	789,75	304,22	2402,58
Class 5	Crustose	2118,51	273,83	5801,12	6030,09	273,83	16512,20
Class 6	Crustose Sparse	8558,91	54,766	4687,37	15195,87	54,766	8322,17
Total				26141,32			30370,60

Figure A27: Estimated total dryweight biomass calculation according to WESSELS continued for the lichen fields No. 1 through No. 6.

Dry weight Biomass acc. to Wessels - Unitemporal Classification 2003 for all Lichen Fields (continued)

Class	Lichen Community	Lichen Field 7 - Omaruru Gravel Plain			Lichen Field 8 - Mile 72		
		Area ha	Biomass g/sqm (Mean)	Total Biomass t	Area ha	Biomass g/sqm (Mean)	Total Biomass t
Class 1	Fruticose	11,79	359,72	42,41	5,85	359,72	21,04
Class 2	Fruticose / Foliose	1000,35	188,53	1885,96	99,00	188,53	186,64
Class 3	Foliose	2813,13	142,62	4012,09	87,75	142,62	125,15
Class 4	Foliose / Crustose	2176,47	304,22	6621,26	160,74	304,22	489,00
Class 5	Crustose	2349,00	273,83	6432,27	59,40	273,83	162,66
Class 6	Crustose Sparse	17745,12	54,766	9718,29	791,64	54,766	433,55
Total				28712,27			1418,05

Class	Lichen Community	Lichen Field 9 - Messum Crater			Lichen Field 10 - Cape Cross		
		Area ha	Biomass g/sqm (Mean)	Total Biomass t	Area ha	Biomass g/sqm (Mean)	Total Biomass t
Class 1	Fruticose	4324,32	359,72	15555,44	27,00	359,72	97,12
Class 2	Fruticose / Foliose	14767,29	188,53	27840,77	742,77	188,53	1400,34
Class 3	Foliose	10530,99	142,62	15019,30	73,44	142,62	104,74
Class 4	Foliose / Crustose	975,06	304,22	2966,33	902,79	304,22	2746,47
Class 5	Crustose	4668,84	273,83	12784,68	0,00	273,83	0,00
Class 6	Crustose Sparse	1989,72	54,766	1089,69	0,00	54,766	0,00
Total				75256,22			4348,68

Class	Lichen Community	Lichen Field 11 - Brandberg West			Lichen Field 12 - Huabmond		
		Area ha	Biomass g/sqm (Mean)	Total Biomass t	Area ha	Biomass g/sqm (Mean)	Total Biomass t
Class 1	Fruticose	0,00	359,72	0,00	0,00	359,72	0,00
Class 2	Fruticose / Foliose	444,42	188,53	837,87	51,03	188,53	96,21
Class 3	Foliose	2523,51	142,62	3599,03	2,43	142,62	3,47
Class 4	Foliose / Crustose	70,38	304,22	214,11	1093,23	304,22	3325,82
Class 5	Crustose	0,00	273,83	0,00	0,00	273,83	0,00
Class 6	Crustose Sparse	0,00	54,766	0,00	0,00	54,766	0,00
Total				4651,01			3425,50

Figure A28: Estimated total dryweight biomass calculation according to WESSELS continued for the lichen fields No. 7 through No. 12.

Net Biomass acc. to Loris

Area related Biomass Contributions per Lichen Community (Mean Values)

Class	Lichen Community	Mean Net Biomass g/sqm
Class 1	Fruticose	192,18
Class 2	Fruticose / Foliose	64,90
Class 3	Foliose	72,55
Class 4	Foliose / Crustose	197,00
Class 5	Crustose	139,297321
Class 6	Crustose Sparse	27,8594642

Unitemporal Classification 2003 for all Lichen Fields

Class	Lichen Community	Total Biomass per Lichen Community t	Outside Lichen Fields		
			Area ha	Biomass g/sqm (Mean)	Biomass total t
Class 1	Fruticose	8900,43	20,88	192,18	40,13
Class 2	Fruticose / Foliose	15521,00	2220,93	64,90	1441,38
Class 3	Foliose	21427,83	6714,63	72,55	4871,52
Class 4	Foliose / Crustose	40703,65	8469,54	197,00	16684,99
Class 5	Crustose	79506,75	8717,85	139,30	12143,73
Class 6	Crustose Sparse	37382,76	61402,50	27,86	17106,41
Total		203442,42			52288,16

Figure A29: Estimated total net biomass calculation according to LORIS.

Net Biomass acc. to Loris - Unitemporal Classification 2003 for all Lichen Fields (continued)

Class	Lichen Community	Lichen Field 1 - Southern Naukluft Plateau			Lichen Field 2 - Northern Naukluft Plateau		
		Area	Biomass	Total Biomass	Area	Biomass	Total Biomass
		ha	g/sqm (Mean)	t	ha	g/sqm (Mean)	t
Class 1	Fruticose	0,00	192,18	0,00	0,00	192,18	0,00
Class 2	Fruticose / Foliose	0,00	64,90	0,00	0,00	64,90	0,00
Class 3	Foliose	0,00	72,55	0,00	0,00	72,55	0,00
Class 4	Foliose / Crustose	970,65	197,00	1912,18	1633,14	197,00	3217,29
Class 5	Crustose	13038,12	139,30	18161,75	15984,72	139,30	22266,29
Class 6	Crustose Sparse	9082,53	27,86	2530,34	9575,01	27,86	2667,55
Total				22604,28			28151,12

Class	Lichen Community	Lichen Field 3 - Nonidas			Lichen Field 4 - Mile 8/Mile 12		
		Area	Biomass	Total Biomass	Area	Biomass	Total Biomass
		ha	g/sqm (Mean)	t	ha	g/sqm (Mean)	t
Class 1	Fruticose	0,00	192,18	0,00	37,17	192,18	71,43
Class 2	Fruticose / Foliose	0,99	64,90	0,64	1898,19	64,90	1231,93
Class 3	Foliose	137,25	72,55	99,58	1381,86	72,55	1002,55
Class 4	Foliose / Crustose	215,01	197,00	423,57	1408,95	197,00	2775,63
Class 5	Crustose	1129,41	139,30	1573,24	2981,07	139,30	4152,55
Class 6	Crustose Sparse	1150,56	27,86	320,54	8691,48	27,86	2421,40
Total				2417,57			11655,49

Class	Lichen Community	Lichen Field 5 - Wlotzkasbaken			Lichen Field 6 - Jakkalsputz		
		Area	Biomass	Total Biomass	Area	Biomass	Total Biomass
		ha	g/sqm (Mean)	t	ha	g/sqm (Mean)	t
Class 1	Fruticose	201,51	192,18	387,27	2,70	192,18	5,19
Class 2	Fruticose / Foliose	2441,52	64,90	1584,55	248,76	64,90	161,45
Class 3	Foliose	3408,39	72,55	2472,81	1861,56	72,55	1350,58
Class 4	Foliose / Crustose	1796,04	197,00	3538,20	789,75	197,00	1555,81
Class 5	Crustose	2118,51	139,30	2951,03	6030,09	139,30	8399,75
Class 6	Crustose Sparse	8558,91	27,86	2384,47	15195,87	27,86	4233,49
Total				13318,32			15706,26

Figure A30: Estimated total net biomass calculation according to LORIS continued for the lichen fields No. 1 through No. 6.

Net Biomass acc. to Loris - Unitemporal Classification 2003 for all Lichen Fields (continued)

Class	Lichen Community	Lichen Field 7 - Omaruru Gravel Plain			Lichen Field 8 - Mile 72		
		Area	Biomass	Total Biomass	Area	Biomass	Total Biomass
		ha	g/sqm (Mean)	t	ha	g/sqm (Mean)	t
Class 1	Fruticose	11,79	192,18	22,66	5,85	192,18	11,24
Class 2	Fruticose / Foliose	1000,35	64,90	649,23	99,00	64,90	64,25
Class 3	Foliose	2813,13	72,55	2040,95	87,75	72,55	63,66
Class 4	Foliose / Crustose	2176,47	197,00	4287,65	160,74	197,00	316,66
Class 5	Crustose	2349,00	139,30	3272,09	59,40	139,30	82,74
Class 6	Crustose Sparse	17745,12	27,86	4943,70	791,64	27,86	220,55
Total				15216,27			759,10

Class	Lichen Community	Lichen Field 9 - Messum Crater			Lichen Field 10 - Cape Cross		
		Area	Biomass	Total Biomass	Area	Biomass	Total Biomass
		ha	g/sqm (Mean)	t	ha	g/sqm (Mean)	t
Class 1	Fruticose	4324,32	192,18	8310,62	27,00	192,18	51,89
Class 2	Fruticose / Foliose	14767,29	64,90	9583,97	742,77	64,90	482,06
Class 3	Foliose	10530,99	72,55	7640,32	73,44	72,55	53,28
Class 4	Foliose / Crustose	975,06	197,00	1920,87	902,79	197,00	1778,50
Class 5	Crustose	4668,84	139,30	6503,57	0,00	139,30	0,00
Class 6	Crustose Sparse	1989,72	27,86	554,33	0,00	27,86	0,00
Total				34513,67			2365,72

Class	Lichen Community	Lichen Field 11 - Brandberg West			Lichen Field 12 - Huabmond		
		Area	Biomass	Total Biomass	Area	Biomass	Total Biomass
		ha	g/sqm (Mean)	t	ha	g/sqm (Mean)	t
Class 1	Fruticose	0,00	192,18	0,00	0,00	192,18	0,00
Class 2	Fruticose / Foliose	444,42	64,90	288,43	51,03	64,90	33,12
Class 3	Foliose	2523,51	72,55	1830,83	2,43	72,55	1,76
Class 4	Foliose / Crustose	70,38	197,00	138,65	1093,23	197,00	2153,66
Class 5	Crustose	0,00	139,30	0,00	0,00	139,30	0,00
Class 6	Crustose Sparse	0,00	27,86	0,00	0,00	27,86	0,00
Total				2257,90			2188,54

Figure A31: Estimated total net biomass calculation according to LORIS continued for the lichen fields No. 7 through No. 12.

Total Net Primary Production per Lichen Field according to Lange et al. 1994

Precondition:
1. each fog event results in the same average amount of photosynthetic gain
2. annual average of 250 Fog Days
3. 100 % coverage of biological soil crust

Results:
Productivity approx. 32 g C /qm soilcrust p.a.
Respiratory Loss during nights: ca. 50%
Total amount NPP p.a. 16 g C / qm

	Outside LF	LF-1	LF-2	LF-3	LF-4	LF-5	LF-6	LF-7
Total Lichen Area (ha)	87546,33	23091,30	27192,87	2633,22	16398,72	18524,88	24128,73	26095,86
Total NPP at 100% Cover (t)	14007,41	3694,61	4350,86	421,32	2623,80	2963,98	3860,60	4175,34
Total NPP at 20% Cover (t)	2801,48	738,92	870,17	84,26	524,76	592,80	772,12	835,07

	LF-8	LF-9	LF-10	LF-11	LF-12	**Total**	**Total Lichen Fields only**
Total Lichen Area (ha)	1204,38	37256,22	1746,00	3038,31	1146,69		
Total NPP at 100% Cover (t)	192,70	5961,00	279,36	486,13	183,47	**43200,56**	**29193,15**
Total NPP at 20% Cover (t)	38,54	1192,20	55,87	97,23	36,69	**8640,11**	**5838,63**

Figure A32: Estimated total net primary productivity according to LANGE ET AL. (1994).

Max. Daily Carbon Gain per Lichen Species acc. to Lange et al. 1991

Species	Max. Daily Carbon Gain (mgc/gc/d)	Carbon Gain on April, 24 1988 (mgc/gc/d)	Carbon Content % Dry Weight
Teloschistes capensis	2,491	1,158	35,0
Ramalina lacera	1,821	0,861	39,3
Heterodermia ef. Erinacea	0,539	0,517	36,5
Caloplaca elegantissima	0,806	0,496	37,1
Neofuscelia namaensis	0,425	0,373	37,3
Alectoria spec.	1,055	0,336	38,7
Xanthoparmelia walteri	0,456	0,229	37,7
Santessonia hereroensis	0,481	0,151	40,3
Xanthomaculina convoluta	0,281	0,113	40,2
Xanthomaculina hottentotta	0,417	0,095	38,5

Biomass acc. to Wessels 2003 (Gross Dry Weight)

Class	Lichen Community	Total Biomass (t)
Class 1	Fruticose	16659,42
Class 2	Fruticose / Foliose	45087,42
Class 3	Foliose	42122,73
Class 4	Foliose / Crustose	62857,18
Class 5	Crustose	156293,98
Class 6	Crustose Sparse	73486,85
Total		396507,58

Figure A33: Maximum daily carbon gain per lichen species according to LANGE ET AL. (1991) and dryweight biomass according to WESSELS.

Net primary production per species within the Lichen Communities according to Lange et al. 1991 (Data acc. Wessels)

Species	**Class 1 - Fruticose** Mean Cover in %	Total Biomass t	Biomass per Species t	Carbon Content % Dry Weight	Total Carbon Content per Species g	Max. daily Carbon Gain (mgc/gc/d)	Carbon Gain /a (250 Fog days) t
Acarospora cf. Schleicheri	0,00	16659,42	0,00	0,00	0,00	0,00	0,00
Alectoria sp.	4,40	16659,42	733,01	38,70	283676681,82	1,06	74,82
Buellia sp. Crustose	0,00	16659,42	0,00	0,00	0,00	0,00	0,00
Caloplaca elegantissima	0,11	16659,42	18,33	37,10	6798711,17	0,81	1,37
Caloplaca namibiensis	0,00	16659,42	0,00	0,00	0,00	0,00	0,00
Caloplaca volkii	0,18	16659,42	29,99	0,00	0,00	0,00	0,00
Diploschistes sp.	0,00	16659,42	0,00	0,00	0,00	0,00	0,00
Heterodermia ef. Erinacea	0,00	16659,42	0,00	36,50	0,00	0,54	0,00
Lecidea sp. Chasmoendolithic	0,00	16659,42	0,00	0,00	0,00	0,00	0,00
Lecidella cristallina	0,44	16659,42	72,47	0,00	0,00	0,00	0,00
Neofuscelia namaensis	1,81	16659,42	300,98	37,30	112265641,01	0,43	11,93
Ramalina lacera	0,00	16659,42	0,00	39,30	0,00	1,82	0,00
Santessonia hereroensis	0,00	16659,42	0,00	40,30	0,00	0,48	0,00
Teloschistes capensis	36,69	16659,42	6111,79	35,00	2139125648,00	2,49	1332,14
Xanthomaculina convoluta	0,03	16659,42	5,00	40,20	2009126,60	0,28	0,14
Xanthomaculina hottentotta	0,00	16659,42	0,00	38,50	0,00	0,42	0,00
Xanthoparmelia evernica	0,00	16659,42	0,00	0,00	0,00	0,00	0,00
Xanthoparmelia serusiauxii	0,00	16659,42	0,00	0,00	0,00	0,00	0,00
Xanthoparmelia walteri	4,00	16659,42	665,82	37,70	251014769,29	0,46	28,62
Total							**1449,02**

Figure A34: Estimated sum of net primary production per lichen species according to LANGE ET AL. (1991) and within the fruticose lichen community. Mean cover according to WESSELS.

Net primary production per species within the Lichen Communities according to Lange et al. 1991 (Data acc. Wessels)

Species	**Class 2 - Fruticose / Foliose** Mean Cover in %	Total Biomass t	Biomass per Species t	Carbon Content % Dry Weight	Total Carbon Content per Species g	Max. daily Carbon Gain (mgc/gc/d)	Carbon Gain /a (250 Fog days) t
Acarospora cf. Schleicheri	0,00	45087,42	0,00	0,00	0,00	0,00	0,00
Alectoria sp.	0,00	45087,42	0,00	38,70	0,00	1,06	0,00
Buellia sp. Crustose	0,00	45087,42	0,00	0,00	0,00	0,00	0,00
Caloplaca elegantissima	0,00	45087,42	0,00	37,10	0,00	0,81	0,00
Caloplaca namibiensis	0,00	45087,42	0,00	0,00	0,00	0,00	0,00
Caloplaca volkii	0,00	45087,42	0,00	0,00	0,00	0,00	0,00
Diploschistes sp.	0,00	45087,42	0,00	0,00	0,00	0,00	0,00
Heterodermia ef. Erinacea	0,00	45087,42	0,00	36,50	0,00	0,54	0,00
Lecidea sp. Chasmoendolithic	0,00	45087,42	0,00	0,00	0,00	0,00	0,00
Lecidella cristallina	10,98	45087,42	4950,60	0,00	0,00	0,00	0,00
Neofuscelia namaensis	4,60	45087,42	2074,02	37,30	773609966,52	0,43	82,20
Ramalina lacera	0,00	45087,42	0,00	39,30	0,00	1,82	0,00
Santessonia hereroensis	0,48	45087,42	216,42	40,30	87217106,84	0,48	10,49
Teloschistes capensis	0,09	45087,42	40,58	35,00	14202537,56	2,49	8,84
Xanthomaculina convoluta	0,00	45087,42	0,00	40,20	0,00	0,28	0,00
Xanthomaculina hottentotta	79,83	45087,42	35993,29	38,50	13857415897,17	0,42	1444,64
Xanthoparmelia evernica	0,00	45087,42	0,00	0,00	0,00	0,00	0,00
Xanthoparmelia serusiauxii	0,00	45087,42	0,00	0,00	0,00	0,00	0,00
Xanthoparmelia walteri	3,48	45087,42	1569,04	37,70	591528926,26	0,46	67,43
Total							**1613,60**

Figure A35: Estimated sum of net primary production per lichen species according to LANGE ET AL. (1991) and within the fruticose /foliose lichen community. Mean cover according to WESSELS.

Net primary production per species within the Lichen Communities according to Lange et al. 1991 (Data acc. Wessels)

Species	**Class 3 - Foliose** Mean Cover in %	Total Biomass t	Biomass per Species t	Carbon Content % Dry Weight	Total Carbon Content per Species g	Max. daily Carbon Gain (mgc/gc/d)	Carbon Gain /a (250 Fog days) t
Acarospora cf. Schleicheri	0,67	42122,73	282,22	0,00	0,00	0,00	0,00
Alectoria sp.	0,00	42122,73	0,00	38,70	0,00	1,06	0,00
Buellia sp. Crustose	0,00	42122,73	0,00	0,00	0,00	0,00	0,00
Caloplaca elegantissima	11,72	42122,73	4934,68	37,10	1830765533,10	0,81	368,90
Caloplaca namibiensis	7,29	42122,73	3070,75	0,00	0,00	0,00	0,00
Caloplaca volkii	2,12	42122,73	893,00	0,00	0,00	0,00	0,00
Diploschistes sp.	0,00	42122,73	0,00	0,00	0,00	0,00	0,00
Heterodermia ef. Erinacea	0,00	42122,73	0,00	36,50	0,00	0,54	0,00
Lecidea sp. Chasmoendolithic	0,00	42122,73	0,00	0,00	0,00	0,00	0,00
Lecidella cristallina	19,57	42122,73	8243,42	0,00	0,00	0,00	0,00
Neofuscelia namaensis	8,40	42122,73	3538,31	37,30	1319789421,10	0,43	140,23
Ramalina lacera	0,07	42122,73	29,49	39,30	11587963,42	1,82	5,28
Santessonia hereroensis	0,00	42122,73	0,00	40,30	0,00	0,48	0,00
Teloschistes capensis	0,50	42122,73	208,51	35,00	72977632,20	2,49	45,45
Xanthomaculina convoluta	2,32	42122,73	977,25	40,20	392853442,39	0,28	27,60
Xanthomaculina hottentotta	22,36	42122,73	9418,64	38,50	3626177457,71	0,42	378,03
Xanthoparmelia evernica	0,40	42122,73	168,49	0,00	0,00	0,00	0,00
Xanthoparmelia serusiauxii	2,07	42122,73	871,94	0,00	0,00	0,00	0,00
Xanthoparmelia walteri	18,46	42122,73	7773,75	37,70	2930703782,06	0,46	334,10
Total							**1299,58**

Figure A36: Estimated sum of net primary production per lichen species according to LANGE ET AL. (1991) and within the foliose lichen community. Mean cover according to WESSELS.

Net primary production per species within the Lichen Communities according to Lange et al. 1991 (Data acc. Wessels)

Species	**Class 4 - Foliose / Crustose** Mean Cover in %	Total Biomass t	Biomass per Species t	Carbon Content % Dry Weight	Total Carbon Content per Species g	Max. daily Carbon Gain (mgc/gc/d)	Carbon Gain /a (250 Fog days) t
Acarospora cf. Schleicheri	0,86	62857,18	540,57	0,00	0,00	0,00	0,00
Alectoria sp.	0,03	62857,18	18,86	38,70	7297718,12	1,06	1,92
Buellia sp. Crustose	0,00	62857,18	0,00	0,00	0,00	0,00	0,00
Caloplaca elegantissima	0,10	62857,18	64,95	37,10	24097345,98	0,81	4,86
Caloplaca namibiensis	1,22	62857,18	763,71	0,00	0,00	0,00	0,00
Caloplaca volkii	5,41	62857,18	3398,48	0,00	0,00	0,00	0,00
Diploschistes sp.	0,00	62857,18	0,00	0,00	0,00	0,00	0,00
Heterodermia ef. Erinacea	0,00	62857,18	0,00	36,50	0,00	0,54	0,00
Lecidea sp. Chasmoendolithic	0,00	62857,18	0,00	0,00	0,00	0,00	0,00
Lecidella cristallina	61,51	62857,18	38665,54	0,00	0,00	0,00	0,00
Neofuscelia namaensis	18,73	62857,18	11773,15	37,30	4391384590,69	0,43	466,58
Ramalina lacera	0,00	62857,18	0,00	39,30	0,00	1,82	0,00
Santessonia hereroensis	0,00	62857,18	0,00	40,30	0,00	0,48	0,00
Teloschistes capensis	0,12	62857,18	72,29	35,00	25300013,28	2,49	15,76
Xanthomaculina convoluta	0,50	62857,18	312,19	40,20	125500637,30	0,28	8,82
Xanthomaculina hottentotta	22,36	62857,18	14054,86	38,50	5411122840,22	0,42	564,11
Xanthoparmelia evernica	0,00	62857,18	0,00	0,00	0,00	0,00	0,00
Xanthoparmelia serusiauxii	0,00	62857,18	0,00	0,00	0,00	0,00	0,00
Xanthoparmelia walteri	1,59	62857,18	1001,52	37,70	377574674,37	0,46	43,04
Total							**1105,09**

Figure A37: Estimated sum of net primary production per lichen species according to LANGE ET AL. (1991) and within the foliose / crustose lichen community. Mean cover according to WESSELS.

Net primary production per species within the Lichen Communities according to Lange et al. 1991 (Data acc. Wessels)

Species	**Class 5 - Crustose** Mean Cover in %	Total Biomass t	Biomass per Species t	Carbon Content % Dry Weight	Total Carbon Content per Species g	Max. daily Carbon Gain (mgc/gc/d)	Carbon Gain /a (250 Fog days) t
Acarospora cf. Schleicheri	1,44	156293,98	2250,63	0,00	0,00	0,00	0,00
Alectoria sp.	0,00	156293,98	0,00	38,70	0,00	1,06	0,00
Buellia sp. Crustose	0,81	156293,98	1265,98	0,00	0,00	0,00	0,00
Caloplaca elegantissima	12,98	156293,98	20286,96	37,10	7526461472,72	0,81	1516,58
Caloplaca namibiensis	3,08	156293,98	4813,85	0,00	0,00	0,00	0,00
Caloplaca volkii	0,00	156293,98	0,00	0,00	0,00	0,00	0,00
Diploschistes sp.	0,81	156293,98	1265,98	0,00	0,00	0,00	0,00
Heterodermia ef. Erinacea	0,00	156293,98	0,00	36,50	0,00	0,54	0,00
Lecidea sp. Chasmoendolithic	1,01	156293,98	1578,57	0,00	0,00	0,00	0,00
Lecidella cristallina	33,33	156293,98	52092,78	0,00	0,00	0,00	0,00
Neofuscelia namaensis	1,67	156293,98	2610,11	37,30	973570808,91	0,43	103,44
Ramalina lacera	0,00	156293,98	0,00	39,30	0,00	1,82	0,00
Santessonia hereroensis	0,00	156293,98	0,00	40,30	0,00	0,48	0,00
Teloschistes capensis	0,00	156293,98	0,00	35,00	0,00	2,49	0,00
Xanthomaculina convoluta	3,50	156293,98	5470,29	40,20	2199056249,12	0,28	154,48
Xanthomaculina hottentotta	0,00	156293,98	0,00	38,50	0,00	0,42	0,00
Xanthoparmelia evernica	0,00	156293,98	0,00	0,00	0,00	0,00	0,00
Xanthoparmelia serusiauxii	0,00	156293,98	0,00	0,00	0,00	0,00	0,00
Xanthoparmelia walteri	0,45	156293,98	695,51	37,70	262206589,65	0,46	29,89
Total							**1804,40**

Figure A38: Estimated sum of net primary production per lichen species according to LANGE ET AL. (1991) and within the crustose lichen community. Mean cover according to WESSELS.

Net primary production per species within the Lichen Communities according to Lange et al. 1991 (Data acc. Wessels)

Species	**Class 6 - Crustose Sparse** Mean Cover in %	Total Biomass t	Biomass per Species t	Carbon Content % Dry Weight	Total Carbon Content per Species g	Max. daily Carbon Gain (mgc/gc/d)	Carbon Gain /a (250 Fog days) t
Acarospora cf. Schleicheri	1,44	73486,85	1058,21	0,00	0,00	0,00	0,00
Alectoria sp.	0,00	73486,85	0,00	38,70	0,00	1,06	0,00
Buellia sp. Crustose	0,81	73486,85	595,24	0,00	0,00	0,00	0,00
Caloplaca elegantissima	12,98	73486,85	9538,59	37,10	3538817954,17	0,81	713,07
Caloplaca namibiensis	3,08	73486,85	2263,39	0,00	0,00	0,00	0,00
Caloplaca volkii	0,00	73486,85	0,00	0,00	0,00	0,00	0,00
Diploschistes sp.	0,81	73486,85	595,24	0,00	0,00	0,00	0,00
Heterodermia ef. Erinacea	0,00	73486,85	0,00	36,50	0,00	0,54	0,00
Lecidea sp. Chasmoendolithic	1,01	73486,85	742,22	0,00	0,00	0,00	0,00
Lecidella cristallina	33,33	73486,85	24493,17	0,00	0,00	0,00	0,00
Neofuscelia namaensis	1,67	73486,85	1227,23	37,30	457756924,78	0,43	48,64
Ramalina lacera	0,00	73486,85	0,00	39,30	0,00	1,82	0,00
Santessonia hereroensis	0,00	73486,85	0,00	40,30	0,00	0,48	0,00
Teloschistes capensis	0,00	73486,85	0,00	35,00	0,00	2,49	0,00
Xanthomaculina convoluta	3,50	73486,85	2572,04	40,20	1033959951,14	0,28	72,64
Xanthomaculina hottentotta	0,00	73486,85	0,00	38,50	0,00	0,42	0,00
Xanthoparmelia evernica	0,00	73486,85	0,00	0,00	0,00	0,00	0,00
Xanthoparmelia serusiauxii	0,00	73486,85	0,00	0,00	0,00	0,00	0,00
Xanthoparmelia walteri	0,45	73486,85	327,02	37,70	123285210,52	0,46	14,05
Total							**848,40**
					Total NPP p.a. all Lichen Fields (t)		**8120,08**

Figure A39: Estimated sum of net primary production per lichen species according to LANGE ET AL. (1991) and within the crustose sparse lichen community. Mean cover according to WESSELS.

Acarospora spp.

Figure B1:
Acarospora spp.

Location: Central Namib Desert SE of Swakopmund, Namib-Naukluft Park. Along Kuiseb River ca. 25 km NW of Gobabeb. On course sandstone gravel on slope. Southern-Naukluft-Plateau lichen field - No. 1.
Degree ref.: 23 14 BC
Photo: Christoph Schultz, 2004
Scale-Bar: Millimeter
Collection: University of Bayreuth - Museum Botanicum Berolinense

Figure B2:
Acarospora spp.

Location: Central Namib Desert SE of Walvisbay, Namib-Naukluft Park. Canyon of Kuiseb River. On rock. Southern-Naukluft-Plateau lichen field - No. 1.
Degree ref.: 23 14 BC
Photo: Christoph Schultz, 2004
Scale-Bar: Millimeter
Collection: University of Bayreuth - Museum Botanicum Berolinense

Figure B3:
Acarospora spp.

Location: Central Namib Desert 50 Miles E of Swakopmund. Southern-Naukluft-Plateau lichen field - No. 1.
Degree ref.: 23 14 BC
Photo: Christoph Schultz, 2004
Scale-Bar: Millimeter
Collection: University of Bayreuth - Museum Botanicum Berolinense

Buellia spp.

Figure B4:
Buellia spp.

Location: Central Namib Desert 5 km SE of Cape Cross. Cape Cross mountains close to Lagunenberg - sandstone hill close to the sea on SW-facing rocky slope. Cape Cross lichen field - No. 10.
Degree ref.: 21 14 CC
Photo: Christoph Schultz, 2003

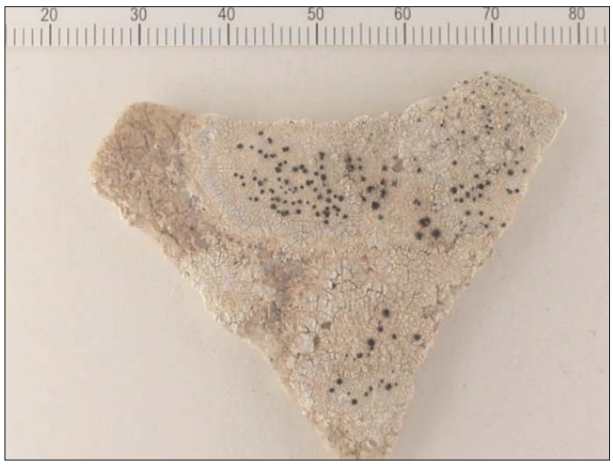

Figure B5:
Buellia spp.

Location: Central Namib Desert SE of Swakopmund, Namib-Naukluft Park. Along Kuiseb River ca. 25 km NW of Gobabeb. On course sandstone gravel on slope. Southern-Naukluft-Plateau lichen field - No. 1.
Degree ref.: 23 14 BC
Photo: Christoph Schultz, 2004
Scale-Bar: Millimeter
Collection: University of Bayreuth - Museum Botanicum Berolinense

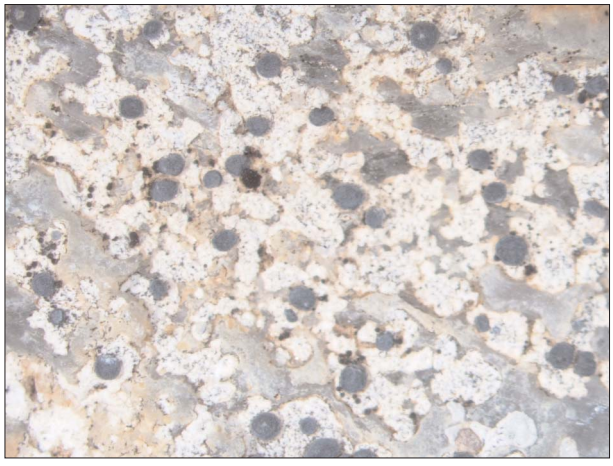

Figure B6:
Buellia spp.

Extreme macro photography of thallus
Photo: Zedda L. & Rambold G. 2000-2005. BIOTA Southern Africa Subproject 04 -Diversity of lichens.
Collection: University of Bayreuth - Museum Botanicum Berolinense

Caloplaca elegantissima (Nyl.) Zahlbr.

Figure B7:
Caloplaca elegantissima (Nyl.) Zahlbr.

Location: Central Namib Desert 20 km NE of Swakopund. On SW-facing rocky slope of Dolerite-Ridge. Nonidas lichen field - No. 3.
Degree ref.: 22 14 BC
Photo: Christoph Schultz, 2002

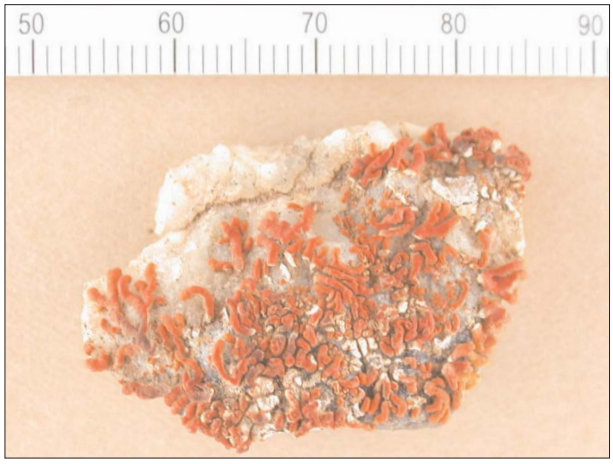

Figure B8:
Caloplaca elegantissima (Nyl.) Zahlbr.

Location: Location: Central Namib Desert SE of Walvisbay, Namib-Naukluft Park. Swartbank on rock. Southern-Naukluft-Plateau lichen field - No. 1.
Degree ref.: 23 15 AA
Photo: Christoph Schultz, 2004
Scale-Bar: Millimeter
Collection: University of Bayreuth - Museum Botanicum Berolinense

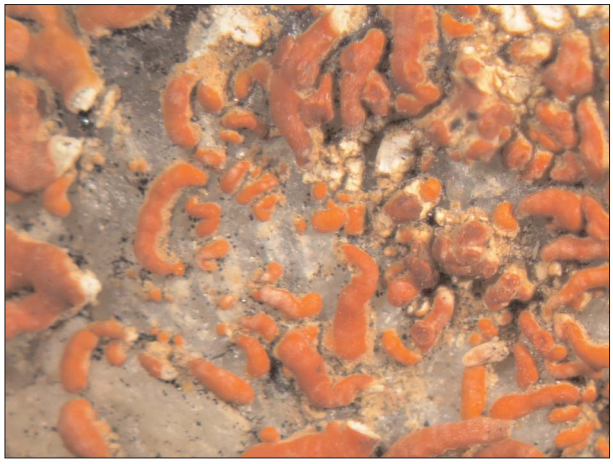

Figure B9:
Caloplaca elegantissima (Nyl.) Zahlbr.

Extreme macro photography of thallus
Photo: Zedda L. & Rambold G. 2000-2005. BIOTA Southern Africa Subproject 04 -Diversity of lichens.
Collection: University of Bayreuth - Museum Botanicum Berolinense

Caloplaca sp.

Figure B10:
Caloplaca sp.

Location: Central Namib Desert E of Swakopund. On fine gravel plain. Nonidas lichen field - No. 3.
Degree ref.: 22 15 AA
Photo: Christoph Schultz, 2004
Scale-Bar: Millimeter
Collection: University of Bayreuth - Museum Botanicum Berolinense

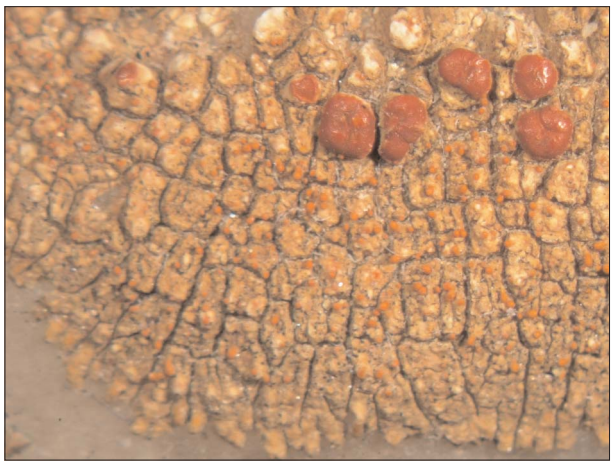

Figure B11:
Caloplaca sp.

Extreme macro photography of thallus
Photo: Zedda L. & Rambold G. 2000-2005. BIOTA Southern Africa Subproject 04 -Diversity of lichens.
Collection: University of Bayreuth - Museum Botanicum Berolinense

Caloplaca namibiensis Kärnefelt

Figure B12:
Caloplaca namibiensis Kärnefelt

Location: Central Namib Desert 40 km N of Swakopund. On SW-facing rocky slope of Dolerite-Ridge. Wlotz-kasbaken lichen field - No. 5.
Degree ref.: 22 14 AD
Photo: Christoph Schultz, 2002

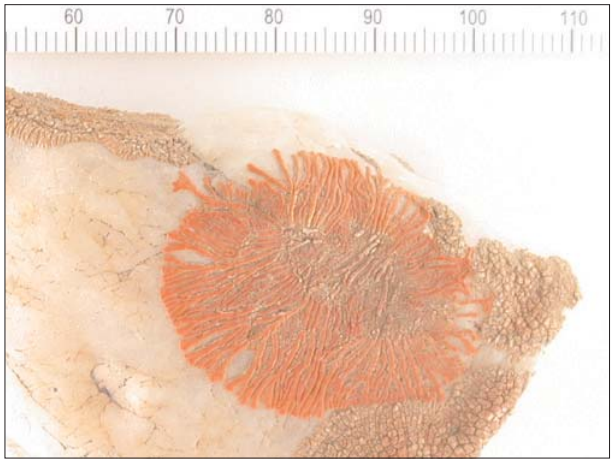

Figure B13:
Caloplaca namibiensis Kärnefelt

Location: Central Namib Desert E of Swakopund. On gravel plain. Nonidas lichen field - No. 3.
Degree ref.: 22 15 AA
Photo: Christoph Schultz, 2004
Scale-Bar: Millimeter
Collection: University of Bayreuth - Museum Botanicum Berolinense

Figure B14:
Caloplaca namibiensis Kärnefelt

Extreme macro photography of thallus
Photo: Zedda L. & Rambold G. 2000-2005. BIOTA Southern Africa Subproject 04 -Diversity of lichens.
Collection: University of Bayreuth - Museum Botanicum Berolinense

Caloplaca regalis

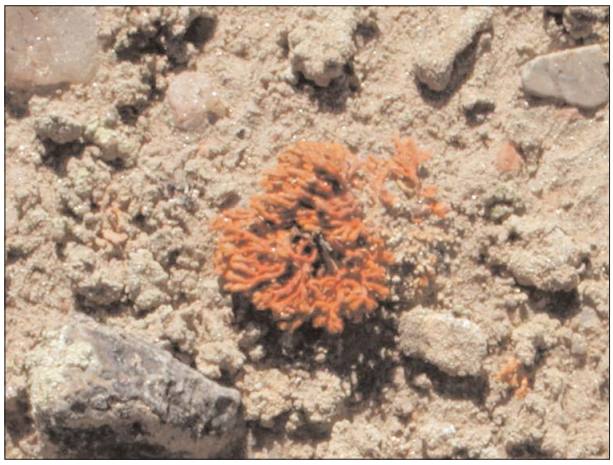

Figure B15:
Caloplaca regalis

Location: Central Namib Desert 20 km SE of Swakopund. On undulating course gypsum / gravel plain. Northern-Naukluft-Plateau lichen field - No. 2.
Degree ref.: 22 14 DA
Photo: Christoph Schultz, 2003

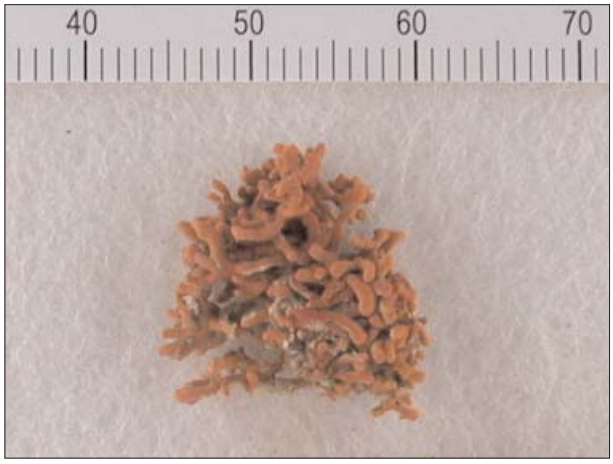

Figure B16:
Caloplaca regalis

Location: Central Namib Desert E of Swakopund. On gravel plain. Nonidas lichen field - No. 3.
Degree ref.: 22 15 AA
Photo: Christoph Schultz, 2004
Scale-Bar: Millimeter
Collection: University of Bayreuth - Museum Botanicum Berolinense

Figure B17:
Caloplaca regalis

Extreme macro photography of thallus
Photo: Zedda L. & Rambold G. 2000-2005. BIOTA Southern Africa Subproject 04 -Diversity of lichens.
Collection: University of Bayreuth - Museum Botanicum Berolinense

Caloplaca volkii Wirth & Vezda

Figure B18:
Caloplaca volkii Wirth & Vezda

Location: Central Namib Desert 20 km SE of Swakopund. On undulating course gyspum / gravel plain. Northern-Naukluft-Plateau lichen field - No. 2.
Degree ref.: 22 14 DA
Photo: Christoph Schultz, 2003

Figure B19:
Caloplaca volkii Wirth & Vezda

Location: Central Namib Desert N of Swakopund. Between Cape Cross and Swakopmund. Fog-rich coastal desert. Jakkalsputz lichen field - No. 6.
Degree ref.: 22 14 AD
Photo: Christoph Schultz, 2004
Scale-Bar: Millimeter
Collection: University of Bayreuth - Museum Botanicum Berolinense

Figure B20:
Caloplaca volkii Wirth & Vezda

Extreme macro photography of thallus
Photo: Zedda L. & Rambold G. 2000-2005. BIOTA Southern Africa Subproject 04 -Diversity of lichens.
Collection: University of Bayreuth - Museum Botanicum Berolinense

Combea mollusca

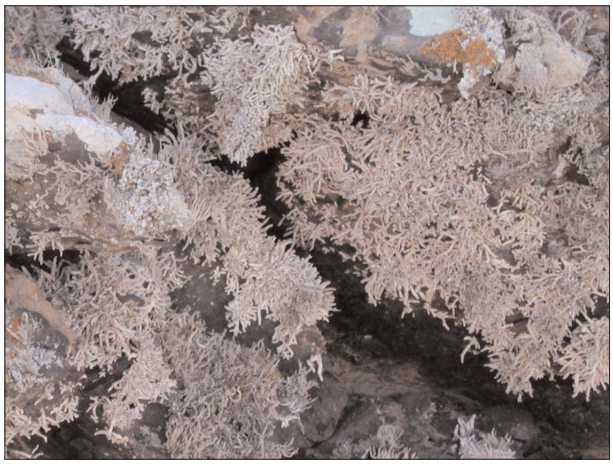

Figure B21:
Combea mollusca

Location: Central Namib Desert 5 km SE of Cape Cross. Cape Cross mountains close to Lagunenberg - sandstone hill close to the sea on SW-facing rocky slope. Cape Cross lichen field - No. 10.
Degree ref.: 21 14 CC
Photo: Christoph Schultz, 2003

Figure B22:
Combea mollusca

Location: Central Namib Desert 5 km SE of Cape Cross. Cape Cross mountains close to Lagunenberg. Cape Cross lichen field - No. 10.
Degree ref.: 21 14 CC
Photo: Christoph Schultz, 2004
Scale-Bar: Millimeter
Collection: University of Bayreuth - Museum Botanicum Berolinense

Figure B23:
Combea mollusca

Extreme macro photography of thallus
Photo: Zedda L. & Rambold G. 2000-2005. BIOTA Southern Africa Subproject 04 -Diversity of lichens.
Collection: University of Bayreuth - Museum Botanicum Berolinense

Coronoplectrum namibicum

Figure B24:
Coronoplectrum namibicum

Location: Central Namib Desert 5 km SE of Cape Cross. Cape Cross mountains close to Lagunenberg - sandstone hill close to the sea on SW-facing rocky slope. Cape Cross lichen field - No. 10.
Degree ref.: 21 14 CC
Photo: Christoph Schultz, 2003

Figure B25:
Coronoplectrum namibicum

Location: Central Namib Desert 5 km SE of Cape Cross. Cape Cross mountains close to Lagunenberg. Cape Cross lichen field - No. 10.
Degree ref.: 21 14 CC
Photo: Christoph Schultz, 2004
Scale-Bar: Millimeter
Collection: University of Bayreuth - Museum Botanicum Berolinense

Figure B26:
Coronoplectrum namibicum

Location: Central Namib Desert 5 km SE of Cape Cross. Cape Cross mountains close to Lagunenberg. Cape Cross lichen field - No. 10.
Degree ref.: 21 14 CC
Photo: Christoph Schultz, 2004
Scale-Bar: Millimeter
Collection: University of Bayreuth - Museum Botanicum Berolinense

Diploschistes sp.

Figure B27:
Diploschistes sp.

Location: Central Namib Desert SE of Swakopmund, Namib-Naukluft Park. Along Kuiseb River ca. 25 km NW of Gobabeb. On soil on slope. Southern-Naukluft-Plateau lichen field - No. 1.
Degree ref.: 23 14 BC
Photo: Christoph Schultz, 2004
Scale-Bar: Millimeter
Collection: University of Bayreuth - Museum Botanicum Berolinense

Figure B28:
Diploschistes sp.

Extreme macro photography of thallus
Photo: Zedda L. & Rambold G. 2000-2005. BIOTA Southern Africa Subproject 04 -Diversity of lichens.
Collection: University of Bayreuth - Museum Botanicum Berolinense

Paraparmelia spp.

Figure B29:
Paraparmelia spp.

Location: Central Namib Desert 20 km NE of Horing Bay. On course gravel plain. Brandberg-West lichen field - No. 11.
Degree ref.: 21 14 AC
Photo: Christoph Schultz, 2003

Figure B30:
Paraparmelia spp.

Location: Central Namib Desert 30 km NE of Henties Bay. On course gravel plain. Jakkalsputz lichen field - No. 6.
Degree ref.: 21 14 DC
Photo: Christoph Schultz, 2003

Figure B31:
Paraparmelia spp.

Location: Central Namib Desert N of Swakopund. Between Cape Cross and Swakopmund. Fog-rich coastal desert.. Brandberg-West lichen field - No. 11.
Degree ref.: 21 14 AC
Photo: Christoph Schultz, 2004
Scale-Bar: Millimeter
Collection: University of Bayreuth - Museum Botanicum Berolinense

Lecidea s. lat.

Figure B32:
Lecidea s. lat.

Location: Central Namib Desert 40 km NE of Horing Bay. On Messum River Terraces. Brandberg-West lichen field - No. 11.
Degree ref.: 21 14 AC
Photo: Christoph Schultz, 2003

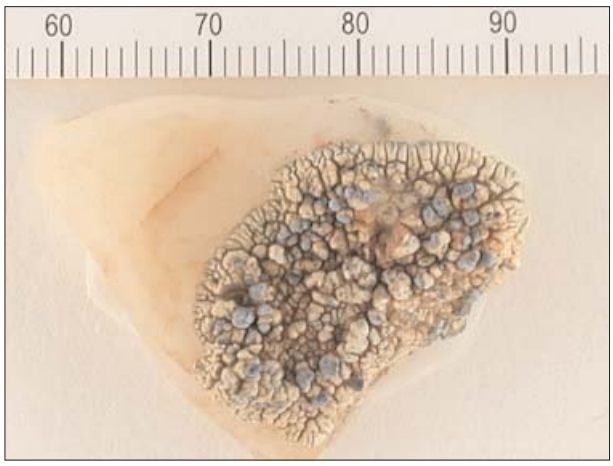

Figure B33:
Lecidea s. lat.

Location: Central Namib Desert E of Swakopund. On fine gravel plain. Nonidas lichen field - No. 3.
Degree ref.: 22 15 AA
Photo: Christoph Schultz, 2004
Scale-Bar: Millimeter
Collection: University of Bayreuth - Museum Botanicum Berolinense

Figure B34:
Lecidea s. lat.

Extreme macro photography of thallus
Photo: Zedda L. & Rambold G. 2000-2005. BIOTA Southern Africa Subproject 04 -Diversity of lichens.
Collection: University of Bayreuth - Museum Botanicum Berolinense

Lecidella crystallina Wirth & Vezda

Figure B35:
Lecidella crystallina Wirth & Vezda

Location: Central Namib Desert 10 km SE of Swakopund. On undulating course gyspum / gravel plain. Northern-Naukluft-Plateau lichen field - No. 2.
Growth Form: Extremely wind blown pattern of loose thalli, with maximum diameters of 1 cm.
Degree ref.: 22 14 DB
Photo: Christoph Schultz, 2003

Figure B36:
Lecidella crystallina Wirth & Vezda

Location: Central Namib Desert 20 km SE of Swakopund. On undulating course gyspum / gravel plain. Northern-Naukluft-Plateau lichen field - No. 2.
Growth Form: Wind blown pattern of loose thalli, with maximum diameters of 2 cm.
Degree ref.: 22 14 DB
Photo: Christoph Schultz, 2003

Figure B37:
Lecidella crystallina Wirth & Vezda

Location: Central Namib Desert 30 km SE of Swakopund. On undulating course gyspum / gravel plain. Northern-Naukluft-Plateau lichen field - No. 2.
Growth Form: Thalli firmly fixed to the ground with maximum diameters of 4 cm. In some areas many thalli have grown to cover an area of 10 to 30 cm - see Figure B38 for example. Almost full ground coverage.
Degree ref.: 22 14 DB
Photo: Christoph Schultz, 2003

Lecidella crystallina Wirth & Vezda

Figure B38:
Lecidella crystallina Wirth & Vezda

Location: Central Namib Desert 20 km SE of Swakopund. On undulating course gyspum / gravel plain. Northern-Naukluft-Plateau lichen field - No. 2.
Degree ref.: 22 14 DB
Photo: Christoph Schultz, 2003

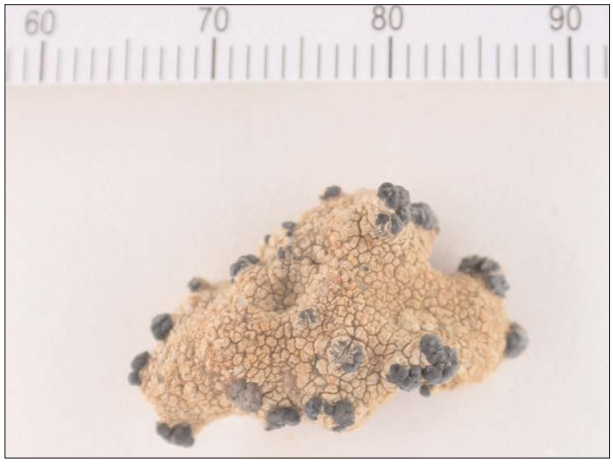

Figure B39:
Lecidella crystallina Wirth & Vezda

Location: Central Namib Desert E of Swakopund. On gravel plain. Nonidas lichen field - No. 3.
Degree ref.: 22 15 AA
Photo: Christoph Schultz, 2004
Scale-Bar: Millimeter
Collection: University of Bayreuth - Museum Botanicum Berolinense

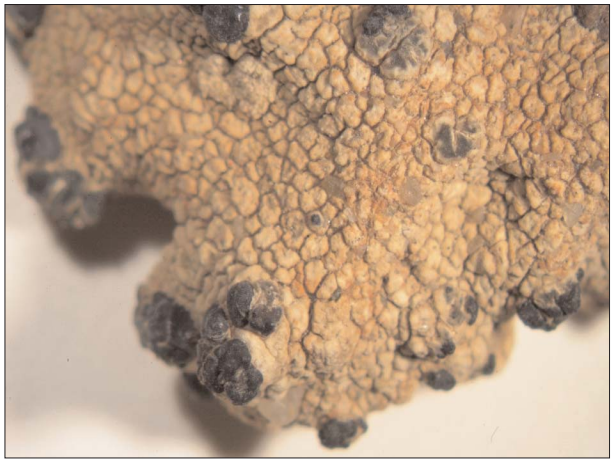

Figure B40:
Lecidella crystallina Wirth & Vezda

Extreme macro photography of thallus
Photo: Zedda L. & Rambold G. 2000-2005. BIOTA Southern Africa Subproject 04 -Diversity of lichens.
Collection: University of Bayreuth - Museum Botanicum Berolinense

Neofuscelia dregeana gr.

Figure B41:
Neofuscelia dregeana gr.

Location: Location: Central Namib Desert SE of Walvisbay, Namib-Naukluft Park. On coarse gravel undulating gravel plain. Southern-Naukluft-Plateau lichen field - No. 1.
Degree ref.: 22 14 DB
Photo: Christoph Schultz, 2003

Figure B42:
Neofuscelia dregeana gr.

Location: Central Namib Desert 10 km E of Swakopund. On fine gravel plain. Northern-Naukluft-Plateau lichen field - No. 2.
Degree ref.: 22 14 DA
Photo: Christoph Schultz, 2004
Scale-Bar: Millimeter
Collection: University of Bayreuth - Museum Botanicum Berolinense

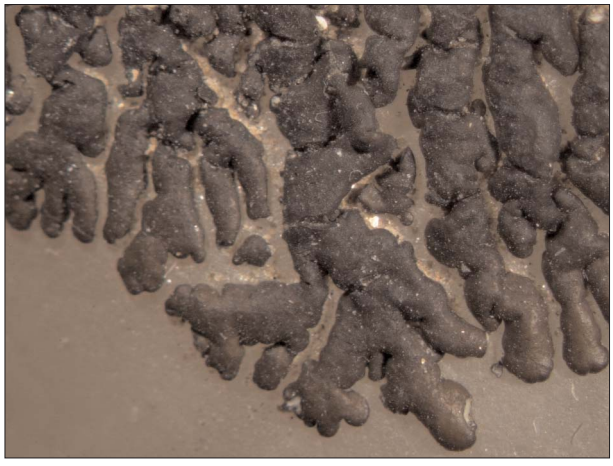

Figure B43:
Neofuscelia dregeana gr.

Extreme macro photography of thallus
Photo: Zedda L. & Rambold G. 2000-2005. BIOTA Southern Africa Subproject 04 -Diversity of lichens.
Collection: University of Bayreuth - Museum Botanicum Berolinense

Ramalina sp.

Figure B44:
Ramalina sp.

Location: Central Namib Desert, Skeleton-Coast Park. On low marble outcrops close to the sea, N of entrace gate at Ugabmond. Huabmond lichen field - No. 12.
Degree ref.: 21 13 BA
Photo: Christoph Schultz, 2003

Figure B45:
Ramalina sp.

Location: Central Namib Desert 10 km NE of Cape Cross. Grouped with Teloschistes Capensis. Cape Cross lichen field - No. 10.
Degree ref.: 22 13 DB
Photo: Christoph Schultz, 2003

Figure B46:
Ramalina sp.

Location: Central Namib Desert 37 km S of Henties Bay near Wlotzkasbaken. Grouped with Teloschistes Capensis. Wlotzkasbaken lichen field - No. 5.
Degree ref.: 22 14 AD
Photo: Christoph Schultz, 2004
Scale-Bar: Millimeter
Collection: University of Bayreuth - Museum Botanicum Berolinense

Santessonia spp.

Figure B47:
Santessonia spp.

Location: Location: Central Namib Desert SE of Walvisbay, Namib-Naukluft Park. On coarse gravel undulating gravel plain. Southern-Naukluft-Plateau lichen field - No. 1.
Degree ref.: 22 14 DB
Photo: Christoph Schultz, 2003

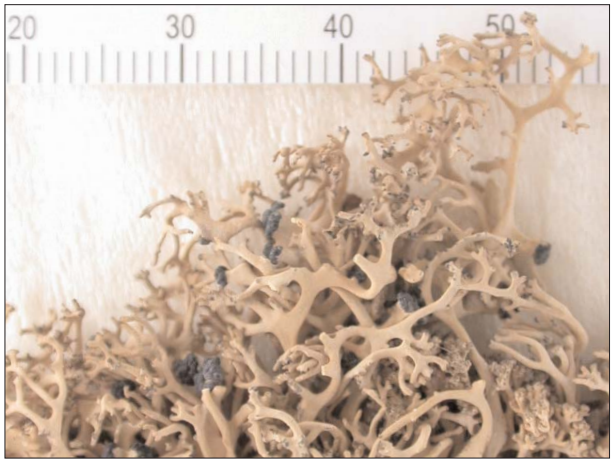

Figure B48:
Santessonia spp.

Location: Location: Central Namib Desert, Skeleton-Coast Park. On low marble outcrops close to the sea, N of entrace gate at Ugabmond. Huabmond lichen field - No. 12.
Degree ref.: 21 13 BA
Photo: Christoph Schultz, 2004
Scale-Bar: Millimeter
Collection: University of Bayreuth - Museum Botanicum Berolinense

Figure B49:
Santessonia spp.

Extreme macro photography of thallus
Photo: Zedda L. & Rambold G. 2000-2005. BIOTA Southern Africa Subproject 04 -Diversity of lichens.
Collection: University of Bayreuth - Museum Botanicum Berolinense

Santessonia sorediata

Figure B50:
Santessonia sorediata

Location: Central Namib Desert 40 km NE of Horing Bay. On Messum River Terraces. Brandberg-West lichen field - No. 11.
Degree ref.: 21 14 AC
Photo: Christoph Schultz, 2003

Figure B51:
Santessonia sorediata

Location: Location: Central Namib Desert, 2 km N of Cape Cross. On boulders on NW-facing hillslope ca. 2 km E of the road. Cape Cross lichen field - No. 10.
Degree ref.: 21 14 CA
Photo: Christoph Schultz, 2004
Scale-Bar: Millimeter
Collection: University of Bayreuth - Museum Botanicum Berolinense

Figure B52:
Santessonia sorediata

Extreme macro photography of thallus
Photo: Zedda L. & Rambold G. 2000-2005. BIOTA Southern Africa Subproject 04 -Diversity of lichens.
Collection: University of Bayreuth - Museum Botanicum Berolinense

Teloschistes capensis (L.f.) Müll. Arg.

Figure B53:
Teloschistes capensis (L.f.) Müll. Arg.

Location: Central Namib Desert 20 km NE of Cape Cross. On coarse gravel plain. Messum Crater / Orawab lichen field - No. 9.
Growth Form: Clusters of individual thalli are grown together as a tuft and are up to 5cm tall with a diameter of up to 8 cm.
Degree ref.: 21 14 CB
Photo: Christoph Schultz, 2003

Figure B54:
Teloschistes capensis (L.f.) Müll. Arg.

Location: Central Namib Desert 20 km N of Cape Cross. On fine gravel plain. Cape Cross lichen field - No. 10.
Growth Form: Numerous thalli growing in close association as cushions covering an area of 10 to 30 cm. As an amalgation some of these cushions form mats with ribbon-like or polygon shape.
Degree ref.: 21 13 DB
Photo: Christoph Schultz, 2003

Figure B55:
Teloschistes capensis (L.f.) Müll. Arg.

Location: Central Namib Desert 40 km N of Swakopund. On fine gravel plain. Wlotzkasbaken lichen field - No. 5.
Growth Form: After recent strong Foehn-Winds many thallus pieces have accumulated around single low lying cormophytes or higher plants as well as their dead remains. This wind-blown growth form is believed to be the begining of lichen mats.
Degree ref.: 22 14 AD
Photo: Christoph Schultz, 2003

Teloschistes capensis (L.f.) Müll. Arg.

Figure B56:
Teloschistes capensis (L.f.) Müll. Arg.

Location: Central Namib Desert 20 km N of Cape Cross. On fine gravel plain. Cape Cross lichen field - No. 10.
Degree ref.: 21 13 DB
Photo: Christoph Schultz, 2003

Figure B57:
Teloschistes capensis (L.f.) Müll. Arg.

Location: Central Namib Desert 40 km N of Swakopund. On fine gravel plain. Wlotzkasbaken lichen field - No. 5.
Degree ref.: 22 14 AD
Photo: Christoph Schultz, 2004
Scale-Bar: Millimeter
Collection: University of Bayreuth - Museum Botanicum Berolinense

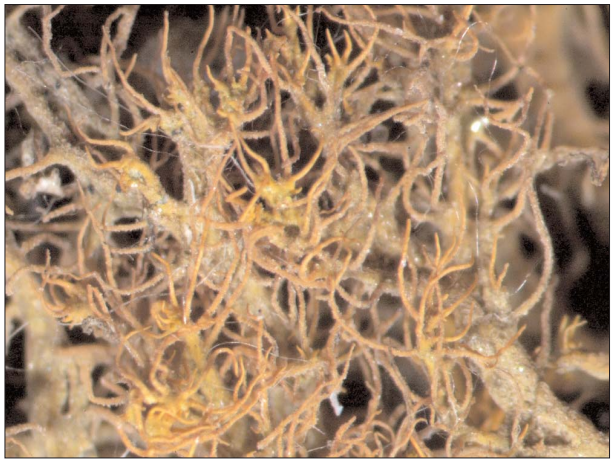

Figure B58:
Teloschistes capensis (L.f.) Müll. Arg.

Extreme macro photography of thallus
Photo: Zedda L. & Rambold G. 2000-2005. BIOTA Southern Africa Subproject 04 -Diversity of lichens.
Collection: University of Bayreuth - Museum Botanicum Berolinense

Xanthomaculina hottentotta

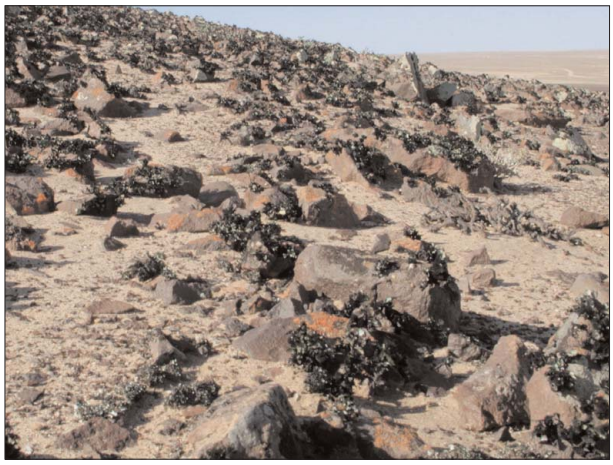

Figure B59:
Xanthomaculina hottentotta

Location: Central Namib Desert 30 km NE of Cape Cross. On SW-facing hill-slope. Messum Crater / Orawab lichen field - No. 9.
Degree ref.: 21 13 DB
Photo: Christoph Schultz, 2003

Figure B60:
Xanthomaculina hottentotta

Location: Central Namib Desert 20 km NE of Cape Cross. On coarse gravel. Messum Crater / Orawab lichen field - No. 9.
Degree ref.: 21 14 CB
Photo: Christoph Schultz, 2003

Figure B61:
Xanthomaculina hottentotta

Location: Central Namib Desert 10 km E of Swakopund. On coarse gravel. Southern-Naukluft-Plateau lichen field - No. 2.
Degree ref.: 22 14 DA
Photo: Christoph Schultz, 2004
Scale-Bar: Millimeter
Collection: University of Bayreuth - Museum Botanicum Berolinense

Xanthomaculina convoluta

Figure B62:
Xanthomaculina convoluta

Location: Central Namib Desert 30 km SE of Swakopund. On undulating course gyspum / gravel plain. Northern-Naukluft-Plateau lichen field - No. 2.
Degree ref.: 22 14 DB
Photo: Christoph Schultz, 2003

Figure B63:
Xanthomaculina convoluta

Location: Central Namib Desert 30 km SE of Swakopund. On undulating course gyspum / gravel plain. Northern-Naukluft-Plateau lichen field - No. 2.
Degree ref.: 22 14 DB
Photo: Christoph Schultz, 2002

Figure B64:
Xanthomaculina convoluta

Location: Central Namib Desert 10 km SE of Swakopund. On undulating course gyspum / gravel plain. Northern-Naukluft-Plateau lichen field - No. 2.
Degree ref.: 22 14 BD
Photo: Christoph Schultz, 2004
Scale-Bar: Millimeter
Collection: University of Bayreuth - Museum Botanicum Berolinense

Xanthoparmelia spp.

Figure B65:
Xanthoparmelia spp.

Location: Central Namib Desert 10 km NE of Jakkalsputz. On fine quartz gravel plain. Jakkalsputz lichen field - No. 2.
Growth Form: With small fruticose and crustose lichens interspersed *Xanthoparmelia walteri Knox*-thalli of about 3 cm in diameter shows almost full ground coverage.
Bare soil shows on dirt-road where cover has been distroyed.
Degree ref.: 22 14 DB
Photo: Christoph Schultz, 2003

Figure B66:
Xanthoparmelia spp.

Location: Central Namib Desert 2 km E of Mile 72. Mile 72 lichen field - No. 8.
Growth Form: Almost pure stand of *Xanthoparmelia walteri Knox* of about 5 cm in diameter shows high ground coverage. For detail see Figure B67 below.
Degree ref.: 22 14 AB
Photo: Christoph Schultz, 2003

Figure B67:
Xanthoparmelia spp.

Location: Central Namib Desert 2 km E of Mile 72. Mile 72 lichen field - No. 8.
Degree ref.: 22 14 AB
Photo: Christoph Schultz, 2003

Xanthoparmelia spp.

Figure B68:
Xanthoparmelia spp.

Location: Central Namib Desert 20 km NE of Swakopund. On undulating course gyspum / gravel plain. Nonidas lichen field - No. 3.
Degree ref.: 22 14 DA
Photo: Christoph Schultz, 2003

Figure B69:
Xanthoparmelia spp.

Location: Central Namib Desert 5 km SE of Cape Cross. Cape Cross mountains close to Lagunenberg. Cape Cross lichen field - No. 10.
Degree ref.: 21 14 CC
Photo: Christoph Schultz, 2004

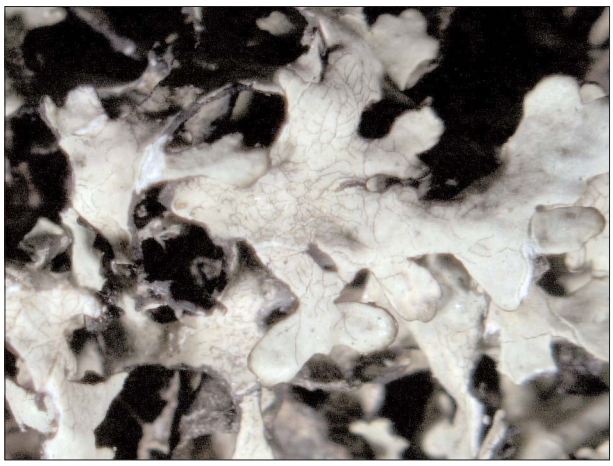

Figure B70:
Xanthoparmelia spp.

Extreme macro photography of thallus
Photo: Zedda L. & Rambold G. 2000-2005. BIOTA Southern Africa Subproject 04 -Diversity of lichens.
Collection: University of Bayreuth - Museum Botanicum Berolinense

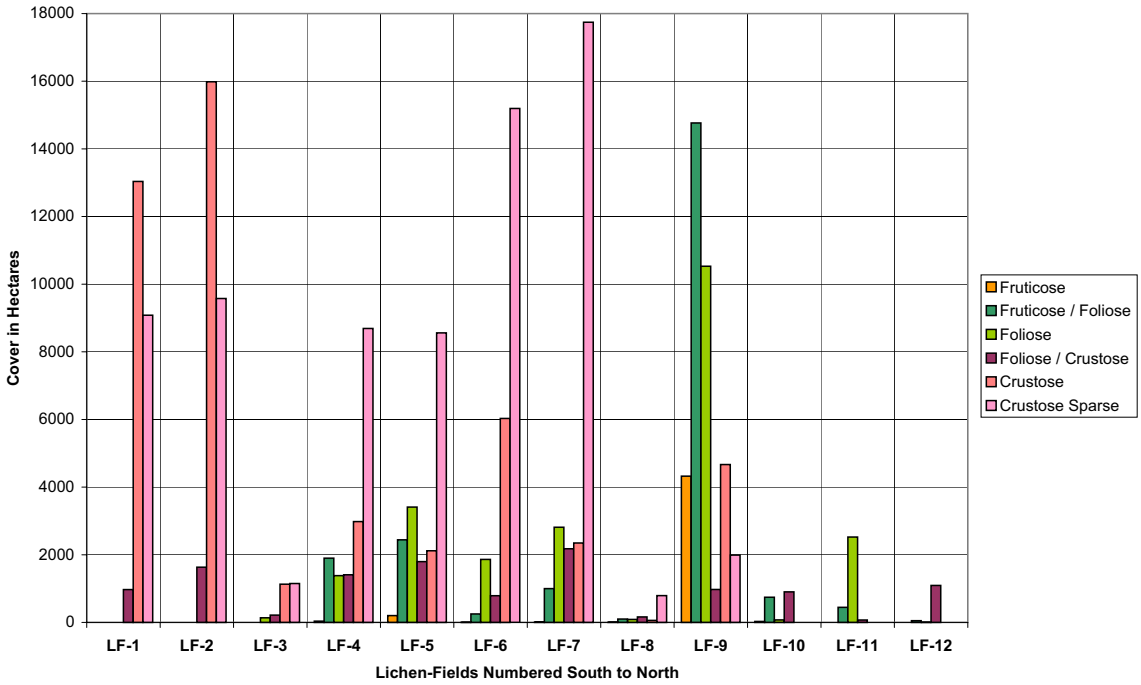

Figure C1: Unitemporal classification 2003 - Comparison of lichen community coverage per lichen-field.

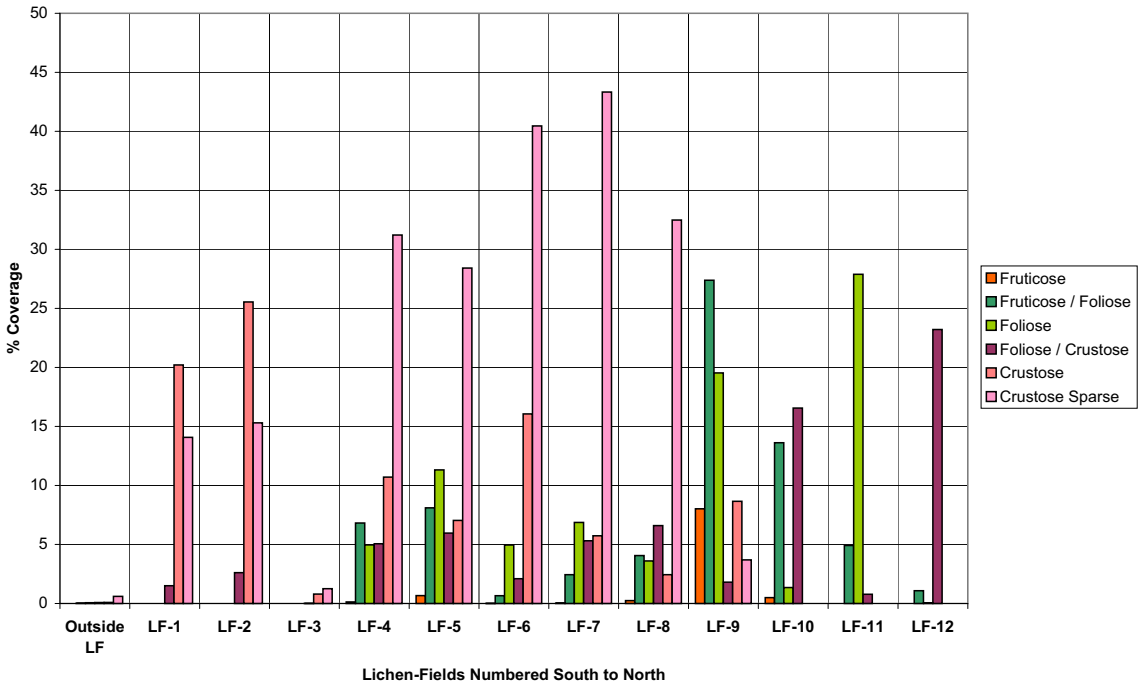

Figure C2: Unitemporal classification 2003 - Comparison of lichen community coverage per total lichen-field area.

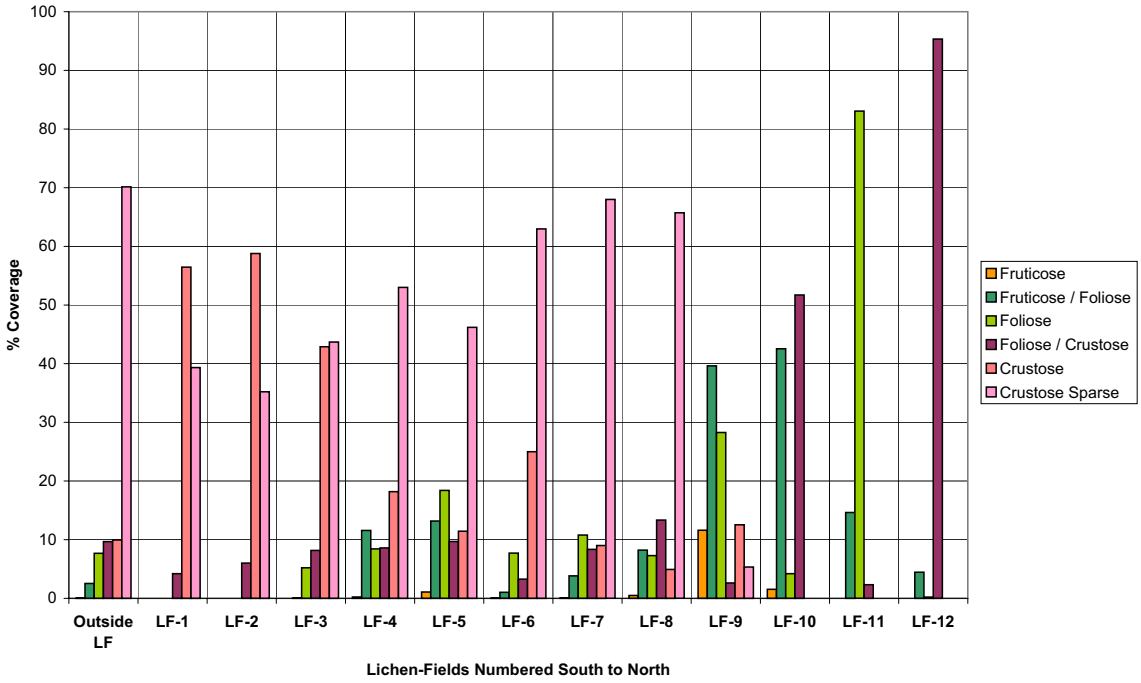

Figure C3: Unitemporal classification 2003 - Comparison of lichen community coverage per lichen-covered area per lichen-field.

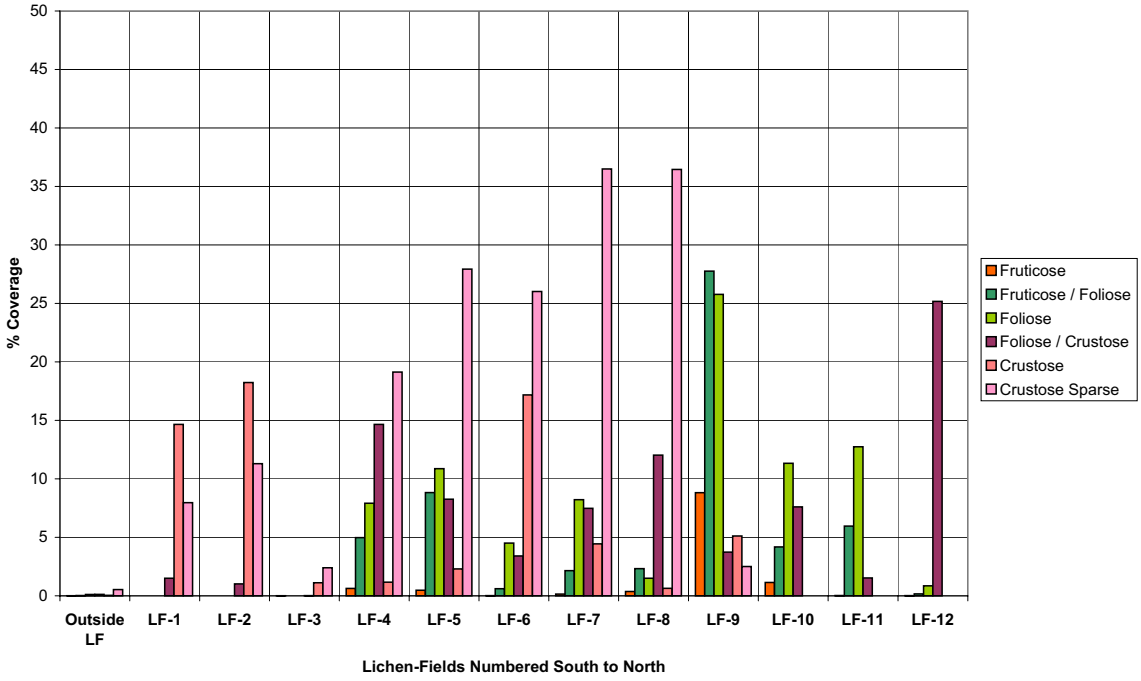

Figure D1: Multitemporal Classification 2003 - Comparison of Lichen Community Coverage per Total Lichen-Field Area.

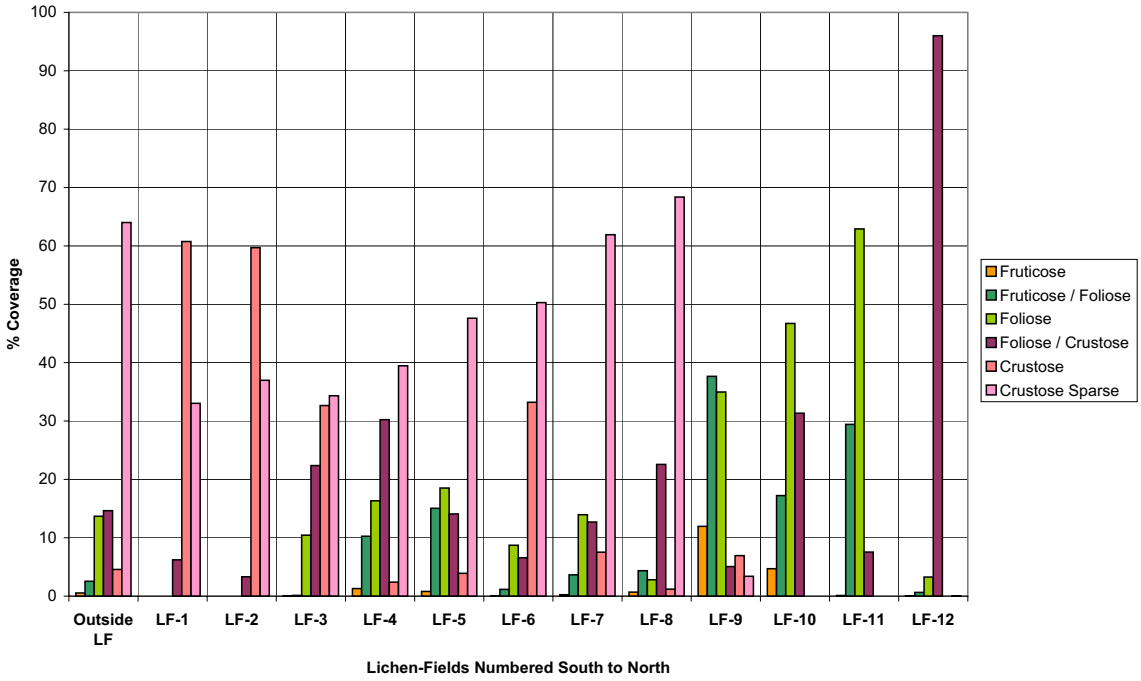

Figure D2: Multitemporal Classification 2003 - Comparison of Lichen Community Coverage per Lichen-Covered Area per Lichen-Field.

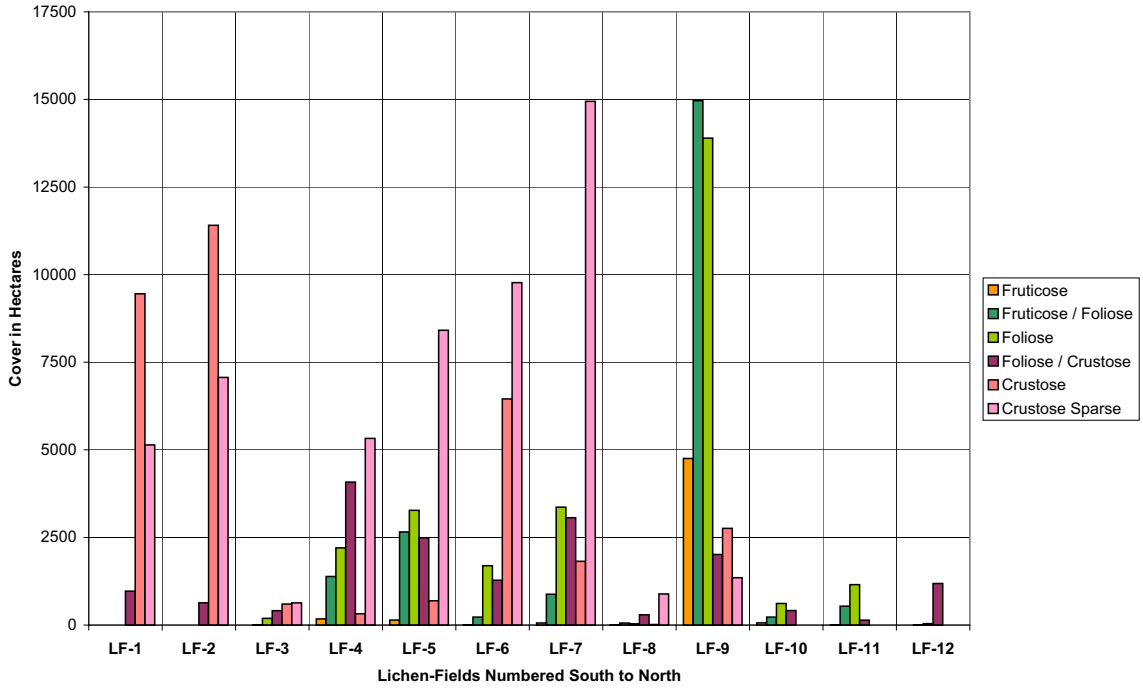

Figure D3: Multitemporal Classification 2003 - Comparison of Lichen Community Coverage per Lichen-Field.

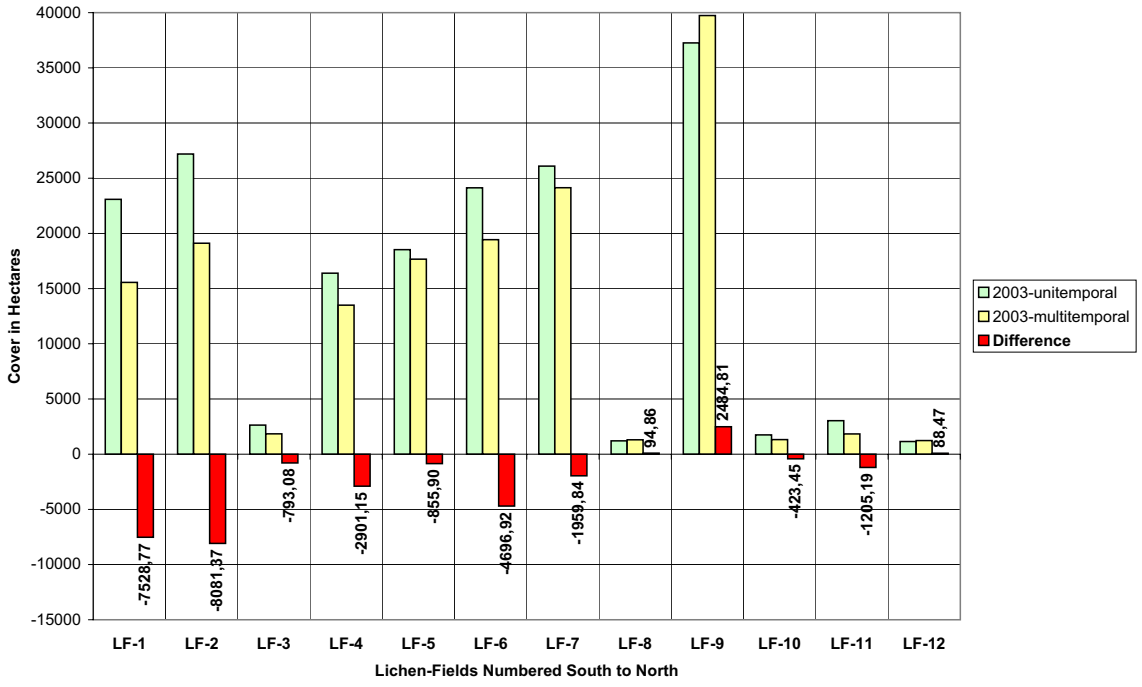

Figure D4: Comparison of Total Lichen Coverage per Lichen-Field 2003-multitemporal MINUS 2003-unitemporal.

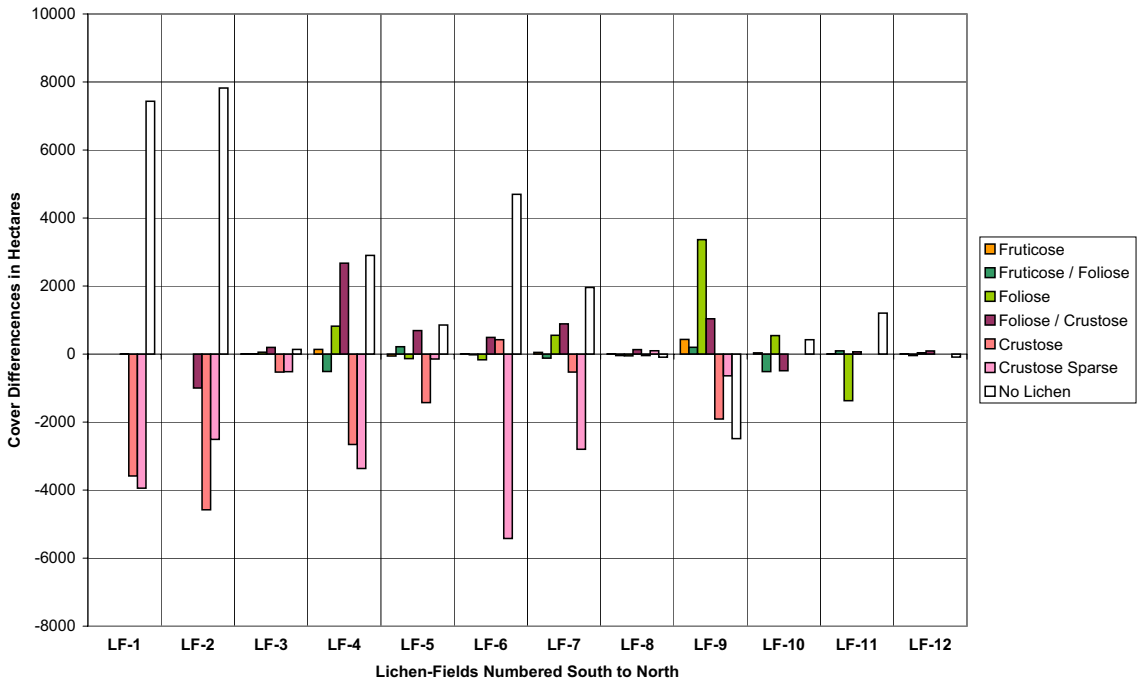

Figure D5: Comparison of Lichen Community Coverage per Lichen-Field 2003-multitempral MINUS 2003-unitemporal.

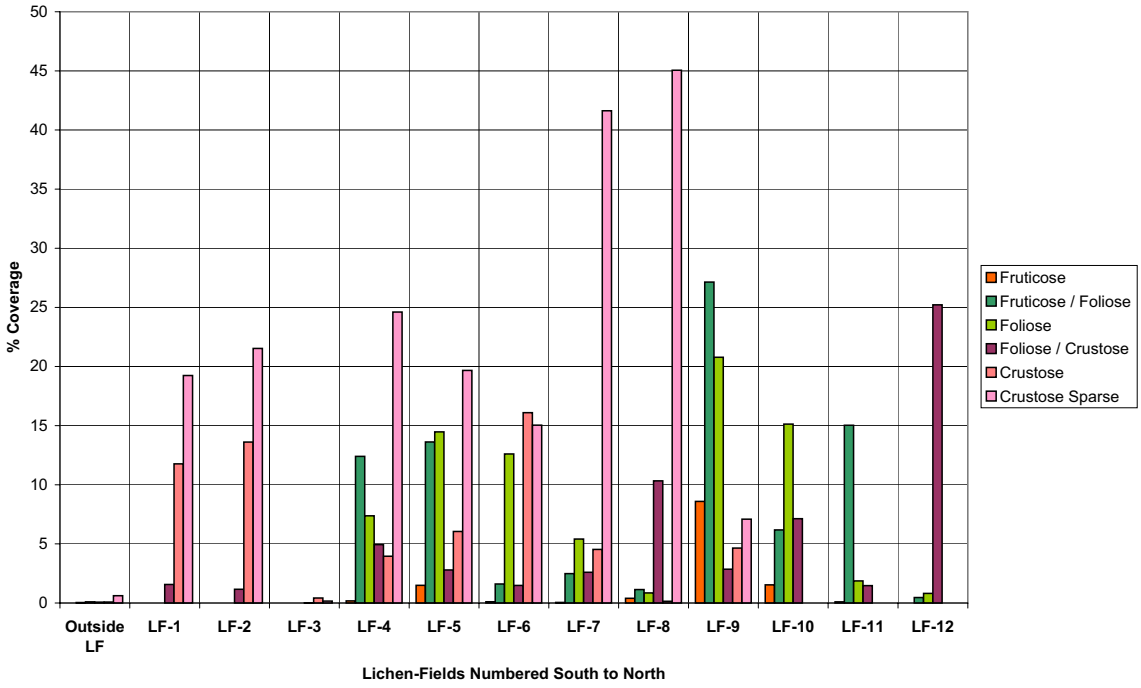

Figure D6: Multitemporal Classification 2000 - Comparison of Lichen Community Coverage per Total Lichen-Field Area.

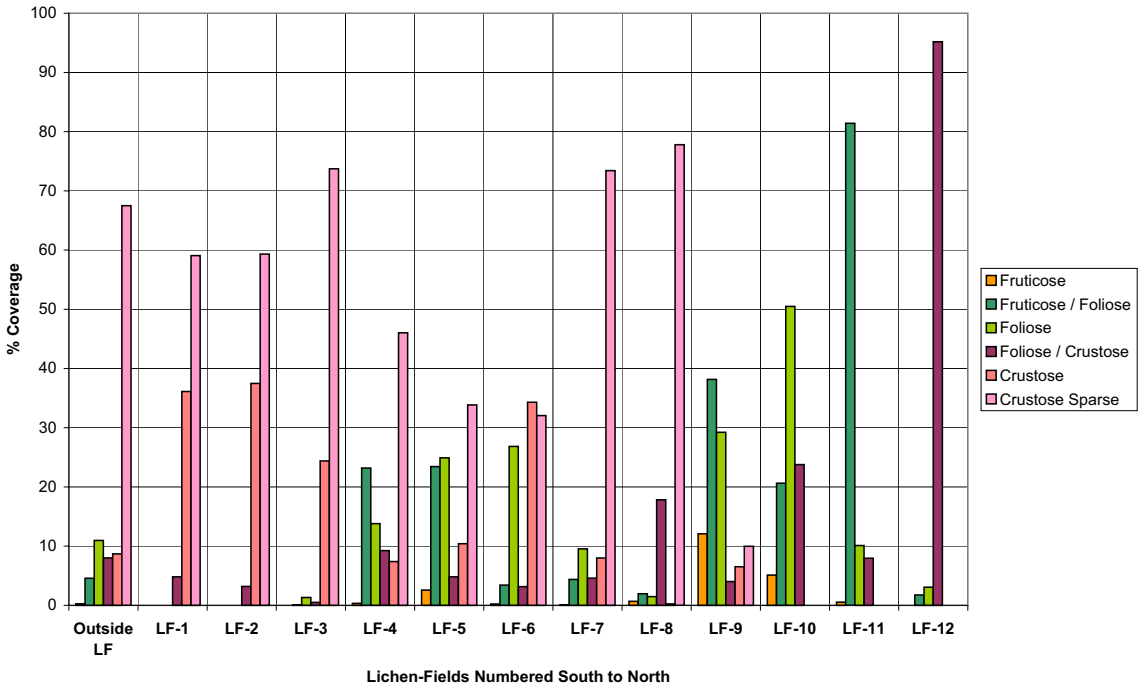

Figure D7: Multitemporal Classification 2000 - Comparison of Lichen Community Coverage per Lichen-Covered Area per Lichen-Field.

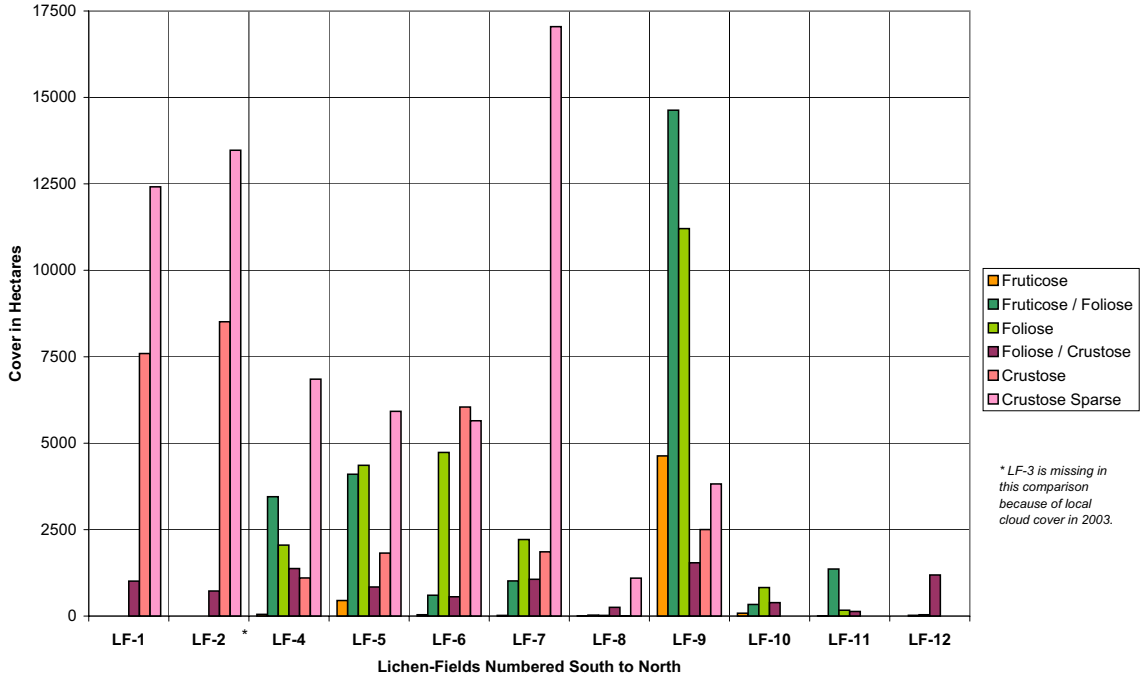

Figure D8: Multitemporal Classification 2000 - Comparison of Lichen Community Coverage per Lichen-Field.

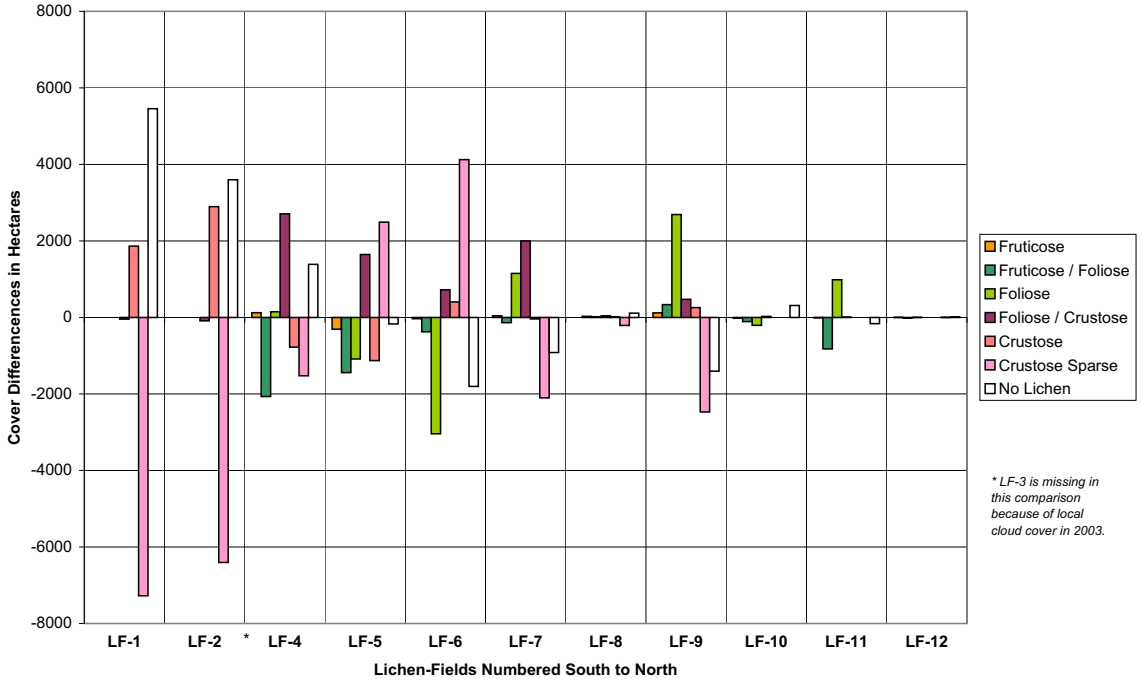

Figure D9: Classification Comparison of Lichen Community Coverage per Lichen-Field 2003-multitemporal MINUS 2000-multitemporal.

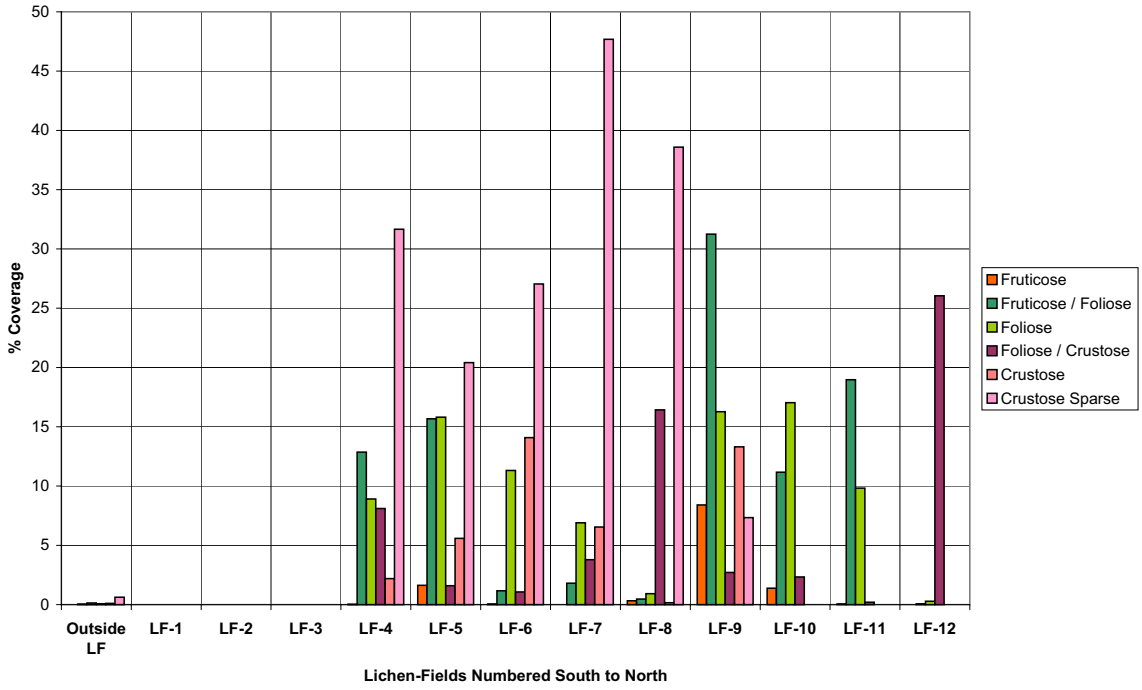

Figure D10: Multitemporal Classification 1999 - Comparison of Lichen Community Coverage per Total Lichen-Field Area.

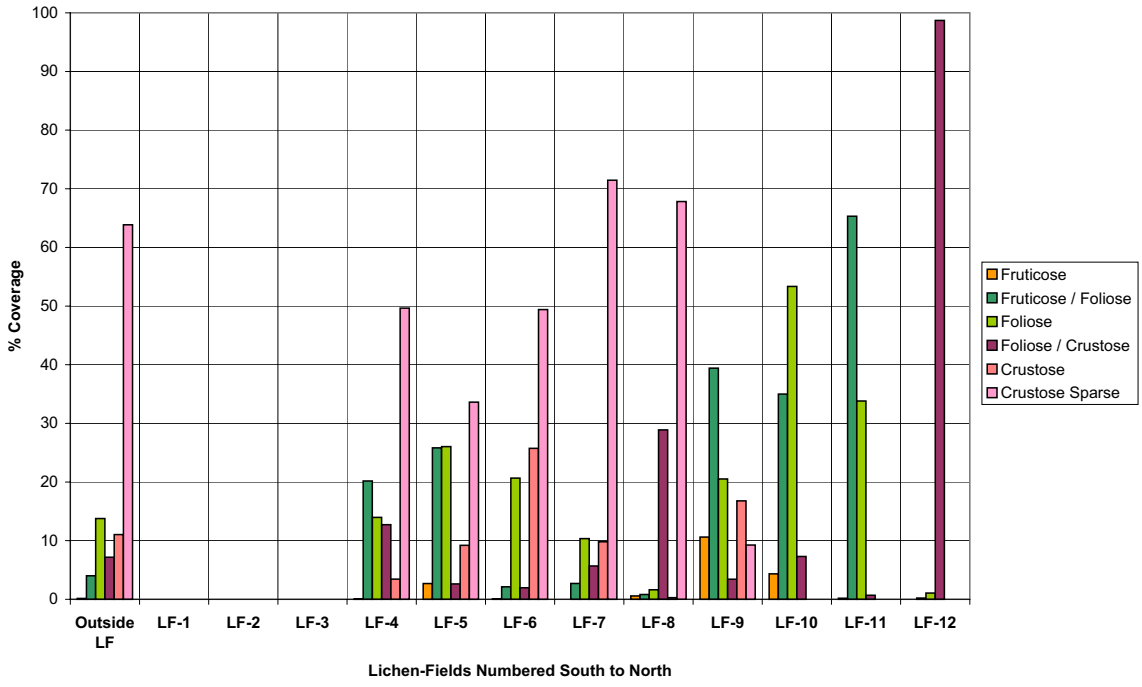

Figure D11: Multitemporal Classification 1999 - Comparison of Lichen Community Coverage per Lichen-Covered Area per Lichen-Field.

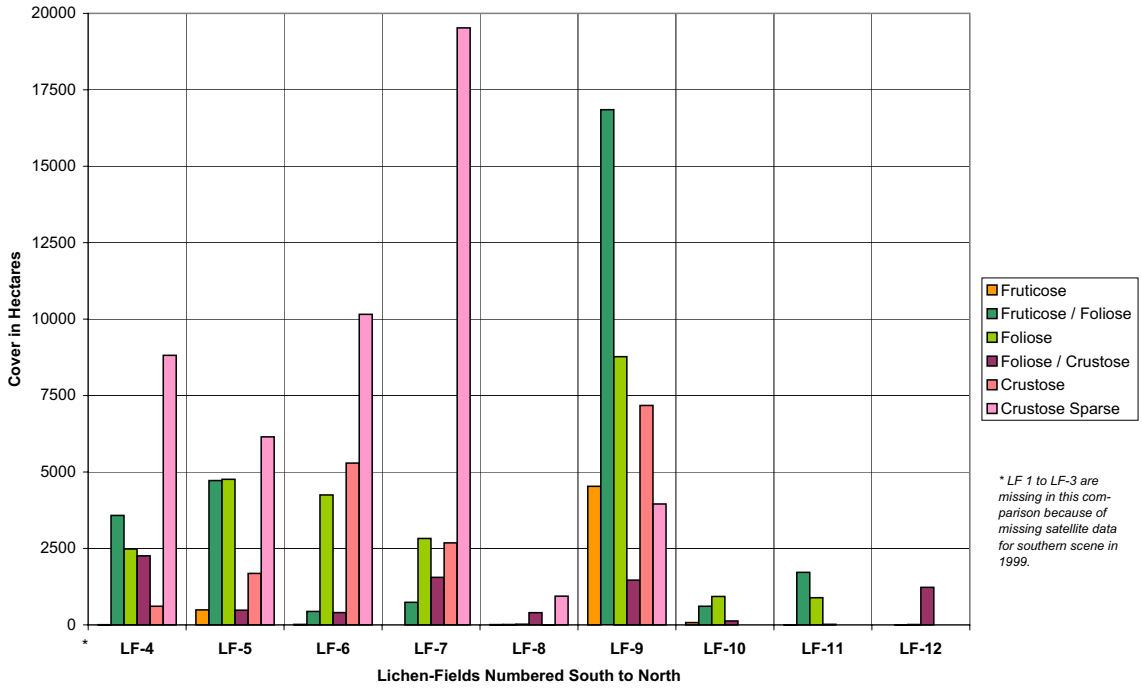

Figure D12: Multitemporal Classification 1999 -Comparison of Lichen Community Coverage per Lichen-Field.

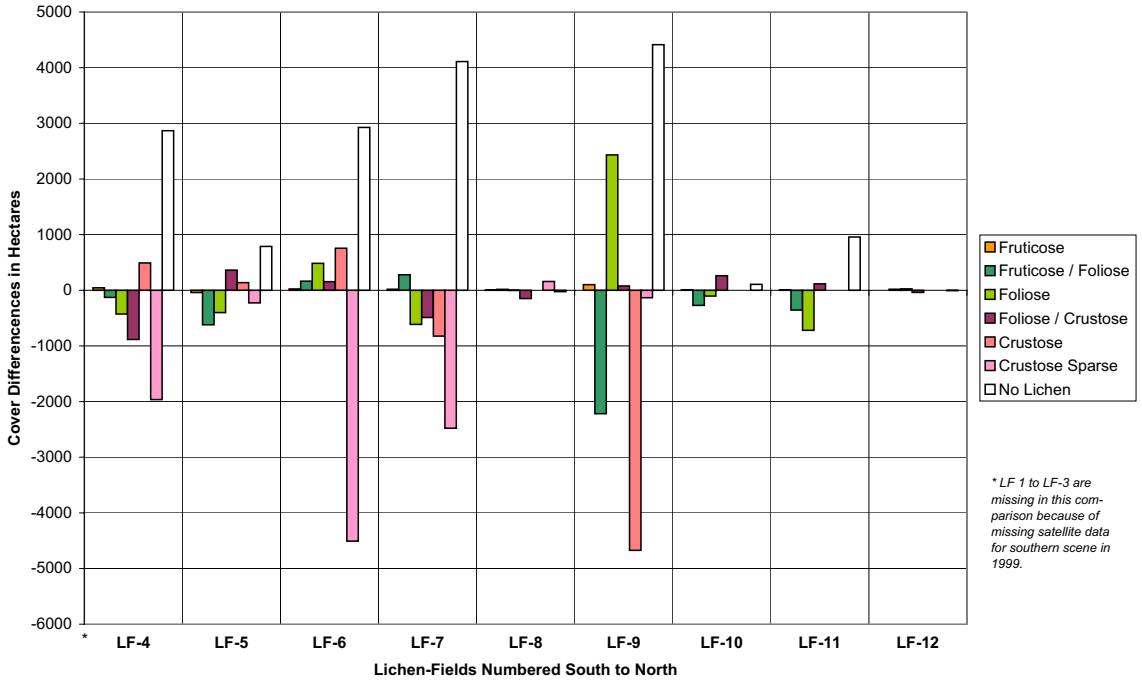

Figure D13: Classification Comparison of Lichen Community Coverage per Lichen-Field 2000-multitemporal MINUS 1999-multitemporal.

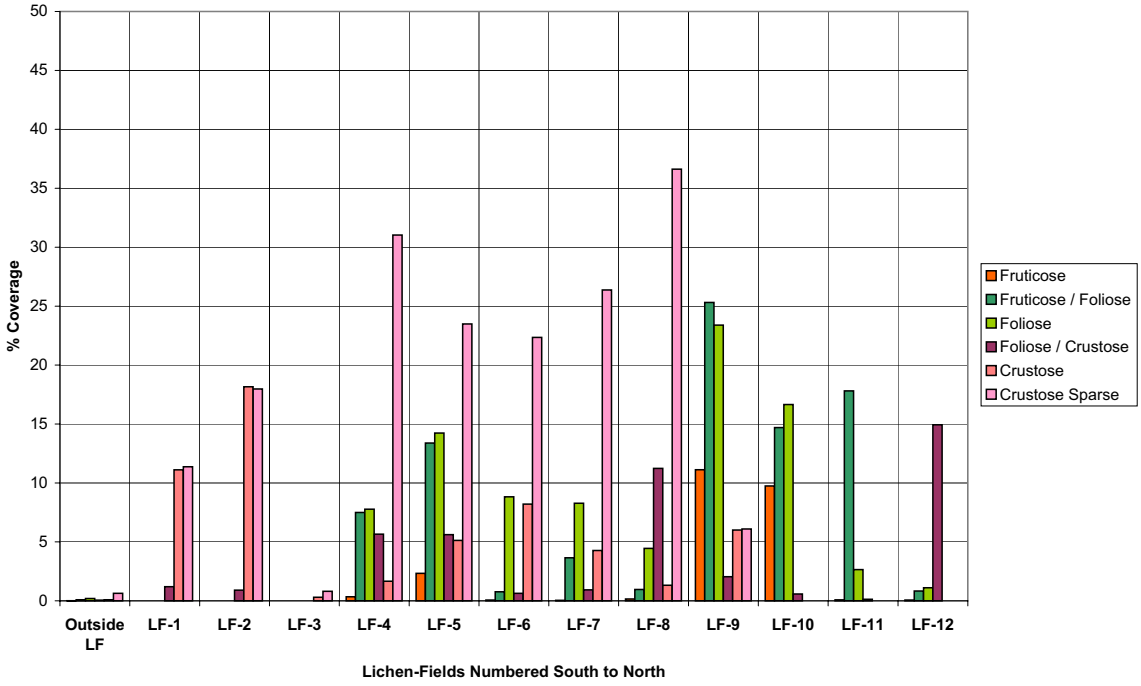

Figure D14: Multitemporal Classification 1991/92 - Comparison of Lichen Community Coverage per Total Lichen-Field Area.

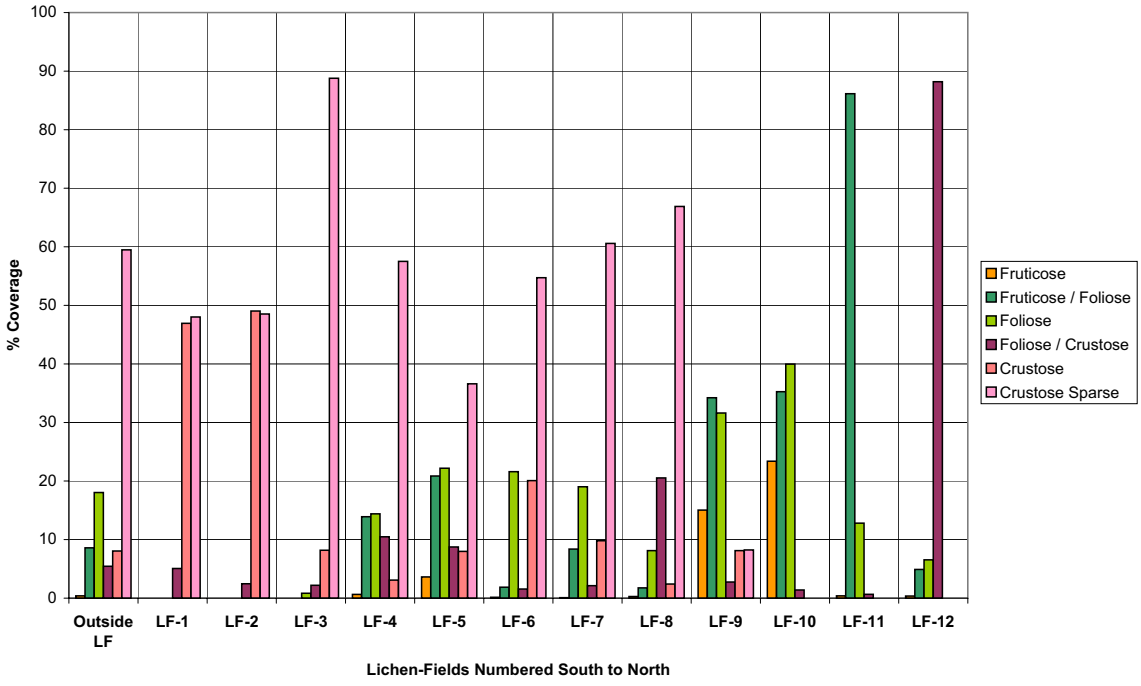

Figure D15: Multitemporal Classification 1991/92 - Comparison of Lichen Community Coverage per Lichen-Covered Area per Lichen-Field.

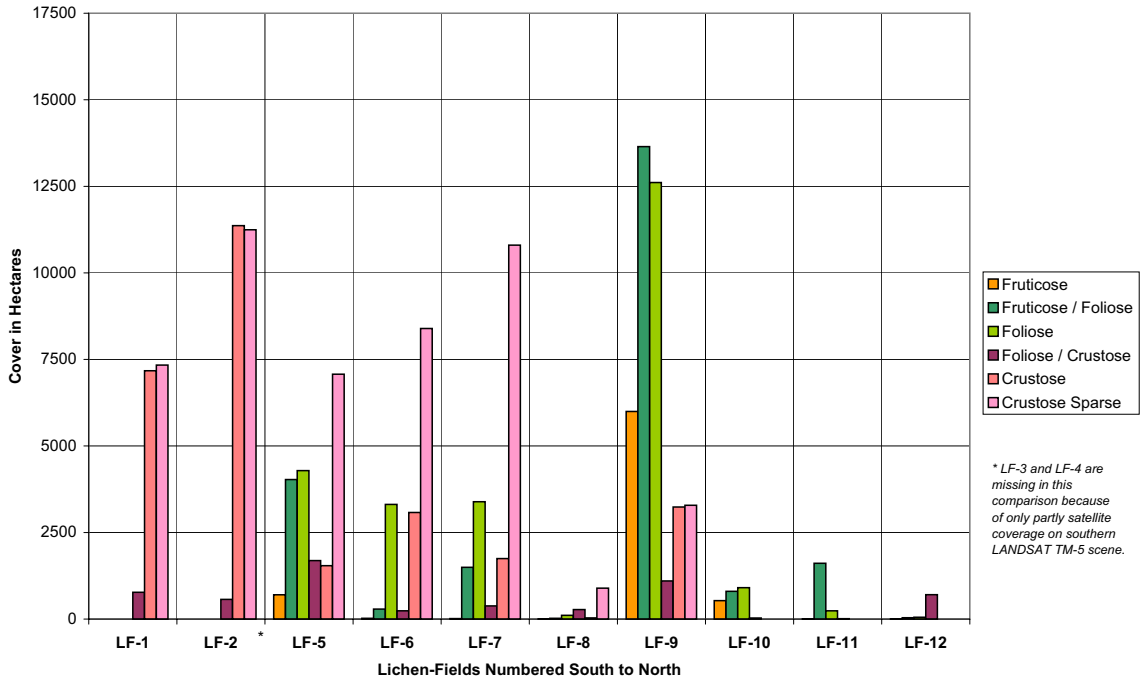

Figure D16: Multitemporal Classification 1991/92 - Comparison of Lichen Community Coverage per Lichen-Field.

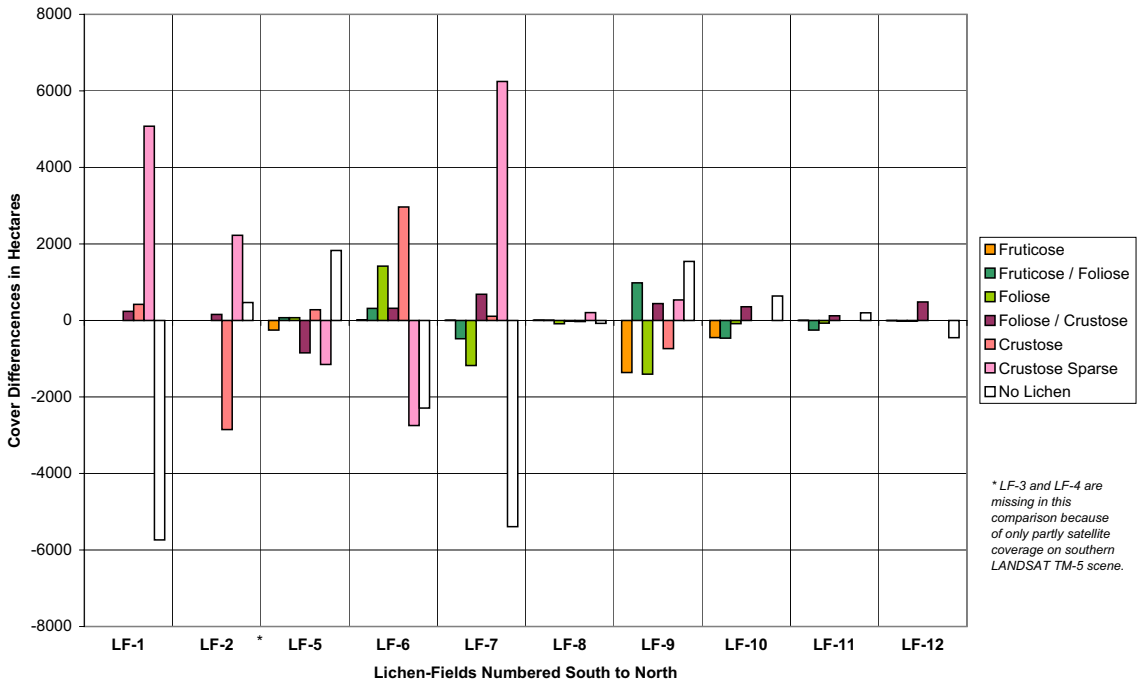

Figure D17: Classification Comparison of Lichen Community Coverage per Lichen-Field 2000-multitemporal MINUS 1991/92-multitemporal.

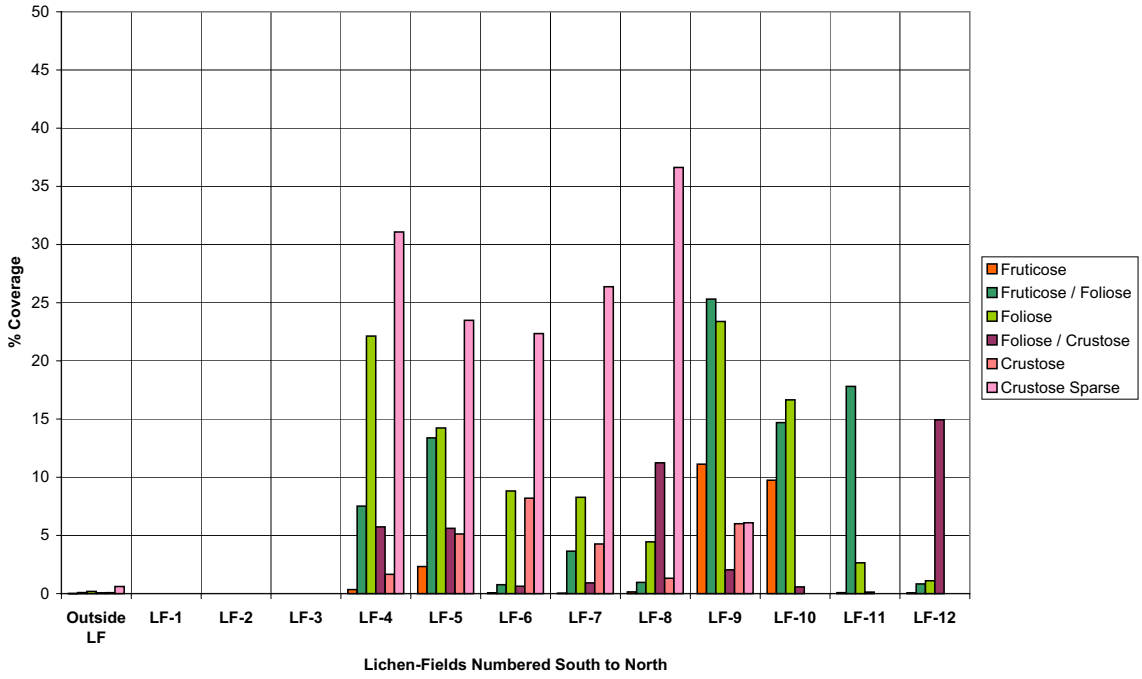

Figure D18: Multitemporal Classification 1991 - Comparison of Lichen Community Coverage per Total Lichen-Field Area.

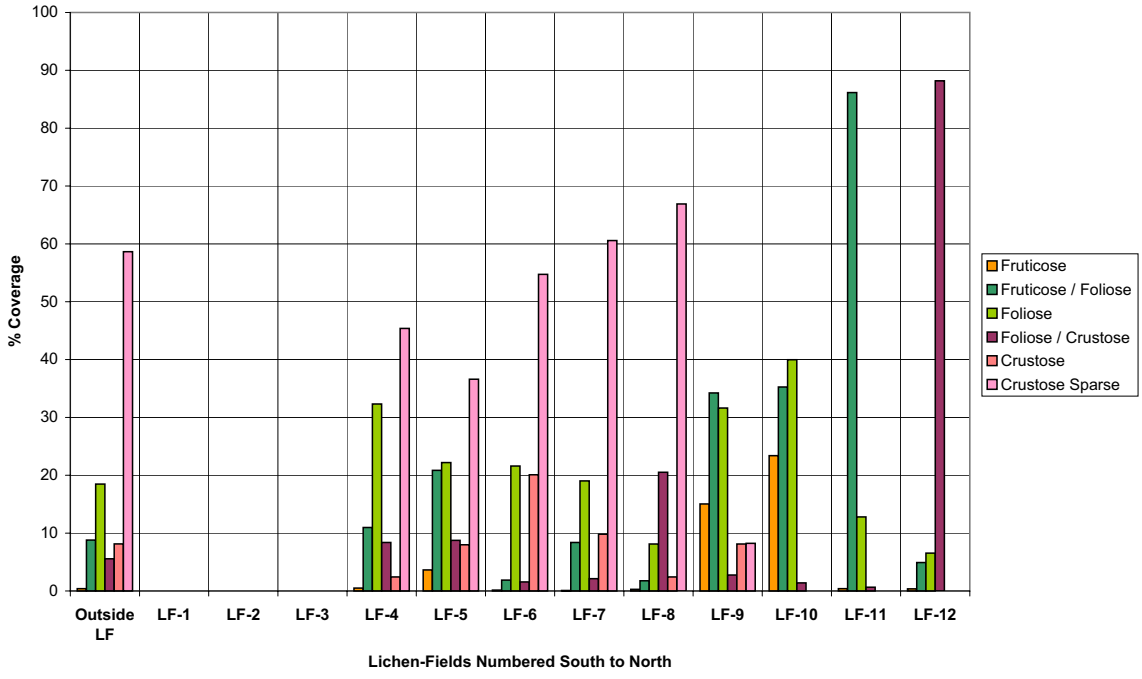

Figure D19: Multitemporal Classification 1991 - Comparison of Lichen Community Coverage per Lichen-Covered Area per Lichen-Field.

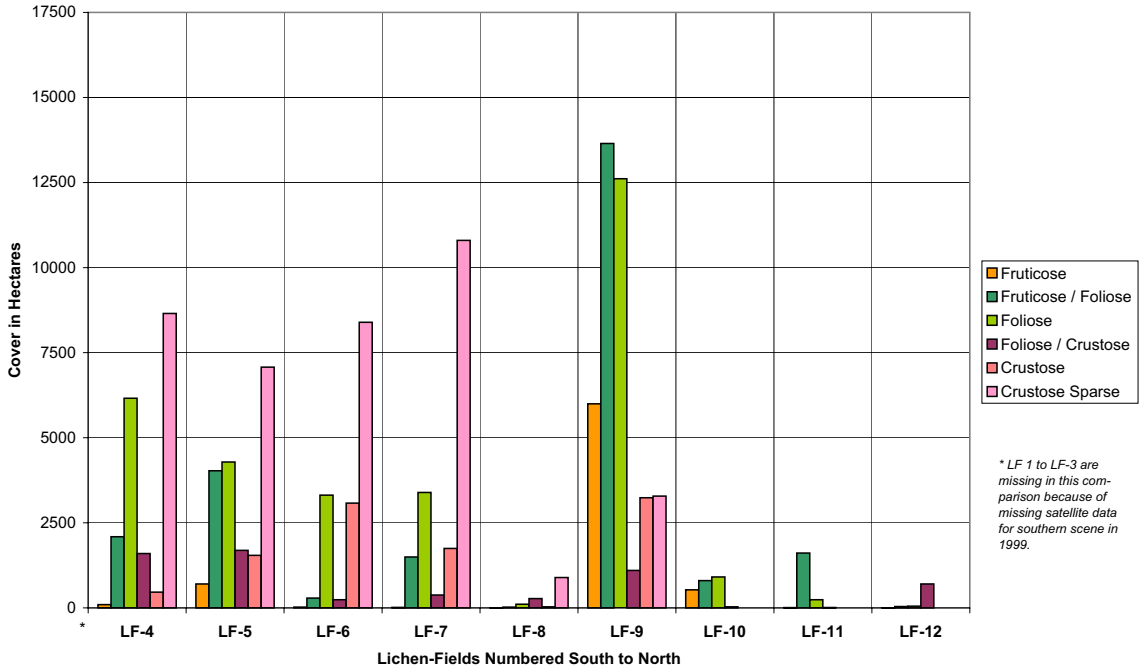

Figure D20: Multitemporal Classification 1991 - Comparison of Lichen Community Coverage per Lichen-Field.

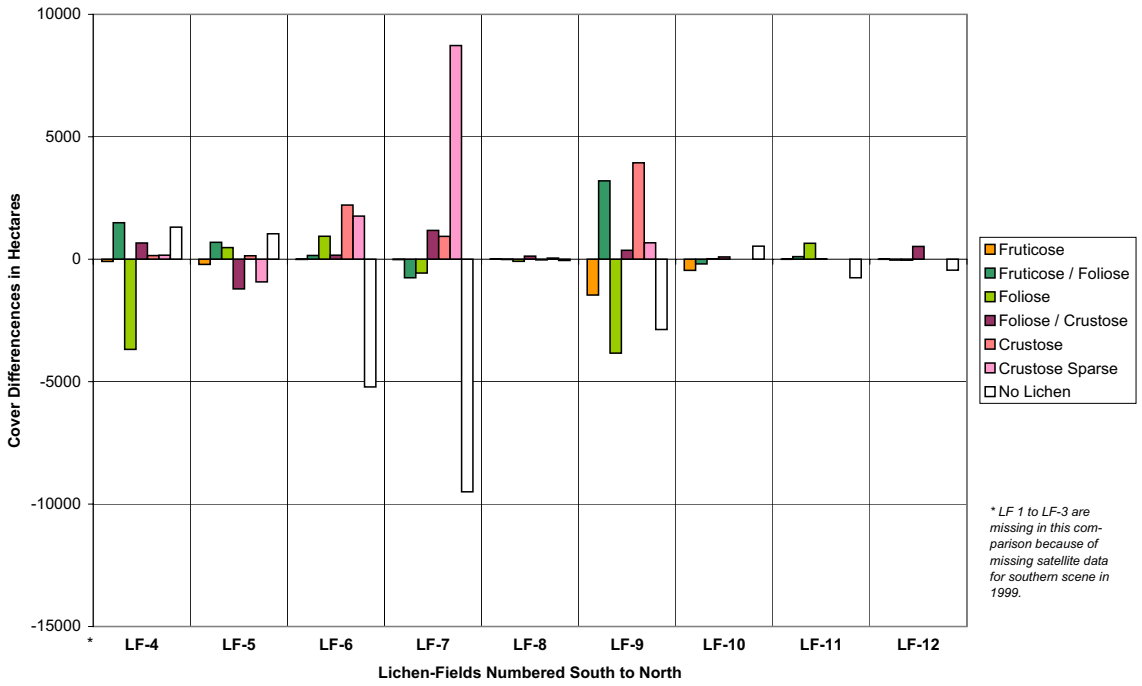

Figure D21: Classification Comparison of Lichen Community Coverage per Lichen-Field 1999-multitemporal MINUS 1991-multitemporal.

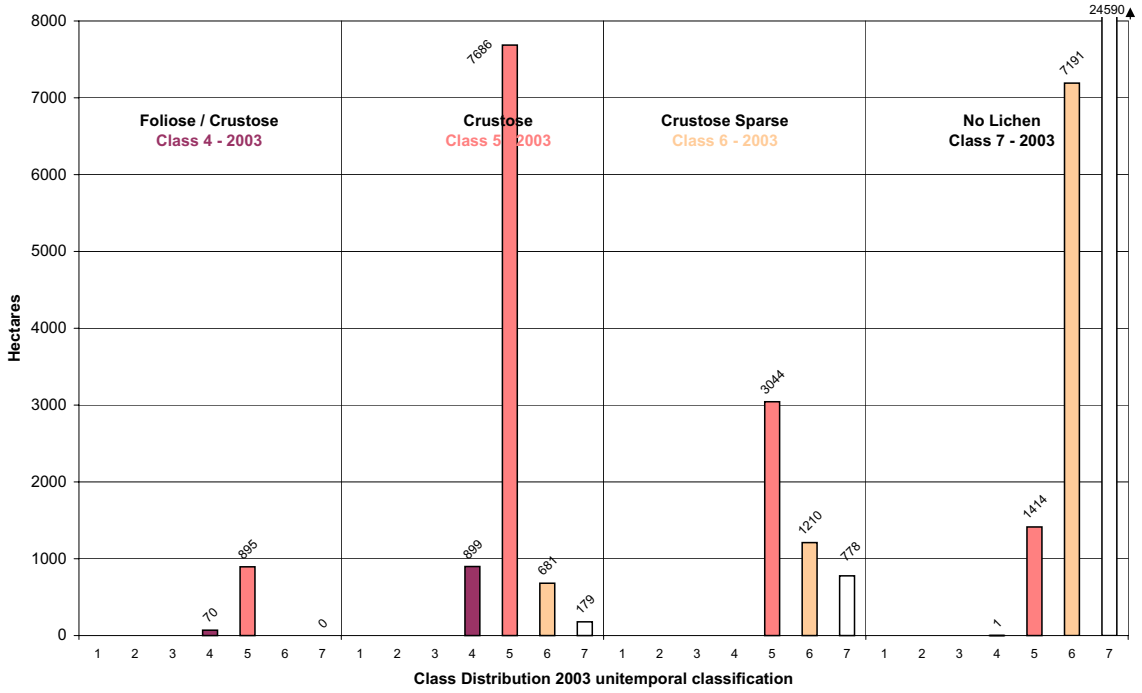

Figure E1: Changes in mapped class distribution of lichen communities between 2003 multi- and 2003 unitemporal classification for the lichen-field of the Southern Naukluft Plateau - No. 1.

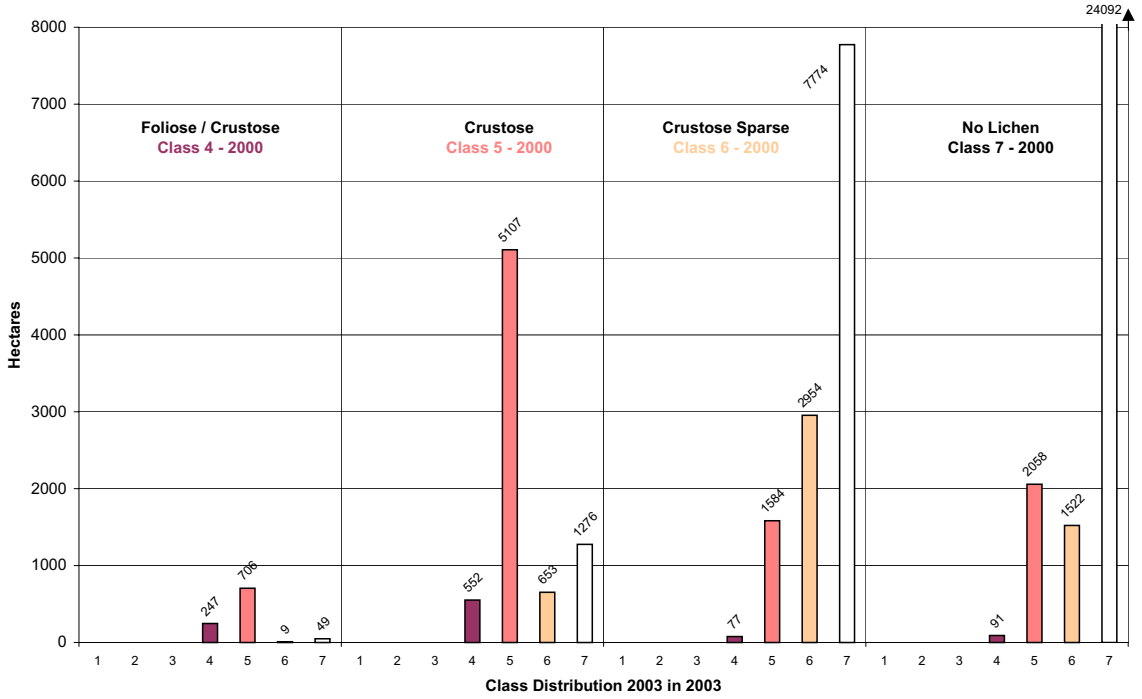

Figure E2: Changes in mapped class distribution of lichen communities between 2000 and 2003 for the lichen-field of the Southern Naukluft Plateau - No. 1.

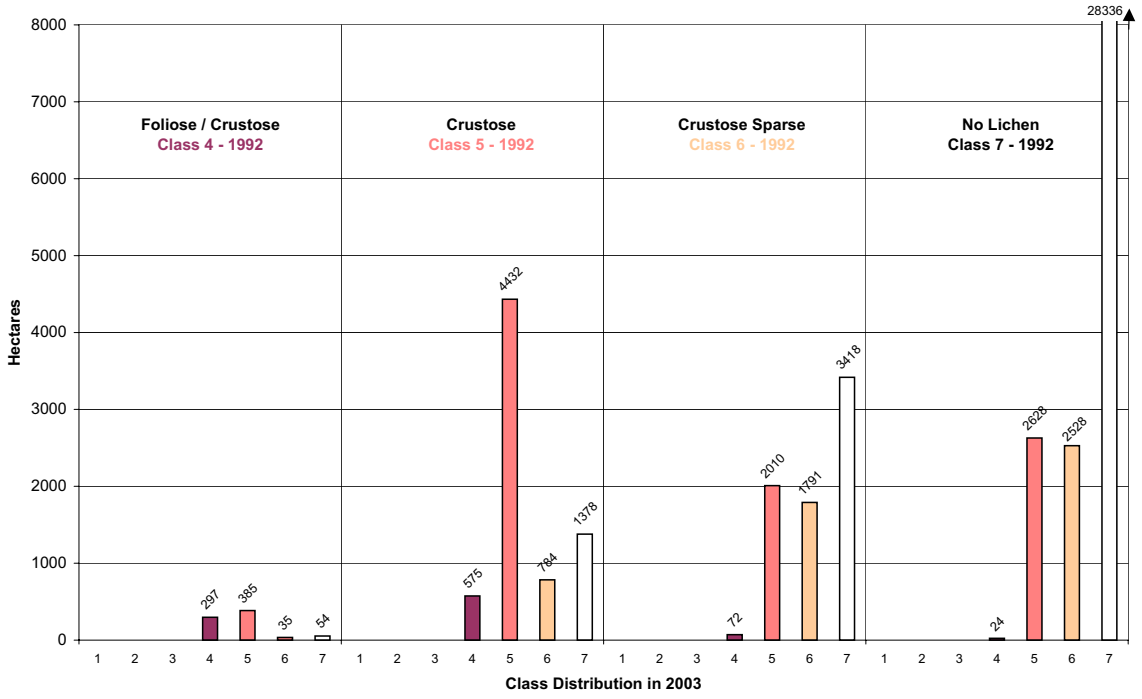

Figure E3: Changes in mapped class distribution of lichen communities between 1992 and 2003 for the lichen-field of the Southern Naukluft Plateau - No. 1.

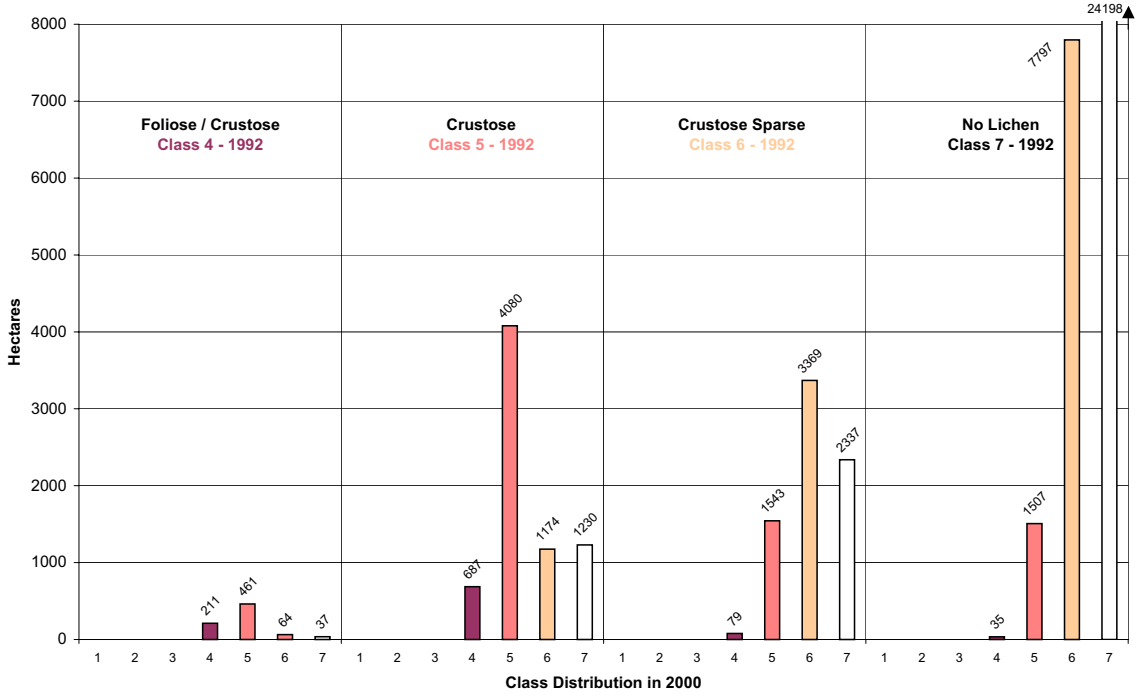

Figure E4: Changes in mapped class distribution of lichen communities between 1992 and 2000 for the lichen-field of the Southern Naukluft Plateau - No. 1.

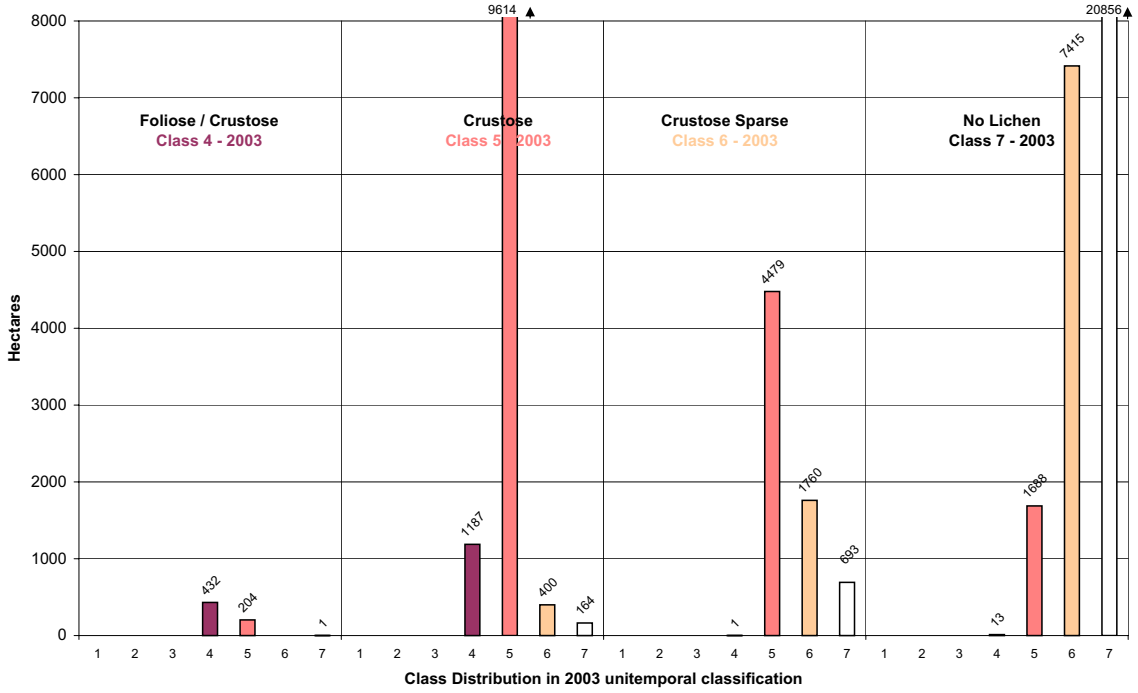

Figure E5: Changes in mapped class distribution of lichen communities between 2003 multi- and 2003 unitemporal classification for the lichen-field of the Northern Naukluft Plateau - No. 2.

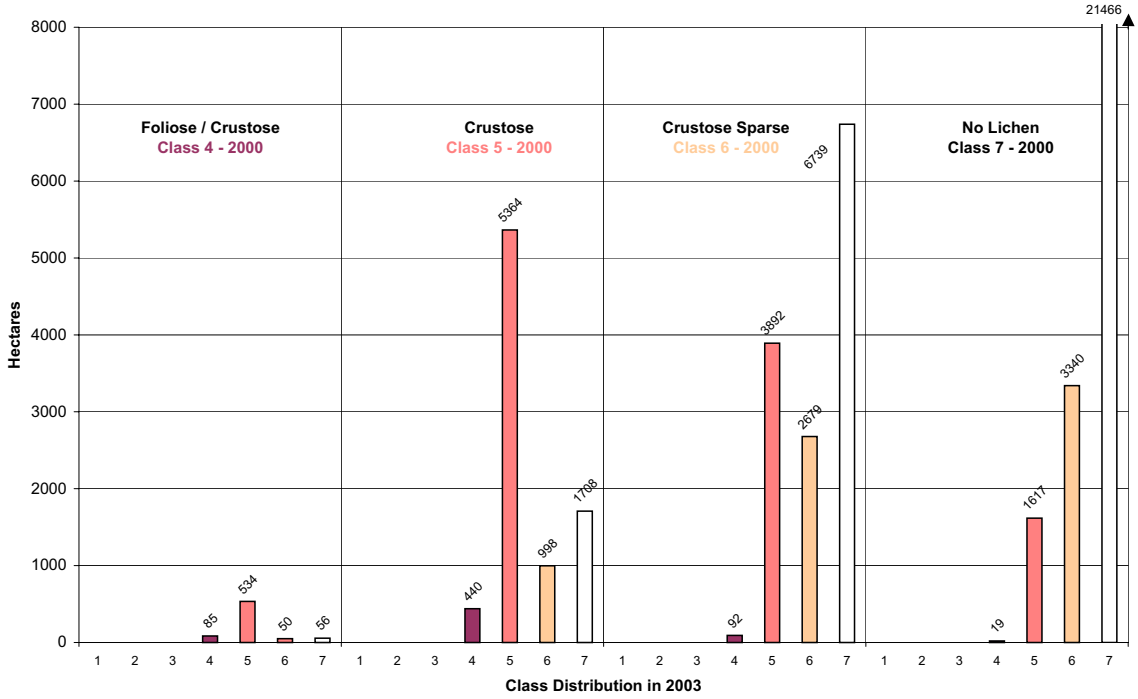

Figure E6: Changes in mapped class distribution of lichen communities between 2000 and 2003 for the lichen-field of the Northern Naukluft Plateau - No. 2.

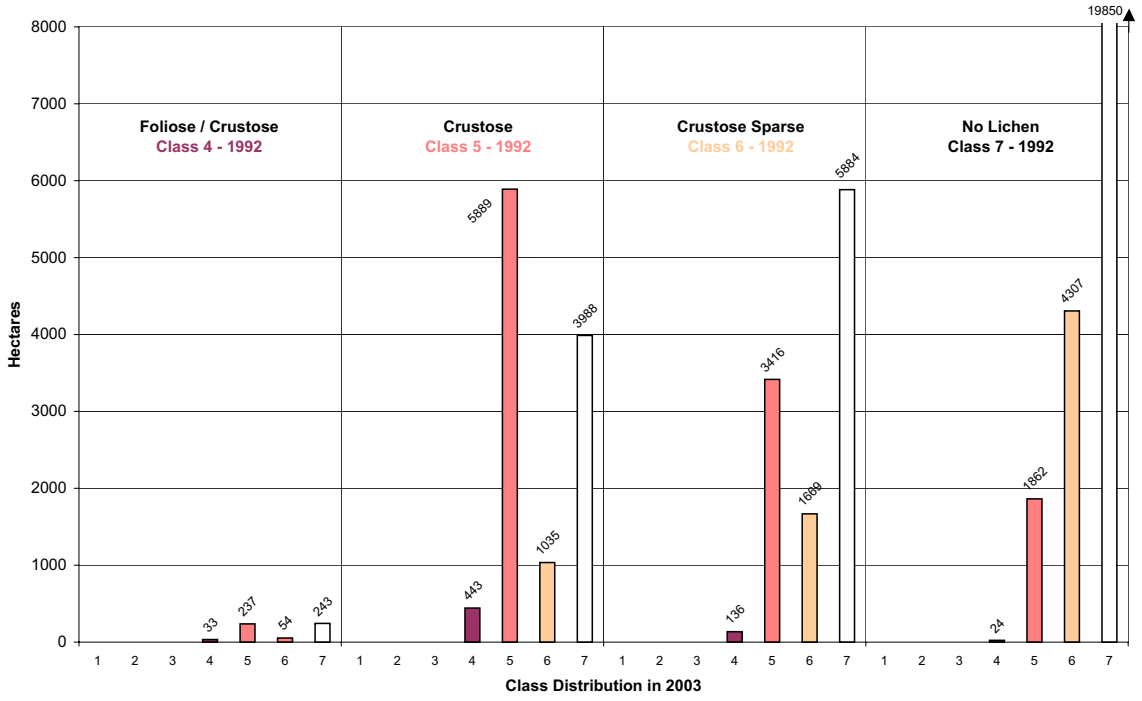

Figure E7: Changes in mapped class distribution of lichen communities between 1992 and 2003 for the lichen-field of the Northern Naukluft Plateau - No. 2.

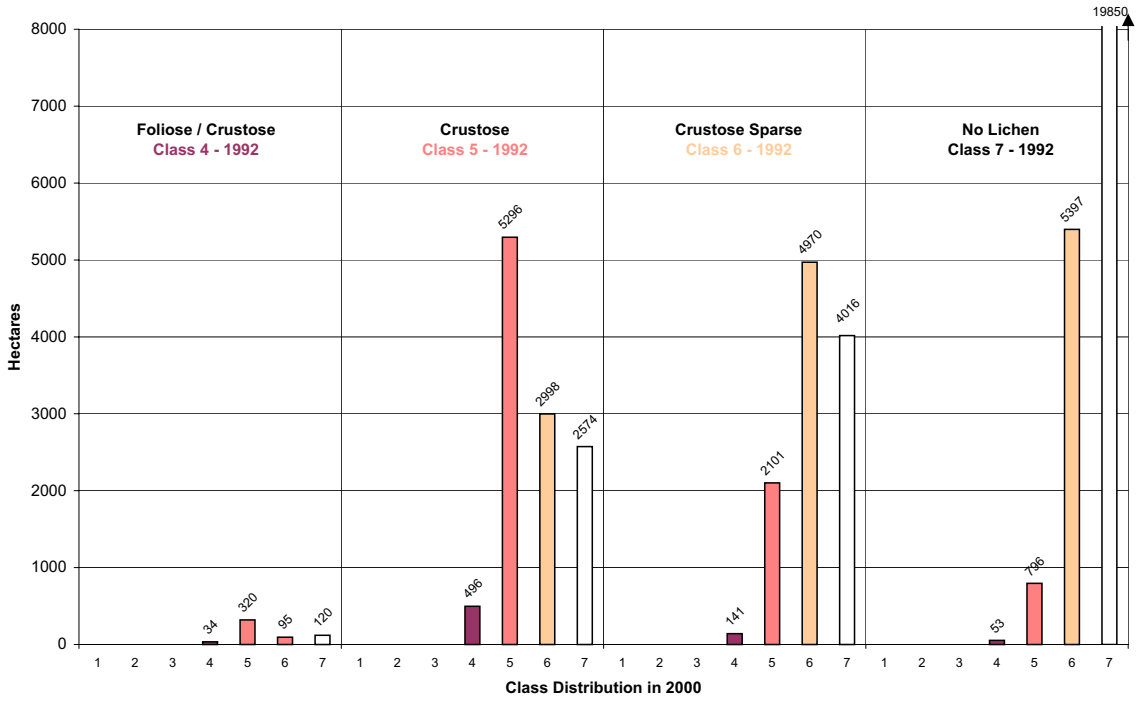

Figure E8: Changes in mapped class distribution of lichen communities between 1992 and 2000 for the lichen-field of the Northern Naukluft Plateau - No. 2.

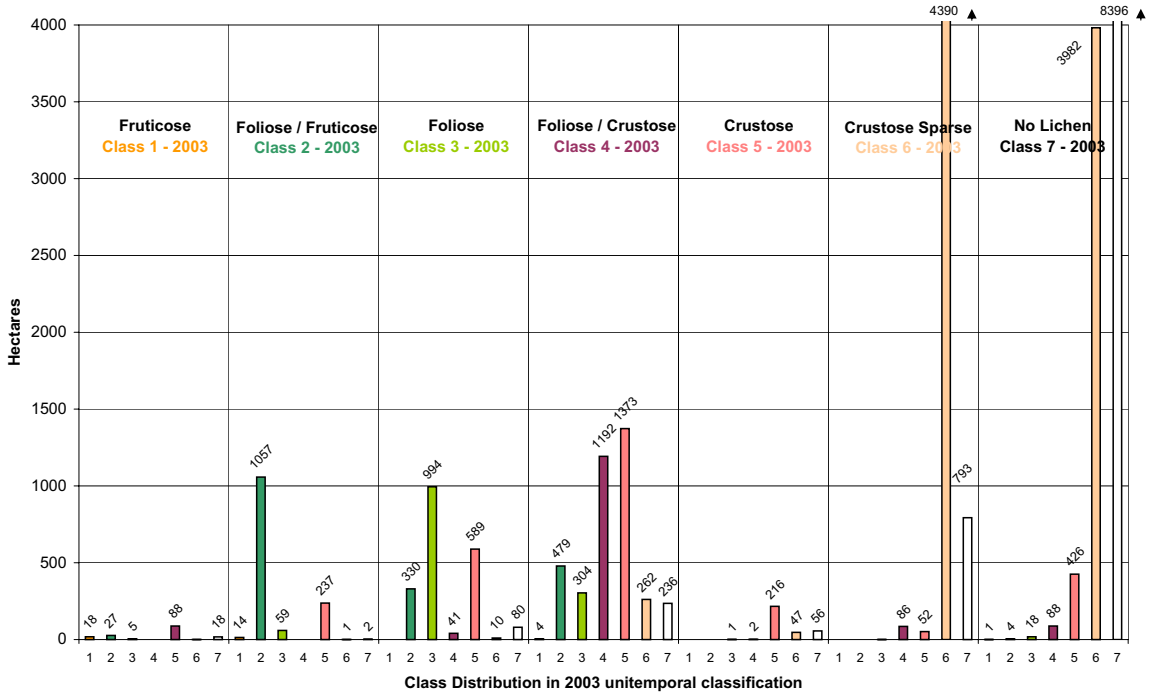

Figure E9: Changes in mapped class distribution of lichen communities between 2003 multi- and 2003 unitemporal classification for the lichen-field of Mile 8 / Mile 12 - No. 4.

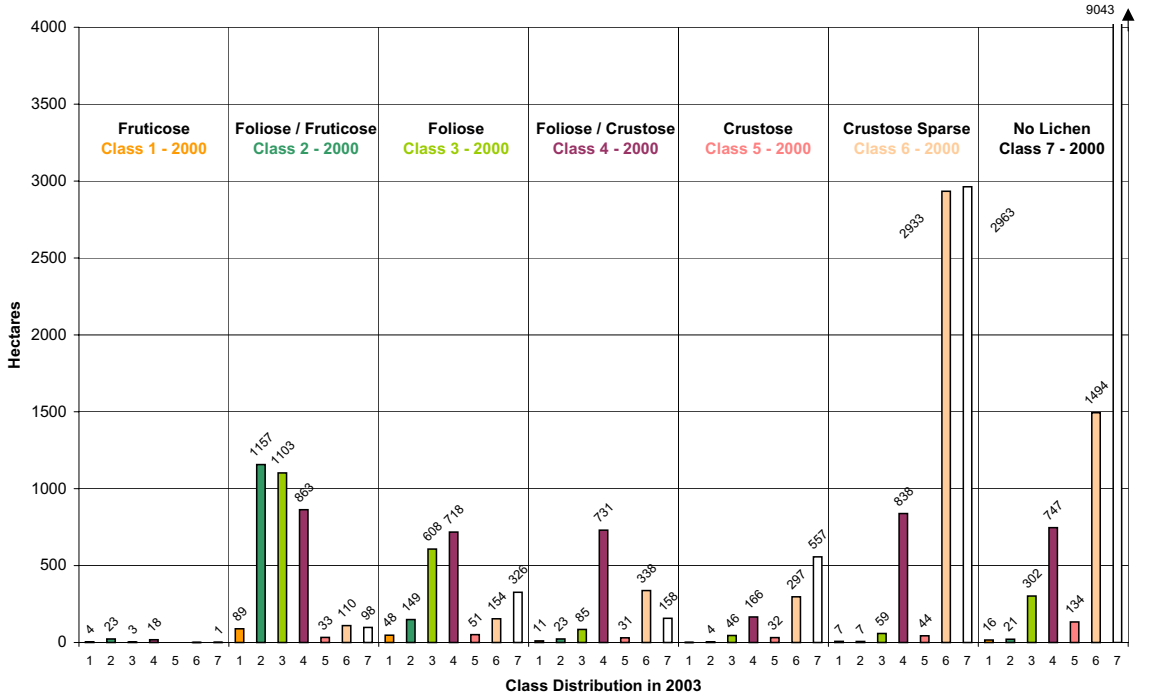

Figure E10: Changes in mapped class distribution of lichen communities between 2000 and 2003 for the lichen-field of Mile 8 / Mile 12 - No. 4.

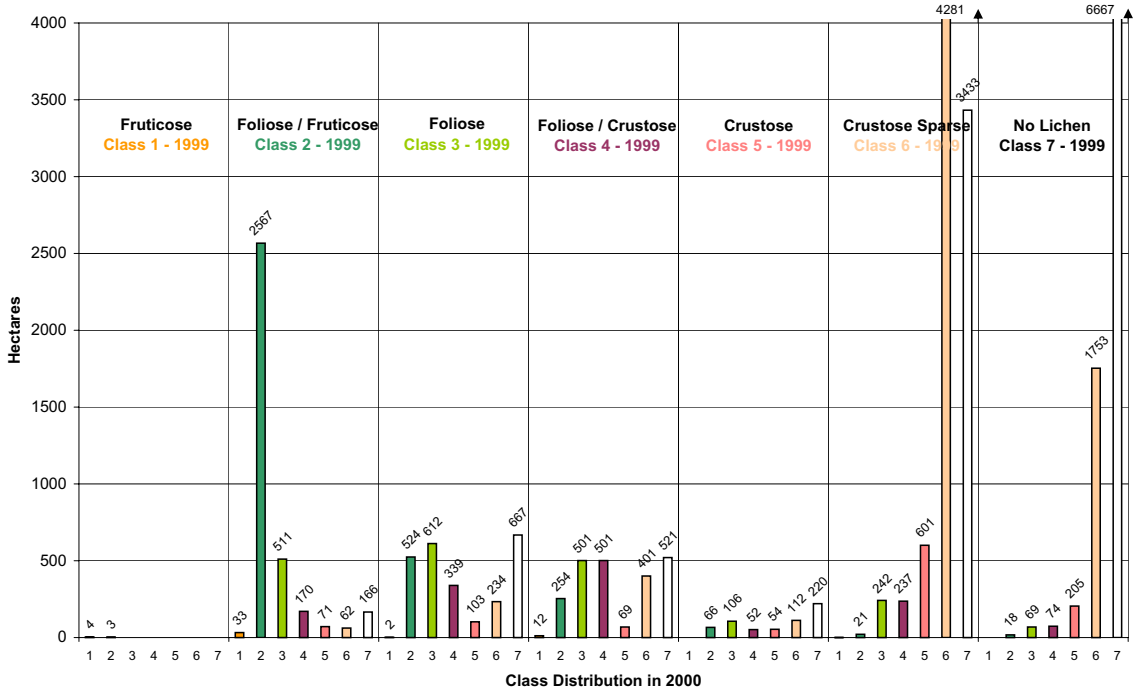

Figure E11: Changes in mapped class distribution of lichen communities between 1999 and 2000 for the lichen-field of Mile 8 / Mile 12 - No. 4.

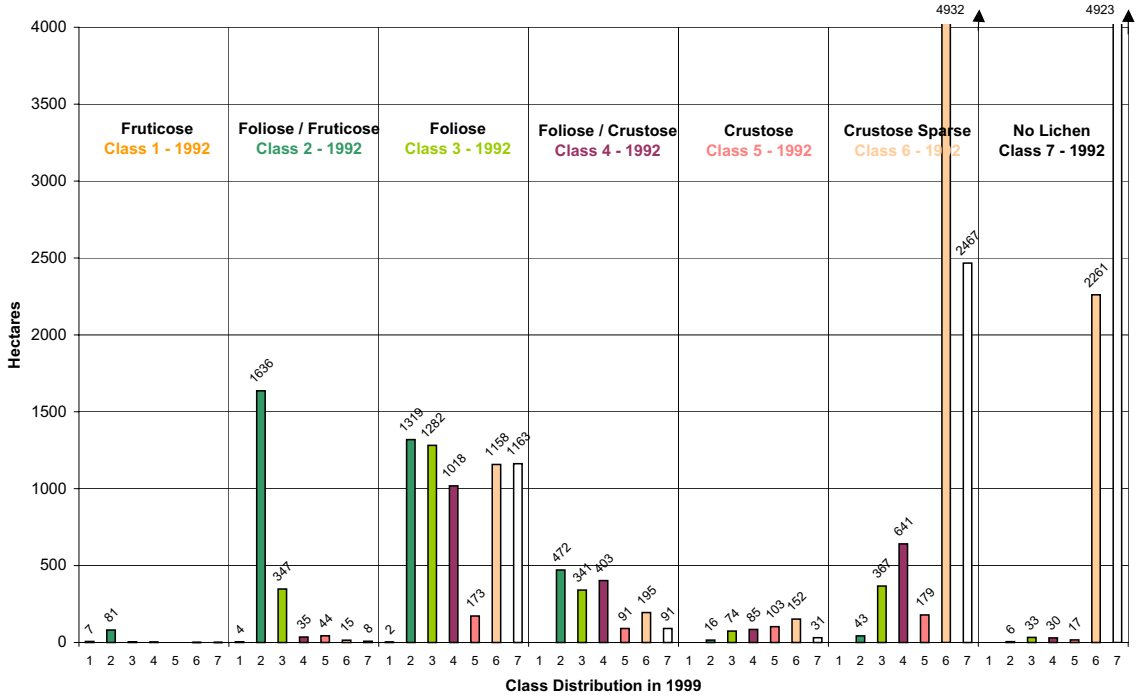

Figure E12: Changes in mapped class distribution of lichen communities between 1991 and 1999 for the lichen-field of Mile 8 / Mile 12 - No. 4.

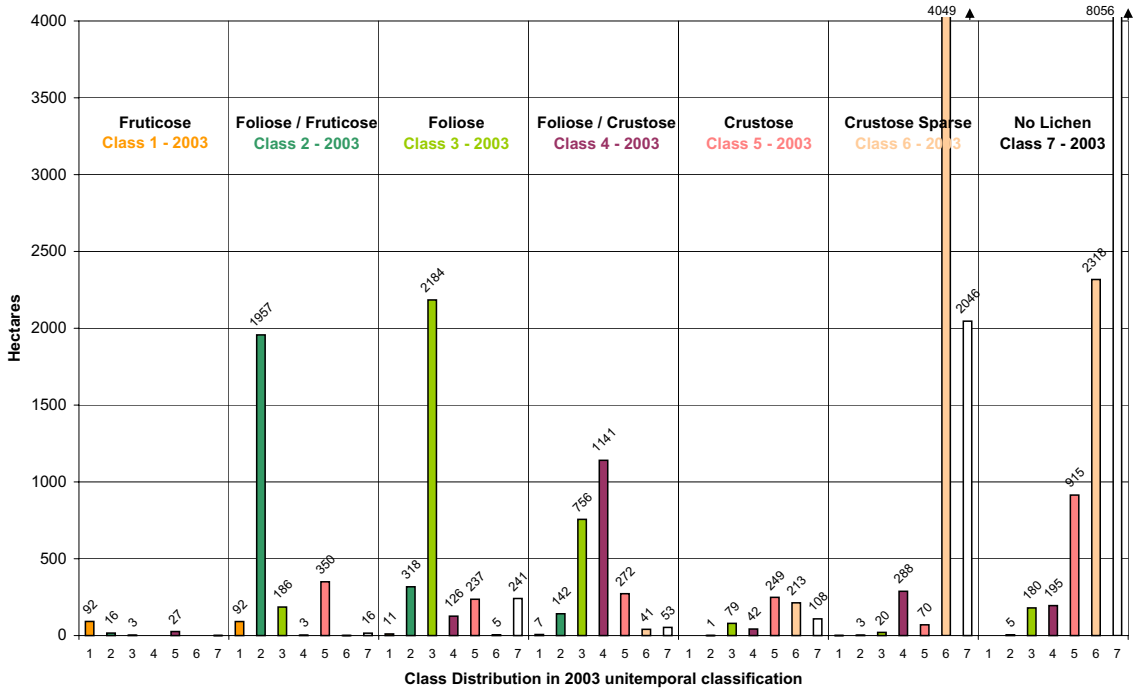

Figure E13: Changes in mapped class distribution of lichen communities between 2003 multi- and 2003 unitemporal classification for the lichen-field of Wlotzkasbaken - No. 5.

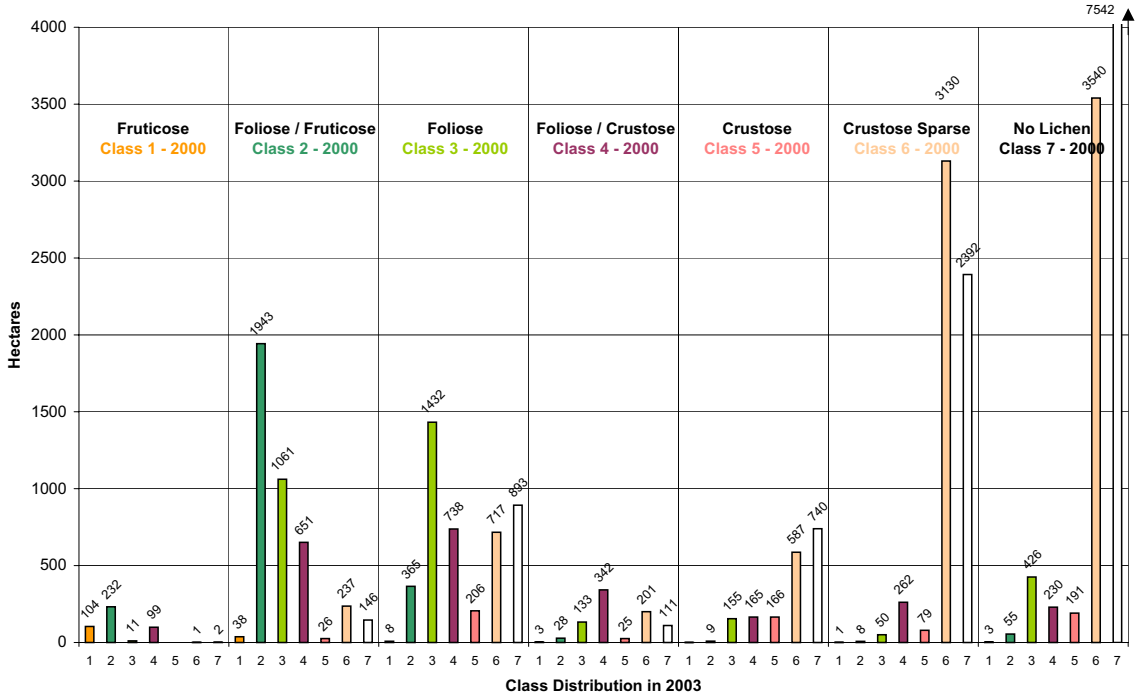

Figure E14: Changes in mapped class distribution of lichen communities between 2000 and 2003 for the lichen-field of Wlotzkasbaken - No. 5.

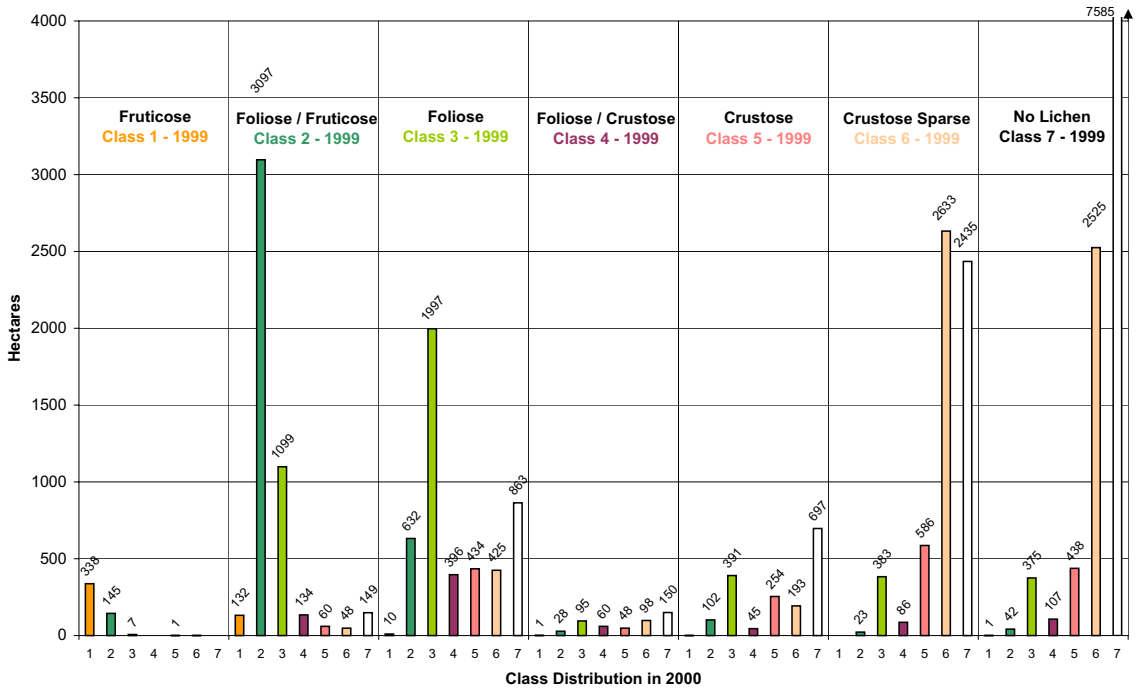

Figure E15: Changes in mapped class distribution of lichen communities between 1999 and 2000 for the lichen-field of Wlotzkasbaken - No. 5.

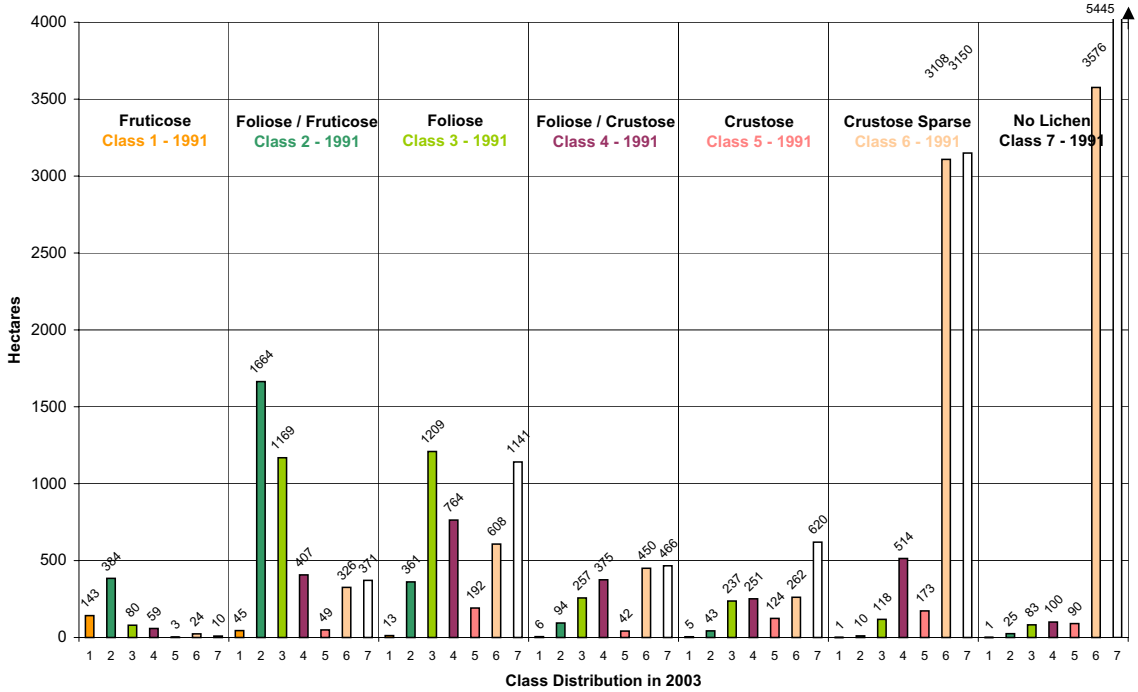

Figure E16: Changes in mapped class distribution of lichen communities between 1991 and 2003 for the lichen-field of Wlotzkasbaken - No. 5.

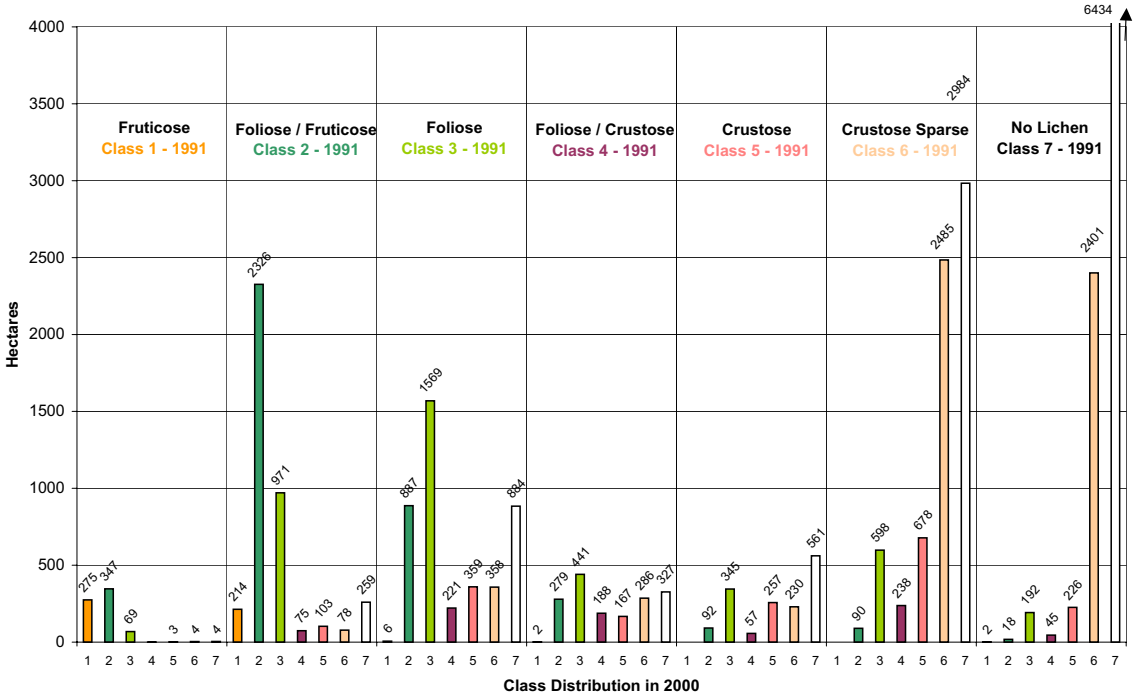

Figure E17: Changes in mapped class distribution of lichen communities between 1991 and 2000 for the lichen-field of Wlotzkasbaken - No. 5.

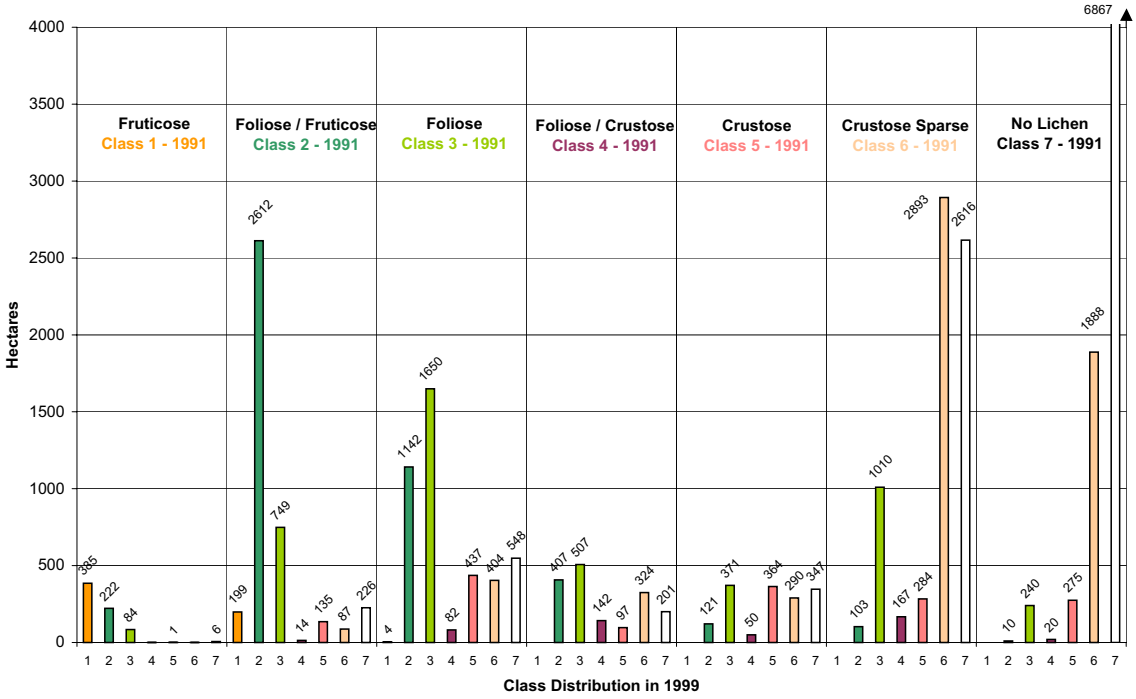

Figure E18: Changes in mapped class distribution of lichen communities between 1991 and 1999 for the lichen-field of Wlotzkasbaken - No. 5.

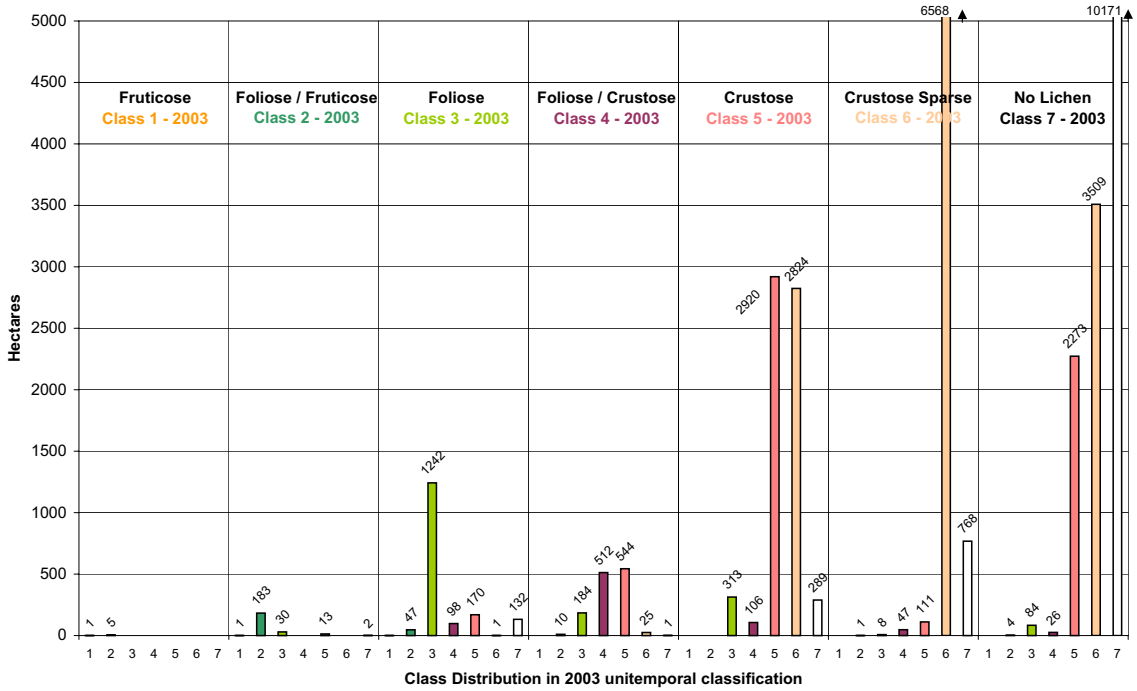

Figure E19: Changes in mapped class distribution of lichen communities between 2003 multi- and 2003 unitemporal classification for the lichen-field of Jakkalsputz - No. 6.

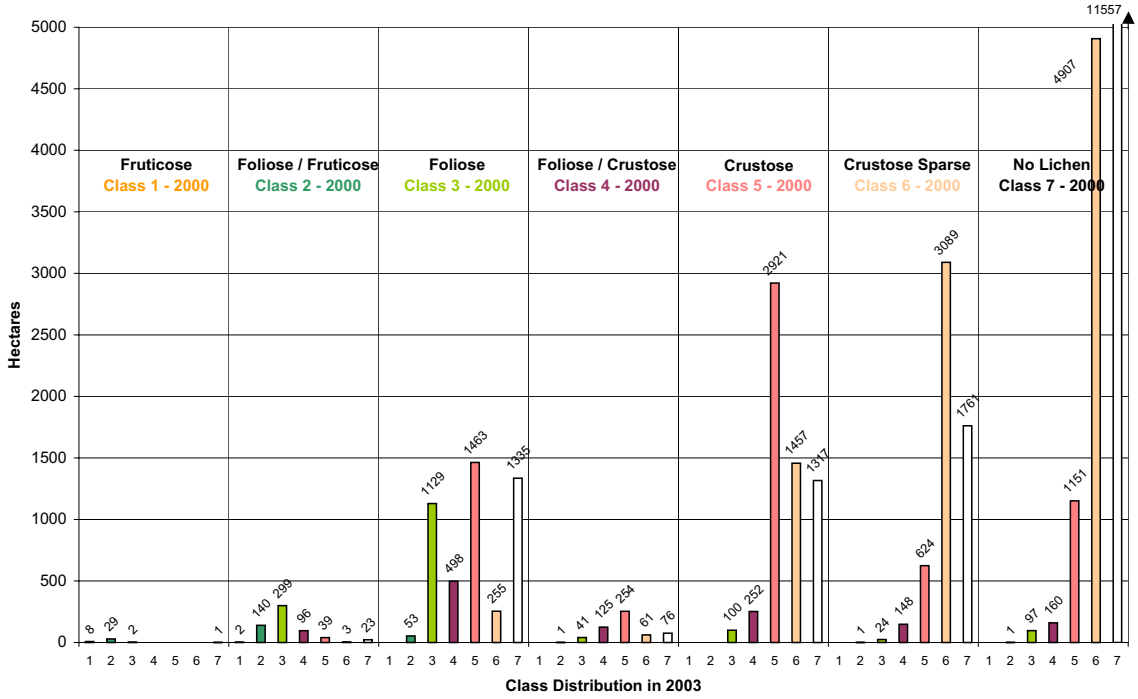

Figure E20: Changes in mapped class distribution of lichen communities between 2000 and 2003 for the lichen-field of Jakkalsputz - No. 6.

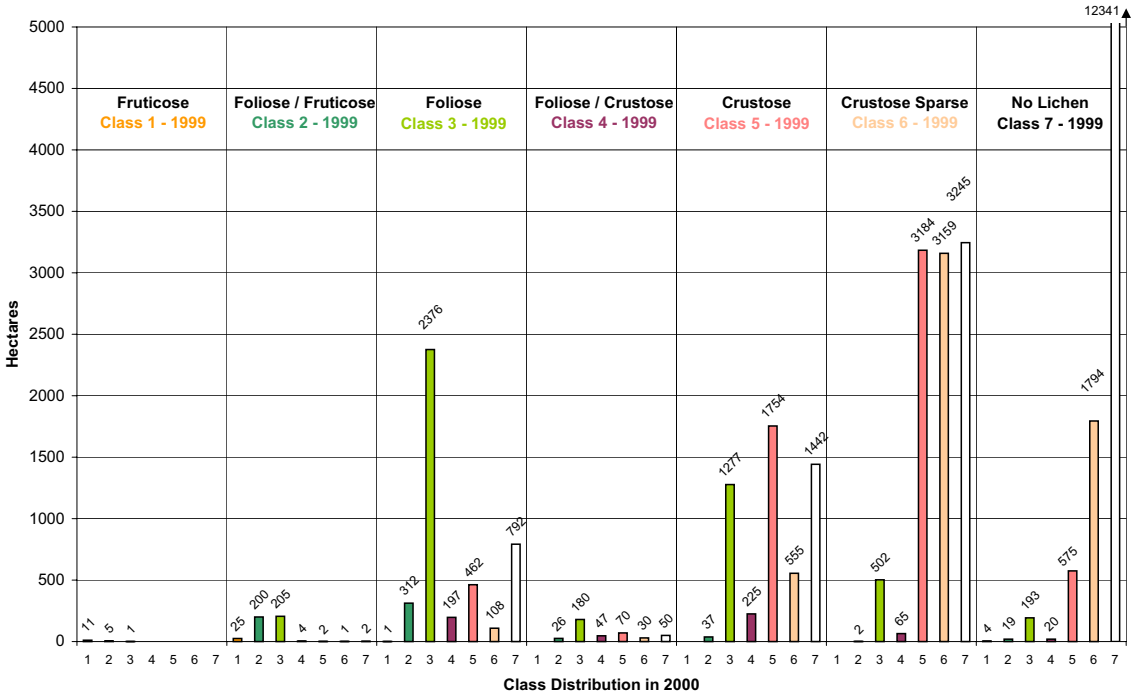

Figure E21: Changes in mapped class distribution of lichen communities between 1999 and 2000 for the lichen-field of Jakkalsputz - No. 6.

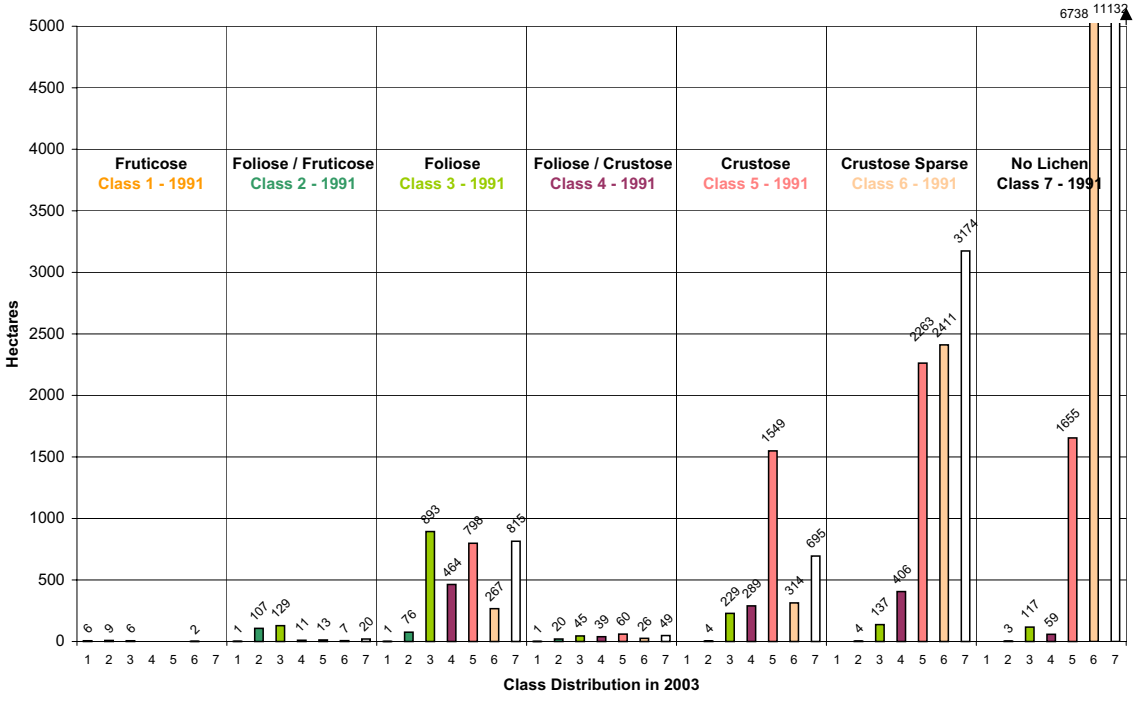

Figure E22: Changes in mapped class distribution of lichen communities between 1991 and 2003 for the lichen-field of Jakkalsputz - No. 6.

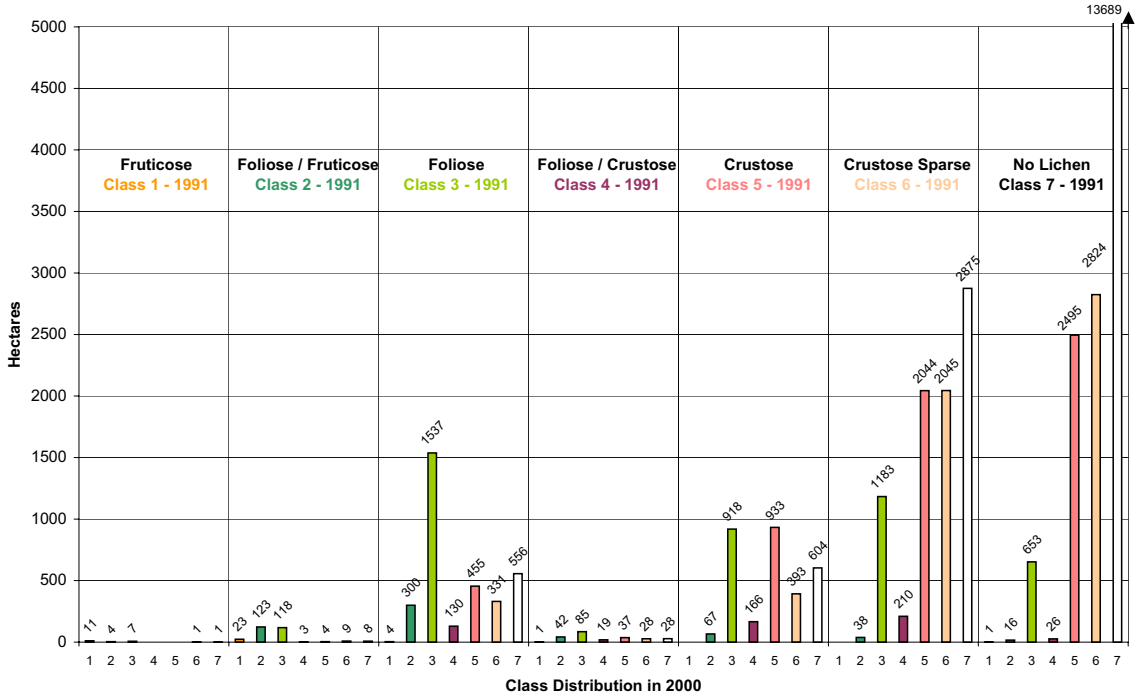

Figure E23: Changes in mapped class distribution of lichen communities between 1991 and 2000 for the lichen-field of Jakkalsputz - No. 6

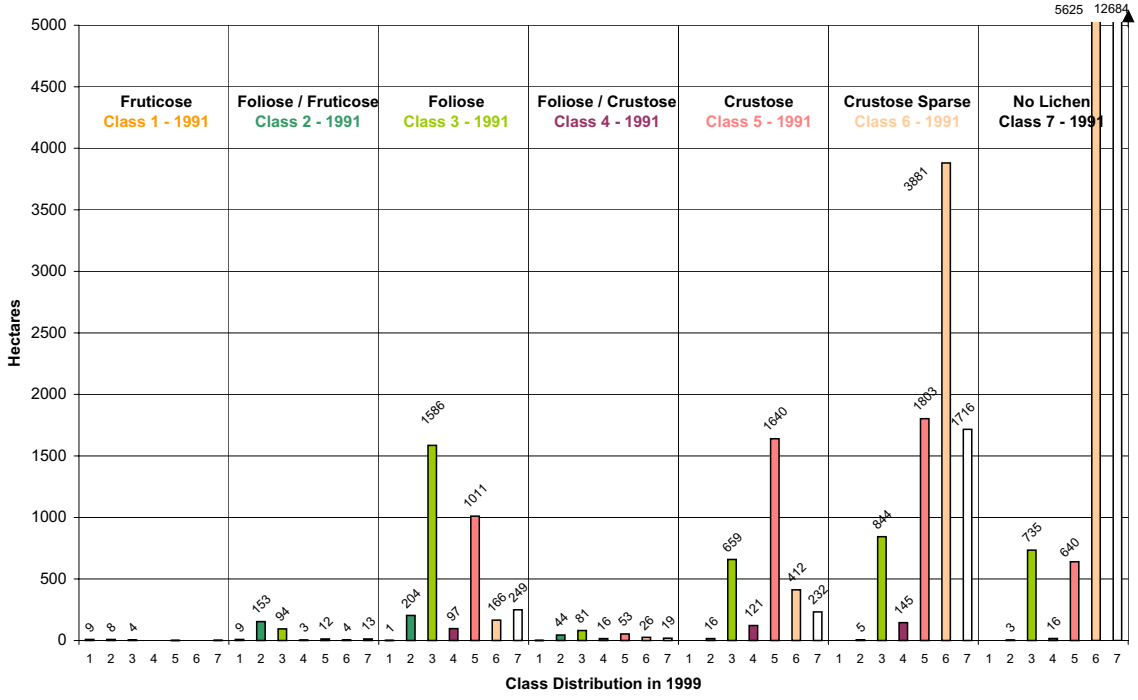

Figure E24: Changes in mapped class distribution of lichen communities between 1991 and 1999 for the lichen-field of Jakkalsputz - No. 6.

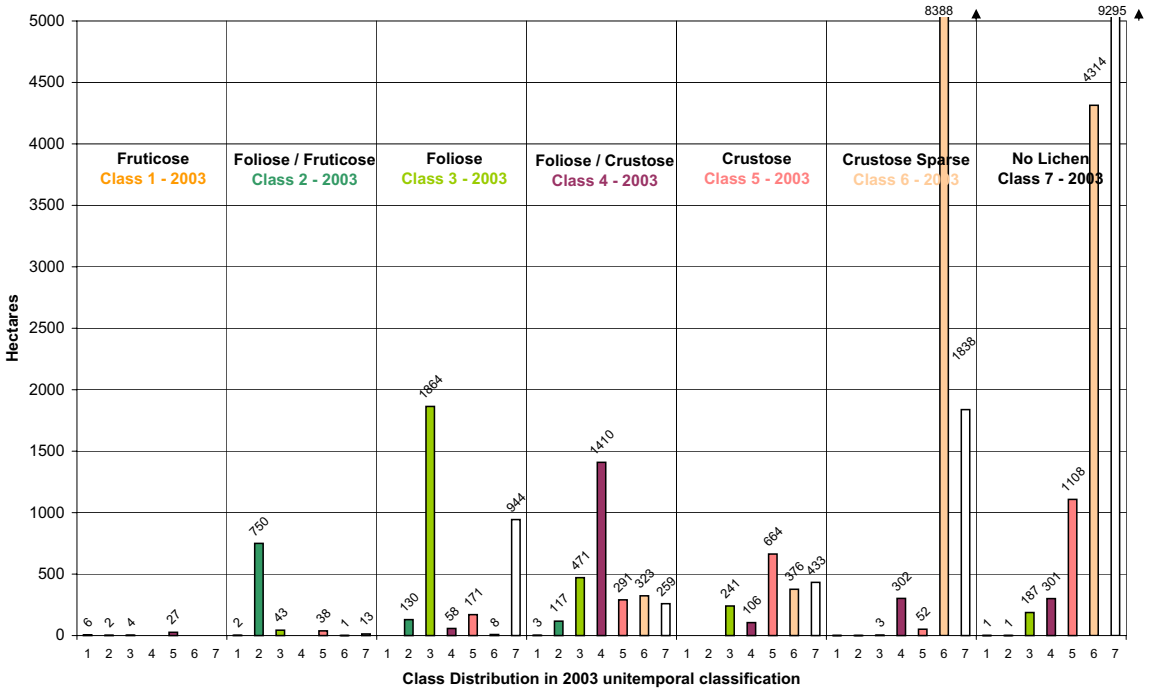

Figure E25: Changes in mapped class distribution of lichen communities between 2003 multi- and 2003 unitemporal classification for the lichen-field of the Omaruru Gravel Plain - No. 7.

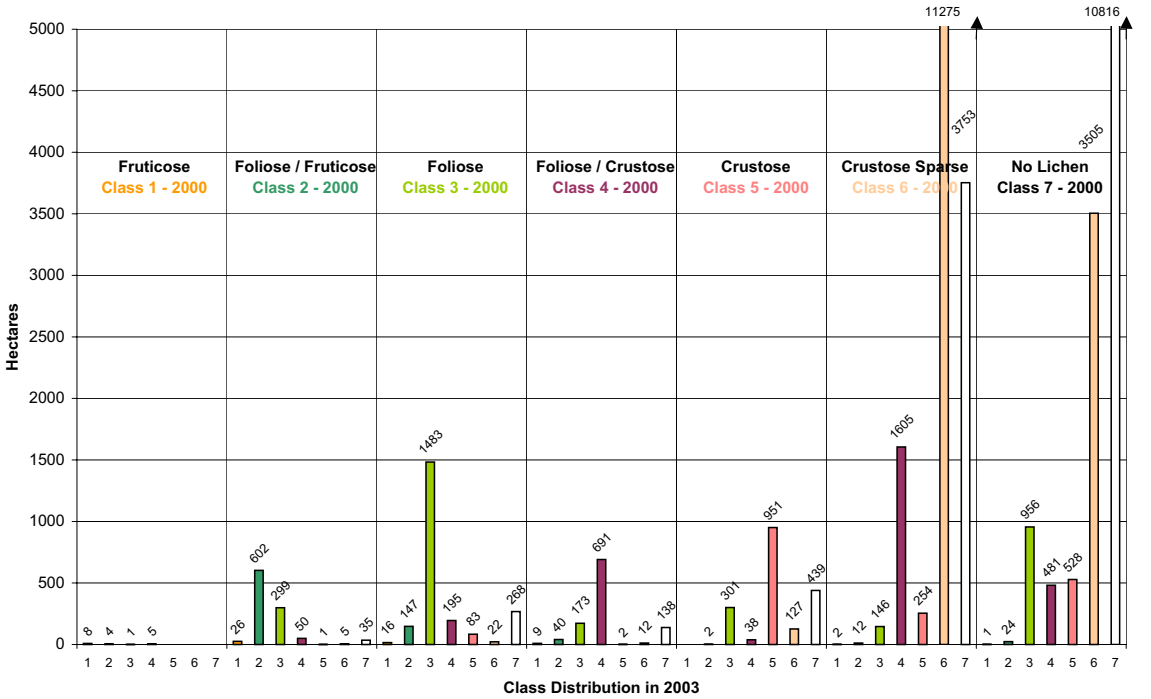

Figure E26: Changes in mapped class distribution of lichen communities between 2000 and 2003 for the lichen-field of the Omaruru Gravel Plain - No. 7.

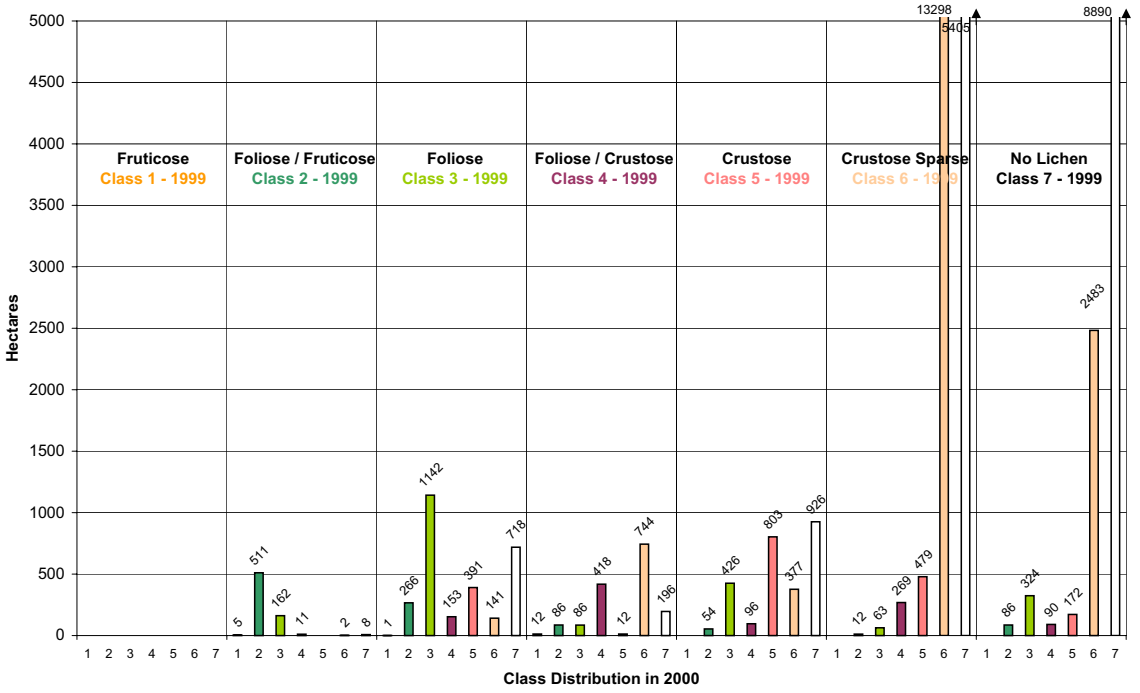

Figure E27: Changes in mapped class distribution of lichen communities between 1999 and 2000 for the lichen-field of the Omaruru Gravel Plain - No. 7.

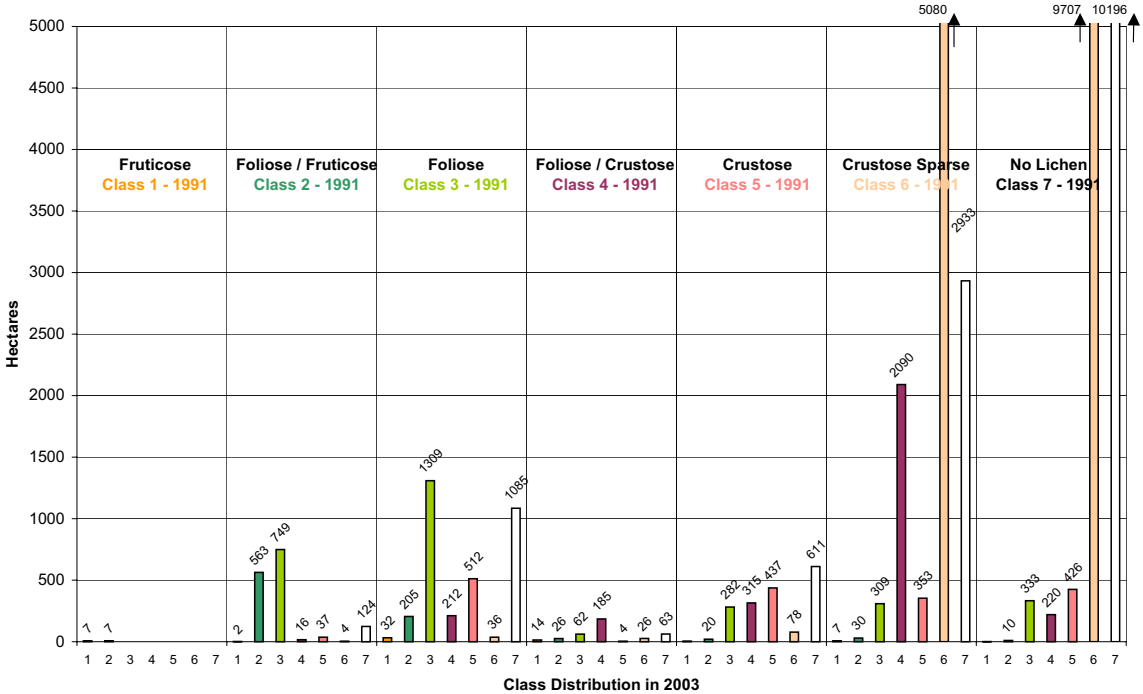

Figure E28: Changes in mapped class distribution of lichen communities between 1991 and 2003 for the lichen-field of the Omaruru Gravel Plain - No. 7.

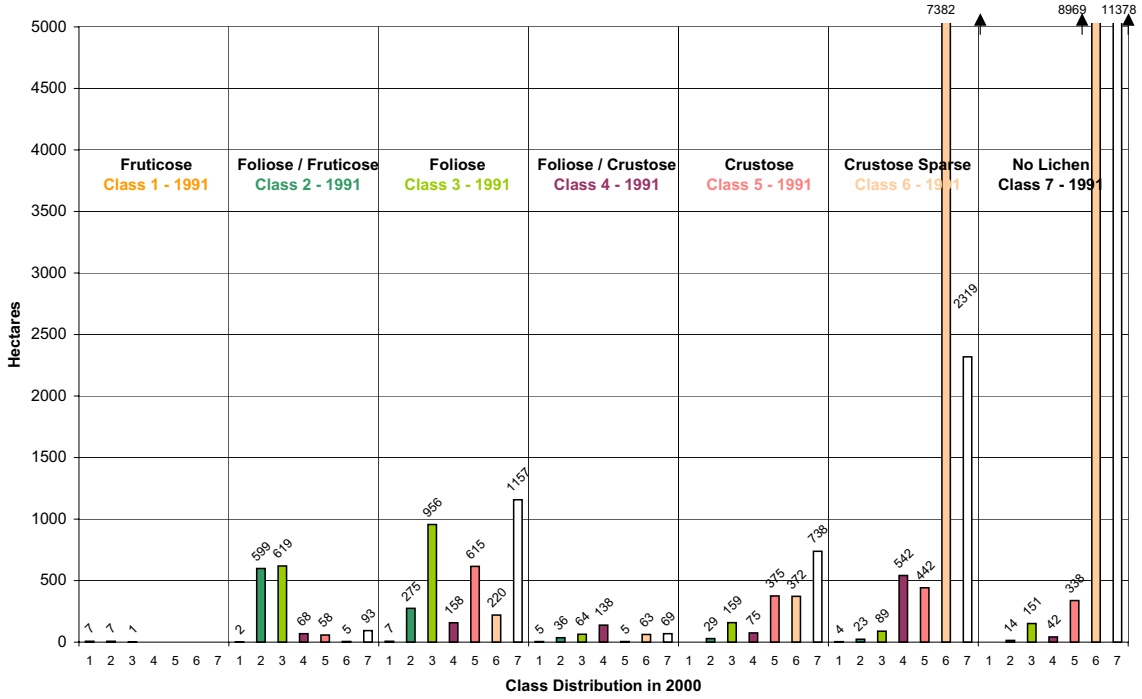

Figure E29: Changes in mapped class distribution of lichen communities between 1991 and 2000 for the lichen-field of the Omaruru Gravel Plain - No. 7.

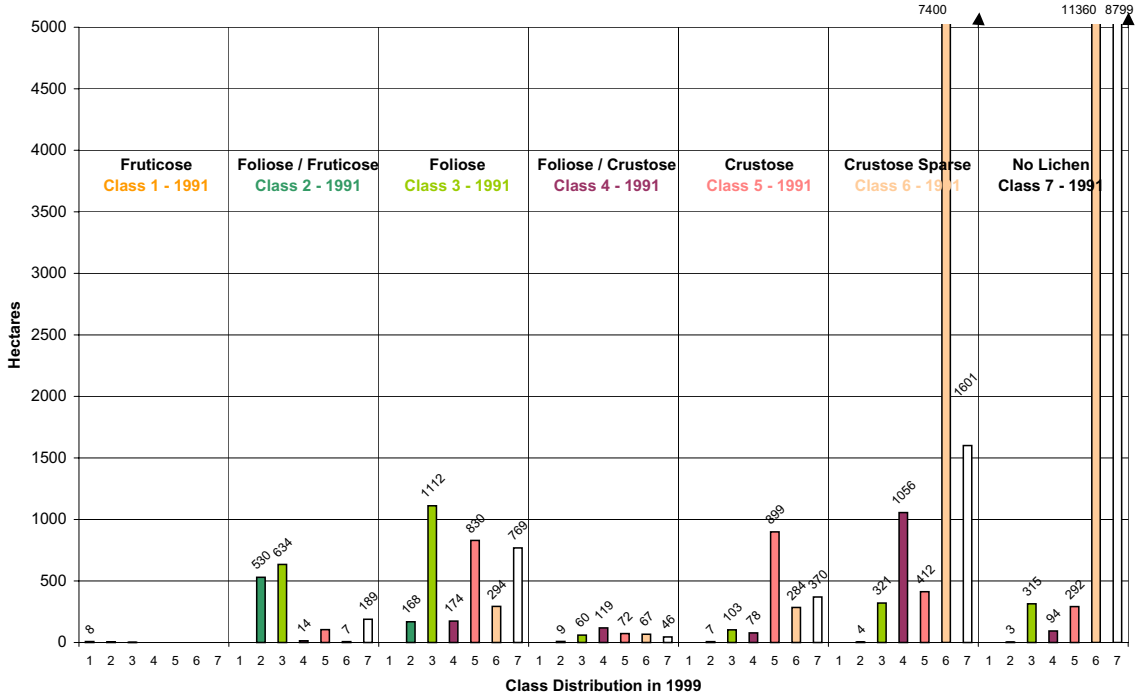

Figure E30: Changes in mapped class distribution of lichen communities between 1991 and 1999 for the lichen-field of the Omaruru Gravel Plain - No. 7.

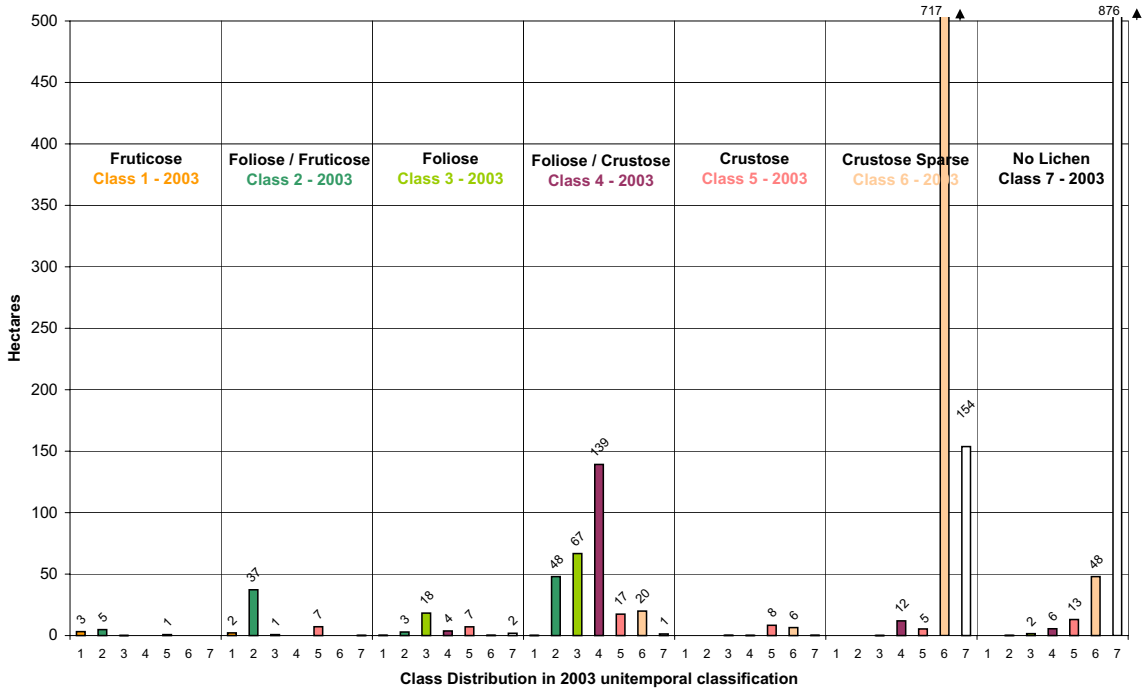

Figure E31: Changes in mapped class distribution of lichen communities between 2003 multi- and 2003 unitemporal classification for the lichen-field of Mile 72 - No. 8.

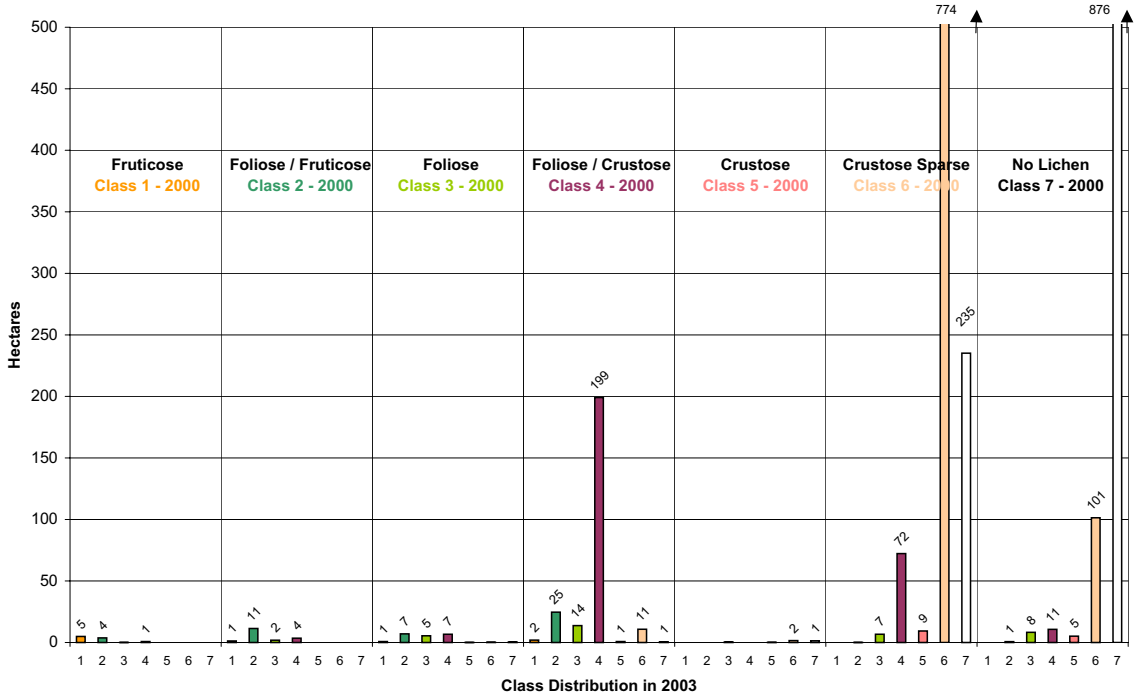

Figure E32: Changes in mapped class distribution of lichen communities between 2000 and 2003 for the lichen-field of Mile 72 - No. 8.

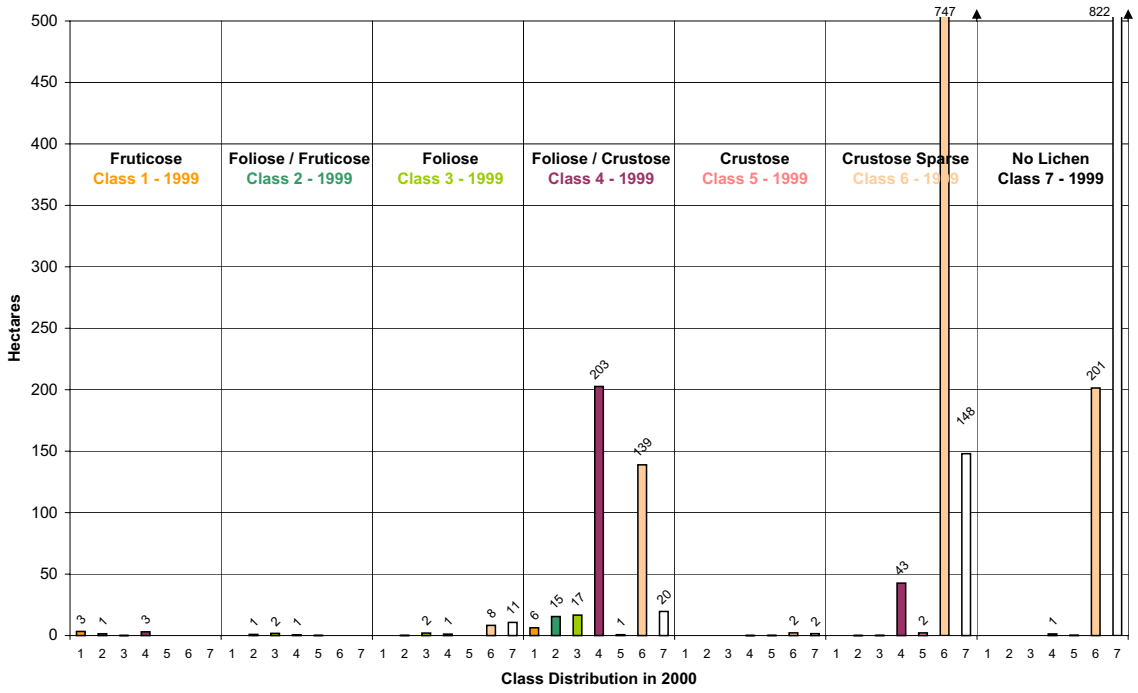

Figure E33: Changes in mapped class distribution of lichen communities between 1999 and 2000 for the lichen-field of Mile 72 - No. 8.

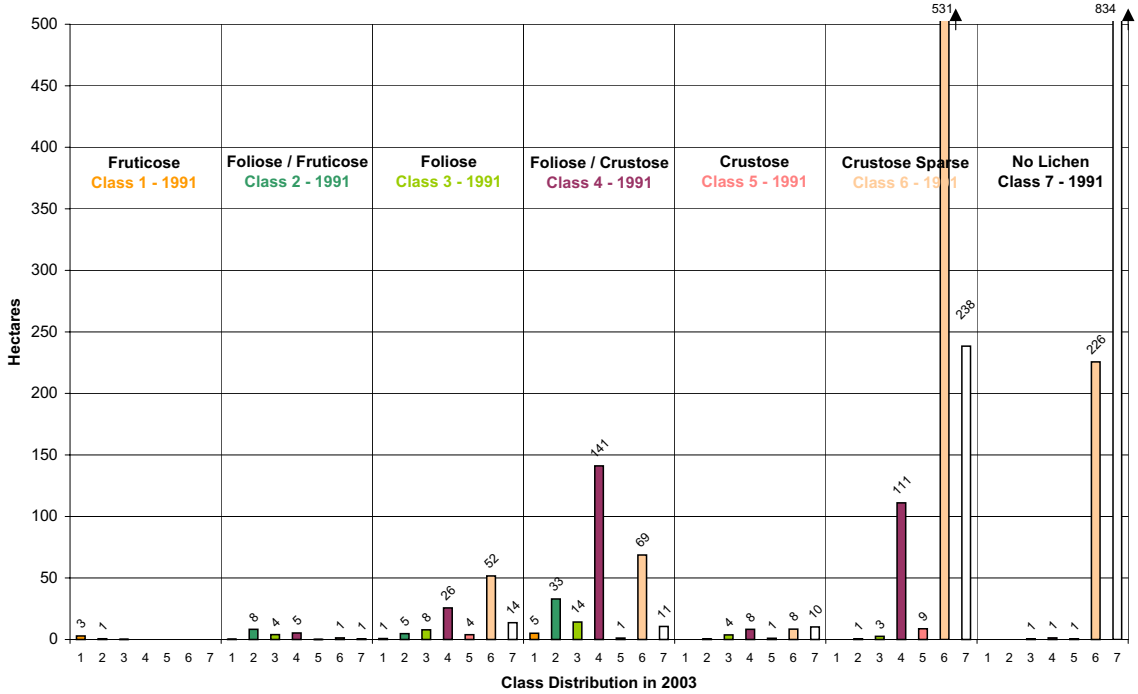

Figure E34: Changes in mapped class distribution of lichen communities between 1991 and 2003 for the lichen-field of Mile 72 - No. 8.

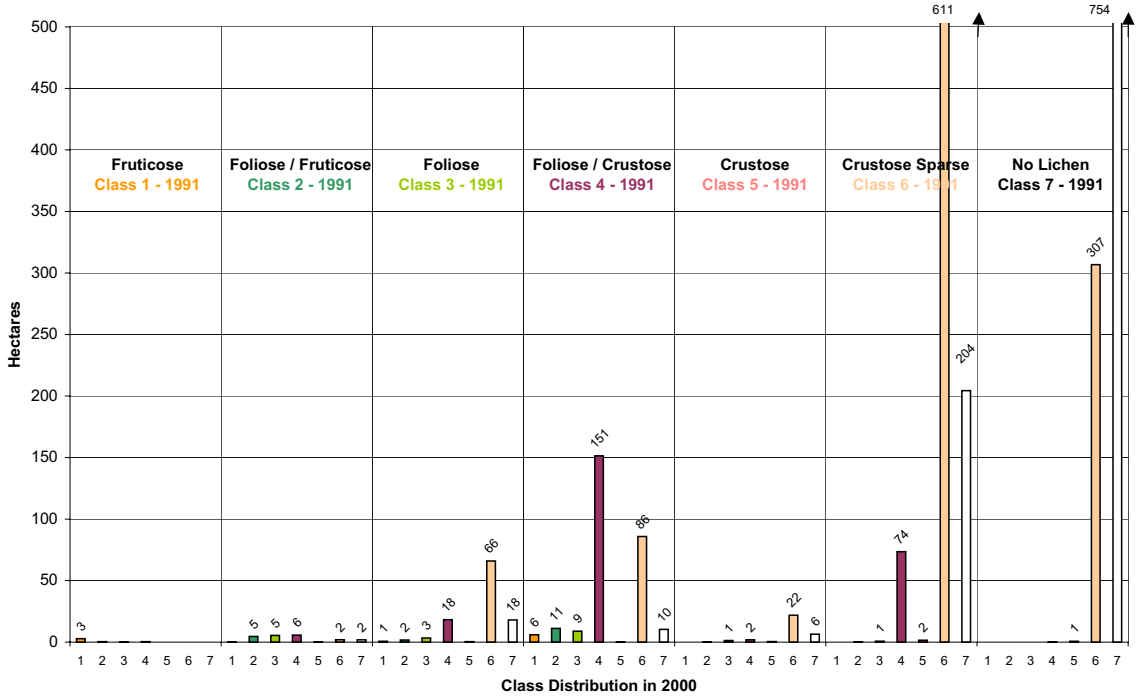

Figure E35: Changes in mapped class distribution of lichen communities between 1991 and 2000 for the lichen-field of Mile 72 - No. 8.

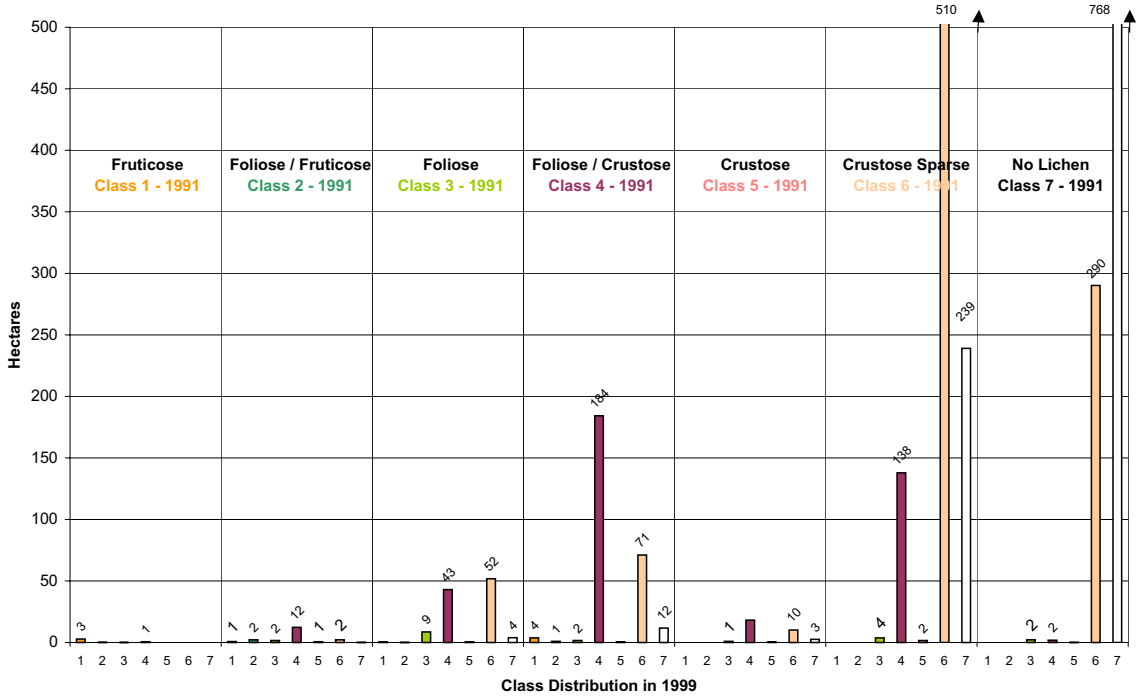

Figure E36: Changes in mapped class distribution of lichen communities between 1991 and 1999 for the lichen-field of Mile 72 - No. 8.

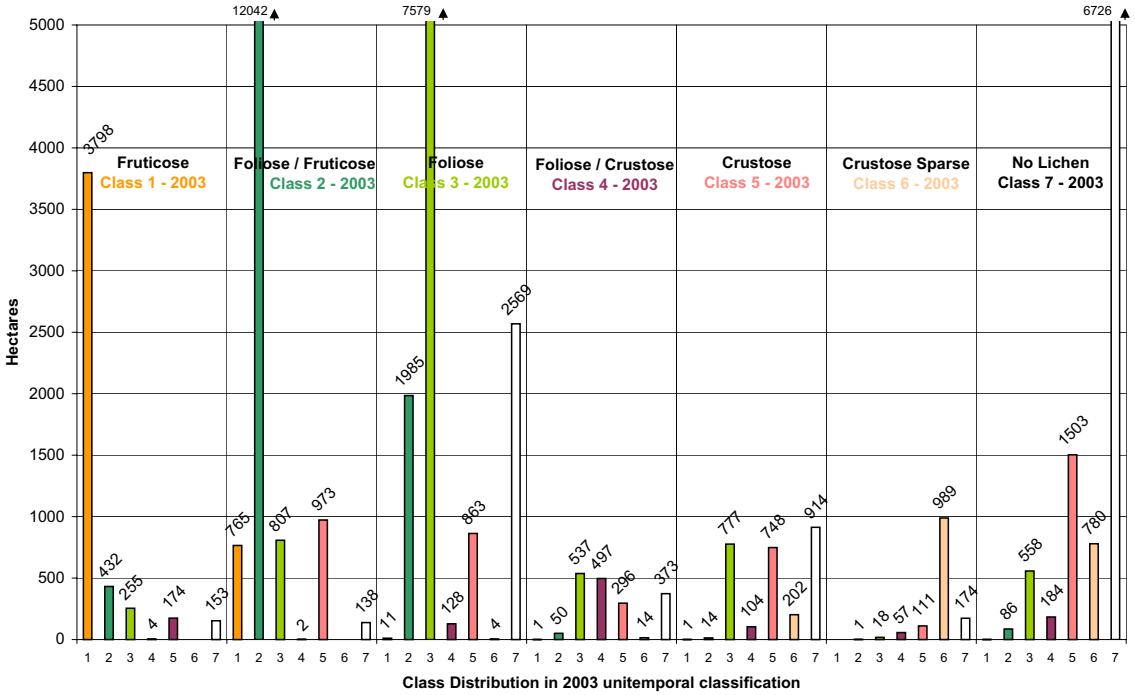

Figure E37: Changes in mapped class distribution of lichen communities between 2003 multi- and 2003 unitemporal classification for the lichen-field of the Messum Crater / Orawab - No. 9.

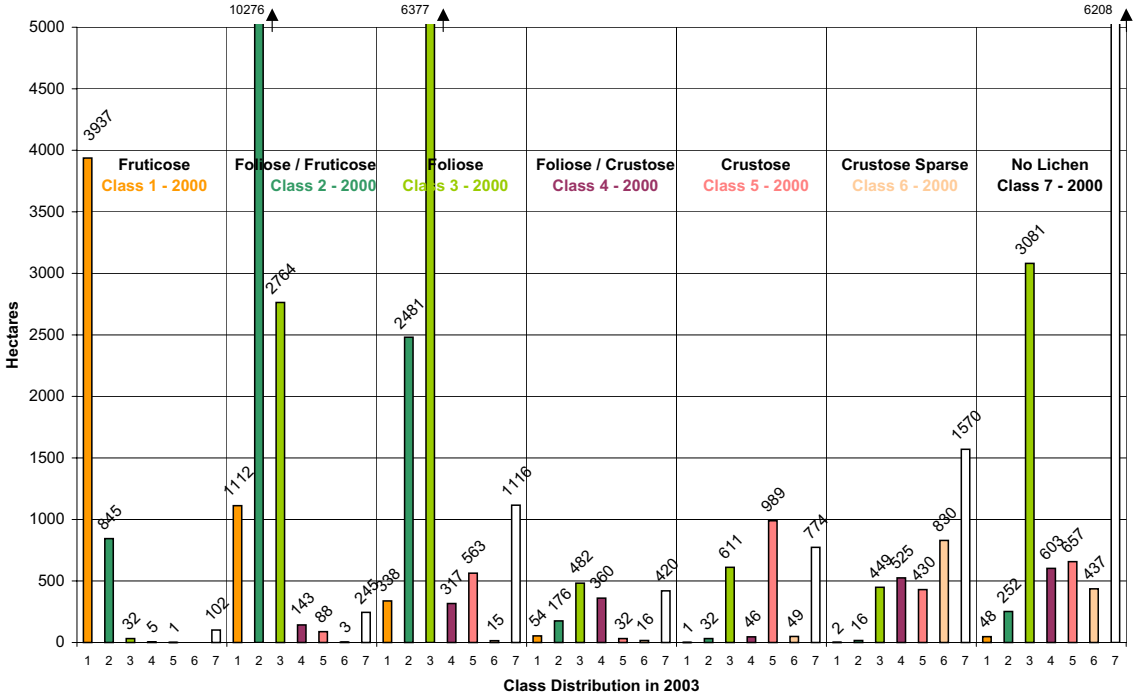

Figure E38:Changes in mapped class distribution of lichen communities between 2000 and 2003 for the lichen-field of the Messum Crater / Orawab - No. 9.

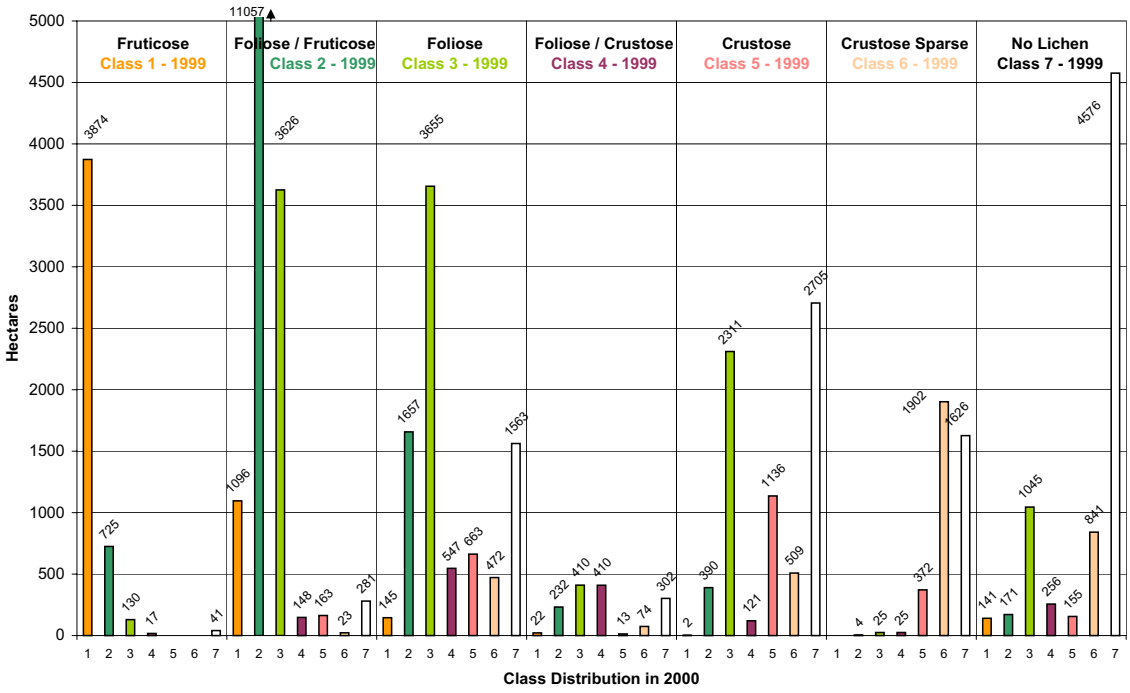

Figure E39: Changes in mapped class distribution of lichen communities between 1999 and 2000 for the lichen-field of the Messum Crater / Orawab - No. 9.

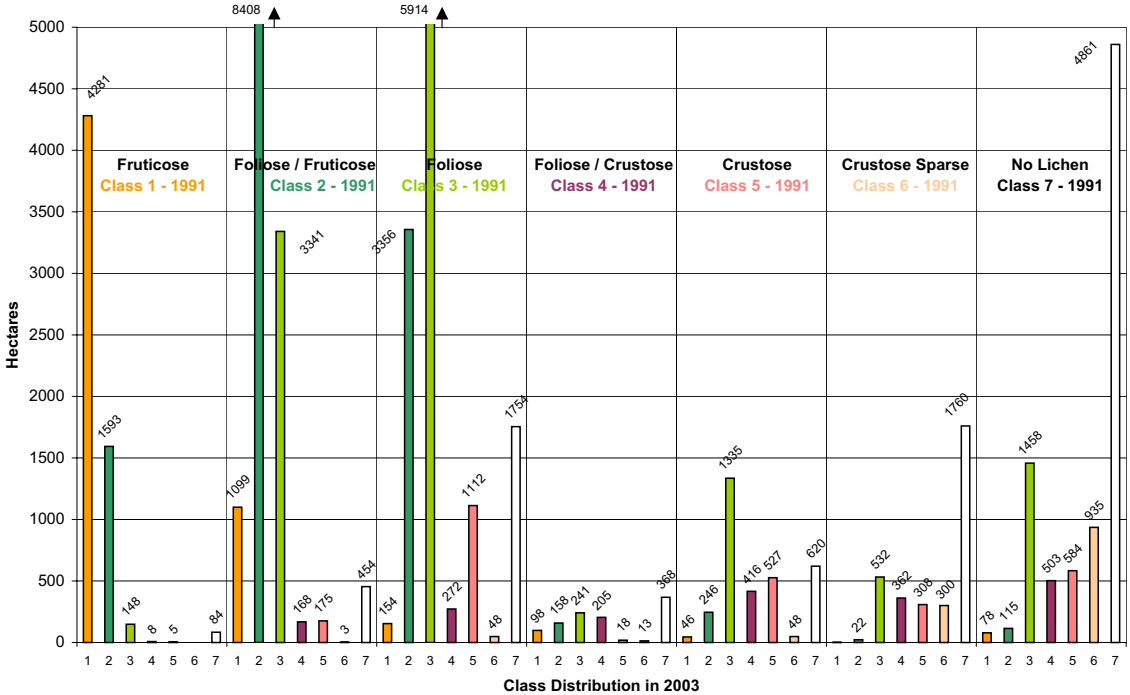

Figure E40: Changes in mapped class distribution of lichen communities between 1991 and 2003 for the lichen-field of the Messum Crater / Orawab - No. 9.

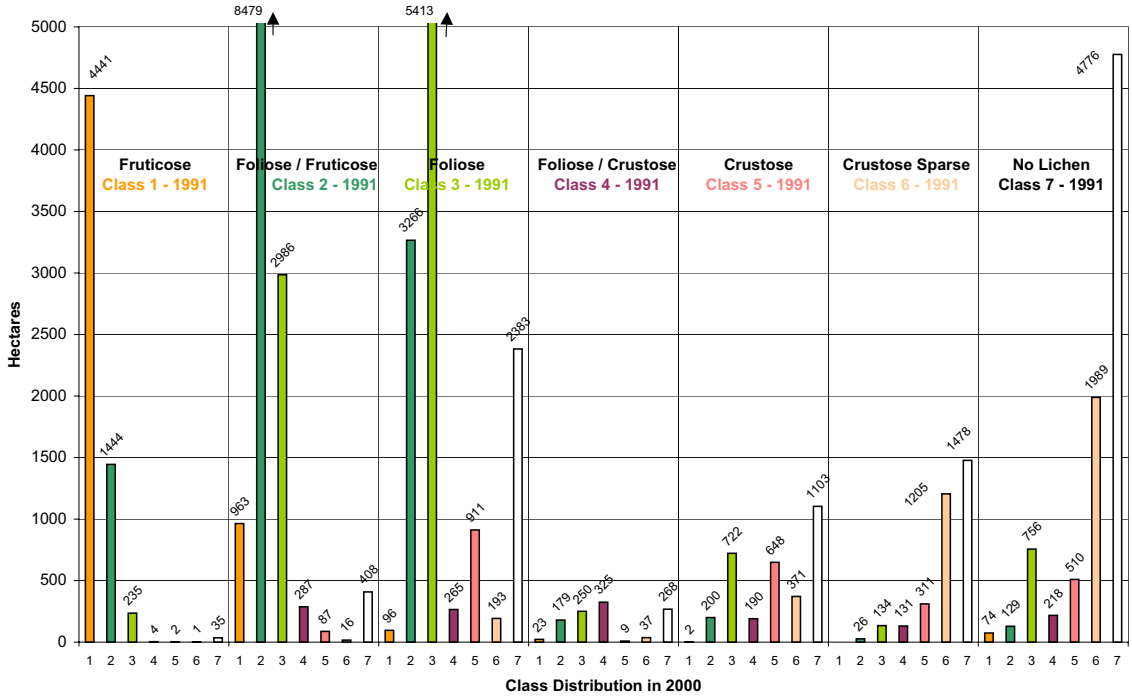

Figure E41: Changes in mapped class distribution of lichen communities between 1991 and 2000 for the lichen-field of the Messum Crater / Orawab - No. 9.

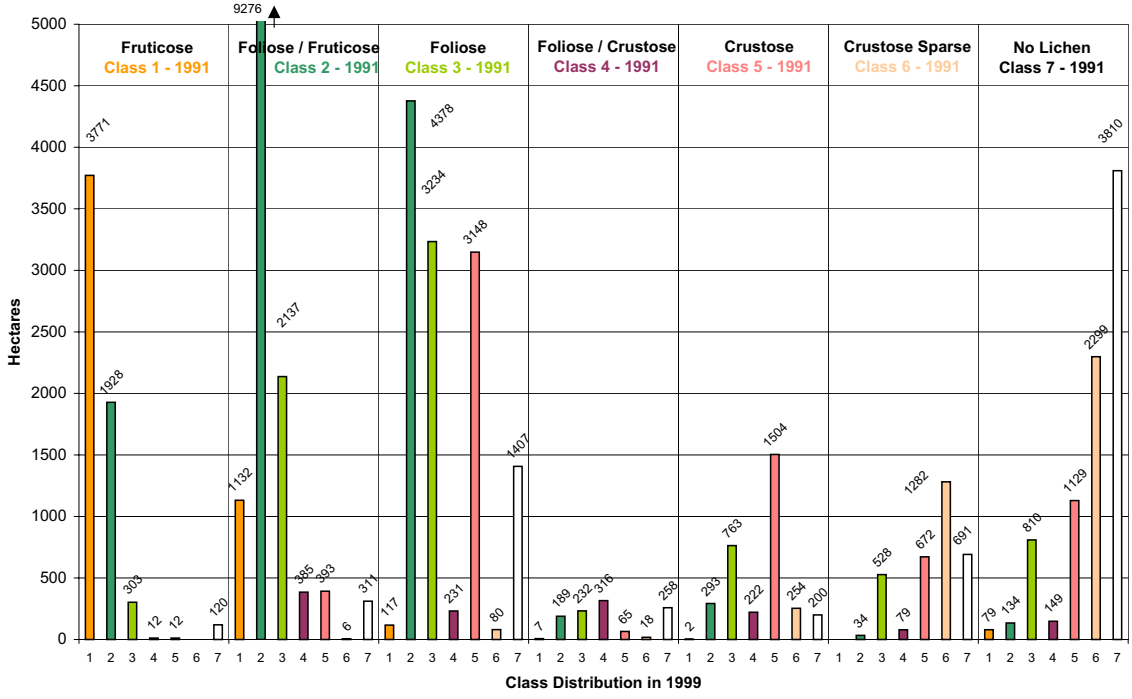

Figure E42: Changes in mapped class distribution of lichen communities between 1991 and 1999 for the lichen-field of the Messum Crater / Orawab - No. 9.

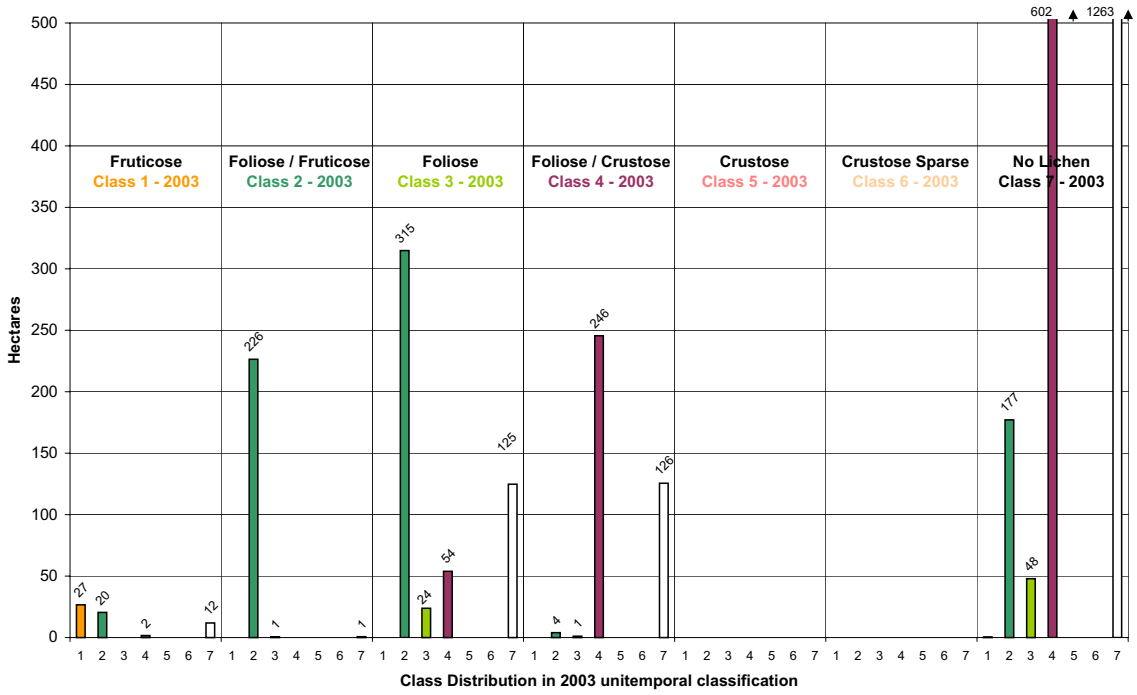

Figure E43: Changes in mapped class distribution of lichen communities between 2003 multi- and 2003 unitemporal classification for the lichen-field of Cape Cross - No. 10.

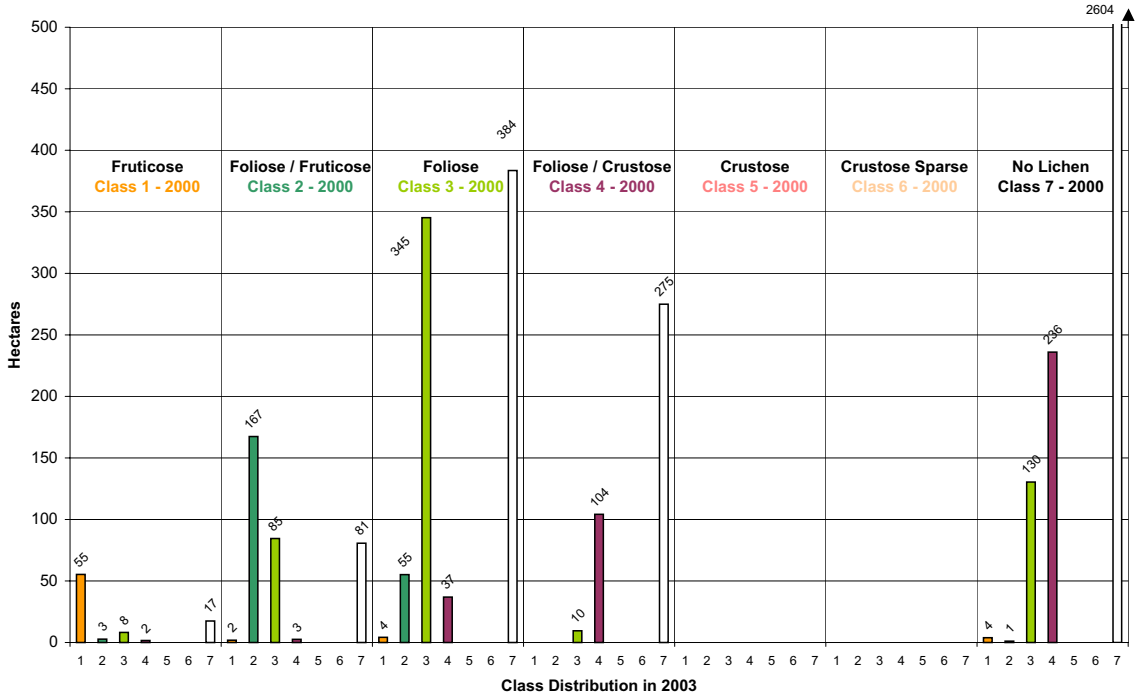

Figure E44: Changes in mapped class distribution of lichen communities between 2000 and 2003 for the lichen-field of Cape Cross - No. 10.

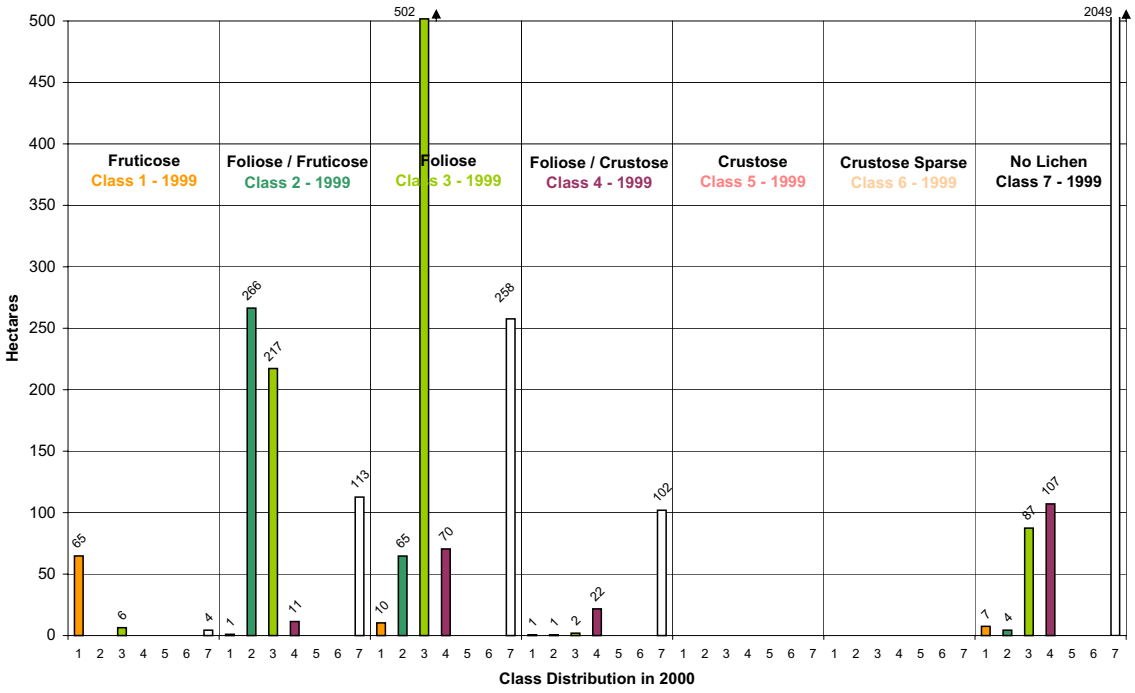

Figure E45: Changes in mapped class distribution of lichen communities between 1999 and 2000 for the lichen-field of Cape Cross - No. 10.

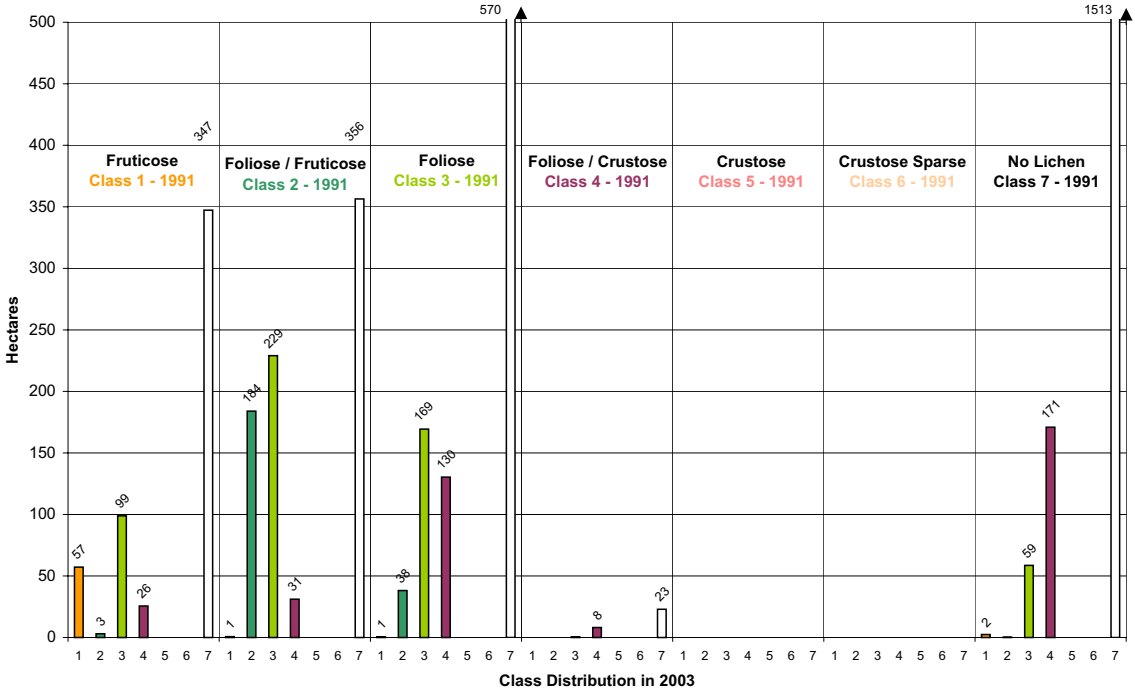

Figure E46: Changes in mapped class distribution of lichen communities between 1991 and 2003 for the lichen-field of Cape Cross - No. 10.

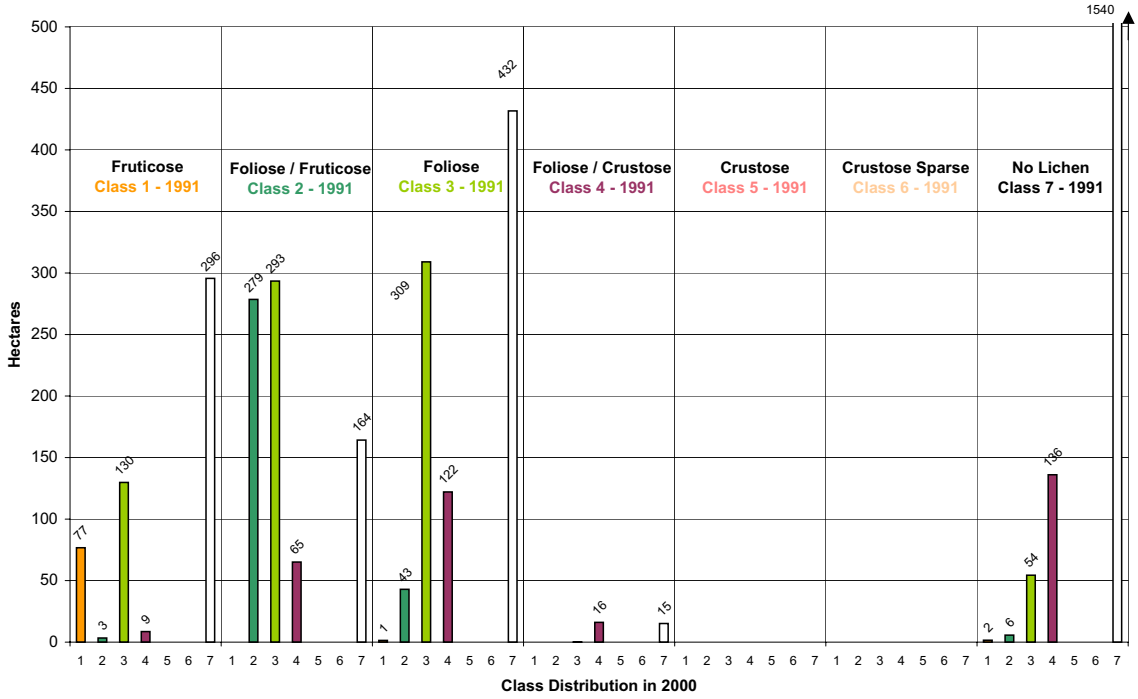

Figure E47: Changes in mapped class distribution of lichen communities between 1991 and 2000 for the lichen-field of Cape Cross - No. 10.

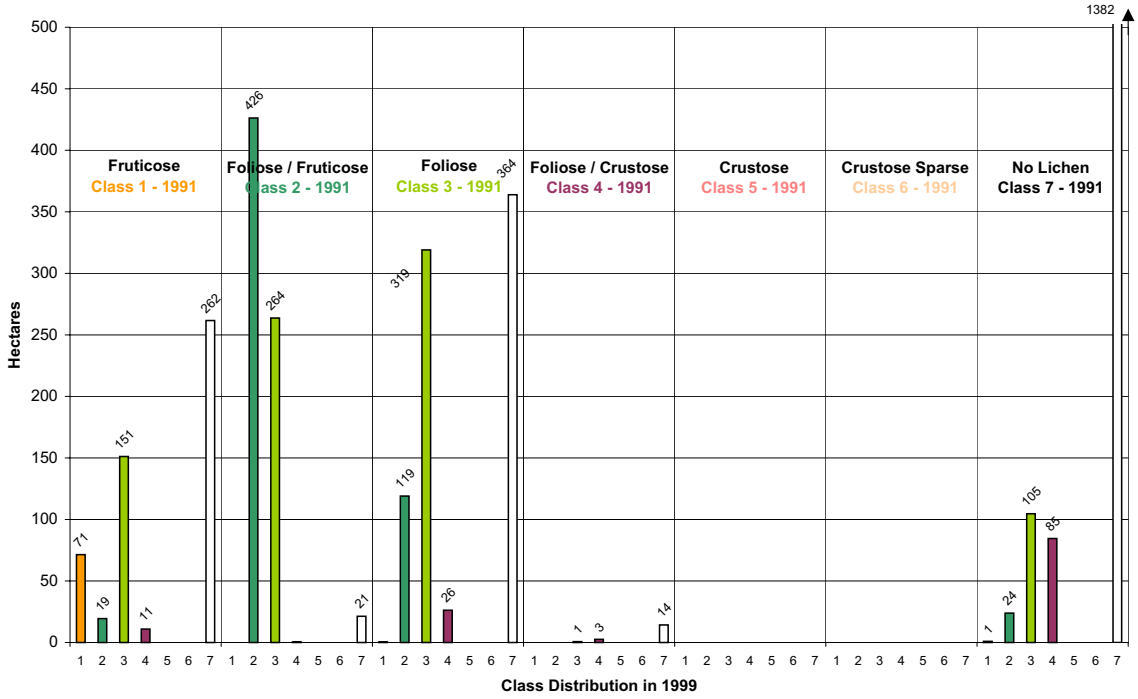

Figure E48: Changes in mapped class distribution of lichen communities between 1991 and 1999 for the lichen-field of Cape Cross - No. 10.

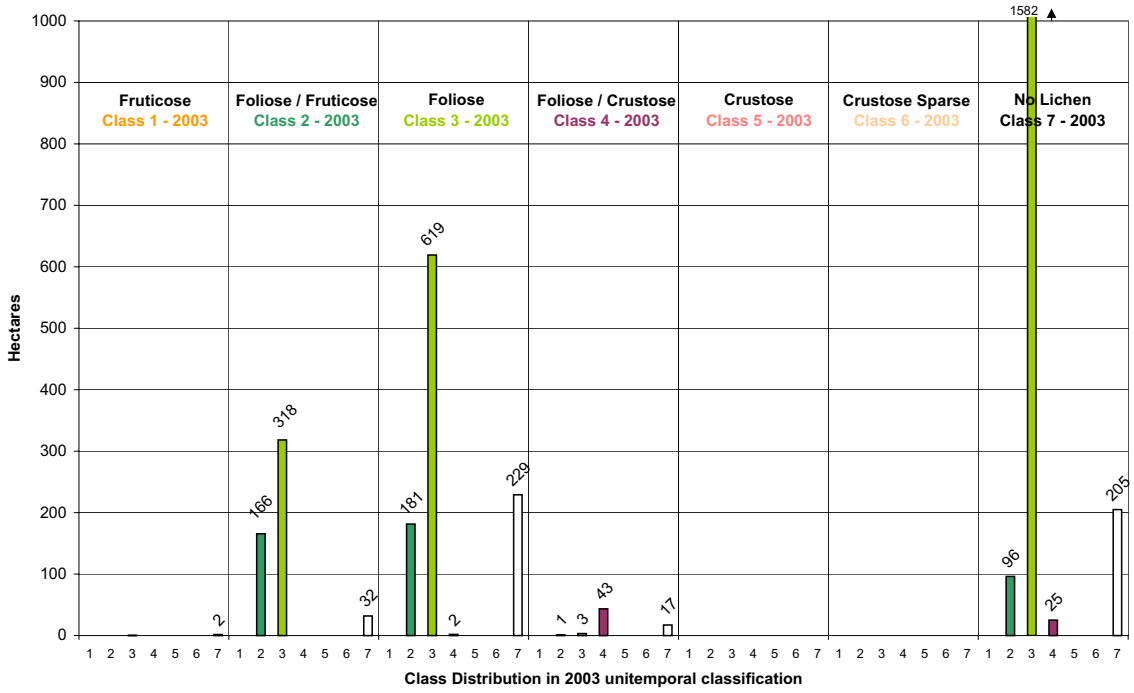

Figure E49: Changes in mapped class distribution of lichen communities between 2003 multi- and 2003 unitemporal classification for the lichen-field of the Brandberg West - No. 11.

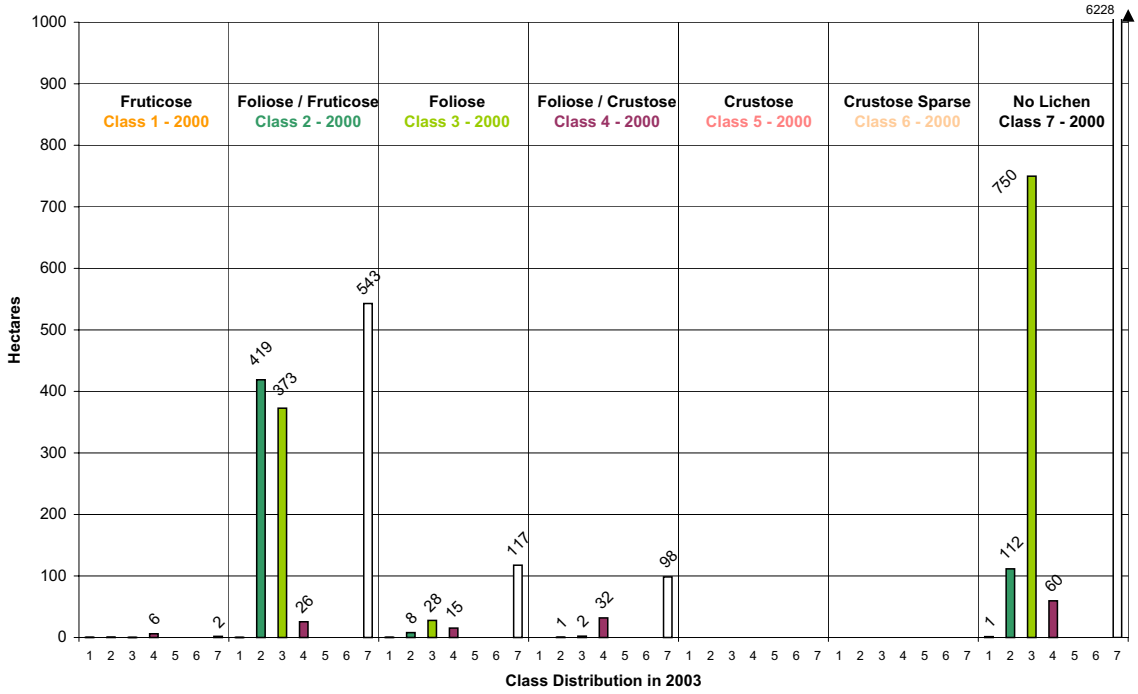

Figure E50: Changes in mapped class distribution of lichen communities between 2000 and 2003 for the lichen-field of the Brandberg West - No. 11.

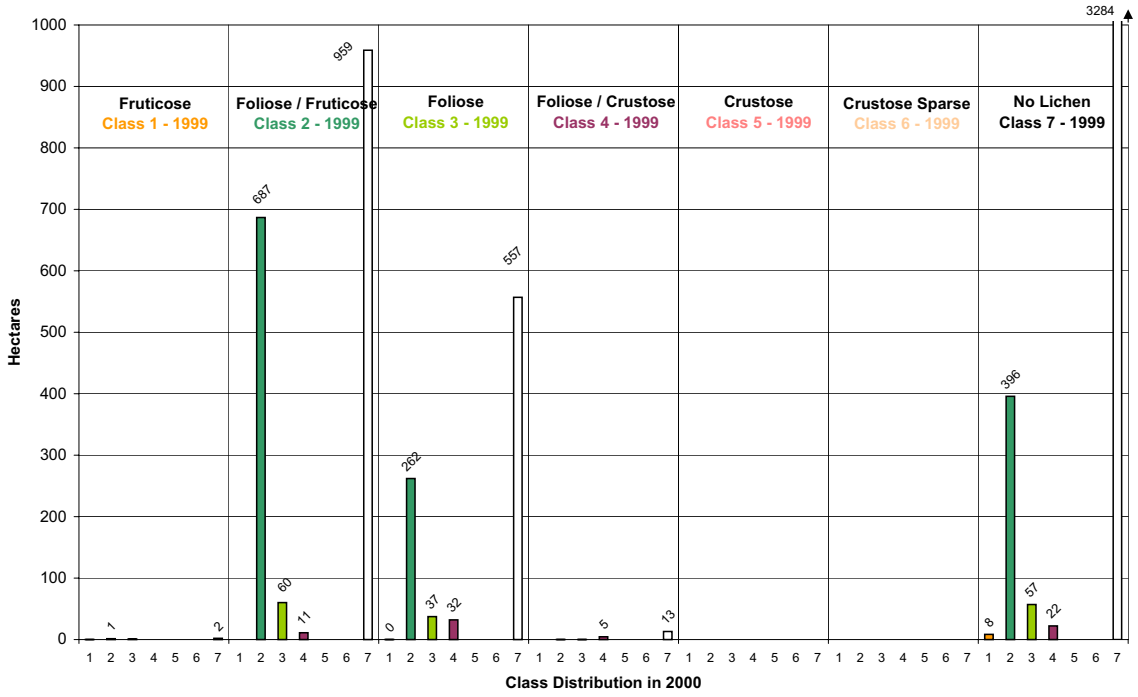

Figure E51: Changes in mapped class distribution of lichen communities between 1999 and 2000 for the lichen-field of the Brandberg West - No. 11.

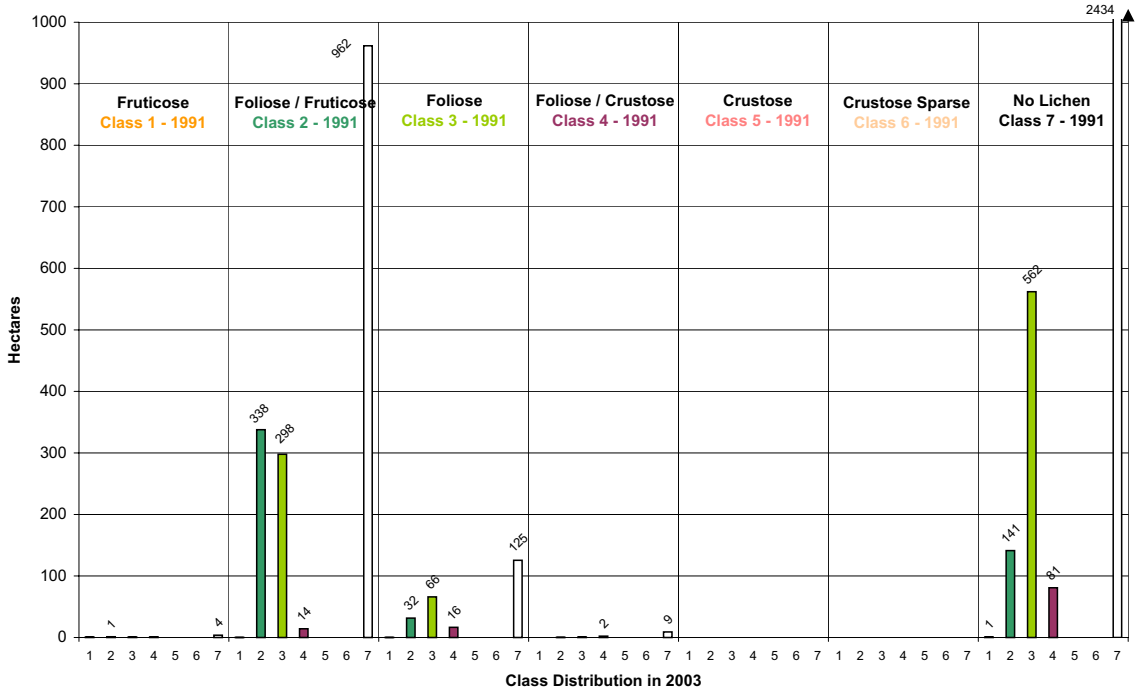

Figure E52: Changes in mapped class distribution of lichen communities between 1991 and 2003 for the lichen-field of the Brandberg West - No. 11.

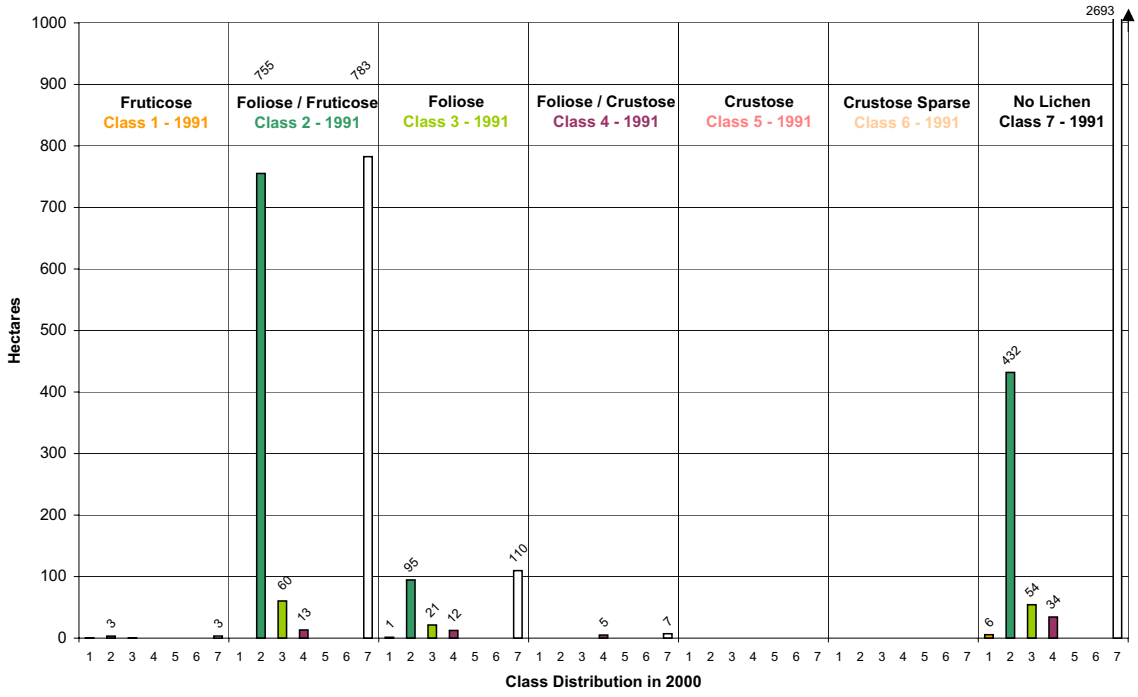

Figure E53: Changes in mapped class distribution of lichen communities between 1991 and 2000 for the lichen-field of the Brandberg West - No. 11.

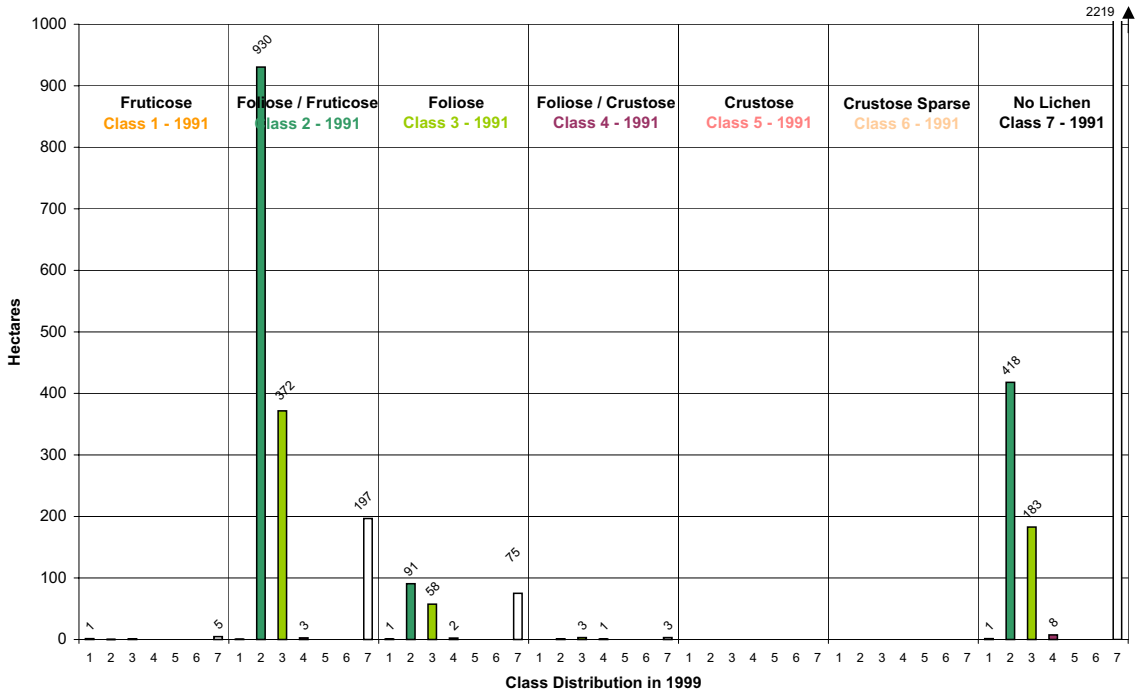

Figure E54: Changes in mapped class distribution of lichen communities between 1991 and 1999 for the lichen-field of the Brandberg West - No. 11.

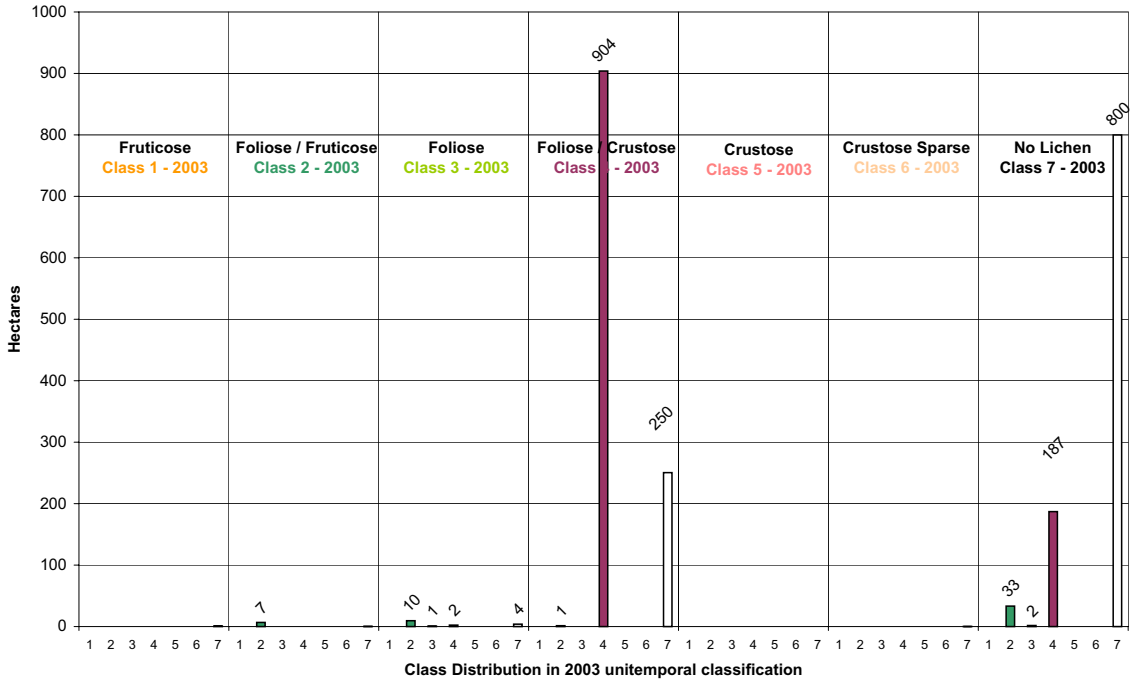

Figure E55: Changes in mapped class distribution of lichen communities between 2003 multi- and 2003 unitemporal classification for the lichen-field of the Huabmond - No. 12.

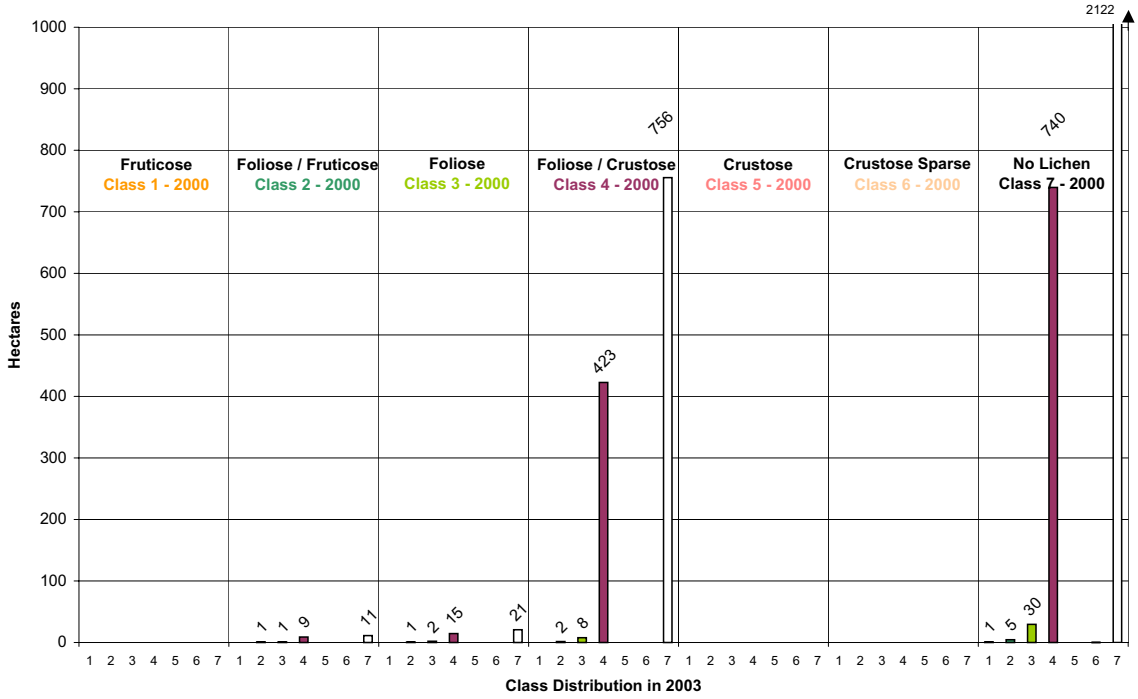

Figure E56: Changes in mapped class distribution of lichen communities between 2000 and 2003 for the lichen-field of the Huabmond - No. 12.

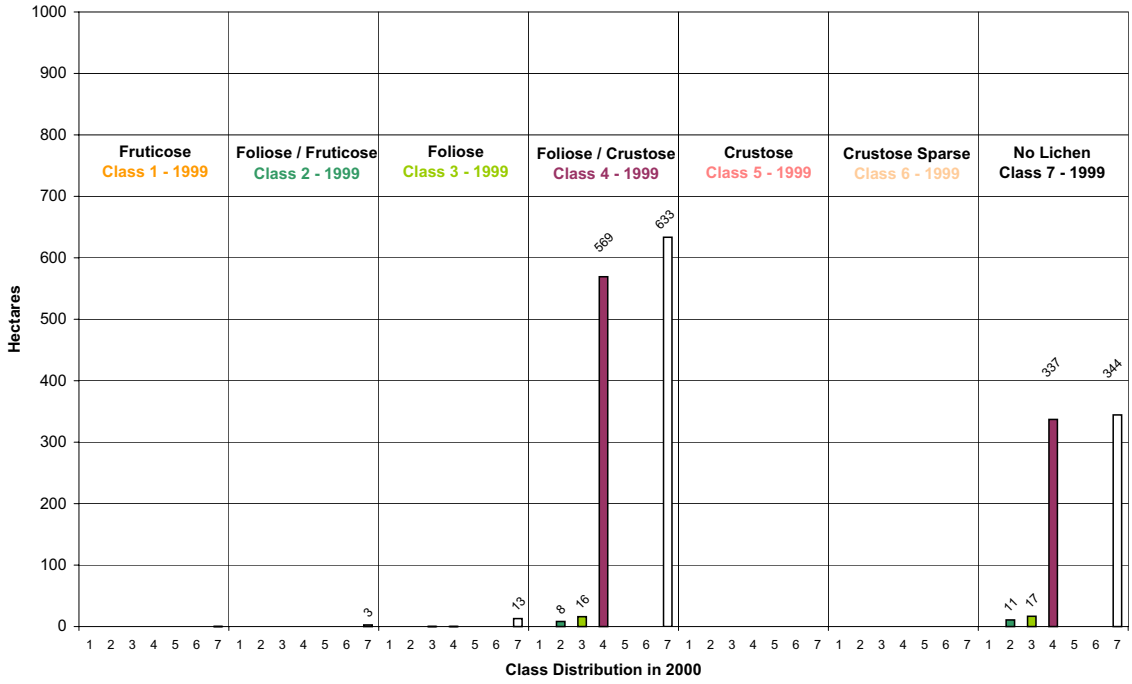

Figure E57: Changes in mapped class distribution of lichen communities between 1999 and 2000 for the lichen-field of the Huabmond - No. 12.

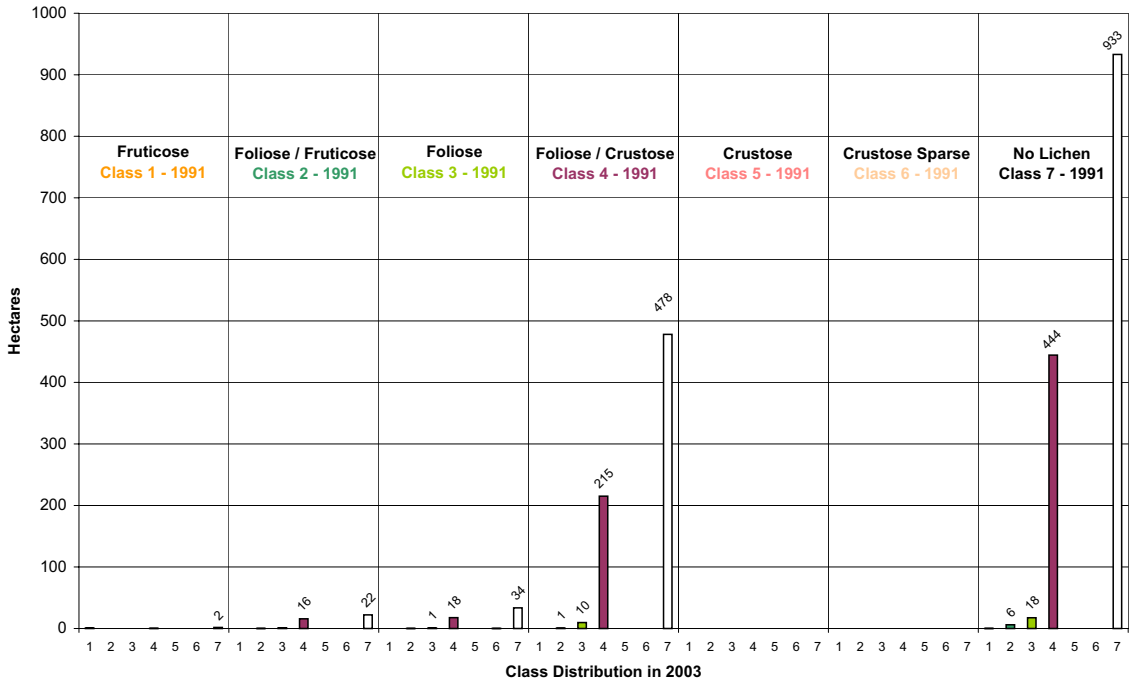

Figure E58: Changes in mapped class distribution of lichen communities between 1991 and 2003 for the lichen-field of the Huabmond - No. 12.

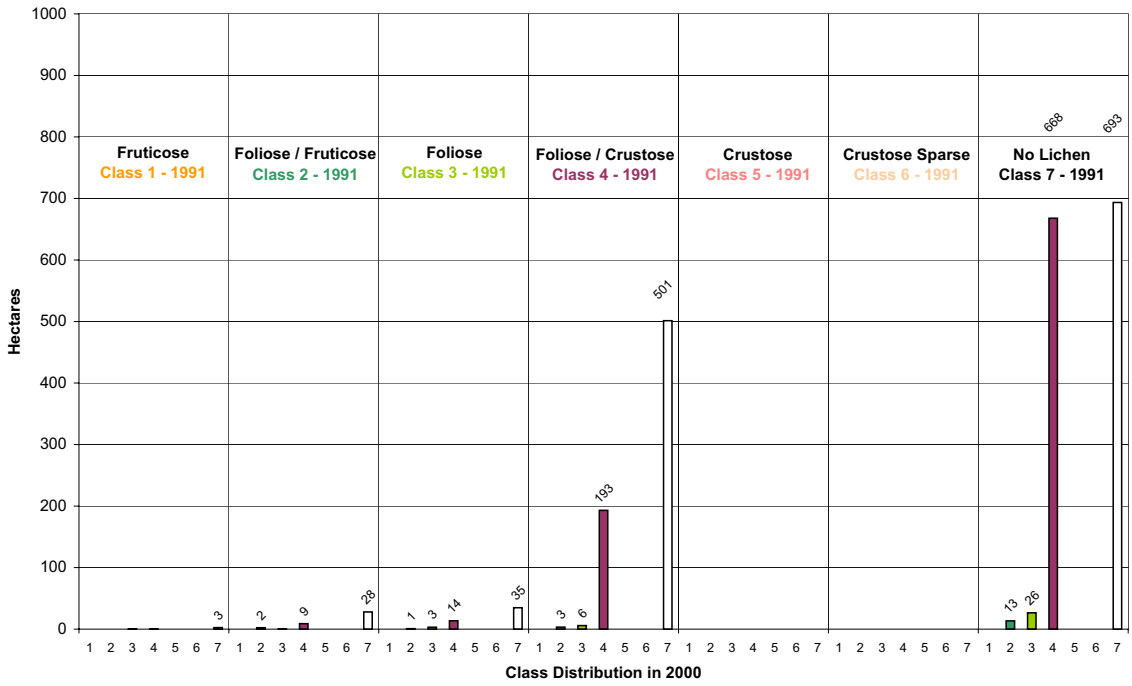

Figure E59: Changes in mapped class distribution of lichen communities between 1991 and 2000 for the lichen-field of the Huabmond - No. 12.

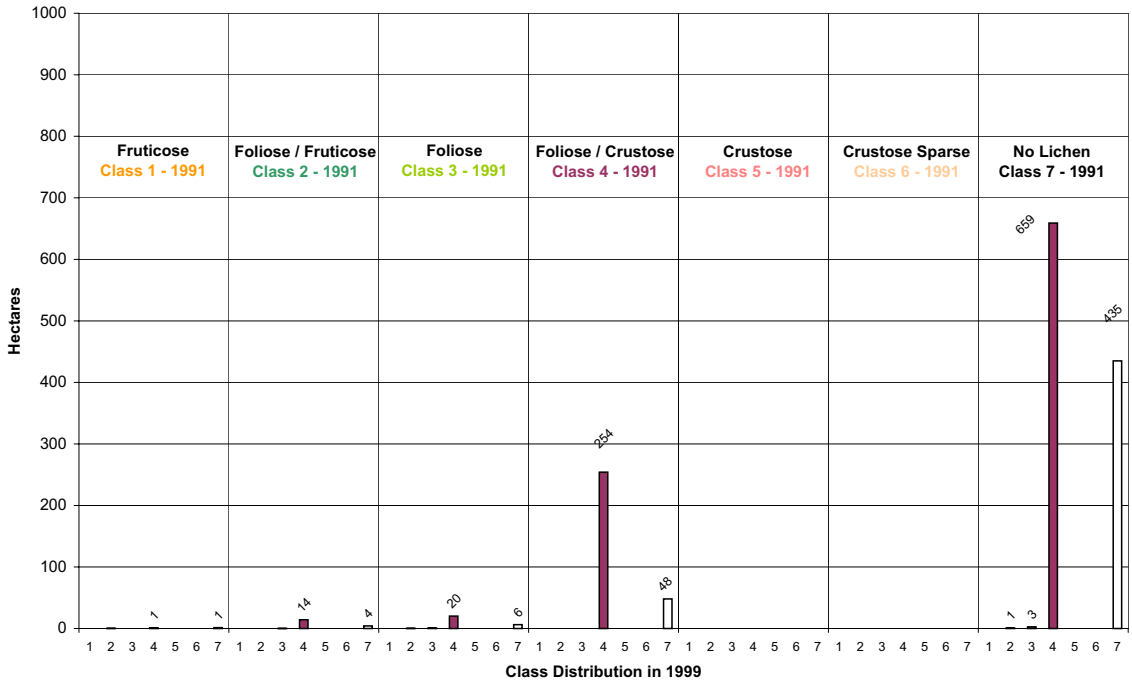

Figure E60: Changes in mapped class distribution of lichen communities between 1991 and 1999 for the lichen-field of the Huabmond - No. 12.

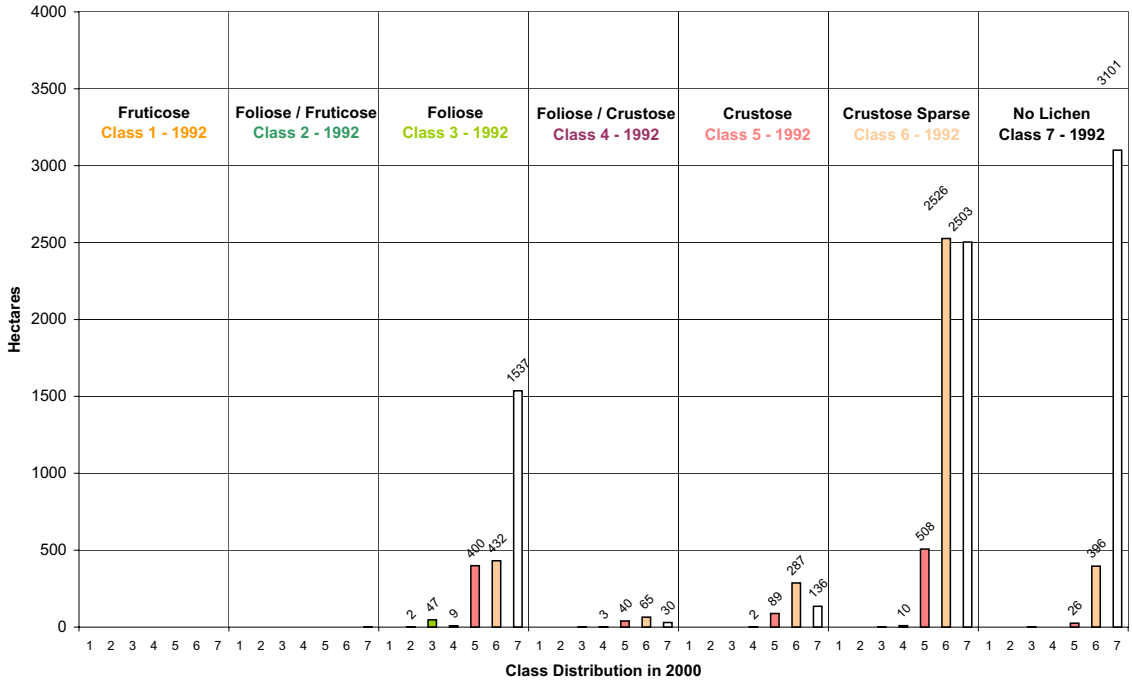

Figure E61: Changes in mapped class distribution of lichen communities between 1992 and 2000 for the Non-idas lichen-field - No. 3.

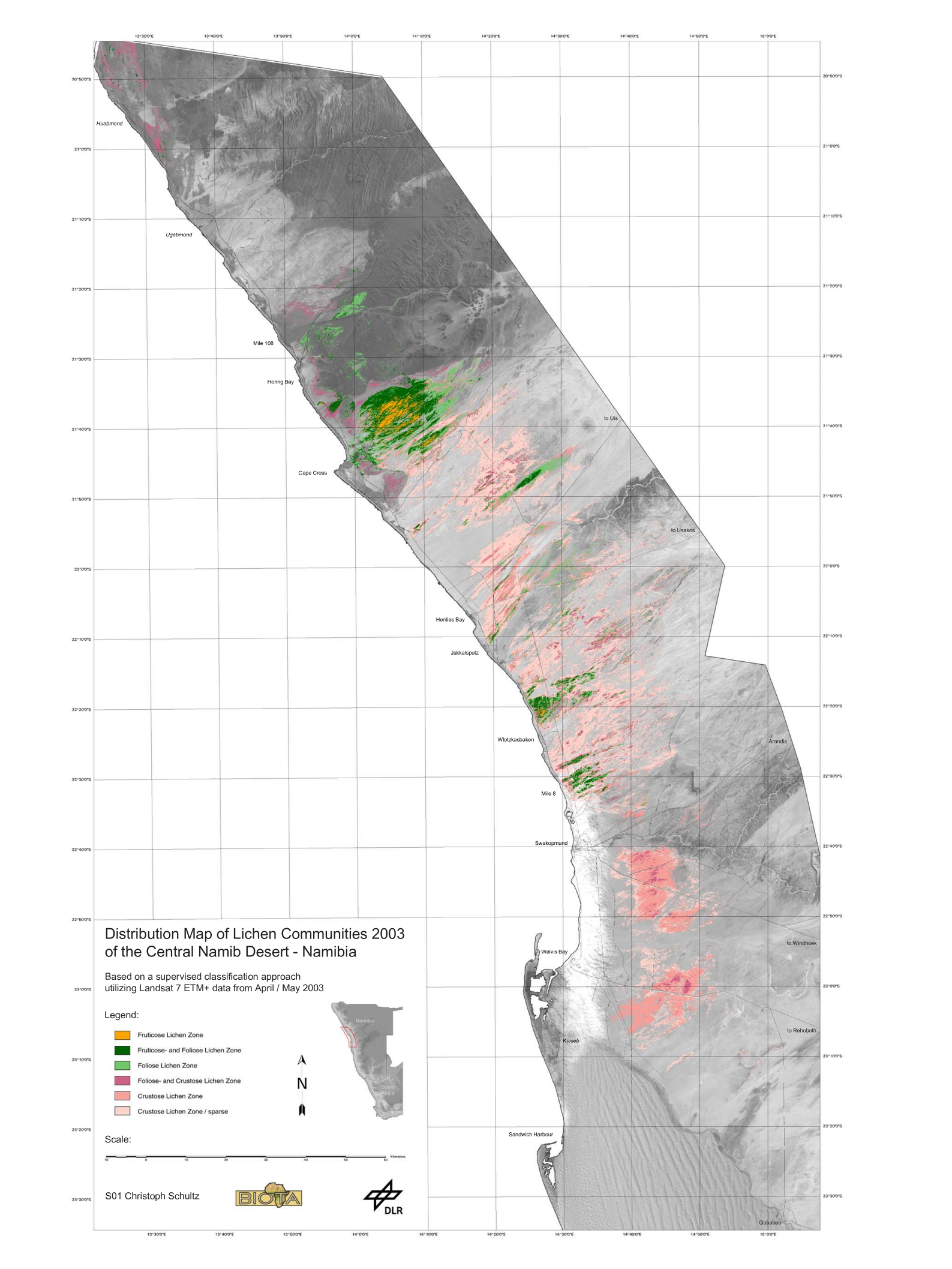
Huabmond
Ugabmond
Mile 108
Horing Bay
to Uis
Cape Cross
to Usakos
Henties Bay
Jakkalsputz
Wlotzkasbaken
Arandis
Mile 8
Swakopmund
Walvis Bay
to Windhoek
to Rehoboth
Kuiseb
Sandwich Harbour
Gobabeb
Distribution Map of Lichen Communities 2003
of the Central Namib Desert - Namibia
Based on a supervised classification approach
utilizing Landsat 7 ETM+ data from April / May 2003
Legend:
Fruticose Lichen Zone
Fruticose- and Foliose Lichen Zone
Foliose Lichen Zone
Foliose- and Crustose Lichen Zone
Crustose Lichen Zone
Crustose Lichen Zone / sparse
N
Namibia
South Africa
Scale:
S01 Christoph Schultz
BIOTA
DLR

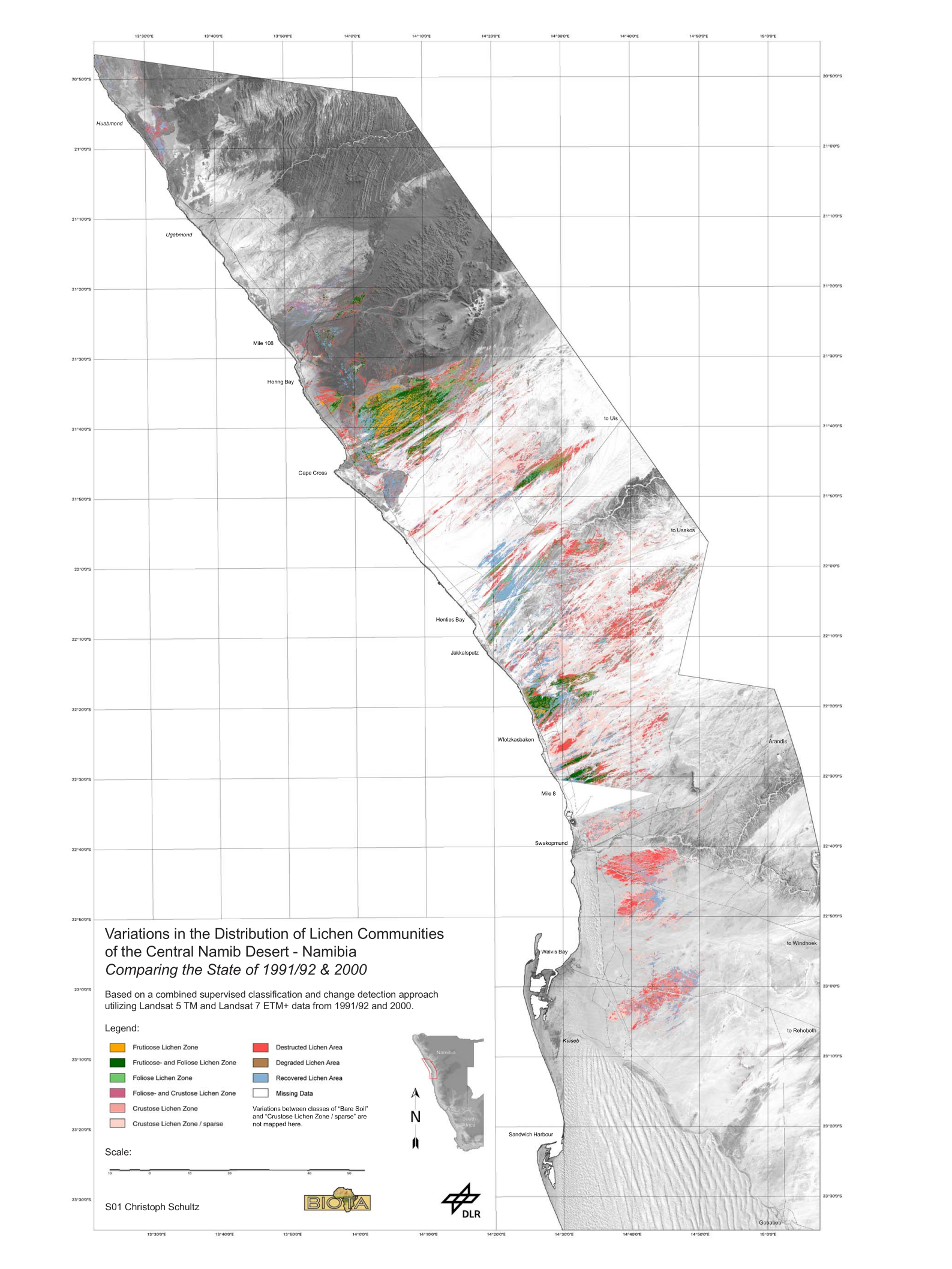
13°30'0"E
13°40'0"E
13°50'0"E
14°0'0"E
14°10'0"E
14°20'0"E
14°30'0"E
14°40'0"E
14°50'0"E
15°0'0"E
20°50'0"S
21°0'0"S
21°10'0"S
21°20'0"S
21°30'0"S
21°40'0"S
21°50'0"S
22°0'0"S
22°10'0"S
22°20'0"S
22°30'0"S
22°40'0"S
22°50'0"S
23°0'0"S
23°10'0"S
23°20'0"S
23°30'0"S
Huabmond
Ugabmond
Mile 108
Horing Bay
to Uis
Cape Cross
to Usakos
Henties Bay
Jakkalsputz
Wlotzkasbaken
Arandis
Mile 8
Swakopmund
Walvis Bay
to Windhoek
to Rehoboth
Kuiseb
Sandwich Harbour
Gobabeb
Variations in the Distribution of Lichen Communities
of the Central Namib Desert - Namibia
Comparing the State of 1991/92 & 2000
Based on a combined supervised classification and change detection approach
utilizing Landsat 5 TM and Landsat 7 ETM+ data from 1991/92 and 2000.
Legend:
Fruticose Lichen Zone
Fruticose- and Foliose Lichen Zone
Foliose Lichen Zone
Foliose- and Crustose Lichen Zone
Crustose Lichen Zone
Crustose Lichen Zone / sparse
Destructed Lichen Area
Degraded Lichen Area
Recovered Lichen Area
Missing Data
Variations between classes of "Bare Soil"
and "Crustose Lichen Zone / sparse" are
not mapped here.
Namibia
South Africa
N
Scale:
10
0
10
20
40
60
S01 Christoph Schultz
BIOTA
DLR

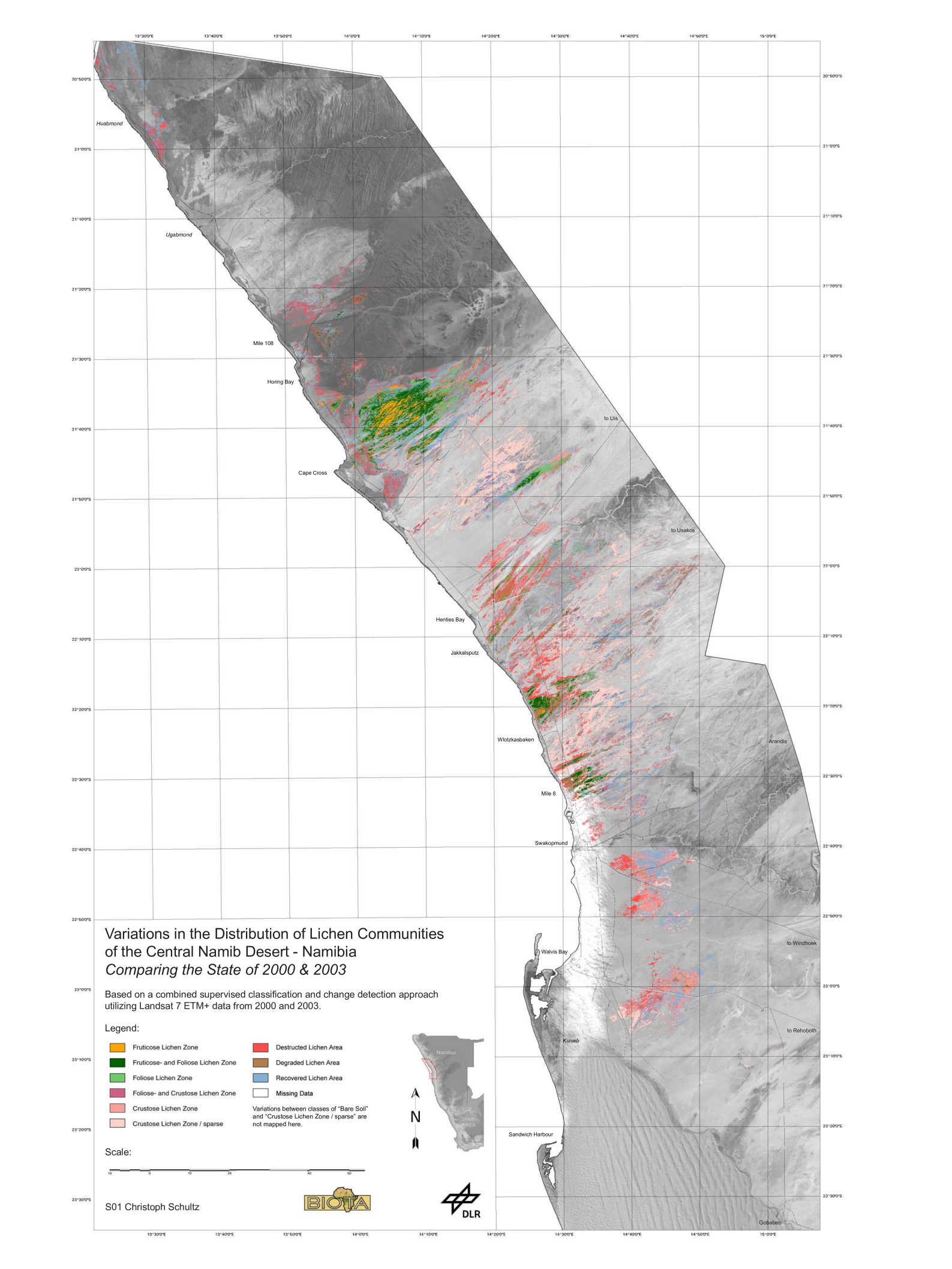
13°30'0"E
13°40'0"E
13°50'0"E
14°0'0"E
14°10'0"E
14°20'0"E
14°30'0"E
14°40'0"E
14°50'0"E
15°0'0"E
20°50'0"S
21°0'0"S
21°10'0"S
21°20'0"S
21°30'0"S
21°40'0"S
21°50'0"S
22°0'0"S
22°10'0"S
22°20'0"S
22°30'0"S
22°40'0"S
22°50'0"S
23°0'0"S
23°10'0"S
23°20'0"S
23°30'0"S
Huabmond
Ugabmond
Mile 108
Horing Bay
to Uis
Cape Cross
to Usakos
Henties Bay
Jakkalsputz
Wlotzkasbaken
Arandis
Mile 8
C34
Swakopmund
to Windhoek
Walvis Bay
B2
to Rehoboth
Kuiseb
Sandwich Harbour
Gobabeb
Variations in the Distribution of Lichen Communities
of the Central Namib Desert - Namibia
Comparing the State of 2000 & 2003
Based on a combined supervised classification and change detection approach
utilizing Landsat 7 ETM+ data from 2000 and 2003.
Legend:
Fruticose Lichen Zone
Fruticose- and Foliose Lichen Zone
Foliose Lichen Zone
Foliose- and Crustose Lichen Zone
Crustose Lichen Zone
Crustose Lichen Zone / sparse
Destructed Lichen Area
Degraded Lichen Area
Recovered Lichen Area
Missing Data
Variations between classes of "Bare Soil"
and "Crustose Lichen Zone / sparse" are
not mapped here.
Namibia
South Africa
N
Scale:
10
0
10
20
40
60
S01 Christoph Schultz
BIOTA
DLR